Role and regulation of the Poly(ADP-ribose)Glycohydrolase (PARG) in the cell response to DNA damages

Eléa Heberle

▶ **To cite this version:**

Eléa Heberle. Role and regulation of the Poly(ADP-ribose)Glycohydrolase (PARG) in the cell response to DNA damages. Genomics [q-bio.GN]. Université de Strasbourg, 2017. English. NNT : 2017STRAJ106 . tel-03934531

HAL Id: tel-03934531
https://theses.hal.science/tel-03934531

Submitted on 11 Jan 2023

HAL is a multi-disciplinary open access archive for the deposit and dissemination of scientific research documents, whether they are published or not. The documents may come from teaching and research institutions in France or abroad, or from public or private research centers.

L'archive ouverte pluridisciplinaire **HAL**, est destinée au dépôt et à la diffusion de documents scientifiques de niveau recherche, publiés ou non, émanant des établissements d'enseignement et de recherche français ou étrangers, des laboratoires publics ou privés.

UNIVERSITÉ DE STRASBOURG

ÉCOLE DOCTORALE Vie et Santé (ED414)

Thèse présentée par :

Éléa HÉBERLÉ

Soutenue publiquement le : 11 décembre 2017

Pour obtenir le grade de : Docteur de l'Université de Strasbourg

Discipline/Spécialité :

Sciences du Vivant – Aspects Moléculaires et Cellulaires de la Biologie

Etude du rôle et de la régulation de la Poly(ADP-Ribose) Glycohydrolase (PARG) dans la réponse cellulaire aux dommages à l'ADN

THÈSE dirigée par :

Dr. SCHREIBER Valérie — Directeur de Recherche, Université de Strasbourg

RAPPORTEURS EXTERNES :

Dr. RIBEYRE Cyril — Chargé de recherche, Institut de Génétique Humaine de Montpellier – CNRS, UMR9002

Pr. ZIEGLER Mathias — Professeur, Department of Biomedicine University of Bergen

EXAMINATEUR INTERNE :

Dr. SOUTOGLOU Evi — Directeur de recherche, Institut de Génétique et de Biologie Moléculaire et Cellulaire - CNRS, UMR 7104

Equipe « Poly(ADP-ribosyl)ation et Intégrité du Génome »

UMR7242-BSC-CNRS – Biologie et Signalisation Cellulaire

300, Boulevard Sébastien Brant, BP10413 – 67412, Illkirch Cedex - FRANCE

J'ai beaucoup appris. Je continue.
Je n'en sais guère plus.

René Barjavel.

Table of contents

Acknowledgements 9

Table of figures 15

Tables : 15

Introduction 17

Chapter 1: Poly(ADP-ribosyl)ation, a versatile post-translational modification. 17

1. Post-translational modifications: roles and common features 20

2. Reaction of ADP-ribosylation and Poly(ADP-ribosyl)ation 22

3. Writers of ADP-ribosylation 24

3.1 The PARP superfamily 27

3.2 DNA dependent PARPs 27

3.2.1 PARP1 27

3.2.2 PARP2 28

3.2.3 PARP3 28

3.3 Tankyrases 29

3.4 CCCH-type Zinc finger PARPs 29

3.4.1 PARP7 30

3.4.2 PARP12 30

3.4.3 PARP13 30

3.5 Macro PARPs 31

3.5.1 PARP9 31

3.5.2 PARP14 31

3.5.3 PARP15 32

3.6 Other MARTs 32

3.6.1 PARP4 32

3.6.2 PARP6 32

3.6.3 PARP8 32

3.6.4 PARP10 34

3.6.5 PARP11 34

3.6.6 PARP16 34

4. Readers of PARylation 36

4.1 PAR binding motif (PBM) 36

4.2 Macro domain 36

4.3 PAR binding Zinc finger (PBZ) 37

4.4 WWE motif 37

4.5 Other ADP ribose readers: 37

4.5.1 FHA and BRCT 37

4.5.2 RNA recognition motif and SR/KR repeats splicing factors 38

4.5.3 OB-fold 38

4.5.4 PIN domain 38

4.5.5 RGG/GAR domains and other reported interactions 38

5. Erasers of PARylation 40

5.1 PARG 40

5.1.1 A Brief history of PARG discovery 40

5.1.2 Genomic structure 40

5.1.3 PARG: “One gene to gen them all” 42

5.1.4 Other structural features ... 42
5.1.5 PARG: catalytic domain ... 44
5.1.6 PARG and genomic integrity ... 44
5.2 ARH proteins: ADP-ribose-acceptor hydrolases ... 46
5.3 MacroD1, MacroD2 and TARG1 ... 48
5.4 Other ADP-ribose erasers ... 48
6. Feeders and consumers of ADP ribosylation ... 48
6.1 Feeders of NAD: Salvage pathway and De Novo biosynthesis. ... 50
6.2 Consumers of NAD+: PARPs and sirtuins ... 50
7. ADP-ribosylation everywhere ... 51
7.1 PARylation in bacteria and fungi ... 51
7.2 PARylation in archaea ... 52
7.3 PARylation in viruses ... 52
7.4 PARylation in plants ... 52
7.5 PARylation in other eukaryotic organisms ... 54
7.6 General features of PARylation ... 54
Chapter 2: Roles of PARylation in the the maintenance of genome integrity ... 56
1. The ever increasing roles and targets of PARylation ... 56
2. DNA Damage Response (DDR) ... 58
2.1 Types of DNA damage and main repair pathways ... 58
2.2 Nucleotide excision repair ... 58
2.2.1 Global Genome NER (GG-NER) ... 60
2.2.2 Transcription-coupled NER (TC-NER) ... 60
2.2.3 PARylation and NER ... 60
2.3 Single Strand Break Repair ... 61
2.3.1 Mechanism ... 61
2.3.2 PARylation in SSBR ... 62
2.4 Base Excision Repair ... 62
2.4.1 Mechanism ... 62
2.4.2 PARylation and BER ... 64
2.5 Double strand break repair (DSBR) ... 64
2.5.1 Homologous recombination ... 64
2.5.1.1 Mechanism ... 64
2.5.1.2 PARylation in HR ... 65
2.5.2 Non-homologous end joining ... 66
2.5.2.1 Classical NHEJ ... 66
2.5.2.2 Alternative NHEJ ... 66
2.5.2.3 PARylation and NHEJ ... 66
2.3.3 PARPs in the choice between the DSB pathways ... 68
2.6 PARP Mismatch repair ... 70
2.6.1 Mechanism: ... 70
2.6.2 PARylation and MMR ... 70
3. Replicative stress Response (RSR) ... 70
3.1 Cell cycle progression ... 70
3.2 The life of a replication fork. ... 72
3.2.1 Fork initiation ... 72
3.2.2 Fork elongation ... 72
3.2.3 Fork termination ... 74
3.2.4 Challenges for the replicative fork ... 74
3.3 Stalling, collapsing, reversal, restart: the faith of replication forks ... 76
3.4 PARylation and replicative stress. ... 78
4. Signalling kinases to maintain genome integrity ... 80

5. PARP and PARG in other interface processes during DNA repair ... *81*
5.1 Controlling cell cycle checkpoints ... 81
5.2 Controlling chromatin structure ... 82
5.3 Controlling transcription ... 84
5.4 PAR in inflammation ... 86
5.5 PARylation in cell death ... 86
5.5.1 Necrosis ... 86
5.5.2 Apoptosis ... 87
5.5.3 Parthanathos ... 87
5.5.4 Autophagy ... 88
5.6 PARylation in metabolism, aging and cancer: ... 88
Chapter 3: PARP and PARG inhibitors in chemotherapeutics ... 90
1. Keeping balance in polymer levels: a trail for treating cancer? ... *90*
2. The targeting of PARP1 in cancer therapeutics ... *92*
2.1 Development of inhibitors ... 92
2.2 Clinical trials ... 94
2.3 Resistance and alternatives ... 96
3. The targeting of PARG in cancer therapeutics ... *98*
3.1 Development of inhibitors ... 98
3.2 Synthetic lethality ... 100
3.3 Towards clinical trials? ... 100
Aims of my research project: ... **102**
Results ... **104**
Aim one: Generation of new cellular tools for the study of the contribution of PARG isoforms in DNA repair ... 104
Introduction ... *104*
Fast track generation of a library of constructs and cell lines expressing wild type or mutated single PARG isoforms: new tools for studying PARG ... **106**
Discussion ... *128*
1. Choice of cell line ... 128
2. Efficiency of PARG depletion ... 128
3. Expression levels of complemented PARG isoforms ... 129
4. Tet-system leakage ... 129
5. Endogenous PARG levels VS complemented cell lines PARG levels ... 130
6. Is PCNA a PIP-degron? ... 131
Conclusion ... *132*
Aim two: Study of the regulation of PARG by post-translational modifications. ... 134
Introduction ... *134*
DNA-PKcs is a new protein partner of PARG. ... **136**
Discussion ... *157*
1. New protein partners for PARG ... 157
2. Monitoring labile interactions ... 158
3. Identification of phosphorylation sites: still a challenge ... 158
4. Functional impact of DNA-PK phosphorylation on PARG ... 160
5. PARG and DNA-PK functional interaction ... 161
6. DNA-PK and PARylation ... 161
Conclusions ... *162*
Aim three: Impact of PARG deficiency on the cell response to camptothecin-induced DSB ... 164
Introduction ... *164*

Impact of PARG deficiency on the cell response to camptothecin-induced DSB 166
Discussion and perspectives 200
1. Escaping replicative stress: a hard task 200
2. Fork reversal as a general response to replicative stress. 202
3. Fork repriming as the way out? 204
4. RPA-P-S4S8 defect results from a direct effect on RPA 205
4. IPond technique as the golden standard? 206
Conclusion 206
General Conclusion: 208
Bibliography: 209
APPENDIX 236
Appendix I: 236
Appendix II: 236
Appendix III: 236

Acknowledgements

Alors voilà. C'est fini.

C'est déjà fini. Et c'est déjà le moment d'écrire ces fameux remerciements. La seule partie d'une thèse que tout le monde lit, car elle est la plus personnelle et la plus émouvante… et sûrement la plus compréhensible, il faut bien le dire. Alors que dire ? A qui dois-je cette thèse ? Qui remercier ? Tellement de gens que je ne sais ni par où commencer, ni si j'arriverai à mentionner tout le monde. J'espère que les absents me pardonneront.

Puisqu'il faut commencer quelque part, commençons par toi **Valérie**. Je n'ai pas eu beaucoup de directrices de thèse, je dois bien l'avouer. Malgré cela, je réalise chaque jour la chance que j'ai eu de tomber sur toi. Depuis le début, tu m'as supporté dans chacune des étapes de ma thèse, de la préparation du concours de l'Ecole doctorale jusqu'à la correction de la dernière ligne de ce manuscrit sur tes jours de congés. En quatre ans, de jour en jour, de manip en manip, tu m'as encouragé, tu m'as conseillé, tu m'as appris, tu m'as montré un nombre incalculable de choses et rattrapé un nombre incalculable de fois, lorsque le projet ne marchait pas comme on voulait. Je sais que j'ai été très loin de la doctorante idéale, avec mon sale penchant pour faire trop de choses à côté de ma thèse, et ma tendance à ne pas savoir dire non. Mais malgré cela, tu es restée patiente et tu m'as permis de faire toutes sortes de choses, du monitorat, des interventions dans les lycées, de la vulgarisation, des formations, des congrès… Malgré cela, tu as continué à me supporter à chacun de mes pas, tout en me montrant toujours le bon exemple. Je ne m'épanche pas beaucoup sur mes sentiments à l'égard des gens en général, mais ici je pense que je peux le dire : tu es et tu resteras l'une des personnes que j'admire le plus. Après tant d'années de recherche, alors que le métier de chercheur, disons-le, n'est franchement pas facile, tu as su rester passionnée, curieuse et toujours avide d'expérimenter. Si un jour je ne t'arrive ne serait-ce qu'à la cheville en tant que chercheuse… je pense que je pourrai m'estimer très heureuse. Pour toutes ces raisons, merci de m'avoir laissé une chance en intégrant l'équipe PARP. J'espère que ton prochain changement de sujet scientifique te satisfera pleinement et que tu continueras d'être formidable.

The second person I'd like to thank is you, my dear **Giuditta**. You were here to watch my first steps as a baby-PhD, you were here to teach me my first words in science, straight at the bench. You were probably the greatest post-doc I met. Hard working and passionate, you were always there to guide my steps. It has been more than a pleasure to have you as a colleague, right behind me for our scientific conversations. And more than a colleague, it was amazing to know you as a friend. I can't explain how much you saved my PhD, but I think if you hadn't been here, I would have given up a long time ago. Saying goodbye when you left for Cambridge was almost as hard as writing my manuscript! But I know we'll see each other again, and I can't wait to see what kind of a great scientist you've become! Thank you so much for everything.

Passons à toi **Jean-Christophe**, toi sans qui cette thèse n'aurait pas eu la même saveur. Toi qui a su tout à la fois, en tant que voisin de bureau, décortiquer mes manips d'immunofluorescence comme un pro, et m'initier aux merveilles de la surface de Mars, des anneaux de Saturne ou des tempêtes de Jupiter. Merci d'avoir patiemment encaissé chacune de mes questions. R a encore beaucoup de secrets pour moi, mais je pense pouvoir dire que grâce à toi, j'en sais un peu plus sur le monde formidable de la bio-informatique. Merci pour ta curiosité quotidienne et ton enthousiasme contagieux sur des sujets parfois très éloignés de ma thèse !

Françoise, même si tu ne m'encadrais pas directement, merci d'avoir répondu à chacune de mes questions lorsque j'en avais. Merci d'avoir été disponible, enthousiaste, encourageante, et merci d'avoir été un véritable modèle de chercheuse également. Toi et Valérie, vous faites vraiment un duo de chercheuses hors-pair, et le fait qu'elle traverse la route qui nous sépare de l'IGBMC n'y changera rien, courage ! J'espère que tu auras la motivation de reproduire ces spectacles de qualité qui caractérisaient notre club théâtre éphémère.

Anne, même si tu n'y es pas resté longtemps, j'espère que mon ancien appartement t'a plu. Merci pour ton franc-parler en toutes circonstances, ton soutien administratif jusqu'au bout de la thèse et surtout, merci de m'avoir donné des prétextes pour faire de la communication scientifique en me recrutant « de force »

à la fête de la science ! Si jamais je n'ai pas d'avenir en tant que chercheur, que tu continues d'organiser des tas d'opérations grand public avec le CNRS ou l'IGBMC et qu'il te manque du monde… considère que je suis partante !

Je passe aux anciens et aux nouveaux doctorants de la famille PARP, et je pense que je dois commencer par toi **Thomas**. Toi qui fût mon premier maître de stage pendant mon cursus de fac, je pense que c'est en partie à toi que je dois cette thèse. Si je n'avais pas fait un petit séjour au labo en 2ème année de licence, jamais je n'y aurais repensé plus tard. Grâce à toi, j'ai rencontré Mike, Elise, Christian… et chacun à votre manière, vous m'avez un peu inspiré. Même si j'étais encore bien trop jeune pour le réaliser, vous m'avez probablement, à l'époque, donné un peu envie d'être une doctorante moi aussi. Et c'est ainsi que j'ai commencé cette aventure quand tu terminais la tienne. Même si tu n'as pas poursuivi plus loin ta carrière de chercheur, je suis certaine que tu es à présent un prof qui déchire, comme tu l'as été à l'époque. Merci pour ça.

Christian, une pensée toute particulière pour toi qui m'a suggéré de demander s'il y avait de la place pour moi au labo. Sans toi, je n'aurais peut-être pas fait cette thèse. Tu as toujours cru en moi, tu as toujours su me remonter le moral quand ce projet n'avançait pas et tu as toujours su me rassurer sur mes propres capacités à faire de la science. Même si je ne sais pas encore ce que je ferai après, tu avais raison sur un point : j'ai réussi à aller au bout de cette thèse vivante. Merci pour nos soirées ciné, merci pour nos soirées nanar, merci pour ton soutien indéfectible. Merci d'avoir refait le monde avec moi au McDo, et à notre prochain rencard, Dr. Dent.

Mike, même si tu es parti depuis un moment, je n'oublierai jamais ta gentillesse et ta patience. Merci pour ton humour et ta bienveillance à mon égard. J'espère toujours qu'un jour, je pourrai venir faire une petite randonnée du côté du Luxembourg !

Carole. Quasi seule doctorante restante à mon arrivée, j'aurais vraiment aimé que les choses se passent mieux entre nous. Une chose est sûre, tu m'as appris le vrai sens du mot « obstination », dans tous les sens que ce terme peut avoir. Comme une leçon de vie n'est jamais mauvaise à prendre, merci pour ça. Je te souhaite une belle réussite scientifique, de beaux voyages dans le monde entier… mais comme j'ai l'impression qu'aucun obstacle n'est trop difficile à grimper pour toi, je ne me fais pas top de soucis !

Kathline, que dire de ton enthousiasme, de ta bonne humeur et de ton légendaire rire contagieux ? Merci d'avoir été une collègue si enjouée, merci d'avoir partagé certaines longues soirées de travail au labo avec moi. Je pense que les pizzas en ta compagnie font partie des moments mémorables de cette thèse ! J'espère qu'on aura l'occasion de retourner faire de la Zumba ou d'aller danser en ville. On l'a fait trop peu de fois, mais j'ai encore pas mal de pas à apprendre auprès de l'experte que tu es ! Bon courage pour la dernière ligne droite de ta thèse (TU PEUX LE FAIRE), et encore mille fois bon courage pour le deuxième accouchement qui suivra ! Je pense que tu te lances dans un projet tout aussi prenant que le doctorat, et même si je ne veux pas l'admettre, j'admire quiconque se lance dans cette fastidieuse entreprise qu'est la conception d'un petit humain. J'espère être encore dans les parages pour pouvoir te souhaiter plein de bonheur pour cette nouvelle étape de ta vie !

José, let me thank you here, even if you're not a PhD student anymore ! I was delighted to have you as a colleague and I hope we will meet again on our path to « Science », with a big « S ». It was great fun to have you as a neighbour in the lab, and even if I still speak spanish like an english cow, I enjoyed TRYING to speak to you in your own language, at least. Thank you for your kindness, advice and help, and I wish you good luck with both of your projects « PARP » and « BABY ». You are the greatest series advisor in the world, by the way. Now I have a whole list of things to watch in case I end up unemployed. I hope we will be able to schedule this famous Paëlla of yours someday !

Olga, même si nous n'avons pas beaucoup fait connaissance, sache que j'ai admiré à la fois ta rigueur scientifique et ta capacité à gérer une vie de famille en parallèle de ton post-doc !

Léonel, tu es arrivé depuis si peu de temps… et c'est bien dommage ! J'aurais vraiment aimé passer plus d'années de doctorat en ta compagnie. Tu es une personne adorable et passionnante, et j'ai réellement apprécié toutes nos conversations politiques des derniers mois. Je te souhaite de cartonner pour ton doctorat, et plein de bonheur dans ta collocation jusqu'à la fin !

Maria, do you know about this french idiomatic, saying that something was « brief, but intense » ? That's the fealing I have ! You're only here for a few months, but I really enjoyed going out with you and your friends ! I hope we can do more of that once I'm finished, because it was a true pleasure to meet you.

Passons aux autres membres de l'équipe, passés ou présents…

Barbara, merci de m'avoir montré la technique et les astuces secrètes du dotblot, ainsi que le meilleur exemple d'organisation de laboratoire du monde. Je n'ai pas vraiment réussi à suivre l'exemple, je dois bien l'avouer, mais maintenant je sais où se situe la barre du top niveau et ce vers quoi je dois tendre pour pouvoir dire que je suis organisée.

Aurélia, merci d'avoir patiemment supporté FIP à la radio toutes ces années. Merci pour ton humour un peu cynique, ta franchise et ton soutien moral pour toutes les expériences qui n'ont pas fonctionné pendant cette thèse… et tu es bien placée pour savoir qu'il y en a eu. Merci de m'avoir aidé à percer le mystère des belles clonos, de m'avoir initié à plein de techniques de labo, d'avoir géré plein de commandes, et de toujours savoir où sont rangées les choses. Je sais que faire copain avec tes collègues, ce n'est pas trop crédo, mais j'en suis venue à espérer te manquer un peu une fois que je serai partie. ;)

Najat, merci en tout premier lieu pour tes conseils vestimentaires. Je pense que grâce à toi, j'ai toutes les cartes en main pour devenir quelqu'un de vraiment bien habillé. Il ne me manque plus que le porte-monnaie pour aller faire du shopping ! Comme Aurélia, merci d'assurer un gros bout de la logistique dans ce labo, c'est grâce à vous en grande partie qu'on peut travailler au quotidien. Merci pour nos longues conversations depuis que nous sommes voisines de bureau.

Nadège, s'il devait y avoir un mode d'emploi sur Terre de « comment tout bien faire », je pense que c'est toi qui l'aurais rédigé. Animatrice de choc, maman idéale, cuisinière de compétition, scientifique de combat… honnêtement, tout mes respects. J'espère que tu trouveras un labo digne de toi après celui-ci, bon courage !

Marie-Elise, on ne s'est pas croisé longtemps, mais merci à toi aussi d'avoir été une collègue super sympa et de m'avoir appris à transfecter correctement, grâce au pouvoir de PolyPlus.

Justine, je pense à toi aussi. Merci de m'avoir permis de m'exercer à la lourde tâche d'encadrer un étudiant pendant ma thèse. J'ai été ravie de te rencontrer, dans ce contexte et en dehors. Même si tu n'as pas pu rester au labo, j'espère que tu t'éclates au Québec et je te souhaite plein de courage pour finir ta thèse !

En sortant un peu des bureaux de notre équipe pour prendre le détour d'un couloir, on peut voir passer certains REIC que j'aimerais également remercier.

Michaël, merci infiniment de m'avoir aidé à préparer le concours de l'Ecole Doctorale et d'avoir brillament défendu l'épigénétique pour une soirée Pint of Science.

Ghislain, merci d'avoir été ce genre de collègue avec qui on peut partager des sujets de discussion pas très scientifiques et aller se promener en Terres d'Askarl. J'espère que ton projet « lumineux » aura énormément de succès, de même que ton Fablab, et que tous tes futurs projets scientfiques aideront à sauver le monde !

Elouan, grâce à toi je peux dire que je connais quelqu'un dans la police scientifique. Ca te va bien, et j'espère que tu t'y plais. Merci pour toutes nos conversations, pour le tour en moto, pour les jeux de société… et au plaisir de te recroiser !

Ambre, merci d'avoir animé tant de nos repas avec ton humour décapant et ton franc-parler. Tu es une véritable battante et un grand bravo d'être venue à bout de thèse !

Manon et Andréa, vous êtes une sacrée paire de doctorantes. Votre arrivée a été un grand courant d'air frais pour l'ambiance du labo, et je ne saurai vous remercier assez pour votre aide sur Pint of Science, vos encouragements pendant ma rédaction, votre bonne humeur constante… vraiment, vous êtes géniales. Une mention spéciale pour tes crêpes et ton caramel au berre salé Manon, j'avoue que ça va me manquer.

Thomas et **Hala**, vous voir disputer dans le labo comme un vieux couple me fera toujours rire. Vous aurez tous les deux été des collègues fort sympathiques, Thomas pour ta calme lucidité, Hala pour ton opti-

misme à toute épreuve, merci d'avoir égayé cet étage et d'avoir souvent partagé des soirées de labo. Merci du fond du cœur pour votre aide sur Pint of Science !

Judith, merci de m'avoir tenu compagnie pendant les longues heures en salle de culture.

Mini-Mike, merci d'avoir patiemment répondu aux questions idiotes que je pouvais avoir en programmation. J'espère que tu cultiveras longtemps ton talent d'artiste-peintre !

Anaïs, merci de tout cœur pour tes précieuses leçons de bioinformatique !

Patrick and **Jitesh**, we don't know each other very well, but thank you for being living examples of the fact that you can handle both a post-doc and a family.

Puis promenons-nous un peu dans le reste de l'étage :

Jo-Ann, it's such a shame that I have to leave when you just arrived. You're such a cool person, I wish we'll have the chance to meet again ! Thank you for playing Santa's part in our first Christmas party, and thanks for cheering me up during the writing of my manuscript !

Agnès, merci pour tes retours sur mon projet en labmeeting. Tu figures également parmi mes modèles de chercheuses-mères de famille exemplaires. Bonne continuation dans les projets du labo !

Frank, merci pour nos conversations très geek autour du jeu vidéo. J'espère qu'avant la fin de ma thèse, tu n'auras pas poney, et qu'on pourra te sortir prendre un verre !

Etienne, une petite pensée pour toi aussi, même si tu es parti – et encore merci pour ta cuisinière qui m'a bien servi depuis.

Bruno, Marc, Mariel, merci pour nos longues conversations géo-politiques autour de l'Odyssey. Et rassurez-vous, la rébellion anti-système n'est pas morte avec la génération Y. On va sauver la recherche un jour, mais pas demain. Demain y'a chômage. ;)

Régine, Jérôme, Véronique, Renaud, et toute la team « Hygiène et sécurité », merci de m'avoir recruté comme présentatrice de show télévisé. Je dois admettre que je me suis bien marrée.

Armand, Raphaëlle, Glenn, merci d'être toujours partants pour les soirées doc-post-docs !

Frédéric et **Safia**, **Gaëtan** et **Aurélie**, merci d'avoir porté brillamment les couleurs de notre Institut pour Pint of Science.

Sandra, merci de m'avoir mobilisé pour Sciences en Marche, j'espère que la lutte pour la défense des droits des chercheurs ne s'arrête pas là !

Christel, merci pour ton aide à l'Incucyte et merci pour la gestion infaillible des stocks d'azote !

Jacky, Raphaël, Claire, Sylvie et tous les membres du service technique et administratif, merci de lutter pour que notre beau bâtiment ne s'effondre pas, et de gérer la paperasse au quotidien, heureusement que vous êtes là !

Sortant des murs du labo, merci à l'équipe de **Bernardo**, **Vincent** pour le clonage, **Isabelle, Mélanie, Jacques**, **Rocio** et surtout **Léa,** pour le soutien moral sans faille et votre aide pour Pint of Science.

Merci à toute mon équipe d'Openlabistes : **Gaëtan, Angélique, Romain, Daphné, Romumu-cœur.** C'était un sacré moment de rigolade.

Merci à tous les copains de **Pint of science** passés ou présents, et parlant de ce projet, merci à Serge Potier et Mélanie Muser pour leur soutien depuis le début de l'initiative.

Une petite pensée à mes deux professeurs de SVT du Lycée Louis Massignon, **Gilles** et **Delphine**, qui m'ont contaminé avec le virus de la biologie. A vous, je décerne le titre de meilleurs profs du monde.

Si chacun d'entre vous a participé à faire de ma thèse ce qu'elle était professionellement, au quotidien, il y a des dizaines d'autres personnes que je dois remercier pour leur soutien.

En tout premier lieu, merci **Papa** et **Maman**, de m'avoir toujours encouragé sur la voie de la curiosité. Vous m'avez appris à devenir une personne ouverte et c'est un peu grâce à vous que j'en suis arrivé là. Même si on ne se voit pas beaucoup, je sais que vous serez toujours là pour moi, et ça n'a pas de prix.

Mamie Christianne, Papy André, Mamie Anne-Marie et Papy François, merci d'être les grands-parents les plus gentils du monde. Je sais que je n'ai pas été très présente pendant mes années de thèse, mais

malgré ça je sais que vous serez toujours présents pour moi. Je vous aime très fort et je vous remercie de votre constant soutien.

Max… j'aurais aimé que tu me voies finir ce que tu m'as vu commencer. Je te dois beaucoup, je ne l'oublie pas. J'espère pouvoir te voir accomplir ton rêve de devenir chimiste un de ces quatre.

Albane, Charley, Lucile, Gaëtan, Jonathan, mes chers colocataires. Merci d'avoir égayé nos soirées au Quai Rouget de Lisle, merci d'avoir refait le monde avec moi, merci pour tous les souvenirs qu'on a accumulé à force de vivre ensemble. Malgré mes absences alors que j'étais prise par ma thèse, vous avez toujours été patients et encourageants à mon égard. Je ne l'oublierai jamais. Passer un bout de vie avec vous à été un véritable privilège donc... bref, gros cœur avec les doigts.

Lucie, de tous mes amis, tu es celle à qui je dois le plus d'avoir survécu à cette thèse. Merci pour ton soutien sans faille. Merci pour les fous rires, pour les pleurs, pour les confidences, pour les chants, pour les gifs nuls pendant ma rédaction. Merci.

Victor, François, Pierre, Poupsy, Patricia, Pierre-Paul, merci d'être devenus un peu comme ma deuxième famille ces dernières années, merci d'avoir cru en moi, merci pour tous vos encouragements et toute votre aide sur chacun de mes projets.

Thomas, tu as vécu l'angoisse de cette thèse au quotidien, pendant des mois.
Pour toi, je pense que merci ou plusieurs merci ne suffiront jamais.
Alors je vais me contenter de te dire que je t'aime.

Ainsi s'achève un beau projet, probablement le projet le plus long, le plus fastidieux et le plus casse-tête que j'ai entrepris.

Je n'aurais jamais pu terminer ce projet sans vous, et sans vous il n'aurait pas été le même.

Alors une dernière fois,

Merci.

Eléa.

Table of figures

Chapter 1 :

Figure 1: The Poly(ADP-ribosyl)ation reaction (PARylation) – p.22

Figure 2: The PARP superfamily, domain architectures – p. 24

Figure 3: Summary of the subcellular localization and roles of the different classes of human PARPs – p.32

Figure 4: Poly (ADP-ribose) readers – p.34

Figure 5: Erasers of Poly(ADP-ribosyl)ation in human genome – p.38

Figure 6: PARG, from gene to isoforms – p.40

Figure 7: PARG signature and structure of PARG's catalytic domain– p.42

Figure 8: Subcellular localization of the ADP-ribose degrading activities in human cells– p.44

Figure 9: Feeders and consumers of PARylation– p.46

Figure 10: Overview of the seven members of the human sirtuin family– p.48

Figure 11: The ever-extending roles and complexity of PARylation– p.52

Chapter 2 :

Figure 12: Types of DNA damages and DNA repair pathways– p.56

Figure 13: Roles of PARP1 in Global-Genome NER and Transcription-Coupled NER– p.58

Figure 14: Roles of PARP1 in BER, SSBR and TOP1-clivage complex removal. – p.62

Figure 15: Roles of PARP1 in Double Strand Break Repair. – p.66

Figure 16: Cell cycle phases– p.68

Figure 17: Schematic structure of the replisome – p.70

Figure 18: Steps for the replication fork machinery– p.72

Figure 19: Obstacles challenging the replication forks – p.74

Figure 20: Roles of PARylation in the different outcomes of replicative stress. – p.76

Figure 21: The apical PI3K kinases in regulating genome integrity. – p.78

***Figure 22: Role of PARP1 in chromatin regulation*. – p.82**

Figure 23: Roles of PARP1 in transcription regulation and gene expression– p.84

Chapter 3 :

Figure 24: Genetic concepts for targeting tumour cell – finding cancer's Achilles' heel. – p.88

Figure 25: The hormetic pattern of PAR accumulation after cellular stress. – p.90

Figure 26: Using PARP inhibitors in cancer therapy. One molecule: a broad range of beneficial effects. – p.92

Figure 27: Resistance mechanisms to PARP inhibitors. – p.96

Discussion

Figure 28: Doxycycline induction of stable cell lines expressing flag-tagged PARG isoforms. – p.129

Figure 29: RUVBL1 co-purifies with PARG and the interaction increases after oxidative stress. – p.156

Figure 30: Phosphorylation site predictions on PARG sequence– p.158

Figure 31: Reported phosphorylation sites on PARG sequence– p.158

Figure 32: DNA-PK sequence logo– p.159

Figure 33: Experimental procedure for evaluating the effect of PARG depletion in the cell response to camptothecin. – p.163

Figure 34: Different outcomes of CPT-induced Top1 poisoning– p.198

Figure 35: Scenario for the replicative stress escape in U2OS shPARG cells. – p.202

Tables :

Chapter 1 :

Table 1: Frequent post-translational modifications, writers, readers, erasers, and biological features - p.20

Table 2: The PARP family: nomenclature, activity, and biological features. – p.25

Chapter 3 :

Table 3: Summary of the main PARP inhibitors available for clinics, and their structures. – p.94

Table 4: Summary of PARG inhibitors developed so far. – p.98

Introduction

Before showing the results I obtained during this thesis project, aiming at understanding the role and regulation of human poly(ADP-ribose) glycohydrolase (PARG) in the cellular response to DNA damages, I would like to introduce the fascinating world of poly(ADP-ribosylation), a remarkable post-translational modification, heavily contributing in many cellular aspects, from DNA repair to cell death.

- **Chapter 1** covers all the aspects of Poly(ADP-ribosylation), from its synthesis to degradation, and provides a detailed description of all the main protein actors of this essential post-translational modification.
- **Chapter 2** aims at defining the different repair pathways in which PARylation has a role, distinguishing mecanisms related with strand breaks and replicative stress.
- **Chapter 3** briefly replaces the importance of studying PARylation in the therapeutic field, and reviews the current inhibitors available for PARP and PARG.

After the introduction, you will find the result section, divided into three projects. Each part can be read independently, and results are presented as article drafts. Three published articles to which I contributed are provided in the Appendix. Introductions and discussions of each result sections are provided in french at the end of the Manuscript.

Wishing you a pleasant reading of this manuscript.

Chapter 1: Poly(ADP-ribosyl)ation, a versatile post-translational modification.

1. Post-translational modifications: roles and common features

Since Francis Crick introduced the concept of the central dogma of biochemistry (Crick, F.H.C, 1958), and even though it was quite appealing for its aesthetic simplicity, data has fastly complexified the basic model involving DNA as the sole source of genetic coding information leading to proteins through an RNA molecule synthesis.

While DNA bears information for an estimated, and constantly shrinking number of around 19'000 protein-coding genes (Ezkurdia *et al*. 2014), providing a basic layer of information encoding, scientists easily acknowledge that over 100'0000 different proteins could ultimately be produced in human cells (Savage, 2015). This number is difficult to estimate, but mechanisms such as mRNA splicing, alternative translational starting or proteolytic cleavage allow enlarging the possibilities available with this basic amino acid toolbox, from a limited sized genomic information set.

In addition to these mechanisms, it appears evident that allowing subsequent modulation of all the levels of gene expression, from DNA expression to the ultimate protein product, unlocks a much broader panel of possibilities and functionalities. In this purpose, post-translational modifications (PTMs) of many different chemical natures are responsible for modifying protein targets, which can result in the regulation of their activity, cellular localization, folding, stability, binding and interaction with other proteins, all of this in a very reactive fashion and within a limited timeframe. This allows the efficient signalling and transducing of environmental cues, as well as an accurate regulation of the downstream cellular pathways. Post-translational modifications of histones, these core protein-components of chromatin are now considered as key actors of this now-called "epigenetic" layer of gene expression regulation (Gayon, 2016), and we even started talking about the "histone code" as additional layer of information encoding (Jeunuwein and Allis, 2001). Some authors beautifully refered to post-translational modifications as "nature's escape from genetic imprisonment and the basis for dynamic information encoding" (Prabakaran *et al.* 2012).

The most widely spread modification is probably phosphorylation, as quantified from proteome wide databases (Khoury *et al*. 2011). Phosphorylation of proteins can regulate their activity and cellular localization. Being rapidly catalysed by several groups of kinases, and rapidly removed by phosphatases, this PTM is widely used in most of cells' signalling cascades, requiring quick and efficient reactions. While more than 230 000 phosphorylation sites have been recently estimated (Vlastaridis *et al*. 2017), that can be classified in 178 sequence motifs and are conserved throughout eukaryotes (Yoshizaki and Okuda, 2016), most of them lack a functional significance. Ubiquitination is also a common PTM, catalysed by ubiquitin ligases and degraded by deubiquitinating enzymes. Poly-ubiquitination is mainly involved in addressing proteins to the 26S proteasome

PTM	Writers	Readers (domains)	Eraser	Feeders	Consumers	Cofactor	Targets	Functional role
Phosphorylation	Kinases	WW, SH, PTB, FHA, MH2, WD40, BRCT, Polo box, FF	Phosphat-ases	ATP synthase	ATP hydrolases	ATP, GTP	Protein, histones Ser, Thr, Tyr	Signaling cascade, Activity, Localization
Methylation	Methyl-transferase	MBD ; C2H2 ; SRA	De-methylase Glyco-hydrolases	Methionine adénosyl-transferase	Methyl-transferases	SAM	Protein, histones, DNA cytosines, Lys	Chromatin structure, metabolism, activity
Acetylation	Acetyl-transferases	BRD, double PHD, YEATS, non canonical BD	Des-acétylases	PHDC ; ACL ; ACS	Krebs cycle, Acetyl-transferase	Acetyl-CoA	Protein, histones, Lys	Chromatin Structure Protein strability, localization, metabolism
Ubiquitination	Ubiquitin ligases	UBD, UIM, UBA	De-ubiquitin-ating enzymes	Protein synthesis	DUB	Ubiquitin peptide	Protein, histones, Lys, Cys, Thr, Ser, Met	Proteasome targeting (poly) signalisation, repair, chromatin remodelling (mono)
Sumoylation/ Neddylation	"	"	SENP CSN	Protein synthesis	Carboxy hydrolases	SUMO/ NEDD8	"	"
Glycosylation	Glycosyl-transférases	CBM, Sugar receptors	Glyco-sydases Endo-Exo Poly Saccharid-ases	Sugar meta-bolism	Sugar/Lipid metabolism	Sugar moieties	Asn, Asp (N-Glc) Ser/Thr (O-Glc) Trp (C-Glc)	Protein adressing (Golgi), folding Receptor Signaling
PARylation	PARP, MART, ARTD	PBM, WWE, PBZ, CCCH, MD ...	PARG, ARH3, TARG, MacroD1, MacroD2	NMNAT	NAD^+, glyco-hydrolases, CD38, sirtuins	NAD^+	Protein, DNA; Asp, Glu, Arg, Lys, Ser	DNA repair, protein activity, chromatin structure, transcription...

Table 1: Frequent post-translational modifications, writers, readers, erasers, and biological features.

The three letter code of amino acids is used in the «targets» columns. PTM, post-translational modification; WW, pSer/Thr binding WW domain; SH, pTyr binding Src Homology domain; PTB, Phospho Tyrosine Binding domain; FHA, Fork Head Associated domain; MH2, MAD Homology 2 domain; WD40, WD repeat domain; BRCT, BRCA1 C Terminus Domain; FF, Double Phenylalanine containing domain; ATP, Adenosine Triphosphate; GTP, Guanosine Triphosphate; BRD, bromodomain ; Double PHD, Phe, His, Asp Containing Finger Domain; YEATS, Yaf9, ENL, AF9, Taf14, Sas5 domain; PHDC, Pyruvate Dehydrogenase Complex ; ACL, Acetyl-CoA Lyase ; ACS, Acetyl CoA synthase; UBD, Ubiquitin Binding Domain ; UIM, Ubiquitin Interacting Motif ; UBA, Ubiquitin Associated Domain ; DUB, Deubiquitinylase ; SUMO, Small Ubiquitin-Like Modifier; NEDD8, Neural Precursor Cell Expressed, Developmentally Down-Regulated 8; CBM, Carbohydrate Binding Module ; Glc, Glycosylation; PARP, Poly(ADP-ribose) Polymerase ; MART, Mono(ADP-ribose) Transferase ; ARTD, ADP-ribose Transferase Diphtheria Toxin Like ; PBM, PAR binding motif ; WWE, WWE containing PAR binding domain ; PBZ, PAR-binding Zinc finger domain ; CCCH, CCCH-Zinc finger domain; MD, Macrodomain ; PARG, Poly(ADP-ribose) glycohydrolase ; ARH3, ADP-ribose Hydrolase 3 ; TARG, Terminal ADP-ribose glycohydrolase ; NAD, Nicotinamide Adenine Dinucleotide; NMNAT, Nicotinamide mononucleotide adenylyltransferase.

for degradation, and mono-ubiquitination involved in DNA repair and chromatin remodelling. The list goes on with methylation, acetylation, glycosylation and new trending PTM such as O-linked-N-acetyl glucosamine (O-GlcNAcylation; Yang and Qian, 2017).

Although these modifications are all very different, chemically and functionally, they all display similarities in the way they all require proteins catalysing it, interacting with it, and metabolising it. These proteins are generally referred to as « writers », « readers » and « erasers ». All these post-translational modifications also require molecular co-factors or precursors that need to be factored and processed. Proteins involved in the regeneration or degradation of these co-factors can be referred to as « Feeders » and « Consumers » (Hyun *et al*. 2017, Wu *et al*. 2017; Verheugd *et al.* 2016). In **Table 1**, I intended to illustrate this concept with a non-exhaustive list of the main writers, readers, erasers, feeders and consumers of the most important PTMs described in the litterature. To these proposed PTMs we could add propionylation, crotonylation, hydroxylation, butyrylation, citrullination… and maybe others in the years to come.

Being pluripotent modifications of protein activities, PTMs are now actively studied. It appears that many neurological diseases, cancers and infections are linked with PTM unbalance. Therefore, targeting them for therapeutics opens new possibilities and hopes (Cole *et al.* 2016; Li and Seto, 2016; Hamamoto and Nakamura, 2016).

Our lab has historically been working on Poly(ADP-ribosyl)ation (PARylation). This PTM has emerged as a versatile regulation feature added on several proteins. For the past fifty years, it has trended in several fields of research such as DNA damage repair and cancer biology. Yet, many biological roles are still emerging, and most of the mechanisms it is involved in remain to be deciphered. As I will mention in chapter 3, PARylation inhibitors are currently of great interest in therapies against a broad range of diseases, starting with cancer.

In the following paragraphs, I intend to draw an accurate portrait of this incredible cellular feature, in all its complexity, versatility and potentiality in living cells. I will describe the main PAR writers, readers, erasers, feeders and consumers, as well as their main biological roles.

2. Reaction of ADP-ribosylation and Poly(ADP-ribosyl)ation

ADP-ribosylation is a unique and reversible post-translational modification catalysed by several writers, and triggering the addition of either single ADP-ribose moieties (Mono(ADP-ribosyl)ation or MARylation) or long chains of ADP-ribose, upon a broad panel of acceptor proteins.

Historically, first evidence for Poly(ADP-ribosyl)ation came from Chambon *et al.* 1963. Through two experiments in rat liver extracts, they showed that a DNA-dependent protein could generate a nucleic acid like polymer from NAD^+ and described it as a « new DNA dependent polyadenylic acid synthesising nuclear enzyme ». Within years, the molecular basis for this PTM emerged (Virag *et al.* 2013).

The ADP-ribosylation reaction is catalysed by a family of enzymes termed Poly(ADP-ribose) Polymerases (PARPs), of which PARP1 (Poly(ADP-ribose) Polymerase 1) is the founding member. It uses Nicotinamide Dinucleotide (NAD^+) as a co-factor, a molecule that will be further described in the « Feeders and consumers » paragraph (**§6**). Mechanistically, PARylation involves a cleavage of the glycosidic bond between ribose and

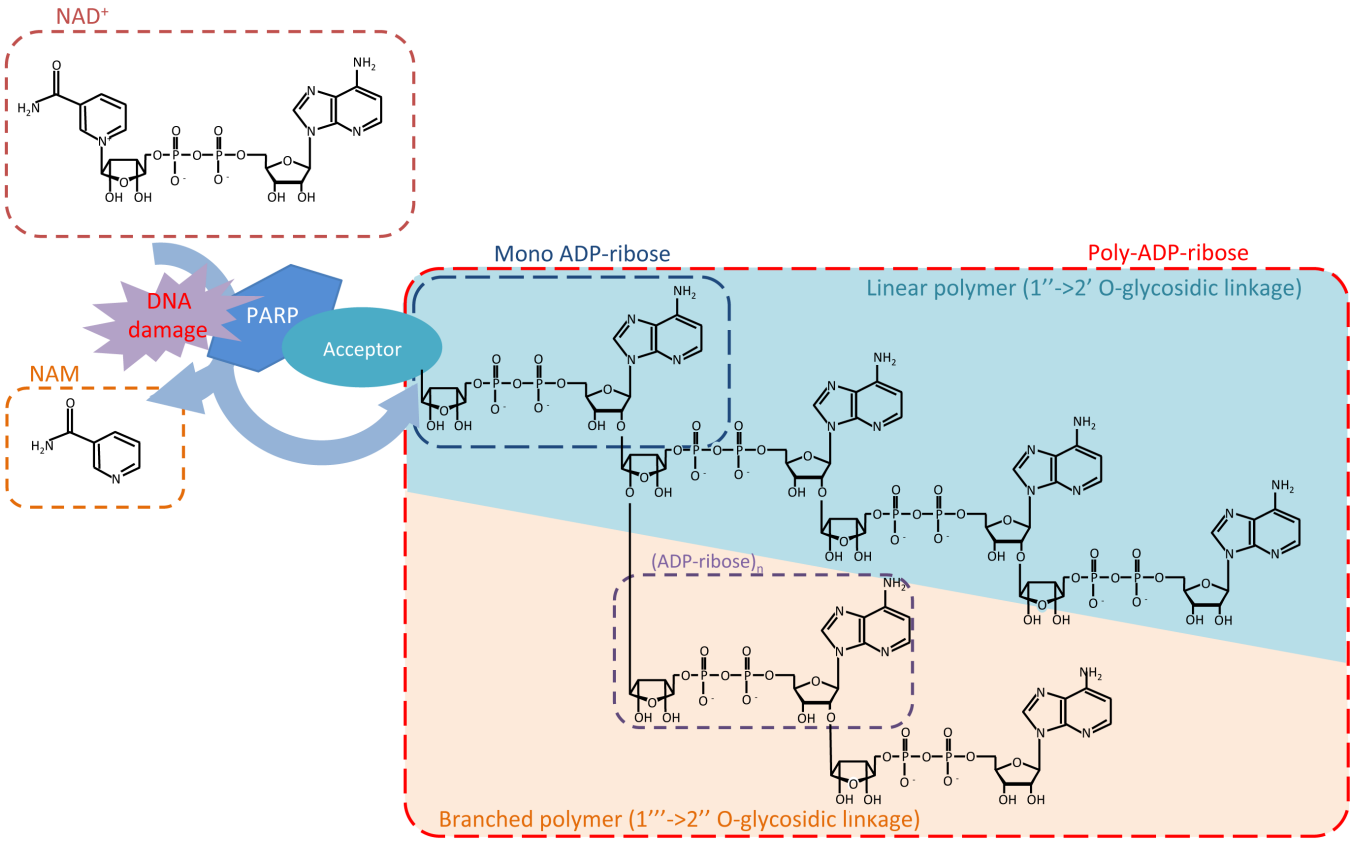

Figure 1: The Poly(ADP-ribosyl)ation reaction (PARylation)

Upon an adequate signal (mainly DNA damage), proteins with PARylation activity are able to use NAD+ moieties to catalyse the condensation of a mono(ADP-ribose) residue on target residues of an acceptor protein. The reaction releases nicotinamide (NAM) The PARylation reaction results in polymerization of several ADP-ribose intro a long linear chain, bond by 1''-2' O-glycosidic linkage. Some writers of PARylation can also trigger branching via 1'''->2'' O-glycosidic linkage. Poly(ADP-ribose) can encompass hundreds of ADP-ribose units.

nicotinamide, releasing nicotinamide (NAM). The ADP-ribose moiety is covalently bound to target amino acids: mainly to carboxyl functional groups in aspartate or glutamate residues through an ester link, or to amine functional groups in lysine or arginine residues through a ketamine link. To these consensual residues, thanks to extensive work done in order to identify new PARylation targets, cysteine (Vyas *et al.* 2014) and serine (Leidecker *et al.* 2016) have recently been added. It has been shown that the presence of HPF1 (Histone PARylation Factor 1) protein, discovered by Gibbs-Seymour *et al.* (2016) switches PARP1 specificity to Serine residues (Bonfiglio *et al.* 2017), highlighting the importance of understanding PARylation partners to implement our current paradigm around this modification.

PARylation can be divided into three phases (for a review, see Gibson and Kraus, 2012): During the initiation step, PARP transfers a first ADP-ribose unit on the acceptor protein (that can be itself). During the elongation step, 1''->2' O-glycosidic bonds are created, concatenating hundreds of ADP-ribose units. Additionally, if PAR exceeds 20 to 50 residues, PARP can generate branchings, adding ADP-ribose units through 2''->1 ''' O-glycosydic bonds and complexifying the molecule. The final size of the polymer depends on the PARP catalysing the reaction (**Figure 1**). The PAR molecule, through its potent helicoidal shape and its negative charges can display nucleic acid-like properties. In addition to covalently modifying and regulating acceptor proteins, it can also non-covalently affect cellular processes through steric hindrance and charge effects, presumably impacting protein-DNA interaction through charge repulsion or protein-protein interaction. Many protein domains are able to non-covalently interact with PAR (see **§4** on PAR readers). In the basic paradigm, proteins are the only macromolecules being PARylated. I think we must add to our knowledge that DNA ends have been shown to be PARylated in vitro (Talhaoui *et al.* 2016, Munnur and Ahel, 2017). In vivo evidence in mammals lacks, but DNA PARylation was reported in bacteria (Jankevicius *et al.* 2016). This perspective enables new putative roles and regulation modes of action for an already versatile modification.

3. Writers of ADP-ribosylation

Proteins able to catalyse the formation of PAR from NAD+ are commonly referred to as PARPs. The first described PARP was PARP1, and its study kept scientists busy for almost 30 years. It was not until 1998, when Jacobson and colleagues studied embryonic fibroblasts from PARP1 deficient mice models, which could still accumulate PAR after damage with DNA alkylating agent MNNG that it became obvious that other PARylating activity bearing proteins had to exist (Shieh *et al.* 1998). Evidence arose quickly after, with the discovery of new PARPs such as PARP2, PARP3, tankyrases and vPARP. With the increasing access to genomic sequences, we then became able to predict proteins with PARP activity, based on sequence homology conservation with the PARP1 catalytic domain. Alignments between organisms allowed to shed light on a « PARP signature », conserved among vertebrates, in all PARylating proteins. The first PARP superfamily classification was proposed by Amé *et al.* 2004, based on this PARP signature. This PARP domain has structural properties resembling the bacterial diphtheria toxin, with a β-α-loop-β-α fold able to bind NAD^+ that is very different from the traditional NAD^+ binding Rossman fold.

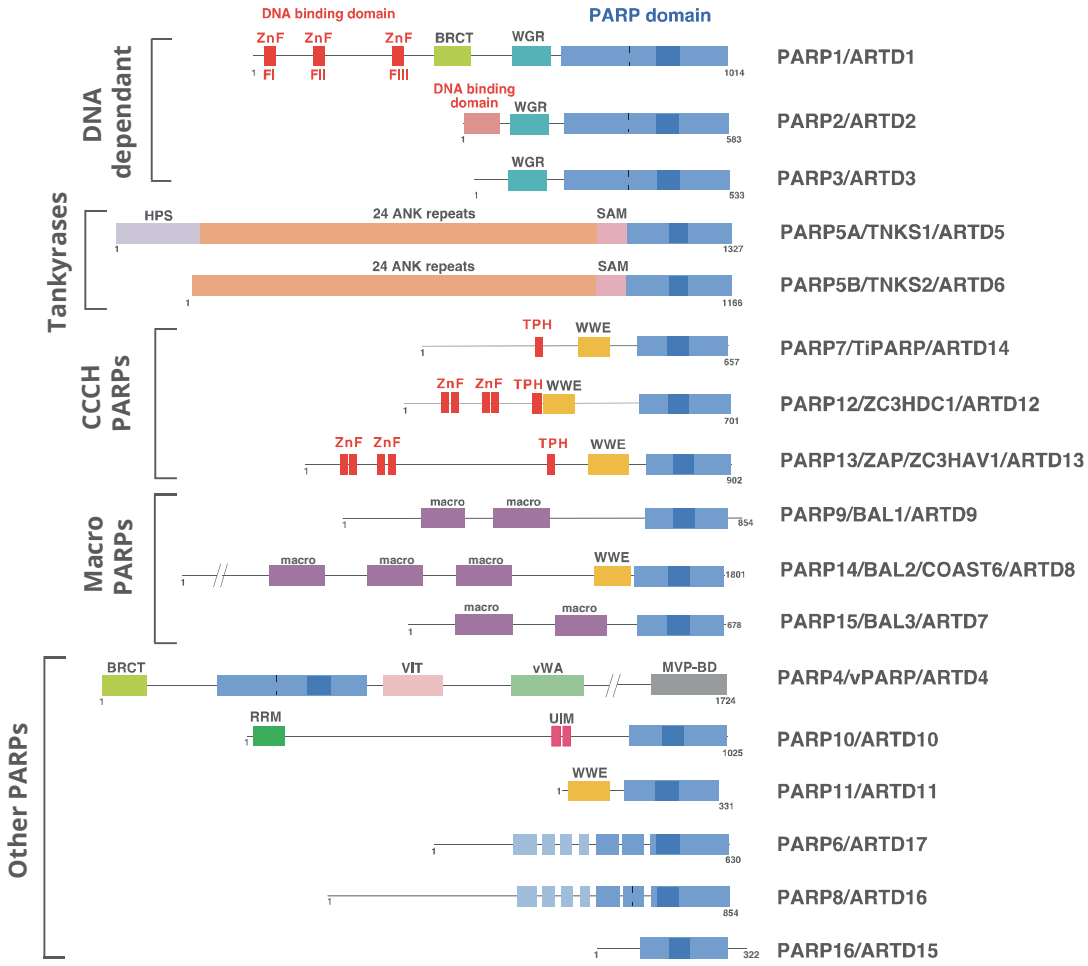

Figure 2: The PARP superfamily, domain architectures.

The PARP signature, common to all PARPs (859-908 in PARP1 sequence) is shown in dark blue. BRCT, SAM, UIM, MVP-BD, VWA and ANK are protein-interaction modules. ANK, ankyrin; BRCT, BRCA1-carboxy-terminus; HPS, homopolymeric runs of His, Pro and Ser; macro, domain involved in ADP-ribose and poly(ADP-ribose) binding; MVP-BD, MVP-binding; PARP poly(ADP-ribose) polymerase; RRM, RNA-binding motif; SAM, sterile α-motif; TPH, TiPARP-homology; UIM, ubiquitin-interacting motif; VIT, vault inter-α-trypsin; vWA, von Willdebrand factor type A; WGR, conserved W, G and R residues; WWE, conserved W, W and E residues, domain involved in ADP-ribose and poly(ADP-ribose) binding; ZnF, DNA or RNA binding zinc fingers (except PARP-1 ZnFIII, which coordinates DNA-dependent enzyme activation). Scheme adapted from Héberlé *et al*. 2015 (Appendix I)

Class of PARP	PARP family member	Alternative names	Uniprot Accession	Genomic locus	Protein lenght (aa)	Isoforms (Alternative splicing)	Cellular	Catalytic Triad motif	Activity
DNA dependant	PARP1	ARTD1	P09874	1q41-42	1014	1	N	HYE	P, B
	PARP2	ARTD2	Q9UGN5	14q11.2	583	2	N	HYE	P, B
	PARP3	ARTD3	Q9Y6F1	3p21.2	533	2	N,Ct	HYE	P, M
Tankyrases	PARP5A	ARTD5 Tankyrase 1, TNSK1	O95271	8p23.1	1327	2	N, C	HYE	P, O
	PARP5B	ARTD6 Tankyrase 2, TNSK2	Q9H2K2	10q23.3	1166	1	N, C	HYE	P, O
CCCH PARPs	PARP7	ARTD14 TiPARP	Q7Z3E1	3q25.32	657	1	N, C	HYI	M
	PARP12	ARTD12 ZC3HDC1	Q9H0J9	7q34	701	1	C, SG, G	HYI	M
	PARP13	ARTD14 ZC3HAV1, ZAP	Q7Z2W4	7q34	902	5	C, SG	HYV	inactive
Macro PARPs	PARP9	ARTD9 BAL1	Q8IXQ6	3q21	854	3	N, C, PM	QYT	inactive
	PARP14	ARTD8 BAL2, COAST6	Q460N5	3q21.1	1801	6	C, SG, FA	HYL	M
	PARP15	ARTD7 BAL3	Q460N3	3q21.1	678	2	C, SG	HYL	M
Other PARPs	PARP4	ARTD4 vPARP	Q9UKK3	13q11	1724	1	C, N	HYE	P
	PARP10	ARTD10	Q53GL7	8q24.3	1025	1	C	HYI	M
	PARP11	AERTD11	Q9NR21	12p13.3	331	3	N, C, Cl	HYI	M
	PARP6	ARTD17	Q2NL67	15q22.3	630	3	C	HYY	M
	PARP8	ARTD16	Q8N3A8	5q11.2	854	2	C, S, NE	HYI	M
	PARP16	ARTD15	Q8N5Y8	15q22.2	322	1	ER	HYI	M

Table 2: The PARP family: nomenclature, activity, and biological features.

Single letter code of amino acids is used in the «Catalytic triad motif» ; aa, amino acids; N, nucleus; Ct, centrosome; C, cytoplasm; SG, stress granule; G, Golgi; PM, plasma membrane; FA, focal adhesion; Cl, centriole; NE, nuclear envelope; ER, endoplasmic reticulum; P, Poly(ADP-ribosylation); B, branching; M, Mono(ADP-ribosyl)ation; O, Oligo(ADP-ribosyl)ation; PARP, Poly(ADP-ribose) Polymerase; ARTD, ADP-ribose transferase Diphtheria Toxin Like; TiPARP, TCDD-inducible poly(ADP-ribose) Polymerase; ZC3DC1, Zinc Finger CCCH domain-containing 1; ZC3HAV1, Zinc Finger CCCH domain-containing antiviral protein 1; ZAP, Zinc Finger Antiviral Protein; BAL1, B-aggressive lymphoma 1; COAST6, Collaborator of Stat6 (CoaSt-6)-associated PARP; vPARP, vault PARP. Table adapted from Héberlé et al. 2015.

Structural studies additionally enabled to highlight a conserved triad of catalytic amino acid residues (H862, Y896, E988 in PARP1) that are crucial for both NAD^+ recognition and polymer elongation activity. In some PARPs, E is replaced with either I, Y, T, V or L, which obviously predicts a mono-ADP ribosylation activity (Kleine *et al.* 2008). Experimental evidence was provided for each PARP activity years later (Vyas *et al.* 2014). Accounting for these differences in the catalytic activities, Hottiger *et al.* (2010) have proposed a new nomenclature for PARPs: they renamed these proteins « ADP-ribosyl Transferases Diphtheria Toxin Like » or ARTDn with n being the number of the protein (See **Table 2** for correspondence). Based on structural and catalytic arguments, the new nomenclature suggested a detailed classification of all the proteins displaying ADP-ribosylation capacities, in all kinds of living organisms. Although it was a remarkable work, I will use the « PARP » nomenclature throughout the present manuscript for simplicity. « PARP » is still widely used in the literature, especially when dealing with the therapy field, topic I will mention in chapter 3.

3.1 The PARP superfamily

The Poly(ADP-ribose) family now encompasses seventeen described members. They were identified by alignment with the « PARP signature » within the catalytic domain of PARP1, and numbered according to the degree of sequence similarity they shared with this founding protein family member (Amé *et al.* 2004). In reviews, PARPs are often grouped into sub-classes according to the different protein domains they share. In the present manuscript, I proceeded accordingly, dividing the PARP family into 5 sub-classes: DNA-dependent PARPs, tankyrases, CCCH-Zinc finger displaying PARPs, macro domain containing PARPs, and finally the other PARPs that cannot be classified in the previous categories (**Figure 2, Table 2**). A more detailed description of all PARP family members was the subject of a book chapter I wrote during my thesis (Héberlé *et al.* 2015). It is provided as an appendix at the end of this manuscript (**Appendix I**).

3.2 DNA dependent PARPs

DNA dependent class of PARPs encompasses the proteins whose catalytic activity is dependent on DNA and stimulated after DNA breaks. This includes PARP1, PARP2 and PARP3.

3.2.1 PARP1

PARP1 was originally termed PARS (Poly(ADP-ribose) synthase) and was the first ever studied member of the PARP family. In humans the PARP1 gene is 3,98kb and mapped on chromosome 1 (1q41-q42). The gene is composed of 23 exons and encodes a 1014 amino acid protein of 116kDa that accounts for 90% of the PARylation activity in cells (Amé *et al.* 1999). The protein is divided in three main domains:

- The N-terminal DNA binding domain contains two CCHC-type zinc fingers and a Zinc Binding domain (ZBD) allowing PARP1 to bind different DNA structures. It contains a Nuclear Localization Signal (NLS) and a caspase cleavage site, generating apoptotic fragments that can inhibit PARP1 activity and regulate cell death.

- The central automodification domain contains a BRCT motif involved in interaction with other BRCT domain containing proteins (ex: DNA repair factors such as XRCC1) and a WGR domain (rich in tryptophan, glycine and

arginine), that is involved in RNA-binding, required for PARP activity and that can be PARylated (Huambachano *et al.* 2011; Loeffler *et al.* 2011). Between BRCT and WGR domains, a basic unfolded region called DsDB (Double strand break DNA binding domain) allows binding to DNA upon damage.

- **A C-terminal catalytic domain** bearing the PARP signature and the three critical amino acids for catalysis of PARylation from NAD^+. A regulatory sub-region containing an alpha helix structure called HD (helical domain), is necessary for catalysis, by making a hinge between the substrate to be PARylated and the catalytic domain (Dawicki-McKenna *et al.* 2015).

The first PARP1 deficient mutant mice (Wang *et al*. 1997, Shall and de Murcia, 2000) highlighted its importance in DNA repair and in several other processes (detailed in **Chapter 2**), requiring the protein to be tightly regulated in human cells. This modular structure allows PARP1 to adopt a globular shape, exposing several domains and allowing several surface interactions such as automodification by PARylation (Langelier *et al.* 2012). PARP1 is indeed the target of many PTMs (recently reviewed in Piao *et al.* 2017), and subjected to a very tight regulation. In human cells, PARP1 can regulate its own expression through negative feedback, by modulating the SP1 transcription factor promoting activity on its own gene promoter (Zaniolo *et al.* 2007).

3.2.2 PARP2

PARP2 is a 570 amino acid and 66kDa protein that is responsible for 5-10% of PARP activity. It displays a short N-terminal basic domain containing both a NLS and a NoLS (Nucleolar Localization Signal), a DNA binding domain (DBD) and a WGR domain. The C-terminal catalytic domain shares 69% similarity with PARP1 (Amé *et al.* 1999, Meder *et al.* 2005). A caspase cleavage site lies in between the DNA binding domain and the WGR domain. PARP2 and PARP1 are able to dimerize and share functional redundancy towards their DNA-structure affinities, for they both bind double strand breaks (DSB), replication or recombination intermediates (Schreiber *et al.* 2002; Kutuzov *et al*. 2013; Langelier *et al.* 2014). They have overlapping roles in DNA repair pathways (See Kutuzov *et al.* 2014 and Beck *et al.* 2014). More recently, it was shown that PARP1 and PARP2 were both sufficient to generate small amounts of polymer needed for the recruitment of both XRCC1 and PNKP, two repair factors, to H_2O_2 induced single strand break (SSB) (Hanzlikova *et al.* 2017). Nonetheless, PARP2 deficient mice models have revealed specific functions for PARP2, mainly in cell differentiation or transcription regulation, but also it has been involved in chromatin integrity, X chromosome stability, transcription regulation, cell death, inflammation and differentiation (Ménissier-de Murcia *et al.* 2003)

3.2.3 PARP3

PARP3 has been discovered and described years after PARP1, with which it shares 35% similarity (Augustin *et al.* 2003). The PARP3 gene encodes for two protein isoforms with a difference of seven amino acids that are either addressed to the nucleus or to the centrosome. In the nucleus, it interacts with the Polycomb chromatin-remodelling complex, strongly suggesting a role for chromatin structure and transcription regulation (Rouleau *et al*. 2007). PARP3 deficiency leads to defects in cell cycle and mitotic progression (Boehler *et al.* 2011). It acts in DNA repair by regulating the DNA repair pathway choice between NHEJ and HR (Beck *et al.* 2014) and has also been identified as a promoter of chromosomal rearrangements by limiting G4 quadruplexes in DNA, thus facilitating DNA repair (Day *et al.* 2017). PARP3 is activated by DNA-breaks (Langelier *et al.* 2014)

and has a MART activity (Loseva *et al.* 2010). It is able to target H2B and to act as nicked-nucleosomes sensor (Grundy *et al*. 2016). Very recently, it has been reported to directly mono-ADP-ribosylate double-stranded DNA-ends. Since PARP3 can interact with both Ku70 and Ku80, two double strand DNA-binding proteins involved in NHEJ, this observation opens new interesting ways of regulating DNA repair (Munnur and Ahel, 2017). PARP3 seems to have a crucial role in development, being requested to specify the neural crest in embryos (Rouleau *et al.* 2011). It is also involved in TGF-ß and ROS (radical oxygen species) driven epithelial-to-mesenchymal transition (EMT) in human epithelial and breast cancer cells (Karicheva *et al.* 2016) and negatively regulates IgG class switch recombination during antibody formation (Robert *et al.* 2015).

3.3 Tankyrases

TNSK1 and TNSK2 (TRF1 interacting ankyrin-related ADP-ribose polymerase), also called PARP5a and PARP5b display solely a linear PARylating activity (Rippmann *et al.* 2002). These two 142kDa proteins both contain 24 ankyrin repeats forming 5 ankyrin repeat clusters (ARCs) involved in protein-protein interaction, thus forming adaptable binding platform for targets of ADP ribosylation (Eisemann *et al.* 2016). They were both identified and localized at human telomeres, in interaction with TRF1 (telomeric repeat binding factor 1) that is PARylated. Acting as heterodimers in telomere homeostasis, their DNA-independent PARylation activity towards TRF1 triggers its release from telomere, allowing telomerase to extend telomeric repeats.

They both bear a SAM domain (Sterile alpha motif) responsible for their homo and heterodimerization (DaRosa *et al.* 2016), that is also required for acting in the Wnt/ß-catenin pathway, regulating important processes such as cell differentiation and cell polarity and embryogenesis (McGonigle *et al.* 2015; Karner *et al.* 2010). They only differ from each other by the absence of the N-terminus HPS rich region (histidine, proline, serine) in TNSK2. This domain bears a MAP kinase consensus phosphorylation site (PXSP) that can be modified after insulin stimulation, thus increasing its PARylation activity (Chi and Lodish, 2000). TNSK1 has been involved in mitosis by regulating mitotic spindle and centrosome function (Chang *et al.* 2009, Ozaki *et al.* 2012). Recently it has also been shown to have a role in pexophagy, the autophagic degradation of peroxisomes (Li *et al.* 2017) Because of its role as a regulator of the Wnt-signalling pathway, it has emerged as an interesting new therapeutic target to fight against WNT dependent tumours (Thorvaldsen, 2017). Finally, their role in DNA repair has been highlighted: Tankyrases promote homologous recombination and checkpoint activation after double strand break damages (Nagy *et al.* 2016) and TNKS1BP1, a TNSK1 interactor facilitates DNA-PK autophosphorylation and contributes to double-strand break repair (Zou *et al.* 2015).

3.4 CCCH-type Zinc finger PARPs

Within the CCCH-type Zinc finger PARPs sub-family, there are three proteins, namely PARP7, PARP12 and PARP13, all bearing at least one CCCH-type Zinc finger domain (Cys-X7-11-Cys-X3-9-Cys-X3-His), one or two WWE motifs and the conserved PARP domain. All the members of this sub-family display antiviral activities.

3.4.1 PARP7

PARP7 is also called TiPARP (TCDD-inducible PARP) for it is considered as a TCDD response marker. TCDD (2,3,7,8-tetrachlorodibenzo-p-dioxine) is an important environmental pollutant causing pleiotropic effects in lipid and sugar metabolism, interfering with immune, reproductive and nervous systems. Upon TCDD exposure the AHR nuclear receptor (Aryl Hydrocarbon Receptor) translocates to the nucleus where in induces PARP7 transcription (Ma *et al.* 2001). PARP7 then acts as a negative regulator of AHR, both by binding gene promoters and by impeding the receptor transactivation and regulating its degradation through proteasome (MacPherson *et al.* 2013). . TiPARP is located both in the cytoplasm and in nuclear foci and activates the liver X receptors α and β (LXRα and LXRβ) through mono(ADP-ribosyl)ation, thus indirectly regulating fatty acids and glucose metabolism (Bindesbøll *et al.* 2016)

Additionally to its function in TCDD response, PARP7 also displays antiviral activity, interfering with alpha viruses replication through its MART activity (Atasheva *et al.* 2012), and by causing the downregulation of the viral specific IFN-I response (Yamada *et al.* 2016). Recently, one paper has shown that mitochondrial damage caused by Sindbis virus (SINV) infection could also elicit a PARP7-dependent antiviral response (Kozaki *et al.* 2017).

3.4.2 PARP12

PARP12 is produced as two isoforms in human cells. The short isoform is devoid of catalytic activity for it lacks the catalytic domain, but the longest diplays a MARylation activity that can be induced by interferon and is strongly involved in reducing viral replication, interfering with cellular translation by binding to ribosomes and polysomes (Atasheva et al. 2012; Welsby *et al*. 2014; Atasheva *et al.* 2014). It is overexpressed in the endometrium of gestating mammals, where it co-localizes with Golgi structures, suggesting a role in protein maturation (Bauersachs *et al.* 2006).

3.4.3 PARP13

As for PARP12, PARP13 gene also generates two distinct isoforms. In the rat, both isoforms lack catalytic domain and activity but nonetheless counteract viral replication. Therefore, they were named ZAP (Zinc Finger Antiviral Protein) and ZAPS (Zinc finger antiviral protein shorter isoform). In humans, only the short isoform lacks the catalytic domain and was reported to prevent mRNA accumulation for Moloney Murine Leukemia virus. Mechanistically, it seems that ZAP dimers are capable of binding viral DNA, mainly recognizing stem-loop structures, then triggering the recruitment of RNA exosomes and the RNA helicase p72 that will degrade viral RNA. In addition to promote mRNA decay, it also inhibits translation (Zhu and Gao, 2008; Zhu *et al.* 2012; Chen *et al.* 2012). Upon interaction with the RNA helicase RIG1 (Retinoic acid-inducible gene 1), ZAPS is able to induce interferon production, thus activating innate immune response. Because ZAP promoter contains interferon stimulated response elements (ISRE), ZAP expression increases after interferon stimulation, thus creating a synergistic effect on viral replication (Hayakawa *et al.* 2011).

In nucleus it is found associated with RNA stress granules where it can be transPARylated by PARP12 or TNSK1. S-farnesylation of ZAP targets the protein to endolysosomes where it enhances its antiviral activity (Charron *et al.* 2013). The double activity for PARP13 in degrading RNA virus concomitent with stimulating immune re-

sponse makes it a broad range antiviral effector. In addition, ZAP represses transposition in humans (Goodier *et al.* 2015), regulates cellular mRNA and acts as a pro-apoptotic factor, thus acting as an important RNA regulator, both in immunity and cancer (Todorova *et al.* 2014; Todorova *et al.* 2015).

3.5 Macro PARPs

The macroPARP subfamily encompasses 3 PARP proteins displaying one or several macro domains. PARP9, PARP14 and PAR15 genes are all located in a 200kb region of human 3q21 chromosomal region, predominantly expressed in haematopoietic related cells, suggesting an important function in immunity. Both PARP 9 and PARP14 were indeed identified as novel regulators of macrophage activation (Iwata *et al.* 2014).

Although macro domains have been identified as both readers and erasers of PARylation, none of these PARPs seem to display a degrading activity towards PAR (Aguiar *et al.* 2005).

3.5.1 PARP9

PARP9 was initially identified as BAL1 (B-aggressive lymphoma 1). It displays a QYT catalytic triad, predicting for an inactive enzyme, but was recently shown, in complex with Dtx3L, to ADP-ribosylate Ubiquitin, thus modulating (Yang *et al.* 2017). It has also been shown to bind to free PAR and PARylated PARP1 and upon induction with IFN-, acts as a transcription co-factor in IFN-G signaling (Camicia *et al.* 2013).

PARP 9 has been linked to DNA damage response and double strand break repair through dimerization with its partner BBAP (B-lymphoma and BAL Associated Protein), a histone ubiquitin-ligase that is required for the efficient recruitment of 53BP1 to radiation induced lesions (Yan *et al.* 2009; Yan *et al.* 2013; Yang *et al.* 2017). Despite its apparent role in immunity and DNA repair, it seems however that it doesn't play a role in antibody class switch recombination in mice deficient models (Robert et al. 2017). In addition, an antiviral activity was also reported for PARP9, for it enhances interferon signalling and controls viral infection, similarly as PARP7, PARP12 and PARP13 described above (Zhang *et al*. 2015).

3.5.2 PARP14

PARP14 displays a HYL catalytic triad motif, and displays a auto and hetero MARylation activity. Its macro domains allow it to recognize MARylated proteins. It also displays a WWE domain whose potent interaction with PAR is impeded by the presence of a ß strand covering the hydrophobic binding pocket (He *et al.* 2012). The role of this non-functional WWE domain is still undefined but it may have remained because it is still mediating interactions with other type of molecules (such as ubiquitinations as we shall see in the readers section). PARP14 is a partner protein of STAT6 (Signal Transducer And Activator Of Transcription 6), a transcription activator. In response to an interleukin-4 stimulation, it activates STAT6 transcription, evicting histone deacetylases from STAT6 dependent gene promoters (Goenka and Boothby 2006; Goenka *et al*. 2007; Mehrotra *et al.* 2011; Mehrotra *et al.* 2013). It has also been reported to protect B cells from caspase 3 dependant apoptosis (Cho *et al.* 2009), inhibits JNK1 pro-apoptotic pathway in cancer (Iansante *et al.* 2015), and plays a role in T-cell differenciation, in a PAR dependent way (Mehrotra *et al.* 2013; Mehrotra *et al.* 2015). PARP14 depletion in mice protected them from allergy airway diseases (AAD) further supporting its role in immunity

and inflammation. Finally, PARP14 was shown in interaction with actin filament ends, thus presumably playing a role in adhesion. Therefore, it could stand as a new target for cancer proliferation (Vyas *et al.* 2013).

3.5.3 PARP15

PARP15 (also called BAL3) is a 74kDa protein located in cytoplasmic stress granules, presumably acting in post-translational regulation of genes, in association with TNSK1, PARP12 and PARP13 (Leung *et al.* 2012). PARP15 displays a HYL catalytic triad, responsible for a MART activity. Until now, it remains the less studied macro-PARP. PARP15 is overexpressed in chemoresistant tumors of diffuse large B-cell lymphoma, becoming a target with therapeutic potential, and opening the way to the development of new inhibitors (Venkannagari *et al.* 2013).

3.6 Other MARTs

In this last section of the PARylation writers, I will detail the rest of the PARP family members, which display very diverse features and activities.

3.6.1 PARP4

PARP4 is a 193kDa protein that was first discovered as a core component of the vault particles, the largest ribonucleoprotein ever described (12,9MDa) (Kickhoefer *et al.* 1999). It was thus renamed vPARP (vault PARP). Vaults are involved in multidrug resistance, cancer-linked molecular pathways, nucleo-cytoplasmic shuttling, ribonucleoparticle assembly and immune response (Steiner *et al*. 2006; Berger *et al.* 2009). Each vault comprises 4 to 16 copies of PARP4, in association with MVP (Major Vault Protein). vPARP is present outside vaults, in nucleus where it can interact with TEP1 (telomerase associated protein 1), mitotic spindle and finally in cytoplasm, into clusters called vPARP-rods. However, its half-life increases when into a vault. This suggests that it has evolved to « shuttle » rapidly to different locations of the cell, probably using vault as a shuttle. It is the only PARP whose catalytic domain is in the middle of the sequence, surrounded by a BRCT domain, inter-alpha-trypsin motif, von Willebrand type A domain. PARP4 has been reported to PARylate MVP and itself (Bateman and Kickhoefer, 2003). Absence of vPARP in mice is associated with increased carcinogen induced tumours (Raval-Fernandes *et al.* 2005). MVP is important for drug resistance in ovarian cancer and requires vPARP for full activation (Wojtowicz *et al.* 2017).

3.6.2 PARP6

Very few data were available on PARP6 until recently. As a negative regulator of cell proliferation, it was believed that it could act as a tumor suppressor (Tuncel *et al*. 2012). Indeed, it acts as such via downregulating survivin expression in colorectal cancer (Qi *et al.* 2016). It also regulates hippocampal dendritic morphogenesis (Huang *et al.* 2016). Additionally, knocking down PARP6 promotes cell apoptosis and inhibits cell invasion of colorectal adenocarcinoma cells, making it an interesting therapeutic target (Wang *et al.* 2017).

3.6.3 PARP8

PARP8 is probably the less studied member of the PARP family. We only know that is is localized at centrosomes and reported as a critical nuclear enveloppe protein, in association with lamin C (Vyas *et al.* 2013).

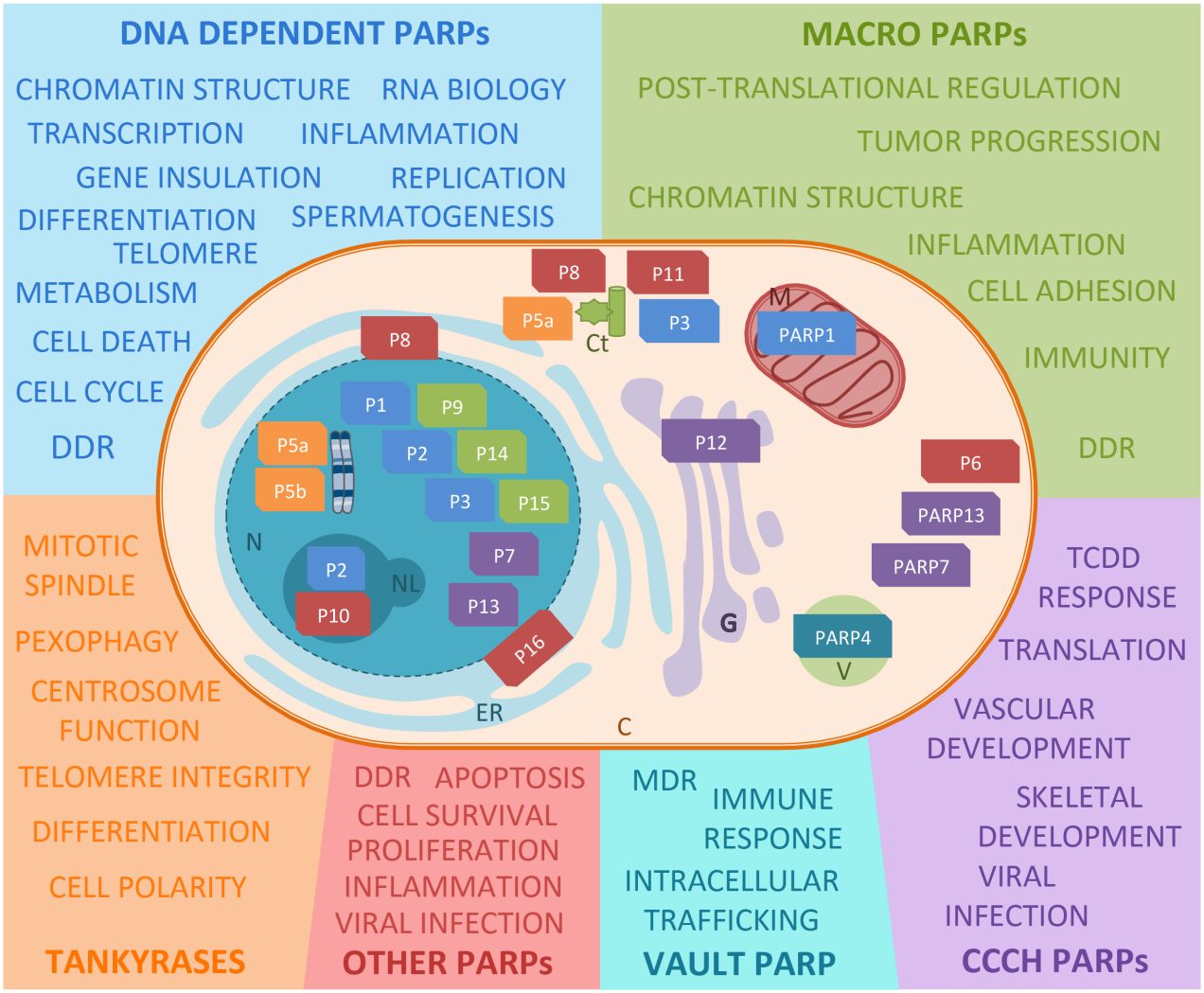

Figure 3: Summary of the subcellular localization and roles of the different classes of human PARPs

DDR, DNA damage response; TCDD, 2, 3, 7, 8-Tetrachlorodibenzo-p-dioxine; MDR, Multiple Drug Resistance; P1-16: Different PARPs. N, nucleus; NL, nucleolus; ER, Endoplamic Reticulum; C, Cytoplasm; G, Golgi; C, Vault Particle; M, Mitochondria; Ct, Centrosome.

3.6.4 PARP10

PARP10 bears a MART activity and has pleiotropic roles in cells (Yu *et al.* 2005). First, it accumulates in poly-ubiquitin containing bodies and interacts wih poly-ubiquitin receptor p62/SQSTM1. In the nucleolus, it is phosphorylated by CDK2 during transition from G1 to S phase, increasing its automodification activity and regulation of cell proliferation, cell survival, transformation or viral infection. It shuttles between cytoplasmic and nucleus through a functional NES and a non-canonical NLS (Kleine *et al.* 2012). Therefore, it seems that a tight regulation of PARP10 level is required for proper cell cycle progression. Interestingly, PARP10 displays a Caspase 6 cleavage site on residue D406, relating it to apopotosis (Herzog *et al.* 2013). It is also linked with cell response to DNA damage, being involved in PCNA (Proliferating Cell Nuclear Antigen) mediated translesion synthesis by interacting through the PIP motif (PCNA interacting peptide) and with mono-ubiquitinated PCNA through its UIM (Ubiquitin interacting motif). This interaction increases after UV damage, and PARP10 depletion in HeLa cells increases their sensitivity to several genotoxic agents and induces fork collapse (Nicolae *et al.* 2014). In humans, clinical cases of PARP10 deficiency link it with a severe developmental delay and DNA repair defect (Shahrour *et al.* 2016). PARP10 is involved in NF-κB (Nuclear factor κB) nuclear translocation and was reported to have an antiviral activity. It is thus another PARP related with inflammatory and viral responses (Verheugd *et al.* 2013; Atasheva *et al.* 2012; Yu *et al.* 2011). Through modifying GSK3ß kinase activity, it also has a role in metabolism (Shen *et al.* 2012). Finally, it has been reported that PARP14 can recognize automodified PARP10 and to MARylate targets such as Ran-GTPase and therefore stands as an interesting example of crosstalk between PARPs (Feijs *et al*. 2013).

3.6.5 PARP11

PARP11 is very weekly expressed in cells, and locates at centrosomes and spindle poles during mitosis (Vyas *et al.* 2013). PARP11 deletion in mice leads to male infertility, and PARP11 MART activity is required for normal spermatid head elongation in mice (Meyer Ficca *et al.* 2015).

3.6.6 PARP16

Lastly, PARP16 is the only PARP bearing a C-terminal transmembrane domain, allowing its localisation in the ER (endoplasmic reticulum) and the nuclear membrane as a tail-anchored protein. PARP16 regulates the unfolded protein response (UPR), by auto-activating by MARylation during ER stress, acting as a stress signal transducer (Jwa and Chang, 2012). It is able to MARylates karyopherin-ß1, acting as a regulator of nucleocytoplasmic shuttling (Girolamo, 2015).

It is interesting to see how a single ADP-ribosyl transferase-bearing protein domain (PARP signature) is declined in a spectrum of protein variants, having pleiotropic functions and cell localisation in humans (**Figure 3**). The study of the « new PARPs » is still an exciting field of research and is likely to open new roles and therapies in the nearest future (for more details see Héberlé *et al.* 2015, **Appendix I**).

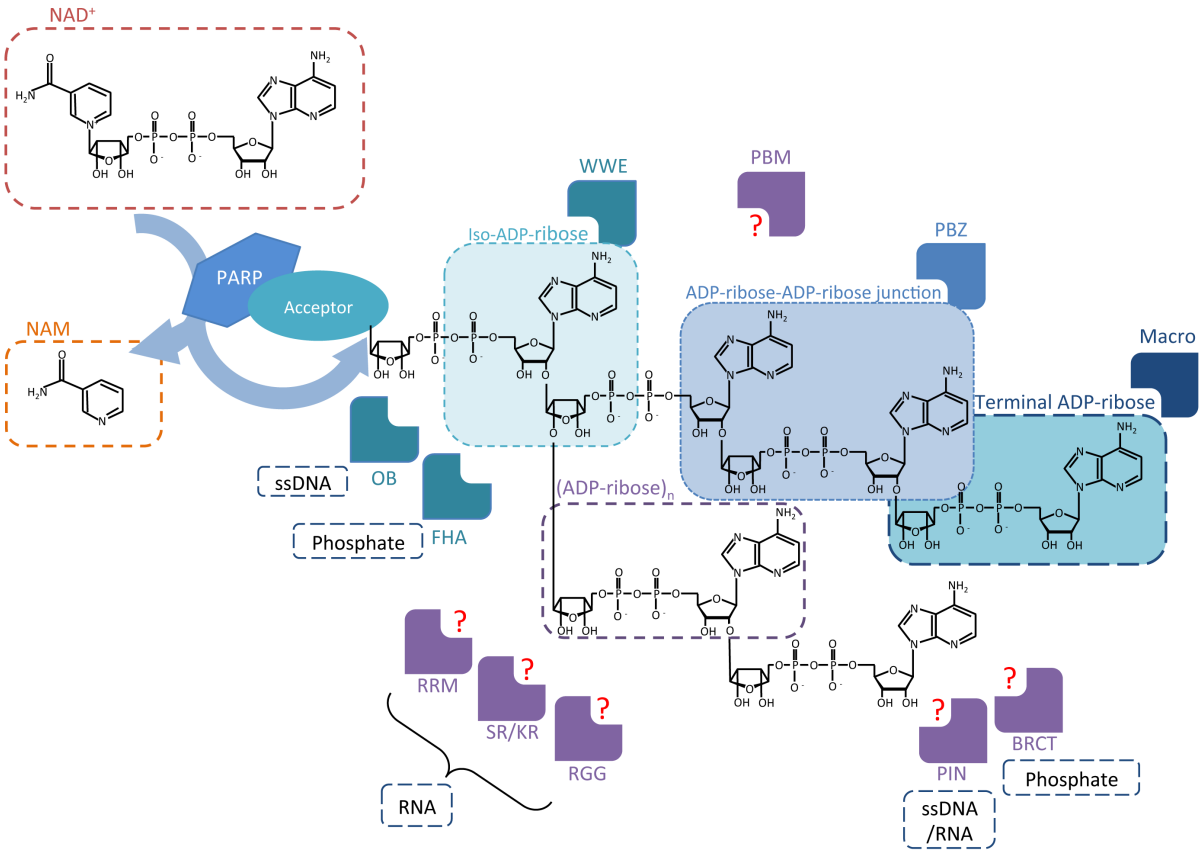

Figure 4: Poly (ADP-ribose) readers.

WWE, OB fold domain (oligosaccharide binding motif), and FHA (fork-head associated) domain containing proteins mainly interact with iso-ADP-ribose. PBZ domain interacts at the vicinity of junctions between two ADP-ribose moieties. Macro domain proteins mainly target Terminal-ADP-ribose extremities. PBM (PAR binding motif)'s interactions have not been clearly identified. RRM (RNA recognition motif), SR/KR (SR repeats and K-rich), RGG (Glycine/Arginine Rich domain), PIN (PiLT N-terminus) and BRCT (BRCA1 C-terminal) domains' interaction have not been precisely defined, but eventually mediate interaction with RNA, single strand DNA or phosphate groups on phosphorylated proteins (adapted from Teloni and Altmeyer, 2016).

Moreover, the discovery of the roles of mono(ADP-ribosyl)ation, that can be catalysed on proteins as well as on DNA, opens new and interesting fields of study (Bütepage *et al.* 2015, Munnur and Ahel, 2017). Part of these different roles is to be attributed to the additional protein domains expressed on the same gene. Some of the domains I mentioned are important for PAR recognition as well as other protein interaction, acting as molecular hinges between interacting proteins in the same catalytic reactions or pathways.

4. Readers of PARylation

As I mentioned in the previous section, PARylation is a macromolecule covalently attached to many proteins, involved in a variety of processes. Proteic domains have also evolved, some being able to interact in a non-covalent fashion with several parts of the polymer. I will describe briefly the main motifs able to recognize PAR (**Figure 4**). All those domains can be referred to as « ADP-ribose binding domains » (ARBD, *Gupte et al.* 2017; Kalisch *et al.* 2013; Zaja *et al.* 2012; Teloni and Altmeyer, 2016)

4.1 PAR binding motif (PBM)

PAR binding motif, although being the first ever identified PAR-interacting protein domain has an interaction mode that is still unknown with the polymer. Hypothesis is that is could interact with PAR through electrostatic interactions, for it is composed of approximately 20 amino acids, with a consensus sequence written as follows: $[HKR]_1$-X_2-X_3-$[AIQVY]_4$-$[KR]_5$-$[KR]_6$-$[AILV]_7$-$[FILPV]_8$

Most of the motif amino acids are positively charged and could account for the interaction with PAR that is negatively charged. X stands for any amino acid (Pleschke *et al.* 2000; Gagné *et al.* 2008). This motif is found in several chromatin structure related proteins (mainly histones: H1, H2A, H2B, H3, H4…), DNA repair factors (XRCC1, XPA, ATM, MRE11, DNA-PKcs, Ku70…), cell-cycle regulators (p53, p21, AIF…) and RNA metabolism (hnRNPs…). Thus, it has important roles in DNA replication, repair, cell cycle maintenance, chromatin architecture and RNA metabolism (Teloni and Altmeyer *et al.* 2016; Kalisch *et al.* 2013).

4.2 Macro domain

The macro domain fold is a mixt globular motif of 130 to 190 amino acids, forming ß-sheets and α-helixes forming a hydrophobic pocket capable of solely interacting with O-acetyl-ADP-ribose, free ADP-ribose or with the terminal moiety of ADP-ribose in a PAR chain (Karras *et al.* 2005). Macro domains are mainly found in chromatin remodeling factors (macroH2A, ALC1, Iduna…) or in PAR degrading enzymes. For those last, the macro domain is bearing a catalytic activity (TARG, MacroD1, MacroD2; Barkauskaite *et al.* 2015; Hassler *et al.* 2011; Jankevicius *et al.* 2013; Feijs *et al.* 2013; Rack *et al.* 2016). As I previously mentioned, some PARPs are also displaying two or three consecutive macro domains (PARP9, PARP15 and PARP14) allowing interaction with mono-ADP-ribose. Interestingly, it seems that very small sequence alterations of the motif are sufficient to switch between an eraser and a reader.

Even some bacteria and viruses have been shown to express macro domain-containing proteins, allowing them to dePARylate host proteins during infections (Gupte *et al*. 2016; Li *et al*. 2016). The most recently identified example is the macro-domain containing non structural proteins of the Chikungunya virus, that can reverse MARylation events catalysed by PARP10, PARP14 or PARP15 (Eckei *et al*. 2017). Understanding the evolution and the peculiarities of this motif will undoubtedly provide new angles of approaches for fighting infections and disease in the years to come. Hepatitis E virus (HEV) also encodes macro-domain proteins, which are determinants for infection (Ohja and Lole, 2016).

4.3 PAR binding Zinc finger (PBZ)

PBZ is a rather short module of 30 aa forming a C2H2-type zinc finger (Lu, 2013), a structure that usually binds DNA, but that in this case is able to bind two adjacent adenines, thus recognizing internal ADP ribose / ADP ribose junctions in the polymer with a very high affinity. It has been discovered in the APLF protein (Aprataxin and PNK-Like Factor), CHFR (Checkpoint with Forkhead Associated) and with a slightly modified sequence in CHK1 (Checkpoint kinase 1), three proteins that are associated with DNA repair and cell cycle control (Ahel *et al.* 2008; Oberoi *et al.* 2010; Isogai *et al*. 2010; Eustermann *et al.* 2010). Its consensus motif is the following: [K/R]-X-X-C-X-[F/Y]-G-X-X-C-X-[K/R]-[K/R]-X-X-X-X-H-X-X-X-[F/Y]-X-H

4.4 WWE motif

WWE motif was named because it contains conserved tryptophan (W) and glutamate (E) residues. It is present in several members of the PARP family (PARP7, PARP11, PARP12, PARP13, PARP14) and most of the existing ubiquitin-ligases (Iduna, Deltex1, Deltex2, Deltex4, HUWE1, TRIP12…). This motif specifically binds to iso-ADP-ribose in PAR chains, thus exclusively targeting oligomers or polymers (Wang *et al.* 2012), and functionnaly bridging ubiquitination and PARylation pathways (Aravind, 2001). The most famous examples of this statement is the RNF146/Iduna E3 ubiquitin ligase, which ubiquitinylates target proteins in a PAR dependent and exclusive fashion (DaRosa *et al.* 2015). PAR dependent ubiquitinylation has extended to the Wnt/ß-catenin signaling pathway, tankyrase being able to PARylate the axin protein, thus allowing its ubiquitination by Iduna. Similar mechanisms have been highlighted for DNA repair proteins: Ku70, DNA-PKcs, XRCC1, DNA-ligase III, PARP1 and PARP2 (Wang *et al.* 2010; Zhou *et al.* 2011; Zhang *et al.* 2011; Kang *et al.* 2011).

4.5 Other ADP ribose readers:

Many other macromolecules or PTM-interacting domains have recently been shown to interact with PAR as well, providing new hinging modalities.

4.5.1 FHA and BRCT

FHA (forkhead associated) and BRCT (BRCA1 C-terminal) for instance were originally reported as readers of phosphorylation (Rheinhardt and Yaffe, 2013). FHA domain mainly interacts with iso-ADP-ribose, and BRCT domain with an ADP-ribosyl moiety. These domains are often found in DNA-repair associated proteins (XRCC1, DNA-ligase III, BRCA1; Breslin *et al.* 2015; Li *et al.* 2013; Li and Yu, 2013) and could thus allow cooperation of

ADP-ribose and phosphorylation cues after DNA damage (γ-H2AX phosphorylation), helping to sequester proteins at the vicinity of DNA breaks.

4.5.2 RNA recognition motif and SR/KR repeats splicing factors

Because of its nucleic acid properties, several RNA and DNA binding motifs have been demonstrated to have affinity for PAR. RNA recognition motif (RRM) is found in many of hnRNPs family protein (heterogeneous nuclear ribonucleoprotein), RNA processing factors and transcription factors (Izhar *et al.* 2015). PAR dependant recruitment of transcription factor is of great interest, thus triggering adequate expression of DNA repair and stress response genesis according to the severity of DNA lesions. In Altmeyer *et al.* 2013, it is suggested that PAR properties, after damage, can outcompete RNA binding, thus assembling RNA binding proteins close to genomic lesion sites in addition to transcription factors. RNA binding Splicing factors such as ASF/ASF2 with positively charged SR repeats or KR rich motifs are also reported to interact with PAR (Malanga *et al.* 2008).

4.5.3 OB-fold

OB-fold (oligonucleotide/oligosaccharide binding fold) is a 70-150 amino acid folded into a ß-barrel that is able to bind single stranded DNA and oligosaccharides and that displays affinity for iso-ADP-ribose. This unique bridge allows the recruitment of SSB1 (single-strand-binding protein 1) and BRCA2 to DNA damage (Zhang *et al.* 2014, Zhang *et al.* 2015).

4.5.4 PIN domain

(PilT N-terminus), interacts both with single stranded DNA and RNA, and PAR, the latter interaction being crucial in order to recruit EXO1, an exonuclease required for DNA end resection in double strand break repair (Zhang *et al.* 2015).

4.5.5 RGG/GAR domains and other reported interactions

MRE11's recruitment to DNA damage, another protein of end resection relies on its arginine and glycine rich motif (RGG) or glycine arginine rich (GAR) domains interaction with PAR (Haince *et al.* 2008).

Increasing examples are available in the litterature of a double usage of protein domains to bridge several mecanistical pathways in cells. It seems that these domains have evolved to favour pluripotent interactions, allowing complex affinity competition between several protein partners. The more evidence we get of multiple interactions through different readers, the more the PAR molecule appears as a beautifully sophisticated and subtle hub for protein complex formation. In the next paragraph, I will focus on PAR erasers that are needed for the rapid turnover and regulation of protein-protein interactions in cells.

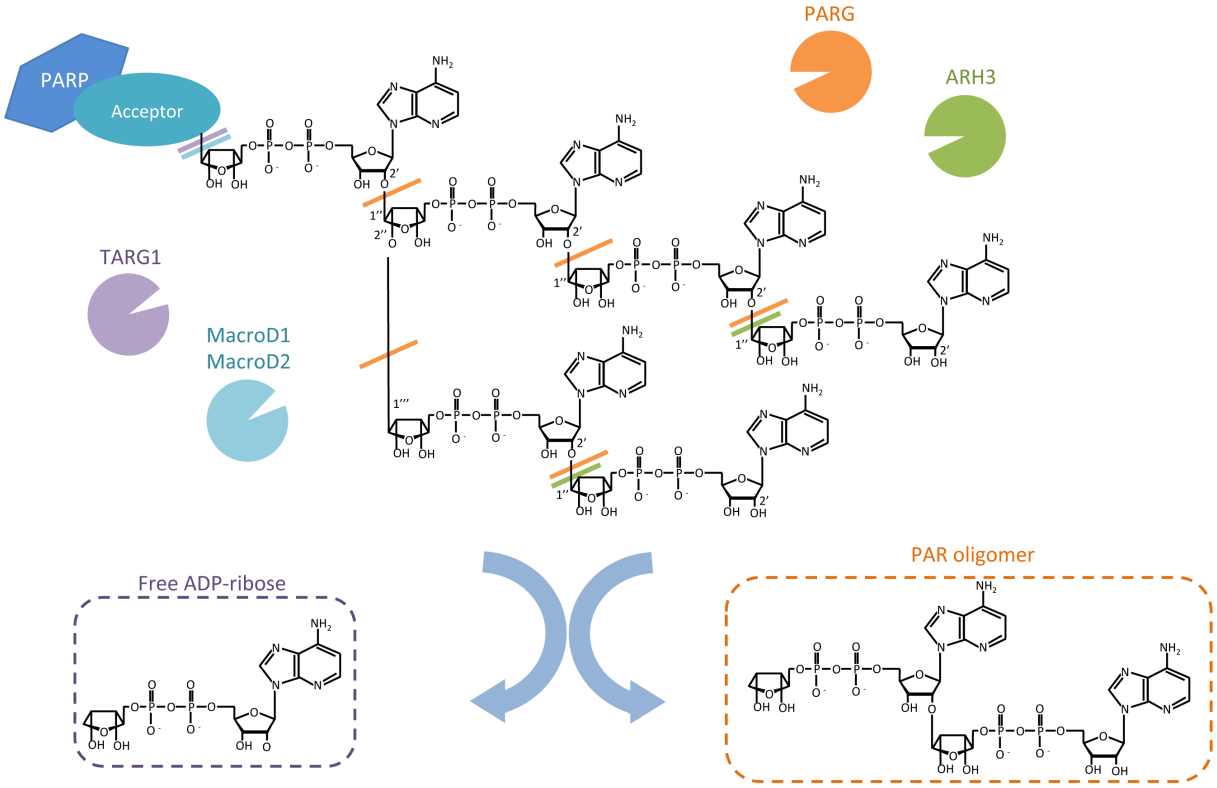

Figure 5: Erasers of Poly(ADP-ribosyl)ation in human genome.

PARG (Poly(ADP-ribose)glycohydrolase), ARH3 (ADP-ribose hydrolase 3) and TARG1 (Terminal ADP-ribose Glycohydrolase 1) display both endonucleolytic and exonucleolytic activities, releasing free ADP-ribose or PAR oligomers, having a signaling role in human cells. Their activities range as follows: PARG > ARH3 > TARG1. TARG1, MacroD1 and MacroD2 are able to cut the bond between target amino acid and terminal mono-ADP-ribose, thus removing the last chain residue of PAR.

5. Erasers of PARylation

Once the reaction of PARylation has occurred, the polymer has a very short lifetime, and the macromolecule is rapidly degraded, within a period of 6 minutes (Jacobson *et al.* 1983), in order to restore normal polymer levels and to regenerate the NAD^+ pool available in the cell. In humans, five main erasers were discovered so far, that all contribute to keep balance in the PAR generated after DNA damage. The main one is the Poly(ADP-ribose) glycohydrolase (PARG), then ARH3 (ARH1 like ADP-ribose hydrolase), TARG1 (Terminal (ADP-ribose) glycohydrolase) and finally the most recently identified : MacroD1 and MacroD2 (see Barkauskaite *et al.* 2015 for a review). They can target different parts of the PAR molecule, releasing either free PAR or single ADP-ribose moieties that can have signaling roles (**Figure 5**).

5.1 PARG

5.1.1 A Brief history of PARG discovery

PARG activity was first characterized in 1970 in rat liver extracts (Shimoyama *et al.* 1970), opening the wide field of PAR catabolism study. Bovine and rat PARG cDNA were cloned 30 years later (Lin *et al.* 1997; Shimokawa *et al.* 1999). Meanwhile, Amé *et al.* mapped PARG gene on human chromosome 10 (10q11.21-23), and mouse chromosome 14B (Amé *et al.* 1999). The cloning of the human gene and the development of several mice and cellular models deficient for PARG allowed to show that PARG was crucial for development, since PARG gene invalidation is embryonic lethal, the spontaneous excessive accumulation of PAR in nuclei resulting in cell death by apoptosis (Koh *et al.* 2004). In this model, PARG depleted embryonic stem cells can only last upon cultivation in PARP inhibitor supplemented medium. This was the first step towards the understanding of the importance of maintaining PAR levels in a cell. PARG is widely conserved across organisms, being shared in several reigns from *Trypanosoma bruceii*, *Drosophila melanogaster*, *Caenorhabditis elegans* or *Arabidopsis thaliana*.

5.1.2 Genomic structure

In humans, the gene comprises 18 exons and 17 introns and shares a bi-directionnal common promoter with the TIM23 gene (Meyer *et al.* 2003), an internal mitochondria membrane associated protein, which is part of a highly dynamic intermembrane complex involved in protein translocation (Bajaj *et al.* 2014a; Bajaj *et al.* 2014b). Although it has been demonstrated that the promoter activity is 3.7 fold higher towards TIM23 expression in comparison with PARG (Meyer *et al.* 2003), no further work has been carried since. Nonetheless, it is interesting to think about this bi-directionality as a putative bacterial operon-like expressing system, since some of the PARG isoforms are targeted to the mitochondria, as we shall see in the next paragraph. Indeed, a single PARG gene encodes at leat five different isoforms in human cells (Meyer-Ficca *et al.* 2004; Niere *et al.* 2012, **Figure 6,** next page).

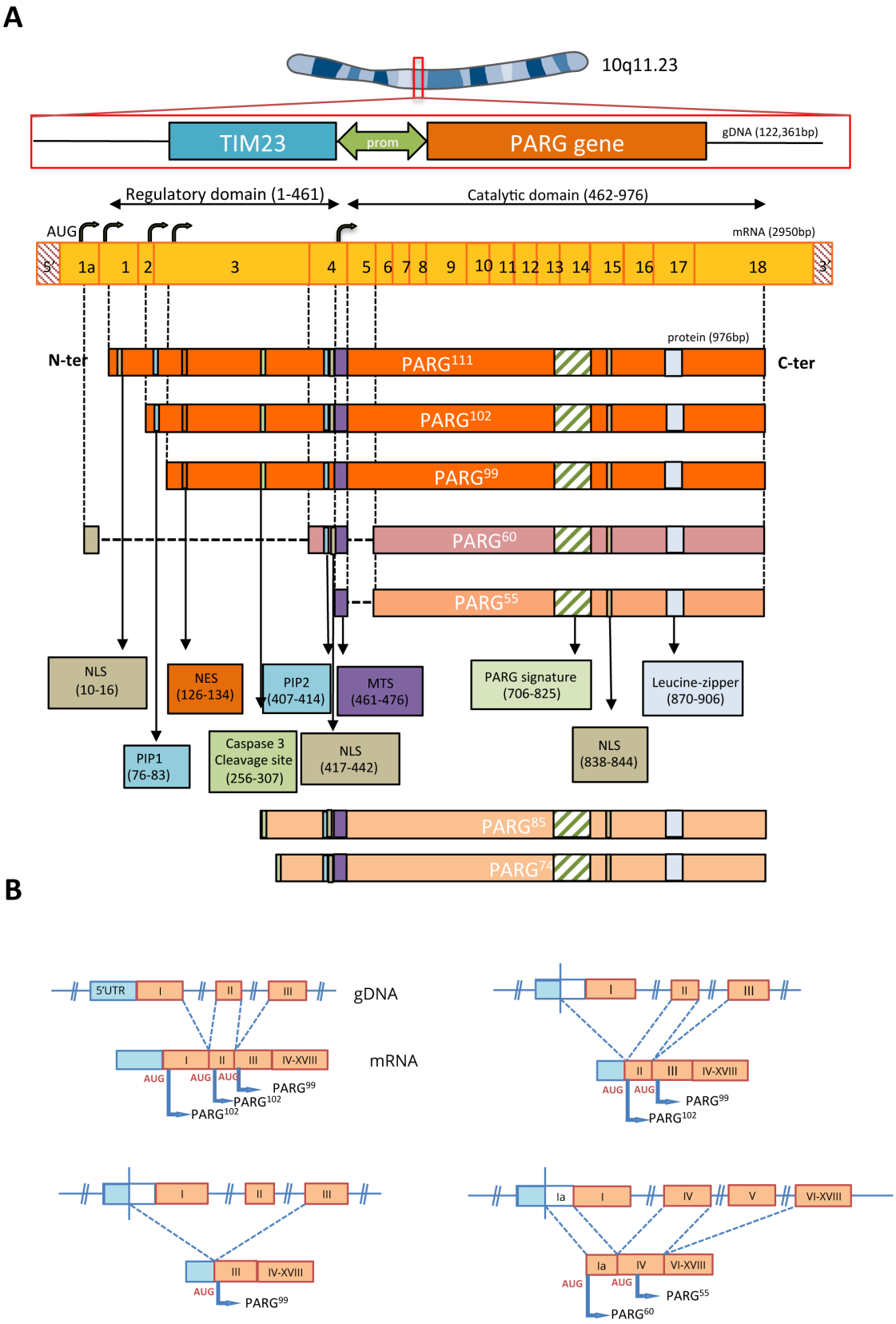

Figure 6: PARG, from gene to isoforms

A) Genomic localization, genomic structure, mRNA and protein isoforms generated from the PARG gene. B) Alternative mecanisms to generate PARG isoforms. Alternative splicing or alternative starting site for translation may play roles in isoform expression. AUG, Start codon.

5.1.3 PARG: "One gene to gen them all"

The PARG gene encodes for a 111kDa protein of 976 amino acids ($PARG^{111}$) that is targeted to the nucleus and comprises two main modular domains. The N-terminal domain (1-460kDa) is considered as a regulatory domain and can be targeted by several kinases for post-translational modifications, while the C-terminal domain (461-976) bears the catalytic activity of the protein, detailed in the next paragraph (Botta and Jacobson, 2010; Gagné *et al.* 2009). In 2004, Meyer-Ficca reported the existence of two additional cytoplasmic isoforms, of 102kDa ($PARG^{102}$) and 99kDa ($PARG^{99}$) respectively (Meyer-Ficca *et al.* 2004). Three years later, they also reported the existence of two mitochondrial isoforms of 60kDa ($PARG^{60}$) and 55kDa ($PARG^{55}$) that lack the N-terminal regulatory domain (**Figure 6A**). These isoforms can be generated by alternative splicing of exons in the mRNA, or presumably by the use of alternative start codons during translation of the mRNA. The different scenarios for generating $PARG^{111}$, $PARG^{102}$, $PARG^{99}$, $PARG^{60}$ and $PARG^{55}$ are reported in **Figure 6B** (Meyer *et al.* 2007, Whatcott *et al.* 2009). The existence of these different isoforms, targeted to different cell compartments, has complicated the study of PARG in the last years. One of the aims of this thesis project is to generate new cellular tools to decipher the roles of these isoforms in DNA repair.

5.1.4 Other structural features

PARG sequence bears several features, which could account for the localization of the different isoforms. A monopartite nuclear localization signal (NLS, 10-18) dwells in the N-terminal domain and is responsible for $PARG^{111}$ nuclear localization (Meyer-Ficca *et al.* 2004). $PARG^{102}$ and $PARG^{99}$ lack this NLS and locate to the cytoplasm. A second putative NLS, homologous to PARP1's NLS, is located between residues 417 and 442 (Lin *et al.* 1997), and a third putative NLS, whose function has not been confirmed, dwells in the C-terminal part of the protein (838-844). PARG also bears one nuclear export signal (NES, 124-132, Shimokawa *et al.* 1999). Treatment with Leptomycine B, an inhibitor of the NES-dependent active export in cells, results in a relocalisation of $PARG^{102}$ from the cytoplasm to the nucleus (Bonicalzi *et al.* 2003). Another putative NES could dwell in the C-terminal leucine-zipper, a motif that can mediate protein-protein interaction (Lin *et al.* 1997). Additionnaly, a mitochondrial transport signal (MTS) lies between residues 461 and 476 (Meyer *et al.* 2007). This MTS accounts for the reported mitochondrial localization of $PARG^{60}$ and $PARG^{55}$. Across the cell cycle, isoforms are dynamically relocalized. One study showed a dynamic relocalization of PARG during mitosis, transiently leaving nucleus as soon as chromatin condensation starts, and rejoining centrosomes (Ohashi *et al.* 2003). In our hands, we never observed such behaviour. Our lab has shown that $PARG^{111}$ mainly accumulates in S phase and co-localizes with replication foci by interacting with PCNA via its PIP domain (Mortusewicz *et al.* 2011). A second PIP2 motif was identified recently (Kauffmann *et al.* 2017). Upon DNA damage, $PARG^{111}$ has been reported to leave the nucleus, meanwhile $PARG^{102}$ and $PARG^{99}$ migrate from the cytoplasm to the nucleus (Mortusewicz *et al.* 2011, Haince *et al.* 2006). Two caspase 3 cleavage sites were also discovered between 253-257(DEIDV) and 304-308 (MDVD), generating two cytoplasmic apoptotic fragments of 85kDa and 74kDa that bear a catalytic activity and could be of use during the apoptosis process (Affar *et al.* 2001). All these features are summarized in **Figure 6A.**

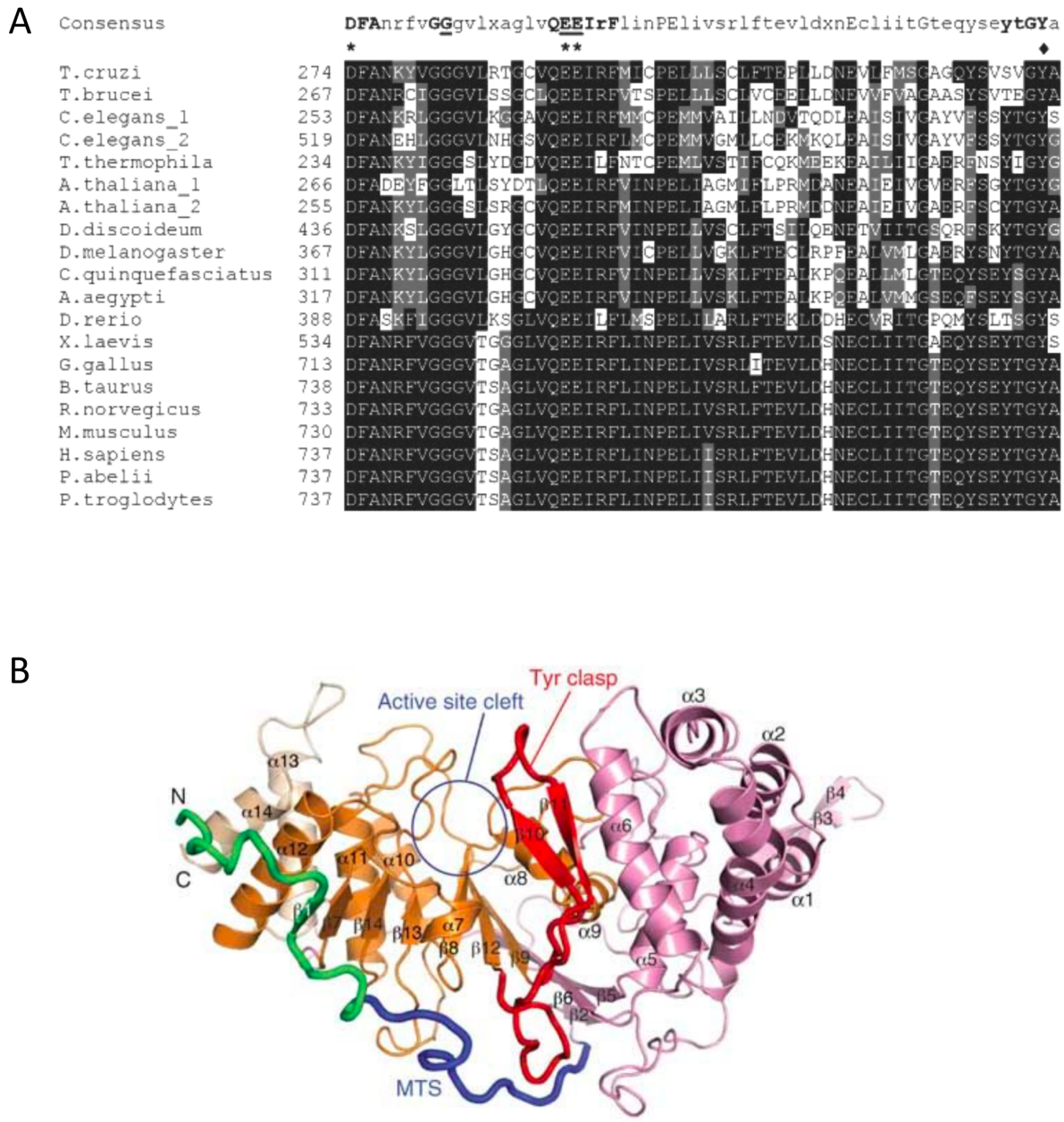

Figure 7: PARG signature and structure of PARG's catalytic domain

A) Amino acid sequence alignement of the PARG catalytic domain, across different organisms. Conserved residues, which are important for PARG catalytic activity, are highlighted with a black asterisk (from Amé *et al.* 1999). B) Three-dimentional structure of the catalytic domain of human PARG. It consists in a core macrodomain fold (displayed in orange), sandwiched between two flanking N-terminal (pink) and C-terminal (beige) helical bundles. The mitochondrial targeting sequence (MTS; blue) wraps around the catalytic domain and stabilizes the tyrosine clasp (Tyr clasp; red), a unique substrate-binding element of mammalian PARG (from Kim *et al.* 2012).

5.1.5 PARG: catalytic domain

PARG activity relies on its "PARG signature" sequence domain (GGG-X_{6-8}-QEE), organized as a macro-fold, which is conserved across organisms and can be written as follows: (see **Figure 7A**). As a macro-domain-containing protein, endowed with both exo and endo glycohydrolase activity (Brochu *et al.* 1994; Zaja *et al.* 2012). The catalytic domain requires three critical residues for the catalysis of PAR degradation: E756, E757 and D738 are necessary for the PAR degrading activity (Patel *et al.* 2005). An additional glycine rich region comprising G745, G746 and G747 is conserved from plants to humans and increases its degrading efficiency (Panda *et al.* 2002). Elucidating and comparing the three-dimensional structure of PARG catalytic domain from several organisms, from bacteria (Slade *et al.* 2011) to mammals, helped understanding the way human PARG is able to degrade polymer. All conserved residues are grouped into a hydrophobic pocket and apart from the catalytic domain, and additional loop structure called the "Tyrosine clasp" allows the endonucleotidic activity of PARG (Tucker *et al.* 2012, Kim *et al.* 2012; Wang *et al.* 2014). PARG preferentially cleaves long PAR chain, and hydrolyzes protein-bound PAR by covalent links, more rapidly than it hydrolyzes free PAR (Uchida *et al.* 1993). The PAR degradation occurs in two steps: during the processive phase, the enzyme shortens each of its PAR branchings, and during the second non-processive step, PARG degrades short polymers. The removal of the terminal ADP-ribose moiety is rate limiting, for PARG in unable to hydrolyze the bond (Wang *et al.* 2014). It is of importance to mention that if PARG is not able to remove the last mono-ADP-ribose moiety on proteins, it is has recently been shown to be, however, capable of reversing mono-ADP-ribosylation on double strand DNA ends (Munnur and Ahel, 2017).

Understanding the details of PARG activity is crucial for the development of PARG inhibitors (James *et al.* 2016) that will help us to refine our understanding of the roles of PAR catabolism. The same inhibitors are currently expected to be of great use for cancer or disease therapies (Fathers *et al.* 2012; Gravells *et al.* 2017; Pascal and Ellenberger, 2015).

5.1.6 PARG and genomic integrity

The role of PARG in the maintenance of genomic integrity first emerged with PARG deficient mice models. First, depletion of all isoforms by deleting exon 4 results in an early death during embryogenesis. Embryos die at 3.5 days of development, and cells derived from the embryos can only survive with the addition of PARP inhibitor in the culture media. This suggested that the overaccumulation of PAR was highly detrimental (Koh *et al.* 2004). Mice models, in which exon 2 and 3 are deleted, lack $PARG^{111}$, $PARG^{102}$ and $PARG^{99}$. The mice are viable and fertile (Cortes *et al.* 2004), but corresponding embryonic stem cells (ES cells) display an increased sensitivity to DNA-damaging agents such as MNNG, an impaired automodification and activation of PARP1 and an impaired recruitment of XRCC1 (Gao *et al.* 2007), a DNA repair factor which is normally recruited by PARP1/PAR (see **Chapter 2**). ES cells of mice in which exon1 was deleted are lacking $PARG^{111}$. These cells are highly sensitive to alkylating agents, irradiation or other carcinogens (Fujihara *et al.* 2009). Deletion of PARG110 in mice results in an increased PAR accumulation, and enhances postischemic brain damage (Cozzi *et al.* 2006), but protects them from renal ischemia/reperfusion injury (Patel *et al.* 2003). The partial loss of PARG in *Drosophila melanogaster* causes progressive neurodegeneration (Hanai *et al.* 2004). Since deleting all isoforms is lethal in organisms, PARG deficient cell models have been developed, using siRNA. These cells were

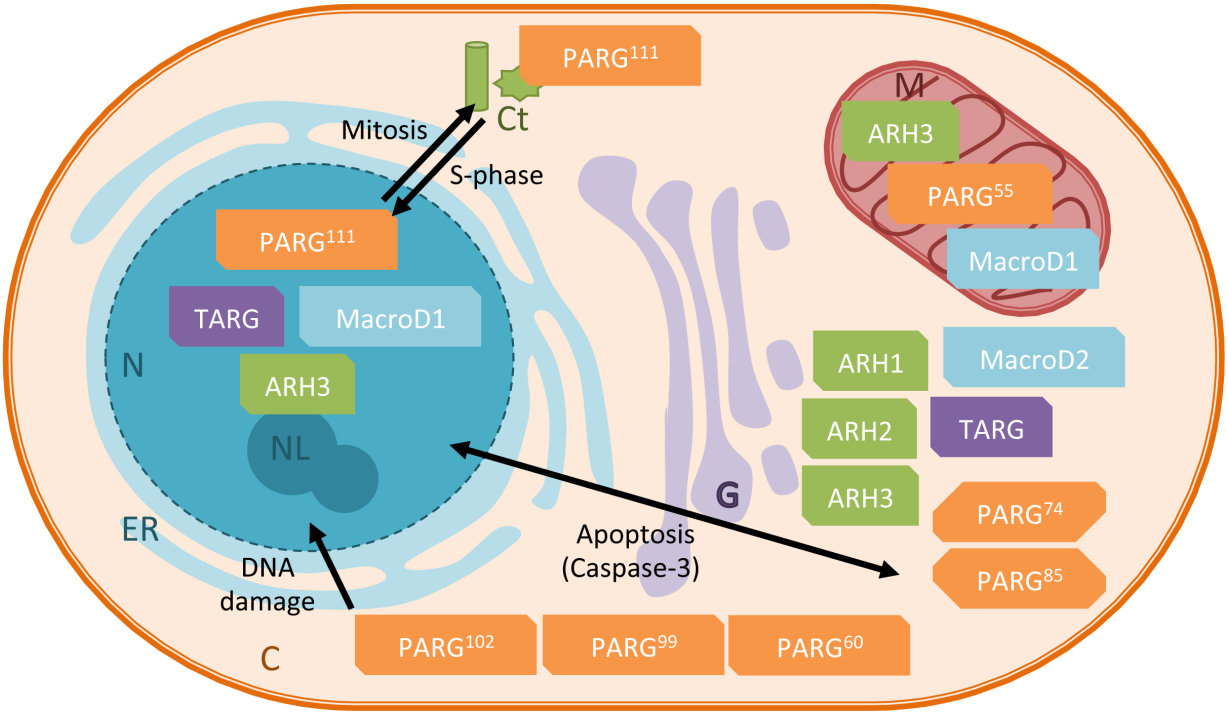

Figure 8: Subcellular localization of the ADP-ribose degrading activities in human cells.

PARG, Poly-ADP-ribose glycohydrolase; ARH1-3, ADP-ribose hydrolases; TARG, Terminal ADP-ribose glycohydrolase MacroD1 and MacroD2, Macro-fold containing proteins with PAR degrading abilities. PARG-111: nuclear isoform of human PARG, can be recruited to centriole in mitosis, PARG-102 : cytoplasmic isoform,can shuttle to the nucleus upon DNA damage. PARG-74 and PARG-85 : apoptotic fragments of PARG. PARG-99, PARG-60 and PARG-55 : other shorter isoforms. N, nulceus; NL, nucleolus; ER, Endoplamic Reticulum; C, Cytoplasm; G, Golgi; C, Vault Particle; M, Mitochondria; Ct, Centrosome.

viable, but displayed increased sensitivity to DNA damage (Blenn *et al.* 2006, Fisher *et al.* 2007). Our lab generated a HeLa cell model, stably expressing an shRNA leading to an efficient PARG depletion (Amé *et al.* 2009). These cells were more sensitive to irradiation, displayed increased levels of DNA damage, linked with a delay of DNA repair, and died from mitotic catastrophe. Using the same cells, the lab also demonstrated that PARG could protect cells from replicative stress, by preventing excessive PARylation of RPA protein after hydroxyurea induced replicaiton fork collapse (Illuzzi *et al.* 2014). These data, plus the fact that $PARG^{102}$ and $PARG^{99}$ isoforms have been reported to shuttle between the cytoplasm and the nucleus, suggest that PARG has important functions in the maintenance of genomic integrity. The subcellular distribution of the isoforms and the other PAR-degrading enzymes is summarized in **Figure 8**. However, the contribution and the regulation of each isoform in these functions are still unclear. Generating cellular models in order to investigate these questions was one of the aims of my PhD project (See **Results section**).

5.2 ARH proteins: ADP-ribose-acceptor hydrolases

The family of ADP-ribosyl acceptor hydrolases (ARH1-3) were named after ARH1. It is the only mammalian ADP-ribosylarginine hydrolase, hydrolysing the N'-glycosidic bond of mono(ADP-ribose) on arginine moieties (Moss *et al.* 1992). ARH1 is ubiquiteously expressed in mammalian cells and tissues as a 39kDa soluble cytoplasmic protein with a ubiquitous expression (Mashimo *et al.* 2014). ARH1 knockout mice develop spontaneous tumors, indicating that control of ARH1 activity is important for tumorigenesis and cell proliferation (Kato *et al.* 2015).

ARH2 shares 68% similarity with ARH1 but is devoid of catalytic activity, although is has been shown to bind ADP-ribose (Kasamatsu *et al.* 2011). The two residues in positions 60 and 61, dwelling in the catalytic site, are aspartate-arginine instead of two aspartates, which may explain its lack of activity (Oka *et al.* 2006).

ARH3 is present only in vertebrates, and shares sequence similarity with both ARH1 and PARG and is ubiquitously expressed in human tissues (Oka *et al.* 2006). The ARH3 cell content parts between cytoplasm, mitochondria and nucleus (65%, 25% and 10% respectively). In humans, it is the only mitochondrial PAR-degrading activity, for $PARG^{60}$ and $PARG^{55}$ have been shown to be inactive (Niere *et al.* 2012). Structure and activity studies show that unlike PARG, ARH3 is able to degrade both ADPr units and chains of ADPr on histones and other proteins, as well as O-acetyl-ADP-ribose (OAADPR), a molecule generated by the sirtuin family of proteins. It seems that the catalytic site enables the sole binding of ARH3 to terminal ADP-ribose, suggesting a exoglycosidase activity, that is dependent on the presence of an Mg^{2+}co-factor (Mueller-Dieckmann *et al.* 2006; Oka *et al.* 2006; Ono *et al.* 2006; Kasamatsu *et al.* 2011).

ARH3 is involved in suppressing PAR-mediated cell death, also called parthanatos, by preventing PAR to translocate and accumulate in the cytoplasm, further triggering the release of AIF (Apoptosis Induced Factor, Wang *et al*. 2011; Mashimo *et al*. 2013). In fact, its functions are tightly linked with PARP1 after oxidative stress (Mashimo and Moss, 2016). Recently, it has been shown to remove serine ADP-ribosylation, thus emerging as an interesting tool to study serine ADP-ribosylation (Fontana *et al.* 2017). Although its PAR degrading activity is lower than PARG, ARH3 needs to be considered when thinking about catalytic degradation of PAR in any study.

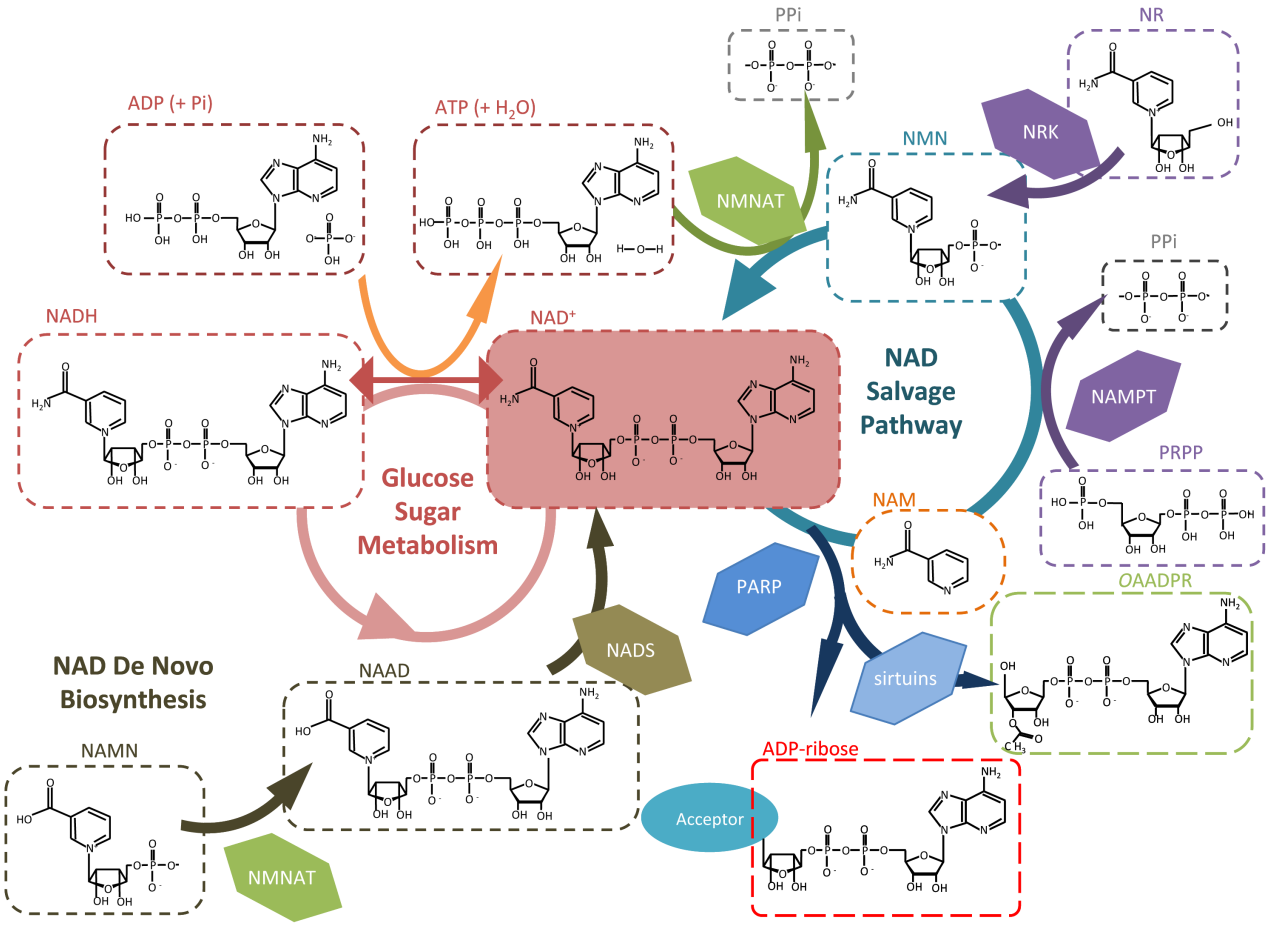

Figure 9: Feeders and consumers of PARylation (adapted from Imai and Guarente, 2014)

NAD+ is a key metabolite for many processes, mainly in sugar metabolism where it regenerates the ATP (Adenosyl Triphosphate) energy pool from ADP (Adenosyl Triphosphate). It is mainly synthetised in two pathways, the NAD de novo biosynthesis and the NAD salvage pathway. In de novo biosynthesis, NAMN (Nicotinic acid mononucleotide) synthetized from tryptophan through several enzymatic steps is used to generate NAAD (Nicotinic acid adenine dinucleotide) through the activity of NMNAT (Nicotinamide Mononucleotide Adenylyl Transferase) NADS (NAD synthase) will regenerate NAD from this precursor.
In the NAD salvage pathway, NMN (Nicotinamide Mononuclotide) can be regenerated from NAM (Nicotinamide Mononucleotide) with the activity of NAMPT (Nicotinamide phosphoribosyltransferase) and using PRPP (Phosphoribosylpyrophosphate) as a cofactor - or using NR (NAM riboside) through the activity of NRK (NAM riboside kinase). NMN is ultimately converted to NAD through the activity of NMNAT. NA (nictotinic acid, not shown) is also a precursor for NAD in the salvage pathway. NAD is mainly consumed in PARylation reactions, through the activity of PARP enzymes and sirtuins. The availability of NAD+ and the equilibrium between its feeders and consumers ensures an adequate level in cellular NAD+ pools.

5.3 MacroD1, MacroD2 and TARG1

Three other human macrodomain proteins are able to reverse MARylation. MacroD1 and MacroD2 display similar structures, with a N-terminal region that consists of an elongated chain of helical segments and short ß-strands. Their macrodomain fold (151-322) consists in three layered α-ß-α sandwich with a central six-stranded ß-sheet, enabling the cleavage of MAR and OAADPR, the reaction product of sirtuins that can act as a signaling molecule (Tong and Denu, 2010).

While MacroD1 displays a N-terminal MTS and localizes in both mitochondria and nucleus, MacroD2 is mainly cytoplasmic. They are therefore addressed to all cellular compartments where OAADPR could be generated, thus competing with nudix hydrolases activities. All macrodomain proteins are tighlty linked with PAR metabolism (Chen *et al.* 2011). MacroD1 deficiency has been linked to breast cancer cell progression and MacroD2 deficiency is associated with cancer and neurological disorders (Rack *et al.* 2016). More importantly, MacroD2 is recruited on DNA damage sites (Rosenthal *et al.* 2013) and ATM induces MacroD2 phosphorylation-dependent export upon DNA damage (Golia *et al.* 2017). Here is another example of PTM being a crucial feature for regulating the localisation of proteins mediating the catabolism of PAR.

TARG1 (C6orf130) was initially reported in a clinical case where its absence was associated with neurologic and developmental defects. Its compact globular macrodomain fold has a different catalytic activity than PARG, removing only the terminal ADP-ribose of PAR chains. It locates in nucleus and its depletion is associated with DNA repair defects (Neuvonen and Ahola, 2009; Sharifi *et al.* 2013). Biochemical assays revealed that MacroD2 and TARG1 have different specifities, and that the sourrounding ADP-ribosylated residues can influence their substrate recognition (Kistemaker *et al.* 2016).

5.4 Other ADP-ribose erasers

Another way of removing ADP-ribosylation consists in converting it into protein-conjugated ribose-5'-p (pR in the litterature). This activity has been first elucidated in vitro, with bacterial proteins. However, two families of human proteins have been found since, that can convert ADP-ribose into pR: ENPP1 (ectonucleotide pyrophosphatase/phosphodiesterase 1) and the Nudix domain bearing protein NUDT16 ((nucleoside diphosphate-linked moiety X)-type motif 16, Palazzo *et al.* 2015; Palazzo *et al.* 2017).

6. Feeders and consumers of ADP ribosylation

Additionally to enzymes that catalyse the ADP ribosylation reaction (writers), interact with ADP-ribose (readers) and remove the modification (erasers), one needs to consider the substrate used as well as the different enzymes that are either increasing the amount of the substrate (feeders) or competing for the substrate to ensure their own catalytic activity (consumers). NAD^+ is the substrate for ADP-ribosylation. Different feeders and consumers of the PARylation reaction are summarized in **Figure 9**.

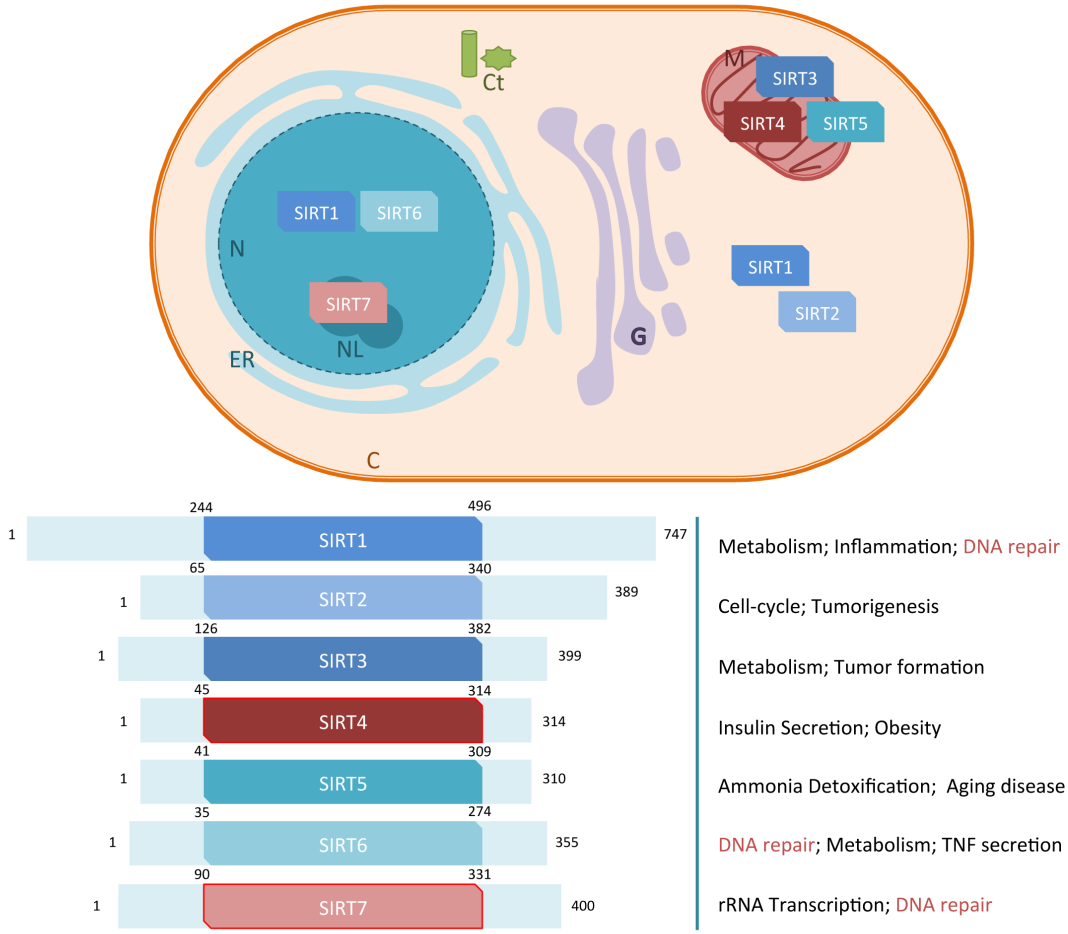

Figure 10: Overview of the seven members of the human sirtuin family (adapted from Mei et al. 2016)

Sirt1, Sirt6 and Sirt7 are located in the nucleus (N) and nucleolus (NL) and are involved in DNA repair. Sirt2 is mainly cytoplasmic (C), Sirt3, Sirt4 and Sirt5 are mitochondrial (M). All of them display de-acetylating activities toward proteins. Sirt4 and Sirt7 also display a ADP-ribosyl transferase activity.

6.1 Feeders of NAD: Salvage pathway and De Novo biosynthesis.

Nicotinamide adenine dinucleotide (NAD^+) was discovered in the early 20th century, by Sir Arthur Harden, as a yeast-extract substance stimulating fermentation and alcool production in vitro (Imai and Guarente, 2014). It is composed of two covalently joined molecules: nicotinamide (NAM) and adenosine monophosphate (AMP). NAD^+ and its reduced version NADH were for a long time considered solely as crucial enzymatic cofactors facilitating hydrogen transfer in metabolic processes, before emerging as the main substrates for PARPs and sirtuins to catalyse chemical modifications and post-translational modifications. NAD^+ can indeed be converted in NADH during the TCA (Tricarboxylic acid) cycle, concomitantly to acetyl-CoA oxidation to CO_2, or during the oxidation of fatty acids in the mitochondria. NADH becomes an electron donor allowing ATP regeneration from ADP in the oxidative phosphorylation process. These biochemical reactions are of major importance in cancer metabolism (see Ciccarone *et al.* 2017; Teoh and Lunt, 2017 for a review). In mammals, NAD^+ can be synthesized by two main pathways (**Figure 9**):

-In the ***de novo* pathway** cells can generate NaMN from tryptophan (in several steps that I will not detail). NaMN (Nicotinic acid mononucleotide) is converted into NAAD (Nicotinic acid adenine dinucleotide) by the NMNAT enzyme (Nicotinamide Mononucleotide Adenylyl Transferase) and then in NAD+ by the NADS (NAD synthase).

-In the **NAD salvage pathway**, cells can use either NR (NAM riboside) that will be converted into NMN by NRK (NAM riboside kinase), or NAM that can be converted into NMN by NAMPT (Nicotinamide phosphoribosyltransferase). NMN is then converted into NAD^+ through the NMNAT activity. NMNAT, NADS or all upstream enzymes are thus limiting-rate factors in the regeneration of NAD pools, and can thus be considered as feeders for the PARylation reaction (Imai and Guarente, 2014; Nikiforov *et al.* 2015). Additionally, it is also interesting to mention that the nuclear enzyme NMNAT1, depending on its phosphorylation state, is able to interact with automodified PARP1 and to stimulate its PARylating activity, thus demonstrating its role as a feeder for the PARylation reaction, bringing NAD^+ directly at the vicinity of its most efficient consumer (Berger *et al.* 2006). Evidence is emerging that PAR formation could act as a biosensor for the levels of the subcellular NAD+ pools (VanLinden *et al.* 2017).

6.2 Consumers of NAD+: PARPs and sirtuins

The main consumers of NAD^+ are PARPs and sirtuins (Silent Information Regulator Two (Sir2) protein) (**Figure 10**). Sirtuins are a family of proteins with two catalytic activities. They can either deacetylate proteins by transferring an acetyl group on NAD^+, thus generating *O*AADPR (O-acetyl-ADP-ribose) by-products, or mono-ADP-ribosylate acceptor proteins. These processes are able to mediate stress response, modulate transcription or cellular metabolism (Feldman *et al.* 2012). This family is conserved in all three evolutionary reigns: bacteria, archaea and eukarya (Greiss and Gartner, 2009). Mammalians have seven sirtuin isoforms (Sirt1-7) that differ in their substrate specificities and subcellular localizations. They are all related with metabolism, DNA repair and cancer (Mei *et al.* 2016).

SIRT1 (Sirtuin1) is the founding member of the SIRT family in humans. Beside from its role in metabolism, it is regulating DNA damage and repair, acting both in single strand break repair and double strand break repair. It has also been linked with stemness and cell differentation mecanisms, which are strongly relying on metabolic activity (Correia *et al.* 2017). SIRT3, SIRT4 and SIRT5 are all mitochondrial sirtuins that have been linked to aging related disease (Van de Ven *et al.* 2017). Interestingly, sirtuin 5 was reported to have a weak deacetylase activity, but to be capable of acting as desuccinylase, demalonylase, and deglutarylase; and associated with diseases such as cancer, Alzheimer and Parkinson (Yang *et al.* 2017). Sirtuin 6 stabilizes DNA-PK at chromatin for double strand break repair and promotes homologous recombination repair during replication (see Beauharnois *et al.* 2013 for a review). Sirtuin 7 has been linked to several pathologies such as cardiac hypertrophy, hepatic steatosis and deafness. It is a key player of genomic integrity by modulating non-homologous end-joining repair (Vazquez *et al.* 2017).

Because of their extending roles and functions, they have been suggested as therapeutic targets and the development of specific inhibitors is on its way, to keep investigating and refining our knowledge on their functional in vivo study (Jiang *et al.* 2017).

In this thesis work, we did not consider sirtuin activity for all the mecanism studied, but it is nevertheless important to keep their contribution to PARylation processes in mind when discussing PARylation matters.

7. ADP-ribosylation everywhere

It has long been known that ADP-ribosylation was occuring both in prokaryotes and eukaryotes. Nonetheless, PARPs were first described only in pluricellular eukaryotes, before being identified in unicellular organisms like *Trypanosoma brucei*, archaebacteria and even viruses (see Palazzo *et al.* 2017 for a review). PARylation now seems to be a general feature of all living organisms, with the peculiar exception of yeast *Saccharomyces cerevisiae* and *Saccharomyces pombe*, suggesting they have lost PARylation during evolution. Consistently, expression of exogenous versions of PARPs in S. cerevisiae or S. pombe seems to interfere with a proper proliferation and to sensitize these fungi to damging agents (Avila *et al.* 1994; Kaiser *et al.* 1992).

Evolutionnary studies suggest that PARP genes have undergone a rapid evolution. Since they display functions that are tightly related with mRNA, viral replication, and more generally nucleic acids, they could be pivotal elements of the host-pathogen relationships across organisms (Daugherty *et al.* 2014).

7.1 PARylation in bacteria and fungi

The first ever discovered ART activities were bacterial toxins able to modify host proteins during pathogenic infection (Holbourn *et al.* 2005; Holbourn *et al.* 2006). Several studies reported the purification of PARP or PARG proteins from different bacteria and filamentous fungi. For instance, the first crystal structure of PARG catalytic domain was identified from T. curvata (Slade *et al.* 2011). Very recently, the DraT/DraG system was discovered, that can trigger ADP-ribosylation of thymidine residues on DNA of nitrogen-fixating bacteria. This phenomenon interferes with DNA replication and triggers DNA damage signaling via the SOS response

(Jankevicius *et al*. 2016). In *Streptomyces,* ADP-ribosylation is important for growth, metabolic processes and morphological differentiation. It has been involved in tRNA dephosphorylation and antibiotic resistance in some species of *Mycobacterium*. A bacterial PARG homologue (SCO0909) was even shown to be induced after ionizing radiation exposure. This event controls DNA damage repair in the radiation resistant *Deinococcus radiodurans* (Liu *et al.* 2003). There is also evidence for the presence of other macrodomain homologues (close to TARG1) and sirtuins. The genus *Streptomyces* is to date the best model so far to study bacterial ADP-ribosylation.

7.2 PARylation in archaea

To date, only one PARP activity-like protein have been purified in *Sulfolobus solfataricus (*Faraone-Mennella *et al*. 1998). There is evidence for the existence of several ART activities and orthologues of the DarT/DarG system. MacroD-type and TARG1-like macrodomain proteins were also found. Overall it seems that most of the archael species display mono-ADP-ribosylation rather than PARylation.

7.3 PARylation in viruses

Viruses have been found capable of manipulating their hosts PARylation mechanisms. In bacteriophages, several ARTs can modify key *E.coli* proteins, interfering with normal replication, protein synthesis and growth (Alawneh *et al.* 2016). Several macrodomain proteins have been found in viral genomes, which can reverse both host MARylation and PARylation, and affect virus replication simultaneously, alongside triggering the ϒ-interferon-response (Li *et al.* 2016). One thing is clear: recognition and removal of ADP ribosylation seems like an underappreciated feature of host-pathogen interactions that will have to be deciphered extensively in the future (Daughery *et al.* 2014).

7.4 PARylation in plants

PARylation functions in humans have been extensively studied in mammals, but there is now increasing evidence for its numerous roles in other higher eukaryotes, such as plants (for a review, see Vaionen *et al.* 2016). PARP activity bearing proteins are conserved from mosses to higher plants, and in the latter PARylation has been linked with circadian rythm regulation (Panda *et al*. 2008); biotic and abiotic stress response (Vanderauwera *et al.* 2007; Vaionen *et al.* 2016), plant immunity (Feng *et al.* 2016), cell division and root development (Liu *et al.* 2017). There is also evidence of other PARylation activities in plants, for knocking out all DNA-dependent PARPs in Arabidopsis thaliana does not abolish PAR accumulation (Rissel *et al.* 2017). Plants have an additional specific family of PARP-like domain bearing proteins: RCD1 and the SRO (similar to RCD One) family (Vaionen *et al.* 2016). Because of an ancestral genome duplication in Angiosperms, each plant PARPs and PARG exist in two copies. PARP2 and PARG1 are the main isoforms involved in DNA-damage polymer metabolism (Song *et al.* 2015; Zhang *et al.* 2015).

It makes no doubt that the PARylation field will soon boom in the plant biology field and that it will result in a little revolution in the future.

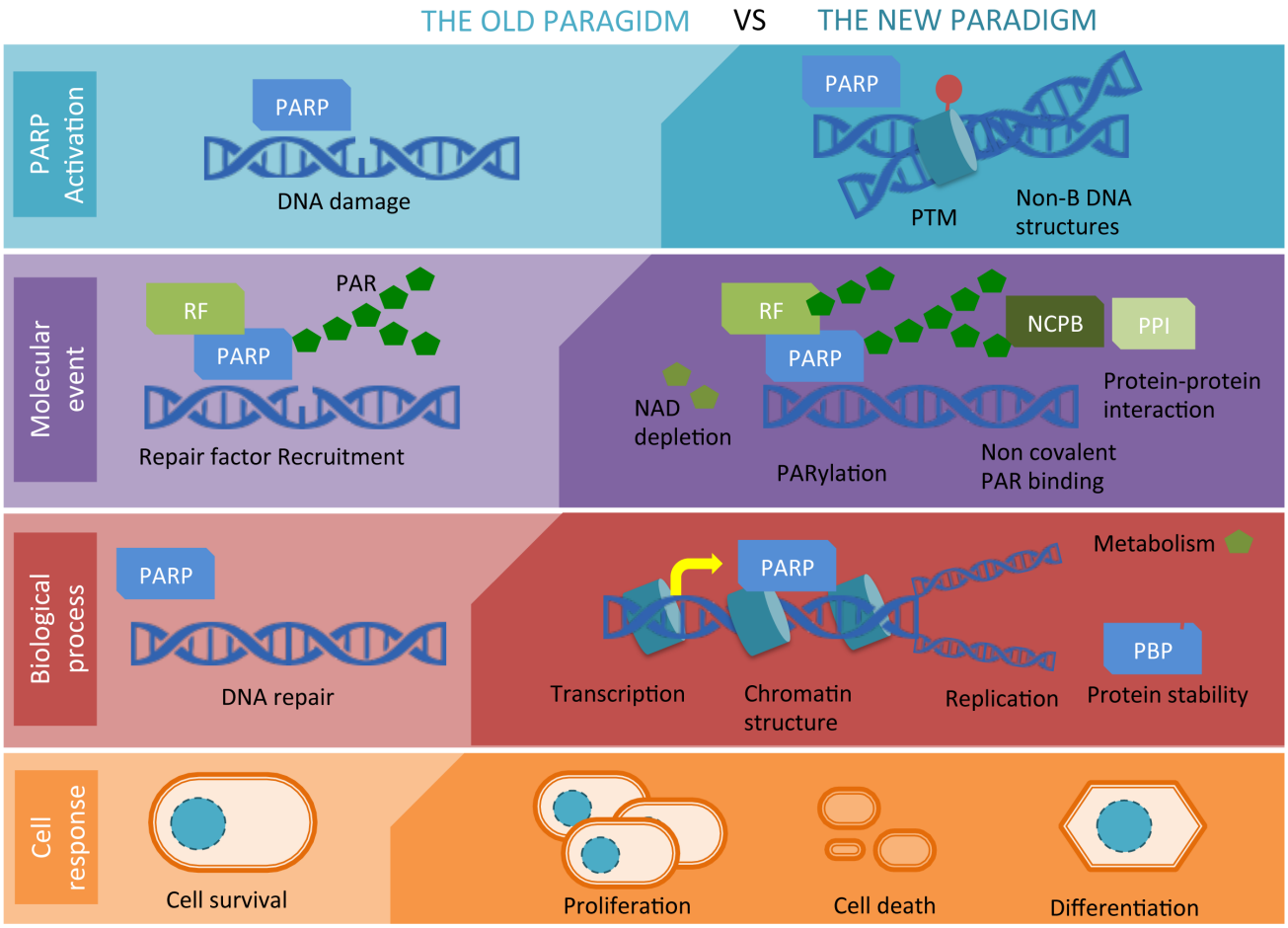

Figure 11: The ever-extending roles and complexity of PARylation (Adapted from Bürkle and Virag, 2013)

During the past decades, the basic consensual mechanism for PARP activation upon DNA damage, recruiting repair factors in order to ensure proper repair and cell survival has evolved to become a more complex and versatile model. Upon activation after either DNA damage, PTM (post-translational modifications) or non-B DNA structures, PARP can PARylate itself and its interactants, thus giving rise to a rich and colourful pattern of interactions.

7.5 PARylation in other eukaryotic organisms

In the past decades, PARylation has extended to several model organisms. The first PARP-encoding cDNA of *Xenopus laevis* was isolated by Uchida *et al.* 1993. In Drosophila melanogaster, just as in humans, PARPs undergo proteolytic cleavage during apoptosis (Poltronieri *et al.* 1997). PARylation of hnRNP A1 controls translational repression (Yingbiao *et al.* 2016). PARG mediates chromatin structure and SIR2 dependent silencing (Tulin *et al.* 2006). PARG deficiency is also associated with neurodegeneration in the fruitfly (Hanai *et al.* 2004). In the worm *C. elegans*, PARG depletion is associated with deficient DNA repair, and reducing PARylation improves axon regeneration (Byrne *et al.* 2016), by acting on the DLK (dual leucine zipper kinase) pathway, a crucial process regulating axon growth, apoptosis and neuron degeneration.

7.6 General features of PARylation

To conclude this chapter, it appears that ADP-ribosylation is a post-translational modification that is conserved in all living reigns, with its own families of writers, readers, erasers, feeders and consumers. In higher organisms, where PARylation is more often found, it seems that the modification has evolved to become a central pillar of genome integrity maintenance (see **Chapter 2**). Indeed, its nucleic-acid like properties allows it to act as a molecule generating charge repulsion, sterical hindrance, regulating the recruitment and the activity of many protein factors in simultaneous covalent and non-covalent fashions. Being a polymer of NAD^+ moieties, and NAD^+ being an important cell metabolite, it could also act as a local pool of energy to feed cellular processes and nutrish other protein modifications (Oei and Ziegler, 2000). Importantly, we must look back at the history of this modification. What was once an anecdotic PTM involved in DNA repair rapidly became, within 60 years, a polyvalent and versatile modification related with mostly any cell process. This change of scientific paradigm is illustrated in **Figure 11**, taking inspiration from Bürkle and Virag, 2013.

What is more exciting is that new roles and functions are still emerging and this field of research is far from being closed. In the years to come, research will probably focus on the interplay of PARylation with other PTM, as well as putative therapeutic opportunities offered by these new discoveries.

Now that I have presented all aspects of the PAR modification, I will focus in the next chapter on the main roles and pathways that are affected by PARylation, especially regarding DNA Damage Response (DDR).

Chapter 2: Roles of PARylation in the the maintenance of genome integrity

1. The ever increasing roles and targets of PARylation

As I mentioned in the previous chapter, PARylation appears as a polyvalent post-translational modification, polarizing many roles especially in DNA repair. During the past ten years, most of its new roles and protein partners were identified with the help of the mass spectrometry (MS) technique. Mass spectrometry appears to be the golden standard to depict an accurate overview of proteins and their post-translational modifications at very precise time points, that can give access to protein abundance changes, PTM changes as well as variation in the interaction partners patterns (von Stechow and Olsen, 2017). In the recent years, many attempts have been done to identify the panel of proteins that are modified by PARPs, also referred as PARylome, in straight line with the other fields of trending « omics » (genomics, proteomics, metabolomics…) (Gagné *et al*. 2008; Jungmichel *et al*. 2013). The main challenge to gain access to the PARylome was the enrichment of modified proteins, for like any PTM, PARylation is a transient event and a reversible chemical modification. One of these recent datasets of PARylome used the PAR-binding macro domain Af1521 identified in *Archaeglobus fulgidus* (Karras *et al.* 2005) in order to increase PARylated proteins from cell samples (Jungmichel *et al.* 2013). While literature is booming on the topic of proteins that interact with PARylation proteins and PARylome studies using mass spectrometry makes a consensus on the fact that PARylation targets are mainly enriched in genes regulating DNA repair, metabolic progress, chromatin structure, transcription, RNA metabolism and cell cycle regulation (Gagné *et al.* 2008; Isabelle *et al.* 2010; Martello *et al.* 2016). New parallel reaction monitoring mass spectrometry even allows following qualitative and quantitative variations in PARylome under different types of stress (Bilan *et al*. 2017; Leutert *et al.* 2017; Larsen *et al.* 2017).

In DNA damage response, a complex network of signalling is acting, where many PTM are synthetized both on lesions, on repair factors involved in the lesion repair and on surrounding proteins that make the chromatin environment. Most of these PTM interact together. The most reported example of this being the links between ubiquitination, sumoylation and PARylation (Pellegrino and Altmeyer, 2016). All these new global genome methods and experiments have interesting outcomes. Most recent discoveries that implemented our knowledge about PARylation allowed depicting serine residues as new common target residues for PARP1 and PARP2, while it was initially thought to occur only on glutamate, aspartic acid or lysine (Bilan *et al.* 2017). Serine ADP-ribosylation strictly relies on HPF1 (histone PARylation factor 1) and seems to be widely spread in processes governing genome stability (Bonfiglio *et al.* 2017a). Serine PARylation is then specifically reversed by ARH3, in an Mg2+ dependent fashion (Fontana *et al.* 2017). Serines also happen to be target residues for phosphorylation, so it is likely that evidences will emerge of PARylation competing with the classical phosphorylation network. This provides new and exciting perspectives about how genome integrity is ensured, and PARP1 and PARG are key players of all the related processes, for they maintain balance over PARylation levels and finely tune this versatile post-translational modification and make an interface for both DNA repair,

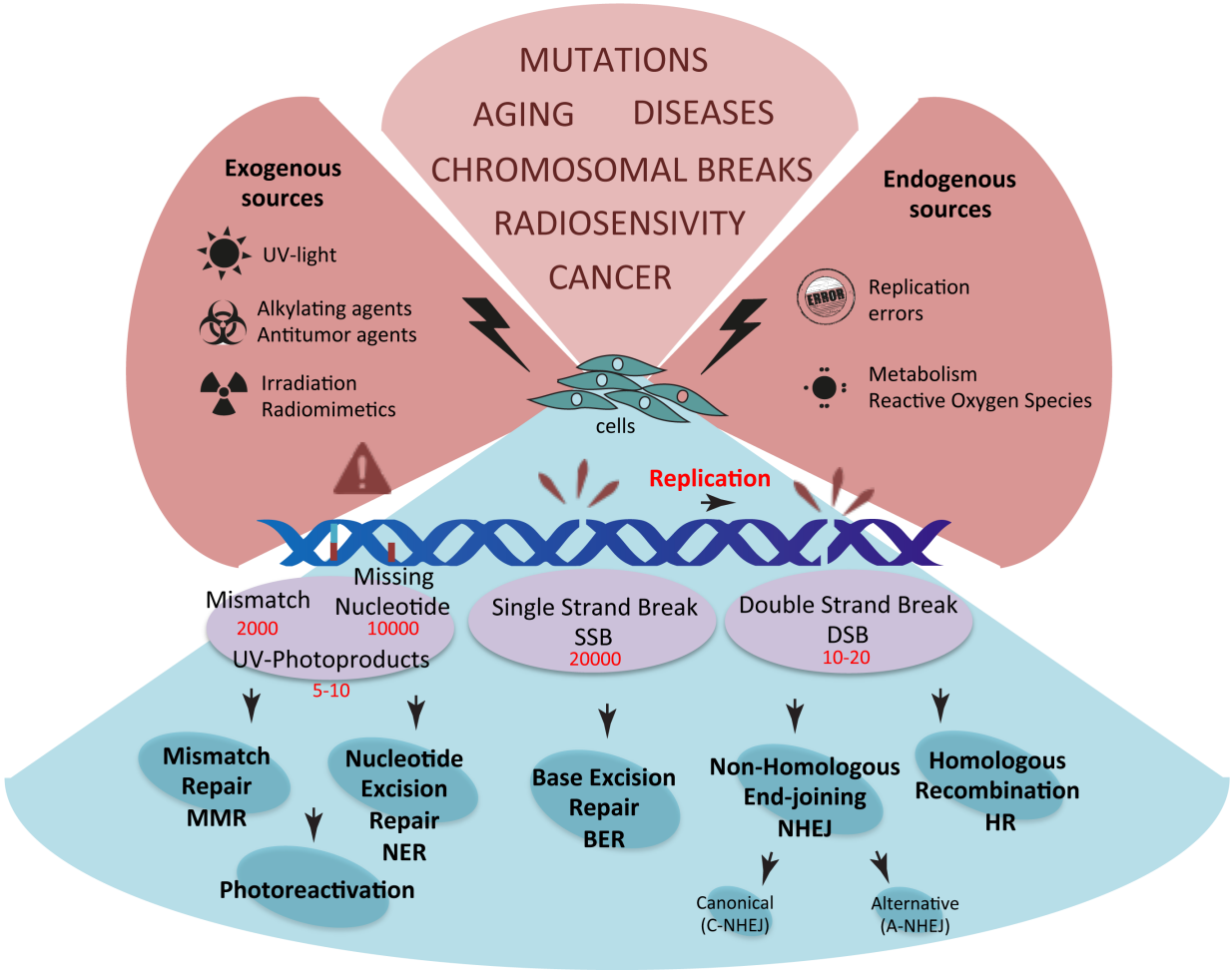

Figure 12: Types of DNA damages and DNA repair pathways.

Average frequencies of each type of damages are shown in red. Cells display a panel of repair pathways to overcome each type of DNA lesions (Adapted from Hoeijmakers, 2001; Polo and Jackson, 2011).

chromatin structure and transcription regulation. In this chapter I will specifically discuss the role of PARG and PARP1 in DNA Damage response (DDR) and Replicative Stress Response (RSR).

2. DNA Damage Response (DDR)

2.1 Types of DNA damage and main repair pathways

We often think as organisms and the cell itself as stably and perfectly working biological machines. At the molecular level, this is though far from being true. Every living cell needs to be fed, replicated and eventually differentiated, in a highly unstable physico-chemical environment. Maintaining genome integrity remains the main challenge for every single living cell, DNA being constantly challenged with many types of endogenous or exogenous stress. For overcoming all types of lesions produced (mismatches, UV photoproducts, single strand breaks, double strand breaks or collapsed replication forks), many different repair pathways exist that share similar main steps: 1) Recognition of the damage; 2) Processing of the damaged DNA extremities; 3) Gap filling or DNA strand restoration and 4) Ligation of DNA ends. The different sources of DNA damage, type of DNA lesions and specific pathway to overcome these genomic injuries are summarized in **Figure 12**.

PARPs, mainly PARP1 have been involved in most of DNA repair pathways, since all cell or mice models deficient for PARP1 are sensitive to radiations, alkylating agents and other damaging agents. It was first involved in SSBR (single strand break repair pathways); mainly BER (Base Excision Repair) and NER (Nucleotide Excision Repair), before emerging as a pluripotent actor in all DNA damage pathways, including DSB (double strand break) and MMR (mismatch repair); (reviewed in Beck *et al.* 2014; Martin-Hernandez *et al.* 2016; Chaudhuri and Nussenzweig, 2017). PARG, as the catalytic counterpart of PARP1 also plays key roles in DNA repair (reviewed in Feng and Koh, 2013), although its contribution has been less extensively studied. In the next paragraphs, I will discuss each of the main repair pathways in vertebrates, and describe the contribution of both PARP1 and PARG to these complex molecular mechanisms.

2.2 Nucleotide excision repair

Nucleotide excision repair is triggered by UV photoproducts formation and allows resolving base cross-linking such as 6-4 photoproducts, covalently bridging cytosine and thymine, thymidine dimers (CPD) or DNA adducts (for a review, see Zhu and Wani, 2016). These lesions, if maintained could impair replication fork progression and trigger genomic instability. Two mechanisms can occur; either global genome NER (GG-NER) or transcription coupled NER (TC-NER), if damage occurs in an actively transcribed area of genome (Diderich *et al.* 2011). Our understanding of these pathways has reached a tremendous complexity (reviewed in Zhu and Wani 2016), but I will simplify the steps. Defects in NER pathway are linked to autosomal recessive human diseases for which patients suffer extreme UV sensitivity and neurological dysfunctions (Emmert and Kraemer, 2013*)*. The name of this diseases are directly linked to the names of the protein factors involved in this repair

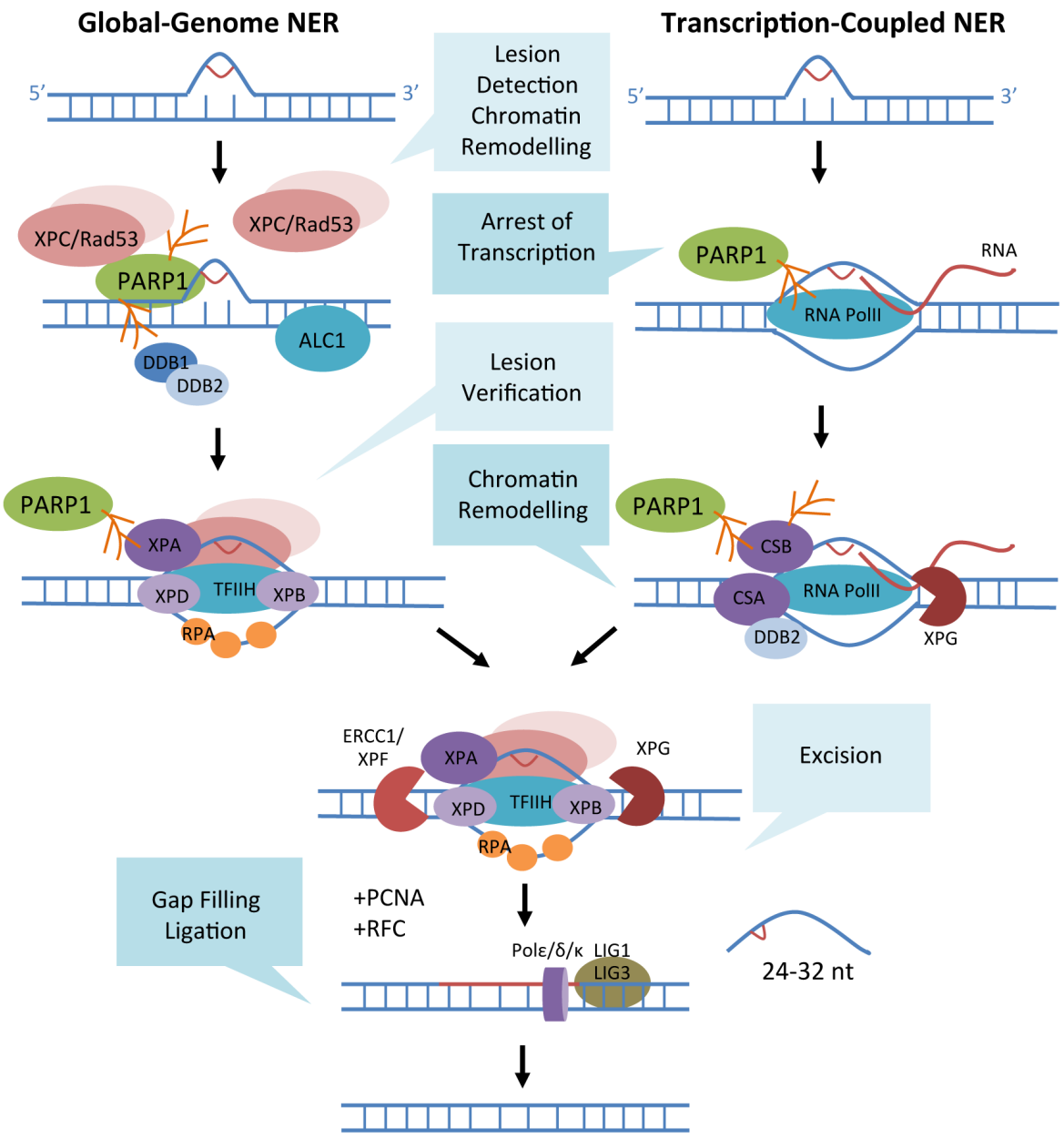

Figure 13: Roles of PARP1 in Global-Genome NER and Transcription-Coupled NER.

This illustration positions PARP1 in the different steps of GG-NER and TC-NER. PARP1 influences mainly damage recognition, chromatin structure surrounding the DNA break. For details, see **section 2.2.3**. Adapted from Chaudhuri and Nussenzweig 2017.

pathway: Xeroderma pigmentosum (XP), Cockayne syndrome (CS), trichothiodystrophy (TTD) are few examples (for a review, see Edifizi and Schumacher, 2015).

2.2.1 Global Genome NER (GG-NER)

- **Lesion detection:** In global genome NER, XPC and Rad23B recognize DNA distortion and binds to the opposite strand of the DNA lesion. This complex mediates DNA opening and recruitment of downstream factors (Rouillon and White, 2011). The DDB1-DDB2 complex of ubiquitin ligases then ubiquitinylates histones, triggering nucleosome displacement and stimulating DNA repair. XPC displays PAR-binding sites that are important for its recruitment to UV-lesions (Maltseva *et al.* 2015). DDB2 also interacts with PARP1, stimulating its activity and amplifying the phenomenon of chromatin decondensation. DDB2 stimulated PARylation of histones also mediates the recruitment of chromatin remodelling helicases (ALC1) that further helps the recruitment of XPC and amplifies the phenomenon (Luijsterburg *et al.* 2012; Pines et al. 2012).
- **Incision:** XPD and XPB are two ATP-dependent helicases that are comprised within a TFIIH complex (Oksenysh and Coin, 2011). They ensure a proper unwinding of DNA at the surroundings of the lesion. XPA protein recognizes the damage and helps the deposition of the single strand binding protein RPA that will stabilize the non-damaged strand. PARP1 helps recruiting XPA at the vicinity of damage (King *et al.* 2012). Once opened, damaged DNA strand will be cut, first by XPG, at 6 nucleotides in 3' of the lesion. XPF associated with ERCC1 then cuts 20 to 22 nucleotides in 5' of the lesion. A 24 to 32 base single strand DNA fragment is thus liberated and degraded.
- **Gap filling:** The nucleotide gap is filled by polymerases (Polδ, Polε or Polκ) that are loaded on DNA with the help of PCNA, in cooperation with RFC (Replication factor C).
- **Ligation:** Ultimately, DNA extremities can be ligated with either Ligase 1 or Ligase 3.

2.2.2 Transcription-coupled NER (TC-NER)

In TC-NER, lesion detection occurs upon RNA-Polymerase II arrest when encountering UV-lesions. CSA and CSB are two ATP-dependent chromatin-remodelling factors of the SWI/SNF family that help adapting the chromatic environment for the purpose of the repair. CSB can interact with several members of the BER pathway, including PARP1 (Thorslund *et al.* 2005). The following downstream steps are conserved with the GG-NER. In the end of the pathway, CSA interacts with DDB1 and forms a complex with CUL4A. It translocates to the damage site, ubiquitinylates CSB that is degraded through the proteasome, thus mediating termination of TC-NER process and restoration of transcription (Groisman *et al.* 2006). Patients bearing mutations in TC-NER genes specifically display neurological disorders, thus suggesting that TC-NER is more important for non-dividing cells (For a review, see Spivak, 2016).

2.2.3 PARylation and NER

The role of PARP1 in NER is summarized in **Figure 13**. Early experiments showed that UV-B and UV-C exposure could induce PARylation in cells and lead to DNA repair of photo-induced lesions by the NER pathway. PARP1 depletion in human fibroblasts results in decreased viability (Ghodgaonkar *et al.* 2008) and PARP1 accelerates NER, since PARP1 inhibition in MEF cells impedes CPD lesions repair after UV-B exposure (Flohr *et al.*

2003). Apart from interacting with PARP1, CSB can be covalently PARylated after oxidative damage (Thorslund *et al.* 2005). XPA protein is reported to bind PAR in vitro, and PARP1 and XPA regulate each other during NER (Pleschke *et al.* 2000; Fischer *et al.* 2014). In GG-NER, PARP1 facilitates lesion recognition by interacting with DDB2, but is has recently been shown that PARP1 could also act in this pathway in a DDB2 independent fashion, by forming a complex with XPC and stimulating its recruitment to UV damage (Robu *et al.* 2017).

2.3 Single Strand Break Repair

2.3.1 Mechanism

Single strand breaks are the most frequent types of lesions. They can occur after several types of events: ROS production by cellular metabolism, radiations, or topoisomerase 1 (TOP1) blocking. Although the initial recognition mechanisms can vary, the main steps of the pathway share many protein effectors:

- **Lesion detection:** Nicked DNA is recognised by the Zinc finger containing DNA binding domain of PARP1, which homo-dimerizes or hetero-dimerizes with PARP2, allowing DNA helix bending with a specific 102° angle. This allows the activation of the protein dimer and the rapid PAR synthesis (De-Murcia and Ménissier-deMurcia, 1994). Accumulation of PAR at the vicinity of damage acts as a molecular platform, allowing recruitment of many DNA repair factors and chromatin remodelers (Polo *et al.* 2010; Schreiber *et al.* 2006; Ciccia and Elledge, 2010). It then triggers a charge repulsion that is sufficient to abolish PARP1 binding, thus allowing the recruitment of downstream enzymes. Additionally, PARP1 PARylates surrounding histones H1 and H2B to allow a better access for repair factors to DNA lesion (Poirier *et al.* 2016). The first protein to be recruited is XRCC1 (Masson *et al.* 1998; Okano *et al.* 2000; El Khamisy *et al.* 2003). It interacts with PAR through its PBM and PARylated PARP1 and becomes PARylated (Dantzer *et al.* 2006).
- **End processing of DNA break**: XRCC1 acts as scaffold protein allowing the efficient recruitment of repair factors, such as DNA ligase III (LIG3), TDP1 enzyme, DNA Polymerase ß (Polß) and the bifunctional Polynucleotide kinase 3'-phosphatase (PNKP). XRCC1 interacts with PNKP in a phosphorylation dependent way through its FHA domain. It can also interact with PNKP through a newly identified RIR motif, which can also interact with PAR (Breslin *et al.* 2017). PNKP has both DNA 5'kinase and 3' phosphatase activities that can convert 3'phosphate and 5'hydroxyle termini to canonical ends (Weinfeld *et al.* 2011). According to the lesions of DNA extremities available, DNA will be processed by different factors. For 3' extremities bound to TOP1, the TDP1 enzyme needs to process the lesion in order to mediate degradation of TOP1 (see Pommier *et al.* 2014).
- **Gap filling:** Usually, only one nucleotide has to be set back, in a process qualified as short-patch repair. In case the filling requires more than one nucleotide, it is called long–patch. DNA Polymerases β/λ/κ can fill such gaps. The switch between short and long sub-pathways (Fortini and Dogliotti, 2007).
- **Ligation:** ultimately, the XRCC1-LIG3α complex restores the bond between the last nucleotide and the DNA chain when the short-patch repair is involved, whereas the PCNA-LIG1 complex will religate in case of long-patch repair.

2.3.2 PARylation in SSBR

The role of PARylation in SSBR is well documented. Both PARP and PARG inhibition result in increasing the rate of SSBR, demonstrating that they act together in single strand break repair (Fisher *et al.* 2007; Gao *et al.* 2007, Amé *et al.* 2009). Indeed, PARP1, PARG and XRCC1 both physically interact in SSBR (Keil *et al.* 2006). PARG binding to PARP1 is independent of its activity and triggers accumulation of short PAR branching. PARG interacts with XRCC1 in vitro and in vivo. Down regulation of PARP1 reduces XRCC1 foci formation after H_2O_2 and PARG down regulation induces spontaneous XRCC1 foci formation even in the absence of damage (Fisher *et al.* 2007). PARP1 activity regulates Polβ in long patch excision repair (Sukhanova *et al.* 2010).

PARG is needed at the vicinity of damage to regulate PAR production and PARP1 and XRCC1 accumulation nearby damage. Deregulation leads to cell death by apoptosis, or other PAR-dependent ways of death that will be discussed later on. In vitro, XRCC1 inhibits PARG activity and stimulates PARP1 activity (Keil *et al.* 2006). The PARylation status of XRCC1 affects the other post-translational modifications regulating the protein, and therefore a good coordination of both PARP1 and PARG is necessary to coordinate XRCC1 scaffolding activity in response to single strand breaks (De Sousa *et al.* 2016). Therefore, PARylation is of the outmost importance for the recognition and the processing of the SSBR pathway (Caldecott *et al.* 2008).

2.4 Base Excision Repair

2.4.1 Mechanism

BER (Base excision repair) is the main repair pathway for base lesions after oxidative or alkylating damage, or DNA ligation intermediates (for a review, see Krokan and Bjøras, 2013). Depending on the chemical nature of base alteration, the damage is detected by a specific DNA glycosidase that cleaves the bond between the base and sugar-phosphate skeleton, creating an abasic site (or apurinic site, also referred as AP) that can then be processed by single strand break repair pathway described above. More than a hundred different types of lesions can arise, that are premutagenic if converted to another base, but can also trigger RNA or DNA Pol blocking and activate cell death response. This pathway can be considered as a sub-type of single strand break repair, because it recognizes specific types of damage induced by alkylating agents, oxidation of bases such as (8-oxo-G), 5-hydroxy cytosines or 5'-hydroxyuracile, instead of immediate single strand breaks. Depending on the type of lesion, an apical mono-functional or bi-functional glycosidase or the endonuclease APE1 will generate a single strand break, allowing normal SSBR process to resume (Almeida and Sobol, 2007). It can go through either short patch BER resulting in the processing of a single nucleotide breach in DNA, or long patch BER, which requires the processing of 2 to 12 nucleotides. Polε/δ carries out LP-BER, with cooperation of the clamp loading factor RFC and the processivity factor PCNA and synthetizes the 2-13 missing nucleotides. The 5'flap structure generated during patch synthesis is removed by FEN1 endonuclease. LIG1 is physically associated with PCNA and seems to be the major nicking enzyme to complete LP-BER.

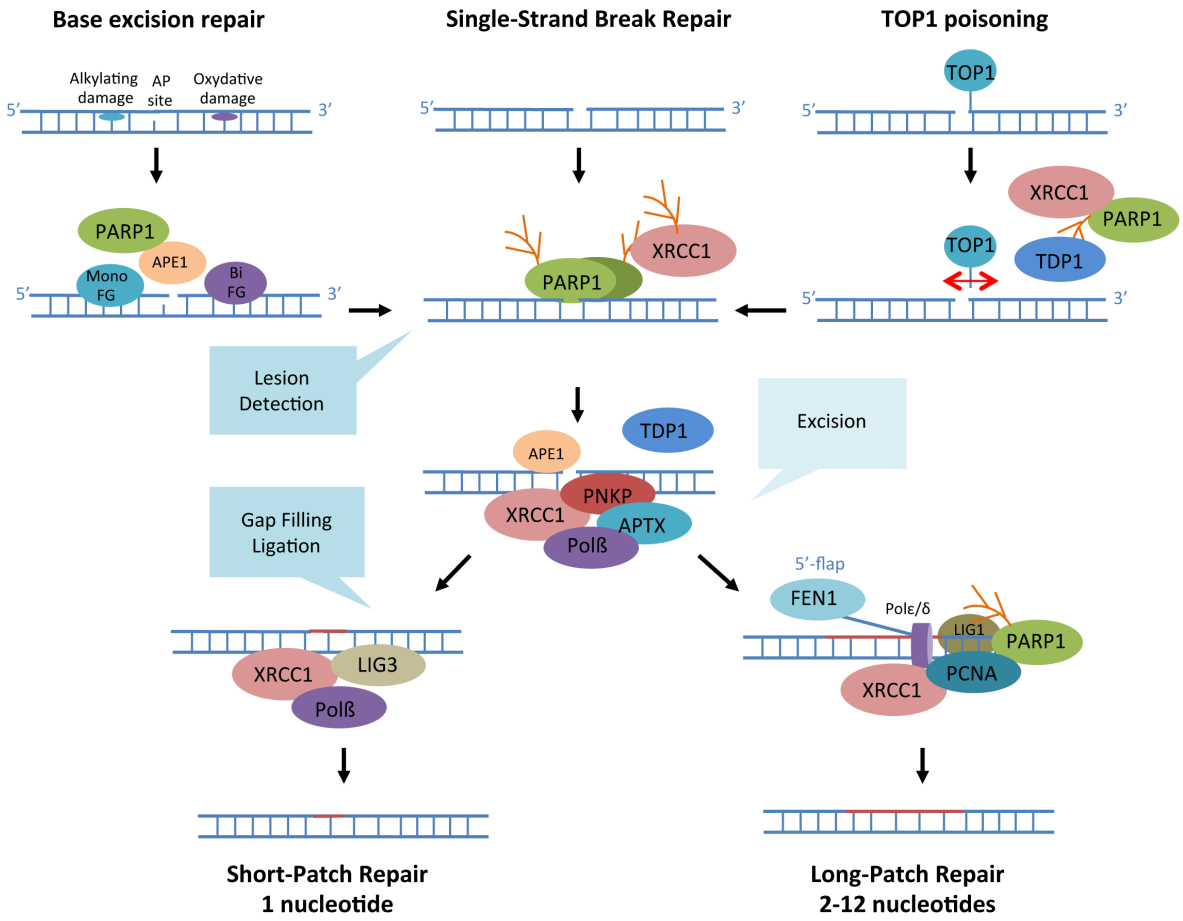

Figure 14: Roles of PARP1 in BER, SSBR and TOP1-clivage complex removal.

Different types of lesions can have different outcomes for DNA repair. PARP1 is mainly involved in damage recognition, but also mediates the activity of the TDP1 enzyme removing TOP1 from DNA, and can regulate LIG1-dependent religation step in Long-Patch Repair. Adapted from Chaudhuri and Nussenzweig, 2017.

2.4.2 PARylation and BER

Contradictory results exist on whether or not PARP1 is involved in BER (Chaudhuri and Nussenzweig, 2017). Some studies suggest that PARP1 is involved in BER. Indeed in the absence of PARP1 in mouse embryonic fibroblasts reduce short patch BER efficiency, and dramatically reduces DNA polymerization for long patch BER (Dantzer *et al.* 1999; Dantzer *et al.* 2000). Other evidence however shows that PARP1 deficiency does not result in an accumulation of apurinic sites (Pachkowski *et al.* 2009), and that BER is efficient in another PARP1-deficient mice cellular model (Vodenicharov *et al.* 2000). It seems that PARP1 is important for the lesion recognition, but not for the damage processing (Allinson *et al.* 2003). The most recent hypothesis is that purine base damage could depend on PARP1, whereas pyrimidine damage could be PARP1 independent (Reynolds *et al.* 2015). PARP1 exists in complex with Polß and APE1, and this complex could allow restoration of DNA ends in BER (Prasad *et al.* 2015).

2.5 Double strand break repair (DSBR)

Double strand breaks are the most deleterious damages that can occur in cells, following ionizing irradiation or replication fork collapse, as well as programmed chromosomal rearrangements such as class-switch recombination or V(D)J recombination, two processes involved in generating new original parts in immunoglobulin formation. Depending on the cell-cycle phase, DSB can be repaired either by homologous recombination (HR), requiring a DNA template in S-phase or G2 phase, or by Non-Homologous End Joining (NHEJ), resulting in the direct re-ligation of DNA extremities. HR is an accurate process whereas NHEJ can be error prone. In DSBR, PARP1 is able to recognize the break directly and, similarly to its role in SSBR, it is involved in the early recruitment of repair factors.

2.5.1 Homologous recombination

Homologous recombination is the most accurate repair pathway, allowing the repair of injured DNA using another undamaged strand of DNA. Because it needs an homologous template, it can only resume during S-phase or G2.

2.5.1.1 Mechanism

Homologous recombination is able to resolve double strand breaks in S and G2 phases of the cell cycle. It employs the DNA template of the sister chromatid, thus allowing an accurate and faithful repair. First, protein sensors recognize DSBs. The MRN complex, composed of Meiotic Recombination 11 (MRE11), RAD50 and Nijmegen breakage syndrome protein 1 (NBS1), acting as a break sensor that recruits the apical kinase ATM. ATM transduces the signal by phosphorylating many target proteins, including cell-cycle checkpoint proteins like Chk2, chromatin remodelers and DNA repair proteins that will coordinate an efficient repair. MRN complex associates with CtBP interacting protein (CtIP) that will execute the 5'-3' end resection at the vicinity of the break. This initial trimming process will be followed by further resection by the EXO1 exonuclease, in cooperation with the BLM helicase that helps unwinding the DNA helix (Symington, 2016). Single strand DNA thus generated will be covered with the single strand binding Replication Protein A (RPA). RPA activates the

Ataxia telangiectasia and Rad3-related protein (ATR) kinase by interacting with its partner ATR-Interacting protein (ATRIP). This activates another cell-cycle kinase checkpoint, by phosphorylation of the checkpoint kinase 1 (Chk1) protein. This checkpoint will avoid an early replication restart.

BRCA2 and RAD52 protein then promote RPA replacement with RAD51, forming a nucleoprotein filament that will be able to invade the homologous corresponding region, using it as a template for repair. A molecular intermediate forms, called a D-loop, that can be resolved by the formation of a Holliday junction, requiring the activity of DNA nucleases like GEN1 or SLX1/SLX4 and helicases of the RecQ family, WRN and BLM (Constantinou *et al.* 2000; Karow *et al.* 2000). Other models of recombination than the Holliday junction exist, but I will not detail them here (To see the mechanism in more details, see Helleday *et al.* 2007; Krejci *et al.* 2012; Kim and Mirkin, 2017).

2.5.1.2 PARylation in HR

PARP1 is important for the control and recruitment of many HR factors. In the absence of PARP1, DT40 chicken cells display reduced HR, following treatment with DSB inducing agents, and PARP1 favours the homologous recombination repair pathway over the NHEJ pathway (Hochegger *et al.* 2006). PARP1 deficiency leads to a delayed activation of DDR proteins, an impaired γ-H2AX, p53 or SMC1 phosphorylation, three proteins that are modified upon DNA damage by the apical kinase ATM (Haince *et al.* 2007). Indeed, ATM displays PAR-binding domains and its interaction with PAR stimulates its catalytic activity in vitro (Aguilar-Quesada *et al.* 2007). PARP1 also triggers the rapid recruitment of MRE11, which has a putative PAR binding domain and NSB1 at DNA damage sites (Haince *et al.* 2008). It is NBS1 ubiquitinylation by the SCF-Skp2 E3 ligase is believed to mediate ATM recruitment and activation upon DNA damage (Lu *et al.* 2012; Zhou *et al.* 2017). Despite these data, it PARP1 deficiency only delays the recruitment of DNA repair proteins. In some PARP1 deficient models, PARP loss even resulted in and increased damage frequency, and in the formation of more Rad51 foci (Schultz *et al.* 2003). Therefore, PARP1 is not a core factor of homologous recombination, but rather a helping factor for double strand break repair. For a review on the role of PARP1, PARP2 and PARP3 in response to DSB, see review Beck *et al.* 2014, Martin-Hernandez *et al.* 2017).

The early recruitment of MRE11 mediated by PARP1 activity contributes to the DNA-end processing step at the extremity of the double strand break. This could help orientating DNA repair towards homologous recombination, for it is believed that PARP1 could protect the homologous recombination process from Ku80 and Ligase IV interference on DNA-ends, which are players of the NHEJ pathway, as we will see afterwards (Haince *et al.* 2008). PARP1 is also involved in the rapid and early recruitment of BRCA1 that helps loading RAD51 on onto DNA (Li and Yu, 2013). On the other hand, one report shows that BRCA1 PARylation promotes the formation of a stable complex BRCA1-RAP80 that inhibits HR (Hu *et al.* 2014). It is likely that PAR levels in HR mechanism have to be timely regulated in order to ensure a proper strand resection activity.

One has to keep in mind that in the absence of PARP1, the amount of single strand breaks increases. These single strand breaks can be converted into single ended double strand breaks upon collision with replication forks. This principle is exploited in the concept of « synthetic lethality » for treatments of cancer with PARP inhibitors in HR deficient cancer-cell types (Presented in **chapter 3**). Interestingly, PARP1 can modify all 5 RecQ

helicases in humans (RCQL1, BLM, WRN, RECQL4, RECQL5), that are a highly conserved family of 3' to 5' DNA unwinding proteins that can unwind and re-anneal DNA strands in DNA repair, replication and recombination processes (reviewed in Croteau *et al.* 2014). WRN has an additional 3' to 5' exonuclease activity. PARP1 modifies helicases covalently and can influence their activities in vivo (reviewed in Veith and Mangerich, 2015).

2.5.2 Non-homologous end joining

NHEJ is the main DSB repair pathway in eukaryotes, because it can be used throughout the cell phases. The mechanism occurs through three main steps: recognition of the two end breaks, processing of the DNA ends and joining of DNA ends. If the ends are not compatible, DNA needs to be processed on several nucleotides and this can result in a loss of information (For a review, see Chang *et al.* 2017).

2.5.2.1 Classical NHEJ

In the classical NHEJ pathway, Ku70/Ku80 (Ku) heterodimers bind at each DNA ends, where they recruit the catalytic subunit of the DNA-PK complex (DNA-PKcs), a PI3K kinase which activates upon dimerization and recruits many target proteins that differ according to the nature of the double strand break. Autophosphorylation of two DNA-PKcs in close vicinity to damage triggers its dissociation and allows the process of DNA ends. DNA-PKcs also phosphorylates a broad range of other protein targets to activate them. The best-known example is the activation of Artemis, an endonuclease that processes 3' and 5' single-stranded overhangs at DNA ends that contain very short complementary nucleotide sequences and will anneal. PNKP is recruited through an interaction with the XRCC4-LigaseIV complex and removes non-canonical DNA ends. If short nucleotide gaps remain, they can be filled by DNA polymerases μ and λ. Ultimately, CLF-Cernunnos complex interacts with XRCC4-LIG4 complex and stimulates DNA end joining (Ahnesorg *et al.* 2006). This process relies on complex and numerous molecular interactions that are timed and regulated. The study of these protein partners are complicated because it involves high molecular weight proteins, but the crystal structures of all NHEJ proteins are now available allowing to increase our knowledge about how it resumes in cells (Liang *et al.* 2017).

2.5.2.2 Alternative NHEJ

A-NHEJ is an alternative pathway that can resume in absence of c-NHEJ core components (Chiruvella *et al.* 2013). In this alternative pathway to classical non-homologous end-joining, the generation of longer microhomology stretches require the use of resection proteins such as the MRN complex, which is responsible for the recognition of the break. PARP1, WRN and LIG3 are also likely to be involved, but the implication of XRCC1 is still controversial. A-NHEJ is considered as a backup pathway for DSBs that couldn't be repaired by c-NHEJ or HR (Iliakis *et al.* 2015).

2.5.2.3 PARylation and NHEJ

Most of NHEJ players are reported to be PARylated, thus suggesting a strong role for PARP1 in this pathway. Mainly Ku70/Ku80 and DNA-PKcs whose kinase activity is stimulated upon PARylation, independently

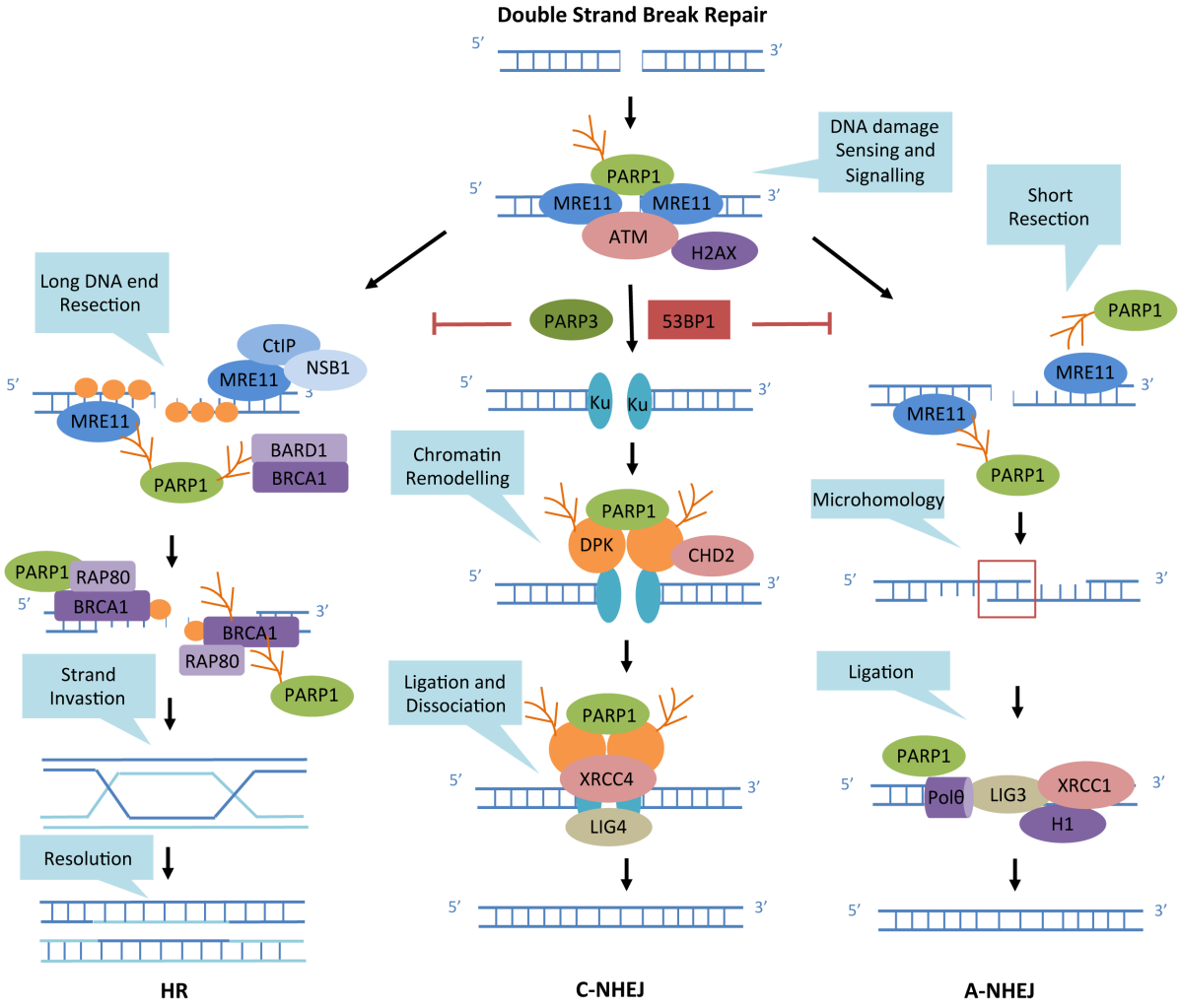

Figure 15: Roles of PARP1 in Double Strand Break Repair.

For details, see in text. PARP1 is mainly involved in damage recognition, and in the decision-making between homologous recombination and NHEJ pathways. PARP1 promotes A-NHEJ and PARP3 promotes C-NHEJ, suggesting an important role for PAR in the way DSB are processed in mammalian cells (Adapted from Beck et al. 2014; Chaudhuri and Nussenzweig, 2017).

of the presence of Ku70/80 usually required for its activity (Ruscetti *et al.* 1998). On the contrary, KU70/80 are less able to bind DNA ends upon PARylation by PARP1 (Li *et al.* 2004). Moreover, PARP1 and DNA-PK are physical interactants (Spagnolo *et al.* 2012). Double depletion of PARP1 and DNA-PK has more severe sensitivity phenotypes to DNA damage than single mutants, showing that they act in synergy in the repair of double strand breaks. PARP1 can facilitate classical NHEJ by recruiting the chromatin remodeller chromodomain helicase DNA binding protein 2 (CHD2) to sites of damage, through the recruitment of XRCC4 (Luijsteburg *et al.* 2016). This way, it could be involved in increasing the efficiency of NHEJ. Studies suggest that PARP1 is unable to affect c-NHEJ in vivo (Yang *et al.* 2004; Noël *et al.* 2003; Robert et *al.* 2009). Instead, PARP1 is believed to promote alternative NHEJ, by competing with the Ku complex for the access to DNA ends. Indeed, in the absence of Ku, studies show that PARP1 binding mediates a-NHEJ (Wang *et al.* 2006; Mansour *et al.* 2013). As I mentioned before, PARP1 activation promotes MRE11 recruitment to DNA damage (Haince *et al.* 2008), but also histone H1 that is a preferential target of PARYlation by PARP1 and will stimulate LIG3 activity in the a-NHEJ (Rosidi *et al.* 2008). PARP1 is involved in the recruitment of Polθ that mediates a-NHEJ through its terminal transferase activity (Matteos-Gomez *et al.* 2015). Ku has a higher affinity for DNA ends than PARP1, so when it is present, c-NHEJ will be favoured (Wang *et al.* 2006; Paddock *et al.* 2011). As we will see later, in case of replicative stress, PARP1 could act in the same mode of competition in order to counteract c-NHEJ and promote HR.

2.3.3 PARPs in the choice between the DSB pathways

As previously mentionned, the presence of PARP1 could influence to which extent resection by Mre11 occurs, thus favoring a-NHEJ over c-NHEJ. The same phenomenon occurs in the choice between HR or C-NHEJ. In addition, PARP3 is also reported to ensure the choice between DSB repair pathways. Our lab demonstrated that PARP3 could bind DNA damage, and PARP3 depletion leads to an accumulation of unrepaired DSB, with no concomitant increase in SSB (Boehler *et al.* 2011). PARP1 and PARP3 interact with each other and activate each other (Rulten et al. 2011) and PARP3 regulates the choice between HR and NHEJ, both by preventing DNA ends from excessive resection by MRE11 and by modulating the balance between BRCA1 and 53BP1 (p53 binding protein 1) around DSB. Overall, PARP3 favours C-NHEJ over A-NHEJ or HR (for a review see Beck *et al.* 2014). Recently, tankyrases (TNSK1 and TNSK2) were also demonstrated to be recruited to DNA lesions, and to promote homologous recombination through regulating the resection events (Nagy *et al.* 2016)

It is interesting in this case to see that PARPs and PARylation can help making an integrated choice for repair pathways, and how PARylation can influence the issue of DNA repair. The involvement of PARP1 in the different pathways is summarized in **Figure 15**.

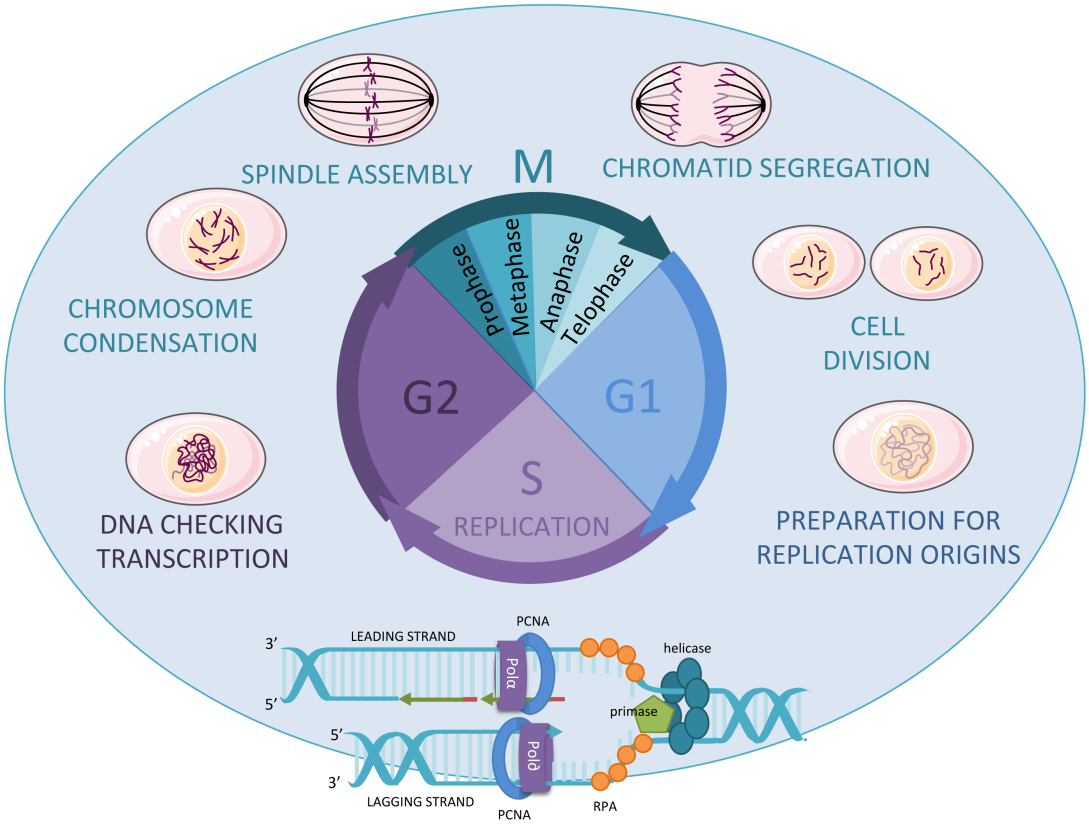

Figure 16: Cell cycle phases

In G1, cells prepare their replication origins to undergo a total replication of their genomic content in S-phase. Origins are fired and the replisome shown above ensures the replication process. In G2 phase, DNA is checked for errors, genes transcribe and cells prepare for division. Ultimately, mitosis occurs in 4 steps: prophase where chromosomes condense, metaphase where the spindle assembles and the chromosomes align on the equatorial axis of the cell; anaphase when chromatids are separated to the cell poles; and telophase when two daughter cells form and chromosomes are embedded into new nuclei.

2.6 PARP Mismatch repair

2.6.1 Mechanism:

Although very accurate, replicative DNA polymerases can make mistakes. The MutSα complex can recognize the structural anomaly, and recruits the MutLα complex in an ATP dependent fashion. Both complexes clamp and slide across the DNA molecule, scanning for the break interruptions between Okazaki fragments to recognize the neo-synthetized strand. The complex then recruits PCNA and exonuclease 1 (EXO1) that will degrade the error-bearing strand. Parental strand covers with RPA protein and Polδ is loaded on DNA by PCNA and fills the gap. The 3' end is ultimately ligated by DNA LIG1 (For a review, see Liu *et al.* 2017).

2.6.2 PARylation and MMR

Both MSH2 and MSH6 of the MutSα complex can bind PAR through non-covalent affinity, suggesting PARP and PARG might have a role in regulating MMR (Gagne *et al.* 2008). EXO1, RPA, RFC and PCNA, key players of mismatch repair, are also known partners of PARP1 (Liu *et al.* 2011).

3. Replicative stress Response (RSR)

Replicative stress is one of the main sources of endogenous DNA lesions and genomic instability. It occurs when replication forks are not properly regulated and result in fork stalling and sometime fork collapsing. In this chapter I will describe the links between PARylation and replication stress.

3.1 Cell cycle progression

Cell cycle is defined by series of complex events, tightly coordinated by hormonal and environmental cues and ultimately results in birth of two daughter cells from a single mother cell. It is divided in 4 phases:

- In **G1 phase,** cells engage in a new division cycle and the starting sites of DNA replication process will be defined. From these zones, called « Origins of replication » that are spread across the eukaryotic genome; replication forks are fired in a sequential cascade, in order to replicate all the genetic integrity only once (Cayrou *et al.* 2011; Guilbaud *et al.* 2011). Just before S phase, centrosomes that will ultimately ensure proper chromosome segregation during cell division undergo duplication.

- In **S-phase**, bi-directional replication forks will start from each one of the hundreds of replication origins. Fork firing and DNA replication is ensured by the replisome. There are several types of replication origins: those that will be opened early in S-phase, late in S-phase or cryptic replication origins that will only be fired in case something occurs during replication, leading to unachieved replication.

- In **G2 phase**, cells can check the replication efficiency and prepare their chromosomes for mitosis by triggering a wave of transcription of mitosis related genes. Centrosomes undergo their last step of maturation.

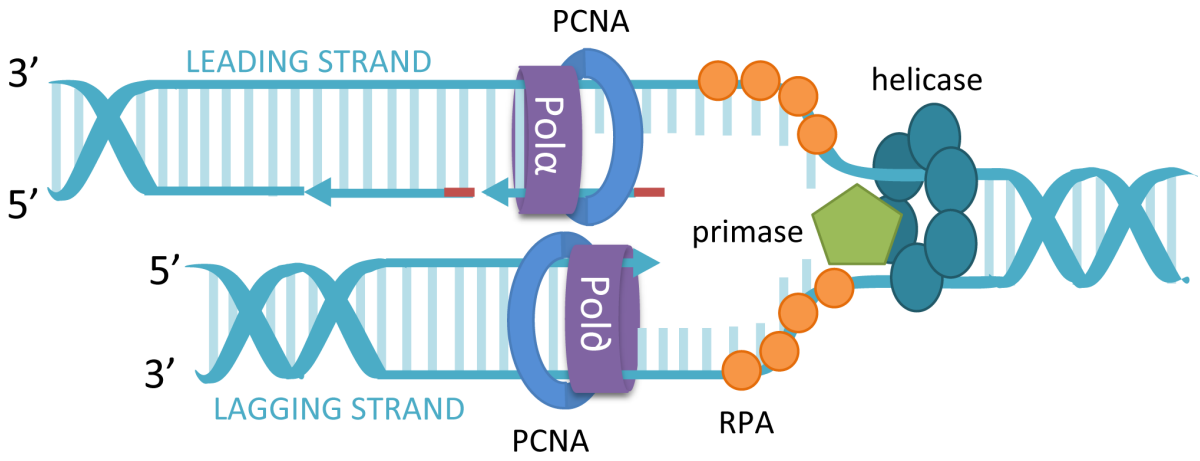

Figure 17: Schematic structure of the replisome

Each replication fork bears many protein factors that are not shown here. Helicases contained in the CMG complex lead the way, unwinding DNA helix. Polε synthetises the leading strand of DNA continuously, while Polδ synthetizes DNA in short patches called Okazaki fragments on the lagging strand, after priming of an RNA oligonucleotide that is synthetized by Polα to prime for DNA synthesis. The single strand DNA that remains between helicase complex and polymerases is covered with RPA protein, a single strand binding protein. RNA primers used for synthesis ultimately need to be degraded by endonucleases and the gaps generated need to be filled before termination of replication.

- **Mitosis** is the ultimate step where cells divide in two. During prophase, centrosomes migrate at cell poles and generate the mitotic spindle to segregate chromosomes. Nuclear envelope breaks during prometaphase, leading to the binding of microtubules on the kinetochores of chromosomes. Chromatids separate in daughter cells during anaphase and are shielded by a new nuclear envelope after telophase. In the ultimate step of cytodieresis, cytoplasm of the two daughter cells separate.

All these steps are regulated by cyclines and cyclin dependent kinases (CDK). In case of DNA-damage, transitions between G1/S and G2/M can be inhibited, notably by p53 phosphorylation that induces p21 expression, resulting in inhibition of CDK-cyclin complexes. This is evidence for any cell biologist, but it is necessary to remember how proper timing of each time-frame of cell life is important, for any malfunction could leave to pathological situations.

3.2 The life of a replication fork.

Human genome consists in over 6 billions base pairs that must be copied once in every cell cycle during the replication process, in which around 30000 to 50000 replication origins must be coordinated to ensure proper duplication. Before explaining how cells can undergo replicative stress, I am briefly going to summarize the basic functioning of the replication complex, also termed « replisome », displayed in **Figure 17**, as well as the different steps of replication fork assembly, elongation and termination (Reviewed in Costa et al. 2013; Dewar and Walter 2017).

3.2.1 Fork initiation

Replication fork story begins in G1, when Origin Replication Complexes (ORC) bind to replication origins throughout genome and acts as a molecular structure to recruit the CDC6 ATPase (Speck *et al.* 2005) and CDT1, that will cooperate to recruit MCM2-7 complex, forming the pre-replicative complex (pre-RC). The precise mechanism is proposed in Frigola *et al.* 2017. MCM2 and MCM7 are two ATPase that will act as helicase motors for DNA-unwinding during replication. Two MCM2-7 are tethered together in opposite directions on each replication origin. Before S-phase, all the pre-replication complexes are thus formed and ready to be fired to trigger the bi-directional replication of DNA. In S-phase, only some of the pre-replicative proteins will be activated by cyclin dependent kinases, allowing the formation of two CDC45-MCM-GINS helicase complex (CMG) that will start unwinding DNA in both directions (reviewed in Dewar and Walter, 2017).

3.2.2 Fork elongation

On each of the two MCM2-7 complexes, the replisome assembles to neo-synthetize DNA strand, starting the progression of two replication forks. Polε, interacting with the CMG complex, replicates the leading strand continuously whereas Polδ whose processivity is ensured by PCNA, in several successive patches of DNA called Okazaki fragments, replicates the lagging strand. Leading strand and Okazaki fragments are primed by a Polα primase that generates a 10 nucleotide RNA fragment. Eukaryotic replisome is rather complicated macromolecular machinery involving many proteic partners.

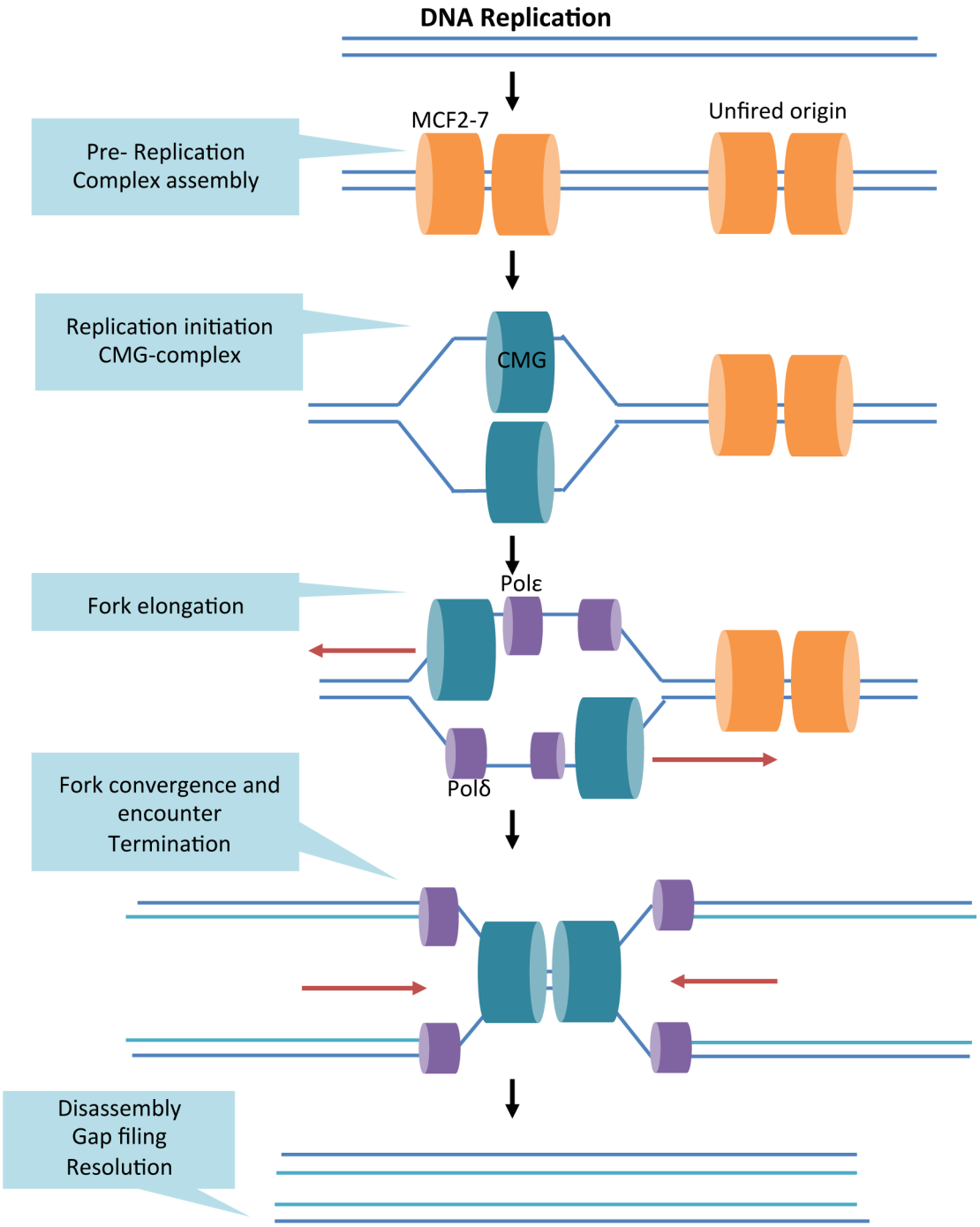

Figure 18: Steps for the replication fork machinery

Just before S-phase, cells assemble pre-replicative MCF2-7 complexes that can be fired upon activation of the cell cycle kinases. This activation leads to a CMG complex containing helicases able to unwind DNA and recruit the recplication machinery (replisome). Once recruited, the replication complexes progress in opposite directions, in two bi-directional forks than can eventually encounter with another replication complex coming from the opposite side. This fork convergence results in replication termination, disassembly of the replisome components, gap filling on the neo-synthetized strands and resolution of DNA structures by Topoisomerases. Adapted from Dewar and Walter, 2017

Replisome contains chromatin remodellers, for instance the BAZ1B-SMARCA5 complex, that helps recruiting protein factors such as topoisomerase 1. Topoisomerase 1 is of the outmost importance near the replication fork, because it must resolve strand tensions during DNA-helix unwinding (Ribeyre *et al.* 2016; reviewed in Dewar and Walter, 2017).

3.2.3 Fork termination

At the end of replication, two replication forks of opposite directions will eventually converge. In normal conditions, CMG converging can bypass each other, until the replisome reaches the priming Okazaki fragment of the opposite starting site. The Okazaki fragment is processed by FEN1 endonuclease and the gap is filled by DNA-Polδ. Replisome is ultimately disassembled by E3 ligase recruitment, triggering ubiquitinylation of MCM7, which is then extracted from chromatin by the ATPase97 (reviewed in Dewar and Walter, 2017). The different steps of replication are summarized in **Figure 18**.

3.2.4 Challenges for the replicative fork

Replisomes can encounter several types of obstacles during their run for replication. DNA damages (abasic sites, UV-photoproducts, crosslinks…), DNA-protein complexes, secondary DNA structures and chromatin condensation can slow the process until replication fork arrests. In case single strand damage occurs on the lagging strand of DNA, synthesis of Okazaki fragments will simply bypass the lesion. But damages occurring on the leading strand are very likely to slow down replication while the helicase goes on. This causes a replication fork uncoupling that can lead to fork arrest. Cells display several genomic loci that are often rich in CpG or enriched with highly expressed genes. These are hotspots of genomic instability and DNA breaks (Barlow *et al.* 2013). Transcription machinery is also a major obstacle for replication fork progression, as both mechanisms share the same DNA template (Garcia-Muse and Aguilera, 2016). First, the R-loops formed by the opening of DNA helix and creating a DNA/RNA hybrid during the process, in parallel to a single strand are physical obstacles that can only be resolved by RNAseH. Additionally, if replication and transcription progression occur in opposite converging ways, highly restrictive DNA supercoils are generated that need the action of both topoisomerases 1 and 2 (Bermejo *et al.* 2007).

Replicative forks blocking or slowing can be due to short supply of proteins or nucleotides ensuring replication machinery and fork structure stability, such as neo-synthetized histones (Mejlvang *et al.* 2014), dNTPs (Anglana *et al.* 2003), or RPA (Replication Protein A) that stabilizes single strand non-template DNA while the other strand is being replicated (Toledo *et al.* 2013).

Fork slowing and blocking can be achieved artificially in cells upon treatment with hydroxyurea (HU), a ribonucleotide reductase inhibitor that creates a situation where cells lack dNTPs for synthesis, as well as with aphidicolin, an inhibitor of the replicative polymerases. Another agent is camptothecin (CPT), that traps topoisomerase I into what is called a cleavage complex (TOP1-cc). This interferes with replisome progression as well. These types of replication stresses, summarized in **Figure 19** (next page) have different outcomes and are likely to be processed by different pathways.

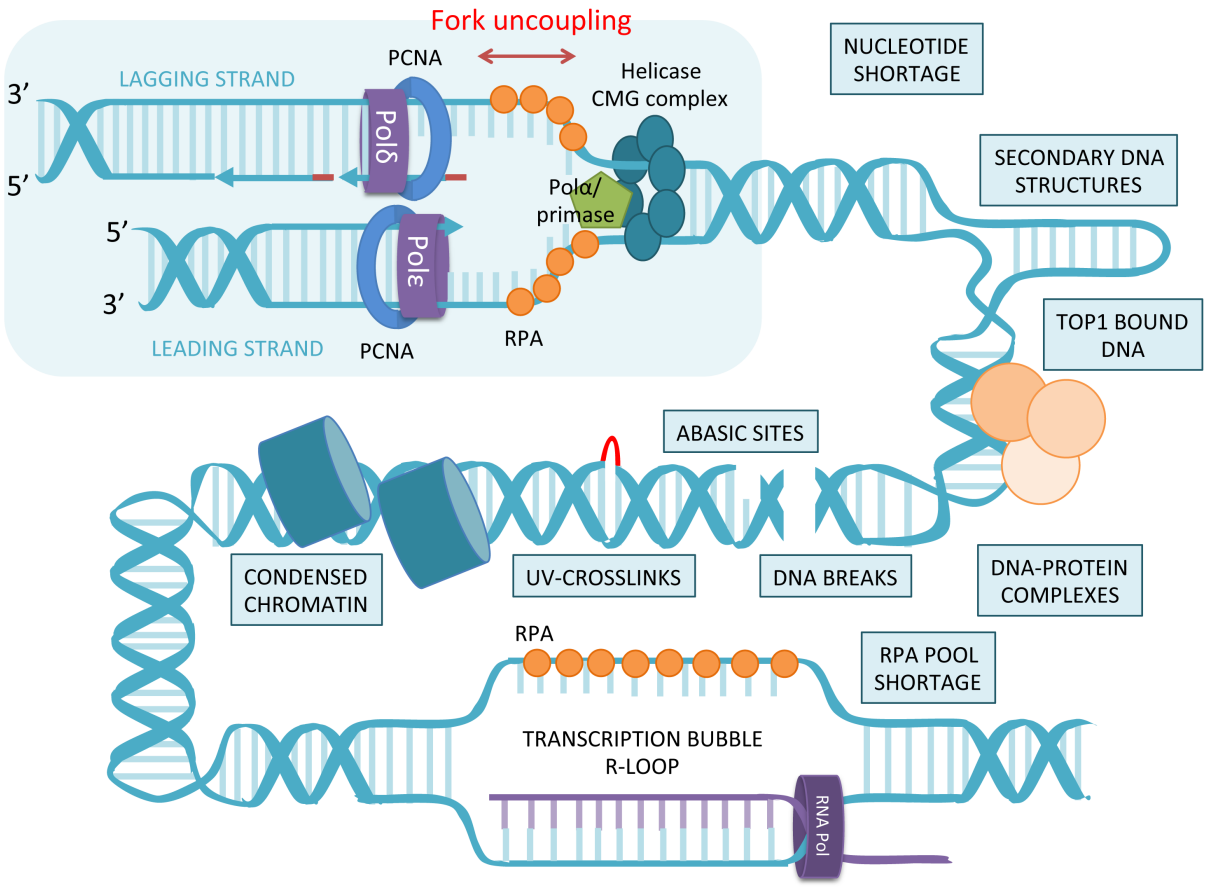

Figure 19: Obstacles challenging the replication forks

Several cellular events can interfere with the replication fork progression and trigger replication fork slowing and uncoupling. Among these: Nucleotide shortage, Secondary DNA structures, Top1-bound DNA, Abasic sites, DNA breaks, UV-crosslinks, condensed chromatin, transcription bubble or the absence of RPA.

3.3 Stalling, collapsing, reversal, restart: the faith of replication forks

Encountering obstacles (**Figure 19**) during replication process can have different outcomes, depending on the nature and the location of the replication challenge. Most of the time, dormant replication origins can be fired to ensure proper replication of areas where fork stopped. However, if no dormant origin is present between two converging forks that are stopped, other mechanisms need to put the replisome "back on the track". Several pathways, reviewed in Berti and Vindigni, 2016, can achieve this. Some of the pathways described above are schemed in **Figure 20**, next page.

In case polymerase slows down, helicase activity is uncoupled and this creates a ssDNA gap that is coated with RPA and recognized by the ATR kinase that will stimulate the activation of Chk1. As a result, cell-cycle progression is blocked, and ATR will mediate regulation of surrounding replication origins and recruitment of the FANCD2 protein with the MCM replication complex, slowing the polymerase and avoiding long tracks of ssDNA to form under conditions of dNTPs shortage (Nam and Cortez, 2011; Lossaint *et al.* 2013, Berti and Vindigni 2016).

In case damage is a base or a nucleotide lesion, replisome can mediate fork repriming through what is called the DNA damage Tolerance pathway (DDT). Either specialized Polymerases called translesion synthesis (TLS) polymerases can help the fork progress through the damage (Sale *et al.* 2012) or by skipping the damage and repriming synthesis elsewhere, leaving a post-replicative ssDNA gap that can be repaired through HR or by TLS polymerases.

Another model was proposed to overcome UV-lesions, called fork reversal, where replication forks reverse their direction to rearrange into a four-way junction. This process allows fork slowing and additional time to repair without triggering any chromosomal break. It is considered as an "emergency brake" in damaged cells (Neelsen and Lopes, 2015). Several helicases (WRN, BLM) and DNA repair factors (Rad51) are required for fork reversal (Zellweger *et al.* 2015). RECQ1 helicase promotes fork restart from this reversed fork (Berti *et al.* 2013). Very interestingly, PARP1 activity suppresses RECQ1 activity until damages are repaired on replication forks (Berti *et al.* 2013; Ray Chaudhuri *et al*. 2012).

Which proteins help the choice between these three pathways is still unknown, however, PCNA state of ubiquitination could be one factor for making the choice, its poly-ubiquitination stimulating fork reversal, whereas its mono-ubiquitination triggering TLS polymerases recruitment and fork repriming (Ciccia *et al.* 2012; Mailand *et al.* 2013).

If the protein factors are unable to stabilize the fork, or if the uncoupling of helicases and polymerases activity is too severe, the components can disassemble in a dramatic process called « Fork collapsing ». Fork collapse would result in the formation of a single ended double strand break that can mainly be resolved by homologous recombination. Fork collapse is not a frequent event in eukaryotic cells, even in the presence of damaging agents and replication inhibitors. However, in yeasts devoid of checkpoint proteins, up to 40% of the forks can collapse and be inactivated (Tercero *et al.* 2001). This suggests that checkpoint proteins are required to prevent fork collapse. The above tolerance mechanisms are crucial to preserve genome integrity.

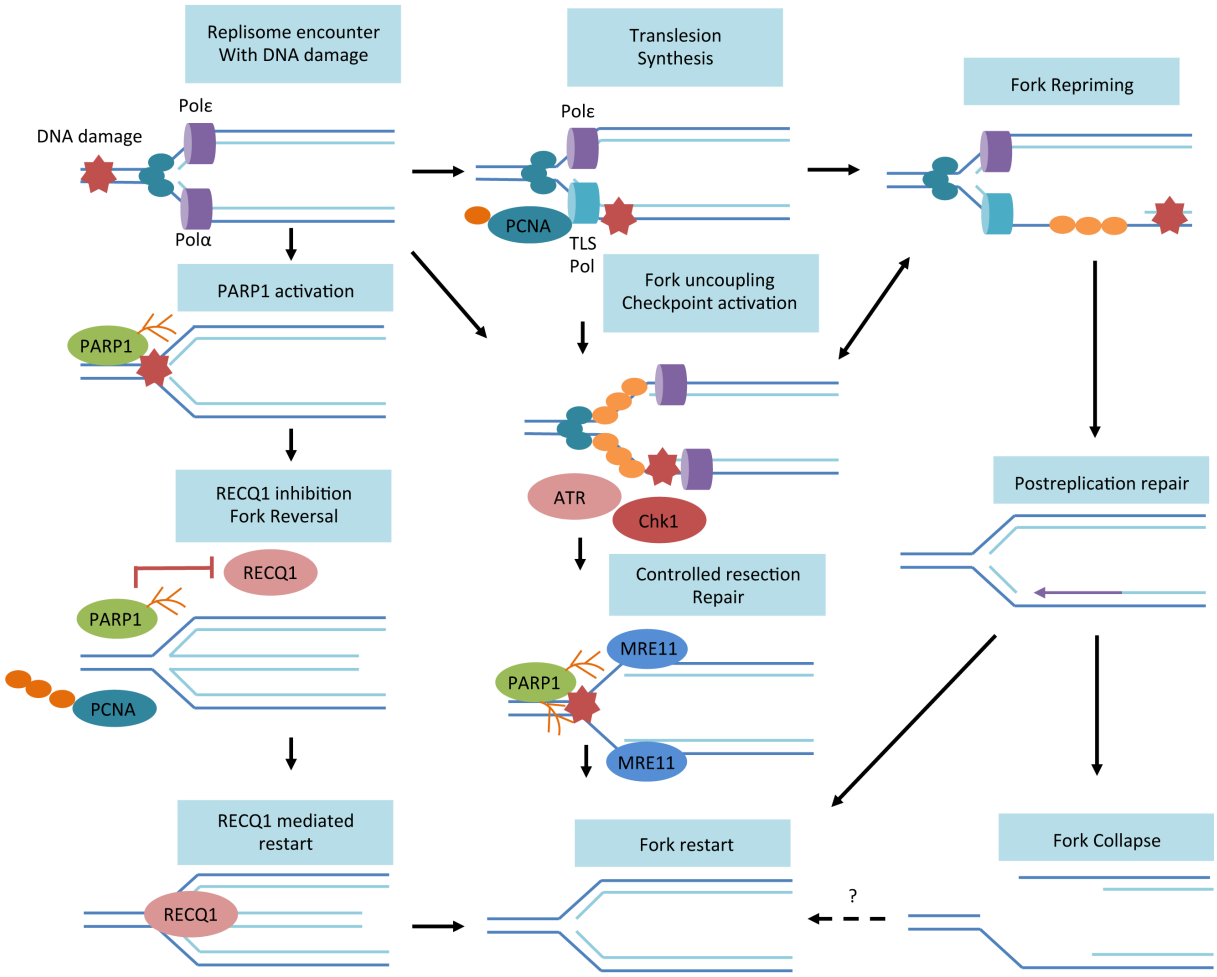

Figure 20: Roles of PARylation in the different outcomes of replicative stress.

When the replication forks encounters DNA lesions, replication fork is stalled, but several strategies can be deployed to resume the process. Mono-ubiquitinated PCNA can recruit trans-lesional polymerase (TLS Pol), and reprime the fork. Alternatively, PARP1 can be recruited and promote fork reversal into a "Chicken foot" four-way junction, which can be restarted through the activity of the RECQ1 helicase. In the case there is an extended fork uncoupling between the replisome and the helicases, single stranded DNA can be covered with the RPA protein (orange spots), activate checkpoint proteins (ATR, Chk1) and promote resection through nuclease activities (MRE11). In case none of these mechanisms allow the fork restart, fork collapse leading to double strand breaks. Adapted from Berti and Vindigni, 2016; Chaudhuri and Nussenzweig, 2017.

3.4 PARylation and replicative stress.

In normal conditions, PARP1 is already present in the replication machinery, throughout the S-phase. It binds PCNA directly, as well as Polα and is able to PARylate over 15 proteins in the replisome, regulating the polymerase activities (Ray Chaudhuri and Nussenzweig, 2017). In absence of damage, cells devoid of PARP1 display an altered activity of the Polα, and are impaired for entry and progression in S-phase (Dantzer *et al.* 1998). In absence of replication stress (basal conditions): PARP1 mouse deficient cells accumulate RPA and Rad51 foci (Yang *et al.* 2004), suggesting that PARP1 is a basal requirement for good replication.

The role of PARP1 in replicative stress however is much more evident. It was highlighted in PARP1 deficient cells that displayed increased sensitivity to HU. These cells displayed an increased fork stalling and collapsing, suggesting incapacity of fork restart through HR mechanism (Yang *et al.* 2004). Indeed, if cells undergo a replicative stress, PARP1 is activated upon interaction with blocked replication forks and mediate Mre11 dependent replication restart and recombination (Bryant *et al.* 2009). On top of this, PAR binding of CHK1 is required for S-phase checkpoint activation (Min *et al.* 2013).

Upon high replicative stress, PARP1 promotes the PAR dependent recruitment of MRE11, and stimulates DNA end resection (Haince *et al.* 2008; Bryant *et al.* 2009). As mentioned above, PARP1 could also simultaneously compete with Ku70/Ku80 dimer binding and thus promote RH instead of NHEJ (Hochegger *et al*. 2006)

In case the fork is paused, in conditions of mild replicative stress without damage, the presence of PARP1 on the contrary seems to prevent excessive resection of MRE11 and thus inhibits HR. It is interesting to see again that PARP1 could have a double role depending on the exact type of damage and the stress state of the cells. The response to CPT exposure is a specific case, which deserves investigation. It has been reported that after CPT treatment, PARP1 could favour fork restart by HR. This mechanism involves PARylation of Ku70 that is liberated from DNA to be replaced with HR machinery (Sugimura *et al.* 2008). Upon short replicative stress, BRCA2 and PARP1 prevent Mre11 dependent degradation of stalled replication forks (Ying *et al.* 2012).

The interaction of PARP1 with the helicases ensuring DNA unwinding during replication is also of importance. After CPT at very low concentrations: PARP1 stabilizes regressed forks and protects from a premature fork restart by RECQ1 helicase-mediated reversion (Berti *et al.* 2013; Ray Chauduri *et al.* 2012). PARP1 and PAR inhibit WRN helicase and exonuclease activities (von Kobbe *et al.* 2004; Popp *et al.* 2013). PARP inhibition also results in abrogating early RECQ5 recruitment to damage. RECQ5 is a helicase that is recruited to sites of damage and promotes DSB repair via an interaction with MRE11 (Zheng *et al.* 2009 ; Popuri *et al.* 2012 ; Paliwal *et al.* 2014). Thus, interference between PARP and helicase might be a general feature for the regulation of DNA repair pathways near replication forks. The different roles for PARP1 in replicative stress are summarized in **Figure 20.**

The role of PARG in this cell process was also examined. Our lab showed that PARG locates at replication foci during S-phase, and that it can be recruited to DNA-damage through PCNA-dependent mechanisms (Mortusewicz et al. 2011). Our team also showed that PARG was not necessary for transient replicative stress, but was needed to avoid detrimental accumulation of PAR on RPA, upon prolonged replicative stress induced

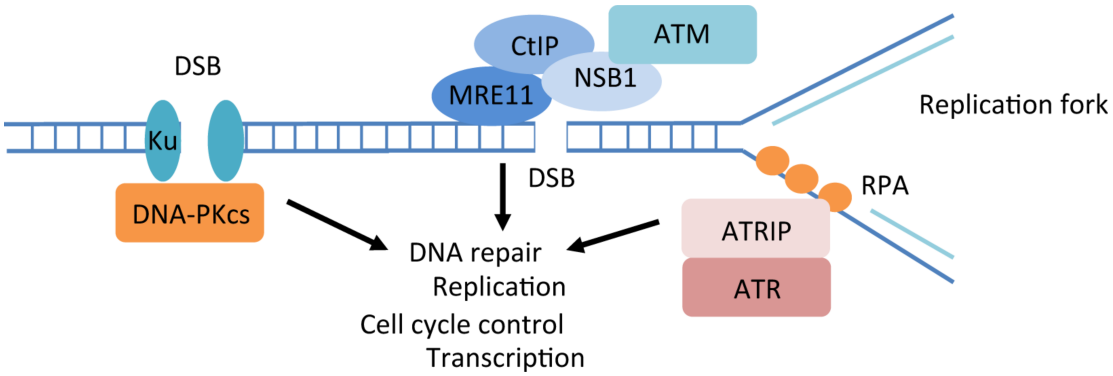

Figure 21: The apical PI3K kinases in regulating genome integrity.

Double strand breaks can be recognized by the Ku complex, that recruits and activate the DNA-PKcs apical kinase. The resection enzymes MRE11, NSB1 and CtIP can recruit and active the ATM kinase at the vicinity of double strand braks (DSB). Single-stranded DNA covered with the RPA protein can recruit ATR through its interacting partner ATRIP. Once activated, ATM, ATR and DNA-PK phosphorylate many downstream effectors, thus activating repair pathways, cell cycle checkpoints, in order to orchestrate cell processes in response to DNA damage. Adapted from Blackford and Jackson, 2017.

by HU (Illuzzi *et al.* 2014). Accumulation of PAR on RPA impairs its binding to stalled forks and promotes fork collapse and breaks, therefore, several lines of evidence were pre-existing suggesting that PARG could help protecting against replicative stress. Other MS data suggest that after replication stress, while both PARP1 and PARG are present near the replisome, PARP1 remains at the vicinity of the fork, while PARG is displaced from the replication fork upon replicative stress (Dungrawala *et al.* 2015). Cells obviously need to accumulate at least low amount of PAR in the process of fork slowing, a mechanism that could be beneficial for the cell, rather than detrimental, as previously suggested (Amé *et al.* 2009). PAR levels need to be tightly regulated at the vicinity of the replication fork, both by PARP1 and PAR. More recently, it was shown that PARG depletion in HeLa or U2OS cells resulted in replication fork slowing and accumulation of ssDNA gaps and fork reversal events, mimicking a CPT-induced mild replication stress, further strengthening the role of PARG in the replication process (Chaudhuri *et al.* 2015). After stress, since PCNA seems to be involved in replication fork outcomes, it makes no doubt that PARG, having the ability to interact with PCNA through two PCNA interacting peptides (PIP) has an important role to play in replication, that needs to be further investigated (Mortusewicz *et al.* 2011; Kaufmann *et al.* 2017).

4. Signalling kinases to maintain genome integrity

In the first chapter, I discussed the importance of post-translational modifications for the signalling of DNA damages. Like many other signalling cascades, this signalling mainly relies on phosphorylation, triggered by three apical kinases of the PI3K family (phospoinositide 3-kinase): ATR, ATM and DNA-PK (see Blackford and Jackson, 2017 for a review). The activation of the three PI3K kinases is displayed in **Figure 21.**

They display common structural and catalytic features, all three displaying N-terminal HEAT repeats, mediating protein-protein interaction (Perry and Kleckner, 2003), a C-terminal catalytic kinase domain, surrounded by a FRAP-ATM-TRRAP (FAT), a PIKK regulatory domain (PRD) followed by a FAT-C terminal motif (Mordes and Cortez, 2008). All three kinases display an affinity for S/T-Q motifs on proteins (Bannister *et al.* 1993; Kim et al. 1999), but kination can also happen outside of this sequence context (Jette and Lees-Miller, 2015).

The three proteins can also auto-phosphorylate. Phosphorylation of either S2056 or T2609 is used as a marker of DNA-PK activation (Chen *et al.* 2005) and these modifications are important for DNA-PK dissociation from DSB (Jette and Lees-Miller, 2015). S2056 phosphorylation could regulate Ku80 binding, whereas T3950 phosphorylation is believed to inhibit kinase activity (Sibanda *et al.* 2017). ATM autophosphorylation on S1981 is less consensual, for there is conflictual reports about whether it activates kinase activity or not (Bakkenist and Kastan, 2003; Kozlov et *al.* 2006; Lau *et al.* 2016). In ATR, T1989 is an automodification site and its phosphorylation is used as an activity marker (Liu *et al.* 2011; Nam *et al.* 2011).

In the current paradigm, all three kinases are recruited to DNA damage sites in different ways. DNA-PK is recruited to DSB by interacting with Ku70/Ku80 dimers during NHEJ. ATM is recruited to DSB by interacting with NSB1 in the MRN complex, and activated upon DNA end resection trigerring the phosphorylation of H2AX variant and Chk2 kinase on Thr68 (Cai *et al.* 2009), modifications that signal double strand breaks. Finally, ATR is recruited via ATRIP interaction on RPA that binds single strand DNA in replication forks (Mordes *et al.* 2008).

ATR is thus recruited to extended tracts of ssDNA covered with RPA (Zou and Elledge 2003). This allows RPA phosphorylation on Ser33 and the cell cycle control kinase CHK1 on Ser345, this post-translational modification being now widely used as a replicative stress marker (Olson *et al.* 2006; Liu *et al.* 2000; Liu *et al.* 2006).

These kinases have redundant targets, making it difficult to assess their involvement in precise mechanism. While DNA-PK and ATM depletions are viable, ATR is essential in replicating cells, showing that it is the major kinase during replication (Brown and Baltimore, 2000; de Klein *et al.* 2000). In case of TOP1 blocking during replication, TOPBP1 (Topoisomerase-1 binding protein) makes a bridge between TOP1 and ATR and activates replicative stress signalling (Kumagai *et al.* 2006; Zhou *et al*. 2013).

However, mass spectrometry studies allow to uncouple their substrates and to refine our understanding of the signalling mechanism (Matsuoka *et al.* 2007), by deciphering specific substrates of ATM and ATR. I won't go much into details in this introduction, but all the crosstalk of these signalling kinases are reviewed in Blackford and Jackson 2017. Because of their multiple roles in DNA repair and replicative stress, PI3K kinases inhibitors have entered clinics for the targeted treatment of lymphomas (for a review see Lampson and Brown, 2017).

Several reports show that ATR, ATM and DNA-PK interact with PARylation mechanisms. I already mentioned the fact that DNA-PK and PARP1 are found in complex and can modify each other (Ariumi *et al.* 1999; Ruscetti *et al.* 1998; Spagnolo *et al.* 2012). PARP1 inhibits ATM activity in vitro, and is able to impede p53 phosphorylation in a DNA dependent manner (Watanabe *et al.* 2004). PARP1 physically interacts with ATM and ATM is able to bind PAR during DNA-damage (Aguilar-Quesada, 2012; Haince *et al.* 2007). Moreover, PARP1 and ATM double knockout mice are embryolethal suggesting that both enzymes act synergistically in DNA repair (Ménissier-de Murcia, 2001). Finally, ATR and PARP1 co-IP, and this interaction is likely to be PAR dependent, for PARP inhibition prevents the interaction (Kedar *et al.* 2008). These data show that PARylation is involved at the very beginning of all the signalling pathways, further guarantying the good orchestration of all DNA Damage and Replication Stress Response.

5. PARP and PARG in other interface processes during DNA repair

5.1 Controlling cell cycle checkpoints

As mentioned in the previous paragraphs, cells can activate checkpoints in order to pause the cell cycle and to verify the integrity of their DNA material before S-phase and before mitosis. Impaired checkpoint regulation can trigger carcinogenesis, for it can result in incorrect chromosome segregation (Burgess *et al.* 2014). In this purpose, PARP1 participates in the proper centrosome biology (Kanai et al. 2003). PARP1 degradation promotes the arrest of cell in mitosis, showing its requirement for resuming cell cycle (Kashima *et al.* 2012). PARP1 regulates Chk1, a kinase that activates S-phase checkpoint control (Min *et al.* 2013). In case of replicative stress induced with HU, the absence of PARP1 destabilises CHk1 from chromatin. Chk1 interacts through a N-terminal PAR binding region that is necessary for a full activation of the S-phase checkpoint. It suggests that PARP1 is necessary for S-phase checkpoint in response to replicative stress, through an activity of Chk1 stabilization that will allow maintaining it on replication forks, so it can be activated by ATR. This model is

solid because ATR is a substrate for PARP1, and PARP1 and ATR interaction is increased in presence of PAR (Kedar *et al.* 2008).

As usual, data for PARG are less evident, but our lab showed that in PARG-deficient HeLa cells, irradiation was increasing the rates of mitotic abnormalities, suggesting a role for PARG in controlling mitotic checkpoint (Amé *et al.* 2009). In PC-14 and A427 lung cancer cell lines, silencing of PARG by the mean of an siRNA results in an impaired checkpoint activation and enhanced radiosensitivity, highligting the role of PAR homeostasis in checkpoint activation (Nakadate *et al.* 2013). Overall, we can see that polymer regulation is important to coordinate repair and cell cycle progression.

5.2 Controlling chromatin structure

Besides controlling DNA repair by acting enzymes, PARylation can also play a critical role at the level of local chromatin rearrangement at the damaged sites.

Histones are the core component of chromatin structure and allow the efficient compaction of DNA molecules in cells. In its most condensed state (heterochromatin), gene expression is repressed, whereas in the relaxed state (euchromatin), transcription machinery has access to genes DNA template. The chromatin landscape is crucial for undergoing cell processes as transcription, regulation and even more importantly DNA repair (for a review see Stadler and Richly, 2017). N-terminal histone tails are subjected to variety of post-translational modifications, impacting chromatin state of condensation. This is excellently reviewed in Ciccarone *et al.* 2017.

PARP1 and PARP2's ability to remodel chromatin structure was observed as early as 1982, by electronic microscopy. PARylation of H1 and H2B triggered chromatin relaxation (Poirier *et al.* 1982). PARG addition was sufficient to reverse the phenomenon in the experiment (De Murcia *et al.* 1986). In absence of NAD^+, PARP1 is able to bind the DNA junctions between nucleosomes, via its DNA binding zinc-finger domains, in a way that is similar to histone H1, and this is sufficient to trigger chromatin condensation (Wacker *et al.* 2007; Langellier *et al.* 2010). After DNA damage it has been shown that PARP1 can PARylate any histone (Messner *et al.* 2010), generating a high amount of PAR that will affect nucleosome spacing by repulsive interactions and help recruiting specialized chromatin-remodelling factors. The resulting amplification of chromatin decondensation helps recruiting the many downstream-required repair factors for processing the damage. Two famous examples are the fact that on the one hand, PARP1 allows rapid recruitment of the SNF2 (Sucrose Non fermented 2) family ATPase protein ALC1 (Amplified in liver cancer), targeting H4 and displacing nucleosome (Ahel *et al.* 2009; Gottshalk *et al.* 2009). On the other hand, SMARCA5 (SWI/SNF related matrix associated actin dependent regulator chromatin subfamily A member 5) is recruited to DSB in a PARP1 dependent manner, by interacting with PARylated E3 ubiquitin ligase RING finger protein 168 (RNF168) involved in NHEJ pathway. CHD2 recruited at the vicinity of DSB repair complex also triggers deposition of histone variant H3.3, inducing chromatin relaxation and promoting NHEJ (Luijsterburg *et al.* 2016). Interestingly, PARP1 induced chromatin decondensation also favours NR4A (nuclear orphan receptor) nuclear translocation, whose phosphorylation by DNA-PK facilitates DSB repair (Malewicz *et al.* 2011).

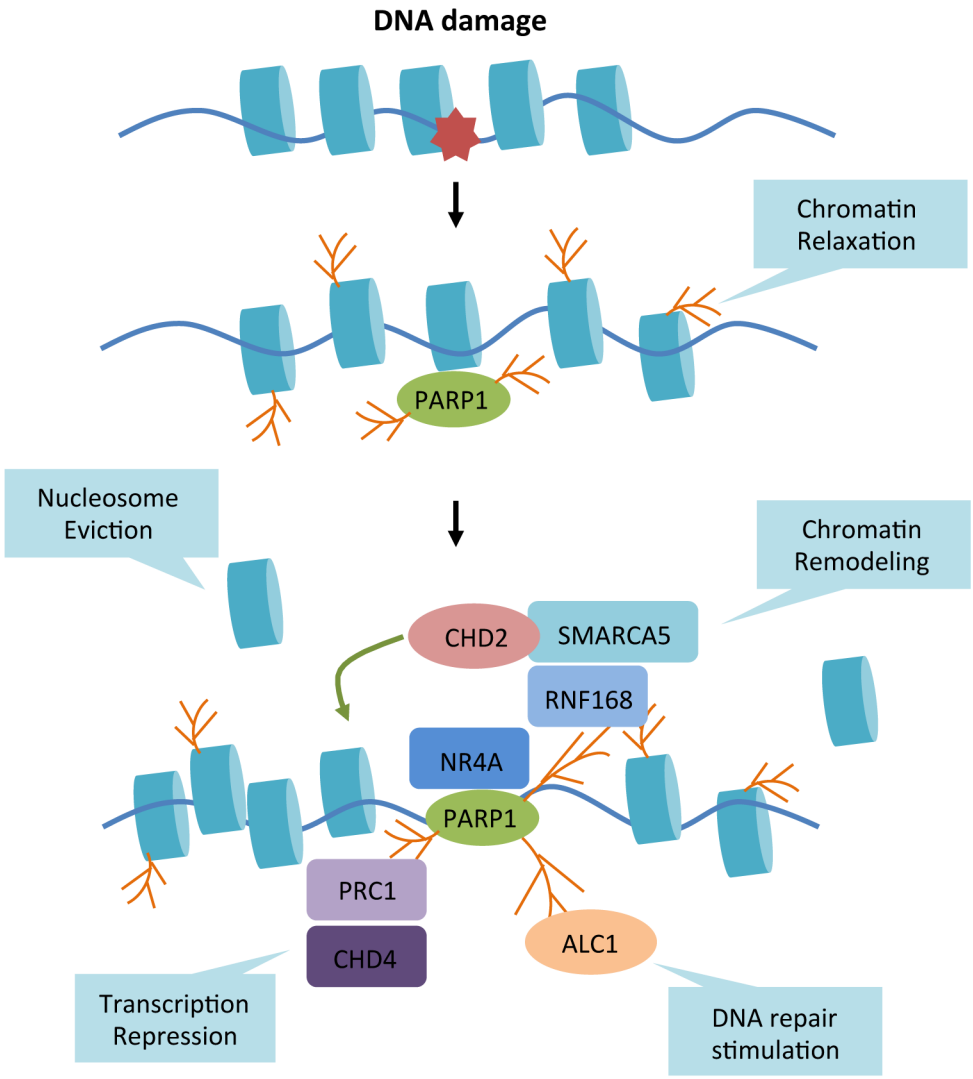

Figure 22: Role of PARP1 in chromatin regulation.

PARylation of chromatin components can favour chromatin relaxation by charge repulsion. Additionnaly, PARP1 can contribute to the eviction of histones, the recruitment of chromatin remodelling complexes (ex: SMARCA5) and transcription repressors thus facilitating the access of the DNA repair pathways components to chromatin. Adapted from Chaudhuri and Nussenzweig, 2017.

PARP1 can also trigger the deposition of the histone variant histone macro H2A1.1 at DNA damage sites, triggering a brief phase of chromatin compaction that reduces recruitment of Ku70 and Ku80 proteins (Timinszky *et al.* 2008).

SSRP1 is a histone H2A/H2B chaperone that triggers chromatin decondensation around single strand breaks after irradiation or alkylating damage. It was recently demonstrated that SSRP1 recruitment to DNA damage was PARP1 dependent. It is retained at sites of damage by interacting with XRCC1 (Gao *et al.* 2017).

The last interesting example is the PARP1 dependent recruitment of the ubiquitin ligase CHFR, containing a PBZ domain that allows its recruitment to damage (Ahel *et al.* 2008). CHFR can ubiquitinylate PARP1 and surrounding histones, further increasing the effect of chromatin decondensation (Kashima *et al.* 2012; Liu *et al.* 2013). This shows how post-translational modifications can cooperate to orchestrate repair responses through both DNA repair and chromatin remodelling (Tallis *et al.* 2013; Ray Chaudhuri and Nussenzweig, 2017). All these examples show different ways for PARP1 to modulate chromatin structure. It is summarized in **Figure 22.**

Another last interesting way of controlling the access of repair factors near chromatin is the recently described phenomenon of "liquid-demixing" (Altmeyer *et al.* 2015). In this process, the negatively charged PAR molecule can "seed" the aggregation of disordered proteins, and is believed to mediate the very early steps of protein recruitment at the vicinity of damages.

5.3 Controlling transcription

Global transcriptomics studies allowed assessing that around 3,5% of the genome is regulated by PARP1, most of the genes being up regulated by PARP1 activation (Ogino *et al.* 2007). Because chromatin structure and transcription activity are tightly correlated, I will just briefly explain several mechanisms by which PARylation can affect transcriptional machineries, summarized in **Figure 23**, next page (Marjanovic *et al.* 2017).

PARP1 can directly promote the transcription machinery recruitment, either by evicting histone H1 that is associated with weakly transcribed regions (Krishnakumar *et al.* 2008; Happel and Doenecke, 2009; Krishnakumar and Kraus 2010), or by recruiting histone demethylases (ex: KDM5B), thus removing histone marks that favour active transcription (Vermeulen *et al.* 2007). PARP1 can also allow the recruitment of transcription repression complexes. The most relevant examples being the recruitment of the nucleosome remodelling and deacetylase (NurD) complex CHD4, metastasis-associated protein 1 (MTA1) and members of the Polycomb repressive complex 1 (PRC1). This results in transcription inhibition and avoids transcription machinery to interfere with a proper DNA repair (Chou *et al.* 2010). In response to oestradiol stimulation, one mecanism involving PARP1, TopIIß and co-activator ASC2 evicts a repressor complex of nucleolin, nucleoplasmin, HsP70, HDAC3 and N-CoR co-repressor (Ju *et al.* 2006). This pathway involves DNA-PK, Ku86 and KU70, because it induces a nick near oestradiol binding site, which stimulates PARP1, evicts H1 from chromatin by PARylation

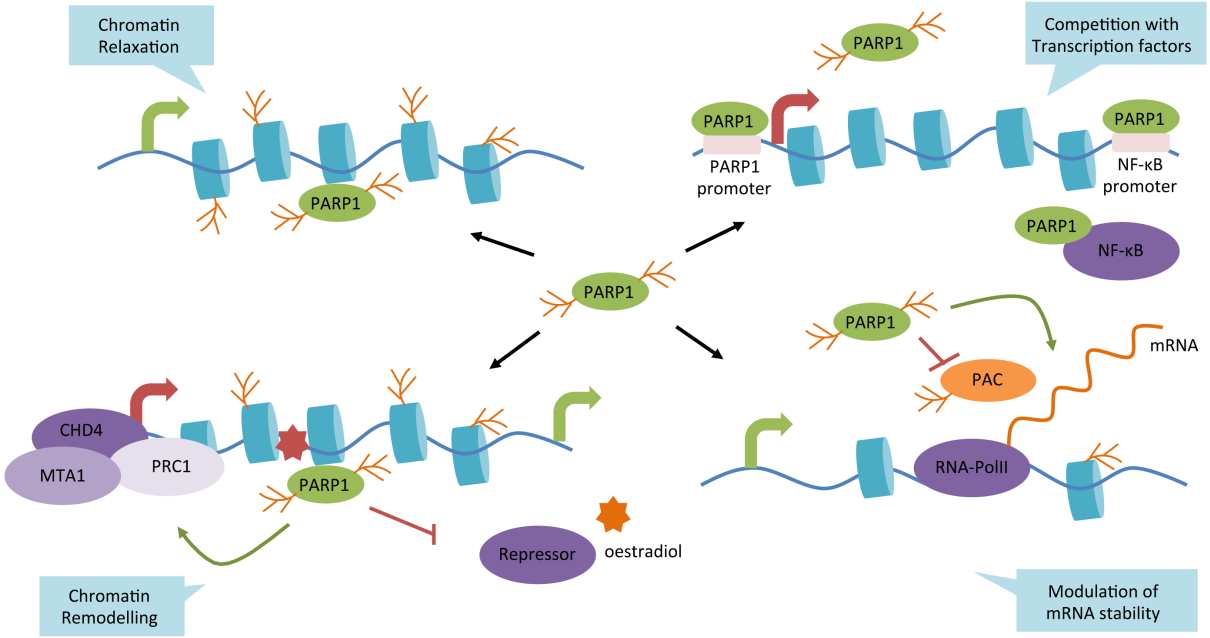

Figure 23: Roles of PARP1 in transcription regulation and gene expression

PARP1 can act in several ways, promoting transcription by the opening of the chromatin after DNA damage, recruiting remodelling factors, activators or repressors, by competitioning with transcription factors for the direct binding of promoter regions, or by modulating mRNA stability.

and trigger replacement of histones. This cascade of event promotes transcription. Recently, it has been showed by comparing ChIP-seq data from WT and PARP1 deficient mouse embryonic stem cells that PARP1 needs to bind a subset of gene promoter motifs usually bound by the pioneer transcription factor Sox2, thus making PARP1 a pre-pioneer transcription factor (Liu and Kraus, 2017). That ability could help transcription factors bind to non-canonical sites throughout the genome. Additionnaly, PARP1 was reported to represses the activity of the Poly-A polymerase (PAP). This regulates the level of a subset of proteins, through a direct destabilisation of mRNAs (Di Giammartino *et al.* 2013). The different mechanisms by which PARP1 regulates transcription are summarized in **Figure 23.**

5.4 PAR in inflammation

Inflammation is a complex mechanism through which cells can signal dysfunction and promote activation of the immune system to sequester the dysfunctional cell. The NF-KB pathway is the main signalling cascade by which inflammation specific genes will be transcribed (see Espinosa *et al.* 2015 for a review). Nonetheless, chronic inflammation promotes carcinogenesis, for it stimulates proliferation and metastasis formation.

Many PARPs have been related to inflammation (see **Chapter 1**). Specifically, PARP1 can activate the NF-KB pathway through two mechanisms. In response to an inflammatory stimulus, PARP1 is acetylated by two histone acetyl transferases, P300 and CBP (CREB binding protein) (Hassa and Hottiger, 2005). This will ultimately result in the activation and translocation of the transcription factor NF-KB to the nucleus where is starts gene transcription. In response to DNA damage, PAR generated by PARP1 can trigger recruitment of ATM and IKK-γ, the natural protein sequestrator of NF-KB (Stilmann *et al.* 2009)

As mentioned before, in inflammation triggered by LPS exposure, PARP1 unstabilizes mRNA of inflammatory genes. For inflammation is not at the centre of this thesis project, I will not go into more details. Signalling mechanisms impacted by PARP1 in inflammatory diseases are reviewed in Chung and Joe, 2014. But interestingly, one can mention that since PARP inhibition allows limiting inflammation produced by chemotherapy (Korkmaz *et al.* 2008), understanding these PAR-related inflammatory mechanisms could be of help in the therapeutic field.

5.5 PARylation in cell death

If cells over accumulate detrimental DNA lesions that remain unrepaired, they can transmit mutations in daughter cells, thus favouring cancer apparition. To avoid this « for the greater good », they can orchestrate their own death through several pathways. PARylation has been linked to 4 modes of cell death so far (Virag *et al.* 2013).

5.5.1 Necrosis

PARylation was first thought to cause necrosis in cells (Sims *et al.* 1983). Necrosis, in contrast with apoptosis is an unscheduled phenomenon where cell swells, plasma membrane degrades, organelles collapse, DNA hydrolyses and cell lyses, releasing cytoplasmic content and triggering inflammation (Galluzzi *et al.* 2011).

Necroptosis is as specific type of PAR dependent death that is also called inflammatory cell death. Over activation of PARP leads to a detrimental accumulation of PAR, which results in depletion of NAD^+ contents in the cell. NAD^+ shortage indirectly leads to short supplies of ATP. As a consequence, cells undergo energy failure and die by necrosis (Virag *et al.* 2013)

5.5.2 Apoptosis

Apoptosis is an ATP-dependent mechanism of programmed cell. It helps removing cells that are no longer needed in development, or to maintain tissue and organs integrity (Orrenius *et al.* 2011). P53 can be activated after cellular stress. It occurs in several steps, first DNA is fragmented and all cell components are converted into apoptotic bodies that do not trigger inflammation (Edinger and Thomson, 2004). Cytochrome c is released from mitochondria, allowing activation of caspases. Caspase 3 and caspase 7 can generate two apoptotic fragments of PARP1. The 89kDa Cter fragment will be excluded from the nucleus, while the 24kDa Nter fragment will retain its DNA binding ability, thus inhibiting further activation of PARP1 binding to DNA breaks, decreasing PAR synthesis, reducing NAD^+ consumption and avoiding DNA repair factors recruitment (Virag *et al.* 2013). Similarly, PARP2 is cleaved by caspase 8, separating its DNA binding domain from the catalytic domain (Benchoua *et al.* 2002)

In addition, PARP1 is a co-activator of NF-KB that promotes apoptosis by regulating several apoptotic genes (Hassa *et al.* 2005; Cohausz and Althaus, 2009). PARP1 cleavage is now broadly used as a marker of apoptosis.

On the other hand, PARG is clived into two Cter fragments of 85 and 74kDa by caspase 3 during apoptosis, induced by several damaging agents. These fragments localize in the cytoplasm and retain their catalytic activities (Bonicalzi *et al.* 2003). Several studies have shown that PAR was regulating caspases activity, mainly by acting on Ca2+ influxes after oxidative stress (Feng *et al.* 2012). As PAR is an agonist of the transient receptor potential 2 cation channel (TRPM2) that facilitates the activation of caspases, depletion of PARP1 or PARG impairs the release of PAR and reduces cell death by apoptosis (Blenn *et al.* 2011).

5.5.3 Parthanathos

PARP1 can also trigger another cell death mechanism that is called Parthanatos. A name that was given in reference to the divinity of death in greek mythology, Thanatos (David *et al.* 2009). Upon severe DNA damage, massive PAR accumulation and NAD^+ and ATP depletion occurs and free PAR can be released with the action of PARG. This free PAR induces the delocalization of a component of the mitochondrial oxidative phosphorylation chain, located in the membrane. AIF (Apoptosis Inducing Factor) translocates into the nucleus where it triggers chromatin condensation, DNA fragmentation and cell death. This delocalization is dependent on PAR binding through its PAR-binding site, and it has been shown that long chains of PAR induce AIF release more efficiently than short chains (Wang *et al.* 2009; Wang *et al.* 2011; Andrabi *et al.* 2006; Galluzzi *et al.* 2012). The role of PARG in PARthanatos is reviewed in Feng and Koh, 2013.

5.5.4 Autophagy

Autophagy is a process by which cells regulate and recycle their own subcellular components through directing them to lysosomes, in conditions of important stress. Metabolic distress activates AMPK (AMP-activated protein kinase) and inhibits mTOR (mammalian target of rapamycin), two kinases involved in initiating autophagy processes. This triggers ROS accumulation by mitochondrial dysfunction that will damage DNA and activate PARP1. Following consumption of NAD^+ and ATP pools reduction further activates AMPK and inactivates mTOR, increasing the phenomenon through a positive feedback loop. In absence of PARP1, this loop is not maintained and cells undergo cell death by apoptosis instead (Rodriguez-Vargas *et al.* 2012). Depletion of the NAD+ pool by overactivation of PAR can also lead to a defective mitophagy phenotype in cells (Scheibye-Knudsen *et al.* 2014).

5.6 PARylation in metabolism, aging and cancer:

Throughout this chapter, we have seen the importance of PAR for regulating all aspects of genomic integrity. In addition to their roles in DNA repair and Replicative Stress Response, PARPs and PARG are involved in chromatin structure, transcription, cell death and cell cycle control. They also display important roles in cell metabolism (reviewed in Vida et al. 2017). If any of these processes are altered, cells can be extensively damaged and genome irreversibly altered. Although genome instability is the main source of mutations and innovation on a long timescale perspective, at the scale of an individual it can lead to highly pathological situations, genetic diseases and eventually cancer development (Jackson and Bartek, 2009; Hoeijmakers et al. 2009). Using inhibitors targeting DNA repair pathways are in focus to treat cancer, such as the PI3K small molecule inhibitors or topoisomerase inhibitors (Pommier *et al.* 2016; Blackford and Jackson 2017).

Because of the utilisation of NAD+ in PARylation process, and because NAD^+ pools have been shown to decrease in aged organisms from C.elegans to mice, the idea of supplementing food with NAD^+ precursors such as NMN (nicotinamide mononucleotide) or NR (nicotinamide riboside) emerged to prevent excessive damage linked with aging (Mendelsohn and Larrick, 2017). Here again, PARylation as the main PTM regulating DNA damage response has roles to play on the outcomes of genomic instability.

Because PARP1 and PARG have pleiotropic roles in maintaining genomic integrity, many inhibitors have been developed to target their specific activity, in order to potentiate cancer therapies. This will be the topic of the next chapter.

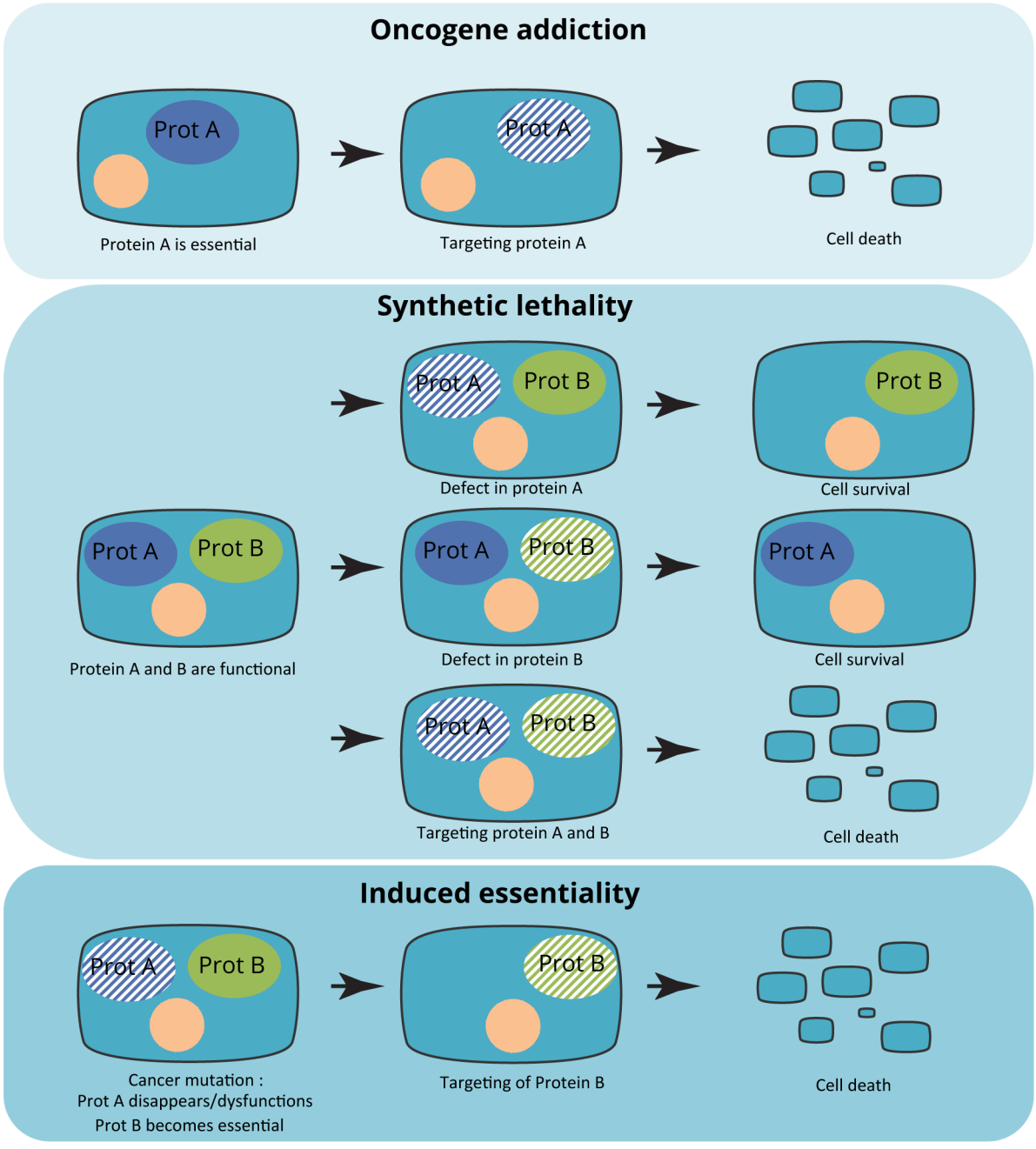

Figure 24: Genetic concepts for targeting tumour cell – finding cancer's Achilles' heel.

Oncogene addiction, synthetic lethality and induced essentiality are three concepts that can be used to understand how to target mutated cancer cell lines (Adapted from Lord *et al.* 2014)

Chapter 3: PARP and PARG inhibitors in chemotherapeutics

1. Keeping balance in polymer levels: a trail for treating cancer?

Cancer can be considered as a group of diseases that are characterized by the uncontrolled growth and spread of abnormal cells. The last worldwide statistics available from the international agency for research on cancer evaluate the occurrence of cancer at over 14 million new cases in 2012. According to the GLOBOCAN 2012 report, this number was expected to increase by 68% by 2030, meaning that cancer will be one of the major therapeutic challenges of the 21th century.

While the occurrences of cancer will increase because of higher exposure to mutagenic agents (smokes, food carcinogens…) the mortality rates are decreasing because of better diagnostic and the emergence of personalized therapies that take genetic features of each type of cancer into account. Targeted therapies aim at understanding each cancer's characteristics and find their Achille's heels.

Several genetic features and concepts can be exploited in treating tumours. Cancer cells often display abnormalities and defects in gene expression comparing with normal cells, therefore their survival can rely on the expression of one single other gene. This is called "**Oncogene addiction**" (Weinstein *et al.* 2002), and allows targeting one gene to trigger specific death of tumour cells.

In some tumours, another thing can happen called "**induced essentiality**". It is a more complex concept, where mutating a gene induces the cell survival to be dependant on another gene, that can thus be targeted to mediate lethality (Tischler *et al.* 2008). Another concept is "**synthetic lethality**", where the simultaneous invalidation of two target genes can lead to death. The concept was proposed as early as 1946 in population genetics studies on Drosophila melanogaster (Dobzhansky, 1946), and is now widely used in therapeutic strategies, depending on the genetic features of each tumour. This allows to target one single gene in cells that are known to lack for another gene it can be synthetic lethal with (For a review of the use of synthetic lethality in clinics, see Lord *et al.* 2014). For each of these mechanisms, resistance can arise in tumour cells, for they often display a high proliferative and mutational rate. Therefore, there is an urgent need of diversifying gene candidates and cellular pathways that can be targeted for resistant tumours, and to broaden our spectra of therapies (see **Figure 24**).

In the previous chapter, I showed how PARylation is a widespread post-translational modification, helping to regulate almost all aspect of cell fate, required for the temporal and spatial orchestration of DNA repair, gene expression, cell metabolism and cell death. This versatility has led to considering enzymes involved in PARylation as potential therapeutic targets for diseases such as cancer.

Both mice models depleted for PARG-110 or mice PARP1 knock-in mutant with a hypo-PARylation activity display increased sensitivity to irradiation, suggesting that even a small modification of PAR homeostasis is essential to influence cell mechanisms (Schuhwerk *et al.* 2017).

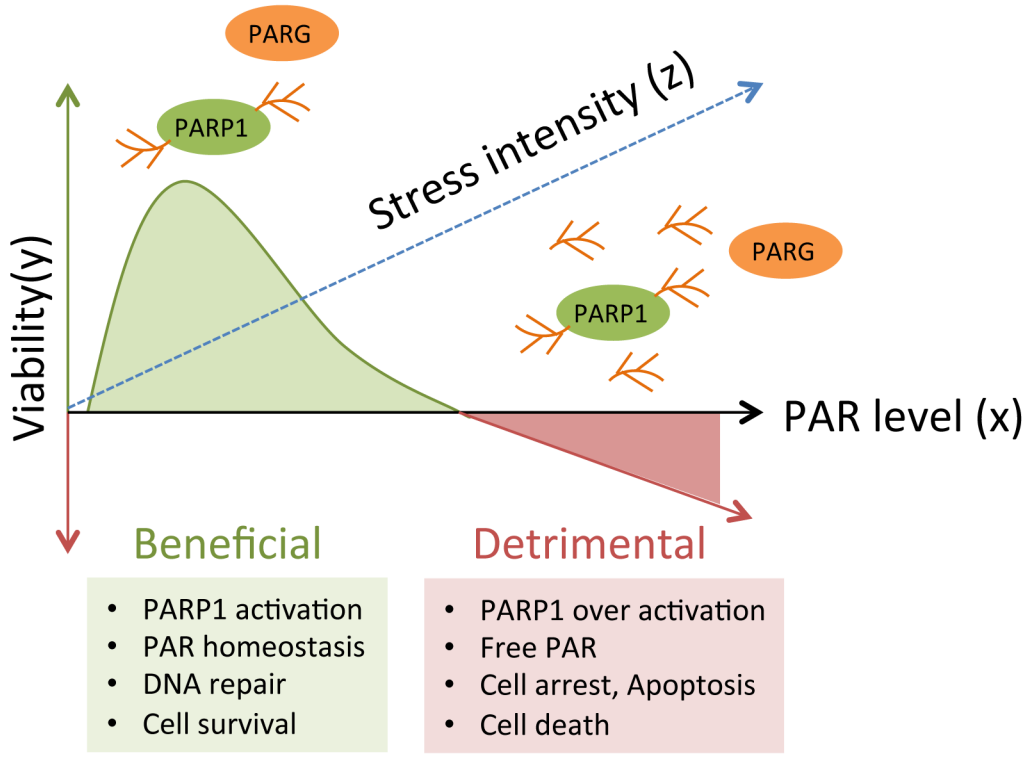

Figure 25: The hormetic pattern of PAR accumulation after cellular stress.

Correlation between the PAR levels accumulated in cells, and cell viability. While upon mild stress, the accumulation of PAR can be beneficial and mediate an efficient repair of DNA strand breaks; the overaccumulation of PAR upon prolonged and intense stress can have detrimental effects and lead to cell death.

Stress induced PARylation indeed displays a hormetic pattern (**Figure 25**): In cases of mild stress, when low PAR amounts are produced, the presence of PAR will favour DNA repair and cell survival. However, upon severe cellular stress, PARP1 will be over activated and a lot of polymer can be accumulated, thus triggering a depletion of the NAD+ cellular pool and a severe energy failure leading to cell death. Free PAR liberated by the endonucleotidic activity of PARG can also lead to programmed cell-death, as mentioned in the previous chapter, channelling the response towards PARthanatos. PARylation can thus simultaneously be a protection and a threat to the cell, further reinforcing the concept of using it in order to influence cancer cell fate (Schuhwerk *et al.* 2017).

Two groups showed the potential of PARP inhibition in treating BRCA-mutated tumours, using a synthetic lethal approach (Farmer *et al.* 2005; Bryant *et al.* 2005), since treatment with an inhibitor in hereditary BRCA1/2 mutated ovarian and breast cancer cells displayed increase chromosome instability, cell cycle arrest and death by apoptosis.

Taking into account the importance of maintaining PAR homeostasis for cell survival and DNA repair, PARG inhibitors are also considered as putative candidates for chemotherapeutic strategies. In the next paragraphs, I will try to summarize the current inhibitors available for targeting PARP1 and PARG activity, as well as their uses for treating cancers.

2. The targeting of PARP1 in cancer therapeutics

As the main enzyme to catalyse PARylation in cells, PARP1 inhibitors were quickly considered as promising targets that could act in cancer therapeutics in several ways:

- In order to **potentiate the effect** of chemotherapeutic or radiotherapeutic treatments by impairing DNA repair, as PARP inhibition sensitizes many cancer cell lines to DNA damaging agents.
- In a **synthetic lethal approach** in HR deficient cells. Occurrence of single strand breaks during cancer therapies can thus be converted to double strand breaks and remain unrepaired, leading to cell death.
- In order to **restrain inflammation** during chemotherapeutic treatments, as it is an important actor of inflammation (see **Chapter 2**)
- In order to **regulate tumoral gene expression** that suppresses angiogenesis or cell proliferation.

These approaches are summarized in **Figure 26**. PARP inhibitors are extensively developed since 1980, and some of them are already used in clinics.

2.1 Development of inhibitors

The first ever-developed PARP inhibitor was 3-aminobenzide (3-AB), a structural analogue of NAD^+ that binds in PARP1 catalytic pocket, and acts as a competitive inhibitor 3-AB (Durkacz *et al.* 1980). On this model, several first generation inhibitors have been developped: veliparib (Abbvie), rucaparib (Pfizer/Clovis), olaparib

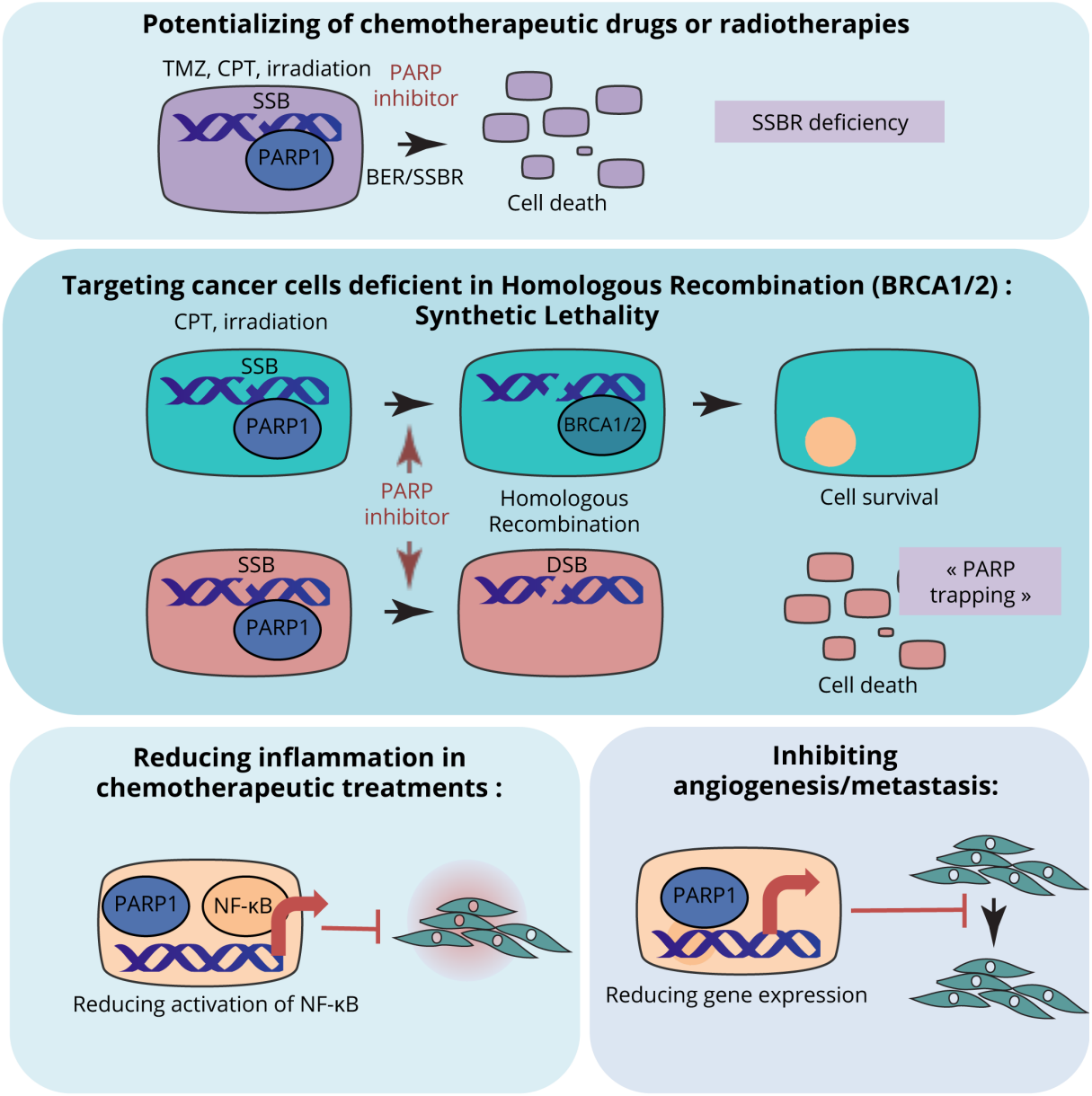

Figure 26: Using PARP inhibitors in cancer therapy. One molecule: a broad range of beneficial effects.

PARP inhibitors can ce used to potentiate the effect of chemotherapeutic drugs and to target homologous recombination defective cells through a synthetic lethality approach. Additionnaly, PARP inhibitors reduce inflammation and inhibit angiogenesis and metastasis of tumours, thus acting as pluripotent anti-cancer agents.

(KuDOS/AstraZeneca) and niraparib (Merck/Tesaro). These first generation inhibitors were efficient, but non-specific for PARP1, for they also inhibited PARP2 and maybe other PARPs.

The discovery of PARP1 catalytic domain structure allowed improving their specificity and efficiency (Ekblad *et al.* 2013), giving rise to new-generation inhibitors such as talazoparib (Lead/Biomarin/medivation/Pfizer), still based on a competitive mode of inhibition (Zaremba and Curtin, 2007). Olaparib and AG1G361 were the first inhibitors used to demonstrate that PARP inhibition was increasing cell death in BRCA1/2 HR deficient cells (Farmer *et al.* 2005; Bryant *et al.* 2005). For a long time, people have thought the lethal effect was essentialy coming from the synthetic lethality effect resulting from the absence of repair of both SSB and DSB. It was then suggested and demonstrated that the effect observed after PARP inhibition was resulting from a PARP « trapping » effect on DNA lesions, impairing PARP1 release after DNA damage sensing and the subsequent repair mechanism (Murai *et al.* 2012). Indeed, it was demonstrated that PARP1 auto modification was needed to generate sufficient electrostatic repulsion to remove PARP1 from DNA damage (Satoh and Lindahl, 1992), and the fact that PARP1 deficient cells are resistant to PARPi treatment further supports this model (Pettitt *et al.* 2013). This model is analogue to the topoisomerase blocking that generates a type of lesion on its own (reviewed in Pommier *et al.* 2016). All of the inhibitors have different trapping efficiencies, which may account for differences in cytotoxicity (see Table 3). Consistently, talazoparib, the most potent PARP inhibitor also displays the highest PARP trapping effect (Murai *et al.* 2014). For a review on their respective trapping potencies, see Lord and Ashworth, 2017. However, PARP1 inhibition sensitizes cells to CPT, and synergizes with topoisomerase blocking, in a process relying on PARP activity rather than PARP1 trapping (Bowman *et al.* 2001)

This has lead to the use of PARPi as a single agent in treating BRCA1/2 tumours, instead of using carcinogens agents that remain deleterious. The development of allosteric inhibitors has been suggested that allosteric inhibitors could be a better way to improve PARP1 targeting (Steffen *et al.* 2014).

2.2 Clinical trials

The first clinical trial was started in 2003 using a combination of temozolomide treatment (an alkylating agent) and PARPi (AGO14699= CO-338 or rucaparib) to treat advanced melanomas (Plummer *et al.* 2008).

Olaparib was the first inhibitor approved by the FDA for phase I clinical tests for treating BRCA1/2 mutant ovarian cell lines using the synthetic lethality approach (Fong *et al.* 2009; Fong *et al.* 2010). Phase II studies further shower PARP inhibition potency in these types of cancers (Tutt *et al.* 2010; Audeh *et al.* 2010 - For a review on the therapeutic use of Olaparib, see Marchetti *et al.* 2012). Rucaparib and niraparib also got an FDA approval recently (Drew *et al.* 2016) and are currently into phase II/III tests with more or less success on different types of tumours. Iniparib, despite showing good results in phase I and II displayed poor results in phase III assessment (Mateo *et al.* 2013). This is a non-exhaustive list of the trials using PARP inhibitors, but the field is currently trending and many lessons for therapies can be retained from the use of PARP inhibitors (Lord and Ashworth, 2017).

PARP inhibitor	Code	Status	Structure	Ki	Relative PARP trapping potency *(Murai et al. 2014)*
NAD^+ (NAM)		Non clinical		PARP1: ND PARP2: ND	
3-Aminobenzamide (3AB)	INO-1001	Non clinical		PARP1: 2µM	ND
olaparib	AZD-2281	2014: FDA/EMA approved	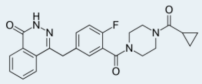	PARP1: 5nM PARP2: 1nM	1
rucaparib	AG-014699	2016: FDA approved	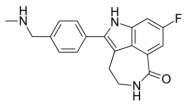	PARP1: 1,4nM	1
niraparib	MK-4827	2017: FDA approved	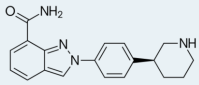	PARP1: 3,2nM PARP2: 4nM	~2
veliparib	ABT-888	2016: FDA Orphan Drug Designation	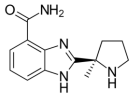	PARP1: 5,2nM PARP2: 2,9nM	<0,2
talazoparib	BMN-673	Phase 3 clinical test	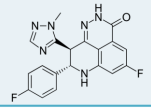	PARP1: 1,2nM PARP2: 0,9nM	~100

Table 3: Summary of the main PARP inhibitors available for clinics, and their structures.

Displayed are the names, codes, structure and inhibition potency (Ki) of the different PARP inhibitors. Their status in clinical trials are also mentionned (FDA: Food and Drug Administration), as well as their putative trapping effects (displayed in arbitrary units, measured in Murai *et al.* 2014)

Interestingly, PARP inhibitors could also target other tumours that show defects in HR, but no obvious mutations in BRCA1/2 genes. These tumours display phenotypes described as "BRCAness" by the experts of the field. Suppression of ATR, FANC, and other DNA repair related genes also confer sensibility to PARP inhibitors and are starting to be exploited in the clinics. PARP inhibition is synthetic lethal with many other genes (Turner *et al.* 2008) such as Rad51, ATRX, RPA1, NBN, ATR, ATM, CHEK1, CHEK2, PNKP, PALB2, CDK1, FANCA, FANCM, all involved in homologous recombination (for a review see Lord and Ashworth, 2016). Additionally, PARP inhibitors could be applied to other types of cancers, such as hepatocarcinoma (Guillot *et al.* 2014). Inhibitors and associated clinical trials are summarized in **Table 3.**

2.3 Resistance and alternatives

Meanwhile using PARP inhibitors in clinics, several mechanisms of resistance were simultaneously identified that could explain the lack of clinical responses in some cases (reviewed in Incorvaia *et al.* 2016). The first mechanism identified was the restitution of BRCA1/2 function through mutations leading to the restoration of BRCA genes open reading frame (Edwards *et al.* 2008). Mutations leading to restoration of the ORF of Rad51 C-terminal binding site also lead to resistance (Norquist *et al.* 2011). Another mechanism is the loss of 53BP1, leading to decreased NHEJ and a restoration of HR activity, taking a shortcut in the pathway choice (Jaspers *et al.* 2013). REV7 loss, another protein involved in NHEJ was also reported to promote HR and lead to PARP1 resistance (Xu *et al.* 2015). This only occurs in cells that are deficient for BRCA1 but keep BRCA2 activity.

The last mechanism identified is the direct pharmacological resistance mediated by the ABC efflux transporters such as Pgp (P-glycoprotein) encoded by the MDR1 gene. The active efflux of PARP1 inhibitor strongly diminished the effect (Binkhathlan *et al.* 2013; Choi and Yu, 2014).

Extensive comprehension of those resistance mechanisms can allow finding strategies to escape this resistance phenotype. For example, development of the PARP inhibitor AZD2461, which is a poor P-glycoprotein substrate displays increased efficiency compared with olaparib in the treatment of breast cancer cells model (Henneman *et al.* 2015).

We must remember that tumours undergo severe selective pressure and that spontaneous mutations can give rise to diverse mechanisms. This can remind us global Darwinian evolution and selection processes, and the solution might be to vary PARP inhibition dosages and to multiply parallel targets in therapies, in order to avoid the emergence of resistant clones (Korolev *et al.* 2014). The emergence of combinatorial therapies is a promising way to overcome cancer resistance to PARP inhibitors, and several strategies are currently under trial (reviewed in Lim and Tan, 2017; Gaducci *et al.* 2017). As mentioned above, combining PARP inhibition and topoisomerase inhibition is also a trending field (reviewed in Pommier *et al.* 2016; Cuya *et al.* 2017). NMNAT inhibition leads to a drastic reduction in cellular NAD^+ pools, increasing the efficiency of olaparib, therefore targeting NAD^+ metabolism enzymes could be another way to target cancer cells by using synthetic lethality (Bajrami *et al.* 2012; Sampath *et al.* 2015). Undoubtedly, all these data will contribute to provide patients with integrative, selective and innovative approaches to cure tumours efficiently, with the minimum side effects. For an extensive review on selective targeting of patients bearing HR-deficient tumours, see Talens *et al.* 2017.

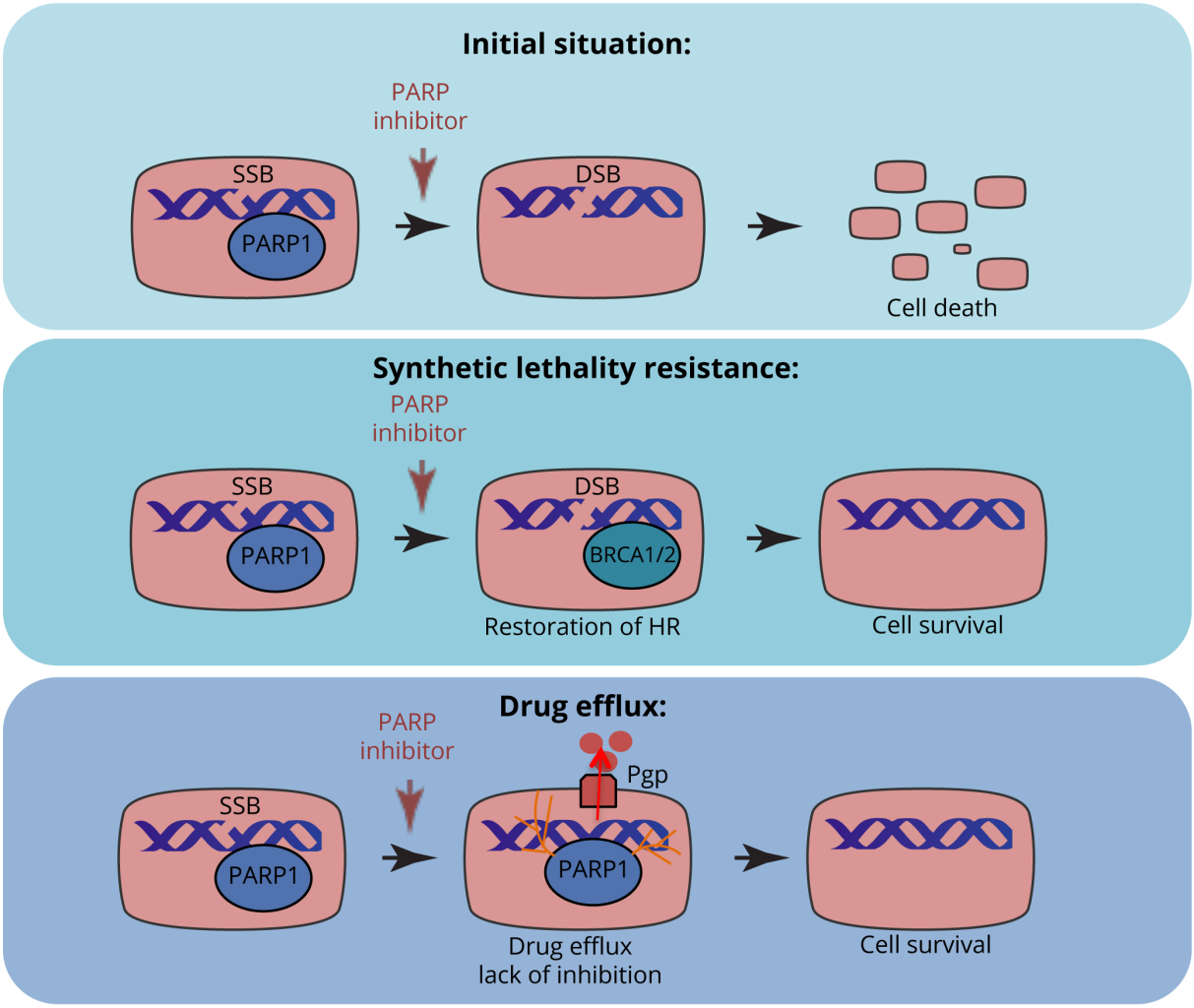

Figure 27: Resistance mechanisms to PARP inhibitors.

Even if PARP inhibition is an interesting strategy for treating cancer cells, several mechanisms of resistance can appear. Spontaneous mutations leading to restoration of homologous recombination components can lead to resistance. P-glycoprotein (Pgp), an ABC efflux transporter can also lead to a decrease of PARP inihibitor molecules in cells.

3. The targeting of PARG in cancer therapeutics

PARG is the main PAR-degrading enzyme, and contrarily to PARPs that have pleiotropic roles and can be unselectively targeted by PARP inhibitors, it consists in a single gene. Despite the fact that this gene copy encodes 5 isoforms, that have different subcellular localizations and possible contributions to DNA repair (see **Chapter 1**), the catalytic domain is highly conserved, and as the main catalytic counterpart for PARPs and regarding its low cellular abundance it could consist in an interesting and easiest target for cancer therapies (Fauzee *et al.* 2010).

3.1 Development of inhibitors

Compared with PARP inhibitors, PARG inhibitors are less well developed. The PARG inhibitors available used to enter into three classes: DNA intercalators, tannins and ADP-ribose analogues. Recently, new inhibitors were developed broadening the possibilities to investigate PARG function in vivo.

DNA intercalators are aromatic compounds that can bind to nucleic acids. The first reported to display inhibitory effects on PARG were compounds such as proflavine, ethacridine, ethidium bromide… (Tassavoli *et al.* 1985). They inhibit PARG indirectly by blocking its interaction with PAR.

The second reported molecule that displayed an effect on PARG activity purified from human placenta were hydrolysable tannins (Tanuma *et al.* 1989). Tannins are complex polyphenol-like molecules that are widely spread in plants that use them as secondary metabolites to defend against parasites. Initial PARG inhibition tests were done with gallotannin, a type of tannin extracted from the Oak species *Quercus robur*. Hundreds of tannin derivatives were tested for their inhibition activities, and it was noticed that an increasing number of galloyl groups was positively correlated with PARG inhibition efficiency (Tsai *et al.* 1991; Aoki *et al.*1995; Formentini *et al.* 2008). However, there are contrasting reports on tannin derivatives bioavailability, for this molecule have a trend to aggregate and are not likely to pass the cell membrane easily, increasing the dose requested to mediate an effect (reviewed in Blenn *et al.* 2011). Gallotannin fails to overcome cell permeability in several assays and moreover, it has been stated that the use of gallotannin was having a steady-state effect on cellular stress (Falsig *et al.* 2004; Bakondi *et al.* 2004), mainly through its antioxidant properties, that can influence the outcome of all studies carried with these types of molecules and should therefore be interpreted with caution. Despite their activity in vitro, and the fact that tannins are “natural” products, tannin derivatives are unlikely to become clinical solutions to cancer.

Other potent inhibitors have been developed such ADP ribose analogues, which work as partial non-competitive inhibitors. The most widely used is ADP-HPD (Adenosine di-phosphate (hydroxyethyl) pyrrolidinediol) that displayed the highest PARG inhibition activity but was incapable of permeabilizing the cell membrane, limiting its use in vivo (Slama *et al.* 1995). It was extensively used in structural biology that allowed unravelling the catalytic structure of bacterial, protozoan and human PARG. This further allowed the improvement of *in silico* screening in order to identify putative inhibitors (Slade *et al.* 2011; Dunstan *et al.*

Class of PARG inhibitor	Name	Cell permeability	Structure	IC50 (µM)
DNA intercalator	Tilorone		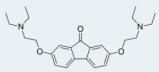	7,3 (Tassavoli *et al.* 1985)
	GPI16552	High	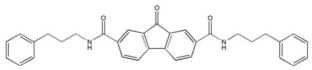	1,7 (Li *et al.* 2002)
	GPI18214	High		3-4,2 (Cuzzocrea *et al.* 2007; Genovese et al. 2004)
	Ethacridine		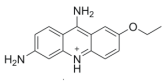	7,2 (Putt and Hergenrother, 2004)
Tannin	Gallotannin	High	NS	17,8-33,4 (Tsai *et al.* 1992)
	3-galloyl-α,β-D-glucose	Low	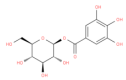	0,95+/-0,02 (Formentini *et al.* 2008)
	Nobotanin B	High	NS	4,4-15 (Aoki *et al.*1992)
	Nobotanin E	Low	NS	1,4-1,8 (Tsai et al. 1992; Aoki et al. 1992)
	Oenothein B	High	NS	3,8+/-1 (Aoki *et al.* 1992)
Substrate analogue	ADP-HPD	Low	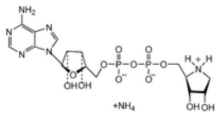	0,12 – 0,66 (Slama *et al.* 1995) (Okita *et al.* 2010)
Salicylanilide	3,5-Dichloro-N-(3-chloro-4-(naphtalen-2-yloxy)phenyl)-2-hydroxybenzamide	High	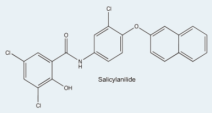	12+/-2 (Steffen *et al.* 2011)
Rhodanine	RBPI2-RBPI6	Low	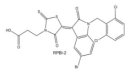	2,9-12,3 (Finch *et al.* 2012)
Hydrazines Hydrazones	3a-f;5a-f and 8a-h	ND	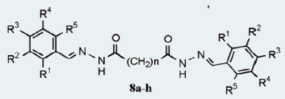	1-75 (Islam *et al.* 2014)
Quinazolinedione	PDD00017273	High	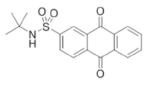	0,2-0,8 (James *et al.* 2016)

Table 2: Summary of PARG inhibitors developed so far.

Displayed are the names, classes, structures and inhibition potency (IC50) of the different PARP inhibitors. Their respective cell permeability is also mentionned (adapted from Feng and Koh, 2013).

2012; Kim *et al.* 2012; Tucker *et al.* 2012). Salicylanides-derivatives were also identified as cell-permeable inhibitors, but they mediate an additional inhibition of PARP1, therefore their use should be limited if a PARG-specific effect is required (Steffen *et al*. 2011). Moreover, salicylanides have a high IC50, requiring doses at the 100µM range (James *et al.* 2016).

Several studies using PARG activity screenings allowed identifying novel small inhibitor compounds targeting PARG activity, such as molecules displaying xanthene scaffolds (Okita *et al.* 2010), rhodamine based PARG inhibitors (RBPI - Finch *et al.* 2012) or hydrazide hydrazones (Islam *et al.* 2014).

The most potent inhibiting capacities were reached only by ADP-HPD and RBPI, but both type of molecules lack cell permeability (Tucker *et al.* 2012).

The most recent and convincing PARG inhibitors developed, both in vitro and in vivo are the anthraquinone derivatives (PDD00013907- James *et al.* 2016), whose cytotoxicity is really low and that display satisfying inhibition activities, within 0,1 - 1µM range. In their study, James et al. show that the use of this inhibitor results to an increase and persistence of PAR levels after DNA damage, increased γH2AX foci and reduced viability in several cell lines, thus proving that PARG inactivation was efficient in several cell lines. In this thesis project, we used this last PARG inhibitor for several experiments (see **Results**).

3.2 Synthetic lethality

Recent work has been done to investigate whether PARG inhibition could be exploited in a synthetic lethality approach. Two studies showed that the simultaneous suppression or inhibition of PARG and several enzymes involved in the last steps of homologous recombination (BRCA1, BRCA2, ABRAXAS and BARD1) by siRNA in MCF7 cells displayed an increased lethality (Gravells *et al.* 2017; Fathers *et al.* 2012).

However, our team has shown that PARG is neither synthetic lethal with BRCA1 nor PTEN deficiency (Noll *et al.* 2016) and that the simultaneous depletion of both PARG and BRCA1 or PTEN did not increase sensitivity in U2OS and MDA-MB-231 cell lines. The study of James *et al.* (2016), testing the new PARG inhibitor also showed that PARG inhibition did not result in increased cell death in several tumour cell lines.

This discrepancy between results shows that one must be very careful with the cell line used and to display careful conclusions, because results cannot be extrapolated for every cell line, and this further reinforces the observations made with PARP inhibitors that therapies must be oriented taking genetic characteristics into account.

3.3 Towards clinical trials?

Although many clinical trials have been conducted for PARP inhibitors, one could not exptrapolate regarding, much less has been done with PARG inhibitors. Tannic acid and gallotannin were reported to potentiate cytotoxicity of chemotherapeutic drugs in different types of cancer (Chen *et al.* 2009, Naus *et al.* 2007, Sun *et al.* 2012). Some studies have shown that gallotannin is toxic to MDA-MB-231 breast cancer cells, and BRCA2

deficient breast cancer cells (Fathers *et al.* 2012; Tikoo *et al.* 2011), but as mentioned before, this effect could be due to the antioxidant properties of tannins. Gallotannin was used in CT26 colon carcinoma cell lines to suppress the expression of tumour growth factors (Lin *et al.* 2009). Very few other PARG inhibitors were tested in experimental trials. We can mention the use of GPI 16552, a DNA intercalator-type PARG inhibitor, in combination with temozolomide to reduce tumour growth, extracellular matrix infiltration and metastasis in B16 melanoma cell lines (Tentori *et al.* 2005). It would be of interest to start clinical trials with the latest PARG inhibitors available (James *et al.* 2016).

Although the use of both PARP inhibition and PARG inhibition are of interest for future treatments, it was demonstrated that their use alone but not in combination was triggering cell death. They do not act synergistically and therefore should remain individually targeted proteins in therapeutic strategies (Feng and Koh, 2013).

In addition to refining our molecular understanding of PARP and PARG contribution to DNA repair and cell processes, development of such inhibitors hold great promises for the future treatment of a wide range of cancer types, broadening our arsenal against one of the deadliest disease in the world.

Aims of my research project:

Over the years, the many roles of the PARP family, and mainly their DNA-dependent representatives (PARP1, PARP2 and PARP3), have been extensively studied. We now know that PARylation has an extensive role in DNA-damage response, replication, transcription, telomere biology, RNA metabolism, cell cycle regulation, cell differentiation and cell death. Acting as a molecular scaffold for sensing, signalling and recruiting repair factors, PAR has become a central post-translational modification for the maintenance of genome integrity. But if polymer synthesis is indeed a crucial event for the outcome of DNA damage accumulation and cell fate, its degradation must be of equal importance. Initial studies regarding the role of PARG in DNA repair came from animal models. Because PARG is present in the human genome as a single gene encoding for five different isoforms displaying several subcellular localizations, and because the simultaneous depletion is embryonic lethal in mice (Koh *et al.* 2004), the contribution of PARG in DNA repair has been difficult to evaluate. For the past decade, the laboratory's projects aimed at elucidating at the molecular and cellular levels the role and regulation of PARG. In former work, the laboratory has generated new PARG-deficient HeLa cells models that were viable, based on an shRNA depletion strategy of all isoforms. These cell lines displayed an increased sensitivity to irradiation, delayed repair of both single and double strand DNA lesions and increased mitotic cell death (Amé *et al.* 2009). The laboratory next revealed a functional link between PARG and the repair/replication factor PCNA, required for efficient localization of the nuclear PARG isoform ($PARG^{111}$) to DNA damage sites and to replication foci (Mortusewicz *et al.* 2011). This study also showed that that the two cytoplasmic isoforms of PARG ($PARG^{102}$ and $PARG^{99}$) could be recruited to laser micro-irradiation induced DNA damages. The identification of an interaction between PARG and PCNA lead to the study of the contribution of PARG to DNA replication, and results showed that PARG was necessary to tightly control PAR levels produced upon prolonged replicative stress to prevent the detrimental effects of PAR over-accumulation that causes RPA exhaustion and DSB accumulation (Illuzzi *et al.* 2014).

The aim of my project was to study the role, regulation and mechanism of action of human PARG in DNA repair and replication, by the formation of isoforms of distinct subcellular localizations and functions, and by post-translational modifications. The first aim (**Aim 1**) was to generate new innovative tools allowing the study of PARG regulation and the precise contribution of each isoform to DNA repair. I generated a library of stable cell lines in a U2OS background constitutively invalidated for all endogenous PARG isoforms and re-expressing upon induction a single PARG isoform or mutant. Some examples of applications that could be done with these constructs are presented.

Another aim of my project (**Aim 2**) was to study whether PARG could be regulated by post-translational modifications. This project led to the discovery of a new protein partner, the DNA damage dependent protein kinase DNA-PK, that was able to phosphorylate PARG *in vitro* on several sites identified by mass spectrometry and by targeted mutagenesis.

In the last part of my project (**Aim 3**), taking advantage of our new cellular models and knowing that PARG and DNA-PK were protein partners, I investigated the role of PARG in the cell response to replicative stress caused by the topoisomerase I inhibitor camptothecin, an anticancer drug known to activate both DNA-PK and PARylation.

Results obtained for each of these aims are presented in the following **Results** section.

Results

Aim one: Generation of new cellular tools for the study of the contribution of PARG isoforms in DNA repair

Introduction

To overcome DNA lesions, constantly occurring in human genome, cells need to mobilize hundreds of protein factors, tightly coordinating their activities in time and space. Poly (ADP-ribosyl)ation, a post-translational modification which is catalysed mainly by the Poly(ADP-ribose) polymerase 1 (PARP1) has a pivotal role in the regulation of DNA-repair. PAR catabolism is primarily mediated by the Poly (ADP-ribose) glycohydrolase (PARG), a conserved protein across mammals, flies, worms and even plants (Amé *et al*. 2000; Davidovic *et al*. 2001). PARG is encoded by a single gene and was early mapped on human chromosome 10 (10q11.23, Amé *et* al. 1999). PARG shares a common promoter with the TIM23 gene (Meyer *et al.* 2003) and encodes five different isoforms of different subcellular localization. Initially, a long nuclear isoform (110kDa), and a short cytoplasmic isoform (65kDa) were identified in vivo (Davidovic *et al.* 2001). It was then demonstrated that alternative mRNA splicing of the transcript could produce two additional cytoplasmic isoforms of 102kDa (lacking exon1) and 99kDa (lacking exon 1 and 2). These isoforms were described as peri-nuclear and present in high abundance (Meyer-Ficca *et al*. 2004). Ultimately, two mitochondrial forms (60kDa and 55kDa) have been identified that could also be produced by alternative splicing (Meyer *et al.* 2007, Whatcott *et al.* 2009). They bear no catalytic activity, for ADP-ribosylhydrolase 3 (ARH3) was described as the main PAR-degrading enzyme in mitochondria (Niere *et al.* 2012). PARG Exon 4 deleted-mice lack all isoforms, leading to an early death of embryos at day 3.5. Derived trophoblast stem cells die by apoptosis because of an overaccumulation of PAR, and can only be maintained upon treatment with a PARP inhibitor (Koh *et al.* 2004). Depletion of exon 2 and 3 in mice lead to viable and fertile mice expressing only the short isoforms of PARG. However, mice-derived embryonic stem cells are sensitized to DNA damaging agents and display DNA repair defects (Cortes *et al.* 2004, Gao *et al.* 2007). Deletion of the exon 1 on the PARG gene in ES cells leads to an increased sensitivity to DNA-damaging agents (Fujihara *et al.* 2009). The first human cell models available were using siRNA strategies to get rid of all PARG isoforms and also displayed increased sensitivity to DNA damage (Blenn *et al.* 2006, Fisher *et al.* 2007). Our lab previously used a HeLa cell model, stably expressing an shRNA leading to an efficient PARG depletion (Amé *et al.* 2009). In these cells, overexpression of GFP-labelled $PARG^{102}$ and $PARG^{99}$ isoforms allowed to demonstrate that they were recruited to DNA-damage foci induced by laser micro-irradiation (Mortusewicz *et al.* 2011). The shuttling ability of these cytoplasmic isoforms was already pointed out in a previous study (Haince *et al.* 2006). Despite these data, there was still a lack of cellular tools to decipher the precise contribution of each isoforms to DNA damage repair. In the following research paper draft, I propose new U2OS cell models and several examples of their use for the study of the regulation of PARG function and activity.

Fast track generation of a library of constructs and cell lines expressing wild type or mutated single PARG isoforms: new tools for studying PARG

E. Héberlé[1], G. Illuzzi[1], J.C. Amé[1], V. Heyer[2], B. Reina-San Martin[2], F. Dantzer[1], V. Schreiber[1]

1. Biotechnology and Cell Signalling, UMR7242 CNRS, Université de Strasbourg, Laboratory of Excellence Medalis, ESBS, 300 Bd Sébastien Brant, CS 10413, 67412 Illkirch, France.
2. Institut de Génétique et de Biologie Moléculaire et Cellulaire, Illkirch, France.

Corresponding author : V. Schreiber, valerie.schreiber@unistra.fr

Highlights:

- Generation of a library of constructs and cell lines allowing the study of PARG biology.
- Confirmation of the subcellular localization of each PARG isoforms.
- $PARG^{102}$ is the main PARG isoform endogenously expressed in U2OS cell lines.
- Although $PARG^{111}$ is the main PAR-degrading enzyme, $PARG^{102}$ and $PARG^{99}$ can also contribute to PAR degradation produced after oxidative stress in the nucleus, while $PARG^{60}$ and $PARG^{55}$ are inactive.
- Identification of a new PCNA-binding PIP box (PIP2m) and residues needed for PCNA interaction.

Abstract (max 200 words):

Poly(ADP-ribose) glycohydrolase is one of the major enzymes involved in the rapid and efficient degradation of the post-translational modification poly(ADP-ribose). A single PARG gene encodes several isoforms displaying distinct subcellular localisations (nucleus, cytoplasm, mitochondria) and functions. We have used the Golden Gate technology to generate a library of PARG modules that, depending on their combination, can lead to the assembly of any PARG isoforms in one step, either wild type or bearing single or multiple targeted mutations. We have then generated a library of plasmids allowing the expression, either constitutive or inducible, of single PARG isoforms, eventually fused to an epitope tag or a reporter protein. To illustrate the interest of this library, we have shuffled some of these constructs into lentivirus-producing plasmids to complement U2OS cells that were constitutively depleted in all PARG isoforms by stable shRNA expression. We have similarly generated cell lines expressing PARG bearing single or double mutations, invalidating its catalytic activity or its interaction with one of its partner, PCNA. Some examples of applications that could be done with these constructs are provided in this article.

Introduction

Poly(ADP-ribosyl)ation (PARylation) is a reversible post-translational modification synthesized by members of the poly(ADP-ribose polymerase (PARP) family. PAR catabolism is mediated mainly by poly(ADP-ribose) glycohydrolase (PARG). PARG is encoded by a single gene but present as multiple isoforms localized to different cellular compartments (Meyer *et al.* 2007; Meyer-Ficca *et al.* 2004; Whatcott *et al*. 2009). Full length $PARG^{111}$ is nuclear; $PARG^{102}$ and $PARG^{99}$ are cytoplasmic, but able to shuttle into the nucleus in response to DNA damage (Haince *et al.* 2006). Two shorter isoforms, one cytoplasmic ($PARG^{60}$) and one mitochondrial ($PARG^{55}$) are catalytically inactive (Niere *et al.* 2012). The relative function of each isoform is still unknown. In mice, depleting all PARG isoforms is embryonically lethal, whereas a hypomorphic mutant is viable, but the mice are sensitive to ionizing radiation and alkylating agents (Cortes *et al*. 2004; Koh *et al.* 2004). We and others have shown that depletion of all PARG isoforms in cellular models using siRNA or shRNA strategies does not affect cell viability. However, upon genotoxic insult, these cells revealed increased cell death and impaired repair of single and double strand breaks and of oxidized bases (Amé *et al.* 2009; Erdelyi *et al.* 2009; Fisher *et al.* 2007), highlighting that PARG, like PARP1, the main enzyme catalysing PARylation, is playing a key role in cell response to DNA damages. All existing isoforms and their reported localisation and activities are summarized in **Figure 1A**.

To investigate the recruitment of PARG isoforms to DNA repair sites we locally introduced DNA damage by laser micro irradiation and showed that $PARG^{111}$, $PARG^{102}$ and $PARG^{99}$ were efficiently recruited but with different kinetics, also different from PARP1 (Mortusewicz *et al*. 2011). PARG recruitment was partially dependent on PARP1 and PAR synthesis, indicating that a second, PAR-independent recruitment mechanism, was taking place. We have revealed a functional link between PARG and the repair/replication factor PCNA, showing that binding to PCNA contributes to the recruitment of PARG not only to laser induced DNA damage sites, but also to replication foci (Mortusewicz *et al.* 2011). We identified a PCNA binding site in the longest nuclear PARG isoform and had evidences for the existence of a second PCNA-binding domain localised in a region common to $PARG^{111}$ and to the cytoplasmic $PARG^{102}$ and $PARG^{99}$. The function of this second PCNA-binding domain and the functional role of the interaction between PCNA and each of all three PARG isoforms remains an open question. Of note, the recruitment of PCNA to laser induced DNA damage was also partially depending on PAR synthesis, pointing to a complex interplay between PARP1/PARG/PCNA, in the DNA damage response. The localisation of nuclear PARG to replication foci, its interaction with PCNA and its requirement for efficient recovery from prolonged replicative stress induced by hydroxyurea (Illuzzi *et al.* 2014) also strongly support the idea that this PARG/PCNA interaction is involved in replication-related processes. Through this project, we provided new cellular tools to study and dissect the contribution of each PARG isoform to DNA-damage response. The constructs and cell lines generated were used to study several aspects of PARG isoforms biology, from their expression to their catalytic activity.

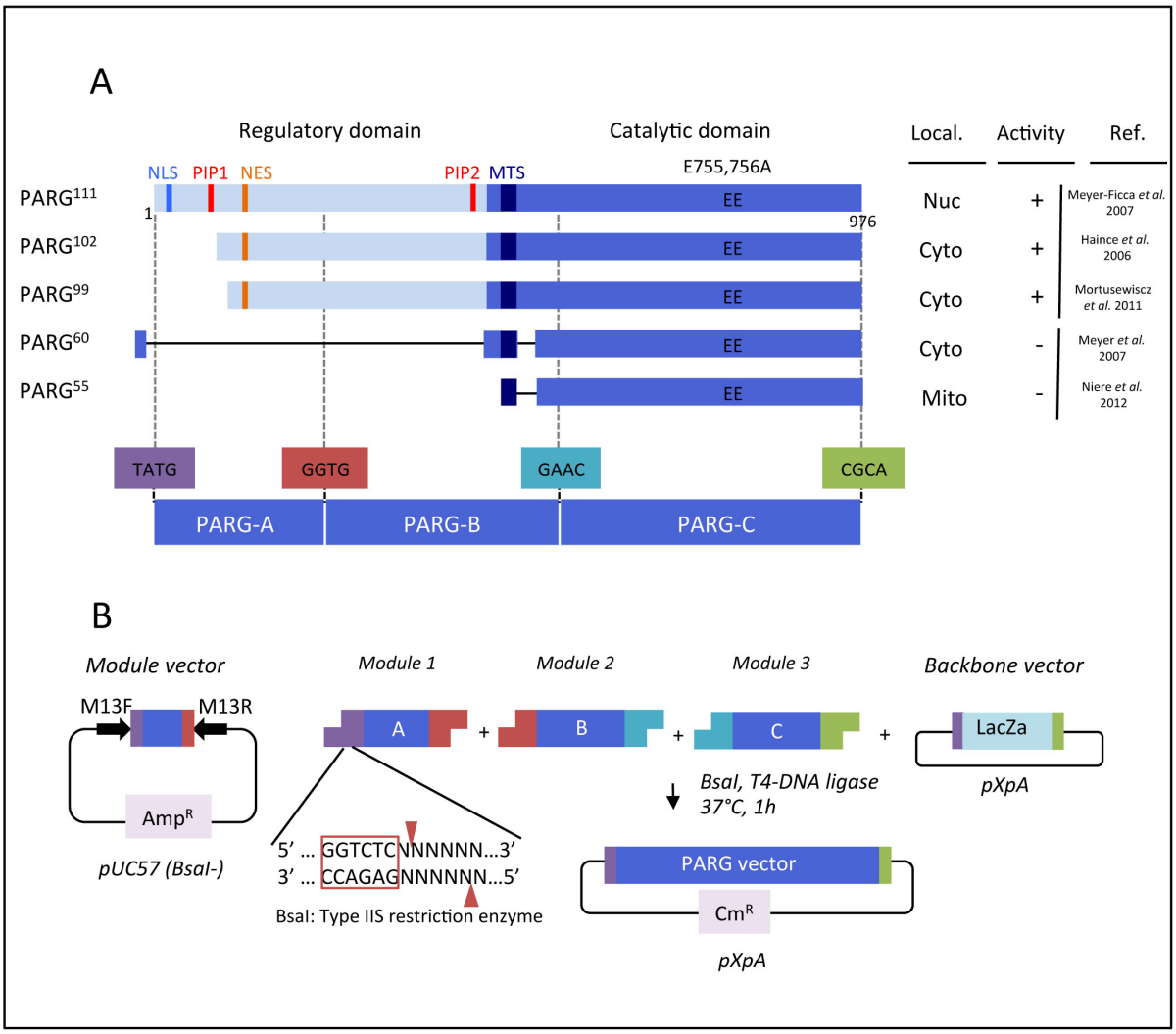

Figure 1: The PARG gene encodes 5 different isoforms. A) Map of the different PARG isoforms and their reported localisation and activity in human cells. PARG[111] is the full-length sequence and is active in the nucleus. PARG[102] and PARG[99] lack the N-terminal sequence with the NLS and the PIP1-box motif. They are cytoplasmic but reported to have a catalytic activity. PARG[60] is cytoplasmic and PARG[55] is mitochondrial. Both lack catalytic activity (Meyer *et al.* 2007, Niere *et al.* 2012). B) Principe of the Golden Gate Cloning-based approach used to generate variants of sequence modules for the fast and simple assembly of new PARG sequences. From pUC57 module vectors, new cDNAs can be generated and cloned in a pXpA backbone vector in a single step reaction using the TypeII-S restriction enzyme BsaI.

Results and discussion

1. Generation of a library of PARG modules using the Golden Gate technology

The PARG gene (10q11.23, Amé *et al.* 1999) encodes five different isoforms that can be expressed either by alternative splicing or translational restart from the same mRNA (Meyer *et al.* 2007). The different isoforms are shown in **Figure 1A**. Because PARG is a low abundant endogenous protein, its direct in cellulo study is complicated and new tools are needed to understand PARG regulation and PARG isoform expression. In collaboration with B.Reina San Martin team (IGBMC, Strasbourg) we designed a new strategy using Golden Gate cloning technology allowing a fast and efficient shuffling of DNA modules to generate combinations of new PARG expression vectors (Engler *et al*. 2009; Weber *et al.* 2011). The principle of Golden Gate technology relies on the use of a type II S restiction enzyme, (BsaI) that recognizes a 6 nucleotide sequence and cuts 4 nucleotides downstream of its recognition site, generating 3'OH cohesive overhangs that can be specifically rejoined. By using consecutive sequence overhangs of different sequences, this method allows the one-step generation of a new DNA sequence that is assembled from many DNA modules that can be combined in a specific order. We dissected the PARG gene into three basic boxes: PARG-A is the N-terminal and regulatory region of PARG containing tge NLS, NES and PIP1 box. PARG-B the middle domain containing the PIP2 box and the MTS (mitochondrial transport signal). Lastly, PARG-C comprises the catalytic domain (**Figure 1A**). Each of these modules are amplified by PCR using oligonucleotides flanked by BsaI sites. The PCR-amplified modules were cloned by Megawhop into the pUC57 plasmid that has no *Bsa*I site (**Figure 1B**). Sequences of the *Bsa*I sites were designed to force each module to ligate in the proper order and orientation with the correct up-stream and downstream modules (**Figure 1B**). The pre-existing BsaI sites on PARG were mutated by introducing silent point mutations by Megawhop during the PCR steps (positions R475; E965) (Miyazaki, 2011).

This method allowed us to generate a small library encoding several versions of PARG-A, B and C. Some examples of these modules are described in **Figure 2A**. In order to generate the assembly of a sequence encoding the $PARG^{60}$ and $PARG^{55}$ small isoforms, we had to generate extra cassettes described as PARG-AB, encoding for the N-terminal part of these PARG variants, and flanked with TATG and GAAC sequence linkers **(Figure 2A).** To generate a plasmid of interest through a single step reaction, selected PARG-A, -B or -AB and -C encoding plasmids can be combined with additional modules and the desired plasmid backbone providing the cassettes of interest (**Figure 2B):** a promoter (a SV40 Large T-constitutive promoter or a tetracycline-inducible promoter), a poly-A, an epitope tag (Flag) or a reporter protein (GFP), a selection cassette (AmpR, KanR, PuroR or HygroR) and eventually a transfection efficiency-reporting fluorescent cassette (SV40-CFP or SV40-GFP). The different assemblies generated are listed in **Table 1 (supplementary data).** To illustrate the interest and possibilities of this library of modules and assemblies, we have designed several experimental approaches to rapidly generate sets of recombinant plasmids encoding PARG isoforms and mutants and test them by transient transfections or after the generation of stable cell lines. For most of the experiments described in this article, strategy is mainly based on a two-plasmid approach **(Figure 2C)**.

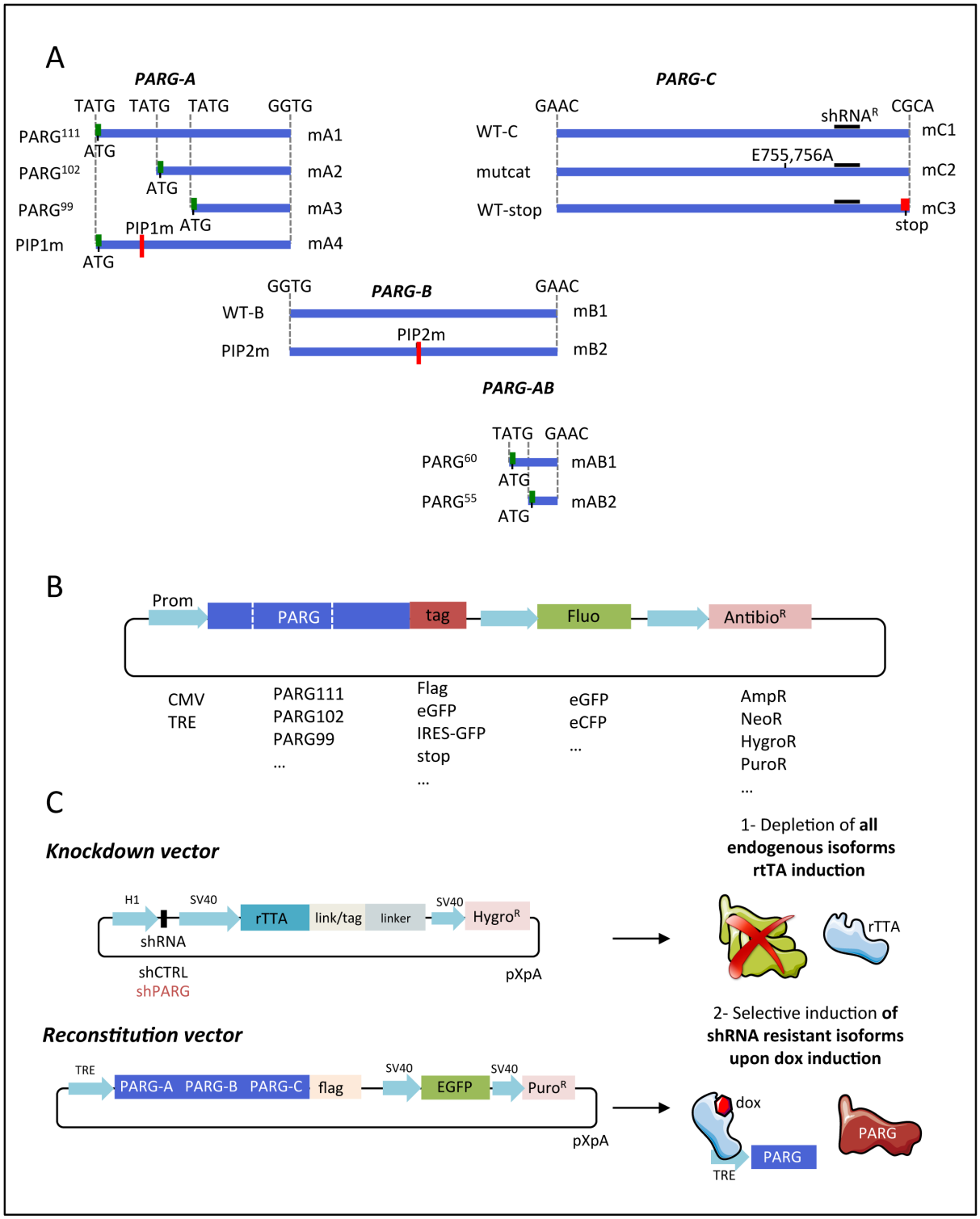

Figure 2: Cloning strategy for studying functional aspects of PARG. A) Modules that can be used to generate a panel of PARG isoforms or PARG mutants in cells. PARG-A is the N-terminal region of PARG. PARG-B is the middle domain. PARG-C is the catalytic domain. PARG-AB is the specific N-terminal region of the shortest PAR^{55} and PARG^{60} isoforms. B) Scheme of the different modules that can be used in combination with PARG for different experimental purposes. PARG cDNA can be combined with different tags (flag, GFP…) under the control of different promoters (CMV, TRE). Plasmids can bear selection markers such as fluorescence (GFP, CFP) or antibiotic restistance (Amp^{R}, Neo^{R}, Hygro^{R}…)

2. Example of application 1: Transient and fast expression of desired PARG isoforms or mutants in cell-lines.

Our first objective was to generate tools allowing the depletion of all endogenous versions of PARG isoforms and the selective re-introduction of each PARG isoform individually. For this purpose, using the same cloning method we generated two-vector system. The first is the **knockdown vector** that expresses either a non-targeted control shRNA or an shRNA targeting the common C-terminus shared by all PARG isoforms (**Figure 2C**), under a H1 promoter. The knockdown vector also expresses the tetracycline-controlled *transactivator* rtTA protein under a SV40 promoter, a transcription factor allowing the selective transcriptional activation of genes under TRE (tetracycline response element) promoters, upon doxycycline treatment. This system is directly derived from the Tet-ON strategy allowing the control of gene expression in mammalian cells upon tetracycline induction (Gossen *et al.* 1995). The second one, called the **reconstitution vector** encodes for the desired PARG version, under the TRE promoter (**Figure 2C**). Each of the PARG versions is a shRNA resistant form that can be co-transfected with the knockdown vector.

To validate our system, we generated constructs allowing the expression of the 5 Flag-tagged PARG isoforms, under the control of the TRE inducible promoter and the stable expression of the rtTA protein under a SV40 promoter (pXR1, pXR3, pXR4, pXR5 and pXR6 in Table 1, supplementary figure). As a proof of concept that our strategy works, we transfected Bosc cell lines with these PARG isoforms and either the shCTRL expression knockdown vector (pXK1) or the shPARG expressing knockdown vector (pXK3). Transfection with the pXK3 (shPARG) alone indeed strongly reduced endogenous PARG levels compared with the pXK1 (shCTRL) transfection (**Figure 3A**), demonstrating that our knockdown vector is functional. When co-transfecting these vectors with the PARG^{60}-flag reconstitution vector (pXR5), and upon addition of doxycycline in the medium, we observed that the PARG^{60}-flag is expressed and that the induction system works (**Figure 3A**). To test the efficiency of this inducible system for all PARG isoforms, we co-transfected BOSC cells with the shCTRL vector with each of the isoforms expressing vector. By Western Blot, we observe the selective induction of each form upon doxycycline addition (**Figure 3B**). With an antibody specifically recognizing PARG N-terminal domain the PARG-Nter antibody, we reveal the 111, 102 and 99 isoforms (highlighted with an asterisk), as well as the endogenous PARG, indicated on the figure with a black arrow. The flag antibody was necessary to reveal the 60 and 55kDa isoforms. All PARG versions migrate to the expected size. Of note, the PARG^{111} lane revealed an additional lower band at the size of the 102 isoform. This observation reinforces the hypothesis that some PARG isoforms can be generated by alternative translation starting in addition to the already described alternative splicing mechanism (Meyer-Ficca *et al.* 2004), although we can not totally exclude that this lower band results from proteolytic cleavage. The same observation can be made regarding the PARG^{60}, that displays a weak lower band at the size of the PARG^{55} isoform, that seems to confirm that PARG^{55} can be generated from the PARG^{60} mRNA, even though this hypothesis had been ruled out in another study (Niere *et al.* 2012). Co-

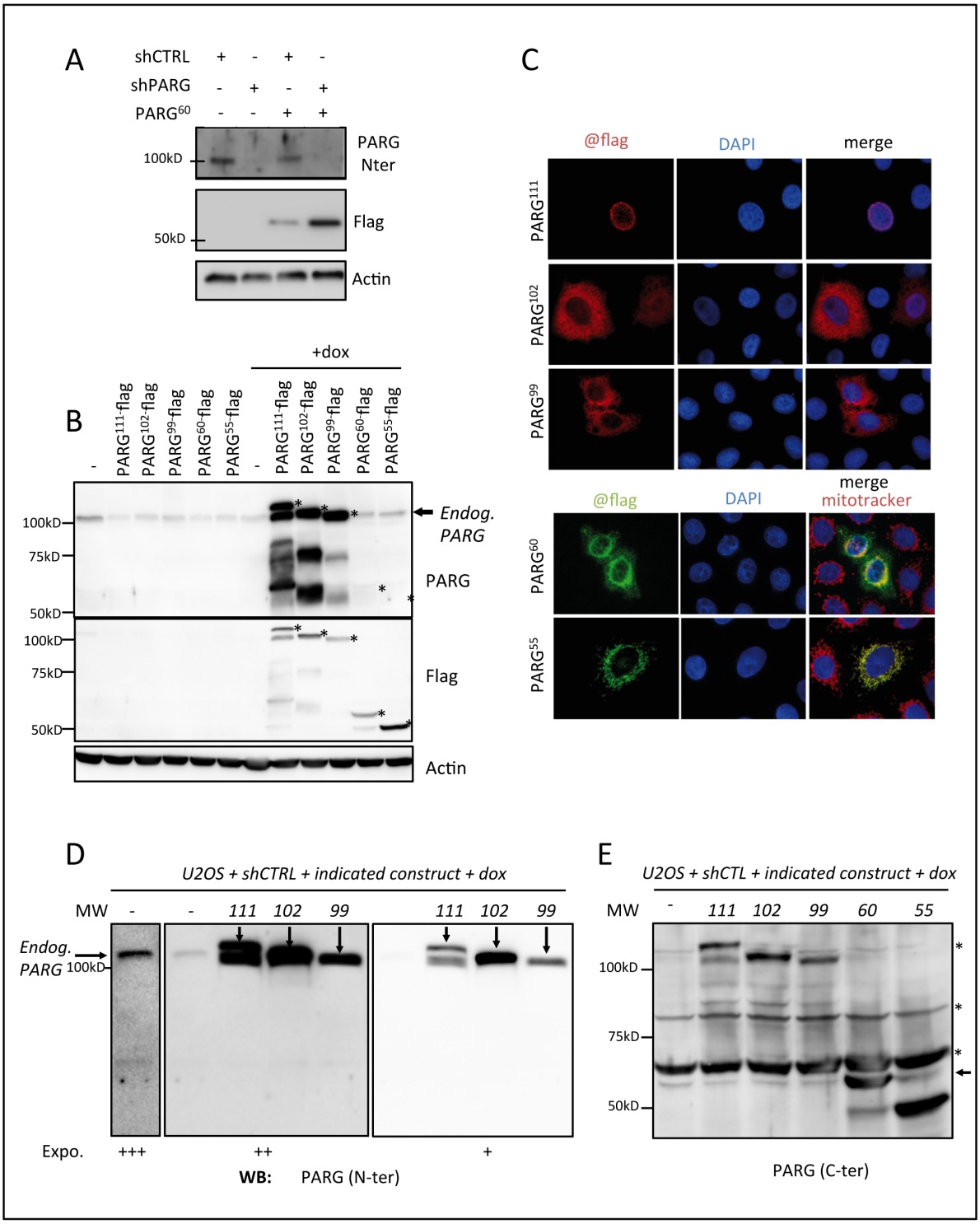

Figure 3: Validation of knockdown and reconstitution vectors. . A) Western blotting on Bosc cell extracts after transfection with shCTRL and shPARG knockdown vectors alone or in co-transfection with the PARG^{60} reconstitution vector. B) Western blot on Bosc cell extracts after co-transfection of the shCTRL knockdown vector with each of the PARG isoforms reconstitution vectors, with or without doxycycline induction, revealed by the PARG-Nter antibody and a flag directed antibody. C) Immunofluorescence in Hela cells after co-transfection of a knockdown plasmid and all flag-tagged PARG isoforms reconstitution vectors in Hela cells. D) and E) Western blot of U2OS cells extracts after co-transfection with the shCTRL knockdown vector and each of the unlabelled PARG-isoforms reconstitution vectors. D) is revealed with an antibody targeting the N-terminal region of PARG (PARG-Nter) and E) is revealed with an antibody targeting the C-terminal region (PARG-Cter), thus revealing the smallest isoforms.

transfection of the double system plasmids in HeLa cells allowed checking for the isoform localization by immunofluorescence taking advantage of the flag tag. As expected to what is described in the literature, PARG^{111} localizes in the nucleus, while PARG^{102}, PARG^{99} and PARG^{60} are cytoplasmic. PARG^{55} is mitochondrial and co-localizes with the control mitotracker. We noticed a slight mitochondrial accumulation of PARG^{60}-Flag that could suggest some internal translation restart at the ATG driving the production of PARG 55 (**Figure 3C**). This is supported by the lower band observed for the PARG^{60} construct on western blot, using the anti-flag antibody (**Figure 3B**) or an antibody raised against the C-terminal part of PARG (**see Figure 3E**) and migrates at the size of PARG^{55}. These experiments show that our system enables the selective depletion of all endogenous PARG isoforms by transient transfection in cells, and the selective re-introduction of PARG isoforms or PARG mutants. This is a new and unique tool allowing the study PARG biology that can be used in many different cell lines.

3. Example of application 2: expression of untagged PARG isoforms demonstrates that PARG102 is the most abundant isoform expressed in cells

Previous study already reported cytoplasmic isoform PARG^{102} and PARG^{99} as the predominant isoforms in HeLa and HEK293T (Meyer-Ficca *et al,* 2004). To address which of the isoforms was the most abundant in U2OS cell lines, where we wish to develop our expression model, we have generated plasmids allowing the expression of all 5 untagged PARG isoforms, under the control of the tetracycline response element (TRE) inducible promoter (plasmids pRX7-11). U20S cells are co-transfected with each of these plasmids, together with the shCTRL plasmid (pXK1) that bears the rtTA protein. After 24 hours of doxycycline treatment, expression of the non-tagged PARG isoforms was analysed by WB in total extracts using an antibody recognizing the N-terminal part PARG, thus detecting only PARG^{111}, PARG^{102} and PARG^{99} (**Figure 3D**). An antibody recognizing the C-terminal part of PARG could detect all PARG isoforms (**Figure 3E**). We could clearly demonstrate that the most abundant endogenous PARG isoform produced within cells is, by far, PARG^{102}, with PARG^{111} being almost undetectable in U2OS cells. This is consistent with the literature in other cell lines (Meyer-Ficca *et al.* 2004). Despite a high background signal, and the impossibility to detect the endogenous PARG, the anti-Cter PARG antibody revealed that whereas PARG^{60} could be present in cells (**Figure 3E**, pointed by a black arrow), PARG^{55} is not detected. Aspecific band signals are highlighted with asterisks. This is again consistent with previous studies and strengthens the validity of our new tool (Meyer *et al.* 2007; Whatcott *et al.* 2009). For further applications linked with DNA repair, which commonly uses the U2OS cell model, we therefore confirmed that the most abundant isoform was the PARG ^{102}.

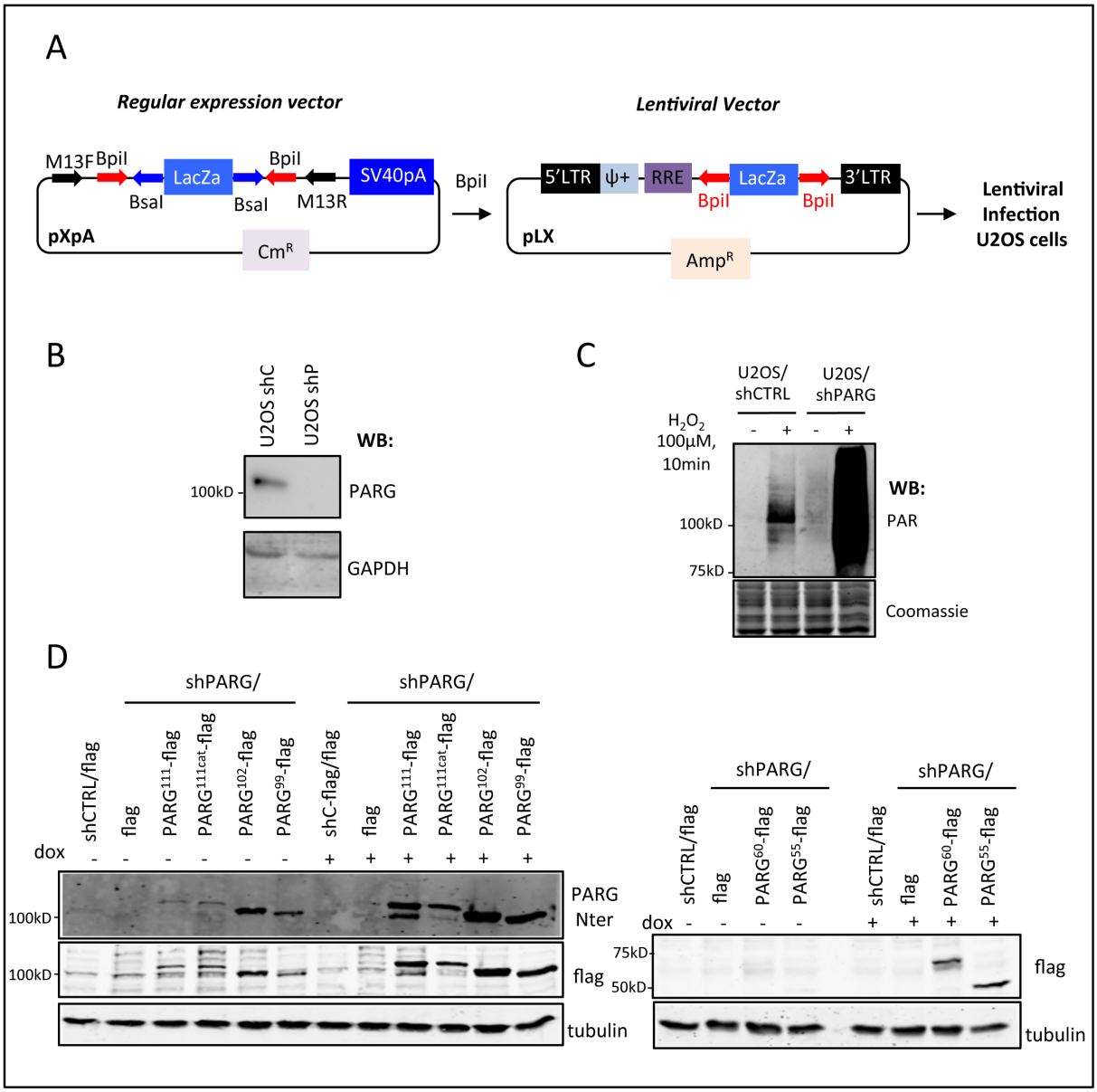

Figure 4: Generation of a collection of stable cell-lines expressing PARG isoforms. A) Plasmid maps of a pXpA expression vector. The cDNA is surrounded with two BpI restriction sites, allowing the one step transfer of the DNA sequence into a lentiviral vector. RRE: Rev Response Element, LTR: Long Terminal Repeat, Psi+: Encapsidation sequence). B) Western blot of stable U2OS cell lines expressing the shCTRL or the shPARG shRNAs. C) Western blot following PAR accumulation in U2OS shC and U2OS shP cell lines after H2O2 treatment (10min, 100µM). D) Western blot of PARG knockdown or PARG reconstituted stable cell U2OS cell lines, before and after induction with doxycyclin (1µg/mL).

4. Example of application 3: generation of a library of cell lines expressing single PARG isoforms to evaluate their contribution in PAR degradation upon genotoxic stress

In order to study functional aspects of PARG isoforms biology, and mainly to evaluate their contribution in the degradation of PAR generated after genotoxic stress we wanted to generate a panel of cell lines expressing each of the isoforms individually. The structure of our knockdown or reconstitution expression vectors allows the direct transfer of the sequence of interest into a lentiviral vector by a single step of restriction with the BpiI enzyme. Lentiviral vectors display encapsidation sequence signals and other features allowing the stable infection of target cell lines. Viral particles were produced by transient transfection of Bosc packaging cells with the lentiviral vectors of interest and used for an immediate infection of U2OS cells (**Figure 4A**).

First pXK1 and pXK3 vectors were converted into lentiviral vectors. Lentiviral particles containing these plasmids were used to infect U20S with both shCTRL and shPARG shRNAs. By western blot, we verified that shCTRL infected cells (U2OS shCTRL) displayed an endogenous PARG signal, whereas shPARG infected cell lines (U2OS shPARG) were constitutively invalidated for the expression of all PARG isoforms (**Figure 4B**). PARG knockdown was efficient in this cell line, as demonstrated by the strong decrease in endogenous PARG levels and the strong increase and persistence of PAR produced after a transient H2O2 treatment (**Figure 4C**).

U2OS shPARG cells were then infected with each of the reconstitution vectors, converted into lentiviral vectors (pXR1, pXR3-pXR6). In addition to all isoforms, we also infected them with a $PARG^{111cat}$ version (pXR2) devoid of catalytic activity, caused by the mutation of the two catalytic glutamic acid residues into alanines (E756, E757, Patel *et al.* 2005). Additionally, we infected both U2OS shCTRL and shPARG cell lines with an empty vector bearing the flag tag alone (pXR27). All of the cell lines generated display the same doubling time (30h+/-2h, data not shown). In a first step, we checked by western blot that these cell lines were expressing each of the constructs after doxycycline induction. Although the expression of all isoforms at the right size strongly increases after induction, $PARG^{111}$-flag, PARG-^{111cat}-flag, $PARG^{102}$-flag and $PARG^{99}$-flag are detectable even without induction, showing that our doxycycline induction system displays some leakage. This is a downside of the doxycyclin strategy that has been observed in other studies. shPARG/$PARG^{60}$-flag and shPARG/$PARG^{55}$-flag are also produced, and the cells display less leakage. These differences of expression among the different cell lines are hardly controllable because we choose to work on whole populations selected after infection, rather than on a clonal population (**Figure 4D**). Interestingly, with the $PARG^{111}$-flag and $PARG^{111cat}$-flag constructs, a band that migrates at the level of $PARG^{102}$ is generated, again suggesting that this isoform might be produced from translational restart using an alternative ATG, or as the result of proteolytic cleavage. Initially, the use of a doxycycline induction system was motivated by the fact that TetON/OFF is a well-known system, allowing a doxycycline dose-dependent induction of gene transcription (Kringstein *et al.* 1998). However, in our hands doxycycline induction proved itself difficult to control, since with the same amount of doxycycline induction, the expression of each PARG isoform was not homogeneous. These differences of the induction expression can be explained by the uncontrolled insertion of cDNA during the lentiviral infection. Despite these discrepancies, we decided to compare the PAR degrading activity of the cell lines by following PAR persistence by immunofluorescence after H_2O_2 treatment (**Supplementary Figure 1**).

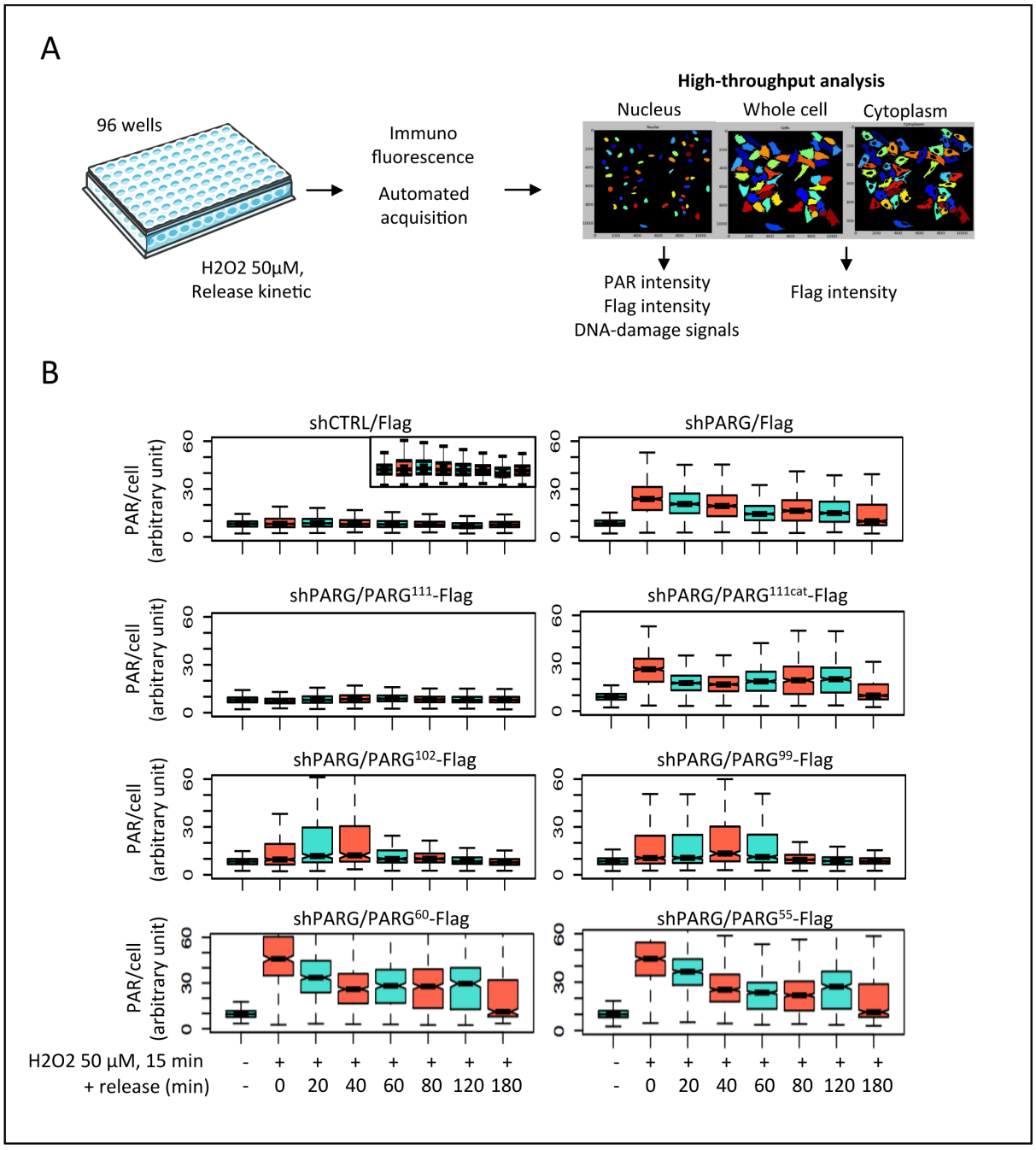

Figure 5: Understanding the contribution of PARG isoforms to PAR degradation in the nucleus. A) Experimental protocol for the high throughput analysis of stable PARG-isoforms expressing cell lines by immunofluorescence after H2O2 treatment. B) Boxplot of PAR accumulation kinetics in PARG-complemented cell lines after H2O2 treatment (50µM, 15min).

First, U2OS cell lines were treated with 50µM for 10min, and flag-tag and PAR signals were monitored through a conventional immunofluorescence experiment immediately after, and after 60 minutes release in fresh medium. Results displayed in Supplementary Figure 1 confirm the absence of flag signal in shCTRL/flag and shPARG/flag cell lines, the nuclear signal of shPARG/PARG^{111}-flag and shPARG/PARG^{111cat}-flag, the cytoplasmic signal of shPARG/PARG^{102}-flag, shPARG/PARG^{99}-flag and shPARG/PARG^{60}-flag and the mitochondrial signal of shPARG/PARG^{55}-flag. However, not all cells express the infected constructs, and the expression pattern in population is highly heterogeneous. Looking at PAR, we observe that the shCTRL/flag cells displayed transient PAR synthesis, with no polymer persistence after 1h, contrarily to shPARG/flag cells. The absence of PAR accumulation and persistence in shPARG/PARG^{111}flag, shPARG/PARG^{102}-flag and shPARG/PARG^{99}-flag suggest that all three forms contribute to PAR degradation. Meanwhile, the accumulation and persistence of PAR in shP-PARG^{111cat}-flag, shP-PARG^{60}-flag and shP-PARG^{55}-flag show that these forms indeed lack PARG activity (**Supplemental Figure 1**). To quantify more precisely the contribution of each PARG isoforms in the degradation of PAR after H_2O_2 treatment in these heterogeneous populations, we set up a high-throughput single cell immunofluorescent assay on 96 wells allowing the simultaneous comparative kinetics analysis of nuclear PAR in all cells lines using an anti-PAR antibody. Cell seeding of every cell lines, treatment with damaging agents and PAR and flag immunofluorescence are carried in parallel. After fixation and staining, 50 images/well are acquired automatically by a 20x objective on a CellInsight microscope (Cellomics), with the HCSStudio software. This step was carried with the generous help of the high-throughput cell-based screening facility of the Institute of Genetics and Molecular and Cellular Biology (IGBMC). Every image was then analysed with the Cell profiler software (Carpenter *et al.* 2006), allowing creating masks for each nuclei, based on DAPI signals in every cell. This allows the quantification of nuclear PAR intensity after a 50µM H2O2 treatment and after release a release kinetic carried until 180min after treatment (**Figure 5A**). At a dose of 50 µM, in shCTRL/Flag cells, only a transient moderate increase in PAR level is observed (**Figure 5B, zoom in**). In shPARG/Flag cells, high PAR levels were observed that only slightly decreased over time. Comparable kinetics of PAR synthesis and persistence was observed in shPARG/PARG^{111cat}-Flag cells, confirming that this inactive PARG isoform cannot degrade PAR. In contrast, complementation with PARG111-Flag in shPARG/PARG^{111}-Flag completely prevented the accumulation of PAR. Interestingly, PARG^{102}-Flag and PARG^{99}-Flag were able to efficiently degrade nuclear PAR, confirming previous observations that the cytoplasmic PARG^{102} and PARG^{99} isoforms can translocate into the nucleus upon irradiation (Haince *et al.* 2006) and are recruited to laser induced DNA damages (Mortusewicz *et al.* 2011). In shPARG/PARG^{60}-Flag and shPARG/PARG^{55}-Flag cells, PAR accumulated and persisted as in shPARG/Flag or shPARG/PARG^{111cat}-Flag cells, confirming that these two short PARG isoforms lack PAR-degrading activity (Niere *et al.* 2007). The existence of these short and inactive PARG mutants is still under debate (Niere *et al.* 2012), but our WB analyses suggest that at least PARG^{60} could be produced (**Figure 3D**). Our library of cell lines allowing the inducible expression of single PARG isoforms is therefore a tool of choice to study the functional role of each and for some still poorly characterized PARG isoforms, that is likely to be extended to other types of DNA damages.

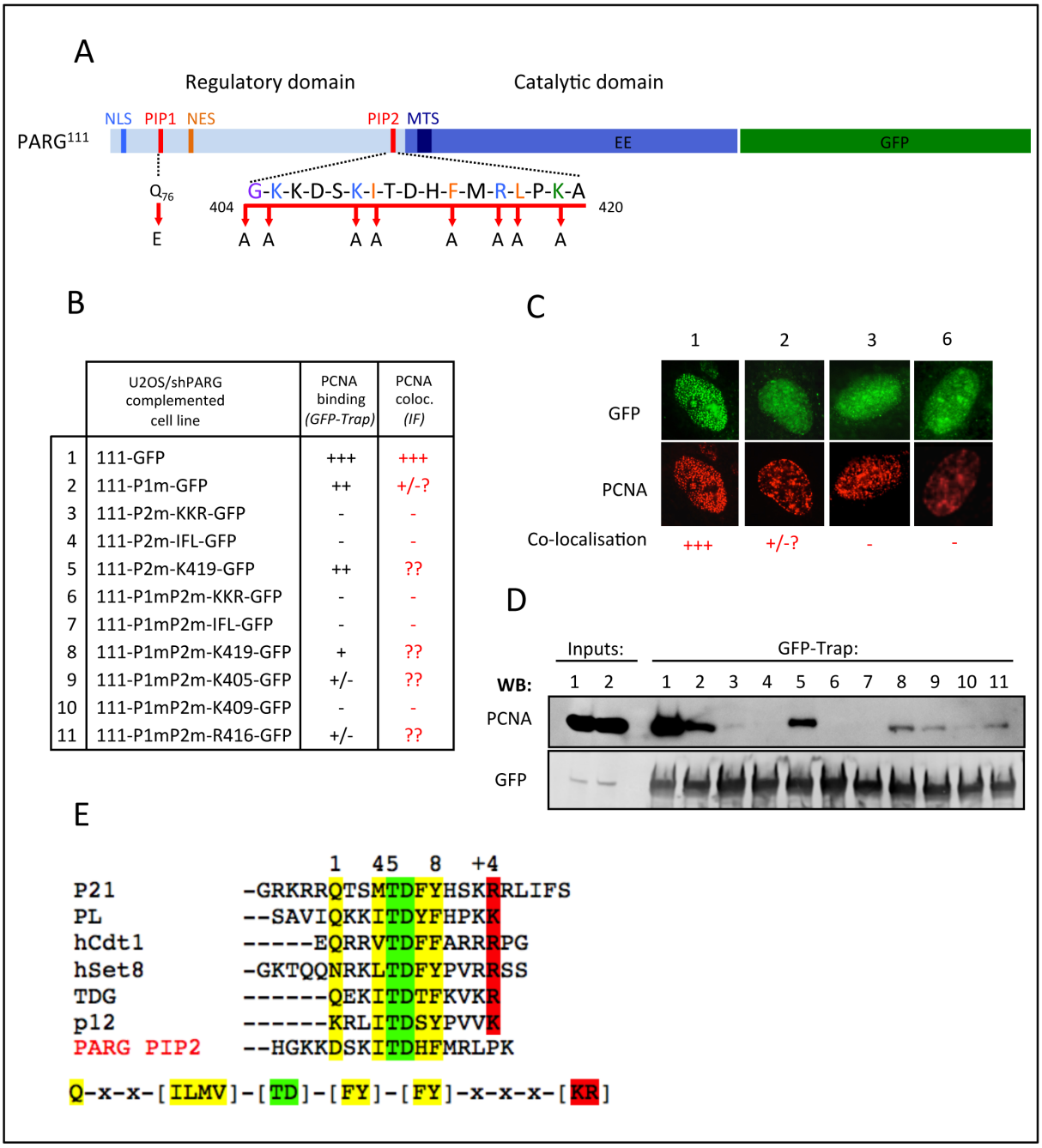

	U2OS/shPARG complemented cell line	PCNA binding *(GFP-Trap)*	PCNA coloc. *(IF)*
1	111-GFP	+++	+++
2	111-P1m-GFP	++	+/-?
3	111-P2m-KKR-GFP	-	-
4	111-P2m-IFL-GFP	-	-
5	111-P2m-K419-GFP	++	??
6	111-P1mP2m-KKR-GFP	-	-
7	111-P1mP2m-IFL-GFP	-	-
8	111-P1mP2m-K419-GFP	+	??
9	111-P1mP2m-K405-GFP	+/-	??
10	111-P1mP2m-K409-GFP	-	-
11	111-P1mP2m-R416-GFP	+/-	??

Figure 6: Generation of cell lines for the study of the PIP2-box domain of PARG. A) Generation of cell lines allowing the inducible expression of GFP-tagged PARG mutated in either one or both PCNA-interacting motifs. B) List of all U2OS cell lines expressing GFP-labelled PIP mutants of PARG and summary of their behaviour regarding PCNA binding assessed by GFP-Trap, or PCNA localization evaluated by immunofluorescence. C) Western blot after GFP-trapping of PIP-mutated PARG isoforms. D) Examples of subcellular localisation of some of the GFP-tagged PARG mutants compared to PCNA. E) Sequence conservation of the PARG PIP2-box and PIP degrons displayed on other proteins.

5. Example of application 4: generation of a library of cell lines expressing PARG single and multiple mutants to study PARG interaction with PCNA.

Note: My personal contribution to this section is restricted to the generation of the constructs and the stable cell lines. Giuditta Illuzzi, a postdoctoral fellow in our laboratory, developed the project in itself.

We have previously revealed a functional interaction between PARG and PCNA, the recruitment of PARG to laser-induced DNA damages partially depending on PARG binding to PCNA (Mortusewicz *et al.* 2011). We have identified a functional PCNA-interacting peptide (PIP) present specifically in the $PARG^{111}$ nuclear isoform. This PIP motif was however not solely responsible for PCNA binding, its mutation strongly reducing PCNA-dependent recruitment of PARG to replication foci and to laser-induced DNA damages but not affecting PCNA co-purification in immunoprecipitation experiments (Mortusewicz *et al.* 2011, and **Supplementary Figure 2A)**.
We therefore suspected the existence of a second region of interaction within PARG, but identified no canonical PIP motif or APIM motif, another described PCNA-interacting motif (Gilljam *et al.* 2009).
By GFP-trap and through the generation of several deletion constructs, we restricted this region to residues 404 to 420 (**Supplementary Figure 2B**). Plotting the amino acid sequence on a helical wheel revealed the possible formation of a hydrophobic surface with I410, F414 and L417 residues and a basic surface with K405, K409 and R416 residues (**Supplementary Figure 2C**). Mutations of these two regions totally prevented PARG and PCNA interaction, whereas mutation of K419 but not G404 had a lesser impact (**Supplementary Figure 2D**). In order to functionally assess *in vivo* the possible contribution of these putative regions in PARG/PCNA interaction, we generated a library of plasmids and corresponding lentiviruses-expressing single or multiple mutants of this second PCNA-interacting motif (named PIP2, **Figure 6A**, **Figure 6B** and **Supplementary Figure 2C**). These mutations were introduced in a GFP-tagged wild type $PARG^{111}$ (111-GFP) or $PARG^{111}$ mutated in its previously identified PIP motif, renamed PIP1 (111-P1m-GFP), driven by the inducible TRE promoter. U2OS stable cell lines were established for representative constructs (**Figure 6B**). By immunofluorescence, we revealed that, as previously reported (Mortusewicz *et al.* 2011), mutation of PIP1 strongly affected PARG localization to replication foci (**Figure 6C**). Triple mutants invalidating completely either the hydrophobic region or the basic region of PIP2 dramatically affected PARG co-localisation to replication foci, even when PIP1 was intact. By GFP-trap experiments, we revealed that this second PIP2 motif is even more crucial for the PARG/PCNA interaction since mutations in its hydrophobic region or basic region completely abolished the interaction, whereas strong residual interaction was still observed when only PIP1 motif was mutated (**Figure 6D**). Within the basic region, K409 appeared to be critical since its mutation was sufficient to abolish PCNA co-purification with PCNA when PIP1 was mutated, whereas K405 and R416 still displayed a weak residual binding. K419, also slightly impacted the interaction, particularly when PIP1 was also mutated. Taken together, these experiments allowed to determine that PARG interaction with PCNA involved two regions: the first canonical PIP1 mutant we previously reported, localised only in $PARG^{111}$ and a non canonical PIP2 motif, present in $PARG^{111}$, $PARG^{102}$ and $PARG^{99}$, involving residues 405 to 419. In the frame of this work, a study came up reporting the characterization of this second PIP2 motif, revealing the importance of K409 that was shown to be a target for acetylation (Kaufmann *et al.* 2017). The authors solved a 3D structure of this PIP2 peptide in complex with PCNA, showing that the

peptide adopts conformation similar to a canonical PIP-box domain, nesting in a hydrophobic pocket within the interdomain connector loop of PCNA. Analyzing the sequence conservation of this PIP2-box with other proteins, we noticed that PARG-PIP2 closely resembles a PIP degron structure, except for a basic residue normally present in the +4 position, which is in +5 position in the case of PARG (**Figure 6E**). A PIP degron is a specialized PIP box that interacts with chromatin bound PCNA, thus providing a scaffold for the recruitment of E3 ubiquitin ligases that can interact, ubiquitinate and mediate the 26S proteasome dependent degradation of protein factors, in a cell phase dependent fashion or in response to DNA damage (Havens and Walter, 2009). This hypothesis of the second PIP-box acting as a PIP degron in PARG is under investigation, but it makes no doubt that our inducible system will provide an interesting tool to answer such functional questions.

Conclusions

Human PARG is an important protein for mediating PAR degradation upon genotoxic stress, whose study was complicated by the existence of five isoforms of different subcellular localization, expressed in low abundance in human cells. Until now, tools were missing in order to decipher the biological functions of PARG isoforms and their relative contribution in mechanisms such as DNA repair. In the present work, we generated libraries of plasmids allowing either the transient or stable expression of PARG isoforms or PARG mutated versions in a variety of cell lines. The two-plasmid strategy developed herein allows the depletion of all endogenous forms of PARG and the re-constitution with any form of the protein. The PARG isoforms generated have cellular localizations and activities that are consistent with the literature, showing the relevance of this approach to study biological questions. We provided new evidence showing that although being cytoplasmic, PARG^{102} and PARG^{99} can both contribute to PAR degradation in the nucleus after DNA damage. We showed that PARG^{102} is the most abundant PARG isoform in cells, and that it can be produced from the PARG^{111} mRNA transcript, most likely by the use of an alternative-starting site. This cloning strategy and construct library also allowed investigating the functional interaction between PCNA and PARG, highlighting the importance of the PIP2-box for PCNA binding. Taken together, these results illustrate that we provided a new versatile molecular tool for the assessment of the role of human PARG in many different cell lines. This library therefore bears a lot of potential, for it might be used to solve many other types of biological questions involving the PARG protein.

Materials and Methods

Cell culture and treatments

All U2OS and HeLa cell lines were cultured in Dulbecco's Modifed Eagle's Medium (DMEM 1 g/l glucose) (Invitrogen) supplemented with 10% foetal bovine serum, 1% gentamicin (Invitrogen) under 5% CO2. BOSC cell lines were cultures in DMEM 4,5g/L supplemented with 10% foetal bovine serum, 1% gentamicin (Invitrogen) under 5% CO2. U2OS shCTRL and shPARG are cultured with the addition of Puromycine, and complemented cell lines are cultured under puromycine (1µg/mL) and hygromycine selection (125µg/mL). Doxycycline induction of stable cell lines is carried for at least 24 hours before each experiment with 1µg/mL doxycycline. For H2O2

treatments, normal culture media is replaced with H2O2 supplemented media at the indicated concentrations. Cells are washed twice with PBS and normal media is added for indicated release times.

Cloning and vector generation

All cloning operations and vector generation were carried following a Golden Gate technology-based protocol developed in B.Reina San Martin's lab in the IGBMC (Strasbourg).

Lentiviral infections

BOSC cells are plated at 50-60% confluency in 6 wells plates (0,3x10^6 cells/well) with, 2mL medium per well. 24h later, cells are transfected with 1µg of the vector of interest, 0,9µg of Helper plasmid-pCMVdR8.91 and 0,1µg Helper plasmid-VSVG using the Fugene (Roche) transfection agent according to the manufacturers instruction with a 1:2 ratio. After 48h to 72h, the media turns yellow and the supernatant is collected and filtered through a Collect the viral SN from BOSC and filter it through a 0,45µM syringe filter. The volume is adjusted to 2mL with DMEM and supplemented with 10µg/mL Polybrene and 20mM HEPES. The U2OS media is replaced with the BOSC supernatant and cells are spin-fected by centrifugation (2500rpm, 90min, RT). Infected cells are cultured for 24h to 48h, and culture media is replaced by a selection media of either Hygromycine (Roche 1 :400 = 125µg/mL) or Puromycine (1µg/mL). Cells are selected for 72h in case of puromycine selection and 10 days for hygromycine selection.

GFP trapping

For each cell line, one P150 is used at 80% confluence, after 48h doxycycline induction. Plates are washed twice with cold PBS on ice. Cells are scrapped on ice with a lysis crosslinking buffer (900µL HEPES buffer + inhibitors + DSP 1,5mM (30mM stock). Lysate is collected in a 2mL eppendorf and pipetted 15 times vigorously. Lysates are left at 2h at 4°C on a rotating wheel for crosslinking. Crosslinking reaction is stopped by adding Tris (50mM final – 50µL for each tube with Tris-HCl 2M). Lysates are left for an additional time of 15min rotation at 4°C. Samples are centrifuged (13,200 rpm, 4°C, 15min) and supernatant in a new 1,5mL eppendorf. 1/10 of the sample is kept aside as an input and completed with Laemmli buffer. 10µL of GFP trap beads washed in HEPES Lysis Buffer with no DSP are added to remaining supernatant, and left under rotation (ON, 4°C). GFP trap beads are Collected by centrifugaton, (2min, 2000rpm, 4°C). Beads are washed thrice with 300µL HEPES lysis buffer + inhibitors (no DSP). During the last wash, beads are dried using special flat tips. Beads are collected in 12µL Laemmli buffer, boiled 5min at 95°C before analysis by western blotting.

Western blotting

Samples are boiled for 5min at 95°C in Laemmli buffer, loaded on a 4-20% gradient gel (Biorad) and migrated for 1h30 at 130V at ambient temperature in running buffer (25mM Tris, 190mM glycine, 0,1% SDS). Gels are transferred on nitrocellulose membrane in transfer buffer (25mM Tris, 190mM glycine, 20% ethanol). Blots are transferred for 2h at 4°C. Nitrocellulose membranes are blocked in TBS-Tween 0,05%, 5% milk for 30min RT. Membranes are probed with GFP mouse monoclonal antibody (Roche 1/10000), GST antibody (ref), PARG-Nter

polyclonal antibody (homemade, 1:2000), flag monoclonal antibody (1:10000) (ref), PAR H10 antibody (1:2000) and revealed with either fluorescent secondary antibodies and revealed at the odyssey scanner (LICOR), or HRP-coupled antibodies and revealed with a camera (LAS4000).

Immunofluorescence

Hela cells are plated and transiently transfected with knockdown and reconstitution vectors using Fugene reagent according to the manufacturers instructions. U2OS cells used for this experiment are seeded in 24 wells plates, 75000 cells on 12mm coverslips (Greiner). After two days of induction with doxycycline-supplemented media, cells are washed once with PBS on ice. A pre-extraction step using two washes of 5 min with CSK+Triton 0,5% is carried. Cells are fixed with PFA 3,7% for 20min, RT. Slides are blocked in PBS+3%BSA for 15 minutes and cells are permeabilized with 2 washes of PBS-Tween 0,1%. Cover slides are incubated with 250µL of PBS-Tween0,1% + 1% BSA containing primary antibodies over-night at 4°C.

High-throughput Immunofluorescence

U2OS cells (3000 cells/well) of each stable cell lines were plated in 96 wells plates (Greiner CELLSTAR). Cells are induced for 16h with 1ng/µL doxycycline, before doing a reverse kinetic treatment with 50µM H202. Plate is stopped on ice and cells are washed once in cold PBS. Cells are fixed with a Methanol/acetone solution (1:1) for 30min at 20°C. After a blocking step of 1h (PBS-Tween 0,1%, 1%BSA), and three permeabilization washes (PBS-Tween 0,1%) cells are incubated overnight with primary antibodies (Flag-mouse IgG1, 1:10000, PAR-H10 mouse IgG3κ antibody, 1:2000). After 2 washes with PBS, cells are incubated with the appropriate secondary antibody (Alexa). 50 images/well are acquired automatically by a 20x objective on a CellInsight microscope (Cellomics), with the HCSStudio software. Images were analysed with the Cell profiler software (Carpenter *et al.* 2006) and boxplots generated with the R software (R 3.4.2).

Acknowledgements

We wish to thank A. Maglott-Roth from the High Throughput Cell-based screening facility of the IGBMC for her assistance in high throughput immunofluorescence acquisition. This work was supported by the Centre National de la Recherche Scientifique, Université de Strasbourg, Ligue contre le Cancer and Fondation pour la Recherche Médicale. EH was supported by the French Ministère de l'Enseignement Supérieur et de la Recherche and the Fondation pour la Recherche Médicale.

Bibliography :

Amé, J.C., Fouquerel, E., Gauthier, L.R., Biard, D., Boussin, F.D., Dantzer, F., de Murcia, G., and Schreiber, V. (2009). Radiation-induced mitotic catastrophe in PARG-deficient cells. J Cell Sci *122*, 1990-2002.

Cortes, U., Tong, W.M., Coyle, D.L., Meyer-Ficca, M.L., Meyer, R.G., Petrilli, V., Herceg, Z., Jacobson, E.L., Jacobson, M.K., and Wang, Z.Q. (2004). Depletion of the 110-kilodalton isoform of poly(ADP-ribose) glycohydrolase increases sensitivity to genotoxic and endotoxic stress in mice. Mol Cell Biol *24*, 7163-7178.

Erdelyi, K., Bai, P., Kovacs, I., Szabo, E., Mocsar, G., Kakuk, A., Szabo, C., Gergely, P., and Virag, L. (2009). Dual role of poly(ADP-ribose) glycohydrolase in the regulation of cell death in oxidatively stressed A549 cells. Faseb J *23*, 3553-3563.

Fisher, A.E., Hochegger, H., Takeda, S., and Caldecott, K.W. (2007). Poly(ADP-ribose) polymerase 1 accelerates single-strand break repair in concert with poly(ADP-ribose) glycohydrolase. Mol Cell Biol *27*, 5597-5605.

Gilljam, K.M., Feyzi, E., Aas, P.A., Sousa, M.M., Muller, R., Vagbo, C.B., Catterall, T.C., Liabakk, N.B., Slupphaug, G., Drablos, F.*, et al.* (2009). Identification of a novel, widespread, and functionally important PCNA-binding motif. J Cell Biol *186*, 645-654.

Haince, J.F., Ouellet, M.E., McDonald, D., Hendzel, M.J., and Poirier, G.G. (2006). Dynamic relocation of poly(ADP-ribose) glycohydrolase isoforms during radiation-induced DNA damage. Biochim Biophys Acta *1763*, 226-237.

Illuzzi, G., Fouquerel, E., Ame, J.C., Noll, A., Rehmet, K., Nasheuer, H.P., Dantzer, F., and Schreiber, V. (2014). PARG is dispensable for recovery from transient replicative stress but required to prevent detrimental accumulation of poly(ADP-ribose) upon prolonged replicative stress. Nucleic Acids Res *42*, 7776-7792.

Koh, D.W., Lawler, A.M., Poitras, M.F., Sasaki, M., Wattler, S., Nehls, M.C., Stoger, T., Poirier, G.G., Dawson, V.L., and Dawson, T.M. (2004). Failure to degrade poly(ADP-ribose) causes increased sensitivity to cytotoxicity and early embryonic lethality. Proc Natl Acad Sci U S A *101*, 17699-17704.

Meyer, R.G., Meyer-Ficca, M.L., Whatcott, C.J., Jacobson, E.L., and Jacobson, M.K. (2007). Two small enzyme isoforms mediate mammalian mitochondrial poly(ADP-ribose) glycohydrolase (PARG) activity. Exp Cell Res *313*, 2920-2936.

Meyer-Ficca, M.L., Meyer, R.G., Coyle, D.L., Jacobson, E.L., and Jacobson, M.K. (2004). Human poly(ADP-ribose) glycohydrolase is expressed in alternative splice variants yielding isoforms that localize to different cell compartments. Exp Cell Res *297*, 521-532.

Mortusewicz, O., Fouquerel, E., Ame, J.C., Leonhardt, H., and Schreiber, V. (2011). PARG is recruited to DNA damage sites through poly(ADP-ribose)- and PCNA-dependent mechanisms. Nucleic Acids Res *39*, 5045-5056.

Niere, M., Mashimo, M., Agledal, L., Dolle, C., Kasamatsu, A., Kato, J., Moss, J., and Ziegler, M. (2012). ADP-ribosylhydrolase 3 (ARH3), not poly(ADP-ribose) glycohydrolase (PARG) isoforms, is responsible for degradation of mitochondrial matrix-associated poly(ADP-ribose). The Journal of biological chemistry *287*, 16088-16102.

Whatcott, C.J., Meyer-Ficca, M.L., Meyer, R.G., and Jacobson, M.K. (2009). A specific isoform of poly(ADP-ribose) glycohydrolase is targeted to the mitochondrial matrix by a N-terminal mitochondrial targeting sequence. Exp Cell Res *315*, 3477-3485.

Knockdown vector	Promoter	cDNA	Reporter	Selection
pXK1	H1: shCTRL1	SV40- rtTA	GFP	hygro
pXK2	H1: shCTRL2	SV40- rtTA	GFP	hygro
pXK3	H1: shPARG1	SV40- rtTA	GFP	hygro
pXK4	H1: shPARG2	SV40- rtTA	GFP	hygro
pXK5	H1: shCTRL1	SV40- rtTA	-	hygro
pXK6	H1: shCTRL2	SV40- rtTA	-	hygro
pXK7	H1: shPARG1	SV40- rtTA	-	hygro
pXK8	H1: shPARG2	SV40- rtTA	-	hygro
pXK9	H1: shCTRL1	CMV- rtTA	IRES:CFP	hygro
pXK10	H1: shPARG1	CMV- rtTA	IRES:CFP	hygro
Reconstitution vector	**Promoter**	**cDNA**	**Reporter**	**Selection**
pXR1	TRE	$PARG^{111}$-flag	SV40 GFP	puro
pXR2	TRE	$PARG^{111cat}$-flag	SV40 GFP	puro
pXR3	TRE	$PARG^{102}$-flag	SV40 GFP	puro
pXR4	TRE	$PARG^{99}$-flag	SV40 GFP	puro
pXR5	TRE	$PARG^{60}$-flag	SV40 GFP	puro
pXR6	TRE	$PARG^{55}$-flag	SV40 GFP	puro
pXR7	TRE	$PARG^{111}$	SV40 GFP	puro
pXR8	TRE	$PARG^{102}$	SV40 GFP	puro
pXR9	TRE	$PARG^{99}$	SV40 GFP	puro
pXR10	TRE	$PARG^{60}$	SV40 GFP	puro
pXR11	TRE	$PARG^{55}$	SV40 GFP	puro
pXR12	TRE	PARG-Q76/E	SV40 GFP	puro
pXR13	TRE	PARG-KKR/AAA	SV40 GFP	puro
pXR14	TRE	PARG-IFL/AAA	SV40 GFP	puro
pXR15	TRE	PARG-K419/A	SV40 GFP	puro
pXR16	TRE	PARG-Q76/E+KKR/AAA	SV40 GFP	puro
pXR17	TRE	PARG-Q76/E+IFL/AAA	SV40 GFP	puro
pXR18	TRE	PARG-Q76/E+K419/A	SV40 GFP	puro
pXR19	TRE	PARG-K405/A	SV40 GFP	puro
pXR20	TRE	PARG-K409/A	SV40 GFP	puro
pXR21	TRE	PARG-R416/A	SV40 GFP	puro
pXR22	TRE	PARG-WT - IRES	IRES GFP	puro
pXR23	SV40	PARG111	SV40 GFP	puro
pXR24	SV40	PARG111 SSAA	SV40 GFP	puro
pXR25	SV40	PARG111 SSDD	SV40 GFP	puro
pXR27	TRE	flag	SV40 GFP	puro

Supplemental Table 1: List of the pXpA expression vectors generated, using the Golden Gate Cloning Technology. Constructs highlighted in green are used in the present study.

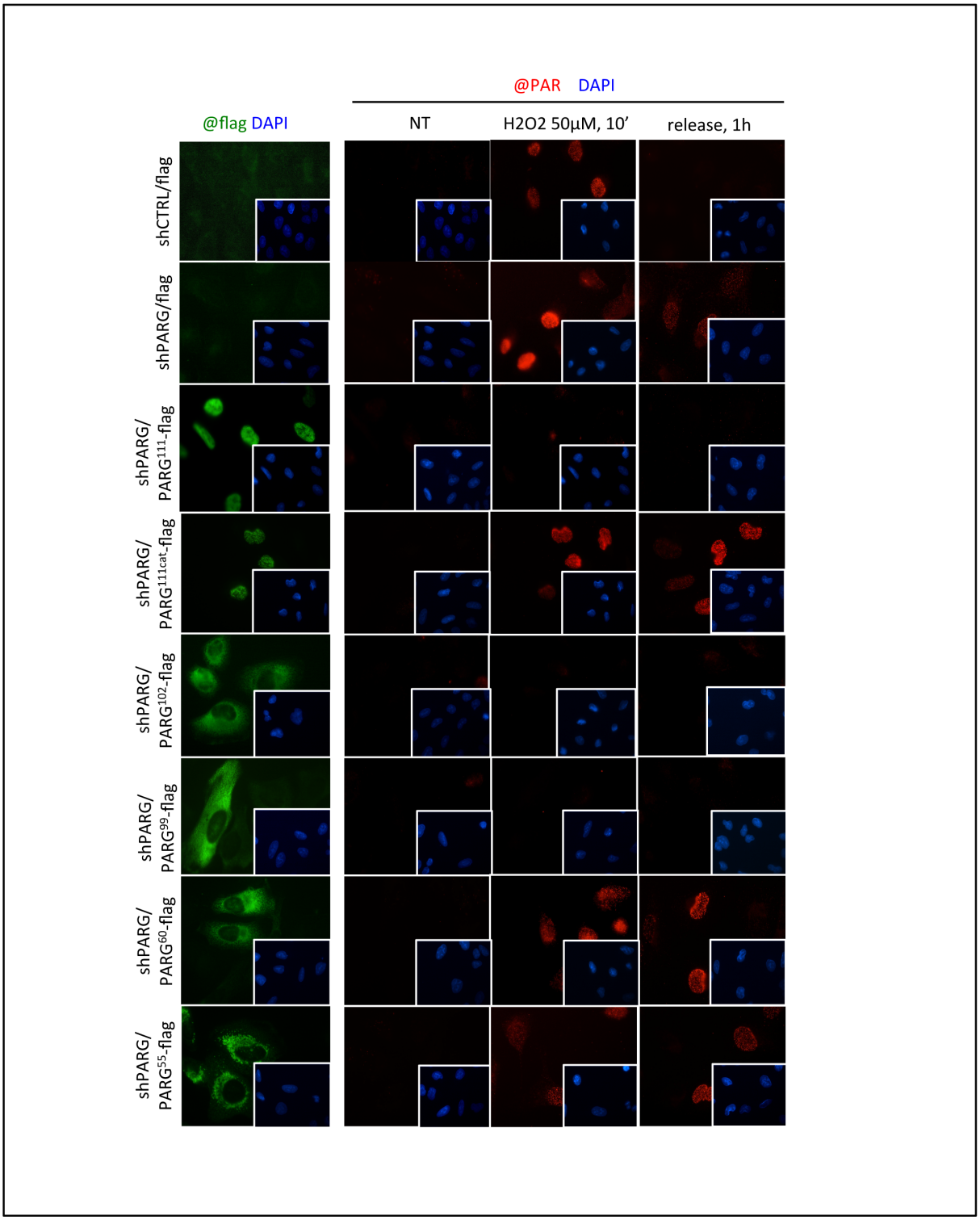

Supplemental Figure 1: Immunofluorescence of shCTRL and shPARG complemented U2OS cell lines after H2O2 treatment (H202, 50µM, 10'). Flag antibody marking (1:10000 green) reveals the cell localization of each construct. PAR degradation is followed in red with an anti-PAR H10 (1:2000)

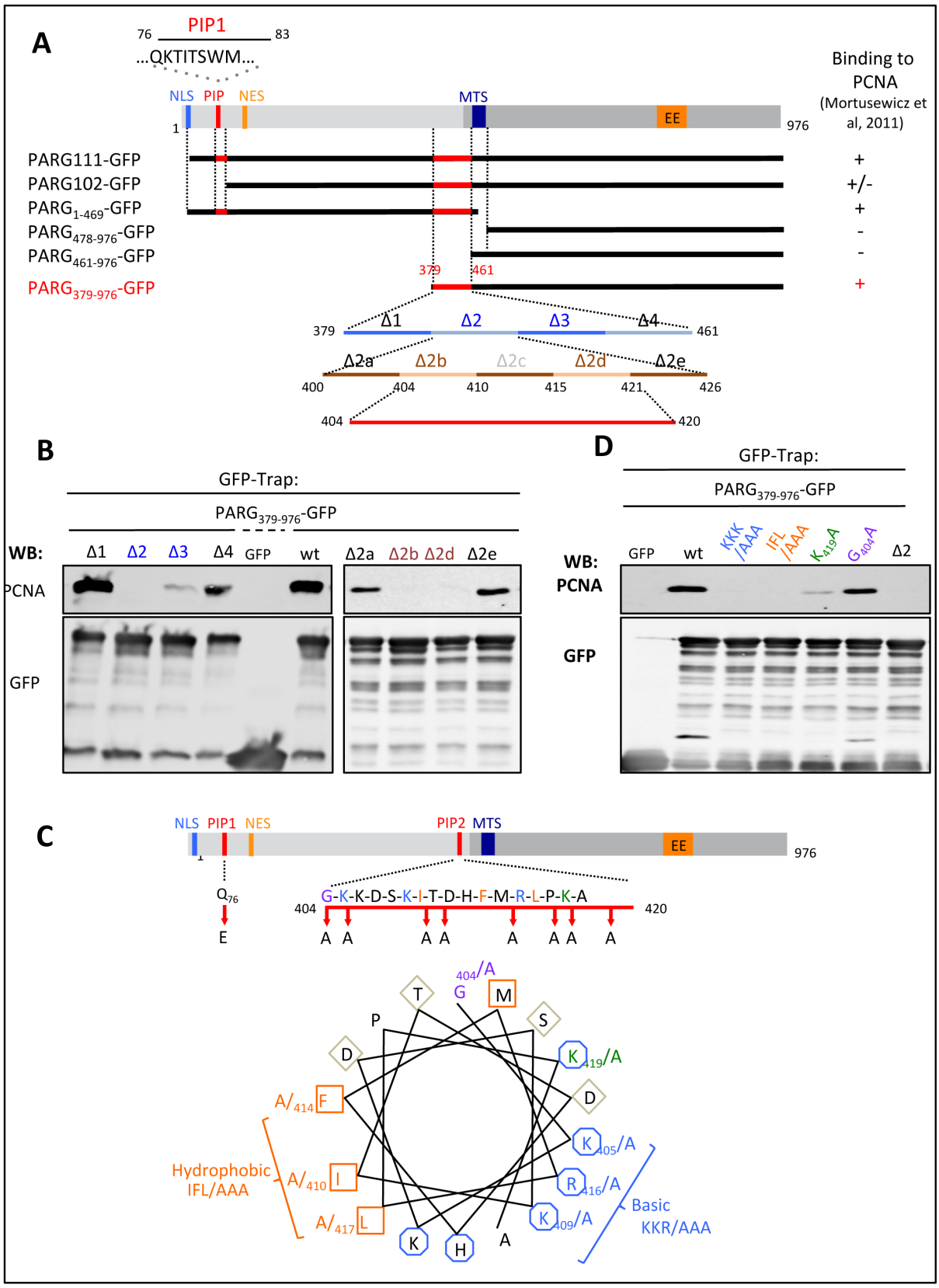

Supplemental Figure 2: A) PIP domains mutations or deletions generated in PARG sequences. B) Western blot after GFP-trapping of PARG-GFP deletion mutants. C) Helical wheel plotting of the PARG PIP2-box domain. This PIP-box displays a hydrophobic IFL region and a basic KKR sub-motif that were mutated. D) Western blot after GFP-trapping of the GFP-labelled PIP2-box mutated versions of PARG

Discussion

1. *Choice of cell line*

Our lab had previously described PARG deficient HeLa cell lines that were used efficiently for asking several questions related with PARG biology (Amé *et al.* 2009, Mortusewicz *et al.* 2011, Illuzzi *et al.* 2014), and many other cell lines deficient for all PARG isoforms already exist. Since we wanted to decipher the role of PARG isoforms in DNA repair, we deliberately chose to create our stable induction system in U2OS cells (ATCC®HTB-96™). U2OS cells (U-2 OS) are Human epithelial adherent cells derived from an osteosarcoma from a 15 year-old Caucasian patient. They are easily transfectable, broadly used for laser micro-irradiation experiments and DNA repair studies in general and thus seemed to fit our purposes perfectly. In addition, we noticed that our previous PARG-deficient HeLa cell model was displaying spontaneous γH2AX accumulation in the absence of damage. Moreover, HeLa cells are mutated for p53, whereas U2OS cells are p53 proficient. Nonetheless, our two-plasmid system can be used either transiently or through stable infections in any cell line. In the study, we demonstrated that the transient expression of our plasmids in either Bosc cells or Hela cells was sufficient to induce the isoform expression at the right size and localization.

2. *Efficiency of PARG depletion*

In our new cell model, PARG depletion with the shRNA targeting all PARG isoforms is non lethal, and cells displayed no growth variations (data not shown). On western blots, we can always see that PARG depletion is efficient, either after transient transfection or after stable infection with the knockdown plasmid. Cells accumulate PAR spontaneously, and PAR induction was remarkably increased after oxidative damage triggered upon H_2O_2 treatment. We used the same shRNA sequence as in the HeLa shPARG cell lines previously described in Amé *et al.* 2009, thus we believe that PARG depletion is efficient. However, when looking at the PAR accumulation kinetics after treatment with H_20_2 and release in shPARG-flag cell lines, either by western blot or by immunofluorescence, we observed that PAR levels decrease over time. After 2h of release, polymer still persists, but the global amount in cells is reduced. Although other PAR-degrading enzymes may contribute to PAR degradation in the nucleus, such as ARH3 or MacroD1 (Massimo *et al.* 2013; Chen *et al.* 2011; Fontana *et al.* 2017), we cannot exclude that PARG depletion is not complete. A convenient way of avoiding such questions would have been to generate a PARG knockout mutant cell line with the CRISPR/Cas9 system. At the time the project started however, CRISPR/Cas9 was not yet fully handled: the design of guide RNAs was complicated by the existence of PARG pseudogenes in the genome (J.C-Amé, personal communication), a lot of off-targets were reported in the literature, and using CRISPR mutants implied the selection of one or several clonal populations, situation which we wanted to avoid. Working with a global cell population seemed more accurate to us, for we can perform statistics on a cell population.

3. *Expression levels of complemented PARG isoforms*

We have to point out the major difficulties encountered during the generation of these cell lines. Upon transient transfection with both the knockdown and the reconstitution vectors, transfection might be heterogeneous, and not all cells express the isoforms at the same levels, as seen in immunofluorescence, or by western blot. The same problem is encountered after lentiviral infection, for we do not know whether cells have integrated one or several copies of each knockdown or reconstitution vectors. We used lentiviral infection rather than retroviral infection because lentiviruses allow the infection of both dividing and non-dividing cells, but both systems usually allow the integration at up to 10 sites in the host genome. We don't master the sites of integration of each construct either, so every cell is likely to display very different expression levels for each vector integrated. Some cells might integrate multiple copies of the knockdown vector and few copies of the reconstitution vectors, generating a broad range of patterns in the expression profile. Additionally, if the reconstitution vector copies are integrated in unfavourable chromatin environments, with a low accessibility for the rtTA protein upon doxycycline induction, cells might also display heterogeneous expression levels. To overcome these problems, we could have rigorously selected cells with the correct copy numbers. This could involve characterizing cell colonies by performing qPCR on every clonal population (Charrier *et al.* 2010), but this still doesn't inform us on the site of integration either, and working on clonal population is what we wanted to avoid. Alternatively, we could have designed our cloning vectors in order to select the cell population for those basally expressing the same amount of rtTA protein, and the same level of reconstituted PARG after doxycycline induction. For this purpose, we could have added fluorescent tags to both rtTA and PARG isoforms, but this is always at the detriment of fluorescent channels available for experiments. Nonetheless, although our PARG-flag constructs were not adequate for this purpose, this was done for the PARG-GFP constructs in order to study the PIP2 interaction motif, in order to gather a cell population that was more homogeneous in their fluorescence level. Yet, another problem arising was to master the doxycycline induction.

4. *Tet-system leakage*

Our cloning strategy in U2OS cellular model was based on the selective expression of PARG isoforms upon doxycycline induction. This is based on the classical Tet-On system, derived from the original comprehension of the bacterial tetracycline responsive Tet Operon, and is a widely used tool in biology, from molecular biology to gene therapy applications (Das *et al.* 2016). The first Tet-On system developed for eukaryotic cells was improved to reduce the doxycycline levels needed to induce expression, and Tetracyclin Responsive Elements (TRE) promoters were engineered to diminish residual binding of the rtTA protein in absence of doxycycline (Gossen *et al*. 1995, Loew *et al.* 2010). Although our vector system uses one of the last generation TRE promoter, based on 7 repeats of the Tet-operator, our stable cell lines displayed a high leakage, with isoforms expression even without doxycycline induction. We initially thought this could be due to a contamination of our DMEM media with residual-doxycycline-containing bovine foetal serum. But even culturing our cell lines in doxycycline-free serum-containing media didn't change the pattern. This leakage seen in western blot is likely

the result of a sub-population of cells in which the rtTA to TRE ratio available is sub-optimal, because of the reasons discussed in the above paragraph. If all induction systems display some basal leakage, it is true that Tet-On was described as having the highest, compared with glucocorticoid responsive or ecdysone-inducible models (*Meyer-Ficca et al. 2004, b*). We kept the Tet-On system for we wanted to be able to modulate gene expression with increasing concentrations of PARG in our assays. Moreover, the quantitiative immunofluorescence techniques we developed were enabling to considerate single cells among the global population, thus circumventing the limitations of our model.

5. Endogenous PARG levels VS complemented cell lines PARG levels

Initially, we thought that doxycycline levels would allow a very fine-tuning of PARG isoforms levels in our cell models. Again, we were very disappointed with the behaviour of our cell lines, for two reasons: first, because the leakage of the system already produced higher reconstituted-PARG levels than the endogenous PARG in some cells; then because we couldn't express the isoforms at similar levels. The standard protocol for doxycycline induction is treating between 24h-48h with 1µg/mL doxycycline, producing very high amounts of PARG isoforms in cells. We did several tests in order to adjust the doxycycline induction dose or the doxycycline treatment time, to reduce it to something close to the endogenous levels. As shown in **Figure 28**, there is already a strong expression of $PARG^{102}$ and $PARG^{99}$ even without induction. $PARG^{111}$ and $PARG^{111cat}$ could be induced at reasonable levels, after 4h induction at 1µg/mL or after 16h induction at 1ng/mL.

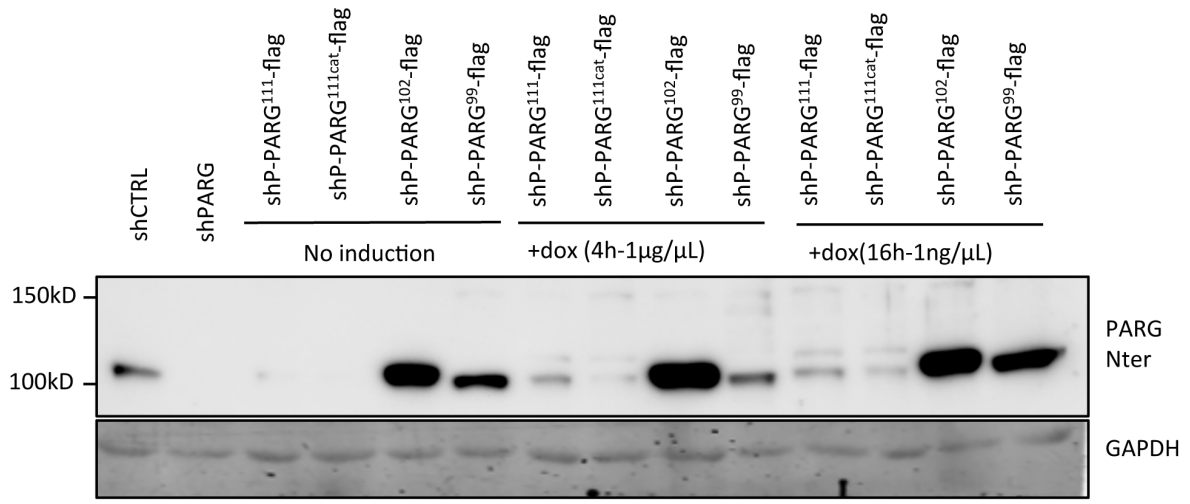

Figure 28: Doxycycline induction of stable cell lines expressing flag-tagged PARG isoforms.

Western blot of U2OS stable cell lines expressing PARG isoforms, after no induction, or treatment with doxycycline for the indicated times.

This is a problem since PARG has a very high activity, and even undetectable amounts of the endogenous protein are sufficient to degrade polymer efficiently in cells. In our PAR degradation assay, we obtained similar results between induced or non-induced cells (data not shown). The analysis of single cells to correlate the flag

expression levels and the PAR degradation was probably the only way to reduce the bias intimately linked with the flaws of the system, however when we tried, we couldn't observe any correlation (data not shown). This suggests indeed that PAR degradation can occur, even in the absence of detectable flag signal.

However, the expression of the untagged versions of the PARG isoforms, regardless of their expression levels allowed us to confirm that PARG^{102} was the most abundant isoform in U2OS cells. This is also the case with Hela cells, HEK293T cells, BOSC cells and HCT116 cells. Since PARG^{102} can contribute to nuclear degradation of PAR after damage, and translocates to the nucleus (Mortusewicz *et al.* 2011; Haince *et al.* 2006), the production and stabilization of PARG^{102} and the regulation of its nucleo-cytoplasmic shuttling could be a way for cells to regulate basal level of damages, while PARG^{111} production in very low amounts could be used to handle more severe damage producing higher levels of PAR. Alternatively, since PARG^{111} is associated with replication foci, it could have a specific function during replication, in response to replication stress. Because PARG is a protein of very low abundance in cells, investigating these questions would require other methods and strategies and could be the object of another research project in its own. CRIPSR-Cas9 knock-in strategies would probably be the golden-standard method to introduce reporter genes and tags to human PARG, in order to refine our understanding of the endogenous situation.

6. Is PCNA a PIP-degron?

For the PCNA project (developed by G. Illuzzi), we tried to get rid of "leaky" cells by selecting a GFP-negative population by FACS before doxycycline induction. After 24h induction with 1µg/mL doxycycline, two populations of "high-GFP" and "low-GFP" were selected for their proper induction capacity. From these inducted cells, it took 72h for the GFP levels to decrease after the removal of doxycycline, suggesting that the PARG^{111} protein is highly stable. Such stability complicates the functional study of the PIP2 motif. We assumed that the PIP2 motif could act as a PIP-degron, a peptide motif allowing the interaction between PCNA and the efficient targeting of PCNA-interacting proteins to the proteasome to mediate their degradation, through the recruitment of the E3 Ubiquitin Ligase CRL4 (Havens and Walter, 2009; Tsanov *et al.* 2014). Indeed, the PIP-motif showed similarity with other PIP-degrons (p21, p12, hSet8…) except it doesn't display the basic arginine or lysine residue in its +4 position. In addition, we discovered an interaction between PARG and the Cullin4A and Cullin4B subunits of the CRL4 enzyme (data not shown). However, despite intensive trial, we did not observe any significant degradation during S-phase progression, or after treatment with various DNA-damaging agents (H202, MNNG, CPT), in contrast to the p21-PIP-degron protein used as a control (data not shown). Only after long HU treatment, PARG levels seemed to decrease, but this was independent on the PIP-degron motif, since its mutation didn't abolish this decrease. Regarding the difficulty to set an efficient experimental procedure to investigate PARG degradation in interaction with PCNA, this question remains to be clearly answered.

Conclusion

Despite all the limitations described above, our cloning system, and vector/cell library enabled to shed light on several aspects of PARG biology. No model is perfect, and we should always keep in mind the limitations of each method used in research. However, we successfully generated a new molecular toolbox to selectively study the contribution of PARG isoforms in DNA repair. Although we limited ourselves to the follow up of PAR degradation after oxidative damage, we could also quantify DNA-damage markers comparatively, in each cell lines and in response to other types of damages. Many more applications await, since we are still lacking of many elements to fully understand the roles of PARG in human cells.

Aim two: Study of the regulation of PARG by post-translational modifications.

Introduction

PARP1 and PARG are two enzymes of opposite catalytic activities, respectively mediating the catalysis and the degradation of Poly(ADP-ribose), a versatile post-translational modification (PTM) that is conserved across eukaryotic organisms. Poly(ADP-ribose), as a nucleic-acid-like molecule, acts as a modulator of protein activity and as a scaffold for the recruitment of many protein factors. Its expanding roles in DNA repair, transcription, replication, cell death and development need it to be finely regulated in time and space (for a review, see Martin-Hernandez *et al.* 2017, Schuhwerk *et al.* 2016, Chaudhuri and Nussenzweig, 2017). More importantly, this modification needs to be dynamically induced or removed, in response to any kind of cellular stress. It has been demonstrated that the kinetics of PARylation was crucial to determine the fate of cells upon DNA damage, and that whereas small transient amounts of PAR are beneficial for they activate DNA-repair, prolonged over-accumulation of PAR is detrimental (Schuhwerk *et al.* 2017; Amé *et al.* 2009; Illuzzi *et al.* 2014). This tight regulation of PAR homeostasis is mainly achieved by the direct and dynamic regulation of its writers and erasers catalytic activities, mainly PARP1 and PARG.

PARP1 has a modular structure, whose modification by PTMs allows a dynamic rearrangement of its different modular amino acid domains (Gibson and Kraus, 2012). Among all PTMs, phosphorylation is the best-described example for regulating PARP1. For instance targeting of serine 372 and threonine 373 by the ERK1/2 kinase reduces PARP1 activity (Kauppinen *et al.* 2006, Cohen-Armon *et al.* 2007), while phosphorylation of serine 785 and Serine 786 by CDK2 are essential for enhancing PARP1's activity (Wright *et al.* 2012). Several other examples are reported, that allow a dynamic regulation (reviewed in Piao *et al.* 2017). Many more sites were identified in a proteomic analysis of phosphorylation sites in PARP1, but the roles for each of them is not yet characterized (Gagné *et al.* 2008). Evidence for PARG phosphorylation have been scarcely gathered from several general proteomic experiments (Beausoleil *et al.* 2006, Villén *et al.* 2007, Imami *et al.* 2008), but to date, only one study really focused on PARG phosphorylation (Gagné *et al.* 2008). This study showed that PARG phosphorylation was predicted mainly on the N-terminal unfolded regulatory domain (predicted as a NORS, NOn Regular Secondary structure, Liu and Rost, 2003), and revealed several phosphorylation sites targeted by the CDKII kinase. In this project, my objective was to find new kinases capable of phosphorylating PARG, to identify phosphorylated residues and to investigate the functional role of PARG phosphorylation. The results I obtained are displayed in the following research article draft.

DNA-PKcs is a new protein partner of PARG.

E. Héberlé[1], G. Illuzzi[1], J.C. Amé[1], B. Camuzeaux[1] F. Dantzer[1], V. Schreiber[1]

1. Biotechnology and Cell Signalling, UMR7242 CNRS, Université de Strasbourg, Laboratory of Excellence Medalis, ESBS, 300 Bd Sébastien Brant, CS 10413, 67412 Illkirch, France.

Corresponding author: V. Schreiber, valerie.schreiber@unistra.fr

Highlights:

- Mass spectrometry and interaction assays revealed DNA-PK as a new protein partner for PARG
- PARG was phosphorylated by DNA-PK in in vitro kination assays
- DNA-PK targets the N-terminal regulatory domain of PARG on at least residues S130, T143 and S335.
- DNA-PK and PARG interaction increases after DNA damage.

Abstract:

Post-translational modifications such as phosphorylation are crucial events regulating protein function, localization and activity. PARP1 is the main enzyme catalysing Poly(ADP-ribosyl)ation, an important post-translational involved in DNA damage signalling and repair. PARG on the other is the main enzyme degrading this post-translational modification. Although the proteome and post-translational modifications linked with PARP1 have been extensively studied, much less work has been done regarding PARG. In this study, we show that the PI3K serine/threonine kinase DNA-PKcs is a new protein partner of PARG. We show that DNA-PKcs modifies PARG residues exclusively on its N-terminal regulatory domain, targeting at least three serine/threonine residues (S130, T143 and S335). These results will be of crucial importance to understand the link between PARG and DNA-PKcs in human cells.

Introduction:

Post-translational modifications are versatile modulators of protein localization and activity. Among these modifications, phosphorylation is the most abundant among higher eukaryotes. Poly(ADP-ribosyl)ation is another post-translational modification of crucial importance for DNA-damage repair, replication, transcription and more generally cell fate regulation in cells. It is formed on acceptor proteins by the activity of Poly(ADP-ribose polymerases (PARPs) and mainly degraded by the activity of the Poly(ADP-ribose) glycohydrolase (Chaudhuri and Nussenzweig, 2017). Interestingly, in the context of DNA damage response, these enzymes need to be tightly regulated in order to orchestrate a proper repair and post-translational modifications are efficient way of regulating proteins. Therefore, the study of the tight interplay between several actors of post-translational modifications has become an emerging and exciting field of research. Until now, studies related with the post-translational regulation of PARylation have focused on PARP1. Evidence for PARP1 phosphorylation, methylation, acetylation and ubiquitination exists in the literature. All these PTM can regulate PARP1's PAR-synthesis activity, nuclear localization or complex interaction with other protein partners (reviewed in Piao *et al.* 2017). For instance, PARP1, the main enzyme catalysing Poly(ADP-ribosyl)ation interacts with all three DNA damage response kinases of the PI3K family. For instance, PARP1 is found in a complex with DNA-PK (Ruscetti *et al.* 1998; Spagnolo *et al.* 2012). ATM and PARP1 interact in vivo after γ-irradiation and PARP inhibition stimulates ATM activity (Aguilar-Quesada *et al.* 2007). ATR and PARP1 co-purify in cell extracts after MMS treatment (Kedar *et al.* 2008).

PARG is the main PAR-degrading enzyme and needs to be tightly regulated in time and space in order to ensure a proper turnover of PAR in cells. However, results regarding its putative regulation through post-translational modifications are scarce. Kination prediction algorithms (PhosphoNet, Phosite, Netphos…) predict phosphorylation sites mainly in the highly disordered N-terminal domain of PARG, which is termed "regulatory domain" (Gagné *et al.* 2009). Mass spectrometry experiments yielded results for CKII (casein-kinase II) phosphorylation sites on residues S197, T199, S261 or S264, S298 and S316 in the N-terminus of PARG (Gagné *et al.* 2009), but other kinases able to phosphorylate PARG were not investigated any further. PARG is also acetylated on multiple lysine residues. Recently, K409 acetylation was revealed as a crucial event for PARG and
PCNA interaction through the second non-canonical PIP-box domain displayed on PARG amino-acid sequence (Kauffmann *et al.* 2017).

To investigate whether PARG undergoes phosphorylation, we performed in vitro kination assays after immunoprecipitation of GFP-labelled PARG constructs. We show that the first 75 residues of PARG are phosphorylated and are sufficient to interact with kinases. Using mass-spectrometry analysis, immuno-precipitation and proximity ligation assay (PLA) we identified DNA-PK as a new protein partner for PARG. DNA-PK ability to phosphorylate PARG was confirmed in vitro, and we identified several target residues on PARG sequence that are indeed phosphorylated by DNA-PK in vitro. Functional interaction between DNA-PK and PARG was assessed by dot-blot assays and clonogenic viability assay experiments on PARG deficient cells, using Nu7441, a specific DNA-PKcs inhibitor or a siRNA targeting DNA-PKcs.

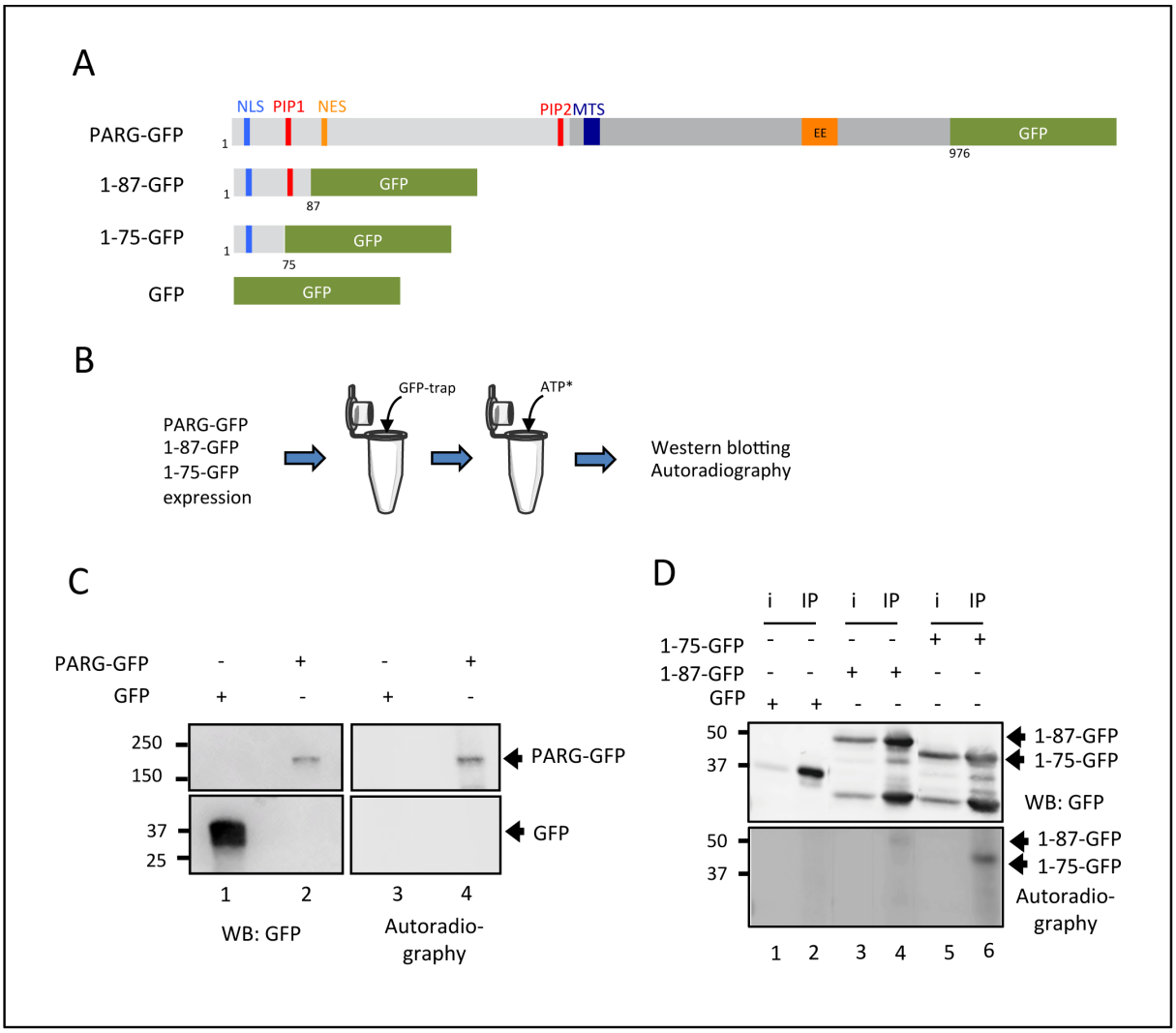

Figure 1: PARG co-purifies with partner kinases. A) PARG-GFP and derived constructs used for GFP affinity precipitation are represented. PARG-GFP encompasses the complete human PARG sequence fused with the GFP tag in C-terminal position. 1-87-GFP encompasses the N-terminal amino acids of human PARG, with the PIP1 (PCNA-interacting peptide). 1-75-GFP encompasses the N-terminal amino acids of human PARG without the PIP1 motif. GFP is used as a negative control. B) Schematic representation of the kinase co-immunoprecipitation experiment. GFP, PARG-GFP, 1-75-GFP and 1-87-GFP constructs are transfected in HeLa cells and enriched through affinity purification with GFP-antibody coupled-beads. Enriched trapped proteins are incubated with radiolabelled ^{32}P-ATP and samples are loaded on acrylamide gels and analysed by western blotting and autoradiography. C) Western Blot and autoradiography analysis of PARG-GFP and GFP samples, analysed as described in B. D) Western Blot and autoradiography of 1-87-GFP, 1-75-GFP and GFP after GFP-trapping and in vitro kinase assay. i: input; IP: immuno-precipitation.

Results and Discussion

1. PARG co-purifies with associated kinases

In order to check for in vivo phosphorylation of PARG, four GFP labelled constructs were transfected in HeLa cells. PARG-GFP is the full-length protein with a GFP fusion in C-terminal. 1-87-GFP encompasses the N-terminal part of PARG, with the PCNA-interacting peptide (PIP1, Mortusewicz *et al.* 2011). Many kinases such as the cyclin-dependent kinases act mainly in a cell cycle dependent manner. Therefore, we believed that putative kinases modifying PARG could likely act indirectly through PCNA and kept the PIP motif in the construct. 1-75 is slightly shorter, excluding the PIP domain but keeping the NLS sequence and thus allowing comparing the kinases co-purifying with the N-terminal part or with the PIP domain. The GFP sequence alone was used as a control (**Figure 1A**). In order to check for general phosphorylation sites, we transfected these constructs (PARG-GFP, 1-87-GFP, 1-75-GFP and GFP) in HeLa cells. After 24 hours of expression of these constructs, we performed immuno-precipitations experiments on the HeLa cell lysates, using GFP-trap beads (ChromoTek). To address the presence of co-purifying kinases in these samples, beads were incubated for 30min in the presence of radiolabelled ^{32}P-ATP. The reaction mixture was separated on a gradient acrylamide gel and analysed through western blotting and autoradiography (**Figure 1B**).

No phosphorylation signal is detectable on the GFP alone (**Figure 1C, lane 1 and 3**). When trapping PARG-GFP however, a phosphorylation signal at the molecular size of PARG-GFP is observed, indicating that full-length PARG can be phosphorylated in vitro by one or co-purifying kinases (**Figure 1C, lane 2 and 4**).

Trapping of the 1-87-GFP and 1-75-GFP results in an enrichment of the GFP signal after immunoprecipitation (**Figure 1D, compare lane "i:input" and "IP:immunoprecipitation"**). The GFP negative control is not phosphorylated (**Figure 1D, lane 1 and 2**). Bands corresponding to each of the construct are labelled with an arrow. After autoradiography, 1-87-GFP yields a phosphorylation signal (**Figure 1D, lane 4**), although weaker than for the 1-75-GFP construct (**Figure 1D, lane 6**). This suggests that the first 1-75 residues of PARG are sufficient for co-purifying with partner kinases. We might even hypothesize than the residues 75-87 bearing the PIP1 motif interfere with the in vitro phosphorylation.

2. Mass spectrometry reveals DNA-PK as a new partner for PARG

To identify the co-purifying kinases responsible for PARG phosphorylation, we performed mass spectrometry analysis on HeLa samples after GFP-trapping of the 1-87-GFP constructs, bearing the PIP1 motif (**Figure 2A**). Co-purification of PCNA would thus serve as a positive control for the experiment. In the mass spectrometry tables, selected results are summarized, with the number of total peptides identified, termed "PSM" (peptide score mass) and the number of different peptides found among the peptide mix for each protein.

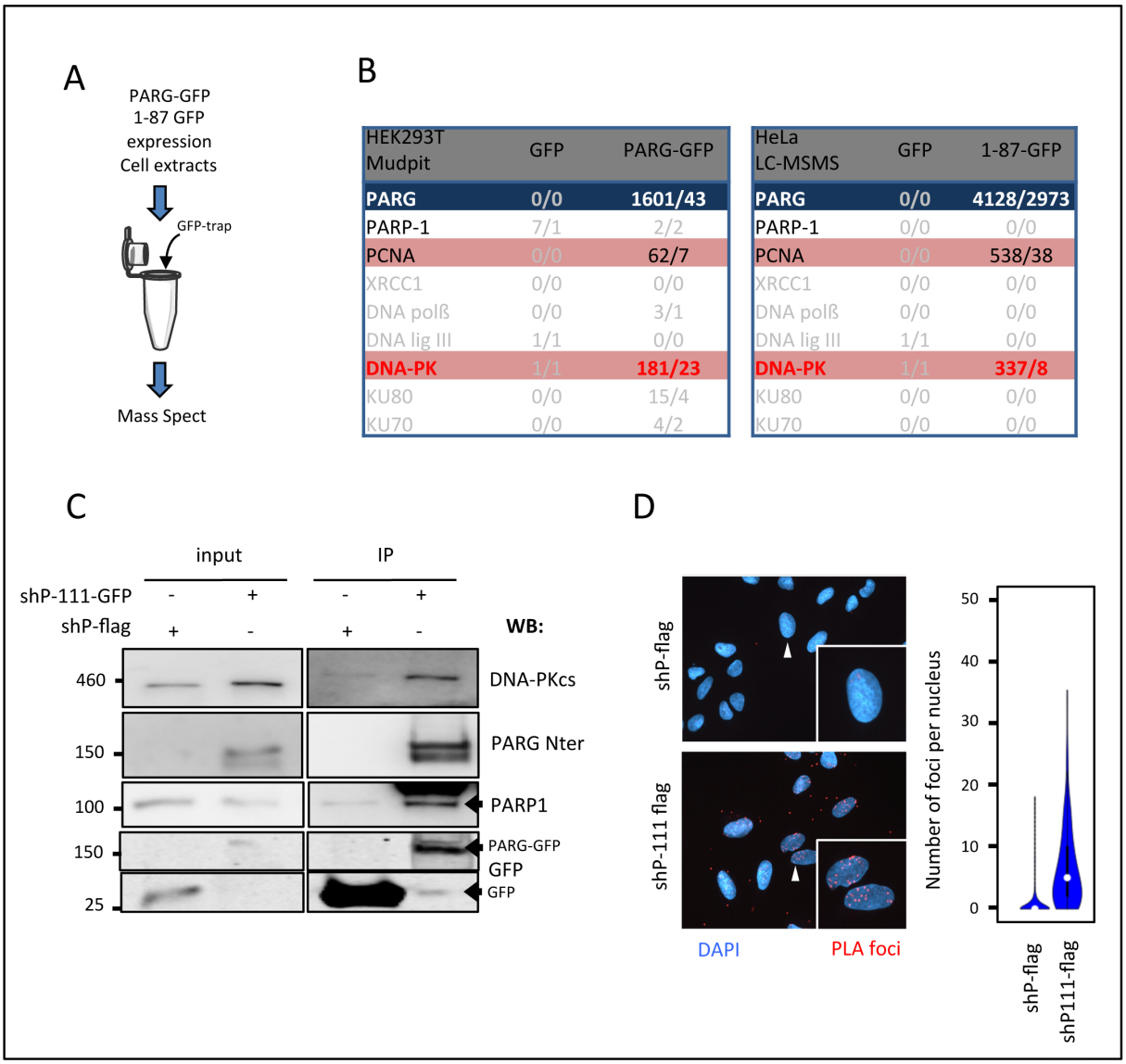

HEK293T Mudpit	GFP	PARG-GFP
PARG	**0/0**	**1601/43**
PARP-1	7/1	2/2
PCNA	0/0	62/7
XRCC1	0/0	0/0
DNA polß	0/0	3/1
DNA lig III	1/1	0/0
DNA-PK	1/1	**181/23**
KU80	0/0	15/4
KU70	0/0	4/2

HeLa LC-MSMS	GFP	1-87-GFP
PARG	**0/0**	**4128/2973**
PARP-1	0/0	0/0
PCNA	0/0	538/38
XRCC1	0/0	0/0
DNA polß	0/0	0/0
DNA lig III	1/1	0/0
DNA-PK	1/1	**337/8**
KU80	0/0	0/0
KU70	0/0	0/0

Figure 2: DNA-PKcs is a new protein partner for PARG. A) PARG-GFP, 1-87-GFP and GFP constructs are transiently transfected in HEK293T or HeLa cells and used for GFP affinity precipitation by GFP-trap (chromoTek). Enriched samples are processed for mass spectrometry analysis. B) Tables showing selected protein partners yielded in two experiments of mass spectrometry analysis in HEK293T and HeLa cell lines. PCNA interaction is retrieved after both PARG-GFP and 1-87-GFP purification and is our positive control. DNA-PK interacts with PARG in both experiments. Interactions are displayed by showing the PSM (peptide spectrum matches)/peptide values. C) Co-immuno-precipitation of DNA-PK in U2OS cell lines stably expressing 111kDa PARG fused to GFP (shP-111-GFP) and cell lines expressing a flag tag alone and GFP (shP-flag). DNA-PKcs co-immunoprecipitates with PARG-GFP. PARP1 efficiently co-purifies with PARG-GFP and is a positive control for this experiment. D) Proximity ligation assay using DNA-PKcs and flag antibodies in U2OS cell lines stably expressing the 111kDa PARG coupled to a flag-tag (shP-111-flag), or flag-tag (shP-flag) alone. Interaction is quantified by counting the number of foci per nucleus yielded after the experiment.

Previous experiments performed in the lab in HEK293-T cells after PARG-GFP expression and mass spectrometry are displayed in the left table (**Figure 2B, J-C. Amé,** personal communication**)**. PCNA was recovered as a protein partner with a PSM of 62, and 7 different peptides identified. It is a positive control for this experiment, since PARG and PCNA interaction were previously shown to interact and to co-localize in replication foci throughout S-phase, even in absence of DNA-damage (Mortusewicz *et al.* 2011). Partners such as PARP-1, XRCC1, DNA Polß or ligase III are barely detectable, but the absence of damaged conditions in the experiments could explain that we do not retrieve these DNA-repair protein partners. Co-immunoprecipitated with the full-length PARG, mass spectrometry reveals over 30 different kinases with low score and peptide numbers (1 or 2 peptides, data not shown). The most reliable score for a kinase partner was yielded by DNA-PK, with 181 peptides identified, among which 23 are unique peptides. When performing the same experiment with the 1-87-GFP construct, we obtained comparable results. PCNA was retrieved with a score of 538 peptides of 38 different sequences, and DNA-PK with 337 peptides of 8 different sequences. This suggests that DNA-PK is indeed a protein partner for PARG, and that the 1-87 residues of PARG are sufficient to mediate the interaction.

3. DNA-PK and PARG co-immuno-precipitate

To provide further biological evidence for DNA-PK and PARG interaction, we used the stable U2OS cell-lines generated in the first part of my thesis project (shP-111-GFP) stably expressing the 111-GFP construct in order to perform a classical immuno-precipitation. shPARG cell lines expressing only the flag tag (shP-flag) were used as a negative control for they express a GFP fluorescent marker that was used for the initial selection and sorting of stably infected cells. Results are shown in **figure 2C**, with initial protein signals shown in the "input" panel and the protein levels after immuno-trapping displayed in lane "IP". After GFP-trapping and western blotting, DNA-PKcs level increases in the PARG-GFP immunoprecipitated samples (IP lane), showing that both proteins indeed interact in this cell line. It is of importance to mention that co-trapping of DNA-PK with PARG-GFP (of PARG-flag, data not shown), did not always allow retrieving strong and reproducible signals by western blotting. First of all, DNA-PKcs is a huge protein (469kDa), complicating its detection by western blotting. Then, interaction between a kinase and its protein substrate is likely to be transient and specific to cellular localization or cell cycle. Therefore, the initial state of the cells can affect the level of basal interaction between both proteins in absence of DNA-damage. The interaction between PARG and DNA-PK in the context of DNA-damage will be discussed in the last paragraph of this article **(§8**).

PARP1 being a partner of both PARG and DNA-PK, we also probed it in our experiment and its level indeed increases after IP. PARP1 interaction with PARG was previously reported, showing that the catalytic domain of PARG interacts with the automodification domain of PARP1 (Keil *et al.* 2006). On the other hand, PARP1 was previously shown to interact with DNA-PK (Spagnolo *et al.* 2012) and that DNA-PK could negatively regulate PARP1 activity (Ariumi *et al.* 1999). We cannot exclude that PARP1, PARG and DNA-PK can therefore exist in a ternary complex.

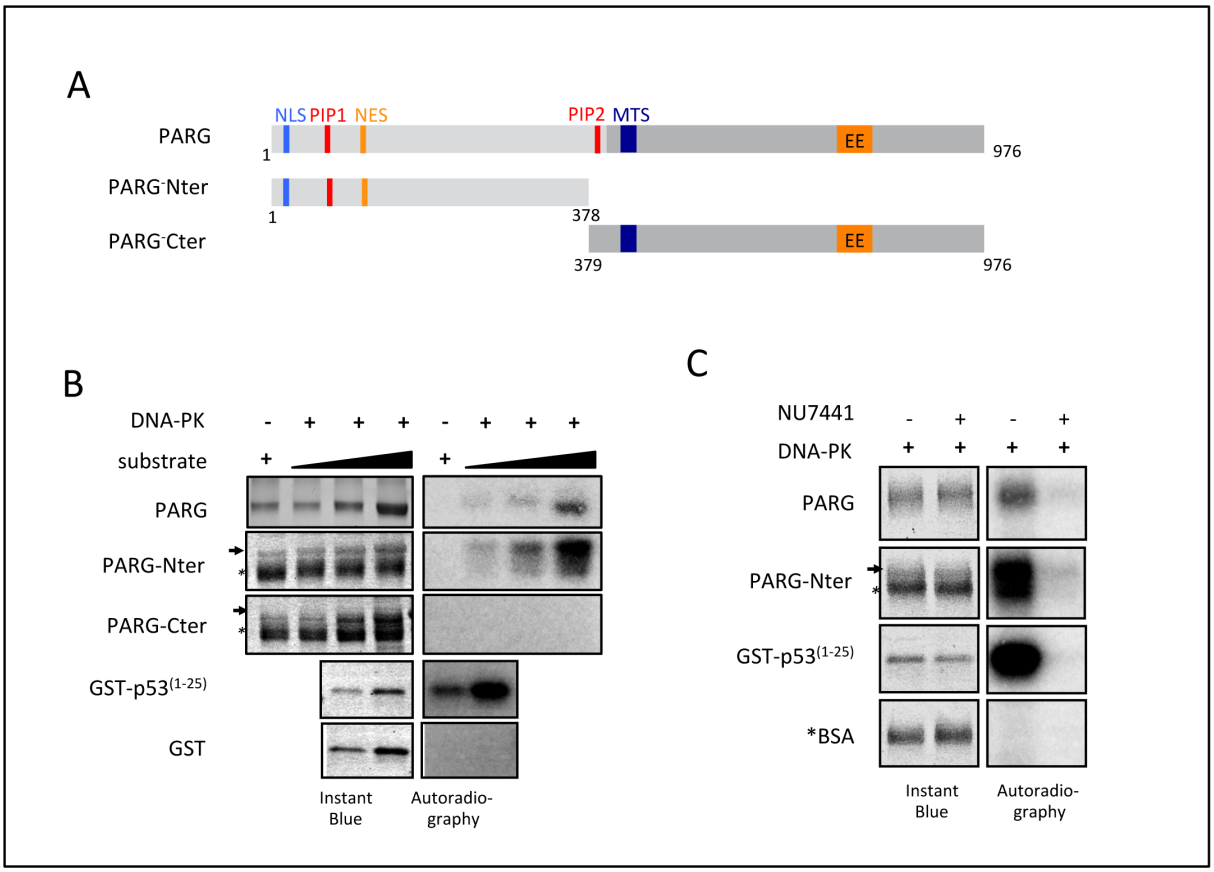

Figure 3: PARG is a phosphorylation substrate of DNA-PKcs. A) PARG is divided into two fragments: its N-terminal regulatory part (1-378), referred to as PARG-Nter and its C-terminal catalytic domain (379-976), referred to as PARG-Cter. These constructs are expressed in *E.coli* and the proteins are purified in order to perform in vitro kination assay. B) In vitro kination assay using increasing amounts of PARG, PARG-Nter or PARG-Cter (250ng, 500ng, 1µg). PARG fragments are highlighted with a black arrow. The lower band marked with an asterisk is the BSA protein added in the reaction mixture. 125ng and 250ng of GST-p53$^{(1-25)}$ are used as a positive control for DNA-PK phosphorylation. 250ng and 500ng of GST alone is used is a negative control. C) In vitro kination assay using fixed concentration of proteins (250ng), with or without addition of Nu7441, a specific DNA-PK inhibitor. GST-p53$^{(1-25)}$ N-terminal peptide is used as a positive control and BSA as a negative control to ensure that BSA is not responsible for a non-specific kination signal in this experiment.

4. DNA-PK and PARG interact directly in vivo

In order to check whether PARG and DNA-PK directly interact in vivo, and taking into account that this interaction can be transient in cells, we carried Proximity Ligation Assays (Duolink) on U2OS stable cell lines expressing the full length PARG fused to a flag tag (shP-111-flag). Cells stably expressing a flag tag alone are used as negative control for the interaction (shP-flag). Using specific antibodies targeting the flag-tag and DNA-PKcs, this method allows the specific detection of isolated interaction events, even transient, directly *in situ* (Leuchowius *et al.* 2011; Greenwood *et al.* 2015). The amount of interaction can be quantified in each cell by counting the number of fluorescent foci per nucleus. Representative microscopy images (**Figure 2D**) show that the 111-flag construct and DNA-PK interact. Relevant examples of the interaction foci, in red, are displayed in microscopy close-ups of cells marked with a white arrow. The number of foci in cell population is represented in a violin graphic. For each condition, over 100 nuclei were counted. The amount of foci increases from 0-3 foci per nucleus in the shP-flag cell line to 5-30 foci in the shP-111-flag cell lines. We thus reveal an interaction between the full-length PARG and DNA-PK *in situ* even in the absence of DNA-damage. DNA-PK being able to modify PARP1, negatively regulating its PARylation activity (Ariumi *et al.* 1999), it is not excluded that this protein could also phosphorylate PARG, which would be an interesting way of regulating polymer degradation and PARG turnover in cells.

5. PARG is a phosphorylation substrate for DNA-PKcs

We showed that PARG and DNA-PK could interact in vivo and in vitro, even in absence of DNA damage. To test whether they functionally interact, we first tried to check whether DNA-PK could directly phosphorylate PARG in vitro. For this we used commercial purified human DNA-PK (Promega), and expressed either the full-length PARG protein fused with GST, the N-terminal (1-378) part of PARG or the C-terminal (379-976) part of PARG fused with GST in BL21 strain of *E.coli* (**Figure 3A**). These proteins were purified on glutathione beads and separated from GST by cleavage with the PreScission Protease (GE Healthcare), as described in Amé *et al.* 2017 (see Appendix III). Increasing concentrations of each construct are incubated with DNA-PK, in the presence of radiolabelled ^{32}P-ATP to check for phosphorylation by incorporation of ^{32}P. The 25 first residues of the N-terminal part of p53 fused to GST (GST-p53$^{(1\text{-}25)}$) is used as a positive control for DNA-PK phosphorylation (Lees-Miller *et al.* 1992), and GST alone is used as a negative control. In our experimental conditions, p53 is strongly phosphorylated and GST is not, indicating that the assay is functional. PARG displays a phosphorylation signal in autoradiography, showing that it is phosphorylated in vitro. PARG-Nter displays even higher phosphorylation levels, whereas PARG-Cter displays no phosphorylation signal. This shows that the N-terminal part of PARG is phosphorylated by DNA-PK in vitro (**Figure 3B**). This result is interesting, for the N-terminal part of PARG is predicted to be a regulatory domain, displaying many putative phosphorylation sites (Gagné *et al.* 2008). Since the phosphorylation signal was always weaker on the PARG construct than on the PARG-Nter, we can hypothesize that the catalytic C-terminal domain has some inhibitory effect on PARG and DNA-PK interaction or on DNA-PK activity.

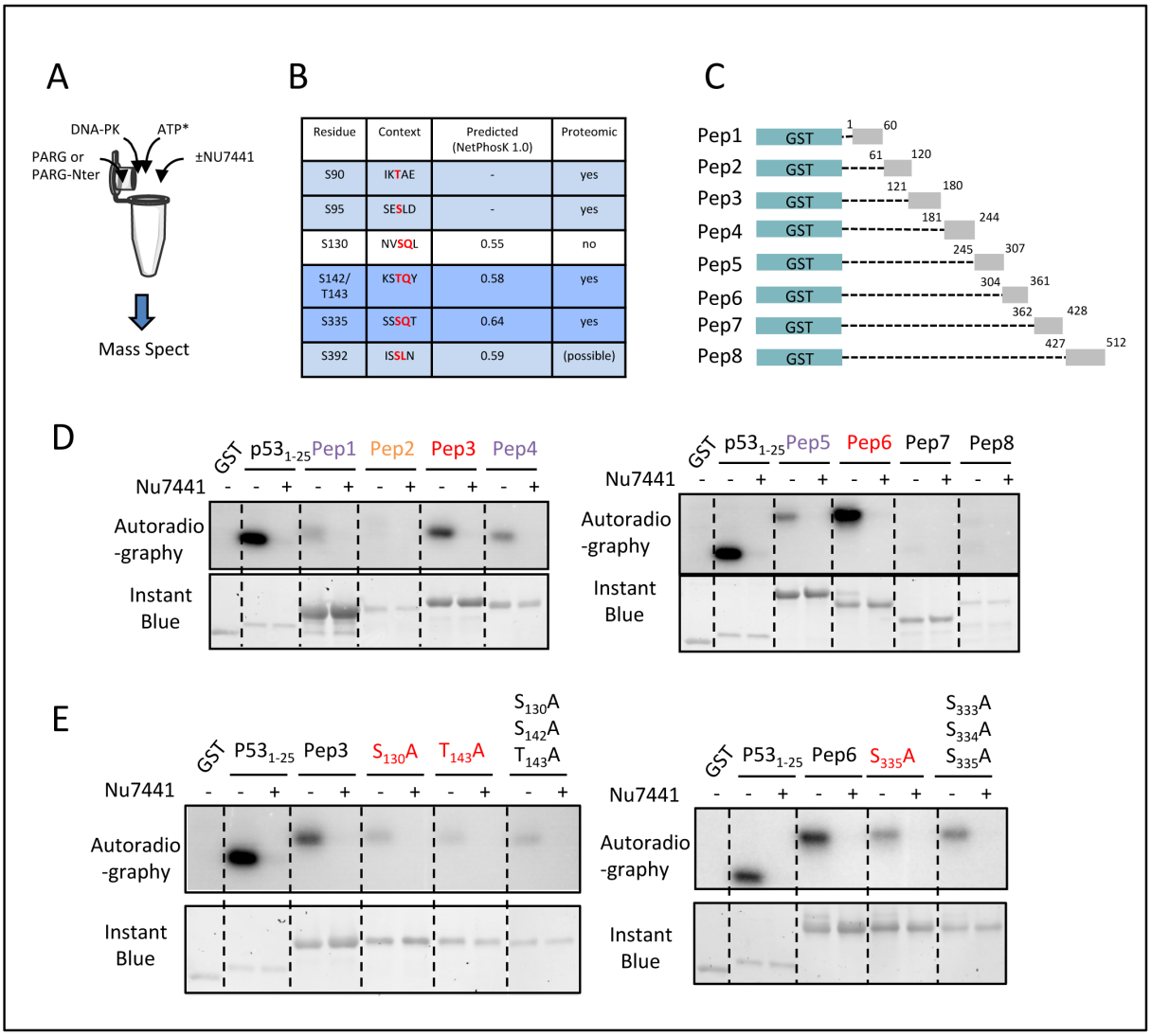

Figure 4: Identification of DNA-PKCs phosphorylation sites on PARG. A) Investigation of the phosphorylation sites was performed after a kination assay in vitro, using PARG or PARG-Nter, purified DNA-PK (Promega) and ATP with or without Nu7441. Samples were sent for mass spectrometry analysis. B) Summary of the target residues identified by mass spectrometry (Light and dark blue). Table also displays the context of the target residues and their prediction score for DNA-PK phosphorylation, if predicted (NetPhosK 1.0). Residues highlighted in dark blue were both identified in mass spectrometry and predicted by algorithms. C) The N-terminal domain of PARG was divided into seven sequence fragments of 60 amino acids long on average (Peptide 1 to Peptide 7) and cover PARG sequence from residue 1 to 428. Peptide 8 overlaps the C-terminal domain of PARG. Each of these protein fragments were expressed and purified from *E.coli*. D) Peptides were incubated with DNA-PK as described in (A), with radiolabelled ^{32}P-ATP. Samples were loaded on acrylamide gels and revealed with instant blue and by autoradiography. GST-p53$^{(1-25)}$ is used as a positive control for DNA-PK phosphorylation, GST as a negative control. E) In vitro kination assay using peptide 3 and 6 displaying target DNA-PKcs serine/threonine mutated into alanine residues.

The DNA-PK protein ordered from Promega Company is purified from HeLa cell extracts. In order to check that the PARG signal obtained was specifically due to DNA-PKcs and not to other contaminating kinases, we performed the kination experiments in the presence of Nu7441 (Sellekchem), a specific DNA-PK inhibitor (Leahy *et al.* 2004). PARG and PARG-Nter phosphorylation is strongly impaired upon addition of the DNA-PK inhibitor in the experiment, thus proving that the phosphorylation event is due to DNA-PK and that PARG-Nter is indeed phosphorylated by this kinase. BSA (Bovine Serum Albumine), marked with an asterisk on the blot, was used in the reaction buffer, and thus was also tested for phosphorylation, because its size (50kDa) is nearly overlapping the PARG-Nter size and is detected when revealing the gel with Instant Blue. BSA generates no parasitic signal in autoradiography (**Figure 3C**), proving that the signal observed for PARG-Nter is specific.

PARP1 is able to PARylate DNA-PK, which increases its phosphorylation activity (Ruscetti *et al.* 1998). Conversely, DNA-PK phosphorylates PARP1, inhibiting its catalytic activity in vitro (Ariumi *et al*. 1999). It is likely that PARG could degrade PAR on DNA-PK, since they interact in vivo. This is complicated to test in vitro, but yet here we show that DNA-PK is able to phosphorylate the regulatory domain of PARG, suggesting that DNA-PK interaction could similarly affect PARG activity and modulate cellular events around PARylation.

6. Narrowing DNA-PK phosphorylation sites in PARG sequence

After identifying DNA-PK as a kinase able to phosphorylate PARG, we wanted to investigate which residues of PARG are targeted by DNA-PK. To have an unbiased approach for identifying these targets, we performed mass spectrometry experiments after kination reactions on PARG or PARG-Nter constructs, in the presence or absence of Nu7441, similarly as in §5 but using non radiolabelled ATP (**Figure 4A**). We recovered S90, S95, S142/T143, S335 and S392 as phosphorylated residues in our experiments (**highlighted in blue, Figure 4B**), but three different experiments never yielded the same phosphorylation targets. When performing phosphorylation site predictions with online algorithms (NetPhosK 1.0), S130, T143, S335 and S392 are predicted with a score >0.5 (**Figure 4B**), suggesting that the amino acid context of these residues would favour DNA-PK phosphorylation. DNA-PK is a serine/threonine kinase that mostly triggers phosphorylation of serine or threonine residues dwelling in a [S/T]-Q context (Collis *et al.* 2005). Accordingly, we assumed that S130, S142, T143 and S335 should be the best candidates for DNA-PK phosphorylation. The most promising residues, confirmed by both mass spectrometry, prediction and favourable sequence context are highlighted in dark blue (**Figure 4B**).

Since the mass spectrometry results were not highly reproducible, we used another complementary strategy to identify the phosphorylated PARG residues. PARG N-terminus (1-425) was divided into six smaller fragments of around 60 amino acids, covering residues 1 to 428 of the human PARG sequence. Peptide 8 (427-512) covers the beginning of the C-terminal domain of PARG and will be used as negative control for phosphorylation (**Figure 4C**). These constructs are fused to GST, allowing their purification from *E.coli*, using the same protocol as described in Amé *et al.* 2017 (**Appendix III**). On each of these constructs, we performed an in vitro kination assay using purified DNA-PK, radiolabelled ^{32}P-ATP in the presence or absence of the DNA-PK inhibitor Nu7441 (**As in Figure 4A**). GST-p53$^{(1-25)}$ is used as a positive control for DNA-PK phosphorylation and GST alone is used as a negative control. Peptides 1, 4 and 5 display a weak phosphorylation signal, that could vary across replicates (**Figure 4D, highlighted in purple**), but peptide 3 and 6 were always strongly phosphorylated in our assays

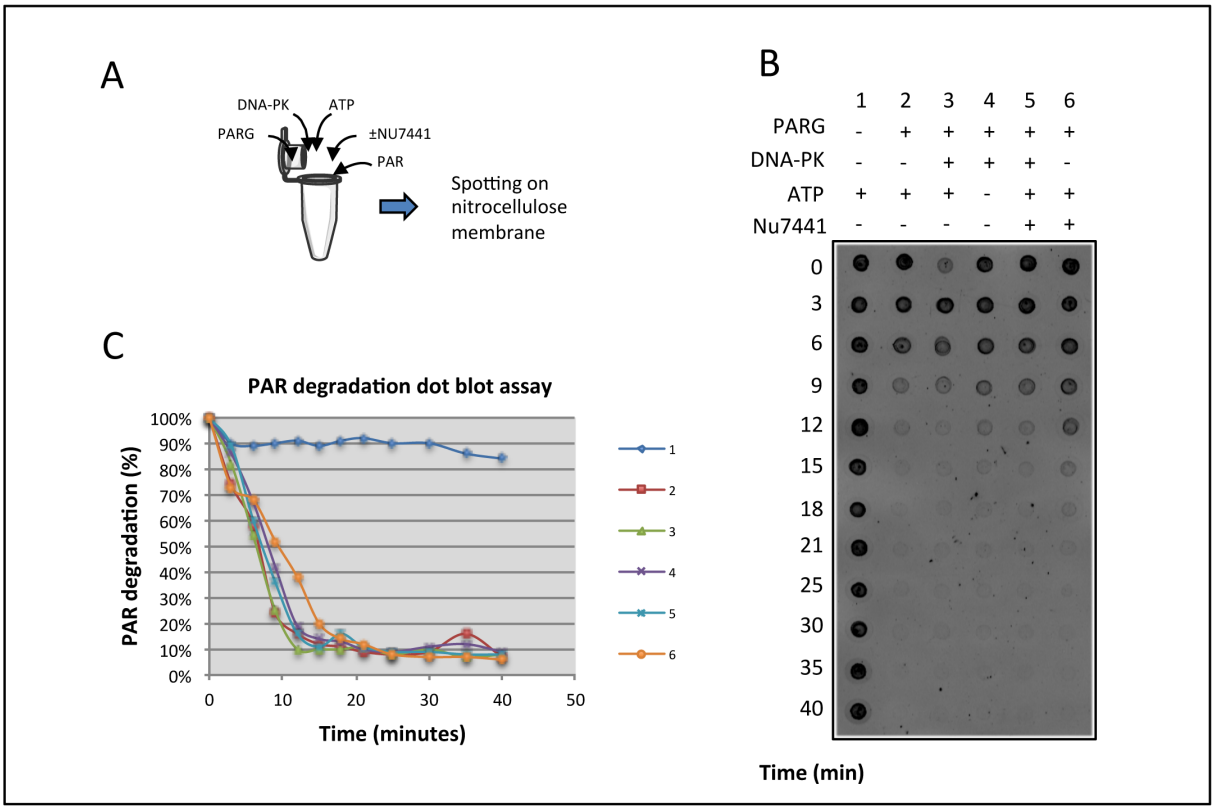

Figure 5: DNA-PK phosphorylation does not affect PARG catalytic activity in a dot blot experiment. A) Purified PARG activity was followed after incubation with DNA-PK with or without DNA-PK inhibitor, through a dot blot activity assay described in Amé *et al.* 2017 B) Representative dot blot membrane probed with an anti polymer antibody. Different conditions are tested, labelled from 1 to 6. Polymer degradation by purified PARG is tested in a kinetic of 40 minutes. C) Quantification of the PAR-degradation kinetics in each condition from 1 to 6. Lane 1 is the negative control without PARG, showing no spontaneous decrease of the polymer.

(**Figure 4D, highlighted in red**). Both algorithms and mass spectrometry data pointed out several serines/thronines mapping in peptide 3 and 6. We thus chose to investigate whether S130, T143 and S335 were indeed phosphorylation targets of DNA-PK. In peptide 3, we generated phosphomutant constructions replacing either serine 130 or threonine 143 by alanine residues that cannot be phosphorylated. Because T143 is near a serine in position 142, we also generated a triple mutant S130A, S142A and T143A. In peptide 6, we generated a S335A mutation, plus an additional triple mutation of the nearby serines (S333A, S334A, S335A). Each of these mutants were expressed, purified from *E.coli* and tested in an in vitro kination assay with DNA-PK. The signal in autoradiography revealed that phosphorylation was strongly reduced when mutating S130, T143 and S335. Multiple mutations do not further increase the phosphorylation signal loss, indicating that these three mutations are all true target residues for DNA-PK (**Figure 4E**). We thus identified precise PARG residues that are modified by DNA-PK in vitro. The role of these phosphorylation events remains to be deciphered in vivo, but we can hypothesize that they have a regulatory function for PARG. However, our results also indicate that additional DNA-PK targets likely exist between amino acids 181 and 307 (peptide 4 and peptide 5), without being predicted nor retrieved in mass spectrometry, thus complicating our investigation. We could not conclude for peptide 2, although phosphorylation on S90 and S95 were retrieved by mass spectrometry, for this fragment was weakly produced in bacteria and seems highly unstable.

7. DNA-PK phosphorylation has no detectable effect on PARG activity in vitro

In order to test the effect of PARG phosphorylation by DNA-PK on its catalytic activity, we developed a dot blot protocol to follow PAR degradation by PARG in vitro. The protocol is as described in Amé *et al.* 2017 (See Appendix III) and was used to evaluate the activity of PARG, previously phosphorylated in vitro by DNA-PK. Non-radioactive ATP was used in the kination experiment. At the beginning of the experiment, purified PAR synthetized in vitro is added in the reaction mixture, and aliquots from the reaction mixture are spotted at regular time on a nitrocellulose membrane (**Figure 5A**). PAR degradation by PARG is revealed by probing the membrane with a specific antibody against the polymer (**Figure 5B**). Kinetics of PAR degradation are quantified with image J and shown in a graph (**Figure 5C**). The obvious conclusion is that the addition of DNA-PK, in the absence or presence of ATP does not affect PARG activity. However, we cannot rule out the possibility that the phosphorylation of PARG is far from being complete or that the enzyme stoichiometry is not optimal. A fraction of unmodified PARG in the reaction with DNA-PK (reaction 3) could therefore be sufficient to degrade the polymer in similar rates than in the control reaction without DNA-PK (reaction 2). Additionally, addition of Nu7441 in the reaction slightly slows polymer degradation even in the absence of DNA-PK (reaction 6). Therefore, this type of experiment does not allow to formally conclude any impact of DNA-PK phosphorylation on PARG activity in vitro. In addition, more sensitive experiments than dot-blot could be carried to monitor PARG activity. Fluorescence-based approaches are good alternatives to this method (Stowell *et al.* 2016). After kination, we could also think about enriching samples with phosphorylated PARG before performing the activity assay. This could be done by using columns or beads coupled to phosphorylation-specific antibodies, or new biomaterials such as spore@Fe3+ microspheres that allow specific enrichment of phosphoproteins (Fei *et al.* 2017).

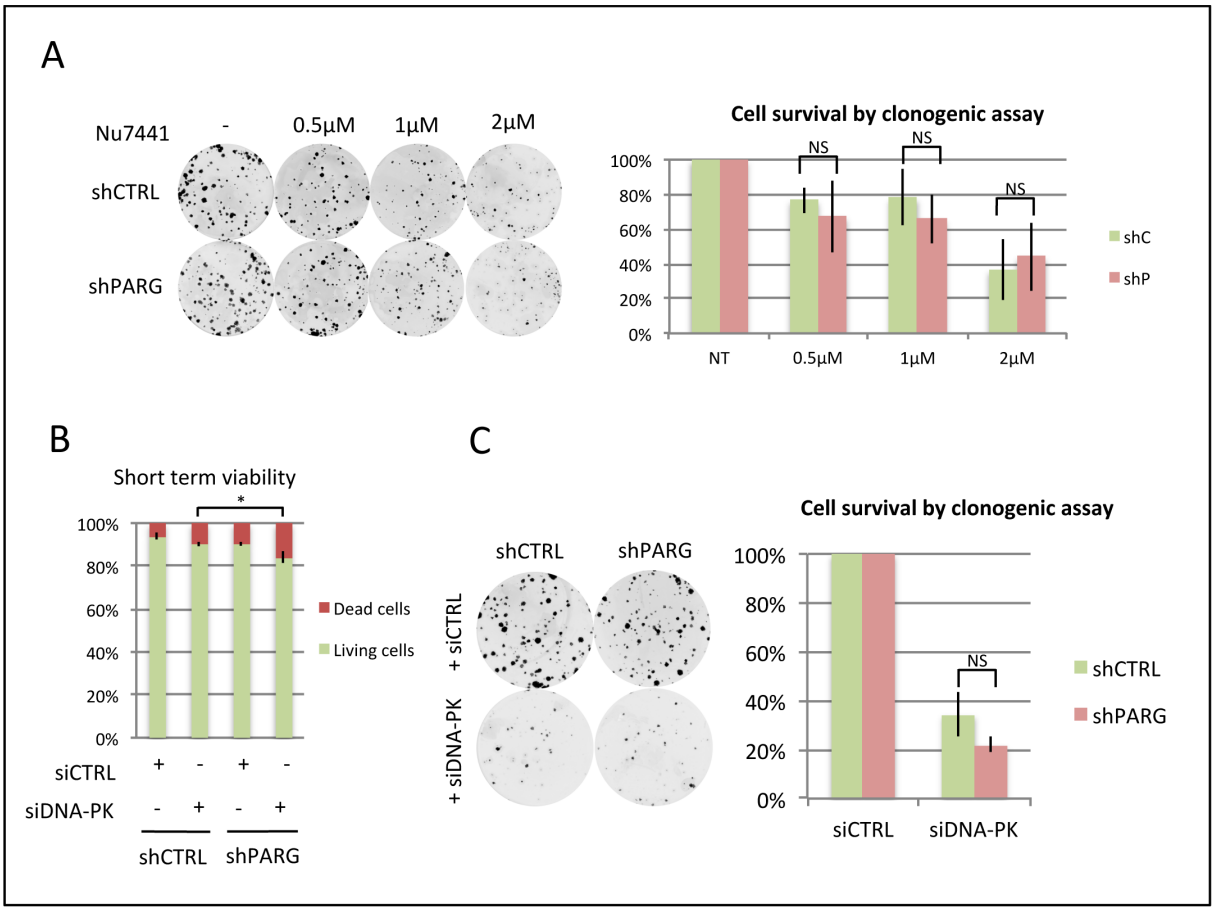

Figure 6: Investigating the functional basal interaction of PARG and DNA-PK. A) Clonogenic assay on shCTRL and shPARG cells treated with increasing concentrations of the DNA-PK inhibitor Nu7441. No significant difference between shCTRL and shPARG (n=5, student t-test, p>5%, NS: non significant). B) Short term viability assay by trypan blue counting of living cells. Although DNA-PK depletion already has an effect on shCTRL cells, it slighlty reduces cell viability in shPARG cells. This result is statistically significant (n=3, student t-test, p=0.037) C) Clonogenic assay on shCTRL and shPARG cells with or without depletion of DNA-PK by siRNA (n=3, student t-test, p=0,348 >5%, NS : non significant).

8. Functional impact of DNA-PK inhibition or depletion in U2OS cells

Since a direct effect of phosphorylation on PARG activity couldn't be shown in vitro, we tried to assess the functional impact of PARG and DNA-PK interaction by performing clonogenic viability assays in U2OS cells stably expressing a control shRNA (shCTRL) or an shRNA targeting PARG (shPARG).

Four hours after seeding, cells were treated with 0; 0.5µM; 1µM or 2µM of the DNA-PK inhibitor Nu7441 and cells are counted 14 days later. At 0.5µM and 1µM, shPARG cells display an average of 10% decrease of their survival rate compared with the shCTRL cells. No statistically significant differences in cell survival were observed across replicates (n= 5;Student test: p>5%). Therefore, we can conclude that the inhibition of DNA-PK activity with increasing doses of Nu7441 does not have a significant impact on cell survival when comparing control shCTRL cell line and PARG-depleted shPARG cell line (**Figure 1A**).

On the other hand, we investigated the effect of direct DNA-PK depletion by siRNA on shCTRL and shPARG cell lines. The short-term viability was measured by a Trypan blue staining of the cells, 72h after transfection with either siCTRL or siDNA-PK. Depletion of DNA-PK decreases cell viability already in CTRL cells, and slightly increases cell death in shPARG cells. However this result was not statistically significant across replicates. Since viability decreases in shPARG already after transfection with the siCTRL, we can only assume that shPARG cells are slightly more sensitive to siRNA transfection compared with shCTRL cells. On long term viability, CTRL cells display a 30% average survival rate and PARG display a 20% average survival rate. shPARG therefore seems slightly more sensitive to DNA-PK depletion, but statistics show that this results is non significant (n=3; Student test: p>5%). Overall, the absence of PARG does not sensitize cells to either DNA-PK depletion or inhibition. PARG and DNA-PK suppression are therefore not synthetic lethal.

9. DNA-PK and PARG interaction increase after DNA damage with NCZ.

Both PARG and DNA-PKcs are well known actors of DNA repair (for a review see Feng and Koh, 2013; Jette and Lees-Miller, 2015). DNA-PKcs acts as repair factor mainly in the non-homologous end-joining double-strand break repair pathway. After having demonstrated that PARG and DNA-PK both interact in cells, we chose to investigate whether or not this interaction was increasing after DNA-damage. For all the reasons mentioned above (See **§4**), Proximity Ligation Assay appeared as the best method to monitor changes in the PARG and DNA-PK interaction. We performed a kinetic experiment on shP-flag and shP-111-flag after treatment with neocarzinostatin (NCZ, 15min, 50ng/mL), an antibiotic that inhibits DNA synthesis and favours DNA strand cleavage, thus creating double strand breaks. As previously shown in figure 2D, interaction increases in shP-111-flag compared with shP-flag, in the absence of damage. Again, this strengthens our observation of a basal interaction between PARG and DNA-PK. Upon treatment with NCZ, the number of foci per nucleus slightly increases. It increases even more after 1h release, suggesting that both proteins are mobilized at the vicinity of

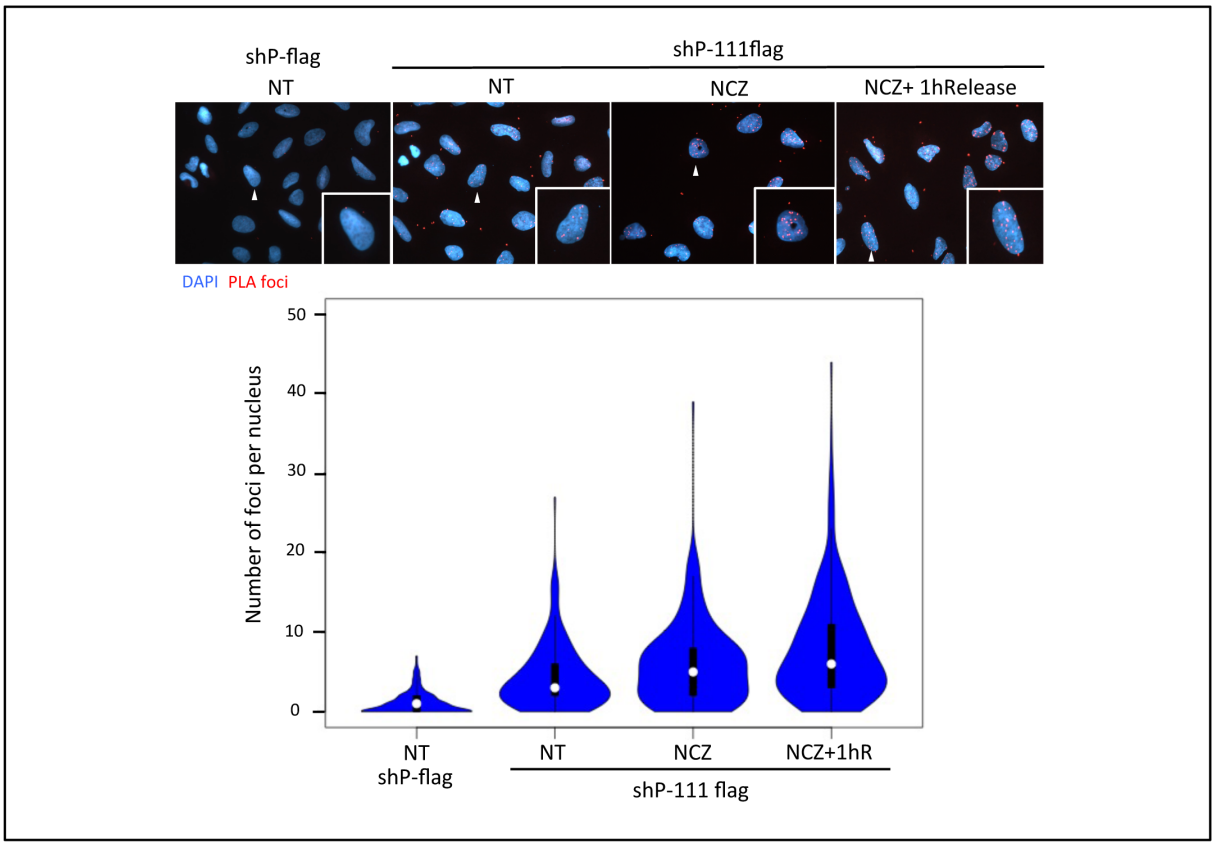

Figure 7: PARG and DNA-PK interaction increase after NCZ induced DNA damage.
Proximity ligation assay in U2OS shP-flag and U2OS shP-111-flag cell lines. NT: No treatment, NCZ: Neocarzinostatin, NCZ+1hR: 1h release after neocarzinostatin treatment (15min, 50ng/mL). Selected images of each condition are shown in the upper panel. Representative nuclei, which are zoomed in, are marked by a white arrow. Quantifications of each condition are represented in the graph below in the form of vioplots, made with R software (version 3.4.2).

each other after double strand break induction (**Figure 7**). To our knowledge, this is the first evidence of a direct physical and functional interaction between the PARG enzyme and DNA-PK. The experiment with NCZ was performed thrice independently with similar tendency (data not shown). We also tested this interaction after treatment with several other damaging agents (H_2O_2, etoposide) or replicative stress inducers (HU, CPT) and in every case, there seemed to be a slight increase between PARG and DNA-PK (data not shown). However, the latest experiments need to be reproduced before making any conclusions. It makes no doubt that these DNA-damage related questions deserve further investigations in the future.

Conclusions

In this project, we identified the PI3K family protein kinase DNA-PKcs as a novel protein partner for PARG, both by mass spectrometry analysis. This novel partner was confirmed by co-immunoprecipitation and proximity ligation assay approaches. Mass spectrometry analysis and in vitro kination assays revealed that PARG was a direct phosphorylation target of DNA-PK. DNA-PK enzyme phosphorylates PARG only in its regulatory N-terminal region, and we were able to identify several target residues that are effectively phosphorylated (S130, T143 and S335). Although we didn't see a direct functional impact of DNA-PK activity on PARG activity in vitro when performing dot blot experiments after the in vitro kination of PARG, we cannot exclude an effect on PAR catabolism. First because we cannot be sure that DNA-PK is able to phosphorylate all the PARG molecules available in the assay for stoichiometry reasons, then because our assay might not be sensitive enough to detect small changes in PARG turnover. Additionally, we didn't observe a statistically significant effect of DNA-PK depletion by siRNA, or of DNA-PK inhibition by Nu7441, on PARG depleted cells viability in the absence of DNA-damage. This suggests that DNA-PK and PARG interaction might not be crucial for cells in basal conditions. However, since PARG and DNA-PK are both important factors for DNA repair (Feng and Koh, 2013; Blackford and Jackson, 2017), it is a priority to investigate their interaction in the context of DNA-damage response. Our first attempt highlighted that after NCZ treatment, PARG and DNA-PK interaction was indeed increasing. We acknowledge that this part deserves more efforts and investigation. In conclusion, we reported the first direct evidence for PARG and DNA-PK interaction both under basal conditions and after DNA damage. This will open the path for new hypothesis linked with PARG regulation by post-translational modifications.

Materials and methods

Cell culture and treatments

HeLa cell lines used for mass spectrometry were cultured in Dulbecco's Modifed Eagle's Medium (DMEM 1 g/l glucose) (Invitrogen) supplemented with 10% foetal bovine serum, 1% gentamicin (Invitrogen) under 5% CO2. Stable CTRL and PARG knockdown U2OS cell lines were described in the previous chapter and cultured under the same conditions, but in DMEM 4,5g/L glucose. For PLA, shP-flag and shP-111-flag cell lines were supplemented with 100µg/mL doxycycline to induce expression of the 111-flag PARG. Induction was carried for at least 24 hours before each experiment. DNA-PK inhibitor Nu7441 (Sellekchem) was suspended in DMSO and added in the media for clonogenic assays at the indicated concentrations. NCZ treatments consisted in 15min

incubations with 50ng/mL NCZ. For release times, cells were washed twice with PBS and allowed to recover in DMEM media.

Short term viability and clonogenic assay

U20S shPARG or U2OS shCTRL (600 cells) were seeded in triplicate on 60mm dishes 5 h prior to treatment with the indicated doses of Nu7441. Alternatively, 250000 cells of each cell line were seeded in a P60 dish 24 hours before transfecting with 20nM of either siCTRL or siDNA-PK (Dharmacon) with Jetprime (Polyplus), according to the manufacturer's instructions. Seventy hours later, cells were washed twice with 4mL PBS (Dulbecco) and detached with 2mL trypsin (Dulbecco). Cells were stained with Trypan blue (Gibco), according to the manufacturer's instruction and dead cells were quantified in each condition. Remaining unstained cells are plated for clonogenic assay. Plates are incubated for 14 days in complete medium. After 2 washes with PBS, colonies were fixed in 3,7% paraformaldehyde (PFA) and stained with 0,1% crystal violet. Dishes were scanned with a Typhoon FLA 7000 and colonies are enumerated with ImageJ (NIH, Bethesda, MD, USA)

Bacterial culture and protein expression

BL21 strain of chemocompetent E.coli were transformed with 2ng of pGEX-6P3 plasmids encoding the full length PARG or fragments of PARG. After transformation, bacteria were cultured in LB+Ampicillin (100µg/mL). Purification of GST-tagged proteins were carried from lysates, as described in the methods paper available in **Appendix III** (Amé *et al.* 2017).

Peptide generation and mutation

Peptide sequences were amplified from the full-length sequence of PARG using PARG-GFP expressing vector as a template, using combinations of PCR oligonucleotides framing the delimited peptide region and bearing BamH1 and EcoRI cloning sites. PCR fragments were cloned in the pGEX-6P3 vector allowing the expression of proteins in bacteria. Primers used for cloning are listed above:

Peptide 1: Pep1-Fwd (ATATGGATCCATGAATGCAGGTCCGGGTTGCG)
Pep1-Rev (ATATGAATTCAAGCTTAACCCGGAACGCAAGCCG);

Peptide 2: Pep2-Fwd (ATATGGATCCCCGTGCTGGTCAACATCGCGGTTC)
Pep2- Rev (ATATGAATTCAAGCTTACTGGTAGAAGTTGTCTTTCTGGACGCTG);

Peptide 3: Pep3-Fwd (ATATGGATCCCCACAACGTCGAGAAACTGGAGAACGT)
Pep3-Rev (ATATGAATTCAAGCTTATTCCGGAACTAAGGTAACGGTCTGC);

Peptide 4: Pep4- Fwd (ATATGGATCCCAGTTCAGCAACGCGAACATTGATCG)
Pep4- Rev: (ATATGAATTCAAGCTTAGCCCGGATCACAGCTTTTGGAGC);

Peptide 5: Pep5 – Fwd (ATATGGATCCGAAGATTGCGCAAGTTGTCAGCAGGAC)
Pep5 – Rev (ATATGAATTCAAGCTTAGTCAACGTCCATCGGAGACTCCGGTTC);

Peptide 6: Pep6 – Fwd (ATATGGATCCATGGACGTTGACAACAGCAAAAACAGC)
Pep6 – Rev (ATATGAATTCAAGCTTAGCCTTTGGTGCTATAGCGTTTGCGG);

Peptide 7: Pep7 – Fwd (ATATGGATCCGGCGAAGTTCGTCTGCATTTTCAGTTTG)

Pep7 – Rev (ATATGAATTCAAGCTTACCACTGCTCTTTGCGACGATCTTCTG);

Peptide 8: Pep8 – Fwd (ATATGGATCCCAGTGGGAAACCAAACATCAGCGCAC)

Pep8- Rev (ATATGAATTCAAGCTTATTTGACGTGTTTGTTGTCCCACAGGTC).

Once the peptide expressing vectors were obtained, we introduced point mutations using a single step Megawhop annealing method with single overlapping primers bearing the desired mutations.

Primers used for mutagenesis :

Peptide 3 : S130A-Fwd: CTGGAGAACGTTGCCCAGTTAAGCCTGG

S130A-Rev: CCAGGCTTAACTGGGCAACGTTCTCCAG

S143A-Fwd: GACCGAAAAAAGCGCCCAGTACCTGAACC

S143A-Rev: GGTTCAGGTACTGGGCGCTTTTTTCGGTC

S142A,T143A-Fwd: GCCCGACCGAAAAAGCCGCCCAGTACCTGAACCAG

S142A,T143A-Rev: CTGGTTCAGGTACTGGGCGGCTTTTTCGGTCGGGC

Peptide 6 : S335A-Fwd: GATGGTAGCAGCGCTCAGACCGCGAATAAAC

S335A-Rev: GTTTATTCGCGGTCTGAGCGCTGCTACCATC

S333, 334, 335A-Fwd : GAACAGGAAGATGGTGCCGCCGCTCAGACCGCGAATAAACCG

S333, 334, 335A-Rev : CGGTTTATTCGCGGTCTGAGCGGCGGCACCATCTTCCTGTTC

GFP pull down assays, immunotrapping.

HeLa cells were seeded (2.10^7) in 150mm plates. Twenty-four hours, later when cells reached 80% confluence, 10µg of each GFP constructs were transfected in cells with Jetprime reagent, according to the manufacturer instructions. After 48h expression, cells are lysed in 1mL lysis buffer (Tris 50mM ph7,5, NaCl 150mM, EDTA 1mM, Triton 1%, Pefabloc 1mM, Phostop (Sigma), Complete Mini EDTA free protease inhibitor cocktail (Sigma)). Samples were pipetted up and down for 15 times in order to break cells and left on ice for 30min. Samples were centrifuged for 20min at 13200 rpm, 4°C and supernatants were collected in a new eppendorf. A fraction of the sample was kept aside as an input (1/20). For each sample, 25µL of GFP-Trap beads (Chromotek) were added. Samples are left at 4°C on a rotating wheel for 2h for GFP binding. Beads are washed three times with the lysis buffer (described above). Beads are then used for activity assay or for western blotting directly, resuspending them in Laemmli buffer.

Proximity ligation assay (PLA)

U2OS cells (75000 cells) used for this experiment are seeded on 12mm coverslips in 24 wells plates (Greiner). After two days of induction with doxycycline-supplemented media, cells are washed once with PBS on ice. A pre-extraction step using two washes of 5 min with CSK+Triton 0,5% is carried. Cells are fixed with PFA 3,7% for 20min, RT. Slides are blocked in PBS+3%BSA for 15 minutes and cells are permeabilized with 2 washes of PBS-Tween 0,1%. Cover slides are incubated with 250µL of PBS-Tween0,1% + 1% BSA containing primary antibodies over-night at 4°C. (Flag rabbit polyclonal antibody, dilution 1:10000; DNA-PK mouse monoclonal antibody, dilution 1:4000). Indirect proximity ligation assay was performed on each slide with the duolink in situ kit (Sig-

ma) on cells stably expressing flag-tag fused U2OS shPARG cell lines, according to the manufacturer's instruction. Cover slides are mounted on glass slides in fluorescence mounting media containing DAPI (Agilent/Dabco). At least 100 nuclei are acquired with a 40x Leica fluorescent microscope. Number of foci for each condition is counted with ImageJ software (NIH, Bethesda, MD, USA). Results are represented in vioplots with R version 3.4.2 software, using the vioplot package (Hintze and Nelson, 1998).

Activity assay

GFP beads are incubated in a kinase buffer (Tris HCl pH7.5 70 mM , $MgCl_2$ 10 mM, DTT 5 mM, Pefabloc 1 mM, OVaNa 1 mM, NaF 2 mM supplemented with 0.06µCi/µl [^{32}P]-gATP or non labelled ATP for 30 minutes at 30°C. Reaction is stopped by addition and incubation at 95°C for 5min. Samples are loaded on a gradient gel (4-15%, Biorad) and migrated for 1h30 at 130V. Gel is stained with Coomassie blue or Instant blue (Expedeon), acquired and then exposed for 16h for an autoradiography revelation in Typhoon LAS 700 (GE Healthcare).

DNA-PK activity assay

Alternatively, purified GST-fused PARG proteins from *E.coli* are incubated directly in 20µL DNA-PK reaction buffer. DNA-PK (Promega) is used as recommended in the manufacturer's instructions, the assay conditions are: 50mM HEPES (pH 7.5), 1mM DTT, 0.1mM EDTA, 0.2mM EGTA, 10mM MgCl2, 0.1M KCl, 1.14mM DNA-PK Peptide Substrate (Cat.# V5671), 80µg/ml BSA, 0.2mM ATP, 10µg/ml linear double-stranded DNA and trace [γ-^{32}P]ATP and 25 units of DNA-PK enzyme.

Mass spectrometry:

Seeking partner kinases with the full length PARG-GFP and the 1-87-PARG GFP (cloned in the pEGFP-C3 vector) was performed by the IGBMC proteomic platform (L. Negroni, M. Decourcelle, F. Ruffenbach), using MUDPIT analysis. Mass spectrometry experiments performed in order to identify phosphorylation sites were carried by the IBMC platform of the University of Strasbourg from our protein samples (P.Hammann, J. Chicher), using LC-MS/MS methodology.

Western blotting

Samples are boiled for 5min at 95°C in Laemmli buffer, loaded on a 4-20% gradient gel (Biorad) and migrated for 1h30 at 130V at ambient temperature in running buffer (25mM Tris, 190mM glycine, 0,1% SDS). Gels are transferred on nitrocellulose membrane in transfer buffer (25mM Tris, 190mM glycine, 20% ethanol). For normal sized proteins, blots are transferred for 2h at 4°C. For large proteins such as DNA-PK, blots are transferred for 4h at 4°C, 80V. Nitrocellulose membranes are blocked in TBS-Tween 0,05%, 5% milk for 30min RT. Membranes are probed with GFP mouse monoclonal antibody (Roche, 1:10000), GST rabbit polyclonal antibody (1:1000), PARG-Nter polyclonal antibody (homemade, 1:2000), PARP1 mouse monoclonal antibody (1:1000) and revealed with fluorescent secondary antibodies and revealed at the odyssey scanner (LICOR).

Acknowledgements:

We wish to thank F. Ruffenbach and M. Decourcelle (Proteomic Facility, IGBMC), as well as P. Hammann and J.Chicher (Proteomic Facility, IBMC), for their help and advice in all proteomic analysis. We also wish to thank C. Spenlé for her wise advice on the PLA technique. This work was supported by the Centre National de la Recherche Scientifique, Université de Strasbourg, Ligue contre le Cancer and Fondation pour la Recherche Médicale. EH was supported by the French Ministère de l'Enseignement Supérieur et de la Recherche and the Fondation pour la Recherche Médicale.

Bibliography :

Aguilar-Quesada, R., Muñoz-Gámez, J.A., Martín-Oliva, D., Peralta, A., Valenzuela, M.T., Matínez-Romero, R., Quiles-Pérez, R., Murcia, J.M., Murcia, G. de, Almodóvar, M.R. de, et al. (2007). Interaction between ATM and PARP-1 in response to DNA damage and sensitization of ATM deficient cells through PARP inhibition. BMC Molecular Biol *8*, 29.

Amé, J.-C., Héberlé, É., Camuzeaux, B., Dantzer, F., and Schreiber, V. (2017). Purification of Recombinant Human PARG and Activity Assays. Methods Mol. Biol. *1608*, 395–413.

Ariumi, Y., Masutani, M., D Copeland, T., Mimori, T., Sugimura, T., Shimotohno, K., Ueda, K., Hatanaka, M., and Noda, M. (1999). Suppression of the poly(ADP-ribose) polymerase activity by DNA-dependent protein kinase in vitro. Oncogene *18*, 4616–4625.

Blackford, A.N., and Jackson, S.P. (2017). ATM, ATR, and DNA-PK: The Trinity at the Heart of the DNA Damage Response. Mol. Cell *66*, 801–817.

Feng, X., and Koh, D.W. (2013). Roles of poly(ADP-ribose) glycohydrolase in DNA damage and apoptosis. Int Rev Cell Mol Biol *304*, 227–281.

Gagné, J.-P., Moreel, X., Gagné, P., Labelle, Y., Droit, A., Chevalier-Paré, M., Bourassa, S., Mcdonald, D., Hendzel, M., Prigent, C., et al. (2009). Proteomic investigation of phosphorylation sites in poly (ADP-ribose) polymerase-1 and poly (ADP-ribose) glycohydrolase. Journal of Proteome Research *8*, 1014–1029.

Hintze, J. L. and R. D. Nelson (1998). Violin plots: a box plot-density trace synergism. The American Statistician, 52(2):181-4.

Greenwood, C., Ruff, D., Kirvell, S., Johnson, G., Dhillon, H.S., and Bustin, S.A. (2015). Proximity assays for sensitive quantification of proteins. Biomol Detect Quantif *4*, 10–16.

Kaufmann, T., Grishkovskaya, I., Polyansky, A.A., Kostrhon, S., Kukolj, E., Olek, K.M., Herbert, S., Beltzung, E., Mechtler, K., Peterbauer, T., et al. (2017). A novel non-canonical PIP-box mediates PARG interaction with PCNA. Nucleic Acids Res *45*, 9741–9759.

Kedar, P.S., Stefanick, D.F., Horton, J.K., and Wilson, S.H. (2008). Interaction between PARP-1 and ATR in mouse fibroblasts is blocked by PARP inhibition. DNA Repair *7*, 1787–1798.

Keil, C., Gröbe, T., and Oei, S.L. (2006). MNNG-induced cell death is controlled by interactions between PARP-1, poly(ADP-ribose) glycohydrolase, and XRCC1. The Journal of Biological Chemistry *281*, 34394–34405.

Leuchowius, K.-J., Weibrecht, I., and Söderberg, O. (2011). In situ proximity ligation assay for microscopy and flow cytometry. Curr Protoc Cytom *Chapter 9*, Unit 9.36.

Mortusewicz, O., Fouquerel, E., Amé, J.-C., Leonhardt, H., and Schreiber, V. (2011). PARG is recruited to DNA damage sites through poly(ADP-ribose)- and PCNA-dependent mechanisms. Nucleic Acids Research *39*, 5045–5056.

Piao, L., Fujioka, K., Nakakido, M., and Hamamoto, R. (2017). Regulation of poly(ADP-Ribose) polymerase 1 functions by post-translational modifications. Frontiers in Bioscience.

Ruscetti, T., Lehnert, B.E., Halbrook, J., Le Trong, H., Hoekstra, M.F., Chen, D.J., and Peterson, S.R. (1998). Stimulation of the DNA-dependent protein kinase by poly(ADP-ribose) polymerase. J. Biol. Chem. *273*, 14461–14467.

Spagnolo, L., Barbeau, J., Curtin, N.J., Morris, E.P., and Pearl, L.H. (2012). Visualization of a DNA-PK/PARP1 complex. Nucleic Acids Res *40*, 4168–4177.

Discussion

1. New protein partners for PARG

A first GFP-trapping and mass spectrometry analysis in KEK293T cells performed in the lab yielded hundreds of putative protein partners, among which we could find dozens of kinases (J-C. Amé, personal communication). Among these we retained DNA-PK, because we found reproducibly found it in several independent mass spectrometry experiments, we also identified it as interacting with the 1-87-GFP PARG fragment, and because DNA-PK had already been reported as protein partner for PARP1. Indeed, PARP1 is found in a complex with DNA-PK and Ku (Spagnolo *et al.* 2012), DNA-PK phosphorylation can regulate PARP1's activity, and conversely, PARP1 PARylation can regulate DNA-PK's activity (Ruscetti *et al.* 1998, Ariumi *et al.* 1999). We noticed that when DNA-PK was retrieved in our datasets, Ku80 peptides were less abundant, and conversely (data not shown). This might suggest that PARG and DNA-PK compete for Ku80 binding the same way PARP1 does. Although our study focused on DNA-PK, some other interesting partners were identified in our datasets.

For instance, PARG-GFP was associated with FAK1 (Focal adhesion kinase 1), a kinase that activates several important signalling pathways such as the PI3K-AKT-mTOR pathway in which PARylation has roles to play (Philip *et al.* 2017). Plk4 and Cdk1 were also retrieved, but we never detected these kinases by western blot after GFP-trapping of the GFP-labelled 1-87-PARG construct. Another interesting example is WSTF (BAZ1B), a tyrosine-protein kinase that associates with PCNA (Poot *et al.* 2004), targets the remodelling complex ISWI to replication foci, and regulates topoisomerase I (TOP1) recruitment at replication forks (Ribeyre *et al.* 2016). In the literature, PARylation is described to regulate the ISWI nucleosome-remodelling complex, and PARP1 strongly contributes to chromatin remodelling (Sala *et al.* 2008; Hinz and Czaja, 2015; Posavec Marjanovic *et al.* 2017). In this aspect, PARG as well could be an important player in these processes.

We also co-purified the RUVBL1 protein, an ATPase of the remodelling complex INO80 that has diverse functions in maintaining genome integrity (Poli *et al.* 2017). RUVBL1 and RUVBL2 are regulators of the PIKK kinases (among which we can find ATM, ATR and DNA-PK), and our preliminary data show that PARG and RUVBL1 co-immunoprecipitate, the interaction increasing after H_2O_2 treatment (See **Figure 29**). RUVBL1 signal is detected after co-purification with the 1-87-GFP construct in the HCT1116 cell line.

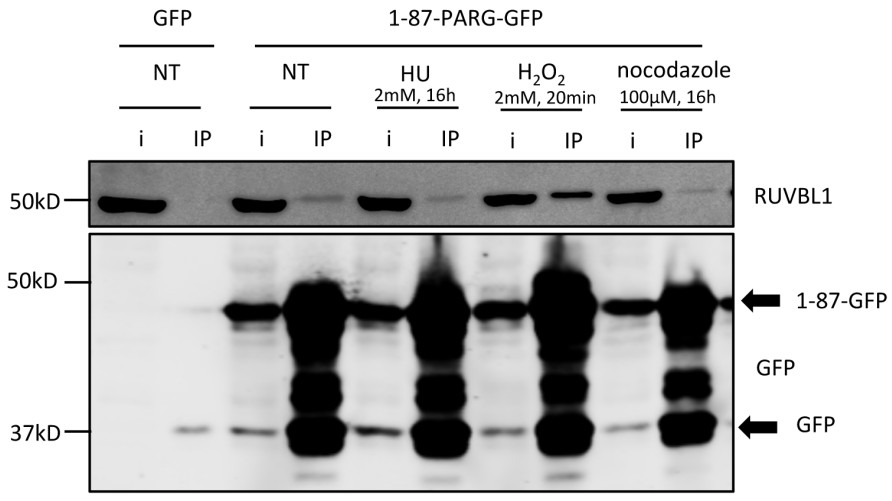

Figure 29: RUVBL1 co-purifies with PARG and the interaction increases after oxidative stress.
Western blotting of GFP and 1-87-PARG-GFP transfected HCT1116 cell extracts after GFP-trapping. I: input, IP: immunoprecipitation fraction.

Collectively, our data confirms that PARG has many other roles and protein partners, yet unravelled. Gene ontologies analysis and previous studies linked PARG with RNA biology and metabolism, functions we also retrieved in our datasets (Gagné *et al.* 2005; Gagné *et al.* 2010).

2. Monitoring labile interactions

With DNA-PK as our new putative partner, we intended many co-purification experiments, in the absence or presence of DNA-damages. When purifying the endogenous DNA-PK, we never managed to see a co-precipitation of endogenous PARG in our conditions. PARG being a very low abundance protein, we can imagine that the putative interaction stays below the western blot detection signal. However, when purifying PARG, it was possible to trap DNA-PK. However, the results were hardly reproducible, for it appears that DNA-PK is a huge protein (469kDa, Brewerton *et al.* 2004). Huge proteins can be destabilized from complexes during IP, and transfer slower during the western blot operations. In addition, kinase interaction with their substrate is very transient, which further complicates the visualization of the interaction. We decided to take advantage of our flag-tagged expressing PARG cell lines (shPARG-flag and shPARG-111-flag, described in **Aim1**), in order to refine the interaction between PARG and DNA-PK interaction events directly in cells, using PLA. Although this method needs some setting-up before finding the most efficient primary antibody couple to use for our purpose, it was the best method to monitor and quantify PARG and DNA-PK interaction. Alternatively, we could have used BiFC, FRET or other proximity-dependent assays (Lönn and Landergren, 2017). To get a full understanding of the protein environment of PARG, we could have derived our double-plasmid cell model in order to fuse PARG with the BirA enzyme, allowing the biotin labelling of all surrounding proteins in vivo, to analyse them by mass spectrometry. This method is called BioID and has been strongly envisaged during this project as an alternative to PLA (Varnaité and MacNeill, 2016). In the future perspectives of this project, it will be of the first importance to assess the variations in PARG and DNA-PK interaction in response to several types of cellular stresses.

3. Identification of phosphorylation sites: still a challenge

If the identification and validation of partner kinases was already a challenging task, the identification of phosphorylation residues was even trickier. In this study we focused on DNA-PK phosphorylation sites and to identify target residues, we used three different approaches. The first one is to predict all the phosphorylation sites on PARG. On Phosphosite.org (See **Figure 30**), we can indeed see that reported phosphorylation events in PARG are concentrated in the N-terminal part, which is an acidic region (isoelectric point, pI=6.0). The region between reisudes 250 and 350 is even more acid, with a pI of 3.94, whereas the catalytic C-terminal domain is more basic (pI=8.63). Our in vitro assays confirm that DNA-PK phosphorylates the N-ter PARG exclusively.

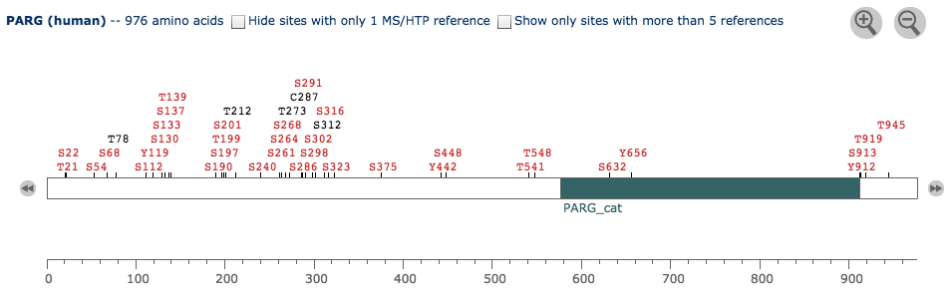

Figure 30: Phosphorylation site predictions on PARG sequence

PARG putative phosphorylation site was predicted on www.phosphosite.org

This is confirmed in Gagné *et al.* 2008, paper in which similar predictions were found with other algorithms. The phosphorylations that were found in this study are summarized in the figure below (**Figure 31**).

Phosphorylated residue(s)	For each phosphorylation experiment: Phosphorylation sites as revealed by either MS/MS (black rectangle) or MALDI-TOF MS (gray rectangle). (« x » : reported in the litterature)							Phoscan kinase prediction	Netphosk kinase prediction	Phospho-rylation potential	References
	Endo-genous	*Erk1*	*CKII*	*PKCβ*	*CaMK -II*	*JNK1*	*CDK5*				
PARG											
S^{22}	X							CDK, MAPK	CDK5, GSK3	High	Beausoleil *et al.*[49]
S^{137}	X							MAPK	CDK5, GSK3	High	Villen *et al.*[48]
S^{139}	X							PKC, CaMK-II, DNA-PK	PKC	High	Imami *et al.* [50]
T^{164} or S^{170} or T^{174}			■					CKII / Not predicted / Not Predicted	CKII / CKI, CDC2 / Not predicted	Low / High / Low	This study
S^{197} and T^{199}			■					CKII / CKII	CKII / CKII	High / High	This study
S^{261} and S^{264}	X							MAPK, ERK / CKII	P38MAPK,GSK3 / CKI	High / High	Villen *et al.*[48]
S^{261} or S^{264}			■					MAPK, ERK / CKII	P38MAPK,GSK3 / CKI	High / High	This study
S^{298}			■					CKII	CKII, PKG	High	This study
S^{316}			■					CKII	CKII	High	This study + Beausoleil *et al.*[47]
S^{962} or T^{966}			■					Not predicted / Not predicted	CKII / Not predicted	High / Low	This study

Figure 31: Reported phosphorylation sites on PARG sequence

(adapted from Gagné *et al.* 2008)

Of note, among the kinases identified in this article and in the literature, only one site is predicted to be a DNA-PK target site with the Phoscan kinase prediction algorithm. The same site can obviously be predicted as a PKC or as a CamK-II kinase target. When we used the NetPhosK 1.0 algorithm, we didn't yield the same phosphorylation sites. Predictions can be made on the basis of peptide sequences that were identified in mass spectrometry datasets. The comparison of such sequences gives an idea of the similarity between target sites, and helps to generate what is called "sequence logos". For DNA-PK, the sequence logo is shown above (**Figure 32**), and shows that DNA-PK almost exclusively targets serine or threonine residues that are followed by a glutamine residue (Bennetzen *et al.* 2010).

Three of our predicted serines fitted this sequence logo (S130, T143 and S335) however we couldn't exclude the others because we know of several examples of DNA-PK phosphorylation occurring in other sequence con-

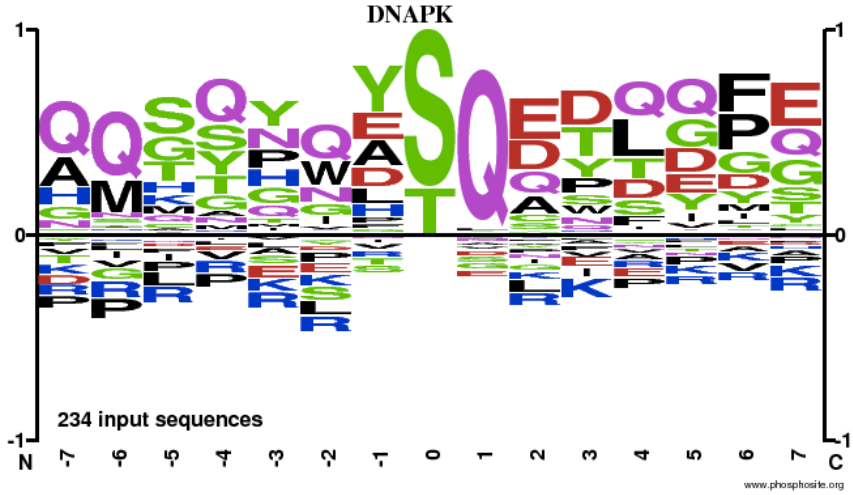

Figure 32: DNA-PK sequence logo
(from www.phosphosite.org)

texts, such as SL instead of SQ. As such we can mention that DNA-PK phosphorylates Artemis in vitro, on residue S503, in a ESLE context (Soodarzi *et al.* 2006). DNA-PK also targets the SAF-A/hnRNP U protein on residue S59 in response to DNA damage in a GSLD context, thus bridging non-homologous end-joining and RNA metabolism (Britton *et al.* 2009). In Ku80, S580 dwells in a SSLA context and is also a target for DNA-PK in vitro (Chan *et al.* 1999), and the serine S260 in XRCC4, dwelling in SSLD context is also targeted in vitro (Yu *et al.* 2003). Therefore, the choice of phosphorylation sites should not rely solely on predictions but also on direct mass spectrometry evidence. S90, S95 or S393 residues in PARG were not in an optimal sequence context but were nonetheless yielded in our experiments. In our parallel approach of dissecting PARG-Nterminal sequence into 7 smaller fragments, we detected weak phosphorylation signals in Peptide 1, Peptide 4 and Peptide 5 where no DNA-PK site was predicted nor yielded in mass spectrometry. We weren't able to detect strong phosphorylation signals in Peptide 7, although S392 was predicted. In Peptide 2, we couldn't rule out the fact that S90 and S95 were true phosphorylation sites, but couldn't test it in vitro by mutating, since peptide 2 appeared highly unstable, for unknown reasons, when we tried to purify it from bacteria.

For all these reasons, the choice of S130, S142/T143 and S335 mutations to alanine residues was reasoned, but still arbitrary. Then, I must mention that even if we confirmed that the single S130A or T143A mutations were decreasing phosphorylation levels on Peptide 3, the simultaneous mutation of S130, S142 and T143 did not further decrease the signal in autoradiography. This suggests the existence of other DNA-PK phosphorylation sites on Peptide 3. Accordingly, if the S335A mutation decreases Pep6 phosphorylation in vitro, the S333,334,335A mutation has not a stronger impact. Other sites are thus likely to exist, that remain to be identified. A phylogenetic sequence alignment of PARG sequence could similarly help us to identify conserved serine or threonine residues that could match DNA-PK specificity. Mutating these residues in N-ter and Full-length PARG would help confirming the DNA-PK target sites in longer peptide sequence context.

4. Functional impact of DNA-PK phosphorylation on PARG

Although we didn't identify and confirm all the possible DNA-PK target sites in vitro, we can make several assumptions about how these modifications could influence PARG activity. S130, that was predicted and confirmed in our in vitro assay, but was not yielded in our proteomic experiments, maps the putative nuclear export (NES) signal of PARG. We could imagine that phosphorylating the NES could regulate PARG localization in the cell. Indeed, we and others have shown that $PARG^{102}$ and $PARG^{99}$ were cytoplasmic isoforms, able to shut-

tle to the nucleus in order to degrade nuclear polymer (Haince *et al.* 2006, Mortusewicz *et al.* 2011, **Aim1**). While we detected no impact on PARG^{111} subcellular localization upon DNA-PK inhibition (data not shown), it would be interesting to investigate the localization of PARG^{102} and PARG^{99} in the same conditions.

The S335 site we identified lies between the CK-II-targeted S316 in PARG's caspase3-cleavage sites (Gagné *et al.* 2008), and a putative second bipartite NLS, conserved across organisms (421-441, Amé *et al.* 1999).

Alternatively, phosphorylation could regulate PARG activity or PARG stability. Although our dot-blot method did not allow us to conclude (for reasons discussed in the article), we could compare the PAR-degrading activities of phosphomutated versions of purified PARG in vitro, or even evaluate the impact of the reconstitution of phosphomutant or phosphomimetic versions of PARG-flag or PARG-GFP constructs, by complementing our PARG-deficient U2OS cell lines, generated in **Aim1**. Since PARG PTM in key domains (ex: PIP motif) can influence its interaction with other protein partners such as PCNA (Kaufmann *et al.* 2017), it would be interesting to monitor changes in the interactome of these kind of PARG mutants.

5. PARG and DNA-PK functional interaction

Our results show that in basal conditions, the inhibition or siRNA depletion of DNA-PK in PARG deficient cells does not significantly affect cell viability in clonogenic assay. The short term viability after transfection with siDNA-PK, however, slightly decreases compared with a shCTRL transfection. Preliminary results of short term viability and clonogenic assays performed on M059J-Fus9 DNA-PK deficient cells, compared with Fus1 cells, which are complemented with a portion of chromosome 8 bearing the DNA-PK gene (described in Hoppe *et al.* 2000), also suggest that the absence of DNA-PK sensitizes cells to the siRNA depletion of PARG (data not shown). In our hands though, Fus9 cells' growth rate was much lower than Fus1 cells, complicating the work with these cell lines. Since PARG and DNA-PK are both DNA-damage repair-linked enzymes, the importance of this interaction would probably be better highlighted in the context of damage, as suggested by the increase of PLA interaction foci after NCZ treatment. Other interesting data available in the lab suggest that PARG recruitment to laser-micro-irradiation induced DNA-damage is slower in 3T3 DNA-PK deficient mice cells, and that it remains longer at repair foci. Although these experiments need to be confirmed, the hypothesis that DNA-PK phosphorylation could affect PARG mobility could be a quite interesting lead for future researches.

6. DNA-PK and PARylation

Over the years, growing evidence show that PARP1 and DNA-PK are functionally linked, even beyond their physical interaction (Spagnolo *et al.* 2012) and their ability to catalyse post-translational modifications on each other (Ruscetti *et al.* 1998; Ariumi *et al.* 1999). DNA-PK is indeed a key component of the NHEJ pathway, in interaction with the KU70/KU80 proteins. PARP1 was identified in complex with KU as well as with DNA-PK (Li *et al.* 2004), and PARP regulates the NHEJ pathway through a competition with KU at double strand breaks (Wang *et al.* 2006). In the described model, Ku80 presence at double strand breaks favour classical-NHEJ, while PARP1 favours alternative-NHEJ (Audebert *et al.* 2004; Hochegger *et al.* 2006; Mansour *et al.* 2013). The tight links between PARylation and NHEJ components have even been described as an alternative pathway to mediate the PARP inhibitor synthetic lethality in homologous recombination deficient cells (Patel *et al.* 2011), and

conversely, deficiency of NHEJ components results in PARP inhibitor resistance in ovarian cancer cells (McCormick *et al.* 2017). Of note, the combined use of PARP and DNA-PK inhibitors sensitize cells to ionizing radiations and inhibit DNA repair, thus emerging as a powerful strategy to target tumours in the context of radiotherapies (Veuger *et al.* 2003; Veuger *et al.* 2004; Miura *et al*. 2012; Arad *et al.* 2014).

Therefore, a putative effect of PARG depletion on DNA-PK could be mediated by an effect on KU, which is a question we did not investigate.

Conclusions

In this article, we provided evidence that the first 87 amino acids of the N-terminal domain of PARG was sufficient to interact with co-purifying kinases, and notably DNA-PK, which is a new protein partner for PARG. We identified three residues (S130, S142/T143 and S335) that are targeted by DNA-PK in-vitro. Although we did not elucidate the functional impact of these phosphorylation sites, yet PARG phosphorylation could likely be an efficient leverage for the rapid and reversible modulation of PARG isoforms localization, stability or catalytic activity. While PARP1 was already demonstrated as a protein partner for DNA-PK (Spagnolo *et al.* 2012), this project demonstrated that PARG and DNA-PK interact as well, and suggest that the interaction increases in conditions of DNA-damage. We now know that DNA-PK is tightly linked to double strand break repair, and replicative stress (Ashley *et al.* 2014, Ying *et al.* 2016). DNA-PK complex defects trigger SCID syndrome (Severe Combined Immunity Deficiency), because it is involved in V(D)J recombination. It has functions in the appearance of cancer since it protects cells from genomic instability (Grundy *et al.* 2014, Goodwin and Knudsen, 2014). Since it is now a putative target for treating cancers, understanding its interactions with the PARylation pathways is now essential (Harnor *et al.* 2017). In the next chapter, we investigate the link between PARG deficiency and DNA-PK in the cell response to the anticancer drug camptothecin (**Aim3**).

Aim three: Impact of PARG deficiency on the cell response to camptothecin-induced DSB

Introduction

In the first part of this thesis project, I have generated new tools for the study of PARG (see **Aim 1**). Among these tools, U2OS cellular models were established, stably expressing an shRNA targeted against the C-terminal domain of PARG, shared by all its isoforms. This shRNA had already been successfully used to generate a PARG deficient HeLa cell line (Amé *et al.*2009). Our U2OS shPARG cell model can be complemented with GFP-labelled or flag-tagged PARG isoforms versions. These cell models allowed us to investigate many questions related with PARG biology. Particularly, we confirmed that DNA-PK was a new protein partner of PARG in vivo (see **Aim2**). DNA-PK is a serine/threonine kinase of the PI3-K family, which has a central role in double strand break (DSB) repair, acting in coordination with ATR and ATM for the maintenance of genomic integrity (for a review Blackford and Jackson, 2017). We were interested by this interaction, because several reports indicate that DNA-PK interacts with PARP1, and that PARylation could stimulate its activity (Spagnolo *et al.* 2012; Ruscetti *et al.* 1998). Although DNA-PK's kinase activity is mainly involved in the non-homologous end-joining pathway, it can also regulate homologous recombination and many other pathways, from metabolism to immunity, through V(D)J recombination (Kong *et al.* 2011). DNA-PK inhibitors are now serious candidates for the development of new cancer therapies (for a review, see Harnor *et al.* 2017). Importantly, DNA-PK is able to target the RPA 32kDa subunit, RPA2 and to mediate its hyper-phosphorylation. S4S8 phosphorylation is an important step in homologous recombination, and is also triggered upon replicative stress caused by HU and CPT that leads to the generation of DSB (Liaw *et al.* 2011, Ashley *et al.* 2014). Our lab has previously shown that PARG deficiency triggers a strong reduction in RPA2-S4S8 phosphorylation upon long HU treatment leading to DSB that was attributable to high PAR levels preventing RPA2 loading to ssDNA on chromatin (Illuzzi *et al.* 2014). For all these reasons, and taking advantage of our new U2OS shPARG model, we decided to investigate the role of PARG in the cell response to the anticancer drug camptothecin (CPT). CPT triggers replicative stress when replication forks collide with a blocked Topoisomerase I cleavage-complex (Pommier *et al.* 2010).

In order to decipher the role of PARG after CPT treatment, we decided to investigate several markers of stress and damage response (checkpoint activation, DNA damage…) just after an acute treatment and during a kinetic release from CPT, following a protocol scheme illustrated in **Figure 33**. Results obtained are presented in the following research paper draft.

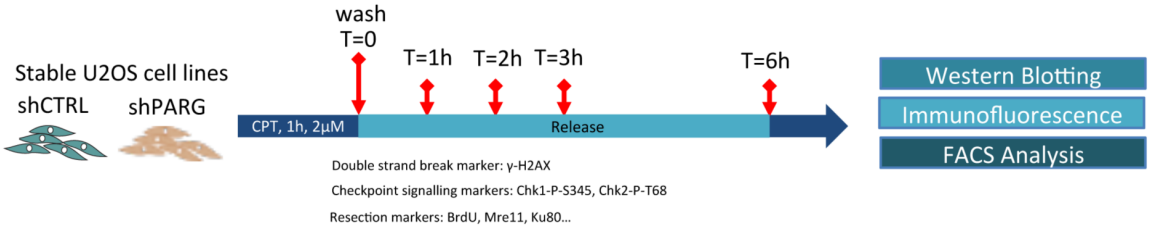

Figure 33: **Experimental procedure for evaluating the effect of PARG depletion in the cell response to camptothecin**
U2OS shCTRL and U2OS shPARG cells undergo an acute CPT treatment (2µM, 1h). DNA-damage repair steps are monitored during a 6h-release kinetics by standard cellular and molecular biology techniques.

Impact of PARG deficiency on the cell response to camptothecin-induced DSB

E. Héberlé[1], J.C. Amé[1], G. Illuzzi[1], F. Dantzer[1], V. Schreiber[1]

1. Biotechnology and Cell Signalling, UMR7242 CNRS, Université de Strasbourg, Laboratory of Excellence Medalis, ESBS, 300 Bd Sébastien Brant, CS 10413, 67412 Illkirch, France.

Corresponding author: V. Schreiber, valerie.schreiber@unistra.fr

Highlights

- PARG depletion slightly decreases DNA double strand breaks levels after CPT-induced replicative stress
- PARG depletion slightly reduces S-phase checkpoint activation after CPT treatment
- PARG depletion does not impair CPT-induced ATM and DNA-PK activity
- PARG activity is needed for CPT-induced RPA2-P-S4S8 and T21 phosphorylation
- PARG inhibition slightly protect from mild doses of CPT

Abstract:

Poly(ADP-ribose) is a post-translational modification catalyzed by a group of enzymes called Poly(ADP-ribose) polymerases (PARPs) and mainly degraded by Poly(ADP-ribose) glycohydrolase (PARG). Poly(ADP-ribose) homeostasis is important for the regulation of a broad range of cellular processes, including DNA repair, transcription, cell death and replication. Inhibitors targeting Poly(ADP-ribose) polymerases have entered clinical trials for the treatment of homologous recombination deficient tumours, in combination with antitumor drugs. In order to evaluate the interest of PARG inhibitors in this type of combined treatment, we investigated the role of PARG in the cell response to the anticancer drug camptothecin, which triggers replicative stress. For this purpose, we conducted a systematic molecular analysis of all steps of DNA damage response within a 6-hour kinetic response after camptothecin treatment in PARG-deficient U2OS cells. These cells displayed a strong decrease in RPA2-S4S8 phosphorylation with no comparable effect on DNA damage levels, DNA damage checkpoint activation and DNA resection. At least upon PARG inhibition, cell viability was slightly increased. These results suggest the existence of a camptothecin-induced replication stress resistance mechanism in PARG deficient cells, which compensates for the lack of RPA2-S4S8 phosphorylation.

Introduction:

Poly (ADP-ribose) (PAR) is an important post-translational modification (PTM) in the control of genomic integrity, which contributes to the proper coordination of repair factors and their activities at the vicinity of DNA damage. As such, it has several protein writers, readers and erasers. The Poly(ADP-ribosyl)ation (PARylation) event is mainly catalyzed by Poly(ADP-ribose) polymerase 1 (PARP1), the founding member of the PARP family (for a review, see Gupte *et al.* 2017; Chaudhuri and Nussenzweig, 2017). Cells accumulate PAR near sites of DNA damage to modulate the DNA damage response, before its erasers degrade this reversible PTM. The role Poly(ADP-ribose) glycohydrolase (PARG) in DNA damage response and replicative stress remains under-investigated. PARG is encoded as a single gene expressing several isoforms of different subcellular localizations in low abundance (Meyer-Ficca *et al.* 2004; Niere *et al.* 2008). Despite these constraints several milestone studies have been published on PARG role in DNA repair (reviewed in Feng and Koh, 2013). In mice, the disruption of all PARG isoforms is lethal at the embryonic stage (Koh *et al.* 2004). However, in cells, siRNA or shRNA depletion approaches targeting all isoforms is not lethal unless cells are treated with damaging agents. Our team showed that PARG-deficient HeLa cells are sensitive to irradiation, display a delayed repair of both single strand breaks and double strand breaks, and die by mitotic catastrophe (Amé *et al.* 2009). In human A549 cells, PARG depletion triggers sensitivity to oxidative damage (Fisher *et al.* 2007; Erdélyi *et al.* 2009). PARG invalidated mice cells display increased sensitivity to alkylating agents and irradiation (Shirai *et al.* 2013a; Shirai *et al.* 2013b). Thus, alike PARP1, PARG has important functions in DNA damage response. An exciting field of research arose when linking replication stress to DNA damage. Indeed, replicative stress occurs when replication forks encounter an obstacle. Upon HU treatment, replication fork slow and arrest, triggering an uncoupling between the replisome machinery and the upstream helicases unwinding DNA (Liew *et al.* 2016). This generates stretches of single stranded DNA (ssDNA) that need to be protected by the single strand binding protein RPA (Replication Protein A), a hetero-trimeric protein complex (RPA1: 70kDa; RPA2: 32kDa and RPA3: 40kDa) that has dynamic interactions with the DNA matrix and acts as a core component of replication, DNA repair and DNA recombination (Binz *et al.* 2004; Krasikova *et al.* 2016).

RPA coated ssDNA stimulates the activation of the DNA-damage checkpoint kinase ATR and Chk1 through interaction with the ATRIP protein (Berti and Vindigni, 2015). This mechanism helps stabilizing the stalled replication fork by coordinating the recruitment of accessory proteins until replication. While upon transient replicative stress, forks can restart or cells can fire new replication origins, upon prolonged replicative stress, replication forks eventually collapse; replication machinery dissociates ultimately generating single ended DSBs that need to be repaired, mainly by homologous recombination. To artificially trigger replicative stress, two agents are mainly used: hydroxyurea (HU) or camptothecin (CPT). HU is a ribonucleotide reductase inhibitor triggering a deprivation in the nucleotide pool and inducing transient fork stalling to fork collapse, depending on the exposure time (Petermann and Helleday, 2010). PARP1 inhibition in mouse fibroblasts or human cells sensitizes cells to HU treatment, and PARP1 favours replication fork restart from prolonged replicative stress by recruiting MRE11 enzyme in a PAR dependent manner (Yang *et al.* 2004, Bryant *et al.* 2009). After transient HU replication stress, PARP1 protects replication forks from extensive resection of the MRE11 containing MRN complex,

together with BRCA2 (Ying *et al*. 2012). The anticancer agent CPT selectively targets and stabilizes the Topoisomerase I-cleavage complexes formed upstream replication forks to relieve DNA supercoils (Pommier *et al.* 2013). Upon collision with the replication fork, Top1-linked single strand breaks can be converted into double strand break that need to be repaired. PARP1-deficient cells are hypersensitive to CPT treatment (Pommier *et al*. 2006), and PARylation is tightly linked to replication response at different levels. PARP1 is required for the recruitment and stabilization and activation of the TDP1 enzyme that directly removes TOP1-cc (Pommier et al. 2006, Das et al. 2016; Murai *et al.* 2014; Lebedeva *et al.* 2015). After TOP1 poisining by camptothecin, PARP1 is involved in a fork reversal mechanism, by slowing fork progression and inhibiting the RECQ1 helicase-dependent early restart of reversed forks (Ray Chaudhuri *et al.* 2012; Berti *et al.* 2013). Although PARG localizes at replication foci throughout cell phase through its two PCNA-interacting Motifs, suggesting a replication dependent role for this protein, its function in replication stress remains less studied than for PARP1 (Mortusewicz *et al.* 2011; Kaufmann *et al.* 2017). PARG-/- (deleted in exon 1) hypomorphic mice ES cells and PARG depleted human pancreatic cancer cell lines display increased S-phase arrest and DSB formation after treatment with alkylating agents, suggesting an enhanced replication stress (Shirai *et al.* 2013). PARG 2,3 -/- lacking exons 2 and 3 displayed persistant of Rad51 foci after short HU treatment, and gallotannin PARG inhibition resulted in increased spontaneous replication fork collapse, thus suggesting a rather protective role for PARG after replication stress (Min *et al.* 2010, Cortes *et al.* 2004).

Our lab has previously shown that PARG protects cells against prolonged replicative stress induced by HU. PARG deficient HeLa cell lines are more sensitive to long HU treatments, and accumulate detrimental amounts of PAR that prevents RPA2 loading to ssDNA and its subsequent hyper-phosphorylation (Illuzzi *et al.* 2014). PARG has also been shown to prevent the accumulation of abnormal replication structures in S-phase, in absence of damage (Ray Chaudhuri *et al.* 2015).

Here, we examined the impact of PARG deficiency on the cell response to the topoisomerase I inhibitor CPT. We demonstrate that U2OS shPARG cells present a strong defect in RPA2-S4S8 phosphorylation after replication stress induced by an acute treatment with CPT. We tested several hypotheses in order to explain the strong RPA2-P-S4S8 decrease: since PAR regulates TOP1 activity and favours the recruitment of TDP1, there could be a reduced formation of DSB in shPARG cells (**Hypothesis 1**). RPA2-P-S4S8 being a generally admitted marker of resection at stalled fork, there could be a reduced resection in shPARG cells (**Hypothesis 2**). As RPA2-P-S4/S8 phosphorylation is generally attributed to either ATM or DNA-PK, the RPA2-P-S4/S8 phosphorylation defect could be due to a reduced activity of these kinases (**Hypothesis 3**). Another hypothesis could be that it is due to a direct effect on RPA2 (**Hypothesis 4**), alike what was observed in long HU-triggered replicative stress (Illuzzi *et al.* 2014). These hypotheses were tested using, different markers of DNA repair and DNA damage signalling, comparatively followed during a 6-hour kinetics after release from a CPT treatment.

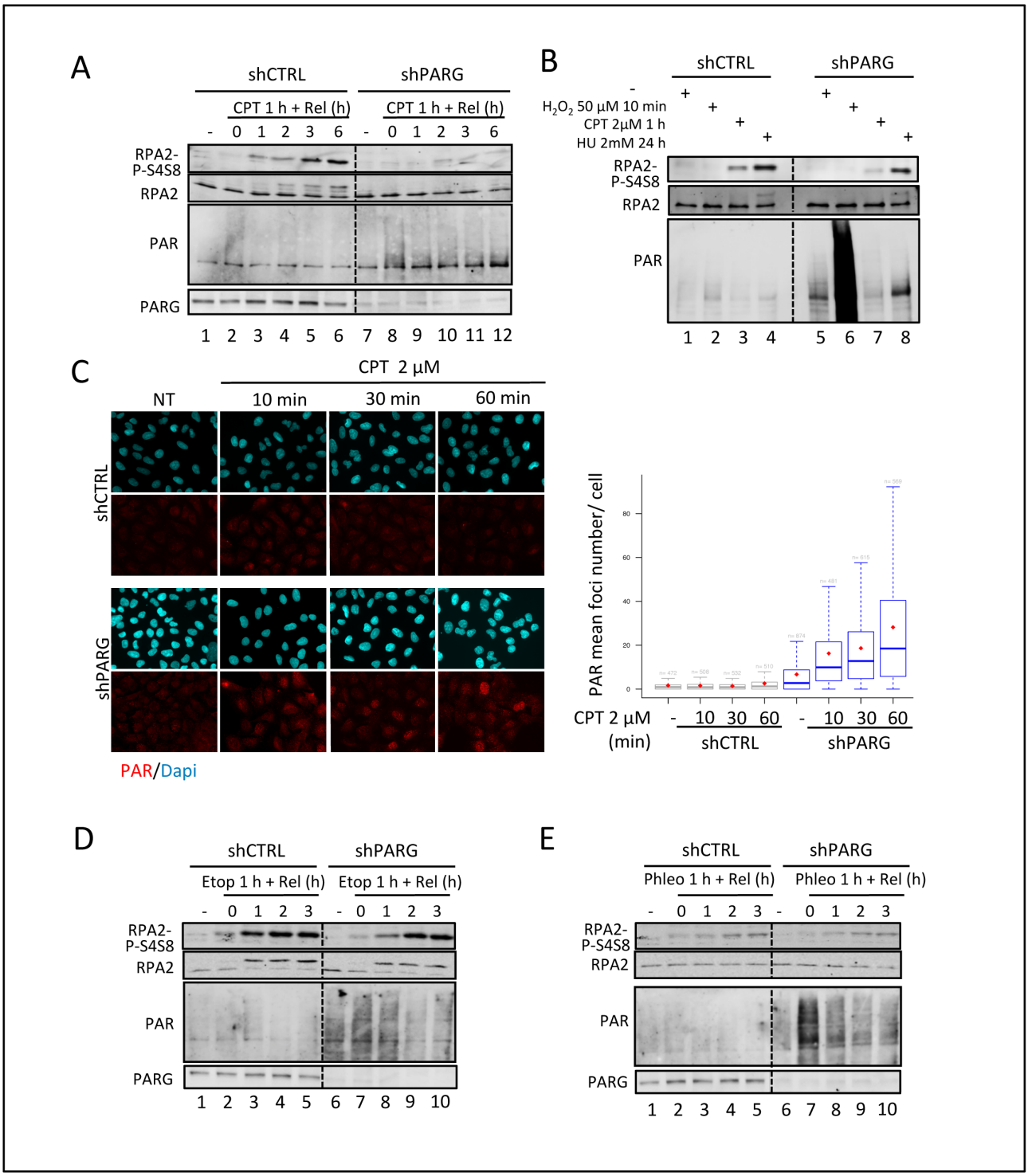

Figure 1: U2OS shPARG display a defect in RPA2-S4S8 phosphorylation after replicative stress induced by camptothecin. A) Western blotting of whole cell extracts in shCTRL and shPARG cells after a kinetic release after camptothecin treatment (2µM for 1 h). B) Comparison of RPA2, RPA2 phosphorylation and PAR accumulation after genotoxic stress in shCTRL and shPARG by western blotting on whole cell extracts (H2O2, 50µM; CPT, 2µM; HU, 2mM). C) Left: Immunofluorescence experiments monitoring PAR synthesis in shCTRL and shPARG cells treated with 2µM CPT for the indicated time. Red: PAR, Blue: DAPI staining. Right: Boxplot showing the PAR mean foci number per cell. The number of cell analysed is indicated for each condition. D) Western blotting of whole cell extracts of shCTRL and shPARG cells after a kinetic response to etoposide (20 µM for 1 h). E) Western blotting of whole cell extracts in shCTRL and shPARG cells after a kinetic response to phleomycin (25 µg/ml for 1 h).

Results

1. PARG is required for RPA2 hyperphosphorylation after camptothecin treatment

Our team has previously shown that upon prolonged replicative stress triggered by HU, RPA loading on chromatin was impaired in shPARG-deficient HeLa cells because of an over accumulation of polymer reducing RPA DNA binding capacity (Illuzzi *et al.* 2014). To study the role of PARG in the cell response to another trigger of replicative stress, the topoisomerase I inhibitor camptothecin (CPT), we have established U2OS cellular models in which all endogenous PARG isoforms were depleted by constitutive shRNA expression. The efficient PARG depletion was controlled by western blot (**Figure 1A**, compare lanes 7-12 to 1-6). To examine the impact of PARG deficiency on CPT-induced replicative stress, we followed the phosphorylation of RPA2 on Ser4/Ser8 (RPA2-P-S4S8) at different time points after the release from a one-hour cell treatment with 2 µM CPT. PARG-deficient cells exposed to CPT displayed a dramatic reduction of RPA2-S4S8 phosphorylation up to at least 6 h after the treatment. This defect is also observable by the absence of an upper-migrating band in the RPA2 revelation. PAR accumulated after 1h treatment in both shCTRL and shPARG, but persisted in shPARG (**Figure 1A**, lanes 8 to 12) whereas it immediately decreased in shCTRL (**Figure 1A**, lanes 2 to 6).

To compare the CPT-induced RPA2-S4S8 phosphorylation and PAR production with that of a prolonged HU treatment (Illuzzi *et al.* 2014), we performed parallel treatments in both cell lines with CPT (2µM, 1h) or HU (2mM, 24h). A treatment with oxidative damage (H_2O_2, 50µM, 10min) was done in parallel as a positive control for PAR synthesis. Steady state levels of PARylation were higher in shPARG cells, as expected (**Figure 1B**, compare lanes 1 and 5). In shPARG cells, H_2O_2 triggered a massive accumulation of PAR, as expected because PARP1 is strongly activated after oxidative damage. Upon CPT treatment, there was no clear accumulation of PAR, rather a decrease in shPARG, (**Figure 1B**, compare lanes 3 and 7). PAR accumulation was much higher in HU treated shPARG cells (**Figure 1D**, lane 8), in agreement with our previous data (Illuzzi *et al.* 2014). RPA2-S4S8 phosphorylation was strongly reduced in shPARG cells compared to shCTRL cells for both CPT and HU treatments (**Figure 1B**). However, whereas the strong impact of PARG deficiency on RPA2-P-S4S8 could be attributed to massive PAR produced upon prolonged HU-treatment, it is very unlikely that the limited amount of PAR produced upon CPT treatment explains the strong reduction in RPA2-P-S4S8 upon CPT treatment.

Since PAR accumulation after CPT has been reported previously (Zhang *et al.* 2011, Patel *et al.* 2012, Das *et al.* 2014), we monitored PAR levels using a more sensitive method, immunofluorescence. We observed a notable accumulation of the number PAR foci per cell, from 10 to 30 min of CPT treatment in shPARG cells, whereas PAR was hardly detectable in shCTRL cells (**Figure 1C**). This further supports the hypothesis that the reduction of CPT-triggered RPA2-S4S8 phosphorylation in shPARG cells is unlikely explained by such limited increased PAR levels.

We next examined whether reduction of RPA2-S4S8 phosphorylation in shPARG cells was restricted to conditions leading to replication stress or could reflect a more general outcome of DSB generation. We performed cell treatments with the DSB-inducing agents Etoposide and Phleomycine. After the release from a 1h treatment with 20 µM Etoposide, U2OS shCTRL cells displayed a gradual increase in RPA2-S4S8 phosphorylation

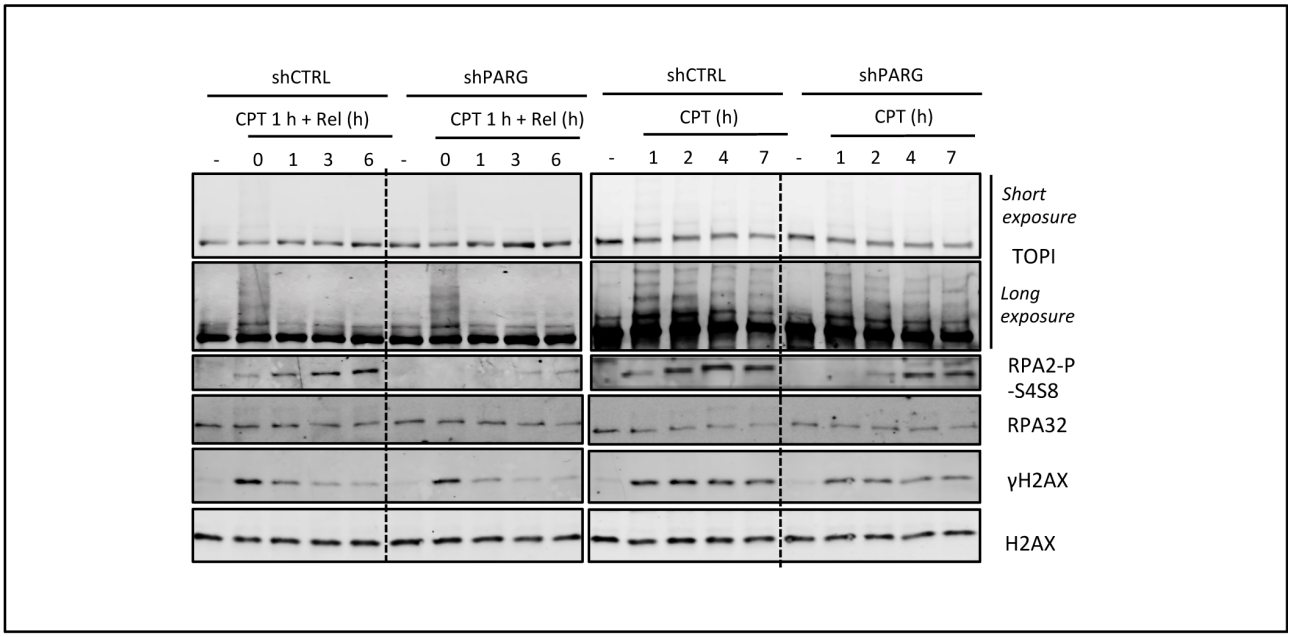

Figure 2: TOP1 accumulation, RPA2 and YH2AX accumulation after long or short exposure to CPT
Western blotting after CPT treatment and release. TOP1 accumulation, RPA2, RPA2-P-S4S8, γH2AX and H2AX levels are monitored after transient exposure to CPT and release (2µM, 1h, left panel) or prolonged CPT treatment (2µM for the indicated times, right panel), in shCTRL and shPARG cells.

(**Figure 1D**, lanes 1 to 5). In U2OS shPARG cells (**Figure 1D**, lanes 6 to 10). RPA2-S4S8 phosphorylation also accumulated, although with a slightly delayed kinetics.

As expected in shPARG cells, the overall polymer levels were higher than in shCTRL cells. After release from a 1h treatment with 25 µg/ml Phleomycin, we observed a similar slight reduction of RPA2 phosphorylation and a strong accumulation of polymer in shPARG cells compared to shCTRL cells (**Figure 1D**, lanes 7 to 10 compared to 2 to 5). However, the reduction in RPA2-P-S4S8 observed in shPARG cells upon Etoposide and Phleomycin treatment if far less than the one observed upon CPT treatment, suggesting that the absence of PARG more significantly affect the cell response to replicative stress induced by CPT.

2. shPARG cells and shCTRL cells display similar TOP1 dynamics after CPT treatment

Topoisomerase I relieves tensions in DNA at sites of torsions, upstream replication forks and transcription bubbles. It acts by creating a nick in DNA allowing the unwinding of the DNA helix. The reaction intermediate is called TOP1 cleavage complex, and CPT treatment results in TOPI-cc blocking and covalent binding to DNA (Laev *et al*. 2016). Early studies demonstrated that TOP1-cc was ubiquitinated and destroyed by the proteasome after CPT treatment (Desai *et al.* 1997). TOP1 activity and regulation have been tightly linked to PARylation. TOP1 is a PAR acceptor and PAR was proposed to reduce the formation of TOP1-cc but also to favour the religation activity of TOP1 (Malanga *et al*, 2002; Park and Chang, 2005; D'Onofrio *et al.* 2011). More recently, PARP activity was reported to regulate TOP1 dynamics within the nucleus (Das *et al*. 2016).

We analysed by western blot the kinetics of TOP1 ubiquitination and degradation in CPT-treated shCTRL and shPARG cells by the appearance of upper bands corresponding to ubiquinated forms of TOP1 (Desai *et al.* 1997). Upon short CPT treatment, in both cell lines, Ub-Topo1 accumulated transiently during the one-hour exposure to camptothecin and then disappeared, but the overall TOP1 level did not vary suggesting that TOP1 is not massively degraded (**Figure 2**, left panels). A persistent CPT treatment was necessary to detect a CPT-induced TOP1 degradation, that appeared to be similar in both cell lines, with Ubi-TOP1 similarly formed throughout the treatment (**Figure 2**, right panels). By immunofluorescence, we also observed a normal subcellular redistribution of TOP1 that normally exited the nucleolus after CPT treatment in both cell lines (data not shown). Therefore, our results suggest that the absence of PARG does not impact on CPT-induced TOP1 subcellular distribution. As mentioned above, PARP1 activity was reported to regulate TOP1 activity. In addition, PAR produced upon CPT treatment was shown to promote the recruitment of the XRCC1/TDP1 complex aimed to resolve the TOP1-DNA covalent link (Das *et al.* 2014). It was therefore tempting to propose that in the absence of PARG, the increased PAR level would facilitate these steps, increasing the repair efficiency and thus reducing the fork collapsing and formation of DSB. To test this hypothesis, we tried to examine by immunofluorescence the recruitment of XRCC1 and TDP1 to CPT-induced lesions following published protocols (Das *et al.* 2014; Ying *et al.* 2016). Despite several attempts, we never obtained conclusive data; no specific foci could be observed with the recommended anti-XRCC1 and anti-TDP1 antibodies we have tested (data not shown). To overcome this problem, and to evaluate the amount of DSB generated after CPT treatment in our cell lines, we examined the kinetics of γH2AX signal, a consensual marker of DSB occurrence. We reasoned that monitoring DSB formation would indirectly reflect the conversion of TOP1-cc to DSB.

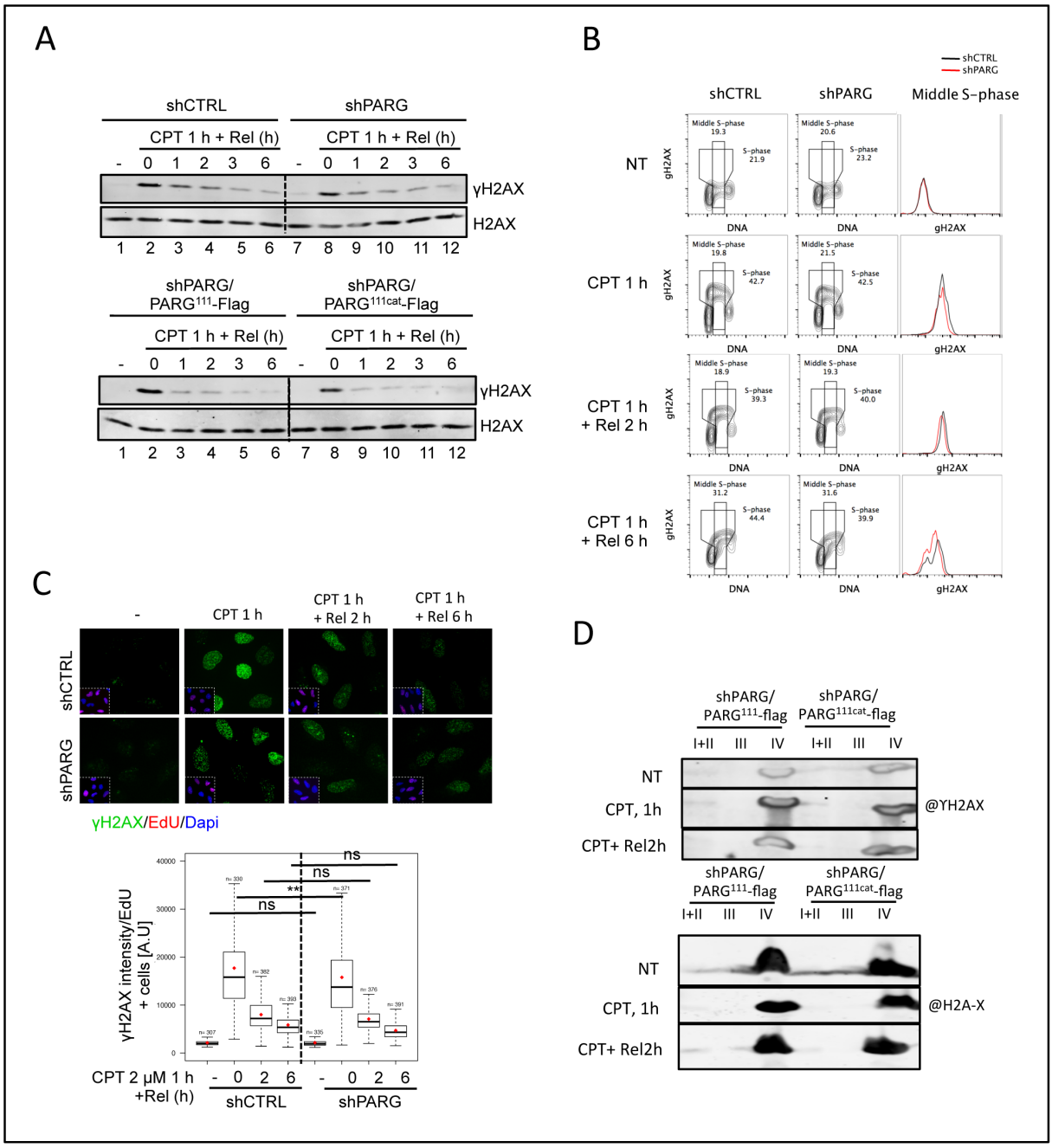

Figure 3: The absence of PARG is associated with a slight reduction in ϒH2AX levels. A) Western blotting of whole cell extracts of shCTRL and shPARG cells, shPARG/PARG^{111}-flag and shPARG/PARG^{111cat}-flag cells after a kinetic response to camptothecin. B) FACS analysis of the γH2AX levels in shCTRL and shPARG cell lines after CPT treatment and release. C) Quantitative immunofluorescence of γH2AX intensity in shCTRL and shPARG. S-phase are stained with EdU labelling. D) Chromatin fractionation of shPARG/PARG^{111}-flag and shPARG/PARG^{111cat}-flag cell extracts. I+II: soluble fraction, III: nuclear soluble fraction, IV: chromatin unsoluble fraction.

3. shPARG cells display a slight decrease in CPT-induced γH2AX levels

To evaluate the amount of CPT-induced DSB, we followed γH2AX accumulation and persistence after a transient CPT treatment in control and PARG deficient cells. By Western blot, we observed for both cell lines an accumulation of γH2AX levels directly after the treatment followed by a progressive reduction till 6h of release (**Figure 3A**, upper panel). Of note, a slight reduction in γH2AX levels was observed in shPARG cells just after the CPT treatment (**Figure 3A**, compare lanes 2 and 8). In order to prove that what is observed in shPARG cells compared to shCTRL cells is due to the invalidation of PARG catalytic activity, we have complemented shPARG cells by re-expressing either wild type active $PARG^{111}$ ($PARG^{111}$-Flag) or a catalytically inactive $PARG^{111}$ mutant ($PARG^{111cat}$-Flag) harbouring the E755,756A mutations (Mortusewicz *et al.* 2011). Both are expressed upon doxycyclin induction as Flag-tagged proteins (see Chapter 1 for their description). Again, we observed a slight reduction in γH2AX signal after 1 h of CPT in shPARG cells complemented with the inactive PARG111, compared to cells complemented with the wild type PARG111, suggesting that this slight reduction of γH2AX is a direct consequence of PAR accumulation (**Figure 3A**, lower panel).

We next examined the presence of CPT-induced γH2AX on chromatin by performing chromatin fractionation assays in shPARG/$PARG^{111}$-flag and shPARG/$PARG^{111cat}$-flag cell lines. First, detection of γH2AX on total lysates revealed the similar slight reduction of γH2AX levels in shPARG/$PARG^{111cat}$-flag compared to shPARG/$PARG^{111}$-flag cells (**Figure 3B**). However, the accumulation of H2AX and γH2AX in fraction IV (chromatin bound fraction) was not significantly different between the two cell lines (**Figure 3B**).

Western blotting on total lysates and on chromatin fractionations gives only an average view of a cell population. To have a more precise view at the level of individual cells, we followed CPT-induced γH2AX formation by FACS and by immunofluorescence (**Figure 3C and 3D**). By FACS analyses, DNA content measurement by PI staining revealed a similar cell cycle distribution for both cell lines in absence of CPT treatment (**Figure 3C**). Fitting with this observation is the similar average doubling time of 30 +/- 2 hours for both cell lines (data not shown). After CPT treatment, for both cell lines, γH2AX strongly increased immediately after the treatment and progressively decreased with time throughout the duration of the experiment. Again, γH2AX signal was slightly reduced in shPARG cells compared to shCRL cellss (**Figure 3C**). Of note, γH2AX was specifically increased in S-phase cells, which is in agreement with published data showing that CPT induces DSB specifically in S-phase of replicating cells (Chanut *et al.* 2016). Quantitative immunofluorescence microscopy confirmed the FACS analyses, also showing a slight but significant reduction of γH2AX signal after 1h CPT treatment in S-phase cells labelled with EdU (**Figure 3D**). Taken together, these results are in favour of a slight reduction in CPT-induced DSB formation upon PARG catalytic inactivation, however unlikely to be sufficient to explain the observed drastic reduction of RPA2-S4S8 phosphorylation.

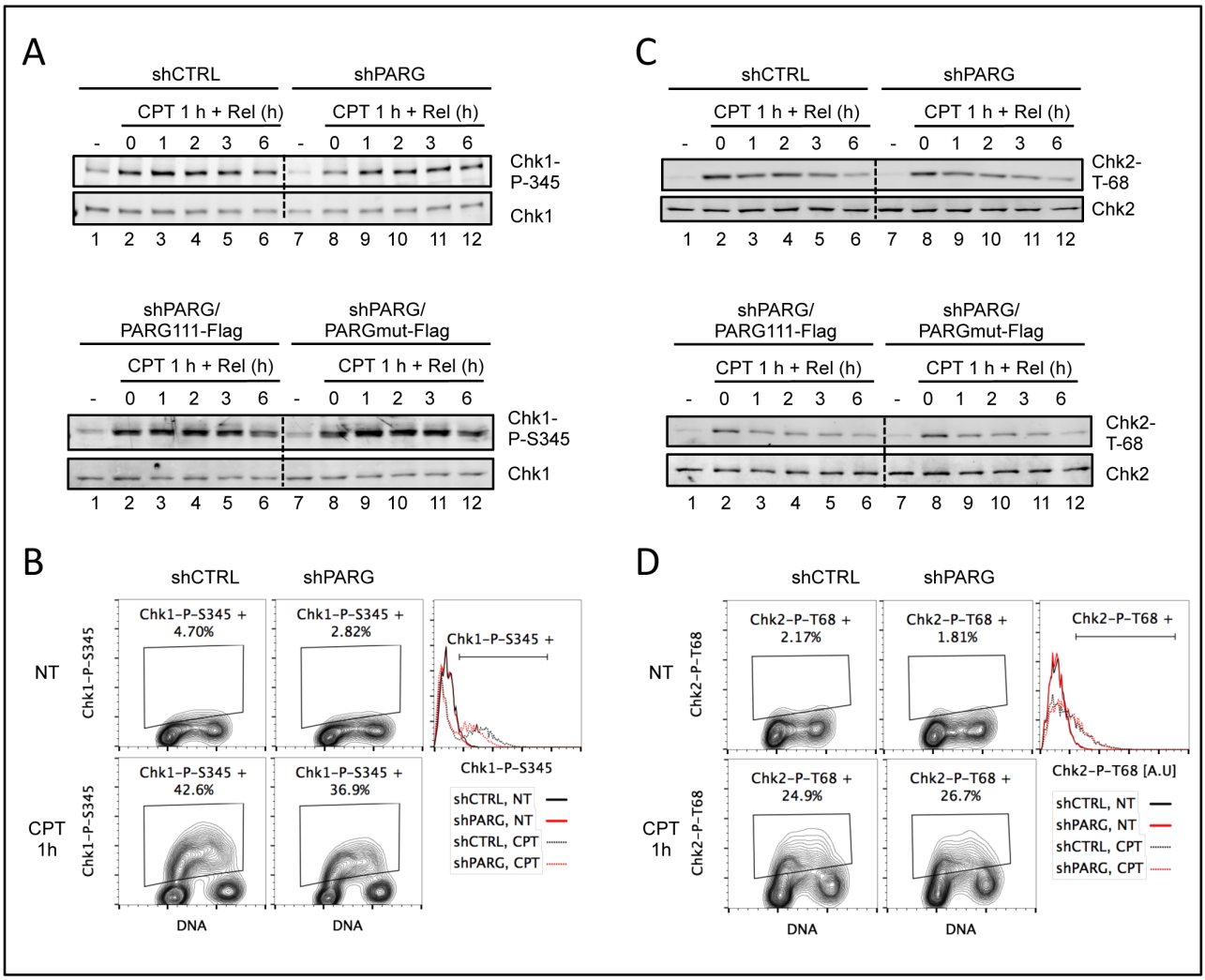

Figure 4: shPARG cells display no defect DNA damage checkpoint signalling but a slight delay in replication stress checkpoint activation.

A) Western blotting of CHk1-P-S345 phosphorylation and Chk1 levels in shCTRL, shPARG and complemented shPARG/PARG111-Flag and shPARG/PARG111cat-flag whole cell extracts. B) FACS analysis of CHk1 phosphorylation levels in S-phase shCTRL and shPARG cells in response to CPT. C) Western blotting of CHk2-P-T68 phosphorylation and Chk2 levels in shCTRL, shPARG and complemented shPARG/PARG111-Flag and shPARG/PARG111cat-flag whole cell extracts. D) FACS analysis of CHk2 phosphorylation levels in S-phase shCTRL and shPARG cells in response to CPT.

4. shPARG cells display a slight reduction in S-phase checkpoint activation but a normal activation of DSB-induced checkpoint after CPT treatment

To prevent the accumulation of mutations, cells respond to DNA lesions by inhibiting cell cycle progression in order to allow DNA repair. Chk1 kinase is required for the S-phase checkpoint; it is mainly activated by ATR phosphorylation of S317 and S345 (Cimprich and Cortez, 2008). This Chk1 phosphorylation triggers downstream phosphorylation events to stabilize replication forks and to arrest cell-cycle progression to avoid an early entry into mitosis. We compared the replication checkpoint activation in shCTRL and shPARG cells throughout the kinetics of CPT treatment by monitoring Chk1-S345 phoshorylation by Western blot. In shCTRL cells, Chk1 activation was seen already just after CPT treatment, peaked after 1h release and reduced between 3 or 6 hours. The early activation of Chk1 was reduced in shPARG cell line (**Figure 4A,** upper panel, compare lanes 8 and 2). The same experiment was performed in shPARG cell lines complemented with either the flag-tagged version of $PARG^{111}$ (shPARG/$PARG^{111cat}$-flag) or the flag-tagged $PARG^{111}$ mutated in its catalytic domain (shPARG/$PARG^{111cat}$-flag). Similar conclusions were made, with a reduced activation of Chk1 just after CPT treatment, but a similar kinetic after release (**Figure 4A**, lower panel, compare lanes 8 and 2). These results suggest that the lack of PARG activity reduced the early CPT-induced activation of Chk1. At later time points after the release from CPT treatment, P-Chk1-S345 was similar between both lines. FACS analyses confirmed that there was less Chk1-P-S345 in shPARG cells after 1h of CPT treatment (**Figure 4B**). Of note, it is the intensity of Chk1-phosphorylation that was significantly reduced, not the number of cells, since almost all S-phase cells were Chk1-P-S345 positive for both cell lines. Taken together, these results suggest a delayed activation of the S-phase checkpoint in PARG-deficient cells in response to CPT.

The Chk2 kinase is also activated in response to replication block and DNA damages leading to DSB. Activation of Chk2 is measured by following its phosphorylation on threonine 68. This phosphorylation event is mainly attributed to the ATM kinase. In both shCTRL and shPARG cell lines, Chk2-P-T68 phosphorylation increases after CPT treatment, and slowly decreases during the release. There was no significant difference between shCTRL and shPARG cells, nor between shPARG/$PARG^{111}$-flag and shPARG/$PARG^{111cat}$-flag complemented cell lines (**Figure 4C**). The same observation was made by FACS analyses with a similar number of cells positive for Chk2-T68 phosphorylation and similar intensity. In conclusion, shCTRL and shPARG cells display similar kinetics and levels of Chk2 activation in response to CPT. As Chk2 activation is associated with DSB signalling, this supports the hypothesis that the CPT-induced DSB levels should be rather equivalent in both cell lines. Therefore, the fact that PARG deficiency could have a slight protective effect on CPT-induced stalled forks, to prevent them from collapsing, is probably not sufficient to account for the drastic reduction of RPA2-S4S8 phosphorylation observed.

5. DNA resection at CPT-induced DSB is not dramatically altered in shPARG cells

The second addressed hypothesis was that shPARG cells could display an impaired resection at CPT-induced collapsed forks. Indeed, cells must deal with single ended DSB that have no equivalent end to be

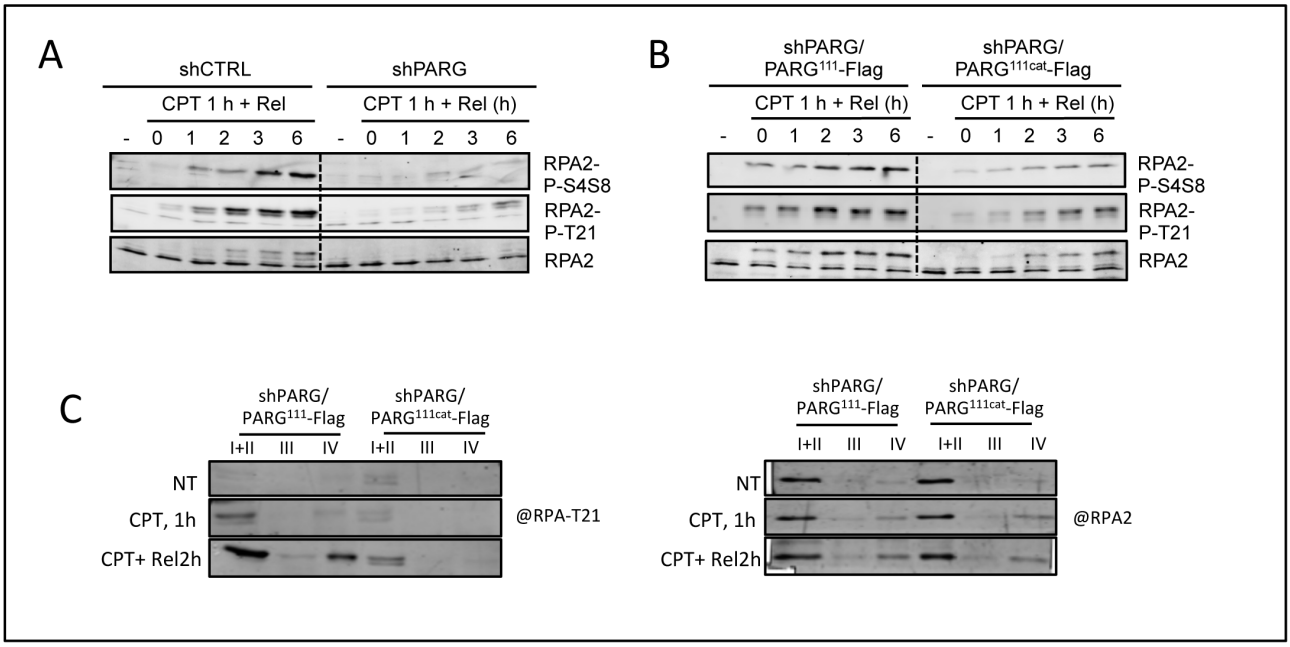

Figure 5: The absence of PARG is associated with a dramatic defect of RPA2 phosphorylation that is not correlated to RPA2 loading on chromatin (1/2) A) Western blotting of whole cell extracts of shCTRL and shPARG cells after a kinetic response to camptothecin. B) Western blotting of whole cell extracts of shPARG/PARG^{111}-flag and shPARG/PARG^{111cat}-flag cells after a kinetic response to CPT. C) Chromatin fractionation of shPARG/PARG^{111}-flag and shPARG/PARG^{111cat}-flag cell extracts. I+II: soluble fraction, III: nuclear soluble fraction, IV: chromatin unsoluble fraction.

joined with. Therefore, they need to inhibit repair through non-homologous end joining and to favour DNA-end resection and homologous recombination repair in order to avoid detrimental asymmetric joining (Zeman *et al.* 2014). RPA2-P-S4S8 is commonly used as a marker of DNA-end resection, RPA being rapidly recruited to protect single-strand DNA arising from DNA resection with bound RPA2 becoming hyper-phosphorylated on several sites, among them Ser4, Ser8 and Thr21 (Block *et al.* 2004; Anantha *et al.* 2007; Liaw *et al.* 2011; Chanut *et al.* 2016).

To investigate in more details resection efficiency in CPT-treated shPARG cells, we monitored RPA2 phosphorylation on Ser4, Ser8 and Thr21 and compared it with the chromatin loading of RPA2. As previously shown in **Figure 1**, RPA2-S4S8 phosphorylation increased with time after CPT treatment and release in shCTRL cells, whereas this increase was much lower in shPARG cells (**Figure 5A**). RPA2-T21 phosphorylation was similarly impaired in shPARG cells (**Figure 5A**). We observed a similar defect of RPA hyperphosphorylation in shPARG/PARG^{111cat}-flag cell lines when comparing to shPARG/PARG^{111}-flag, again suggesting that it is PARG activity, not protein, that is necessary for normal RPA2-S4S8 and T21 phosphorylation (**Figure 5B**). We next examined the recruitment of RPA2 on chromatin and its phosphorylation on T21 by performing chromatin fractionation assays in CPT-treated shPARG/PARG^{111}-flag and shPARG/PARG^{111cat}-flag cell lines. The accumulation of RPA2 in fraction IV (chromatin bound fraction) was not significantly different between the two cell lines (**Figure 5C**), whereas phosphorylation of RPA2 on T21 was again dramatically impaired in shPARG cells (**Figure 5C**).

To have a more precise view of RPA2 recruitment and phosphorylation at the level of individual cells, we performed FACS and immunofluorescence microscopy on CPT-treated cells after a pre-extraction of soluble proteins to visualize chromatin bound proteins (**Figure 6A and B**). FACS analyses confirmed the strong defect on RPA2-S4S8 phosphorylation in CPT-treated shPARG cells and after 3 and 6 hours of release (**Figure 6A**). For RPA2, there was no remarkable difference between cell lines in the percentage of positive RPA2 cells throughout the kinetics (**Figure 6B**), but RPA2 intensity was slightly decreased at all time points after treatment (compare median intensity of RPA2 positive cells for CPT-treated shCTRL and shPARG cells, respectively). Again, both RPA2 and RPA2-P-S4S8 signals were specifically increased in S-phase cells, confirming that CPT induces DSB specifically in S-phase of replicating cells.

Quantitative immunodetection of chromatin associated RPA2-P-S4S8 by fluorescence microscopy was performed after a CSK pre-extraction of the soluble proteins and combined with an EdU labelling of S-phase cells. Results confirmed this dramatic phosphorylation defect in shPARG cells compared to shCTRL cells (**Figure 6C**). With a similar protocol, we followed by immunofluorescence microscopy RPA2 foci formation in pre-extracted cell lines. Superimposition of EdU signal with RPA2 signal nicely correlated, confirming that CPT-induced lesions affect essentially replicating cells. Quantification analyses confirmed that neither RPA2-S4S8 nor RPA2 foci were efficiently detected in the EdU-negative non-S phase cells (data not shown). Results showed that in shCTRL cells, RPA2 foci formed after CPT treatment, their intensity (not shown) and number further increasing 2 and 6 hours after the release from the treatment (**Figure 6D**). In shPARG cells, RPA2 foci also efficiently accumulated, at however slightly lower levels than shCTRL, the difference being significant only at late time-point release after CPT (2 and 6 hours), confirming FACS analyzes. Taken together, these results suggest

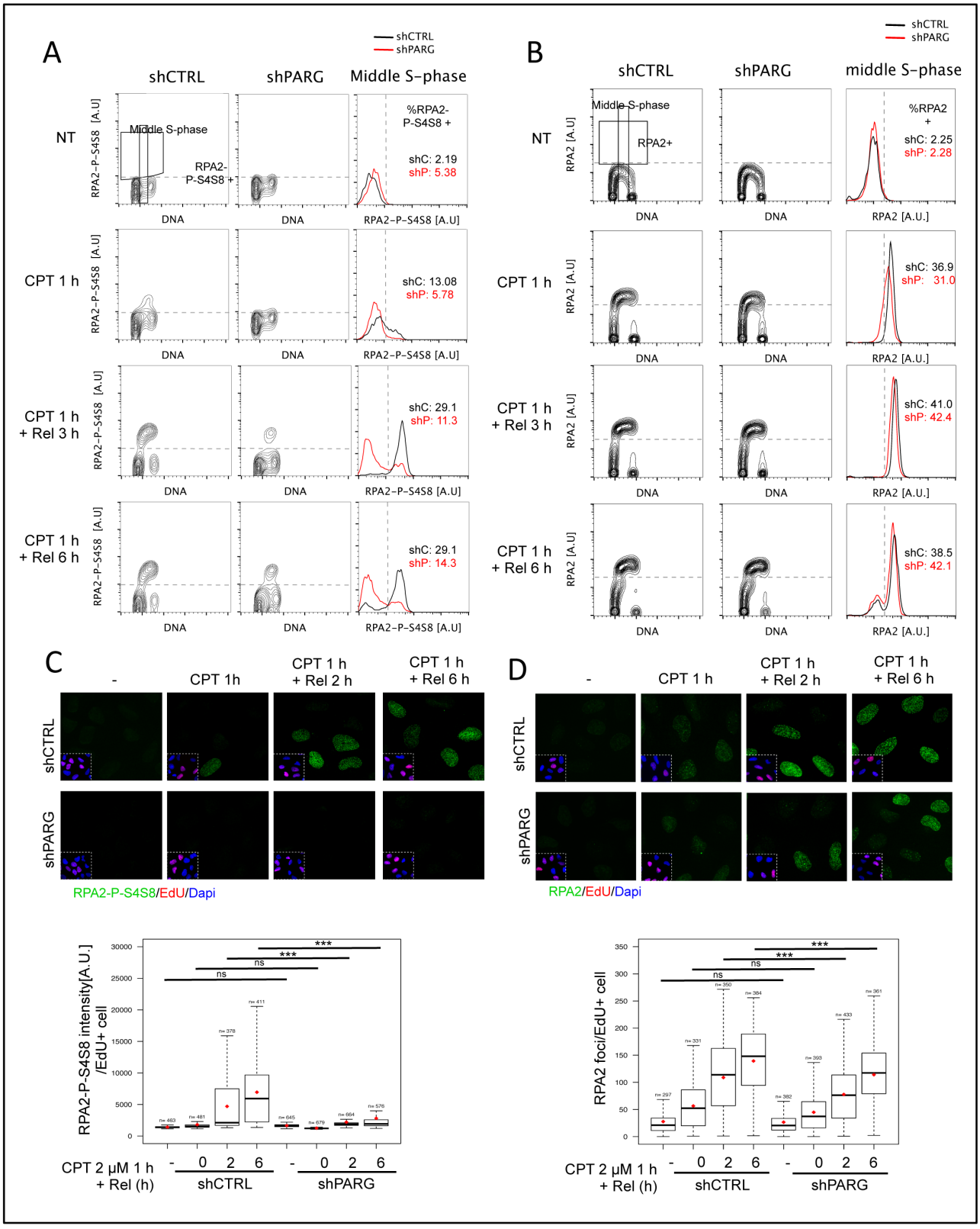

Figure 6: The absence of PARG is associated with a dramatic defect of RPA2 phosphorylation that is not correlated to RPA2 loading on chromatin (2/2) A) FACS analysis of RPA2-S4S8 signal on chromatin in shCTRL and shPARG cells. Western blotting of whole cell extracts of shCTRL and shPARG cells. B) FACS analysis of the RPA2 levels in shCTRL and shPARG cell lines after CPT treatment and release. C) Quantitative immunofluorescence of the RPA2-S4S8 phosphorylation intensity in Edu positive S-phase shCTRL and shPARG cell lines after CPT treatment and release. RPA2-S2S8 is stained in green, S-phase cells are stained in red, and nucleuses are DAPI stained in blue. D) Quantitative immunofluorescence of the RPA2 l-foci number in Edu positive S-phase shCTRL and shPARG cell lines after CPT treatment and release. RPA2-S2S8 is stained in green, S-phase cells are stained in red, and nucleuses are DAPI stained in blue.

that whereas part of RPA2 hyperphosphorylation defect could thus be explained by the slight reduction in RPA2 recruitment to chromatin, it is however very unlikely that this mild difference account for the dramatic impact on RPA2 hyperphosphorylation in CPT-treated shPARG cells.

To support further these observations and to have a more precise view on DNA resection, we attempted to monitor directly single strand DNA formation by immunodetecting previously incorporated BrdU in the absence of DNA denaturation, so that only BrdU present in ssDNA can be detected (Raderschall *et al.* PNAS 1999). The high antibody background and the low amount of resection observed after CPT treatment compared for example with prolonged HU treatment (data not shown) precluded to conclude. Following by immunofluorescence the recruitment of the endogenous major resecting enzyme Mre11 was also an option, but the difficulties we faced with this approach when studying PARG implication in the HU response (low signal, high background) did not encourage us to try it (Illuzzi *et al,* 2014). We have however some preliminary observations using chromatin fractionation that CPT-induced Mre11 recruitment to chromatin is effective but not significantly different between shPARG/PARG^{111}-flag and shPARG/PARG^{111cat}-flag cells (data not shown). Although this last result needs to be confirmed, the efficient loading of RPA2 onto chromatin already invalidates the hypothesis that an impaired resection would explain the defect in RPA-S4S8 and T21 phosphorylation in CPT-treated PARG deficient cells.

6. In shPARG cells, the kinases known to phosphorylate RPAS4S8 are functional.

A third possible explanation for the observed phosphorylation defect on RPA2-S4S8 in shPARG cells could come from defective activity of the upstream kinases. DNA-PK, ATM and ATR, the three kinases of the PI3K family, have been reported to act in replicative stress signalling. In the literature, DNA-PK and ATM are described as being the most important for RPA2 phosphorylation on Ser4, Ser8 and Thr21, but the consensus on which kinase targets which residue is unclear and seems to depends on the cell type and the DNA damaging agent or trigger of replicative stress (Block *et al*. 2004; Sakasai *et al*. 2006; Anantha *et al.* 2007; Chanut *et al.* 2016; Liu *et al.* 2012; Ashley *et al.* 2014 ; Liaw *et al.* 2011). DNA-PK seems however considered as the major kinase for RPA2-S4S8 phosphorylation induced by CPT (Shao *et al.* 1999; Anantha *et al.* 2007; Chanut *et al.* 2016). To have an unbiased idea of which kinase is responsible for the phosphorylation of each sites in our U20S-derived cell lines, we assessed RPA2 phosphorylation levels by western-blot immediately after a one hour CPT treatment and after a 2 hours release in cells simultaneously treated with specific inhibitors of DNA-PK (NU7441, 10 µM), ATM (KU55933 10 µM) or ATR (VE31 10 µM). PAR and γH2AX levels were also examined (**Figure 7A**). We first validated the effective inhibition of the different kinases in our experiments, by examining the phosphorylation of the ATR target Chk1-S345 and the ATM target Chk2-T68 (**Figure 7B**). As expected, only ATM inhibition reduced the Chk2 phosphorylation levels, in both shCTRL and shPARG cells (**Figure 7B**, lanes 7-8 and 19-20). ATM inhibitor also reduced Chk1-S345 phosphorylation, but not as efficiently as ATR inhibitor (lanes 9-10 and 21-22). DNA-PK inhibition had no effect on Chk1 phosphorylation, but seemed to increase CHk2 phosphorylation in shPARG cells (**Figure 7B**, compare lanes 6 to 4 and 18 to 16). However, this result was not reproducible in other replicates and should therefore not be considered.

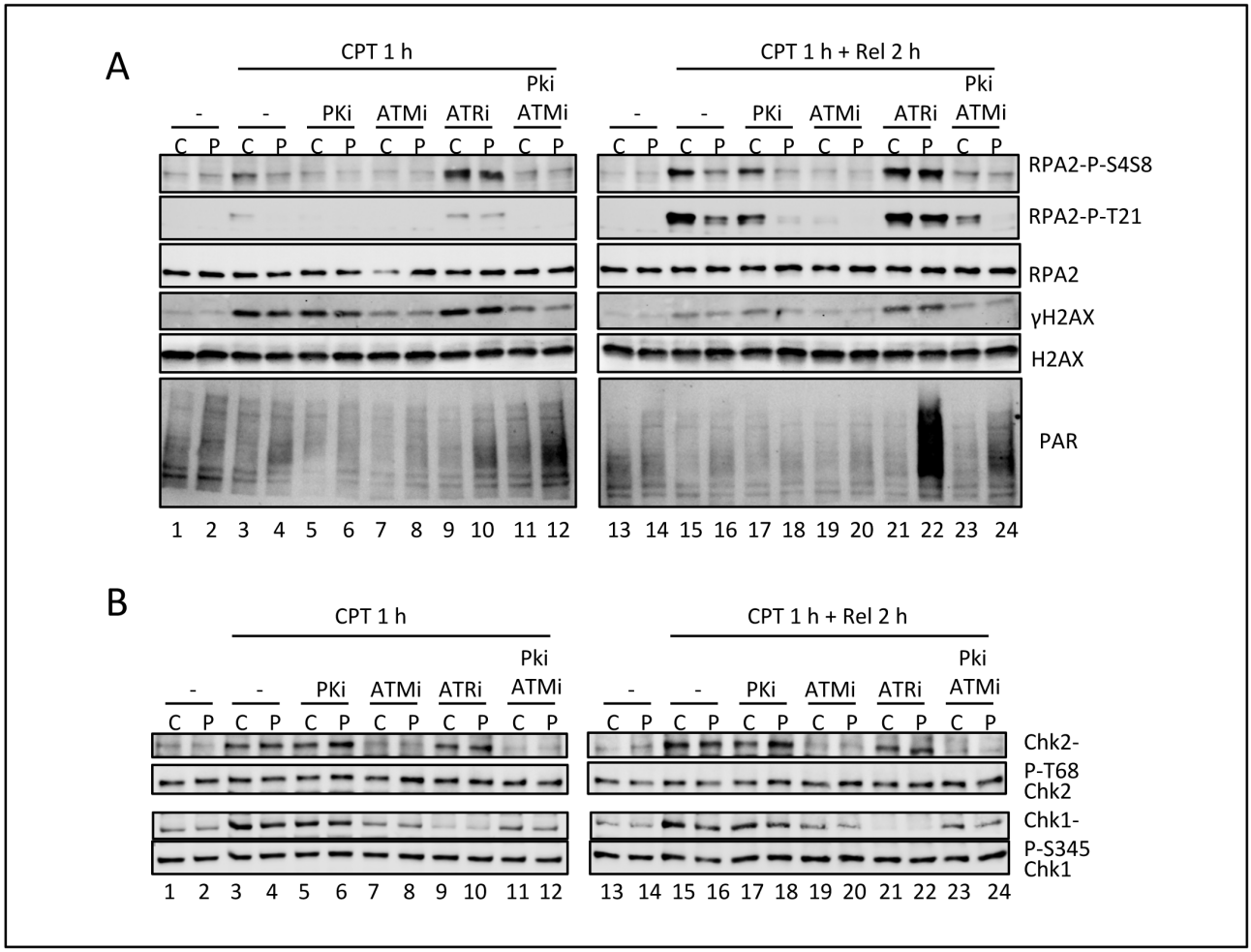

Figure 7: Contribution of ATR, ATM and DNA-PK kinases in shCTRL and shPARG cells after CPT
A-B) Western blot of U2OS shCTRL and shPARG cell extracts after CPT treatment (2µM, 1h) and release (2h), in combination with kinase inhibitors. RPA2, RPA2-P-S4S8, RPA2-P-T21, γH2AX, H2AX, PAR, CHk2-P-T68 and CHk2-P-S345 are monitored (CPT, 2µM; Pki, DNA-PK inhibitor (Nu7441, 10µM); ATRi, ATR inhibitor (VE31, 10µM); ATMi, ATM inhibitor (KU55933, 10µM).

Probing for RPA2 phosphorylations, both modifications appear and accumulate in CPT-induced shCTRL cells whereas at dramatically lower levels in shPARG cells, as previously observed (**Figure 7A**, compare lanes 3 with 4 and 15 with 16). Upon DNA-PK inhibition, RPA phosphorylation was reduced for both cell lines, but did not return to initial levels especially after 2h release (**Figure 7A**, compare lanes 17 and 18 with 15 and 16 and with 13 and 14). Of note, γH2AX levels were not significantly affected by DNA-PK inhibition. In contrast, the ATM inhibitor almost completely abolished both RPA2 phosphorylation and H2AX phosphorylation, at both time points, and for both cell lines (**Figure 7A**, lanes 7 and 8, 19 and 20). This suggests that unlike what is more commonly stated in the literature, ATM seems to be the main kinase responsible for RPA phosphorylation (and H2AX phosphorylation) in response to CPT in U2OS cells.

In contrast to DNA-PK and ATM inhibition, ATR inhibition dramatically increased RPA2-S4S8 phosphorylation and γH2AX in shCTRL. This was expected since ATR inhibition is known to increase CPT- and HU- induced fork collapse and DSB formation (Trenz *et al.* 2006; Toledo *et al.* 2011; Toledo *et al.* 2013). Interestingly, no more difference was observed between the two cell lines upon ATR inhibition: the levels of RPA2 hyper-phosphorylation and of γH2AX also strongly increased and were maintained at similar levels in both lines 2 h after the release from CPT treatment (**Figure 7A**, lane 10, 11 and lane 21, 22). However, only for shPARG cells, a huge production of PAR was observed two hours after the release from CPT treatment. These results indicate that 1) both DNA-PK but mainly ATM are involved in the CPT- induced hyper-phosphorylation of RPA2; 2) none of these kinases seems sufficiently defective in shPARG cells to solely explain the defect in RPA2 hyper-phosphorylation, since both their single inhibition reduce the residual RPA2 phosphorylation in shPARG cells; and upon ATR inhibition, hyper-phosphorylation is completely restored in shPARG cells; 3) this strong RPA2 hyper-phosphorylation observed upon ATR inhibition that leads to massive PAR production excludes that PAR directly act on RPA2 to prevent its phosphorylation. This latter observation allowed to reject the hypothesis that accumulated PAR molecules could directly prevent RPA2 hyper-phosphorylation.

To further monitor DNA-PK activity in shPARG cells, we examined S2056 auto-phosphorylation of DNA-PK, described as a marker of DNA-PK activation (Javvadi *et al.* 2012; Yajima *et al.* 2006; Davis *et al.* 2014; Neal and Meak, 2011; Neal *et al.* 2014). S2056 phosphorylation signal was impossible to follow in whole cell extracts because the signal was too weak and needed enrichment. We therefore prepared chromatin enriched extracts and soluble fractions from CPT-treated shCTRL and shPARG cells accumulated in S-phase by a single thymidine block. We observed a similar level of activated DNA-PK on soluble and chromatin enriched fractions after CPT treatment in both cell lines, suggesting that DNA-PK activation is not altered in shPARG cells (**Figure 8A**, compare lane 7-8 and lane 5-6). Quantitative immunofluorescence of DNA-PK S2056 in S-phase cells after CPT treatment revealed only a slight but not significant reduction of DNA-PK S2056 phoshorylation in shPARG cells. (Figure 8B) We noticed that DNA-PK S2056 is localized into undefined clusters just after the CPT treatment and progressively after release; it accumulates into foci, some co-localizing perfectly with RPA foci (Figure 8B). When we examined the recruitment of DNA-PK and Ku80 proteins onto chromatin, we surprisingly observed that both seemed to be enriched on chromatin in undamaged cells and evicted upon CPT treatment (Figure 8A). We explain this unexpected observation by the strong accumulation of both proteins in nucleolus of undamaged cells that was lost upon CPT treatment (immunofluorecence microscopy data not shown). It is

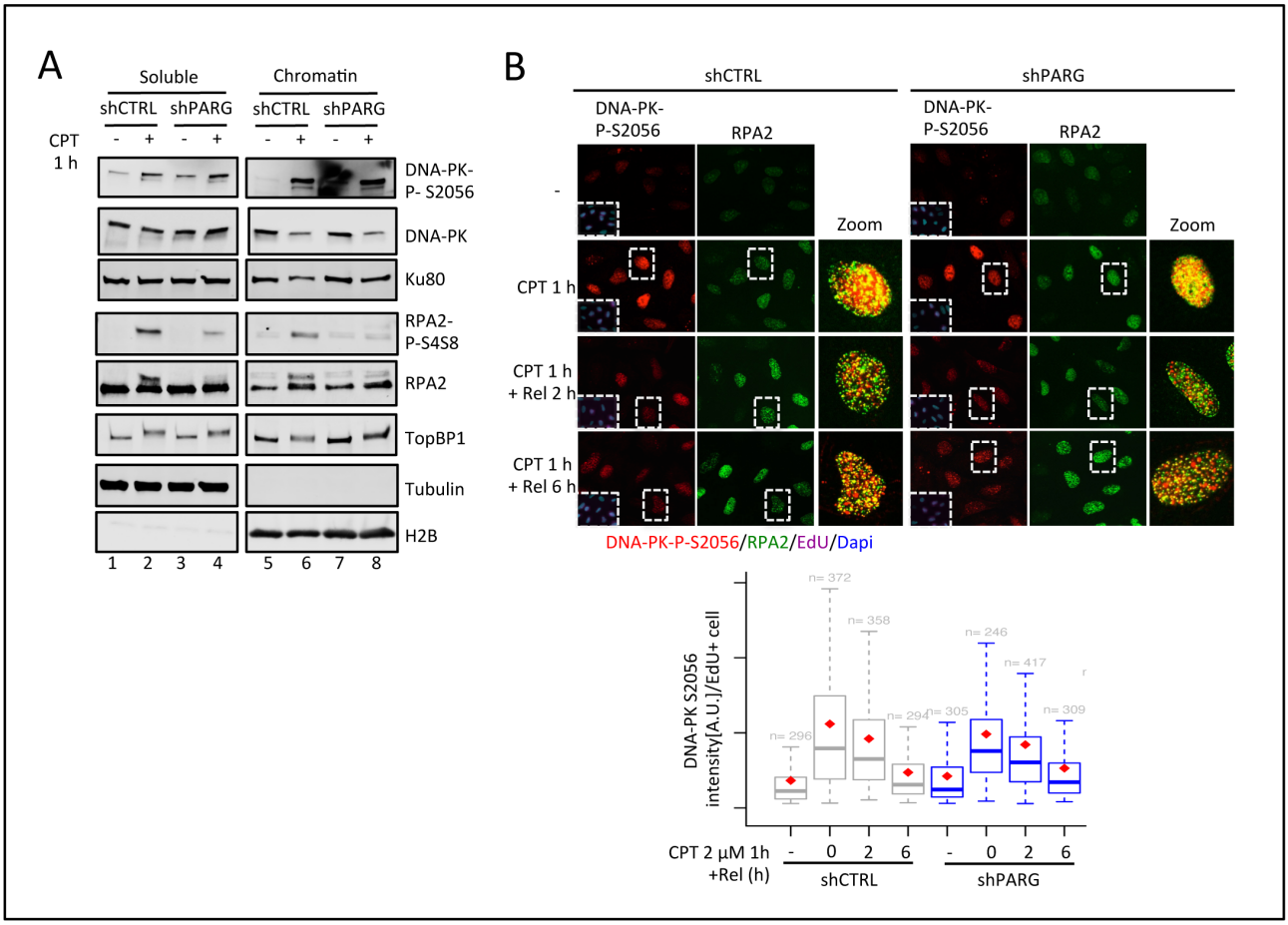

Figure 8: DNA-PK is activated in shPARG cells A) Western blotting of shCTRL and shPARG cell extracts after CPT treatment and chromatin fractionation. Tubulin is a marker of soluble fraction and H2B a marker of the chromatin fraction. B) Quantitative immunofluorescence of DNA-PK-P-S2056 intensity and RPA2 localization in Edu positive cells.

probably this nucleolar fraction that contaminates the "chromatin enriched" fraction, prepared here with a CSK treatment performed in absence of RNAse treatment, known to be required to remove all soluble Ku80 from chromatin fractions (Britton *et al.* 2013; Chanut *et al.* 2016). RPA phosphorylation defect in soluble and chromatin fractions was again observable in shPARG cell lines (**Figure 8A**, compare lane 8 to 6). Interestingly, TopBP1 protein phosphorylation after CPT, generally attributed to ATM, was similarly observable in both shCTRL and shPARG cell lines, as seen with the shift of TopBP1 band (**Figure 8A**, lane 6 and 8). This again supported a normal ATM activity in shPARG cells in response to CPT. Taken together, these results show that neither ATM nor DNA-PK activity are defective in shPARG cells upon CPT treatment. Overall, the defect in RPA-S4S8 and T21 seems not a consequence of defective kinase activation in shPARG cells

7. PARG deficiency might slightly protect from prolonged mild CPT treatment, but not from transient acute treatment

In order to measure the physiological impact of PARG deficiency on cell response to CPT, we performed clonogenic viability assays. The treatment was performed for 1 h with high concentrations of CPT, to generate a transient replication stress similar to the conditions used throughout this study. Results showed that PARG deficient U2OS cells are similarly sensitive to CPT than shCTRL cells (**Figure 9A**). Recently, an efficient PARG inhibitor with the capacity to enter cells has been reported (James *et al.* 2016; Gravells *et al*. 2017). We first confirmed that the chemical inhibition of PARG also dramatically reduced CPT-induced RPA2-S4S8 and T21 phosphorylation (data not shown). We next compared the effect of PARG inhibition with that of PARP inhibition, known to sensitise cells to CPT

(Patel *et al.* 2012; Davidson *et al.* 2012, Das *et al.* 2014). We performed clonogenic assays on shCTRL cells treated with either PARP inhibitor (olaparib, 10nM) or PARG inhibitor (0.3µM), in conditions of prolonged exposure to CPT but with mild doses (5 to 15nM, 18h), following the protocol described by Chanut *et al*. 2016.

As expected, we confirmed the increased sensitivity of shCTRL cells upon combination of PARP inhibitor and CPT (Patel *et al.* 2012, Das *et al.* 2014). In contrast, PARG inhibition did not sensitize U2OS shCTRL cells to CPT, but had a rather significant protective effect. These results suggest that PARG deficiency does not affect cell sensitivity to transient treatment with high doses of CPT, known to trigger fork collapse and DSB (Chaudhuri *et al.* 2012), but protect (at least when chemically inhibited) from prolonged treatment with mild doses of CPT.

Discussion

In this study, we analysed the response of a U2OS cell line stably depleted of all PARG isoforms to replicative stress, induced by a transient acute treatment with CPT. In these shPARG cells, we observed a dramatic decrease in RPA2-S4S8 and -T21 phosphorylation but only a slight reduction in DNA double breaks formation, and associated DNA resection. Neither RPA loading on chromatin, nor PI3-K kinases activities involved in RPA2 hyper-phosphorylation were sufficiently impaired to account for this effect. Moreover, this strong reduction in RPA2 phosphorylation was specific to DSB generated during replication stress, since DSB generated by Etoposide or Phleomycine did not elicit a similar defect.

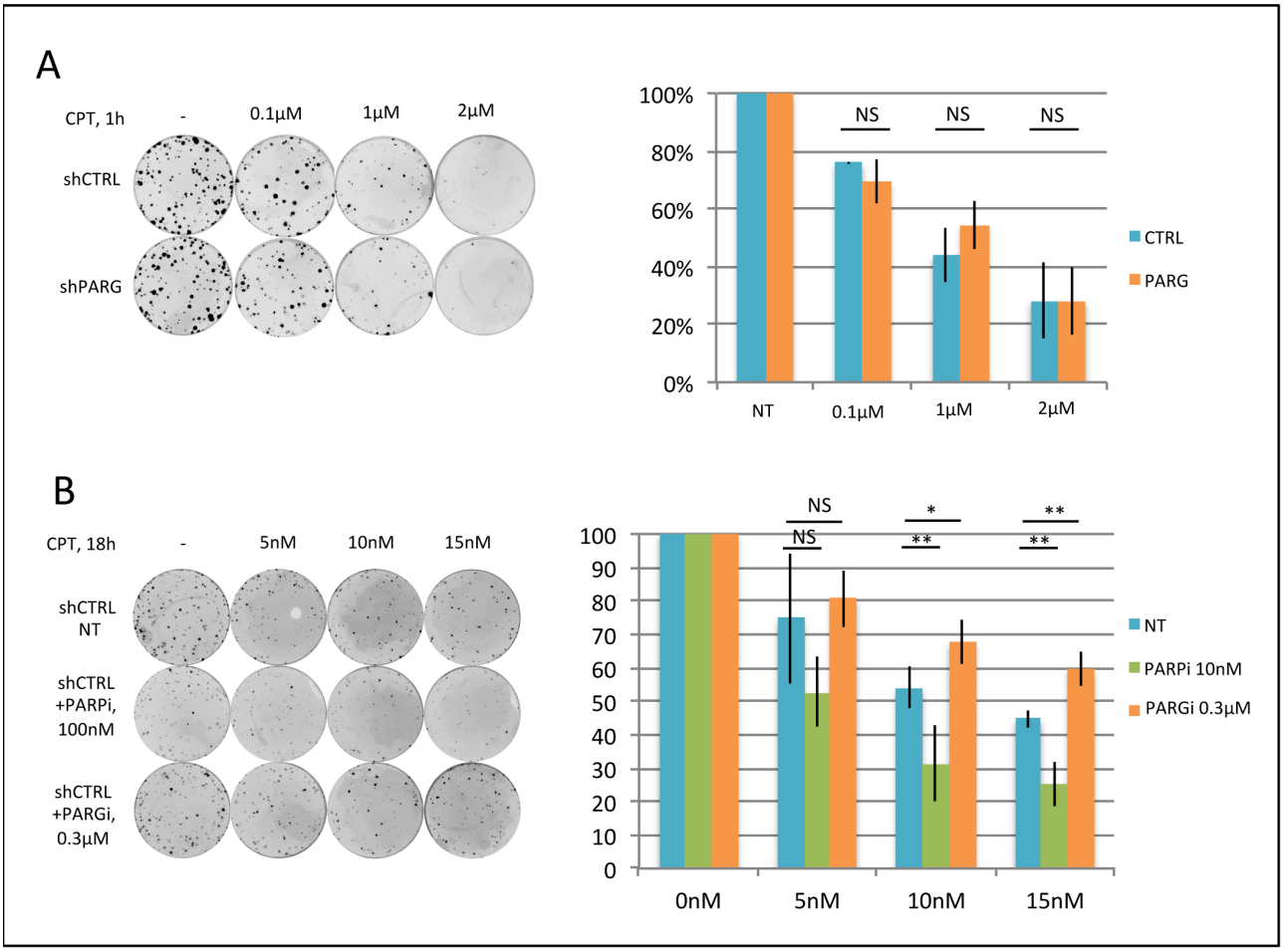

Figure 9: PARG deficiency is not associated with CPT sensitivity. A) Clonogenic assay on shCTRL and shPARG cells after 1h treatment of increasing doses of CPT (0.1µM, 1µM, 2µM). B) Clonogenic assay on shCTRL cells treated with increasing doses of CPT (5nM, 10nM, 15nM) for 18h, with no inhibitors, PARP inhibitor (10nM) or PARG inhibitor (0.3µM).

Our initial hypothesis of a reduced formation of DSB to explain this reduction in RPA2 hyperphosphorylation was the most tempting one. It is supported by the literature reporting that PARP1 and PAR directly act on Top1 activity. CPT triggers PAR synthesis, and *in vitro*, PAR polymers can inhibit the formation of Top1cc and reactivates stalled Top1 (Malanga *et al.* 2004; Zhang *et al.* 2011; Patel *et al.* 2012; Das *et al.* 2014). PAR polymers produced upon CPT treatment also favour the recruitment and stabilization of TDP1, the protein required to cleave the covalent link between the Top1 tyrosyl moiety and the 3' end of DNA (Das *et al*. 2014). In contrast, PARP inhibition impedes the repair of CPT-induced lesions leading to the generation of DSB resulting from collapsed forks. Inhibition of Top1 by CPT slows fork progression and PARP1/PAR were proposed to actively contribute to this fork slowing (Hochegger *et al*. 2006; Sugimura *et al.* 2008; Ray Chaudhuri *et al.* 2012; Berti *et al.* 2013). Upon mild CPT treatment, PARP1 was shown to control the reversion and stabilization of forks, by inactivating the RECQL1 helicase in order to prevent premature fork restart and the resulting risk of collision with transcription machinery, the source of fork collapsing and DSB formation (Ray Chaudhuri *et al.* 2012; Berti *et al.* 2013, Ray Chaudhuri *et al.* 2014). This mechanism can explain why PARP inhibition increases DSB formation upon Top1 inhibition. Using the iPOND technology to monitor proteins associated with replication forks, Dungrawala *et al.* (2015) revealed that PARP1 and PARG are associated with undamaged forks in unperturbed cells, but only PARG is evicted upon HU treatment, a way to locally increase protein PARylation at stalled forks. PARG deficiency has been reported to slow down replication fork progression in unperturbed cells with the accumulation of reversed forks, spontaneous γH2AX signal and recruitment of some DSB repair factors (Ray Chaudhuri *et al.* 2014). The accumulation of reversed forks was not further increased by low doses of CPT that are not sufficient to induce DSB, but the effect of high doses of CPT, known to trigger DSB even upon transient treatments (at least at 1 µM for 1 hour, Zellweger *et al*. 2015), was not investigated.

No significant γH2AX signal was observed in U2OS shCTRL and shPARG S-phase cells in absence of CPT treatment, in contrast to what has been previously observed in PARG deficient HeLa cells (Chaudhuri *et al.* 2015, Amé *et al.* 2009). Additionally, FACS analyses and EdU staining in immunofluorescence microscopy experiments revealed that the number of S-phase cells was similar for both cell lines throughout the CPT kinetics experiment (data not shown). Therefore, PARG deficiency did not seem to perturb replication process in untreated cells. Upon transient acute CPT treatment, we observed a slight but significant reduction of γH2AX accumulation in shPARG cells, suggestive of small reduction in DSB levels. This apparent protective effect of PARG depletion might result collectively from a more efficient repair of Top1cc via the PAR-dependent TDP1 recruitment and a slow down of fork progression with the accumulation of reversed forks. Interestingly, the variation of γH2AX signal followed the same shape in both cell lines: high burst of γH2AX level during the CPT treatment that rapidly decreased with time when CPT was removed. In contrast, RPA2 foci formation and RPA2 phosphorylation gradually increased from the CPT treatment to at least 6 hours after the release. This suggests that probably a large fraction of the CPT-induced damages were rapidly repaired without the need for DNA resection. We noticed that the correlation between γH2AX foci and RPA2-P-S4S8 foci increased with time (data not shown), likely highlighting that some breaks need more time to be repaired, most likely by HR.

However, using γH2AX as a readout for DNA damage has limitations: it doesn't form in nucleoli or poorly chromatinized regions (Kim *et al.* 2007), its induction can be modulated by several different kinases, as well as being induced by chromatin structures in the absence of DNA damage (Bakkenist and Kastan, 2003; Soutoglou and Misteli, 2008). For all these reasons, the slight differences observed between shCTRL and shPARG cells could be due to changes in the chromatin structure, a consequence of the higher steady state levels of PAR in PARG-deficient cells. It is indeed known that the spontaneous increased PAR levels in cells lacking PARG affect chromatin structure (Zhou, Feng and Koh, 2010). Despite these limitations, the normal activation of Chk2 and the slight diminution of γH2AX signals suggest no strong, if any, reduction of DSB in shPARG cells. The only slight reduction in RPA2 loading onto chromatin further supports, even if indirectly, that DSB breaks levels seems to be only slightly lower in CPT-treated shPARG cells compared to control cells. Although we would need to perform COMET assays or TUNEL assays to confirm the amount of breaks in both CPT-treated cell lines, we can suggest that even if there is slightly less DSB, it cannot completely account for the strong decrease in RPA2 hyper-phosphorylation.

Acute CPT treatment and prolonged HU treatment both trigger replicative stress with generation of single-end DSB that need to be repaired by HR. However, this work and our previous work demonstrate that the mechanisms involved are completely different. In PARG-deficient cells treated with HU, a high PAR production correlated with high γH2AX, high Chk1 activation, RPA PARylation, impeding its binding to chromatin and its subsequent hyperphosphorylation (Illuzzi *et al.* 2014). The hypothesis of RPA exhaustion (Toledo *et al.* 2014) caused by the high PAR levels that could explain this particular cell response to HU is not suitable to explain what we observe here with CPT: in shPARG cells treated with CPT, a moderate PAR production lead to slightly lower γH2AX levels, Chk1 activation and RPA2 chromatin loading, but a dramatically lower RPA2 hyper-phosphorylation.

Another hypothesis for the reduced RPA2 hyper-phosphorylation was that PAR could directly act on RPA subunits, preventing their phosphorylation. RPA subunits can be PARylated or bind PAR is some contexts (Eki and Hurwitz, 1991; Gagne *et al.* 2012, Illuzzi *et al.* 2014). We have reported previously that high PAR levels are needed to prevent RPA binding to single strand DNA, whereas low PAR concentration rather increases binding (Illuzzi *et al.* 2014). That the high PAR levels produced when shPARG cells are treated with CPT in the presence of ATR inhibitor do not further reduce, but conversely restore, high levels of RPA2-P-S4S8, argues against a direct effect of PAR on RPA here.

Impaired resection was also an attractive hypothesis to explain why RPA2 hyper-phosphorylation was so low in CPT-treated shPARG cells. PARP1 can recruit the Mre11 resecting enzyme in response to prolonged fork stalling (Bryant *et al.* 2009), whereas upon transient HU treatment, PARP1 together with BRCA2 rather protect from extensive resection by Mre11 (Ying *et al.* 2012). Despite this point should deserve further examination, the fact that RPA2 recruitment to chromatin was far less reduced than its hyper-phosphorylation argues against flawed resection. RPA loads on single stranded DNA formed upon DNA resection before getting

phosphorylated (Sartori *et al.* 2007). RPA2-S4S8 phosphorylation is commonly used as a marker of resection. Our results suggest considering this mark with caution, since its absence does not necessarily reflect lack of resection. Taken together, our data do not support that the strong defect in RPA2 hyper-phosphorylation in CPT-treated shPARG result from a defective resection.

Another DNA resection enzyme, CtIP, is required for the sustained ATR-Chk1 checkpoint signalling in response to CPT treatment, whereas dispensable for its initiation (Kousholt *et al.* 2012). Interestingly, in shPARG cells, activation of this checkpoint by transient CPT treatment was delayed but then sustained; again supporting that DNA resection is not impaired. Since the early activation of Chk1 by ATR upon acute CPT treatment has been separated from DNA end resection (Kousholt *et al*. 2012; Zellweger *et al.* 2015) it remains to be determined how ATR is early activated and why this early activation is reduced in the absence of PARG, with meanwhile no difference in the activation of Chk2. Moreover, since Chk1 is supposed to bind long chains of PAR at replication forks, stimulating its kinase activity (Min *et al.* 2013), we could have rather expected an increase in Chk1 phosphorylation levels in shPARG cells. The initial activation of ATR depends on TOPBP1 (Kousholt *et al.* 2012) and its MRN dependent loading at DNA-break sites (Yoo *et al.* 2009). TOPBP1 interacts with PARP1 (Wollmann *et al.* 2007), PARG (Liu *et al*. 2017 and our personal observations) and PAR (our personal observations). Because of the tight links between MRN, PARP1 and TOPBP1, PARG deficiency could be responsible for a reduced TOPBP1 loading at collapsed forks and account for the slight defect of early Chk1 activation. Since TOPBP1 phosphorylation by ATM was not reduced in CPT-treated shPARG, an eventual effect on TOPBP1 would therefore occur downstream. This needs however further examination.

One hypothesis we need to consider is that the only slight reduction in γH2AX levels and apparent normal Chk2 and TOPBP1 phosphorylation could originate from an increased ATM activity that would compensate and therefore mask a stronger reduction in DSB formation than we think. A spontaneous increased ATM activity was observed in HeLa shPARG cells (Amé *et al.* 2009; Chaudhuri *et al.* 2014) and PARP1/PAR are described as regulating the ATM activity (Aguilar-Quesada *et al.* 2007; Haince *et al.* 2007). Again, a direct visualization of DSB breaks by TUNEL or COMET is necessary to challenge this hypothesis.

RPA2-S4S8 phosphorylation is used as a marker, not only of resection, but also of HR. HR is the mechanism that is privileged to repair the single-ended DSB generated at replication forks. Since NHEJ requires two ends, this mechanism would perform long-distance religation, leading to chromosomes rearrangements, with deletions and translocations. However, the NHEJ enzyme DNA-PK with its DNA-binding subunits Ku70/Ku80 (KU) is present at DSB generated at replication forks (Dungrawala *et al.* 2015; Ribeyre *et al.* 2016; Chanut *et al.* 2016). In NHEJ, the presence of KU is a prerequisite for the presence and activity of DNA-PKcs at the vicinity of DNA-damage. Upon CPT treatment, KU is described as transiently localizing to single-ended DSB, bringing DNA-PKcs to phosphorylate RPA2, but then being evicted by the ATM-regulated CTIP-mediated DNA resection (Britton *et al.* 2013; Chanut *et al.* 2016). However, these studies did not examine time points beyond the 1 h CPT treatment, where RPA2-S4S8 phosphorylation levels strongly increase with time. Our results with PI3K inhibi-

tors show that even if DNA-PK contributes to RPA2 hyper-phosphorylation, ATM is the major kinase involved. Our data thus provide evidence that RPA-S4S8 cannot be considered as a mark of KU presence at stalled replication forks, as proposed by Chanut *et al.* 2016. However, CPT-activation of DNA-PK is not dramatically affected in shPARG cells, as seen with the normal DNA-PK-P-S2056 signal. But the link between PARylation and DNA-PK is rather complex, since PARylation can activate DNA-PKcs (Ruscetti *et al.* 1998, Sajish *et al.* 2012), but PARP1 and KU compete for DNA ends (Wang *et al.* 2006; Hochegger *et al.* 2006; Mansour *et al.* 2013). Whether CPT-induced KU recruitment differs in our shCTRL and shPARG cellular models is currently under investigation.

Our study reveal that in contrast to PARP inhibition (Patel *et al.* 2012; Davidson *et al.* 2012; Das *et al.* NAR 2014), PARG inhibition does not sensitize U2OS shCTRL cells to mild sustained treatment with CPT, but has a rather protective effect. A protective effect towards CPT has been previously reported for PARG-/- murine ES cells deleted of the longer PARG isoform (Fujihara *et al.* 2009). This cellular tolerance was however not observed with the acute CPT treatment that leads to a dramatic reduction in RPA2-S4S8 phosphorylation in shPARG cells. The kinetics of γH2AX appearance and clearance was comparable between shCTRL and shPARG cell lines, suggesting global similar repair efficiency. What happens to the breaks where RPA-S4S8 phosphorylation is low or absent in shPARG cells? How are they repaired? Are there alternative mechanisms by which HR can resolve these damages without involving RPA2 hyper-phosphorylation? An alternative route has been reported involving Rad18 and FANCD2 to recruit BRCA2 and subsequently RAD51 (Palle and Vaziri, 2011, Tripathi *et al.* 2016). Some studies have described a new role for TOPBP1, which binds to and activates PLK1 to phosphorylate Rad51 on Ser14, promoting RAD51 chromatin loading (Yata *et al.* 2012; Moudry *et al*. 2016; Liu and Smolka, 2016). Its absence impacts RAD51 recruitment, without affecting resection and RPA loading. TOPBP1 depletion sensitizes to PARPi *(*Yata *et al.* 2012*).* Finally, TOPBP1 was shown to interact with BRCA1, 53BP1 but also PARG, and upon HU, the interaction with BRCA1 and PARG increases, whereas decreasing with 53BP1 (Liu *et al.* 2017*).* Additional work is under way to challenge these hypotheses.

While the treatment of certain types of cancer using combination of PARP inhibitors and CPT is a promising chemotherapeutic option (Murai *et al.* 2014), our results argue against the simultaneous use of CPT and PARG inhibitors in therapeutics. This contrasts with the previously described potentiation of cytotoxic effect of irradiation or HU, by PARG invalidation (Amé *et al.* 2009; Fujihara *et al.* 2009; Feng and Koh, 2013, Shirai *et al.* 2013; Illuzzi *et al.* 2014). Future work is necessary to precise the role and mode of action of PARG in cell response to anticancer drugs to evaluate its clinical interest.

Materials and Methods:

Cell culture and treatments

U2OS shCTRL, shPARG, shPARG/PARG^{111}-Flag and shPARG/PARG^{111cat}-Flag cell-lines were cultured in Dulbecco's Modifed Eagle's Medium (DMEM 4.5 g/l glucose) (Invitrogen) supplemented with 10% foetal bovine serum, 1% gentamicin (Invitrogen) under 5% CO2. Kinetic treatments are performed using 2µM of CPT treatment,

and release time starts after 2 washes of PBS. Cells have also been treated with specific inhibitors of DNA-PK (NU7441, 10 µM), ATM (KU55933 10 µM) or ATR (VE31 10 µM).

Clonogenic assay

U2OS shPARG and shCTRL are transfected with U20S shPARG or U2OS shCTRL (600 cells) were seeded in triplicate on 60mm dishes 5 h prior to treatment with the indicated doses of camptothecin, PARP inhibitor or PARG inhibitor. Plates are incubated for 14 days in complete medium. After 2 washes with PBS, colonies were fixed in 3,7% paraformaldehyde (PFA) and stained with 0,1% crystal violet. Dishes were scanned with a Typhoon FLA 7000 and colonies are enumerated with ImageJ (NIH, Bethesda, MD, USA).

Western blotting

Total cell lysates were prepared by adding Laemmli buffer (4% SDS, 20% glycerol, 120 mM Tris-HCl pH 6.8) directly on the culture dishes and sonication of the collected samples. The relative protein content of each sample was estimated by analysing an aliquot on a 10% SDS-PAGE followed by Coomassie Blue staining and quantification with an Odyssey Infrared Imaging System (Li-Cor, Bioscience). After normalization, equal amounts of proteins were separated on a 4-20% gradient gel (Biorad) and transferred to nitrocellulose membranes. Membranes were probed with the appropriate primary antibodies: mouse monoclonal anti-α-tubulin (Sigma), γH2AX-Ser139 (Millipore), Chk1 and Chk2 (Santa Cruz Biotechnology), RPA2 (9H8, Abcam), DNA-PK (Ab4, Intechim), KU80 (Abcam) and rabbit polyclonal anti-PAR (Trevigen), Chk1-P-S345 and Ch2-P-T68 (Cell Signaling), RPA2-P-S4S8 (Bethyl Laboratories), TOP1 and TOPBP1 (Novus Biologicals), H2AX, RPA2-P-T21 and DNA-PK-P-S2056 (Abcam) and H2B (Upstate).

After extensive washing in TBS-0.1% Tween, membranes were incubated with the secondary antibodies: Alexa Fluor 680 goat anti-rabbit or goat anti-mouse antibodies (Molecular Probes, Invitrogen) or Alexa Fluor 790 goat anti-rabbit or goat anti-mouse antibodies (Molecular Probes, Invitrogen) revealed using Odyssey, or horseradish peroxidase coupled goat anti-mouse or anti-rabbit antibodies (Sigma), revealed by chemiluminescence with ECL+ (Amersham) and the images were captured using the Image Quant LAS 400 imaging system (GE Healthcare Life Science). Quantification was performed with ImageJ (NIH, Bethesda).

Immunofluorescence microscopy

Cells grown on glass coverslips were left untreated or treated with 2 µM CPT for 1 h, washed twice and release in fresh medium for the indicated time before fixation. PAR detection was performed as described in Illuzzi *et al*. (2014). To label S-phase cells, EdU 10 µM was added to the medium 20 min prior to the CPT treatment. Cells were washed in PBS and pre-extraction step was carried out by incubating the coverslips in CSK extraction buffer (10 mM PIPES, pH 6.8, 100 mM NaCl, 3 mM MgCl2, 300 mM glucose, 0.5% Triton X-100) twice on ice for 5 min before fixation 20 min in FA 3.7% in PBS. Cells were washed twice in PBS, incubated 10 min in PBS-0.2% Triton (PBS-T) than overnight in PBS-1% BSA. EdU was detected by click chemistry according to the manufacturer (Invitrogen), using a CF680 picolyl azide. All subsequent steps were performed at room temperature protected from light. Cells were incubated with primary antibodies diluted in PBS-0.1% BSA: mouse anti PAR, RPA2

or gH2AX antibodies or rabbit anti RPA2-P-S4S8, DNA-PK-P-S2056 antibodies After washing in PBS-0.2% Triton, cells were incubated for 1 h with the appropriate secondary antibodies: an Alexa Fluor 488 or 594 goat anti-mouse IgG or IgG3, or an Alexa Fluor 488 or 594 goat anti-rabbit IgG (Molecular Probes, Invitrogen). After three washes with PBS, 0.2% Triton and one wash with PBS, slides were mounted in Dapi-Fluoromount (SouthernBiotech).

Image Acquisition and Analysis

Immunofluorescence microscopy was performed using a Leica DMRA2 microscope with the 40X AN=1.0 objective under immersion (Leica Microsystems) equipped with an ORCA-ER chilled CCD camera (Hamamatsu) and the capture software Openlab (Improvision). Merging of images was done using NIH ImageJ or Adobe Photoshop CS5.1. At least 15 fields were imaged for each time and treatment conditions. Automated image analysis was performed using NIH ImageJ using macros we specifically developed in the lab. These macros allow to automatically define from blue Dapi staining the nuclei as ROI. These ROI are subsequently used to precisely measure the signal intensity and count the foci number in the other colours (infra red, red and green labels). The values, global nuclei intensity (mean * std deviation) and foci count and some other nuclei parameters were recorded in a .csv (comma separated) table for further analysis in R statistical package.

Statistical analyses

Statistical analyses were performed using R statistical packages. Data are represented as box plot graph where the lower and upper hinges represent the 25th and 75th percentile respectively. The middle horizontal line represents the median or 50th percentile. Whiskers are drawn to the lower and upper adjacent values. Far out values are not represented in the graphs. Significance tests, such as Anova and TukeyHSD (honest significant difference, for multiple comparisons) were performed in R using the dataset used to draw the box plot. For significance codes *p*: 0 <‘ ***’ <0.001 <‘**’ <0.01 <‘*’ <0.05 <ns (not significant). Signal intensity measured in nuclei is defined as the mean intensity value multiplied by the standard deviation of the signal intensity. Foci numbers are defined as the number of foci (fn) in a nucleus per surface unit and correspond to the number of counted foci (f) divided by the nucleus area (s), multiplied by the mean surface area (ma) of all the nuclei in the experiment, fn = (f/s)*ma.

Flow cytometry

Cells were collected by trypsinization at the time indicated after CPT treatment, washed with PBS and fixed in PFA 3.7% in PBS for 10 min at RT, washed once in PBS-glucose 0.25%, EDTA 1 mM (PGE) and fixed O/N in ETOH 70% in PGE. To detect RPA2, RPA2-S4S8 and gH2AX on chromatin, soluble proteins were removed by a pre-extraction for 10 min on ice in PBS-Triton 0.2% before fixation. Cells were rehydrated in PGE-Triton 0.2% (PGE-T) for 15 min, incubated 15 min in PGE-T BSA 1% (PGE-TB) then at least 2 hours at RT in PGE-1% BSA (PGE-B) containing mouse anti RPA2 or gH2AX antibodies or rabbit anti RPA2-P-S4S8, Chk1-P-S345 or Chk2-P-T68 antibodies. After 2 washes with PGE-TB, cells were incubated for at least 1 h at RT in the dark with Alexa 488 conjugated goat anti-mouse or anti-rabbit antibodies diluted in PGE-B. After two washes in PGE-TB, cells were

incubated for 30 min in PGE containing 40 µl/ml RNAse A and 50 µg/ml propidium iodite to stain nuclear DNA and were analysed on a FACScalibur (Becton Dickinson) using CellQuest software (Becton Dickinson). Data were further analyzed using FlowJo V10.1.

Chromatin fractionation

U2OS shPARG/PARG^{111}-Flag and U2OS shARG/PARG1^{11cat}-Flag are cultured in P100 plates (Greiner) for each condition. After culture and treatments, cells are were twice and scrapped in 1mL cold PBS supplemented with protease, phosphatase and PARP inhibitors(Na3VO4, 1mM, NaF 1mM, KuDOS 948 100nM). Cells were collected by centrifugation (1000g, 5min, 4°C), and resuspended in buffer 1 (50mM HEPES pH7.5; 150mM NaCl; 1mMEDTA; 0,05% NP40; 1mM PefaBloc; Phostop (Roche), CompleteMINI (Roche), 100nM KuDOS). Lysates were centrifuged (1000g, 5min, 4°C). The supernatant was kept as Fraction I (soluble). The pellet was resuspended in Buffer 2 (Buffer 1 containing 100 µg/ml RNAseA) and left 10 min at 20°C. Lysates were centrifuged (1000g, 5min, 4°C) and supernatant kept as fraction II. Pellet was resuspended in Buffer 2 (Buffer 1 + NP40 0.5%). Lysate was left at 4°C for 40 min and centrifuged (13000g, 15min, 4°C). The supernatant was kept as Fraction III. The pellet was washed once with Buffer 3 and centrifuged. The supernatant was discarded and the pellet resuspended in Buffer1 + 1/5 loading Laemmli buffer and sonicated. This was fraction IV of chromatin extracts. Aliquots of the fractions I – IV, derived from equivalent cell numbers for each culture conditions, were added to loading buffer, boiled and loaded on SDS–PAGE to be analysed by western blot as described above.
The protocol used in Figure 8A was the following. Cells were treated for 18 hours with 2.5 mM thymidine, then released for 3 hours in fresh medium to enriched in S-phase cells, before being treated or not 1 hour with 2 µM CPT. Cells were washed twice with cold PBS, scraped in CSK (containing 0.5% Triton) supplemented with 1mM Pefabloc; Phostop (Roche), CompleteMINI (Roche) and incubated 20 min on ice. After centrifugation for 15 min at 13000 g, supernatant was collected (soluble fraction) and kept on ice or at -80°C. The pellet was thoroughly washed once with CSK, resuspended in CSK supplemented with 200 mM NaCl (300 mM final) and 50U/ml benzonase, sonicated 25 s and incubaetd 15 min on ice. After centrifugation for 15 min at 13000g, the supernatant was collected and diluted with one volume of Tris-HCl 100 mM pH7.5 (chromatin enriched fraction). Protein concentration of both soluble and chromatin enriched fractions was determined by Bradford and equal amounts of proteins were analysed by Western blotting with the indicated antibodies.

Acknowledgments:

We wish to thank J.C-Amé for all the immunofluorescence analysis and quantification. This work was supported by the Centre National de la Recherche Scientifique, Université de Strasbourg, Ligue contre le Cancer and Fondation pour la Recherche Médicale. EH was supported by the French Ministère de l'Enseignement Supérieur et de la Recherche and the Fondation pour la Recherche Médicale.

Bibliography:

Amé, J.-C., Fouquerel, E., Gauthier, L.R., Biard, D., Boussin, F.D., Dantzer, F., de Murcia, G., and Schreiber, V. (2009). Radiation-induced mitotic catastrophe in PARG-deficient cells. J. Cell. Sci. *122*, 1990–2002.

Anantha, R.W., Vassin, V.M., and Borowiec, J.A. (2007). Sequential and Synergistic Modification of Human RPA Stimulates Chromosomal DNA Repair. J. Biol. Chem. *282*, 35910–35923.

Ashley, A.K., Shrivastav, M., Nie, J., Amerin, C., Troksa, K., Glanzer, J.G., Liu, S., Opiyo, S.O., Dimitrova, D.D., Le, P., et al. (2014). DNA-PK phosphorylation of RPA32 Ser4/Ser8 regulates replication stress checkpoint activation, fork restart, homologous recombination and mitotic catastrophe. DNA Repair *21*, 131–139.

Bakkenist, C.J., and Kastan, M.B. (2003). DNA damage activates ATM through intermolecular autophosphorylation and dimer dissociation. Nature *421*, 499–506.

Berti, M., and Vindigni, A. (2016). Replication stress: getting back on track. Nat. Struct. Mol. Biol. *23*, 103–109.

Berti, M., Ray Chaudhuri, A., Thangavel, S., Gomathinayagam, S., Kenig, S., Vujanovic, M., Odreman, F., Glatter, T., Graziano, S., Mendoza-Maldonado, R., et al. (2013). Human RECQ1 promotes restart of replication forks reversed by DNA topoisomerase I inhibition. Nat. Struct. Mol. Biol. *20*, 347–354.

Binz, S.K., Sheehan, A.M., and Wold, M.S. (2004). Replication protein A phosphorylation and the cellular response to DNA damage. DNA Repair (Amst.) *3*, 1015–1024.

Block, W.D., Yu, Y., and Lees-Miller, S.P. (2004). Phosphatidyl inositol 3-kinase-like serine/threonine protein kinases (PIKKs) are required for DNA damage-induced phosphorylation of the 32 kDa subunit of replication protein A at threonine 21. Nucleic Acids Res. *32*, 997–1005.

Bryant, H.E., Petermann, E., Schultz, N., Jemth, A.-S., Loseva, O., Issaeva, N., Johansson, F., Fernandez, S., McGlynn, P., and Helleday, T. (2009). PARP is activated at stalled forks to mediate Mre11-dependent replication restart and recombination. EMBO J. *28*, 2601–2615.

Chanut, P., Britton, S., Coates, J., Jackson, S.P., and Calsou, P. (2016). Coordinated nuclease activities counteract Ku at single-ended DNA double-strand breaks. Nat Commun *7*, 12889.

Chiker, S., Pennaneach, V., Loew, D., Dingli, F., Biard, D., Cordelières, F.P., Gemble, S., Vacher, S., Bieche, I., Hall, J., et al. (2015). Cdk5 promotes DNA replication stress checkpoint activation through RPA-32 phosphorylation, and impacts on metastasis free survival in breast cancer patients. Cell Cycle *14*, 3066–3078.

Cimprich, K.A., and Cortez, D. (2008). ATR: an essential regulator of genome integrity. Nat. Rev. Mol. Cell Biol. *9*, 616–627.

Cortes, U., Tong, W.-M., Coyle, D.L., Meyer-Ficca, M.L., Meyer, R.G., Petrilli, V., Herceg, Z., Jacobson, E.L., Jacobson, M.K., and Wang, Z.-Q. (2004). Depletion of the 110-kilodalton isoform of poly(ADP-ribose) glycohydrolase increases sensitivity to genotoxic and endotoxic stress in mice. Mol. Cell. Biol. *24*, 7163–7178.

Cristini, A., Park, J.-H., Capranico, G., Legube, G., Favre, G., and Sordet, O. (2016). DNA-PK triggers histone ubiquitination and signaling in response to DNA double-strand breaks produced during the repair of transcription-blocking topoisomerase I lesions. Nucleic Acids Res *44*, 1161–1178.

Das, B.B., Antony, S., Gupta, S., Dexheimer, T.S., Redon, C.E., Garfield, S., Shiloh, Y., and Pommier, Y. (2009). Optimal function of the DNA repair enzyme TDP1 requires its phosphorylation by ATM and/or DNA-PK. EMBO J. *28*, 3667–3680.

Das, B.B., Huang, S.N., Murai, J., Rehman, I., Amé, J.-C., Sengupta, S., Das, S.K., Majumdar, P., Zhang, H., Biard, D., et al. (2014). PARP1-TDP1 coupling for the repair of topoisomerase I-induced DNA damage. Nucleic Acids Res. *42*, 4435–4449.

Das, S.K., Rehman, I., Ghosh, A., Sengupta, S., Majumdar, P., Jana, B., and Das, B.B. (2016). Poly(ADP-ribose) polymers regulate DNA topoisomerase I (Top1) nuclear dynamics and camptothecin sensitivity in living cells. Nucleic Acids Res *44*, 8363–8375.

Davidson, D., Wang, Y., Aloyz, R., and Panasci, L. (2013). The PARP inhibitor ABT-888 synergizes irinotecan treatment of colon cancer cell lines. Invest New Drugs *31*, 461–468.

Davis, A.J., Chen, B.P.C., and Chen, D.J. (2014). DNA-PK: a dynamic enzyme in a versatile DSB repair pathway. DNA Repair (Amst.) *17*, 21–29.

Desai, S.D., Liu, L.F., Vazquez-Abad, D., and D'Arpa, P. (1997). Ubiquitin-dependent destruction of topoisomerase I is stimulated by the antitumor drug camptothecin. J. Biol. Chem. *272*, 24159–24164.

D'Onofrio, G., Tramontano, F., Dorio, A.S., Muzi, A., Maselli, V., Fulgione, D., Graziani, G., Malanga, M., and Quesada, P. (2011). Poly(ADP-ribose) polymerase signaling of topoisomerase 1-dependent DNA damage in carcinoma cells. Biochem. Pharmacol. *81*, 194–202.

Dungrawala, H., Rose, K.L., Bhat, K.P., Mohni, K.N., Glick, G.G., Couch, F.B., and Cortez, D. (2015). The Replication Checkpoint Prevents Two Types of Fork Collapse without Regulating Replisome Stability. Mol. Cell *59*, 998–1010.

Eki, T., and Hurwitz, J. (1991). Influence of poly(ADP-ribose) polymerase on the enzymatic synthesis of SV40 DNA. J. Biol. Chem. *266*, 3087–3100.

Erdélyi, K., Bai, P., Kovács, I., Szabó, E., Mocsár, G., Kakuk, A., Szabó, C., Gergely, P., and Virág, L. (2009). Dual role of poly(ADP-ribose) glycohydrolase in the regulation of cell death in oxidatively stressed A549 cells. FASEB J. *23*, 3553–3563.

Feng, X., and Koh, D.W. (2013a). Inhibition of poly(ADP-ribose) polymerase-1 or poly(ADP-ribose) glycohydrolase individually, but not in combination, leads to improved chemotherapeutic efficacy in HeLa cells. Int. J. Oncol. *42*, 749–756.

Feng, X., and Koh, D.W. (2013b). Roles of poly(ADP-ribose) glycohydrolase in DNA damage and apoptosis. Int Rev Cell Mol Biol *304*, 227–281.

Fisher, A.E.O., Hochegger, H., Takeda, S., and Caldecott, K.W. (2007). Poly(ADP-ribose) polymerase 1 accelerates single-strand break repair in concert with poly(ADP-ribose) glycohydrolase. Mol. Cell. Biol. *27*, 5597–5605.

Fujihara, H., Ogino, H., Maeda, D., Shirai, H., Nozaki, T., Kamada, N., Jishage, K., Tanuma, S., Takato, T., Ochiya, T., et al. (2009). Poly(ADP-ribose) Glycohydrolase deficiency sensitizes mouse ES cells to DNA damaging agents. Curr Cancer Drug Targets *9*, 953–962.

Gagné, J.-P., Pic, E., Isabelle, M., Krietsch, J., Ethier, C., Paquet, E., Kelly, I., Boutin, M., Moon, K.-M., Foster, L.J., et al. (2012). Quantitative proteomics profiling of the poly(ADP-ribose)-related response to genotoxic stress. Nucleic Acids Res. *40*, 7788–7805.

Gravells, P., Grant, E., Smith, K.M., James, D.I., and Bryant, H.E. (2017). Specific killing of DNA damage-response deficient cells with inhibitors of poly(ADP-ribose) glycohydrolase. DNA Repair (Amst.) *52*, 81–91.

Gupte, R., Liu, Z., and Kraus, W.L. (2017). PARPs and ADP-ribosylation: recent advances linking molecular functions to biological outcomes. Genes Dev. *31*, 101–126.

Hochegger, H., Dejsuphong, D., Fukushima, T., Morrison, C., Sonoda, E., Schreiber, V., Zhao, G.Y., Saberi, A., Masutani, M., Adachi, N., et al. (2006). Parp-1 protects homologous recombination from interference by Ku and Ligase IV in vertebrate cells. EMBO J. *25*, 1305–1314.

Illuzzi, G., Fouquerel, E., Amé, J.-C., Noll, A., Rehmet, K., Nasheuer, H.-P., Dantzer, F., and Schreiber, V. (2014). PARG is dispensable for recovery from transient replicative stress but required to prevent detrimental accumulation of poly(ADP-ribose) upon prolonged replicative stress. Nucleic Acids Res. *42*, 7776–7792.

James, D.I., Smith, K.M., Jordan, A.M., Fairweather, E.E., Griffiths, L.A., Hamilton, N.S., Hitchin, J.R., Hutton, C.P., Jones, S., Kelly, P., et al. (2016). First-in-Class Chemical Probes against Poly(ADP-ribose) Glycohydrolase (PARG) Inhibit DNA Repair with Differential Pharmacology to Olaparib. ACS Chem. Biol. *11*, 3179–3190.

Javvadi, P., Makino, H., Das, A.K., Lin, Y.-F., Chen, D.J., Chen, B.P., and Nirodi, C.S. (2012). Threonine 2609 phosphorylation of the DNA-dependent protein kinase is a critical prerequisite for epidermal growth factor receptor-mediated radiation resistance. Mol. Cancer Res. *10*, 1359–1368.

Kaufmann, T., Grishkovskaya, I., Polyansky, A.A., Kostrhon, S., Kukolj, E., Olek, K.M., Herbert, S., Beltzung, E., Mechtler, K., Peterbauer, T., et al. (2017). A novel non-canonical PIP-box mediates PARG interaction with PCNA. Nucleic Acids Res. *45*, 9741–9759.

Kim, J.-A., Kruhlak, M., Dotiwala, F., Nussenzweig, A., and Haber, J.E. (2007). Heterochromatin is refractory to gamma-H2AX modification in yeast and mammals. J. Cell Biol. *178*, 209–218.

Koh, D.W., Lawler, A.M., Poitras, M.F., Sasaki, M., Wattler, S., Nehls, M.C., Stöger, T., Poirier, G.G., Dawson, V.L., and Dawson, T.M. (2004). Failure to degrade poly(ADP-ribose) causes increased sensitivity to cytotoxicity and early embryonic lethality. Proc. Natl. Acad. Sci. U.S.A. *101*, 17699–17704.

Kousholt, A.N., Fugger, K., Hoffmann, S., Larsen, B.D., Menzel, T., Sartori, A.A., and Sørensen, C.S. (2012). CtIP-dependent DNA resection is required for DNA damage checkpoint maintenance but not initiation. J. Cell Biol. *197*, 869–876.

Krasikova, Y.S., Rechkunova, N.I., and Lavrik, O.I. (2016). [Replication protein A as a major eukaryotic single-stranded DNA-binding protein and its role in DNA repair]. Mol. Biol. (Mosk.) *50*, 735–750.

Laev, S.S., Salakhutdinov, N.F., and Lavrik, O.I. (2016). Tyrosyl-DNA phosphodiesterase inhibitors: Progress and potential. Bioorganic & Medicinal Chemistry *24*, 5017–5027.

Lebedeva, N.A., Anarbaev, R.O., Kupryushkin, M.S., Rechkunova, N.I., Pyshnyi, D.V., Stetsenko, D.A., and Lavrik, O.I. (2015a). Design of a New Fluorescent Oligonucleotide-Based Assay for a Highly Specific Real-Time Detection of Apurinic/Apyrimidinic Site Cleavage by Tyrosyl-DNA Phosphodiesterase 1. Bioconjug. Chem. *26*, 2046–2053.

Lebedeva, N.A., Anarbaev, R.O., Sukhanova, M., Vasil'eva, I.A., Rechkunova, N.I., and Lavrik, O.I. (2015b). Poly(ADP-ribose)polymerase 1 stimulates the AP-site cleavage activity of tyrosyl-DNA phosphodiesterase 1. Biosci. Rep. *35*.

Lees-Miller, S.P., Sakaguchi, K., Ullrich, S.J., Appella, E., and Anderson, C.W. (1992). Human DNA-activated protein kinase phosphorylates serines 15 and 37 in the amino-terminal transactivation domain of human p53. Mol. Cell. Biol. *12*, 5041–5049.

Liaw, H., Lee, D., and Myung, K. (2011). DNA-PK-dependent RPA2 hyperphosphorylation facilitates DNA repair and suppresses sister chromatid exchange. PLoS ONE *6*, e21424.

Liu, Y., and Smolka, M.B. (2016). TOPBP1 takes RADical command in recombinational DNA repair. J. Cell Biol. *212*, 263–266.

Liu, S., Opiyo, S.O., Manthey, K., Glanzer, J.G., Ashley, A.K., Amerin, C., Troksa, K., Shrivastav, M., Nickoloff, J.A., and Oakley, G.G. (2012). Distinct roles for DNA-PK, ATM and ATR in RPA phosphorylation and checkpoint activation in response to replication stress. Nucleic Acids Res. *40*, 10780–10794.

Liu, Y., Cussiol, J.R., Dibitetto, D., Sims, J.R., Twayana, S., Weiss, R.S., Freire, R., Marini, F., Pellicioli, A., and Smolka, M.B. (2017). TOPBP1(Dpb11) plays a conserved role in homologous recombination DNA repair through the coordinated recruitment of 53BP1(Rad9). J. Cell Biol. *216*, 623–639.

Malanga, M., and Althaus, F.R. (2004). Poly(ADP-ribose) reactivates stalled DNA topoisomerase I and Induces DNA strand break resealing. J. Biol. Chem. *279*, 5244–5248.

Malanga, M., Kleczkowska, H.E., and Althaus, F.R. (1998). Selected nuclear matrix proteins are targets for poly(ADP-ribose)-binding. J. Cell. Biochem. *70*, 596–603.

Mansour, W.Y., Borgmann, K., Petersen, C., Dikomey, E., and Dahm-Daphi, J. (2013). The absence of Ku but not defects in classical non-homologous end-joining is required to trigger PARP1-dependent end-joining. DNA Repair (Amst.) *12*, 1134–1142.

Meyer-Ficca, M.L., Meyer, R.G., Coyle, D.L., Jacobson, E.L., and Jacobson, M.K. (2004). Human poly(ADP-ribose) glycohydrolase is expressed in alternative splice variants yielding isoforms that localize to different cell compartments. Exp. Cell Res. *297*, 521–532.

Min, W., Cortes, U., Herceg, Z., Tong, W.-M., and Wang, Z.-Q. (2010). Deletion of the nuclear isoform of poly(ADP-ribose) glycohydrolase (PARG) reveals its function in DNA repair, genomic stability and tumorigenesis. Carcinogenesis *31*, 2058–2065.

Min, W., Bruhn, C., Grigaravicius, P., Zhou, Z.-W., Li, F., Krüger, A., Siddeek, B., Greulich, K.-O., Popp, O., Meisezahl, C., et al. (2013). Poly(ADP-ribose) binding to Chk1 at stalled replication forks is required for S-phase checkpoint activation. Nat Commun *4*, 2993.

Mortusewicz, O., Fouquerel, E., Amé, J.-C., Leonhardt, H., and Schreiber, V. (2011). PARG is recruited to DNA damage sites through poly(ADP-ribose)- and PCNA-dependent mechanisms. Nucleic Acids Res. *39*, 5045–5056.

Moudry, P., Watanabe, K., Wolanin, K.M., Bartkova, J., Wassing, I.E., Watanabe, S., Strauss, R., Troelsgaard Pedersen, R., Oestergaard, V.H., Lisby, M., et al. (2016). TOPBP1 regulates RAD51 phosphorylation and chromatin loading and determines PARP inhibitor sensitivity. J. Cell Biol. *212*, 281–288.

Murai, J., Marchand, C., Shahane, S.A., Sun, H., Huang, R., Zhang, Y., Chergui, A., Ji, J., Doroshow, J.H., Jadhav, A., et al. (2014a). Identification of novel PARP inhibitors using a cell-based TDP1 inhibitory assay in a quantitative high-throughput screening platform. DNA Repair (Amst.) *21*, 177–182.

Murai, J., Zhang, Y., Morris, J., Ji, J., Takeda, S., Doroshow, J.H., and Pommier, Y. (2014b). Rationale for poly(ADP-ribose) polymerase (PARP) inhibitors in combination therapy with camptothecins or temozolomide based on PARP trapping versus catalytic inhibition. J. Pharmacol. Exp. Ther. *349*, 408–416.

Nagasawa, H., Lin, Y.-F., Kato, T.A., Brogan, J.R., Shih, H.-Y., Kurimasa, A., Bedford, J.S., Chen, B.P.C., and Little, J.B. (2017). Coordination of the Ser2056 and Thr2609 Clusters of DNA-PKcs in Regulating Gamma Rays and Extremely Low Fluencies of Alpha-Particle Irradiation to G0/G1 Phase Cells. Radiation Research *187*, 259–267.

Neal, J.A., and Meek, K. (2011). Choosing the right path: does DNA-PK help make the decision? Mutat. Res. *711*, 73–86.

Neal, J.A., Sugiman-Marangos, S., VanderVere-Carozza, P., Wagner, M., Turchi, J., Lees-Miller, S.P., Junop, M.S., and Meek, K. (2014). Unraveling the complexities of DNA-dependent protein kinase autophosphorylation. Mol. Cell. Biol. *34*, 2162–2175.

Niere, M., Kernstock, S., Koch-Nolte, F., and Ziegler, M. (2008). Functional localization of two poly(ADP-ribose)-degrading enzymes to the mitochondrial matrix. Mol. Cell. Biol. *28*, 814–824.

Palle, K., and Vaziri, C. (2011). Rad18 E3 ubiquitin ligase activity mediates Fanconi anemia pathway activation and cell survival following DNA Topoisomerase 1 inhibition. Cell Cycle *10*, 1625–1638.

Patel, A.G., Flatten, K.S., Schneider, P.A., Dai, N.T., McDonald, J.S., Poirier, G.G., and Kaufmann, S.H. (2012). Enhanced killing of cancer cells by poly(ADP-ribose) polymerase inhibitors and topoisomerase I inhibitors reflects poisoning of both enzymes. J. Biol. Chem. *287*, 4198–4210.

Petermann, E., and Helleday, T. (2010). Pathways of mammalian replication fork restart. Nat. Rev. Mol. Cell Biol. *11*, 683–687.

Pommier, Y. (2013). Drugging topoisomerases: lessons and challenges. ACS Chem. Biol. *8*, 82–95.

Raderschall, E., Golub, E.I., and Haaf, T. (1999). Nuclear foci of mammalian recombination proteins are located at single-stranded DNA regions formed after DNA damage. Proc. Natl. Acad. Sci. U.S.A. *96*, 1921–1926.

Ray Chaudhuri, A., and Nussenzweig, A. (2017). The multifaceted roles of PARP1 in DNA repair and chromatin remodelling. Nat. Rev. Mol. Cell Biol. *18*, 610–621.

Ray Chaudhuri, A., Hashimoto, Y., Herrador, R., Neelsen, K.J., Fachinetti, D., Bermejo, R., Cocito, A., Costanzo, V., and Lopes, M. (2012). Topoisomerase I poisoning results in PARP-mediated replication fork reversal. Nat. Struct. Mol. Biol. *19*, 417–423.

Ray Chaudhuri, A., Ahuja, A.K., Herrador, R., and Lopes, M. (2015). Poly(ADP-ribosyl) glycohydrolase prevents the accumulation of unusual replication structures during unperturbed S phase. Mol. Cell. Biol. *35*, 856–865.

Rechkunova, N.I., Lebedeva, N.A., and Lavrik, O.I. (2015). [Tyrosyl-DNA Phosphodiesterase 1 Is a New Player in Repair of Apurinic/Apyrimidinic Sites]. Bioorg. Khim. *41*, 531–538.

Ribeyre, C., Zellweger, R., Chauvin, M., Bec, N., Larroque, C., Lopes, M., and Constantinou, A. (2016). Nascent DNA Proteomics Reveals a Chromatin Remodeler Required for Topoisomerase I Loading at Replication Forks. Cell Rep *15*, 300–309.

Ronco, C., Martin, A.R., Demange, L., and Benhida, R. (2017). ATM, ATR, CHK1, CHK2 and WEE1 inhibitors in cancer and cancer stem cells. Med. Chem. Commun. *8*, 295–319.

Ruscetti, T., Lehnert, B.E., Halbrook, J., Le Trong, H., Hoekstra, M.F., Chen, D.J., and Peterson, S.R. (1998). Stimulation of the DNA-dependent protein kinase by poly(ADP-ribose) polymerase. J. Biol. Chem. *273*, 14461–14467.

Sajish, M., Zhou, Q., Kishi, S., Valdez, D.M., Kapoor, M., Guo, M., Lee, S., Kim, S., Yang, X.-L., and Schimmel, P. (2012). Trp-tRNA synthetase bridges DNA-PKcs to PARP-1 to link IFN-γ and p53 signaling. Nat. Chem. Biol. *8*, 547–554.

Sarkaria, J.N., Busby, E.C., Tibbetts, R.S., Roos, P., Taya, Y., Karnitz, L.M., and Abraham, R.T. (1999). Inhibition of ATM and ATR Kinase Activities by the Radiosensitizing Agent, Caffeine. Cancer Res *59*, 4375–4382.

Sartori, A.A., Lukas, C., Coates, J., Mistrik, M., Fu, S., Bartek, J., Baer, R., Lukas, J., and Jackson, S.P. (2007). Human CtIP promotes DNA end resection. Nature *450*, 509–514.

Sasaki, Y., Hozumi, M., Fujimori, H., Murakami, Y., Koizumi, F., Inoue, K., and Masutani, M. (2016). PARG Inhibitors and Functional PARG Inhibition Models. Curr. Protein Pept. Sci. *17*, 641–653.

Serrano, M.A., Li, Z., Dangeti, M., Musich, P.R., Patrick, S., Roginskaya, M., Cartwright, B., and Zou, Y. (2013). DNA-PK, ATM and ATR collaboratively regulate p53-RPA interaction to facilitate homologous recombination DNA repair. Oncogene *32*, 2452–2462.

Shao, R.G., Cao, C.X., Zhang, H., Kohn, K.W., Wold, M.S., and Pommier, Y. (1999). Replication-mediated DNA damage by camptothecin induces phosphorylation of RPA by DNA-dependent protein kinase and dissociates RPA:DNA-PK complexes. EMBO J. *18*, 1397–1406.

Shirai, H., Fujimori, H., Gunji, A., Maeda, D., Hirai, T., Poetsch, A.R., Harada, H., Yoshida, T., Sasai, K., Okayasu, R., et al. (2013a). Parg deficiency confers radio-sensitization through enhanced cell death in mouse ES cells exposed to various forms of ionizing radiation. Biochem. Biophys. Res. Commun. *435*, 100–106.

Shirai, H., Poetsch, A.R., Gunji, A., Maeda, D., Fujimori, H., Fujihara, H., Yoshida, T., Ogino, H., and Masutani, M. (2013b). PARG dysfunction enhances DNA double strand break formation in S-phase after alkylation DNA damage and augments different cell death pathways. Cell Death Dis *4*, e656.

Soutoglou, E., and Misteli, T. (2008). Activation of the cellular DNA damage response in the absence of DNA lesions. Science *320*, 1507–1510.

Toledo, L., Neelsen, K.J., and Lukas, J. (2017). Replication Catastrophe: When a Checkpoint Fails because of Exhaustion. Mol. Cell *66*, 735–749.

Toledo, L.I., Murga, M., and Fernandez-Capetillo, O. (2011). Targeting ATR and Chk1 kinases for cancer treatment: a new model for new (and old) drugs. Mol Oncol *5*, 368–373.

Toledo, L.I., Altmeyer, M., Rask, M.-B., Lukas, C., Larsen, D.H., Povlsen, L.K., Bekker-Jensen, S., Mailand, N., Bartek, J., and Lukas, J. (2013). ATR prohibits replication catastrophe by preventing global exhaustion of RPA. Cell *155*, 1088–1103.

Trenz, K., Smith, E., Smith, S., and Costanzo, V. (2006). ATM and ATR promote Mre11 dependent restart of collapsed replication forks and prevent accumulation of DNA breaks. EMBO J. *25*, 1764–1774.

Tripathi, K., Mani, C., Clark, D.W., and Palle, K. (2016). Rad18 is required for functional interactions between FANCD2, BRCA2, and Rad51 to repair DNA topoisomerase 1-poisons induced lesions and promote fork recovery. Oncotarget *7*, 12537–12553.

Veith, S., and Mangerich, A. (2015). RecQ helicases and PARP1 team up in maintaining genome integrity. Ageing Research Reviews *23*, 12–28.

Wang, M., Wu, W., Wu, W., Rosidi, B., Zhang, L., Wang, H., and Iliakis, G. (2006). PARP-1 and Ku compete for repair of DNA double strand breaks by distinct NHEJ pathways. Nucleic Acids Res. *34*, 6170–6182.

Wollmann, Y., Schmidt, U., Wieland, G.D., Zipfel, P.F., Saluz, H.-P., and Hänel, F. (2007). The DNA topoisomerase IIbeta binding protein 1 (TopBP1) interacts with poly (ADP-ribose) polymerase (PARP-1). J. Cell. Biochem. *102*, 171–182.

Yang, Y.-G., Cortes, U., Patnaik, S., Jasin, M., and Wang, Z.-Q. (2004). Ablation of PARP-1 does not interfere with the repair of DNA double-strand breaks, but compromises the reactivation of stalled replication forks. Oncogene *23*, 3872–3882.

Yata, K., Lloyd, J., Maslen, S., Bleuyard, J.-Y., Skehel, M., Smerdon, S.J., and Esashi, F. (2012). Plk1 and CK2 act in concert to regulate Rad51 during DNA double strand break repair. Mol. Cell *45*, 371–383.

Ying, S., Hamdy, F.C., and Helleday, T. (2012). Mre11-dependent degradation of stalled DNA replication forks is prevented by BRCA2 and PARP1. Cancer Res. *72*, 2814–2821.

Ying, S., Chen, Z., Medhurst, A.L., Neal, J.A., Bao, Z., Mortusewicz, O., McGouran, J., Song, X., Shen, H., Hamdy, F.C., et al. (2016). DNA-PKcs and PARP1 Bind to Unresected Stalled DNA Replication Forks Where They Recruit XRCC1 to Mediate Repair. Cancer Res. *76*, 1078–1088.

Yoo, H.Y., Kumagai, A., Shevchenko, A., Shevchenko, A., and Dunphy, W.G. (2009). The Mre11-Rad50-Nbs1 complex mediates activation of TopBP1 by ATM. Mol. Biol. Cell *20*, 2351–2360.

ellweger, R., Dalcher, D., Mutreja, K., Berti, M., Schmid, J.A., Herrador, R., Vindigni, A., and Lopes, M. (2015). Rad51-mediated replication fork reversal is a global response to genotoxic treatments in human cells. J. Cell Biol. *208*, 563–579.

Zhang, Y.-W., Regairaz, M., Seiler, J.A., Agama, K.K., Doroshow, J.H., and Pommier, Y. (2011). Poly(ADP-ribose) polymerase and XPF-ERCC1 participate in distinct pathways for the repair of topoisomerase I-induced DNA damage in mammalian cells. Nucleic Acids Res. *39*, 3607–3620.

Zhou, Y., Feng, X., and Koh, D.W. (2010). Enhanced DNA accessibility and increased DNA damage induced by the absence of poly(ADP-ribose) hydrolysis. Biochemistry *49*, 7360–7366.

Zou, Y., Liu, Y., Wu, X., and Shell, S.M. (2006). Functions of human replication protein A (RPA): From DNA replication to DNA damage and stress responses. J. Cell. Physiol. *208*, 267–273.

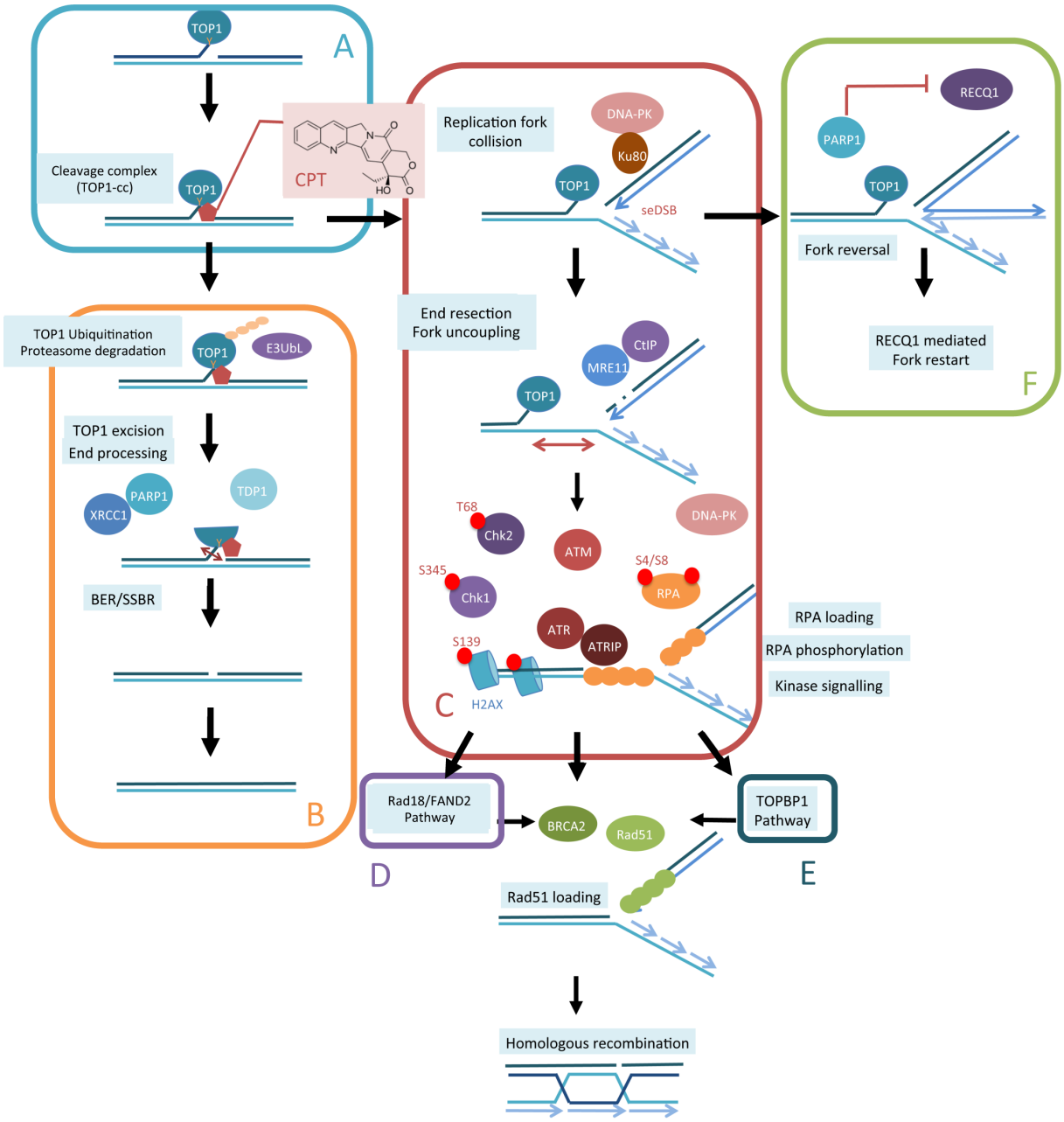

Figure 34: Different outcomes of CPT-induced Top1 poisoning. A) Camptothecin traps TOP1 into a cleavage-complex (Top1cc). B) TOP1 degradation and single strand break repair of the lesion. C) Replication fork collision and homologous end joining repair of stalled forks. D-E) Alternative pathways to lead cells towards HR repair. F) PARP1/RECQ1 dependent fork reversal.

Discussion and perspectives

1. Escaping replicative stress: a hard task

The outcomes and consequences of replication stress are complex mechanisms (Zeman and Cimprich, 2014), and given the incomplete data we provide in this article, we can only formulate several hypotheses of what could happen at every step of the CPT response. Schemed in **Figure 34** are several pathways that can be used to overcome CPT lesions. In this discussion, I will consider some of the possibilities used in shPARG to escape replicative stress even with a defective RPA phosphorylation, discussing the involvement of PARP1 and DNA-PK at each step.

A) CPT treatment results in the trapping of the topoisomerase 1 enzyme into a cleavage complex (Top1-cc), blocking its tension-relief activity on DNA-strands, and resulting in an opened DNA strand (Pommier *et al.* 2010). This initial situation of TOP1 blocking can have different outcomes, which will depend on several factors.

B) The most rapid and consensual way to repair TOP1 lesions is to degrade it through an ubiquitin-dependent pathway, addressing the protein to the proteasome (Desai *et al*. 1997). TOP1 and PARP1 both interact and colocalize in cells and PARylation of Top1 influences its distribution and activity in the nucleus (Das *et al.* 2016; Yung *et al.* 2004). In parallel, the increase of PARylation after CPT treatment also favours the recruitment of the TDP1/XRCC1 complex. TDP1 knocked out cells are highly sensitive to CPT, and one study demonstrated that TDP1 played a pivotal role in NHEJ, through binding of the XLF complex (Li *et al.* 2017). Indeed, TDP1 binds PARP1 and can directly excise Top1-cc, generating a single strand break than can be repaired by base excision repair, owing to the presence of XRCC1 (Das *et al*. 2014). Additionally, TDP1 is able to promote the assembly of NHEJ proteins. It interacts with Ku70/Ku80, promotes DNA-binding of the XLF complex, and stimulates DNA-PK activity (Heo *et al.* 2015). DNA-PK and ATM phosphorylation of the S81 of TDP1 is necessary to mediate the XLF association and required for an optimal TDP1 activity (Das *et al.* 2009). Since DNA-PK also phosphorylates XRCC1 after irradiation, DNA-PK might thus act in SSBR after CPT damage (Lévy *et al.* 2006). Regarding the link between DNA-PK, PARP1 and single strand break repair, we hypothesized that PARG deficiency could lead to an impaired repair of CPT-induced damage by the TDP1 pathway. However, we couldn't assess it precisely because of technical considerations, as discussed in the paper.
This aspect of the CPT response lacks in our study, for TDP1 primarily repairs transcription-coupled Top1-cc (Shiloh *et al.* 2013). Here, we did not consider at all the impact of transcription-coupled Top1-cc lesions, even since PARG deficiency is likely to trigger defects in transcription rates, and therefore to increase the amount of DNA-damages.

C) Upon collision with the replication fork, an important type of lesion is generated: single-ended DSBs (seDSB). Cells must avoid using NHEJ to repair this type of lesion, since there is no opposite strand for re-joining. Chanut *et al* (2016) described a model by which Ku80 and DNA-PK first recognize the single ended DSB, and are then evicted by the coordinated actions of the MRN complex and the CtIP endonuclease, that will me-

diate strand resection allowing Rad51 loading and homologous recombination (Chanut *et al.* 2016). Since PARP1 and PAR have a demonstrated role in regulating resection, PARG deficiency could impair this step. Moreover, resected strands need to be rapidly covered by RPA2 in order to protect them from nucleases, and RPA2 phosphorylation is an important event for HR since hyperphosphorylation of RPA2 increases its affinity with Rad51 and favours the replacement (Wu *et al.* 2005). A phosphorylation-defective version of RPA2 was reported to induce defective Rad51 foci formation and to decrease HR frequency (Shi et al. 2010), explaining why RPA2 hyperphosphorylation favours CPT resistance (Anantha *et al.* 2007). Therefore, while HR should be the main pathway to overcome Top1 lesions and allow the efficient loading of Rad51 in our CTRL cells displaying a RPA2-P-S4S8 signal, our shPARG model seems to be defective for this pathway. However, preliminary results for Rad51 foci formation do not indicate less accumulation in shPARG cells (data not shown).

D) Alternatively to a classical Rad51 loading through and affinity exchange with hyperphosphorylated RPA2, several mechanisms have been suggested to allow an efficient Rad51 loading.
The Rad18 E3 ubiquitin ligase has important functions for the translesion synthesis pathway (TLS), by regulating PCNA monoubiquitination, an event that will favour a polymerase switch, recruiting specialized polymerases able to bypass DNA lesions (Song *et al.* 2010). In itself, Rad18 has been shown to bind Rad51 (Huang *et al.* 2009).

In addition to its direct role on Rad51, Rad18 regulates the Fanconi anemia pathway (Palle and Vaziri, 2011). This pathway mainly intervenes in the repair of interstrand crosslinks, mobilizing dozens of proteins, among which an upstream core complex of 8 Fanconi Anemia proteins, a central ID2 complex composed of the FANCI and FANCD2 complex, that can act as a recruitment platform for the downstream effectors XPF, BRCA2 or Rad51 (for a review see Ceccaldi *et al.* 2016). In the past years, there is growing evidence of the FANC pathway in the stabilization of stalled replication forks, the promotion of fork restart and the inhibition of new firing origins (Schlaker *et al.* 2012, Raghunandan *et al.* 2015; Chaudury *et al.* 2013). Additionally, in yeast, the translesion polymerase REV1, in cooperation with FANCD2 is able to stabilize Rad51 filaments (Yang *et al.* 2015), and another study in human showed that FANCD2 is important for the Rad51 dependent fork restart (Thompson *et al.* 2017). In the absence of either Rad18 or FANCD2, the number of BRCA2 and Rad51 foci decrease after CPT treatment (Tripathi *et al.* 2016).

In chicken DT40 cells, PARP1 and Rad18 simultaneous invalidation have synergistic effect and sensitize cells to CPT treatment, suggesting that they collaborate to recover from this genotoxic treatment (Saberi et al, 2007). Rad18 is also shown to be involved in SSBR (Shiomi *et al.* 2007), a pathway in which PARP1 is central. Regarding the tight link between PARG and PCNA, we can hypothesize than in the absence of PARG, Rad18 and/or FANCD2 might act more efficiently to mediate a RPA independent recruitment of Rad51.

E) TOPBP1 (Topoisomerase IIß-binding protein 1) is a scaffolding protein, endowed with essential functions for genome stability (Sokka *et al.* 2010). It has been reported to enhance ATR activity, by interacting with the ATR- interacting protein ATRIP (Kumagai *et al.* 2006; Mordes *et al.* 2008), and is involved in HR through its interaction with NSB1 of the MRN complex (Morishima *et al.* 2007).

TOPBP1 interacts with PARP1 (Wollmann *et al.* 2007), and is a determinant for PARP inhibitor sensitivity (Moudry *et al.* 2016). Mechanistically, it was shown that TOPBP1 binds to and activates PLK1 to phosphorylate Rad51 on Ser14 (Moudry *et al.* 2016), a pre-requisite for Rad51 phosphorylation by CK2 on T13 and subsequent RAD51 chromatin loading (Yata *et al.* 2012). This TOPBP1-promoted RAD51 loading is independent of the BRCA1/PALB2/BRCA2 complex (Sy *et al.* 2009) necessary for the classical steps of HR (Moudry *et al.* 2016). TOPBP1 absence impacts RAD51 recruitment, without affecting resection and RPA loading (Moudry *et al.* 2016). Interestingly, PLK1 is a kinase that we found associated with PARG in our mass spectrometry datasets (data not shown), CK2 is a kinase that phosphorylates PARG (Gagné *et al.* 2008) and other preliminary data obtained in the lab suggest that PARG and TOPBP1 physically interact and that this interaction is reduced upon CPT treatment (data not shown). Altogether, the absence of PARG could favour the TOPBP1-promoted Rad51 loading, independently of RPA2 phosphorylation. This hypothesis is currently under investigation.

F) Another last scenario for the outcome of CPT poisoning is that forks can reverse into four-way junctions called a "chicken foot" structure. Fork reversal is strongly favoured by PARP1, for it inhibits the early fork restart dependent on the RECQ1 helicase (Berti *et al.* 2013). This hypothesis, detailed below, also needs to be further investigated.

2. Fork reversal as a general response to replicative stress.

Separate and concordant studies have been published in the literature, that lead to consider fork reversal as an evolutionary conserved protective feature to escape from replicative stress (Ray Chaudhuri *et al.* 2012), that can occur after different types of treatment and rely on the presence of Rad51. Interestingly, while CPT was not expected to trigger any fork uncoupling, Zellweger *et al.* 2015 demonstrated that mild doses of CPT could promote the formation of longer ssDNA at fork reversal junctions. They show that a siRNA depletion of Rad51 suppresses fork slowing and reversal after CPT treatment, and therefore might be a key component for stabilizing reversed forks. The latest study using PARG deficient models show that upon basal situations, in the absence of treatment, PARG depletion leads to an increased spontaneous level of fork reversal (Ray *Chaudhuri et al.* 2015). This is an important observation, for it might be the key mechanism to fully explain our own results. Indeed, the accumulation of fork reversal relies on PARP1 activity and polymer levels (Berti *et al.* 2013). Therefore, the increase of spontaneous fork reversal could result from the steady-state accumulation of PAR in our shPARG cells.

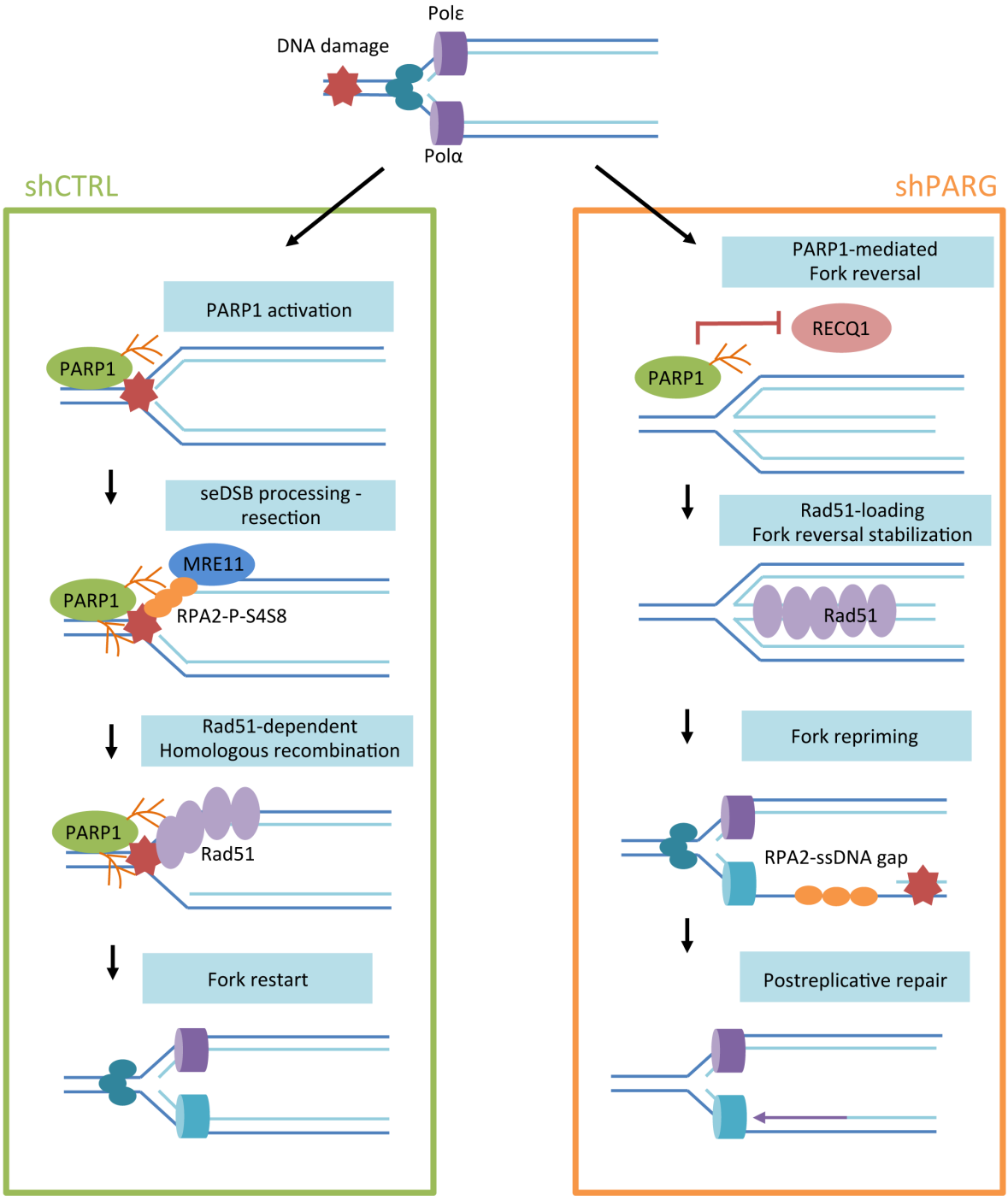

Figure 35: Scenario for the replicative stress escape in U2OS shPARG cells.
Upon CPT-induced replication stress, shCTRL cells undergo normal RPAP-S4S8, Rad51 dependent fork restart. In shPARG cells, there could be an increased proportion of PARP1-Rad51 dependent fork reversal, leading to more fork repriming events in the absence of RPA phosphorylation, and the overaccumulation of post-replicative ssDNA-gaps, covered with RPA, rejoining the observations of Ray Chaudhuri *et al.* 2015.

Moreover, fork reversal is believed to have a protective role for replication forks, acting as an "emergency brake" in cells, in order to give time to the repair machineries to overcome replicative stress, and to mediate fork restart (Higgins *et al,* 1976; Berti and Vindigni, 2013). Given that 1) our U2OS cells are rather protected from CPT treatments; 2) as discussed above, the absence of PARG could favour a RPA-independent recruitment of Rad51 to the forks, through the TOPBP1 or the FANCD2 pathway; 3) Rad51 is needed for fork reversal (Zellweger *et al.* 2015) ; overall we could picture a situation where PARG deficiency favours the Rad51 dependent stabilization of reversed forks, to overcome CPT-induced replicative stress, independently of RPA hyperphosphorylation.

3. Fork repriming as the way out?

After fork reversal, replication fork can either restart by remodeling the structure of the four way junction, or alternatively "reprime" replication, thus generating post-replicative gaps (Heller *et al.* 2006), that also need to be covered with RPA and subsequently repaired by filling with specialized translesion polymerases, through the translesion synthesis (TLS) pathway (Daigaku *et al.* 2010). In humans, the PrimPol protein can restart replication after the damaged fork (Mouron *et al.* 2013), and translesion polymerases (PolH, REV1, POLK, POLI, REV3L, REV7, POLN and POLQ, (for a review see Sale *et al.* 2012), can repair such abnormalities. Since PARG and PCNA interact (Mortusewicz *et al.* 2011; Kaufmann *et al.* 2017), and since PCNA has a key role in TLS (for a review see Kanao and Masutani, 2017), we can suggest that PARG deficiency could somehow favor TLS function after CPT. HeLa deficient shPARG cells display extended ssDNA gaps after no or mild CPT treatment (Ray Chaudhuri *et al.* 2015), and this could be explained by increased proportions of fork repriming, directly linked with the increased proportion of fork slowing and reversal events. Although we didn't measure fork speed nor ssDNA gaps in our U2OS cell model, PARG depletion resulted in such phenotypes in Ray Chaudhuri *et al.* 2015.

With our current data and current understanding of the question, I propose this hypothesis to explain why shPARG cells can escape replicative stress in the absence of RPA phosphorylation (**Figure 35**). While shCTRL display a normal HR-mediated response after CPT, shPARG could favor Rad51 and PARP1 dependent stabilization of fork reversal events, thus leading to an increased fork repriming, with no need for RPA-hyperphosphorylation. The accumulation of post-replicative ssDNA gaps in shPARG could explain while the loss of RPA-S4S8 is not coupled with an impaired recruitment of RPA on chromatin.

4. RPA-P-S4S8 defect results from a direct effect on RPA

In the previous model I described explains how shPARG cells could escape replicative stress without the need of RPA phosphorylation, it doesn't fully explain the origins of this phosphorylation defect.

In a previous work, our lab had demonstrated that PARG activity was necessary to avoid the detrimental accumulation of PAR on RPA, upon prolonged replication stress induced with HU (Illuzzi *et al.* 2014). The fact that CPT treatment does not induce as much polymer synthesis than in HU treatment argued against the hypothesis of an overaccumulation of PAR on RPA. However, we tested both an immunoprecipitation of PAR, in order to reveal RPA and a RPA immunoprecipitation to reveal PAR, after CPT treatment. In both cases, our preliminary data didn't reveal any PARylated RPA (data not shown).

In another scenario, one can imagine the contribution of helicase to this mechanism. Recently, it has been shown that HARP/SMARCAL1, an ATP-dependent helicase is capable of rewinding DNA structure by binding to RPA. Interestingly, HARP co-purifies with RPA bound to DNA-PK and blocks RPA phosphorylation (Quan *et al.* 2014). It would be interesting to see whether HARP is PARylated in shPARG cells, and if this could favour the stabilisation of an unphosphorylated form of RPA.

Monitoring the kinase activity was something we intended, but the impact of each of them on RPA was not clear from the literature, and RPA phosphorylation is under complex regulation, and depends both on the type of DNA-damage and the cell cycle (Maréchal and Zou, 2015). Some of the phosphorylation events need to be "primed" by cycline kinases. A study showed that Cdk5 activity promoted replication checkpoint activation through RPA phosphorylation and was a determinant of PARP inhibitor sensitivity. Cdk5-deficient HeLa and U2OS cells display higher sensitivity to S-phase irradiation. This is due to a reduced priming of Ser23, Ser29 and Ser33 phosphorylation marks, that results in lower levels of RPA-S4S8 phosphorylation and is associated with increased DNA-damage (Chiker *et al.* 2015). Whether our shPARG cells could be slightly defective in priming RPA hyper-phosphorylation needs further investigation

Several studies suggested that DNA-PK is the main kinase involved in RPA hyperphosphorylation (Shao *et al*. 1999), targeting mainly S33 and T21 or S4S8 (Ashley *et al.* 2014). In our study, we showed that ATM was the main kinase responsible for RPA-S4S8 phosphorylation after CPT in U2OS, but its activity was not impaired as revealed by the efficient activation of Chk2. We cannot rule out that ATM activity is stimulated by fork reversal events. ATR activation was slightly delayed, and since an excess of ssDNA has been linked to ATR activation (Zou and Elledge 2003), we can imagine that in shPARG, it is due to the accumulation of ssDNA gaps rather than DNA-damage resection. This gives an additional argument to the hypothesis that after CPT treatment in shPARG, ATM/ATR signalling can be uncoupled from DNA damage accumulation (Ray Chaudhuri *et al.* 2015).

DNA-PK's activity was solely assessed by its autophosphorylation in S2056. DNA-PK displays several clusters of phosphorylation that have many different outcomes for DNA-repair. For instance, phosphorylation of Ser2056 in the "PQR" cluster is reported to restrict DNA-PK's access to DNA ends, while the phosphorylation of Thr2609 in the "ABCD" cluster promotes the access to DNA ends, is Ku dependent and promotes NHEJ (Chan *et al.* 2002). Therefore, monitoring only Ser2056 as a marker of DNA-PK activity is limiting. We thought about monitoring p53 phosphorylation as a better readout of DNA-PK's activity. However, one study has shown that

the simultaneous phosphorylation of p53 by ATR and ATM, and RPA by DNA-PK is necessary to disrupt p53-RPA interaction, allowing them to mediate their function in DNA-damage repair, so even p53 phosphorylation might not be an efficient market for us to conclude (Serrano *et al.* 2013).

5. IPond technique as the golden standard?

Throughout this study, we focused on replicative stress triggered upon collision with the replication fork with TOP1-cc cleavage complexes, but did not consider the role of Top1 in the prevention of R-loop structures formation, that can also interfere with replication (Tuduri *et al.* 2009).

Techniques of nascent DNA proteomics are efficient method to draw the complex network of proteins that are recruited at active or damaged replication forks (Sirbu *et al.* 2011; Drungralawa *et al.* 2015, Ribeyre *et al.* 2016 showed that upon CPT treatment and within minutes, several protein factors are recruited to replication fork, having roles both in DNA damage and replication (DNA-PK, Ku80, Ligase 1, Ligase 3), transcription and RNA processing, and chromatin structure (SMARCA5, BAZ1B, NUMA1). All these functions are tightly related with Poly(ADP-ribosylation). Interestingly, BAZ1B/WSTF is tightly associated with PCNA (Poot *et al.* 2004; Poot *et al.* 2005), a demonstrated partner of PARG (Mortusewicz *et al.* 2011; Kauffmann *et al.* 2017). Preliminary data in our lab has also shown that PARG could directly co-immunoprecipitate with WSTF (G. Illuzzi, personal communication). Because the depletion of WSTF by siRNA results in a reduction of γH2AX phosphorylation, as well as a slight reduction of Chk1 phosphorylation and RPA2-S4S8, we could hypothesize that the absence of PARG could result in an impaired recruitment of WSTF at replication forks.

Another interesting study using IPond revealed the kinetic of several protein factors after replication stress induced by HU (Drungralawa *et al.* 2015). This study shows that while PARP1 levels are stable at replication forks, PARG is evicted from the fork, while H2A.1 and H2A.2, recruited by PAR (Khurana *et al.* 2014) are increasing, possibly contributing to the creation of a permissive chromatin environment allowing the repair and restart of stalled fork. Consistently, pre-treatment with PARP inhibitor before CPT exposure completely restored the RPA-S4S8 phosphorlation level in shPARG (data not shown). Since PARP inhibition also sensitizes cells to CPT treatment, this supports that the accumulation of PAR at the vicinity of replication fork is necessary for a proper restart, or a proper fork repriming, and that it has a protective role (Amé *et al*. 2009).

The best method to decipher what happens in our shPARG cells would be to use the IPond technique, coupled to mass spectrometry, as described in Sirbu *et al.* 2011 and Drungralawa *et al.* 2015.

Conclusion

In this study we used a new U2OS PARG deficient cell line to analyse the response to several DNA-damaging agents or replicative stress inducers. In these shPARG cells, we observed a dramatic defect in RPA-S4S8 phosphorylation that was not associated with a strong decrease in DNA strand breaks, or with a defective damage signalling. Neither RPA loading on chromatin, nor PI3-K kinases activities associated with RPA2-S4S8 or T21 phosphorylation was impaired. While we hypothetised that the RPA phosphorylation defect however reflects an impaired resection, coupled to a diminished level of homologous recombination at collapsed replication forks, our results suggest that these processes are not dramatically affected, and PARG inhibition does

not decrease cell viability. This suggests that PARG deficient cells use alternative pathways to compensate for this RPA-S4S8 defect. Altogether, these results help understanding the mechanisms linking Top1 activity and PARylation, two core features of genomic integrity that can prove to be friend or foe to mammalian cells (Kim and Jinks-Robertson, 2017).

General Conclusion:

During this thesis project, I focused on three axes of research: the initial aim of my project (**Aim 1**) was to generate new innovative cell models allowing the study of PARG regulation and the precise contribution of each isoform to DNA repair. Using the Golden Gate technology, I generated several stable cell lines in a U2OS background allowing the knockdown of all endogenous PARG isoforms and the selective induction of each of PARG isoforms (**Research paper n°1, unpublished**). The project also resulted in the elaboration of a new high-throughput methodology for measuring the dynamic of PAR degradation in isoforms-expressing cell lines. Using these tools, we provided new evidence confirming that PARG^{102} is the most abundant isoforms in human cells, and that it can contribute to DNA repair.

Another aim of my project (**Aim 2**) was to study whether PARG could be regulated by post-translational modifications. This project led to the discovery of a new protein partner, DNA-PK, that could phosphorylate PARG in vitro on several identified target sites, and whose interaction with PARG increases after DNA damage (**Research paper n°2, unpublished**). Although the functional relevance of the phosphorylation sites needs additional investigation, this work provides further evidence that PARG, similarly to PARP1, can probably be regulated by important kinases playing in DNA damage response.

In the last part of my project, taking advantage of our new cellular models and knowing that PARG and DNA-PK were protein partners, I intended to investigate the role of PARG in the cell response to the anticancer drug camptothecin (**Aim 3**). This project was based on a systematic investigation of several markers of DNA repair, after release from an acute treatment with CPT, a drug used in cancer therapies (**Research paper n°3, unpublished**). Our results suggest that shPARG cells, despite displaying a strong defect in RPA phosphorylation, are able to use alternative pathways to overcome CPT-induced replicative stress.

The results yielded in the different parts of this thesis manuscript provide new evidence that PARG, as one of the main enzymes responsible for PAR homeostasis, has a complex regulation. Both isoform generation and post-translational modifications are likely to influence the interaction between PARG and other protein factors involved in the maintenance of genome integrity. Altogether, this project is an additional step in our understanding of the role of PARG in response to DNA damage and replicative stress. This knowledge will be valuable for elaborating new strategies for the therapeutic targeting of DNA repair deficient cancer cell-lines with the combined used of genotoxic agents and protein inhibitors.

Bibliography:

Abudayyeh, O.O., Gootenberg, J.S., Essletzbichler, P., Han, S., Joung, J., Belanto, J.J., Verdine, V., Cox, D.B.T., Kellner, M.J., Regev, A., et al. (2017). RNA targeting with CRISPR–Cas13. Nature *550*, 280–284.

Acevedo, J., Yan, S., and Michael, W.M. (2016). Direct Binding to Replication Protein A (RPA)-coated Single-stranded DNA Allows Recruitment of the ATR Activator TopBP1 to Sites of DNA Damage. J. Biol. Chem. *291*, 13124–13131.

Affar, E.B., Germain, M., Winstall, E., Vodenicharov, M., Shah, R.G., Salvesen, G.S., and Poirier, G.G. (2001). Caspase-3-mediated processing of poly(ADP-ribose) glycohydrolase during apoptosis. J. Biol. Chem. *276*, 2935–2942.

Aguiar, R.C.T., Takeyama, K., He, C., Kreinbrink, K., and Shipp, M.A. (2005). B-aggressive lymphoma family proteins have unique domains that modulate transcription and exhibit poly(ADP-ribose) polymerase activity. J. Biol. Chem. *280*, 33756–33765.

Aguilar-Quesada, R., Muñoz-Gámez, J.A., Martín-Oliva, D., Peralta, A., Valenzuela, M.T., Matínez-Romero, R., Quiles-Pérez, R., Menissier-de Murcia, J., de Murcia, G., Ruiz de Almodóvar, M., et al. (2007). Interaction between ATM and PARP-1 in response to DNA damage and sensitization of ATM deficient cells through PARP inhibition. BMC Mol. Biol. *8*, 29.

Ahel, D., Horejsí, Z., Wiechens, N., Polo, S.E., Garcia-Wilson, E., Ahel, I., Flynn, H., Skehel, M., West, S.C., Jackson, S.P., et al. (2009). Poly(ADP-ribose)-dependent regulation of DNA repair by the chromatin remodeling enzyme ALC1. Science *325*, 1240–1243.

Ahel, I., Ahel, D., Matsusaka, T., Clark, A.J., Pines, J., Boulton, S.J., and West, S.C. (2008). Poly(ADP-ribose)-binding zinc finger motifs in DNA repair/checkpoint proteins. Nature *451*, 81–85.

Ahnesorg, P., Smith, P., and Jackson, S.P. (2006). XLF interacts with the XRCC4-DNA ligase IV complex to promote DNA nonhomologous end-joining. Cell *124*, 301–313.

Al Abo, M., Sasanuma, H., Liu, X., Rajapakse, V.N., Huang, S.-Y.N., Kiselev, E., Takeda, S., Plunkett, W., and Pommier, Y. (2017). TDP1 is critical for the repair of DNA breaks induced by sapacitabine, a nucleoside also targeting ATM- and BRCA-deficient tumors. Mol. Cancer Ther.

Alawneh, A.M., Qi, D., Yonesaki, T., and Otsuka, Y. (2016). An ADP-ribosyltransferase Alt of bacteriophage T4 negatively regulates the Escherichia coli MazF toxin of a toxin-antitoxin module. Mol. Microbiol. *99*, 188–198.

Allinson, S.L., Dianova, I.I., and Dianov, G.L. (2003). Poly(ADP-ribose) polymerase in base excision repair: always engaged, but not essential for DNA damage processing. Acta Biochim. Pol. *50*, 169–179.

Almeida, K.H., and Sobol, R.W. (2007). A unified view of base excision repair: lesion-dependent protein complexes regulated by post-translational modification. DNA Repair (Amst.) *6*, 695–711.

Altmeyer, M., Toledo, L., Gudjonsson, T., Grøfte, M., Rask, M.-B., Lukas, C., Akimov, V., Blagoev, B., Bartek, J., and Lukas, J. (2013). The chromatin scaffold protein SAFB1 renders chromatin permissive for DNA damage signaling. Mol. Cell *52*, 206–220.

Altmeyer, M., Neelsen, K.J., Teloni, F., Pozdnyakova, I., Pellegrino, S., Grøfte, M., Rask, M.-B.D., Streicher, W., Jungmichel, S., Nielsen, M.L., et al. (2015). Liquid demixing of intrinsically disordered proteins is seeded by poly(ADP-ribose). Nat Commun *6*, 8088.

Amé, J.C., Apiou, F., Jacobson, E.L., and Jacobson, M.K. (1999a). Assignment of the poly(ADP-ribose) glycohydrolase gene (PARG) to human chromosome 10q11.23 and mouse chromosome 14B by in situ hybridization. Cytogenet. Cell Genet. *85*, 269–270.

Amé, J.C., Jacobson, E.L., and Jacobson, M.K. (1999b). Molecular heterogeneity and regulation of poly(ADP-ribose) glycohydrolase. Mol. Cell. Biochem. *193*, 75–81.

Amé, J.-C., Spenlehauer, C., and de Murcia, G. (2004). The PARP superfamily. Bioessays *26*, 882–893.

Amé, J.-C., Fouquerel, E., Gauthier, L.R., Biard, D., Boussin, F.D., Dantzer, F., de Murcia, G., and Schreiber, V. (2009). Radiation-induced mitotic catastrophe in PARG-deficient cells. J. Cell. Sci. *122*, 1990–2002.

Anantha, R.W., Vassin, V.M., and Borowiec, J.A. (2007). Sequential and synergistic modification of human RPA stimulates chromosomal DNA repair. J. Biol. Chem. *282*, 35910–35923.

Andrabi, S.A., Kim, N.S., Yu, S.-W., Wang, H., Koh, D.W., Sasaki, M., Klaus, J.A., Otsuka, T., Zhang, Z., Koehler, R.C., et al. (2006). Poly(ADP-ribose) (PAR) polymer is a death signal. Proc. Natl. Acad. Sci. U.S.A. *103*, 18308–18313.

Anglana, M., Apiou, F., Bensimon, A., and Debatisse, M. (2003). Dynamics of DNA replication in mammalian somatic cells: nucleotide pool modulates origin choice and interorigin spacing. Cell *114*, 385–394.

Aoki, K., Maruta, H., Uchiumi, F., Hatano, T., Yoshida, T., and Tanuma, S. (1995). A macrocircular ellagitannin, oenothein B, suppresses mouse mammary tumor gene expression via inhibition of poly(ADP-ribose) glycohydrolase. Biochem. Biophys. Res. Commun. *210*, 329–337.
Aravind, L. (2001). The WWE domain: a common interaction module in protein ubiquitination and ADP ribosylation. Trends Biochem. Sci. *26*, 273–275.
Aravind, L., Zhang, D., De Souza, R., Anand, S., and Iyer, L. (2014). The Natural History of ADP-Ribosyltransferases and the ADP-Ribosylation System. Current Topics in Microbiology and Immunology *384*.
Ariumi, Y., Masutani, M., Copeland, T.D., Mimori, T., Sugimura, T., Shimotohno, K., Ueda, K., Hatanaka, M., and Noda, M. (1999). Suppression of the poly(ADP-ribose) polymerase activity by DNA-dependent protein kinase in vitro. Oncogene *18*, 4616–4625.
Ashley, A.K., Shrivastav, M., Nie, J., Amerin, C., Troksa, K., Glanzer, J.G., Liu, S., Opiyo, S.O., Dimitrova, D.D., Le, P., et al. (2014). DNA-PK phosphorylation of RPA32 Ser4/Ser8 regulates replication stress checkpoint activation, fork restart, homologous recombination and mitotic catastrophe. DNA Repair (Amst.) *21*, 131–139.
Atasheva, S., Akhrymuk, M., Frolova, E.I., and Frolov, I. (2012). New PARP gene with an anti-alphavirus function. J. Virol. *86*, 8147–8160.
Atasheva, S., Frolova, E.I., and Frolov, I. (2014). Interferon-stimulated poly(ADP-Ribose) polymerases are potent inhibitors of cellular translation and virus replication. J. Virol. *88*, 2116–2130.
Audebert, M., Salles, B., and Calsou, P. (2004). Involvement of poly(ADP-ribose) polymerase-1 and XRCC1/DNA ligase III in an alternative route for DNA double-strand breaks rejoining. J. Biol. Chem. *279*, 55117–55126.
Audeh, M.W., Carmichael, J., Penson, R.T., Friedlander, M., Powell, B., Bell-McGuinn, K.M., Scott, C., Weitzel, J.N., Oaknin, A., Loman, N., et al. (2010). Oral poly(ADP-ribose) polymerase inhibitor olaparib in patients with BRCA1 or BRCA2 mutations and recurrent ovarian cancer: a proof-of-concept trial. Lancet *376*, 245–251.
Augustin, A., Spenlehauer, C., Dumond, H., Ménissier-De Murcia, J., Piel, M., Schmit, A.-C., Apiou, F., Vonesch, J.-L., Kock, M., Bornens, M., et al. (2003). PARP-3 localizes preferentially to the daughter centriole and interferes with the G1/S cell cycle progression. J. Cell. Sci. *116*, 1551–1562.
Avila, M.A., Velasco, J.A., Smulson, M.E., Dritschilo, A., Castro, R., and Notario, V. (1994). Functional expression of human poly(ADP-ribose) polymerase in Schizosaccharomyces pombe results in mitotic delay at G1, increased mutation rate, and sensitization to radiation. Yeast *10*, 1003–1017.
Bajaj, R., Munari, F., Becker, S., and Zweckstetter, M. (2014a). Interaction of the intermembrane space domain of Tim23 protein with mitochondrial membranes. J. Biol. Chem. *289*, 34620–34626.
Bajaj, R., Jaremko, Ł., Jaremko, M., Becker, S., and Zweckstetter, M. (2014b). Molecular basis of the dynamic structure of the TIM23 complex in the mitochondrial intermembrane space. Structure *22*, 1501–1511.
Bajrami, I., Kigozi, A., Van Weverwijk, A., Brough, R., Frankum, J., Lord, C.J., and Ashworth, A. (2012). Synthetic lethality of PARP and NAMPT inhibition in triple-negative breast cancer cells. EMBO Mol Med *4*, 1087–1096.
Bakkenist, C.J., and Kastan, M.B. (2003). DNA damage activates ATM through intermolecular autophosphorylation and dimer dissociation. Nature *421*, 499–506.
Bakondi, E., Bai, P., Erdélyi, K., Szabó, C., Gergely, P., and Virág, L. (2004). Cytoprotective effect of gallotannin in oxidatively stressed HaCaT keratinocytes: the role of poly(ADP-ribose) metabolism. Exp. Dermatol. *13*, 170–178.
Bannister, A.J., Gottlieb, T.M., Kouzarides, T., and Jackson, S.P. (1993). c-Jun is phosphorylated by the DNA-dependent protein kinase in vitro; definition of the minimal kinase recognition motif. Nucleic Acids Res. *21*, 1289–1295.
Barkauskaite, E., Jankevicius, G., and Ahel, I. (2015). Structures and Mechanisms of Enzymes Employed in the Synthesis and Degradation of PARP-Dependent Protein ADP-Ribosylation. Mol. Cell *58*, 935–946.
Barlow, J.H., Faryabi, R.B., Callén, E., Wong, N., Malhowski, A., Chen, H.T., Gutierrez-Cruz, G., Sun, H.-W., McKinnon, P., Wright, G., et al. (2013). Identification of early replicating fragile sites that contribute to genome instability. Cell *152*, 620–632.
Bateman, A., and Kickhoefer, V. (2003). The TROVE module: a common element in Telomerase, Ro and Vault ribonucleoproteins. BMC Bioinformatics *4*, 49.
Bauersachs, S., Ulbrich, S.E., Gross, K., Schmidt, S.E.M., Meyer, H.H.D., Wenigerkind, H., Vermehren, M., Sinowatz, F., Blum, H., and Wolf, E. (2006). Embryo-induced transcriptome changes in bovine endometrium reveal species-specific and common molecular markers of uterine receptivity. Reproduction *132*, 319–331.
Beauharnois, J.M., Bolívar, B.E., and Welch, J.T. (2013). Sirtuin 6: a review of biological effects and potential therapeutic properties. Mol Biosyst *9*, 1789–1806.
Beausoleil, S., Villén, J., Gerber, S., Rush, J., and P Gygi, S. (2006). A probability-based approach for high-throughput protein phosphorylation analysis and site localization. Nature Biotechnology *24*, 1285–1292.

Beck, C., Boehler, C., Guirouilh Barbat, J., Bonnet, M.-E., Illuzzi, G., Ronde, P., Gauthier, L.R., Magroun, N., Rajendran, A., Lopez, B.S., et al. (2014a). PARP3 affects the relative contribution of homologous recombination and nonhomologous end-joining pathways. Nucleic Acids Res. *42*, 5616–5632.
Beck, C., Robert, I., Reina-San-Martin, B., Schreiber, V., and Dantzer, F. (2014b). Poly(ADP-ribose) polymerases in double-strand break repair: focus on PARP1, PARP2 and PARP3. Exp. Cell Res. *329*, 18–25.
Benchoua, A., Couriaud, C., Guégan, C., Tartier, L., Couvert, P., Friocourt, G., Chelly, J., Ménissier-de Murcia, J., and Onténiente, B. (2002). Active caspase-8 translocates into the nucleus of apoptotic cells to inactivate poly(ADP-ribose) polymerase-2. J. Biol. Chem. *277*, 34217–34222.
Bennetzen, M.V., Larsen, D.H., Bunkenborg, J., Bartek, J., Lukas, J., and Andersen, J.S. (2010). Site-specific phosphorylation dynamics of the nuclear proteome during the DNA damage response. Mol. Cell Proteomics *9*, 1314–1323.
Berger, F., Lau, C., and Ziegler, M. (2007). Regulation of poly(ADP-ribose) polymerase 1 activity by the phosphorylation state of the nuclear NAD biosynthetic enzyme NMN adenylyl transferase 1. PNAS *104*, 3765–3770.
Berger, W., Steiner, E., Grusch, M., Elbling, L., and Micksche, M. (2009). Vaults and the major vault protein: novel roles in signal pathway regulation and immunity. Cell. Mol. Life Sci. *66*, 43–61.
Bermejo, R., Doksani, Y., Capra, T., Katou, Y.-M., Tanaka, H., Shirahige, K., and Foiani, M. (2007). Top1- and Top2-mediated topological transitions at replication forks ensure fork progression and stability and prevent DNA damage checkpoint activation. Genes Dev. *21*, 1921–1936.
Bilan, V., Selevsek, N., Kistemaker, H.A.V., Abplanalp, J., Feurer, R., Filippov, D.V., and Hottiger, M.O. (2017). New Quantitative Mass Spectrometry Approaches Reveal Different ADP-ribosylation Phases Dependent On the Levels of Oxidative Stress. Mol. Cell Proteomics *16*, 949–958.
Bindesbøll, C., Tan, S., Bott, D., Cho, T., Tamblyn, L., MacPherson, L., Grønning-Wang, L., Nebb, H.I., and Matthews, J. (2016). TCDD-inducible poly-ADP-ribose polymerase (TIPARP/PARP7) mono-ADP-ribosylates and co-activates liver X receptors. Biochem. J. *473*, 899–910.
Binkhathlan, Z., and Lavasanifar, A. (2013). P-glycoprotein inhibition as a therapeutic approach for overcoming multidrug resistance in cancer: current status and future perspectives. Curr Cancer Drug Targets *13*, 326–346.
Binz, S.K., Lao, Y., Lowry, D.F., and Wold, M.S. (2003). The phosphorylation domain of the 32-kDa subunit of replication protein A (RPA) modulates RPA-DNA interactions. Evidence for an intersubunit interaction. J. Biol. Chem. *278*, 35584–35591.
Blackford, A.N., and Jackson, S.P. (2017). ATM, ATR, and DNA-PK: The Trinity at the Heart of the DNA Damage Response. Mol. Cell *66*, 801–817.
Blenn, C., Althaus, F.R., and Malanga, M. (2006). Poly(ADP-ribose) glycohydrolase silencing protects against H2O2-induced cell death. Biochem. J. *396*, 419–429.
Blenn, C., Wyrsch, P., Bader, J., Bollhalder, M., and Althaus, F.R. (2011a). Poly(ADP-ribose)glycohydrolase is an upstream regulator of Ca2+ fluxes in oxidative cell death. Cell. Mol. Life Sci. *68*, 1455–1466.
Blenn, C., Wyrsch, P., and Althaus, F.R. (2011b). The ups and downs of tannins as inhibitors of poly(ADP-ribose)glycohydrolase. Molecules *16*, 1854–1877.
Block, W.D., Yu, Y., and Lees-Miller, S.P. (2004). Phosphatidyl inositol 3-kinase-like serine/threonine protein kinases (PIKKs) are required for DNA damage-induced phosphorylation of the 32 kDa subunit of replication protein A at threonine 21. Nucleic Acids Res *32*, 997–1005.
Boehler, C., Gauthier, L.R., Mortusewicz, O., Biard, D.S., Saliou, J.-M., Bresson, A., Sanglier-Cianferani, S., Smith, S., Schreiber, V., Boussin, F., et al. (2011). Poly(ADP-ribose) polymerase 3 (PARP3), a newcomer in cellular response to DNA damage and mitotic progression. Proc. Natl. Acad. Sci. U.S.A. *108*, 2783–2788.
Bonfiglio, J.J., Colby, T., and Matic, I. (2017a). Mass spectrometry for serine ADP-ribosylation? Think o-glycosylation! Nucleic Acids Res. *45*, 6259–6264.
Bonfiglio, J.J., Fontana, P., Zhang, Q., Colby, T., Gibbs-Seymour, I., Atanassov, I., Bartlett, E., Zaja, R., Ahel, I., and Matic, I. (2017b). Serine ADP-Ribosylation Depends on HPF1. Mol. Cell *65*, 932–940.e6.
Bonicalzi, M.-E., Vodenicharov, M., Coulombe, M., Gagné, J.-P., and Poirier, G.G. (2003). Alteration of poly(ADP-ribose) glycohydrolase nucleocytoplasmic shuttling characteristics upon cleavage by apoptotic proteases. Biol. Cell *95*, 635–644.
Bonicalzi, M.-E., Haince, J.-F., Droit, A., and Poirier, G.G. (2005). Regulation of poly(ADP-ribose) metabolism by poly(ADP-ribose) glycohydrolase: where and when? Cell. Mol. Life Sci. *62*, 739–750.
Botta, D., and Jacobson, M.K. (2010). Identification of a regulatory segment of poly(ADP-ribose) glycohydrolase. Biochemistry *49*, 7674–7682.
Breslin, C., Hornyak, P., Ridley, A., Rulten, S.L., Hanzlikova, H., Oliver, A.W., and Caldecott, K.W. (2015). The XRCC1 phosphate-binding pocket binds poly (ADP-ribose) and is required for XRCC1 function. Nucleic Acids Res. *43*, 6934–6944.

Breslin, C., Mani, R.S., Fanta, M., Hoch, N., Weinfeld, M., and Caldecott, K.W. (2017). The Rev1 interacting region (RIR) motif in the scaffold protein XRCC1 mediates a low-affinity interaction with polynucleotide kinase/phosphatase (PNKP) during DNA single-strand break repair. J. Biol. Chem. *292*, 16024–16031.
Brewerton, S.C., Doré, A.S., Drake, A.C.B., Leuther, K.K., and Blundell, T.L. (2004). Structural analysis of DNA–PKcs: modelling of the repeat units and insights into the detailed molecular architecture. Journal of Structural Biology *145*, 295–306.
Britton, S., Froment, C., Frit, P., Monsarrat, B., Salles, B., and Calsou, P. (2009). Cell nonhomologous end joining capacity controls SAF-A phosphorylation by DNA-PK in response to DNA double-strand breaks inducers. Cell Cycle *8*, 3717–3722.
Brochu, G., Duchaine, C., Thibeault, L., Lagueux, J., Shah, G.M., and Poirier, G.G. (1994). Mode of action of poly(ADP-ribose) glycohydrolase. Biochim. Biophys. Acta *1219*, 342–350.
Brown, E.J., and Baltimore, D. (2000). ATR disruption leads to chromosomal fragmentation and early embryonic lethality. Genes Dev. *14*, 397–402.
Bruck, I., Dhingra, N., Martinez, M.P., and Kaplan, D.L. (2017). Dpb11 may function with RPA and DNA to initiate DNA replication. PLoS ONE *12*, e0177147.
Bryant, H.E., Schultz, N., Thomas, H.D., Parker, K.M., Flower, D., Lopez, E., Kyle, S., Meuth, M., Curtin, N.J., and Helleday, T. (2005). Specific killing of BRCA2-deficient tumours with inhibitors of poly(ADP-ribose) polymerase. Nature *434*, 913–917.
Burgess, R.C., Burman, B., Kruhlak, M.J., and Misteli, T. (2014). Activation of DNA damage response signaling by condensed chromatin. Cell Rep *9*, 1703–1717.
Bütepage, M., Eckei, L., Verheugd, P., and Lüscher, B. (2015). Intracellular Mono-ADP-Ribosylation in Signaling and Disease. Cells *4*, 569–595.
Byrne, A.B., McWhirter, R.D., Sekine, Y., Strittmatter, S.M., Miller, D.M., and Hammarlund, M. (2016). Inhibiting poly(ADP-ribosylation) improves axon regeneration. Elife *5*.
Cai, Z., Chehab, N.H., and Pavletich, N.P. (2009). Structure and activation mechanism of the CHK2 DNA damage checkpoint kinase. Mol. Cell *35*, 818–829.
Camicia, R., Bachmann, S.B., Winkler, H.C., Beer, M., Tinguely, M., Haralambieva, E., and Hassa, P.O. (2013). BAL1/ARTD9 represses the anti-proliferative and pro-apoptotic IFNγ-STAT1-IRF1-p53 axis in diffuse large B-cell lymphoma. J. Cell. Sci. *126*, 1969–1980.
Cayrou, C., Coulombe, P., and Méchali, M. (2010). Programming DNA replication origins and chromosome organization. Chromosome Res. *18*, 137–145.
Ceccaldi, R., Sarangi, P., and D'Andrea, A.D. (2016). The Fanconi anaemia pathway: new players and new functions. Nat. Rev. Mol. Cell Biol. *17*, 337–349.
Chan, D.W., Ye, R., Veillette, C.J., and Lees-Miller, S.P. (1999). DNA-dependent protein kinase phosphorylation sites in Ku 70/80 heterodimer. Biochemistry *38*, 1819–1828.
Chan, D.W., Chen, B.P.-C., Prithivirajsingh, S., Kurimasa, A., Story, M.D., Qin, J., and Chen, D.J. (2002). Autophosphorylation of the DNA-dependent protein kinase catalytic subunit is required for rejoining of DNA double-strand breaks. Genes Dev. *16*, 2333–2338.
Chang, H.H.Y., Pannunzio, N.R., Adachi, N., and Lieber, M.R. (2017). Non-homologous DNA end joining and alternative pathways to double-strand break repair. Nature Reviews Molecular Cell Biology *18*, nrm.2017.48.
Chang, P., Coughlin, M., and Mitchison, T.J. (2009). Interaction between Poly(ADP-ribose) and NuMA contributes to mitotic spindle pole assembly. Mol. Biol. Cell *20*, 4575–4585.
Charrier, S., Ferrand, M., Zerbato, M., Précigout, G., Viornery, A., Bucher-Laurent, S., Benkhelifa-Ziyyat, S., Merten, O.-W., Perea, J., and Galy, A. (2010). Quantification of lentiviral vector copy numbers in individual hematopoietic colony-forming cells shows vector dose-dependent effects on the frequency and level of transduction. Gene Therapy *18*, 479–487.
Charron, G., Li, M.M.H., MacDonald, M.R., and Hang, H.C. (2013). Prenylome profiling reveals S-farnesylation is crucial for membrane targeting and antiviral activity of ZAP long-isoform. Proc. Natl. Acad. Sci. U.S.A. *110*, 11085–11090.
Chaudhuri, A.R., and Nussenzweig, A. (2017). The multifaceted roles of PARP1 in DNA repair and chromatin remodelling. Nature Reviews Molecular Cell Biology *18*, nrm.2017.53.
Chaudhury, I., Sareen, A., Raghunandan, M., and Sobeck, A. (2013). FANCD2 regulates BLM complex functions independently of FANCI to promote replication fork recovery. Nucleic Acids Res. *41*, 6444–6459.
Chen, B.P.C., Chan, D.W., Kobayashi, J., Burma, S., Asaithamby, A., Morotomi-Yano, K., Botvinick, E., Qin, J., and Chen, D.J. (2005). Cell cycle dependence of DNA-dependent protein kinase phosphorylation in response to DNA double strand breaks. J. Biol. Chem. *280*, 14709–14715.

Chen, D., Vollmar, M., Rossi, M.N., Phillips, C., Kraehenbuehl, R., Slade, D., Mehrotra, P.V., von Delft, F., Crosthwaite, S.K., Gileadi, O., et al. (2011). Identification of macrodomain proteins as novel O-acetyl-ADP-ribose deacetylases. J. Biol. Chem. *286*, 13261–13271.
Chen, L.-G., Huang, W.-T., Lee, L.-T., and Wang, C.-C. (2009). Ellagitannins from Terminalia calamansanai induced apoptosis in HL-60 cells. Toxicol In Vitro *23*, 603–609.
Chen, S., Xu, Y., Zhang, K., Wang, X., Sun, J., Gao, G., and Liu, Y. (2012). Structure of N-terminal domain of ZAP indicates how a zinc-finger protein recognizes complex RNA. Nat. Struct. Mol. Biol. *19*, 430–435.
Chi, N.W., and Lodish, H.F. (2000). Tankyrase is a golgi-associated mitogen-activated protein kinase substrate that interacts with IRAP in GLUT4 vesicles. J. Biol. Chem. *275*, 38437–38444.
Chiker, S., Pennaneach, V., Loew, D., Dingli, F., Biard, D., Cordelières, F.P., Gemble, S., Vacher, S., Bieche, I., Hall, J., et al. (2015). Cdk5 promotes DNA replication stress checkpoint activation through RPA-32 phosphorylation, and impacts on metastasis free survival in breast cancer patients. Cell Cycle *14*, 3066–3078.
Cho, S.H., Goenka, S., Henttinen, T., Gudapati, P., Reinikainen, A., Eischen, C.M., Lahesmaa, R., and Boothby, M. (2009). PARP-14, a member of the B aggressive lymphoma family, transduces survival signals in primary B cells. Blood *113*, 2416–2425.
Choi, Y.H., and Yu, A.-M. (2014). ABC transporters in multidrug resistance and pharmacokinetics, and strategies for drug development. Curr. Pharm. Des. *20*, 793–807.
Chou, D.M., Adamson, B., Dephoure, N.E., Tan, X., Nottke, A.C., Hurov, K.E., Gygi, S.P., Colaiácovo, M.P., and Elledge, S.J. (2010). A chromatin localization screen reveals poly (ADP ribose)-regulated recruitment of the repressive polycomb and NuRD complexes to sites of DNA damage. Proc. Natl. Acad. Sci. U.S.A. *107*, 18475–18480.
Chung, H.T., and Joe, Y. (2014). Antagonistic crosstalk between SIRT1, PARP-1, and -2 in the regulation of chronic inflammation associated with aging and metabolic diseases. Integr Med Res *3*, 198–203.
Ciccarone, F., Zampieri, M., and Caiafa, P. (2017a). PARP1 orchestrates epigenetic events setting up chromatin domains. Semin. Cell Dev. Biol. *63*, 123–134.
Ciccarone, F., Vegliante, R., Di Leo, L., and Ciriolo, M.R. (2017b). The TCA cycle as a bridge between oncometabolism and DNA transactions in cancer. Semin. Cancer Biol.
Ciccia, A., and Elledge, S.J. (2010). The DNA damage response: making it safe to play with knives. Mol. Cell *40*, 179–204.
Ciccia, A., Nimonkar, A.V., Hu, Y., Hajdu, I., Achar, Y.J., Izhar, L., Petit, S.A., Adamson, B., Yoon, J.C., Kowalczykowski, S.C., et al. (2012). Polyubiquitinated PCNA recruits the ZRANB3 translocase to maintain genomic integrity after replication stress. Mol. Cell *47*, 396–409.
Cohausz, O., and Althaus, F.R. (2009). Role of PARP-1 and PARP-2 in the expression of apoptosis-regulating genes in HeLa cells. Cell Biol. Toxicol. *25*, 379–391.
Cohen-Armon, M., Visochek, L., Rozensal, D., Kalal, A., Geistrikh, I., Klein, R., Bendetz-Nezer, S., Yao, Z., and Seger, R. (2007). DNA-independent PARP-1 activation by phosphorylated ERK2 increases Elk1 activity: a link to histone acetylation. Mol. Cell *25*, 297–308.
Cole, J., Morris, P., Dickman, M.J., and Dockrell, D.H. (2016). The therapeutic potential of epigenetic manipulation during infectious diseases. Pharmacol. Ther. *167*, 85–99.
Constantinou, A., Tarsounas, M., Karow, J.K., Brosh, R.M., Bohr, V.A., Hickson, I.D., and West, S.C. (2000). Werner's syndrome protein (WRN) migrates Holliday junctions and co-localizes with RPA upon replication arrest. EMBO Rep. *1*, 80–84.
Correia, M., Perestrelo, T., Rodrigues, A.S., Ribeiro, M.F., Pereira, S.L., Sousa, M.I., and Ramalho-Santos, J. (2017). Sirtuins in metabolism, stemness and differentiation. Biochim. Biophys. Acta *1861*, 3444–3455.
Cortes, U., Tong, W.-M., Coyle, D.L., Meyer-Ficca, M.L., Meyer, R.G., Petrilli, V., Herceg, Z., Jacobson, E.L., Jacobson, M.K., and Wang, Z.-Q. (2004). Depletion of the 110-kilodalton isoform of poly(ADP-ribose) glycohydrolase increases sensitivity to genotoxic and endotoxic stress in mice. Mol. Cell. Biol. *24*, 7163–7178.
Costa, A., Hood, I.V., and Berger, J.M. (2013). Mechanisms for initiating cellular DNA replication. Annu. Rev. Biochem. *82*, 25–54.
Couto, C.A.-M., Wang, H.-Y., Green, J.C.A., Kiely, R., Siddaway, R., Borer, C., Pears, C.J., and Lakin, N.D. (2011). PARP regulates nonhomologous end joining through retention of Ku at double-strand breaks. J. Cell Biol. *194*, 367–375.
Cozzi, A., Cipriani, G., Fossati, S., Faraco, G., Formentini, L., Min, W., Cortes, U., Wang, Z.-Q., Moroni, F., and Chiarugi, A. (2006). Poly(ADP-ribose) accumulation and enhancement of postischemic brain damage in 110-kDa poly(ADP-ribose) glycohydrolase null mice. J. Cereb. Blood Flow Metab. *26*, 684–695.
Croteau, D.L., Popuri, V., Opresko, P.L., and Bohr, V.A. (2014). Human RecQ helicases in DNA repair, recombination, and replication. Annu. Rev. Biochem. *83*, 519–552.

Cuya, S.M., Bjornsti, M.-A., and van Waardenburg, R.C.A.M. (2017). DNA topoisomerase-targeting chemotherapeutics: what's new? Cancer Chemother. Pharmacol. *80*, 1–14.
Dai, X., Rulten, S.L., You, C., Caldecott, K.W., and Wang, Y. (2015). Identification and Functional Characterizations of N-Terminal α-N-Methylation and Phosphorylation of Serine 461 in Human Poly(ADP-ribose) Polymerase 3. J. Proteome Res. *14*, 2575–2582.
Daigaku, Y., Davies, A.A., and Ulrich, H.D. (2010). Ubiquitin-dependent DNA damage bypass is separable from genome replication. Nature *465*, 951–955.
Dantzer, F., Schreiber, V., Niedergang, C., Trucco, C., Flatter, E., De La Rubia, G., Oliver, J., Rolli, V., Ménissier-de Murcia, J., and de Murcia, G. (1999). Involvement of poly(ADP-ribose) polymerase in base excision repair. Biochimie *81*, 69–75.
Dantzer, F., de La Rubia, G., Ménissier-De Murcia, J., Hostomsky, Z., de Murcia, G., and Schreiber, V. (2000). Base excision repair is impaired in mammalian cells lacking Poly(ADP-ribose) polymerase-1. Biochemistry *39*, 7559–7569.
DaRosa, P.A., Wang, Z., Jiang, X., Pruneda, J.N., Cong, F., Klevit, R.E., and Xu, W. (2015). Allosteric activation of the RNF146 ubiquitin ligase by a poly(ADP-ribosyl)ation signal. Nature *517*, 223–226.
DaRosa, P.A., Ovchinnikov, S., Xu, W., and Klevit, R.E. (2016). Structural insights into SAM domain-mediated tankyrase oligomerization. Protein Sci. *25*, 1744–1752.
Das, A.T., Tenenbaum, L., and Berkhout, B. (2016a). Tet-On Systems For Doxycycline-inducible Gene Expression. Curr Gene Ther *16*, 156–167.
Das, B.B., Antony, S., Gupta, S., Dexheimer, T.S., Redon, C.E., Garfield, S., Shiloh, Y., and Pommier, Y. (2009). Optimal function of the DNA repair enzyme TDP1 requires its phosphorylation by ATM and/or DNA-PK. EMBO J. *28*, 3667–3680.
Das, B.B., Huang, S.N., Murai, J., Rehman, I., Amé, J.-C., Sengupta, S., Das, S.K., Majumdar, P., Zhang, H., Biard, D., et al. (2014). PARP1-TDP1 coupling for the repair of topoisomerase I-induced DNA damage. Nucleic Acids Res. *42*, 4435–4449.
Das, S.K., Rehman, I., Ghosh, A., Sengupta, S., Majumdar, P., Jana, B., and Das, B.B. (2016b). Poly(ADP-ribose) polymers regulate DNA topoisomerase I (Top1) nuclear dynamics and camptothecin sensitivity in living cells. Nucleic Acids Res. *44*, 8363–8375.
Daugherty, M.D., Young, J.M., Kerns, J.A., and Malik, H.S. (2014). Rapid evolution of PARP genes suggests a broad role for ADP-ribosylation in host-virus conflicts. PLoS Genet. *10*, e1004403.
David, K.K., Andrabi, S.A., Dawson, T.M., and Dawson, V.L. (2009). Parthanatos, a messenger of death. Front Biosci (Landmark Ed) *14*, 1116–1128.
Davidovic, L., Vodenicharov, M., Affar, E.B., and Poirier, G.G. (2001). Importance of poly(ADP-ribose) glycohydrolase in the control of poly(ADP-ribose) metabolism. Exp. Cell Res. *268*, 7–13.
Davis, A.J., Lee, K.-J., and Chen, D.J. (2013). The N-terminal region of the DNA-dependent protein kinase catalytic subunit is required for its DNA double-stranded break-mediated activation. J. Biol. Chem. *288*, 7037–7046.
Davis, A.J., Chen, B.P.C., and Chen, D.J. (2014). DNA-PK: a dynamic enzyme in a versatile DSB repair pathway. DNA Repair (Amst.) *17*, 21–29.
Dawicki-McKenna, J.M., Langelier, M.-F., DeNizio, J.E., Riccio, A.A., Cao, C.D., Karch, K.R., McCauley, M., Steffen, J.D., Black, B.E., and Pascal, J.M. (2015). PARP-1 Activation Requires Local Unfolding of an Autoinhibitory Domain. Mol. Cell *60*, 755–768.
Day, T.A., Layer, J.V., Cleary, J.P., Guha, S., Stevenson, K.E., Tivey, T., Kim, S., Schinzel, A.C., Izzo, F., Doench, J., et al. (2017). PARP3 is a promoter of chromosomal rearrangements and limits G4 DNA. Nat Commun *8*, 15110.
Densham, R.M., and Morris, J.R. (2017). The BRCA1 Ubiquitin ligase function sets a new trend for remodelling in DNA repair. Nucleus *8*, 116–125.
Desai, S.D., Liu, L.F., Vazquez-Abad, D., and D'Arpa, P. (1997). Ubiquitin-dependent destruction of topoisomerase I is stimulated by the antitumor drug camptothecin. J. Biol. Chem. *272*, 24159–24164.
Dewar, J.M., and Walter, J.C. (2017). Mechanisms of DNA replication termination. Nat. Rev. Mol. Cell Biol. *18*, 507–516.
Di Giammartino, D.C., Shi, Y., and Manley, J.L. (2013). PARP1 represses PAP and inhibits polyadenylation during heat shock. Mol. Cell *49*, 7–17.
Diderich, K., Alanazi, M., and Hoeijmakers, J.H.J. (2011). Premature aging and cancer in nucleotide excision repair-disorders. DNA Repair (Amst.) *10*, 772–780.
Dobzhansky, T. (1946). Genetics of natural populations; recombination and variability in populations of Drosophila pseudoobscura. Genetics *31*, 269–290.

D'Onofrio, G., Tramontano, F., Dorio, A.S., Muzi, A., Maselli, V., Fulgione, D., Graziani, G., Malanga, M., and Quesada, P. (2011). Poly(ADP-ribose) polymerase signaling of topoisomerase 1-dependent DNA damage in carcinoma cells. Biochem. Pharmacol. *81*, 194–202.
Drew, Y., Ledermann, J., Hall, G., Rea, D., Glasspool, R., Highley, M., Jayson, G., Sludden, J., Murray, J., Jamieson, D., et al. (2016). Phase 2 multicentre trial investigating intermittent and continuous dosing schedules of the poly(ADP-ribose) polymerase inhibitor rucaparib in germline BRCA mutation carriers with advanced ovarian and breast cancer. Br. J. Cancer *114*, 723–730.
Dungrawala, H., Rose, K.L., Bhat, K.P., Mohni, K.N., Glick, G.G., Couch, F.B., and Cortez, D. (2015). The Replication Checkpoint Prevents Two Types of Fork Collapse without Regulating Replisome Stability. Mol. Cell *59*, 998–1010.
Dunstan, M.S., Barkauskaite, E., Lafite, P., Knezevic, C.E., Brassington, A., Ahel, M., Hergenrother, P.J., Leys, D., and Ahel, I. (2012). Structure and mechanism of a canonical poly(ADP-ribose) glycohydrolase. Nat Commun *3*, 878.
Durkacz, B.W., Omidiji, O., Gray, D.A., and Shall, S. (1980). (ADP-ribose)n participates in DNA excision repair. Nature *283*, 593–596.
Eckei, L., Krieg, S., Bütepage, M., Lehmann, A., Gross, A., Lippok, B., Grimm, A.R., Kümmerer, B.M., Rossetti, G., Lüscher, B., et al. (2017). The conserved macrodomains of the non-structural proteins of Chikungunya virus and other pathogenic positive strand RNA viruses function as mono-ADP-ribosylhydrolases. Sci Rep *7*, 41746.
Edifizi, D., and Schumacher, B. (2015). Genome Instability in Development and Aging: Insights from Nucleotide Excision Repair in Humans, Mice, and Worms. Biomolecules *5*, 1855–1869.
Edinger, A.L., and Thompson, C.B. (2004). Death by design: apoptosis, necrosis and autophagy. Curr. Opin. Cell Biol. *16*, 663–669.
Edwards, S.L., Brough, R., Lord, C.J., Natrajan, R., Vatcheva, R., Levine, D.A., Boyd, J., Reis-Filho, J.S., and Ashworth, A. (2008). Resistance to therapy caused by intragenic deletion in BRCA2. Nature *451*, 1111–1115.
El-Khamisy, S.F., Masutani, M., Suzuki, H., and Caldecott, K.W. (2003). A requirement for PARP-1 for the assembly or stability of XRCC1 nuclear foci at sites of oxidative DNA damage. Nucleic Acids Res. *31*, 5526–5533.
Espinosa, L., Margalef, P., and Bigas, A. (2015). Non-conventional functions for NF-κB members: the dark side of NF-κB. Oncogene *34*, 2279–2287.
Eustermann, S., Brockmann, C., Mehrotra, P.V., Yang, J.-C., Loakes, D., West, S.C., Ahel, I., and Neuhaus, D. (2010). Solution structures of the two PBZ domains from human APLF and their interaction with poly(ADP-ribose). Nat. Struct. Mol. Biol. *17*, 241–243.
Ezkurdia, I., Juan, D., Rodriguez, J.M., Frankish, A., Diekhans, M., Harrow, J., Vazquez, J., Valencia, A., and Tress, M.L. (2014). Multiple evidence strands suggest that there may be as few as 19 000 human protein-coding genes. Hum Mol Genet *23*, 5866–5878.
Falsig, J., Christiansen, S.H., Feuerhahn, S., Bürkle, A., Oei, S.L., Keil, C., and Leist, M. (2004). Poly(ADP-ribose) glycohydrolase as a target for neuroprotective intervention: assessment of currently available pharmacological tools. Eur. J. Pharmacol. *497*, 7–16.
Farmer, H., McCabe, N., Lord, C.J., Tutt, A.N.J., Johnson, D.A., Richardson, T.B., Santarosa, M., Dillon, K.J., Hickson, I., Knights, C., et al. (2005). Targeting the DNA repair defect in BRCA mutant cells as a therapeutic strategy. Nature *434*, 917–921.
Fathers, C., Drayton, R.M., Solovieva, S., and Bryant, H.E. (2012). Inhibition of poly(ADP-ribose) glycohydrolase (PARG) specifically kills BRCA2-deficient tumor cells. Cell Cycle *11*, 990–997.
Fauzee, N.J.S., Pan, J., and Wang, Y. (2010). PARP and PARG inhibitors--new therapeutic targets in cancer treatment. Pathol. Oncol. Res. *16*, 469–478.
Federico, M.B., Campodónico, P., Paviolo, N.S., and Gottifredi, V. (2017). Beyond interstrand crosslinks repair: contribution of FANCD2 and other Fanconi Anemia proteins to the replication of DNA. Mutat. Res.
Feijs, K.L.H., Verheugd, P., and Lüscher, B. (2013a). Expanding functions of intracellular resident mono-ADP-ribosylation in cell physiology. FEBS J. *280*, 3519–3529.
Feijs, K.L.H., Forst, A.H., Verheugd, P., and Lüscher, B. (2013b). Macrodomain-containing proteins: regulating new intracellular functions of mono(ADP-ribosyl)ation. Nat. Rev. Mol. Cell Biol. *14*, 443–451.
Feldman, J.L., Dittenhafer-Reed, K.E., and Denu, J.M. (2012). Sirtuin catalysis and regulation. J. Biol. Chem. *287*, 42419–42427.
Feng, X., and Koh, D.W. (2013). Roles of poly(ADP-ribose) glycohydrolase in DNA damage and apoptosis. Int Rev Cell Mol Biol *304*, 227–281.
Feng, B., Ma, S., Chen, S., Zhu, N., Zhang, S., Yu, B., Yu, Y., Le, B., Chen, X., Dinesh-Kumar, S.P., et al. (2016). PARylation of the forkhead-associated domain protein DAWDLE regulates plant immunity. EMBO Rep. *17*, 1799–1813.

Finch, K.E., Knezevic, C.E., Nottbohm, A.C., Partlow, K.C., and Hergenrother, P.J. (2012). Selective small molecule inhibition of poly(ADP-ribose) glycohydrolase (PARG). ACS Chem. Biol. *7*, 563–570.
Fischer, J.M.F., Popp, O., Gebhard, D., Veith, S., Fischbach, A., Beneke, S., Leitenstorfer, A., Bergemann, J., Scheffner, M., Ferrando-May, E., et al. (2014). Poly(ADP-ribose)-mediated interplay of XPA and PARP1 leads to reciprocal regulation of protein function. FEBS J. *281*, 3625–3641.
Fisher, A.E.O., Hochegger, H., Takeda, S., and Caldecott, K.W. (2007). Poly(ADP-ribose) polymerase 1 accelerates single-strand break repair in concert with poly(ADP-ribose) glycohydrolase. Mol. Cell. Biol. *27*, 5597–5605.
Flohr, C., Bürkle, A., Radicella, J.P., and Epe, B. (2003). Poly(ADP-ribosyl)ation accelerates DNA repair in a pathway dependent on Cockayne syndrome B protein. Nucleic Acids Res. *31*, 5332–5337.
Fong, P.C., Boss, D.S., Yap, T.A., Tutt, A., Wu, P., Mergui-Roelvink, M., Mortimer, P., Swaisland, H., Lau, A., O'Connor, M.J., et al. (2009). Inhibition of poly(ADP-ribose) polymerase in tumors from BRCA mutation carriers. N. Engl. J. Med. *361*, 123–134.
Fong, P.C., Yap, T.A., Boss, D.S., Carden, C.P., Mergui-Roelvink, M., Gourley, C., De Greve, J., Lubinski, J., Shanley, S., Messiou, C., et al. (2010). Poly(ADP)-ribose polymerase inhibition: frequent durable responses in BRCA carrier ovarian cancer correlating with platinum-free interval. J. Clin. Oncol. *28*, 2512–2519.
Fontana, P., Bonfiglio, J.J., Palazzo, L., Bartlett, E., Matic, I., and Ahel, I. (2017). Serine ADP-ribosylation reversal by the hydrolase ARH3. Elife *6*.
Formentini, L., Arapistas, P., Pittelli, M., Jacomelli, M., Pitozzi, V., Menichetti, S., Romani, A., Giovannelli, L., Moroni, F., and Chiarugi, A. (2008). Mono-galloyl glucose derivatives are potent poly(ADP-ribose) glycohydrolase (PARG) inhibitors and partially reduce PARP-1-dependent cell death. Br. J. Pharmacol. *155*, 1235–1249.
Fortini, P., and Dogliotti, E. (2007). Base damage and single-strand break repair: mechanisms and functional significance of short- and long-patch repair subpathways. DNA Repair (Amst.) *6*, 398–409.
Frigola, J., He, J., Kinkelin, K., Pye, V.E., Renault, L., Douglas, M.E., Remus, D., Cherepanov, P., Costa, A., and Diffley, J.F.X. (2017). Cdt1 stabilizes an open MCM ring for helicase loading. Nat Commun *8*, 15720.
Fujihara, H., Ogino, H., Maeda, D., Shirai, H., Nozaki, T., Kamada, N., Jishage, K., Tanuma, S., Takato, T., Ochiya, T., et al. (2009). Poly(ADP-ribose) Glycohydrolase deficiency sensitizes mouse ES cells to DNA damaging agents. Curr Cancer Drug Targets *9*, 953–962.
Gadducci, A., and Guerrieri, M.E. (2017). PARP inhibitors alone and in combination with other biological agents in homologous recombination deficient epithelial ovarian cancer: From the basic research to the clinic. Crit. Rev. Oncol. Hematol. *114*, 153–165.
Gagné, J.-P., Moreel, X., Gagné, P., Labelle, Y., Droit, A., Chevalier-Paré, M., Bourassa, S., McDonald, D., Hendzel, M.J., Prigent, C., et al. (2009). Proteomic investigation of phosphorylation sites in poly(ADP-ribose) polymerase-1 and poly(ADP-ribose) glycohydrolase. J. Proteome Res. *8*, 1014–1029.
Galluzzi, L., Vanden Berghe, T., Vanlangenakker, N., Buettner, S., Eisenberg, T., Vandenabeele, P., Madeo, F., and Kroemer, G. (2011). Programmed necrosis from molecules to health and disease. Int Rev Cell Mol Biol *289*, 1–35.
Galluzzi, L., Kepp, O., Trojel-Hansen, C., and Kroemer, G. (2012). Mitochondrial control of cellular life, stress, and death. Circ. Res. *111*, 1198–1207.
Gao, H., Coyle, D.L., Meyer-Ficca, M.L., Meyer, R.G., Jacobson, E.L., Wang, Z.-Q., and Jacobson, M.K. (2007). Altered poly(ADP-ribose) metabolism impairs cellular responses to genotoxic stress in a hypomorphic mutant of poly(ADP-ribose) glycohydrolase. Exp. Cell Res. *313*, 984–996.
Gao, Y., Li, C., Wei, L., Teng, Y., Nakajima, S., Chen, X., Xu, J., Legar, B., Ma, H., Spagnol, S.T., et al. (2017). SSRP1 Cooperates with PARP and XRCC1 to Facilitate Single-Strand DNA Break Repair by Chromatin Priming. Cancer Res. *77*, 2674–2685.
Garcia-Higuera, I., Taniguchi, T., Ganesan, S., Meyn, M.S., Timmers, C., Hejna, J., Grompe, M., and D'Andrea, A.D. (2001). Interaction of the Fanconi anemia proteins and BRCA1 in a common pathway. Mol. Cell *7*, 249–262.
García-Muse, T., and Aguilera, A. (2016). Transcription-replication conflicts: how they occur and how they are resolved. Nat. Rev. Mol. Cell Biol. *17*, 553–563.
Gayon, J. (2016). From Mendel to epigenetics: History of genetics. Comptes Rendus Biologies *339*, 225–230.
Ghodgaonkar, M.M., Zacal, N., Kassam, S., Rainbow, A.J., and Shah, G.M. (2008). Depletion of poly(ADP-ribose) polymerase-1 reduces host cell reactivation of a UV-damaged adenovirus-encoded reporter gene in human dermal fibroblasts. DNA Repair (Amst.) *7*, 617–632.
Gibbs-Seymour, I., Fontana, P., Rack, J.G.M., and Ahel, I. (2016). HPF1/C4orf27 Is a PARP-1-Interacting Protein that Regulates PARP-1 ADP-Ribosylation Activity. Mol. Cell *62*, 432–442.
Gibson, B.A., and Kraus, W.L. (2012a). New insights into the molecular and cellular functions of poly(ADP-ribose) and PARPs. Nat. Rev. Mol. Cell Biol. *13*, 411–424.

Gibson, B.A., and Kraus, W.L. (2012b). New insights into the molecular and cellular functions of poly(ADP-ribose) and PARPs. Nature Reviews Molecular Cell Biology *13*, nrm3376.
Goenka, S., and Boothby, M. (2006). Selective potentiation of Stat-dependent gene expression by collaborator of Stat6 (CoaSt6), a transcriptional cofactor. Proc. Natl. Acad. Sci. U.S.A. *103*, 4210–4215.
Goenka, S., Cho, S.H., and Boothby, M. (2007). Collaborator of Stat6 (CoaSt6)-associated poly(ADP-ribose) polymerase activity modulates Stat6-dependent gene transcription. J. Biol. Chem. *282*, 18732–18739.
Goodarzi, A.A., Yu, Y., Riballo, E., Douglas, P., Walker, S.A., Ye, R., Härer, C., Marchetti, C., Morrice, N., Jeggo, P.A., et al. (2006). DNA-PK autophosphorylation facilitates Artemis endonuclease activity. EMBO J. *25*, 3880–3889.
Goodier, J.L., Pereira, G.C., Cheung, L.E., Rose, R.J., and Kazazian, H.H. (2015). The Broad-Spectrum Antiviral Protein ZAP Restricts Human Retrotransposition. PLoS Genet. *11*, e1005252.
Gottschalk, A.J., Timinszky, G., Kong, S.E., Jin, J., Cai, Y., Swanson, S.K., Washburn, M.P., Florens, L., Ladurner, A.G., Conaway, J.W., et al. (2009). Poly(ADP-ribosyl)ation directs recruitment and activation of an ATP-dependent chromatin remodeler. Proc. Natl. Acad. Sci. U.S.A. *106*, 13770–13774.
Gravells, P., Grant, E., Smith, K.M., James, D.I., and Bryant, H.E. (2017). Specific killing of DNA damage-response deficient cells with inhibitors of poly(ADP-ribose) glycohydrolase. DNA Repair (Amst.) *52*, 81–91.
Greiss, S., and Gartner, A. (2009). Sirtuin/Sir2 phylogeny, evolutionary considerations and structural conservation. Mol. Cells *28*, 407–415.
Groisman, R., Kuraoka, I., Chevallier, O., Gaye, N., Magnaldo, T., Tanaka, K., Kisselev, A.F., Harel-Bellan, A., and Nakatani, Y. (2006). CSA-dependent degradation of CSB by the ubiquitin-proteasome pathway establishes a link between complementation factors of the Cockayne syndrome. Genes Dev. *20*, 1429–1434.
Guettler, S. (2016). AXIN Shapes Tankyrase ARChitecture. Structure *24*, 1625–1627.
Guilbaud, G., Rappailles, A., Baker, A., Chen, C.-L., Arneodo, A., Goldar, A., d'Aubenton-Carafa, Y., Thermes, C., Audit, B., and Hyrien, O. (2011). Evidence for sequential and increasing activation of replication origins along replication timing gradients in the human genome. PLoS Comput. Biol. *7*, e1002322.
Guillot, C., Hall, J., Herceg, Z., Merle, P., and Chemin, I. (2014). Update on hepatocellular carcinoma breakthroughs: poly(ADP-ribose) polymerase inhibitors as a promising therapeutic strategy. Clin Res Hepatol Gastroenterol *38*, 137–142.
Gupte, R., Liu, Z., and Kraus, W.L. (2017). PARPs and ADP-ribosylation: recent advances linking molecular functions to biological outcomes. Genes Dev. *31*, 101–126.
Haince, J.-F., Kozlov, S., Dawson, V.L., Dawson, T.M., Hendzel, M.J., Lavin, M.F., and Poirier, G.G. (2007). Ataxia telangiectasia mutated (ATM) signaling network is modulated by a novel poly(ADP-ribose)-dependent pathway in the early response to DNA-damaging agents. J. Biol. Chem. *282*, 16441–16453.
Haince, J.-F., McDonald, D., Rodrigue, A., Déry, U., Masson, J.-Y., Hendzel, M.J., and Poirier, G.G. (2008). PARP1-dependent kinetics of recruitment of MRE11 and NBS1 proteins to multiple DNA damage sites. J. Biol. Chem. *283*, 1197–1208.
Hamamoto, R., and Nakamura, Y. (2016). Dysregulation of protein methyltransferases in human cancer: An emerging target class for anticancer therapy. Cancer Sci. *107*, 377–384.
Hanzlikova, H., Gittens, W., Krejcikova, K., Zeng, Z., and Caldecott, K.W. (2017). Overlapping roles for PARP1 and PARP2 in the recruitment of endogenous XRCC1 and PNKP into oxidized chromatin. Nucleic Acids Res. *45*, 2546–2557.
Happel, N., and Doenecke, D. (2009). Histone H1 and its isoforms: contribution to chromatin structure and function. Gene *431*, 1–12.
Harnor, S.J., Brennan, A., and Cano, C. (2017). Targeting DNA-Dependent Protein Kinase for Cancer Therapy. ChemMedChem *12*, 895–900.
Hassa, P.O., and Hottiger, M.O. (2005). An epigenetic code for DNA damage repair pathways? Biochem. Cell Biol. *83*, 270–285.
Hassler, M., Jankevicius, G., and Ladurner, A.G. (2011). PARG: a macrodomain in disguise. Structure *19*, 1351–1353.
Havens, C.G., and Walter, J.C. (2009). Docking of a specialized PIP box onto chromatin-bound PCNA creates a degron for the ubiquitin ligase CRL4Cdt2. Mol Cell *35*, 93–104.
Hayakawa, S., Shiratori, S., Yamato, H., Kameyama, T., Kitatsuji, C., Kashigi, F., Goto, S., Kameoka, S., Fujikura, D., Yamada, T., et al. (2011). ZAPS is a potent stimulator of signaling mediated by the RNA helicase RIG-I during antiviral responses. Nat. Immunol. *12*, 37–44.
He, F., Tsuda, K., Takahashi, M., Kuwasako, K., Terada, T., Shirouzu, M., Watanabe, S., Kigawa, T., Kobayashi, N., Güntert, P., et al. (2012). Structural insight into the interaction of ADP-ribose with the PARP WWE domains. FEBS Lett. *586*, 3858–3864.

Heller, R.C., and Marians, K.J. (2006). Replication fork reactivation downstream of a blocked nascent leading strand. Nature *439*, 557–562.
Henneman, L., van Miltenburg, M.H., Michalak, E.M., Braumuller, T.M., Jaspers, J.E., Drenth, A.P., de Korte-Grimmerink, R., Gogola, E., Szuhai, K., Schlicker, A., et al. (2015). Selective resistance to the PARP inhibitor olaparib in a mouse model for BRCA1-deficient metaplastic breast cancer. Proc. Natl. Acad. Sci. U.S.A. *112*, 8409–8414.
Heo, J., Li, J., Summerlin, M., Hays, A., Katyal, S., McKinnon, P.J., Nitiss, K.C., Nitiss, J.L., and Hanakahi, L.A. (2015). TDP1 promotes assembly of non-homologous end joining protein complexes on DNA. DNA Repair (Amst) *30*, 28–37.
Higgins, N.P., Kato, K., and Strauss, B. (1976). A model for replication repair in mammalian cells. J. Mol. Biol. *101*, 417–425.
Hinz, J.M., and Czaja, W. (2015). Facilitation of base excision repair by chromatin remodeling. DNA Repair (Amst.) *36*, 91–97.
Hochegger, H., Dejsuphong, D., Fukushima, T., Morrison, C., Sonoda, E., Schreiber, V., Zhao, G.Y., Saberi, A., Masutani, M., Adachi, N., et al. (2006). Parp-1 protects homologous recombination from interference by Ku and Ligase IV in vertebrate cells. EMBO J. *25*, 1305–1314.
Hoeijmakers, J.H. (2001). DNA repair mechanisms. Maturitas *38*, 17-22-23.
Hoeijmakers, J.H.J. (2009). DNA damage, aging, and cancer. N. Engl. J. Med. *361*, 1475–1485.
Holbourn, K.P., Sutton, J.M., Evans, H.R., Shone, C.C., and Acharya, K.R. (2005). Molecular recognition of an ADP-ribosylating Clostridium botulinum C3 exoenzyme by RalA GTPase. Proc. Natl. Acad. Sci. U.S.A. *102*, 5357–5362.
Holbourn, K.P., Shone, C.C., and Acharya, K.R. (2006). A family of killer toxins. Exploring the mechanism of ADP-ribosylating toxins. FEBS J. *273*, 4579–4593.
Hoppe, B.S., Jensen, R.B., and Kirchgessner, C.U. (2000). Complementation of the radiosensitive M059J cell line. Radiat. Res. *153*, 125–130.
Hottiger, M.O., Hassa, P.O., Lüscher, B., Schüler, H., and Koch-Nolte, F. (2010). Toward a unified nomenclature for mammalian ADP-ribosyltransferases. Trends Biochem. Sci. *35*, 208–219.
Hu, Y., Petit, S.A., Ficarro, S.B., Toomire, K.J., Xie, A., Lim, E., Cao, S.A., Park, E., Eck, M.J., Scully, R., et al. (2014). PARP1-driven poly-ADP-ribosylation regulates BRCA1 function in homologous recombination-mediated DNA repair. Cancer Discov *4*, 1430–1447.
Huambachano, O., Herrera, F., Rancourt, A., and Satoh, M.S. (2011). Double-stranded DNA binding domain of poly(ADP-ribose) polymerase-1 and molecular insight into the regulation of its activity. J. Biol. Chem. *286*, 7149–7160.
Huang, J., Huen, M.S.Y., Kim, H., Leung, C.C.Y., Glover, J.N.M., Yu, X., and Chen, J. (2009). RAD18 transmits DNA damage signalling to elicit homologous recombination repair. Nat. Cell Biol. *11*, 592–603.
Huang, J.Y., Wang, K., Vermehren-Schmaedick, A., Adelman, J.P., and Cohen, M.S. (2016). PARP6 is a Regulator of Hippocampal Dendritic Morphogenesis. Sci Rep *6*, 18512.
Huang, S.-Y.N., Williams, J.S., Arana, M.E., Kunkel, T.A., and Pommier, Y. (2017). Topoisomerase I-mediated cleavage at unrepaired ribonucleotides generates DNA double-strand breaks. EMBO J. *36*, 361–373.
Hyun, K., Jeon, J., Park, K., and Kim, J. (2017). Writing, erasing and reading histone lysine methylations. Exp. Mol. Med. *49*, e324.
Iansante, V., Choy, P.M., Fung, S.W., Liu, Y., Chai, J.-G., Dyson, J., Del Rio, A., D'Santos, C., Williams, R., Chokshi, S., et al. (2015). PARP14 promotes the Warburg effect in hepatocellular carcinoma by inhibiting JNK1-dependent PKM2 phosphorylation and activation. Nat Commun *6*, 7882.
Iliakis, G., Murmann, T., and Soni, A. (2015). Alternative end-joining repair pathways are the ultimate backup for abrogated classical non-homologous end-joining and homologous recombination repair: Implications for the formation of chromosome translocations. Mutat Res Genet Toxicol Environ Mutagen *793*, 166–175.
Imai, S., and Guarente, L. (2014). NAD+ and sirtuins in aging and disease. Trends in Cell Biology *24*, 464–471.
Imami, K., Sugiyama, N., Kyono, Y., Tomita, M., and Ishihama, Y. (2008). Automated phosphoproteome analysis for cultured cancer cells by two-dimensional nanoLC-MS using a calcined titania/C18 biphasic column. Anal Sci *24*, 161–166.
Incorvaia, L., Bronte, G., Bazan, V., Badalamenti, G., Rizzo, S., Pantuso, G., Natoli, C., and Russo, A. (2016). Beyond evidence-based data: scientific rationale and tumor behavior to drive sequential and personalized therapeutic strategies for the treatment of metastatic renal cell carcinoma. Oncotarget *7*, 21259–21271.
Isabelle, M., Moreel, X., Gagné, J.-P., Rouleau, M., Ethier, C., Gagné, P., Hendzel, M.J., and Poirier, G.G. (2010). Investigation of PARP-1, PARP-2, and PARG interactomes by affinity-purification mass spectrometry. Proteome Sci *8*, 22.

Islam, R., Koizumi, F., Kodera, Y., Inoue, K., Okawara, T., and Masutani, M. (2014). Design and synthesis of phenolic hydrazide hydrazones as potent poly(ADP-ribose) glycohydrolase (PARG) inhibitors. Bioorg. Med. Chem. Lett. *24*, 3802–3806.
Isogai, S., Kanno, S.-I., Ariyoshi, M., Tochio, H., Ito, Y., Yasui, A., and Shirakawa, M. (2010). Solution structure of a zinc-finger domain that binds to poly-ADP-ribose. Genes Cells *15*, 101–110.
Iwata, H., Goettsch, C., Sharma, A., Ricchiuto, P., Goh, W.W.B., Halu, A., Yamada, I., Yoshida, H., Hara, T., Wei, M., et al. (2016). PARP9 and PARP14 cross-regulate macrophage activation via STAT1 ADP-ribosylation. Nat Commun *7*, 12849.
Izhar, L., Adamson, B., Ciccia, A., Lewis, J., Pontano-Vaites, L., Leng, Y., Liang, A.C., Westbrook, T.F., Harper, J.W., and Elledge, S.J. (2015). A Systematic Analysis of Factors Localized to Damaged Chromatin Reveals PARP-Dependent Recruitment of Transcription Factors. Cell Rep *11*, 1486–1500.
Jackson, S.P., and Bartek, J. (2009). The DNA-damage response in human biology and disease. Nature *461*, 1071–1078.
Jacobson, E.L., Antol, K.M., Juarez-Salinas, H., and Jacobson, M.K. (1983). Poly(ADP-ribose) metabolism in ultraviolet irradiated human fibroblasts. J. Biol. Chem. *258*, 103–107.
James, D.I., Smith, K.M., Jordan, A.M., Fairweather, E.E., Griffiths, L.A., Hamilton, N.S., Hitchin, J.R., Hutton, C.P., Jones, S., Kelly, P., et al. (2016). First-in-Class Chemical Probes against Poly(ADP-ribose) Glycohydrolase (PARG) Inhibit DNA Repair with Differential Pharmacology to Olaparib. ACS Chem. Biol. *11*, 3179–3190.
Jankevicius, G., Hassler, M., Golia, B., Rybin, V., Zacharias, M., Timinszky, G., and Ladurner, A.G. (2013). A family of macrodomain proteins reverses cellular mono-ADP-ribosylation. Nat Struct Mol Biol *20*, 508–514.
Jankevicius, G., Ariza, A., Ahel, M., and Ahel, I. (2016). The Toxin-Antitoxin System DarTG Catalyzes Reversible ADP-Ribosylation of DNA. Mol. Cell *64*, 1109–1116.
Jaspers, J.E., Kersbergen, A., Boon, U., Sol, W., van Deemter, L., Zander, S.A., Drost, R., Wientjens, E., Ji, J., Aly, A., et al. (2013). Loss of 53BP1 causes PARP inhibitor resistance in Brca1-mutated mouse mammary tumors. Cancer Discov *3*, 68–81.
Jenuwein, T., and Allis, C.D. (2001). Translating the histone code. Science *293*, 1074–1080.
Jette, N., and Lees-Miller, S.P. (2015). The DNA-dependent protein kinase: A multifunctional protein kinase with roles in DNA double strand break repair and mitosis. Prog. Biophys. Mol. Biol. *117*, 194–205.
Ji, Y., and Tulin, A.V. (2013). Post-transcriptional regulation by poly(ADP-ribosyl)ation of the RNA-binding proteins. Int J Mol Sci *14*, 16168–16183.
Jiang, Y., Liu, J., Chen, D., Yan, L., and Zheng, W. (2017). Sirtuin Inhibition: Strategies, Inhibitors, and Therapeutic Potential. Trends Pharmacol. Sci. *38*, 459–472.
Ju, B.-G., Lunyak, V.V., Perissi, V., Garcia-Bassets, I., Rose, D.W., Glass, C.K., and Rosenfeld, M.G. (2006). A topoisomerase IIbeta-mediated dsDNA break required for regulated transcription. Science *312*, 1798–1802.
Jungmichel, S., Rosenthal, F., Altmeyer, M., Lukas, J., Hottiger, M.O., and Nielsen, M.L. (2013). Proteome-wide identification of poly(ADP-Ribosyl)ation targets in different genotoxic stress responses. Mol. Cell *52*, 272–285.
Jwa, M., and Chang, P. (2012). PARP16 is a tail-anchored endoplasmic reticulum protein required for the PERK- and IRE1α-mediated unfolded protein response. Nat. Cell Biol. *14*, 1223–1230.
Kaiser, P., Auer, B., and Schweiger, M. (1992). Inhibition of cell proliferation in Saccharomyces cerevisiae by expression of human NAD+ ADP-ribosyltransferase requires the DNA binding domain ("zinc fingers"). Mol. Gen. Genet. *232*, 231–239.
Kalisch, T., Amé, J.-C., Dantzer, F., and Schreiber, V. (2012). New readers and interpretations of poly(ADP-ribosyl)ation. Trends Biochem. Sci. *37*, 381–390.
Kanai, M., Tong, W.-M., Sugihara, E., Wang, Z.-Q., Fukasawa, K., and Miwa, M. (2003). Involvement of poly(ADP-Ribose) polymerase 1 and poly(ADP-Ribosyl)ation in regulation of centrosome function. Mol. Cell. Biol. *23*, 2451–2462.
Kanao, R., and Masutani, C. (2017). Regulation of DNA damage tolerance in mammalian cells by post-translational modifications of PCNA. Mutat. Res. *803–805*, 82–88.
Kang, H.C., Lee, Y.-I., Shin, J.-H., Andrabi, S.A., Chi, Z., Gagné, J.-P., Lee, Y., Ko, H.S., Lee, B.D., Poirier, G.G., et al. (2011). Iduna is a poly(ADP-ribose) (PAR)-dependent E3 ubiquitin ligase that regulates DNA damage. Proc. Natl. Acad. Sci. U.S.A. *108*, 14103–14108.
Karicheva, O., Rodriguez-Vargas, J.M., Wadier, N., Martin-Hernandez, K., Vauchelles, R., Magroun, N., Tissier, A., Schreiber, V., and Dantzer, F. (2016). PARP3 controls TGFβ and ROS driven epithelial-to-mesenchymal transition and stemness by stimulating a TG2-Snail-E-cadherin axis. Oncotarget *7*, 64109–64123.
Karner, C.M., Merkel, C.E., Dodge, M., Ma, Z., Lu, J., Chen, C., Lum, L., and Carroll, T.J. (2010). Tankyrase is necessary for canonical Wnt signaling during kidney development. Dev. Dyn. *239*, 2014–2023.

Karow, J.K., Constantinou, A., Li, J.L., West, S.C., and Hickson, I.D. (2000). The Bloom's syndrome gene product promotes branch migration of holliday junctions. Proc. Natl. Acad. Sci. U.S.A. *97*, 6504–6508.
Karras, G.I., Kustatscher, G., Buhecha, H.R., Allen, M.D., Pugieux, C., Sait, F., Bycroft, M., and Ladurner, A.G. (2005). The macro domain is an ADP-ribose binding module. EMBO J. *24*, 1911–1920.
Kasamatsu, A., Nakao, M., Smith, B.C., Comstock, L.R., Ono, T., Kato, J., Denu, J.M., and Moss, J. (2011). Hydrolysis of O-acetyl-ADP-ribose isomers by ADP-ribosylhydrolase 3. J. Biol. Chem. *286*, 21110–21117.
Kashima, L., Idogawa, M., Mita, H., Shitashige, M., Yamada, T., Ogi, K., Suzuki, H., Toyota, M., Ariga, H., Sasaki, Y., et al. (2012a). CHFR protein regulates mitotic checkpoint by targeting PARP-1 protein for ubiquitination and degradation. J. Biol. Chem. *287*, 12975–12984.
Kashima, L., Idogawa, M., Mita, H., Shitashige, M., Yamada, T., Ogi, K., Suzuki, H., Toyota, M., Ariga, H., Sasaki, Y., et al. (2012b). CHFR protein regulates mitotic checkpoint by targeting PARP-1 protein for ubiquitination and degradation. J. Biol. Chem. *287*, 12975–12984.
Kato, J., Vekhter, D., Heath, J., Zhu, J., Barbieri, J.T., and Moss, J. (2015). Mutations of the functional ARH1 allele in tumors from ARH1 heterozygous mice and cells affect ARH1 catalytic activity, cell proliferation and tumorigenesis. Oncogenesis *4*, e151.
Kaufmann, T., Grishkovskaya, I., Polyansky, A.A., Kostrhon, S., Kukolj, E., Olek, K.M., Herbert, S., Beltzung, E., Mechtler, K., Peterbauer, T., et al. (2017). A novel non-canonical PIP-box mediates PARG interaction with PCNA. Nucleic Acids Res. *45*, 9741–9759.
Kauppinen, T.M., Chan, W.Y., Suh, S.W., Wiggins, A.K., Huang, E.J., and Swanson, R.A. (2006). Direct phosphorylation and regulation of poly(ADP-ribose) polymerase-1 by extracellular signal-regulated kinases 1/2. Proc. Natl. Acad. Sci. U.S.A. *103*, 7136–7141.
Kedar, P.S., Stefanick, D.F., Horton, J.K., and Wilson, S.H. (2008). Interaction between PARP-1 and ATR in mouse fibroblasts is blocked by PARP inhibition. DNA Repair (Amst.) *7*, 1787–1798.
Keil, C., Gröbe, T., and Oei, S.L. (2006). MNNG-induced cell death is controlled by interactions between PARP-1, poly(ADP-ribose) glycohydrolase, and XRCC1. J. Biol. Chem. *281*, 34394–34405.
Khurana, S., Kruhlak, M.J., Kim, J., Tran, A.D., Liu, J., Nyswaner, K., Shi, L., Jailwala, P., Sung, M.-H., Hakim, O., et al. (2014). A Macrohistone Variant Links Dynamic Chromatin Compaction to BRCA1-Dependent Genome Maintenance. Cell Reports *8*, 1049–1062.
Kickhoefer, V.A., Siva, A.C., Kedersha, N.L., Inman, E.M., Ruland, C., Streuli, M., and Rome, L.H. (1999). The 193-kD vault protein, VPARP, is a novel poly(ADP-ribose) polymerase. J. Cell Biol. *146*, 917–928.
Kim, K.P., and Mirkin, E.V. (2017). So similar yet so different: The two ends of a double strand break. Mutat. Res.
Kim, B.-J., Chan, D.W., Jung, S.Y., Chen, Y., Qin, J., and Wang, Y. (2017). The Histone Variant MacroH2A1 Is a BRCA1 Ubiquitin Ligase Substrate. Cell Rep *19*, 1758–1766.
Kim, I.-K., Kiefer, J.R., Ho, C.M.W., Stegeman, R.A., Classen, S., Tainer, J.A., and Ellenberger, T. (2012). Structure of mammalian poly(ADP-ribose) glycohydrolase reveals a flexible tyrosine clasp as a substrate-binding element. Nature Structural & Molecular Biology *19*, 653–656.
Kim, S.T., Lim, D.S., Canman, C.E., and Kastan, M.B. (1999). Substrate specificities and identification of putative substrates of ATM kinase family members. J. Biol. Chem. *274*, 37538–37543.
King, B.S., Cooper, K.L., Liu, K.J., and Hudson, L.G. (2012). Poly(ADP-ribose) contributes to an association between poly(ADP-ribose) polymerase-1 and xeroderma pigmentosum complementation group A in nucleotide excision repair. J. Biol. Chem. *287*, 39824–39833.
Kistemaker, H.A.V., Nardozza, A.P., Overkleeft, H.S., van der Marel, G.A., Ladurner, A.G., and Filippov, D.V. (2016). Synthesis and Macrodomain Binding of Mono-ADP-Ribosylated Peptides. Angew. Chem. Int. Ed. Engl. *55*, 10634–10638.
de Klein, A., Muijtjens, M., van Os, R., Verhoeven, Y., Smit, B., Carr, A.M., Lehmann, A.R., and Hoeijmakers, J.H. (2000). Targeted disruption of the cell-cycle checkpoint gene ATR leads to early embryonic lethality in mice. Curr. Biol. *10*, 479–482.
Kleine, H., Herrmann, A., Lamark, T., Forst, A.H., Verheugd, P., Lüscher-Firzlaff, J., Lippok, B., Feijs, K.L., Herzog, N., Kremmer, E., et al. (2012). Dynamic subcellular localization of the mono-ADP-ribosyltransferase ARTD10 and interaction with the ubiquitin receptor p62. Cell Commun. Signal *10*, 28.
von Kobbe, C., Harrigan, J.A., Schreiber, V., Stiegler, P., Piotrowski, J., Dawut, L., and Bohr, V.A. (2004). Poly(ADP-ribose) polymerase 1 regulates both the exonuclease and helicase activities of the Werner syndrome protein. Nucleic Acids Res. *32*, 4003–4014.
Koh, D.W., Lawler, A.M., Poitras, M.F., Sasaki, M., Wattler, S., Nehls, M.C., Stöger, T., Poirier, G.G., Dawson, V.L., and Dawson, T.M. (2004). Failure to degrade poly(ADP-ribose) causes increased sensitivity to cytotoxicity and early embryonic lethality. Proc. Natl. Acad. Sci. U.S.A. *101*, 17699–17704.

Kong, X., Shen, Y., Jiang, N., Fei, X., and Mi, J. (2011). Emerging roles of DNA-PK besides DNA repair. Cell. Signal. *23*, 1273–1280.
Korkmaz, A., Kurt, B., Yildirim, I., Basal, S., Topal, T., Sadir, S., and Oter, S. (2008). Effects of poly(ADP-ribose) polymerase inhibition in bladder damage caused by cyclophosphamide in rats. Exp. Biol. Med. (Maywood) *233*, 338–343.
Korolev, K.S., Xavier, J.B., and Gore, J. (2014). Turning ecology and evolution against cancer. Nat. Rev. Cancer *14*, 371–380.
Kozaki, T., Komano, J., Kanbayashi, D., Takahama, M., Misawa, T., Satoh, T., Takeuchi, O., Kawai, T., Shimizu, S., Matsuura, Y., et al. (2017). Mitochondrial damage elicits a TCDD-inducible poly(ADP-ribose) polymerase-mediated antiviral response. PNAS *114*, 2681–2686.
Kozlov, S.V., Graham, M.E., Peng, C., Chen, P., Robinson, P.J., and Lavin, M.F. (2006). Involvement of novel autophosphorylation sites in ATM activation. EMBO J. *25*, 3504–3514.
Krejci, L., Altmannova, V., Spirek, M., and Zhao, X. (2012). Homologous recombination and its regulation. Nucleic Acids Res *40*, 5795–5818.
Krishnakumar, R., and Kraus, W.L. (2010a). PARP-1 regulates chromatin structure and transcription through a KDM5B-dependent pathway. Mol. Cell *39*, 736–749.
Krishnakumar, R., and Kraus, W.L. (2010b). The PARP Side of the Nucleus: Molecular Actions, Physiological Outcomes, and Clinical Targets. Molecular Cell, Molecular Cell. *39*, 8–24.
Krishnakumar, R., Gamble, M.J., Frizzell, K.M., Berrocal, J.G., Kininis, M., and Kraus, W.L. (2008). Reciprocal binding of PARP-1 and histone H1 at promoters specifies transcriptional outcomes. Science *319*, 819–821.
Krokan, H.E., and Bjørås, M. (2013). Base excision repair. Cold Spring Harb Perspect Biol *5*, a012583.
Kumagai, A., Lee, J., Yoo, H.Y., and Dunphy, W.G. (2006). TopBP1 activates the ATR-ATRIP complex. Cell *124*, 943–955.
Kutuzov, M.M., Khodyreva, S.N., Amé, J.-C., Ilina, E.S., Sukhanova, M.V., Schreiber, V., and Lavrik, O.I. (2013). Interaction of PARP-2 with DNA structures mimicking DNA repair intermediates and consequences on activity of base excision repair proteins. Biochimie *95*, 1208–1215.
Kutuzov, M.M., Khodyreva, S.N., Schreiber, V., and Lavrik, O.I. (2014). [The role of PARP2 in DNA repair]. Mol. Biol. (Mosk.) *48*, 561–572.
Lampson, B.L., and Brown, J.R. (2017). PI3Kδ-selective and PI3Kα/δ-combinatorial inhibitors in clinical development for B-cell non-Hodgkin lymphoma. Expert Opin Investig Drugs *26*, 1267–1279.
Langelier, M.-F., Ruhl, D.D., Planck, J.L., Kraus, W.L., and Pascal, J.M. (2010). The Zn3 domain of human poly(ADP-ribose) polymerase-1 (PARP-1) functions in both DNA-dependent poly(ADP-ribose) synthesis activity and chromatin compaction. J. Biol. Chem. *285*, 18877–18887.
Langelier, M.-F., Planck, J.L., Roy, S., and Pascal, J.M. (2012). Structural basis for DNA damage-dependent poly(ADP-ribosyl)ation by human PARP-1. Science *336*, 728–732.
Langelier, M.-F., Riccio, A.A., and Pascal, J.M. (2014). PARP-2 and PARP-3 are selectively activated by 5' phosphorylated DNA breaks through an allosteric regulatory mechanism shared with PARP-1. Nucleic Acids Res. *42*, 7762–7775.
Larsen, S.C., Leutert, M., Bilan, V., Martello, R., Jungmichel, S., Young, C., Hottiger, M.O., and Nielsen, M.L. (2017). Proteome-Wide Identification of In Vivo ADP-Ribose Acceptor Sites by Liquid Chromatography-Tandem Mass Spectrometry. Methods Mol. Biol. *1608*, 149–162.
Lau, W.C.Y., Li, Y., Liu, Z., Gao, Y., Zhang, Q., and Huen, M.S.Y. (2016). Structure of the human dimeric ATM kinase. Cell Cycle *15*, 1117–1124.
Leidecker, O., Bonfiglio, J.J., Colby, T., Zhang, Q., Atanassov, I., Zaja, R., Palazzo, L., Stockum, A., Ahel, I., and Matic, I. (2016). Serine is a new target residue for endogenous ADP-ribosylation on histones. Nat. Chem. Biol. *12*, 998–1000.
Leung, A., Todorova, T., Ando, Y., and Chang, P. (2012). Poly(ADP-ribose) regulates post-transcriptional gene regulation in the cytoplasm. RNA Biol *9*, 542–548.
Leutert, M., Bilan, V., Gehrig, P., and Hottiger, M.O. (2017). Identification of ADP-Ribose Acceptor Sites on In Vitro Modified Proteins by Liquid Chromatography-Tandem Mass Spectrometry. Methods Mol. Biol. *1608*, 137–148.
Lévy, N., Martz, A., Bresson, A., Spenlehauer, C., de Murcia, G., and Ménissier-de Murcia, J. (2006). XRCC1 is phosphorylated by DNA-dependent protein kinase in response to DNA damage. Nucleic Acids Res *34*, 32–41.
Li, M., and Yu, X. (2013). Function of BRCA1 in the DNA damage response is mediated by ADP-ribosylation. Cancer Cell *23*, 693–704.
Li, Y., and Seto, E. (2016). HDACs and HDAC Inhibitors in Cancer Development and Therapy. Cold Spring Harb Perspect Med *6*.

Li, B., Navarro, S., Kasahara, N., and Comai, L. (2004). Identification and biochemical characterization of a Werner's syndrome protein complex with Ku70/80 and poly(ADP-ribose) polymerase-1. J. Biol. Chem. *279*, 13659–13667.
Li, C., Debing, Y., Jankevicius, G., Neyts, J., Ahel, I., Coutard, B., and Canard, B. (2016). Viral Macro Domains Reverse Protein ADP-Ribosylation. J. Virol. *90*, 8478–8486.
Li, G.-Y., McCulloch, R.D., Fenton, A.L., Cheung, M., Meng, L., Ikura, M., and Koch, C.A. (2010). Structure and identification of ADP-ribose recognition motifs of APLF and role in the DNA damage response. PNAS *107*, 9129–9134.
Li, J., Summerlin, M., Nitiss, K.C., Nitiss, J.L., and Hanakahi, L.A. (2017a). TDP1 is required for efficient non-homologous end joining in human cells. DNA Repair (Amst.) *60*, 40–49.
Li, M., Threadgill, M.D., Wang, Y., Cai, L., and Lin, X. (2009). Poly(ADP-ribose) polymerase inhibition down-regulates expression of metastasis-related genes in CT26 colon carcinoma cells. Pathobiology *76*, 108–116.
Li, M., Lu, L.-Y., Yang, C.-Y., Wang, S., and Yu, X. (2013). The FHA and BRCT domains recognize ADP-ribosylation during DNA damage response. Genes Dev. *27*, 1752–1768.
Li, X., Han, H., Zhou, M.-T., Yang, B., Ta, A.P., Li, N., Chen, J., and Wang, W. (2017b). Proteomic Analysis of the Human Tankyrase Protein Interaction Network Reveals Its Role in Pexophagy. Cell Rep *20*, 737–749.
Liew, L.P., Lim, Z.Y., Cohen, M., Kong, Z., Marjavaara, L., Chabes, A., and Bell, S.D. (2016). Hydroxyurea-Mediated Cytotoxicity Without Inhibition of Ribonucleotide Reductase. Cell Rep *17*, 1657–1670.
Lim, J.S.J., and Tan, D.S.P. (2017). Understanding Resistance Mechanisms and Expanding the Therapeutic Utility of PARP Inhibitors. Cancers (Basel) *9*.
Lin, W., Amé, J.C., Aboul-Ela, N., Jacobson, E.L., and Jacobson, M.K. (1997). Isolation and characterization of the cDNA encoding bovine poly(ADP-ribose) glycohydrolase. J. Biol. Chem. *272*, 11895–11901.
Lindsey-Boltz, L.A. (2017). Bringing It All Together: Coupling Excision Repair to the DNA Damage Checkpoint. Photochem. Photobiol. *93*, 238–244.
Liu, J., and Rost, B. (2003). NORSp: Predictions of long regions without regular secondary structure., NORSp: predictions of long regions without regular secondary structure. Nucleic Acids Res *31*, *31*, 3833, 3833–3835.
Liu, Z., and Kraus, W.L. (2017). Catalytic-Independent Functions of PARP-1 Determine Sox2 Pioneer Activity at Intractable Genomic Loci. Mol. Cell *65*, 589–603.e9.
Liu, C., Wu, J., Paudyal, S.C., You, Z., and Yu, X. (2013). CHFR is important for the first wave of ubiquitination at DNA damage sites. Nucleic Acids Res. *41*, 1698–1710.
Liu, C., Wu, Q., Liu, W., Gu, Z., Wang, W., Xu, P., Ma, H., and Ge, X. (2017a). Poly(ADP-ribose) polymerases regulate cell division and development in Arabidopsis roots. J Integr Plant Biol *59*, 459–474.
Liu, D., Keijzers, G., and Rasmussen, L.J. (2017b). DNA mismatch repair and its many roles in eukaryotic cells. Mutat. Res. *773*, 174–187.
Liu, J.S., Kuo, S.R., McHugh, M.M., Beerman, T.A., and Melendy, T. (2000). Adozelesin triggers DNA damage response pathways and arrests SV40 DNA replication through replication protein A inactivation. J. Biol. Chem. *275*, 1391–1397.
Liu, J.-S., Kuo, S.-R., and Melendy, T. (2006). DNA damage-induced RPA focalization is independent of gamma-H2AX and RPA hyper-phosphorylation. J. Cell. Biochem. *99*, 1452–1462.
Liu, Q., Florea, B.I., and Filippov, D.V. (2017c). ADP-Ribosylation Goes Normal: Serine as the Major Site of the Modification. Cell Chem Biol *24*, 431–432.
Liu, Y., Zhou, J., Omelchenko, M.V., Beliaev, A.S., Venkateswaran, A., Stair, J., Wu, L., Thompson, D.K., Xu, D., Rogozin, I.B., et al. (2003). Transcriptome dynamics of Deinococcus radiodurans recovering from ionizing radiation. Proc. Natl. Acad. Sci. U.S.A. *100*, 4191–4196.
Loeffler, P.A., Cuneo, M.J., Mueller, G.A., DeRose, E.F., Gabel, S.A., and London, R.E. (2011). Structural studies of the PARP-1 BRCT domain. BMC Struct. Biol. *11*, 37.
Loew, R., Heinz, N., Hampf, M., Bujard, H., and Gossen, M. (2010). Improved Tet-responsive promoters with minimized background expression. BMC Biotechnol *10*, 81.
Lönn, P., and Landegren, U. (2017). Close Encounters - Probing Proximal Proteins in Live or Fixed Cells. Trends Biochem. Sci. *42*, 504–515.
Lord, C.J., and Ashworth, A. (2016). BRCAness revisited. Nat. Rev. Cancer *16*, 110–120.
Lord, C.J., and Ashworth, A. (2017). PARP inhibitors: Synthetic lethality in the clinic. Science *355*, 1152–1158.
Lord, C.J., Tutt, A.N.J., and Ashworth, A. (2015). Synthetic lethality and cancer therapy: lessons learned from the development of PARP inhibitors. Annu. Rev. Med. *66*, 455–470.
Lossaint, G., Larroque, M., Ribeyre, C., Bec, N., Larroque, C., Décaillet, C., Gari, K., and Constantinou, A. (2013). FANCD2 binds MCM proteins and controls replisome function upon activation of s phase checkpoint signaling. Mol. Cell *51*, 678–690.

Lu, D. (2013). [C2H2 zinc-finger recognition of biomolecules]. Yao Xue Xue Bao *48*, 834–841.
Lu, C.-S., Truong, L.N., Aslanian, A., Shi, L.Z., Li, Y., Hwang, P.Y.-H., Koh, K.H., Hunter, T., Yates, J.R., Berns, M.W., et al. (2012). The RING finger protein RNF8 ubiquitinates Nbs1 to promote DNA double-strand break repair by homologous recombination. J. Biol. Chem. *287*, 43984–43994.
Luijsterburg, M.S., Lindh, M., Acs, K., Vrouwe, M.G., Pines, A., van Attikum, H., Mullenders, L.H., and Dantuma, N.P. (2012). DDB2 promotes chromatin decondensation at UV-induced DNA damage. J. Cell Biol. *197*, 267–281.
Luijsterburg, M.S., de Krijger, I., Wiegant, W.W., Shah, R.G., Smeenk, G., de Groot, A.J.L., Pines, A., Vertegaal, A.C.O., Jacobs, J.J.L., Shah, G.M., et al. (2016). PARP1 Links CHD2-Mediated Chromatin Expansion and H3.3 Deposition to DNA Repair by Non-homologous End-Joining. Mol. Cell *61*, 547–562.
Ma, Q., Baldwin, K.T., Renzelli, A.J., McDaniel, A., and Dong, L. (2001). TCDD-inducible poly(ADP-ribose) polymerase: a novel response to 2,3,7,8-tetrachlorodibenzo-p-dioxin. Biochem. Biophys. Res. Commun. *289*, 499–506.
MacPherson, L., Tamblyn, L., Rajendra, S., Bralha, F., McPherson, J.P., and Matthews, J. (2013). 2,3,7,8-Tetrachlorodibenzo-p-dioxin poly(ADP-ribose) polymerase (TiPARP, ARTD14) is a mono-ADP-ribosyltransferase and repressor of aryl hydrocarbon receptor transactivation. Nucleic Acids Res. *41*, 1604–1621.
Mailand, N., Gibbs-Seymour, I., and Bekker-Jensen, S. (2013). Regulation of PCNA-protein interactions for genome stability. Nat. Rev. Mol. Cell Biol. *14*, 269–282.
Malanga, M., Czubaty, A., Girstun, A., Staron, K., and Althaus, F.R. (2008). Poly(ADP-ribose) binds to the splicing factor ASF/SF2 and regulates its phosphorylation by DNA topoisomerase I. J. Biol. Chem. *283*, 19991–19998.
Malewicz, M., Kadkhodaei, B., Kee, N., Volakakis, N., Hellman, U., Viktorsson, K., Leung, C.Y., Chen, B., Lewensohn, R., van Gent, D.C., et al. (2011). Essential role for DNA-PK-mediated phosphorylation of NR4A nuclear orphan receptors in DNA double-strand break repair. Genes Dev. *25*, 2031–2040.
Maltseva, E.A., Rechkunova, N.I., Sukhanova, M.V., and Lavrik, O.I. (2015). Poly(ADP-ribose) Polymerase 1 Modulates Interaction of the Nucleotide Excision Repair Factor XPC-RAD23B with DNA via Poly(ADP-ribosyl)ation. J. Biol. Chem. *290*, 21811–21820.
Mansour, W.Y., Borgmann, K., Petersen, C., Dikomey, E., and Dahm-Daphi, J. (2013). The absence of Ku but not defects in classical non-homologous end-joining is required to trigger PARP1-dependent end-joining. DNA Repair (Amst.) *12*, 1134–1142.
Marchetti, C., Imperiale, L., Gasparri, M.L., Palaia, I., Pignata, S., Boni, T., Bellati, F., and Benedetti Panici, P. (2012). Olaparib, PARP1 inhibitor in ovarian cancer. Expert Opin Investig Drugs *21*, 1575–1584.
Maréchal, A., and Zou, L. (2015). RPA-coated single-stranded DNA as a platform for post-translational modifications in the DNA damage response. Cell Res *25*, 9–23.
Martello, R., Leutert, M., Jungmichel, S., Bilan, V., Larsen, S.C., Young, C., Hottiger, M.O., and Nielsen, M.L. (2016). Proteome-wide identification of the endogenous ADP-ribosylome of mammalian cells and tissue. Nat Commun *7*, 12917.
Martin-Hernandez, K., Rodriguez-Vargas, J.-M., Schreiber, V., and Dantzer, F. (2017). Expanding functions of ADP-ribosylation in the maintenance of genome integrity. Semin. Cell Dev. Biol. *63*, 92–101.
Mashimo, M., and Moss, J. (2016). Functional Role of ADP-Ribosyl-Acceptor Hydrolase 3 in poly(ADP-Ribose) Polymerase-1 Response to Oxidative Stress. Curr. Protein Pept. Sci. *17*, 633–640.
Mashimo, M., Kato, J., and Moss, J. (2013). ADP-ribosyl-acceptor hydrolase 3 regulates poly (ADP-ribose) degradation and cell death during oxidative stress. Proc. Natl. Acad. Sci. U.S.A. *110*, 18964–18969.
Mashimo, M., Kato, J., and Moss, J. (2014). Structure and function of the ARH family of ADP-ribosyl-acceptor hydrolases. DNA Repair (Amst.) *23*, 88–94.
Masson, M., Niedergang, C., Schreiber, V., Muller, S., Menissier-de Murcia, J., and de Murcia, G. (1998). XRCC1 is specifically associated with poly(ADP-ribose) polymerase and negatively regulates its activity following DNA damage. Mol. Cell. Biol. *18*, 3563–3571.
Mateo, J., Ong, M., Tan, D.S.P., Gonzalez, M.A., and de Bono, J.S. (2013). Appraising iniparib, the PARP inhibitor that never was--what must we learn? Nat Rev Clin Oncol *10*, 688–696.
Mateos-Gomez, P.A., Gong, F., Nair, N., Miller, K.M., Lazzerini-Denchi, E., and Sfeir, A. (2015). Mammalian polymerase θ promotes alternative NHEJ and suppresses recombination. Nature *518*, 254–257.
Matsuoka, S., Ballif, B.A., Smogorzewska, A., McDonald, E.R., Hurov, K.E., Luo, J., Bakalarski, C.E., Zhao, Z., Solimini, N., Lerenthal, Y., et al. (2007). ATM and ATR substrate analysis reveals extensive protein networks responsive to DNA damage. Science *316*, 1160–1166.
McCormick, A., Donoghue, P., Dixon, M., O'Sullivan, R., O'Donnell, R.L., Murray, J., Kaufmann, A., Curtin, N.J., and Edmondson, R.J. (2017). Ovarian Cancers Harbour Defects in Non-Homologous End Joining Resulting in Resistance to Rucaparib. Clin Cancer Res *23*, 2050–2060.

McGonigle, S., Chen, Z., Wu, J., Chang, P., Kolber-Simonds, D., Ackermann, K., Twine, N.C., Shie, J.-L., Miu, J.T., Huang, K.-C., et al. (2015). E7449: A dual inhibitor of PARP1/2 and tankyrase1/2 inhibits growth of DNA repair deficient tumors and antagonizes Wnt signaling. Oncotarget *6*, 41307–41323.
Mehrotra, P., Hollenbeck, A., Riley, J.P., Li, F., Patel, R.J., Akhtar, N., and Goenka, S. (2013). Poly (ADP-ribose) polymerase 14 and its enzyme activity regulates T(H)2 differentiation and allergic airway disease. J. Allergy Clin. Immunol. *131*, 521-531-12.
Mehrotra, P., Krishnamurthy, P., Sun, J., Goenka, S., and Kaplan, M.H. (2015). Poly-ADP-ribosyl polymerase-14 promotes T helper 17 and follicular T helper development. Immunology *146*, 537–546.
Mei, Z., Zhang, X., Yi, J., Huang, J., He, J., and Tao, Y. (2016). Sirtuins in metabolism, DNA repair and cancer. J. Exp. Clin. Cancer Res. *35*, 182.
Mejlvang, J., Feng, Y., Alabert, C., Neelsen, K.J., Jasencakova, Z., Zhao, X., Lees, M., Sandelin, A., Pasero, P., Lopes, M., et al. (2014). New histone supply regulates replication fork speed and PCNA unloading. J. Cell Biol. *204*, 29–43.
Ménisser-de Murcia, J., Mark, M., Wendling, O., Wynshaw-Boris, A., and de Murcia, G. (2001). Early embryonic lethality in PARP-1 Atm double-mutant mice suggests a functional synergy in cell proliferation during development. Mol. Cell. Biol. *21*, 1828–1832.
Ménissier de Murcia, J., Ricoul, M., Tartier, L., Niedergang, C., Huber, A., Dantzer, F., Schreiber, V., Amé, J.-C., Dierich, A., LeMeur, M., et al. (2003). Functional interaction between PARP-1 and PARP-2 in chromosome stability and embryonic development in mouse. EMBO J. *22*, 2255–2263.
Messner, S., Altmeyer, M., Zhao, H., Pozivil, A., Roschitzki, B., Gehrig, P., Rutishauser, D., Huang, D., Caflisch, A., and Hottiger, M.O. (2010). PARP1 ADP-ribosylates lysine residues of the core histone tails. Nucleic Acids Res. *38*, 6350–6362.
Meyer, R.G., Meyer-Ficca, M.L., Jacobson, E.L., and Jacobson, M.K. (2003). Human poly(ADP-ribose) glycohydrolase (PARG) gene and the common promoter sequence it shares with inner mitochondrial membrane translocase 23 (TIM23). Gene *314*, 181–190.
Meyer, R.G., Meyer-Ficca, M.L., Whatcott, C.J., Jacobson, E.L., and Jacobson, M.K. (2007). Two small enzyme isoforms mediate mammalian mitochondrial poly(ADP-ribose) glycohydrolase (PARG) activity. Exp. Cell Res. *313*, 2920–2936.
Meyer-Ficca, M.L., Meyer, R.G., Kaiser, H., Brack, A.R., Kandolf, R., and Küpper, J.-H. (2004a). Comparative analysis of inducible expression systems in transient transfection studies. Analytical Biochemistry *334*, 9–19.
Meyer-Ficca, M.L., Meyer, R.G., Coyle, D.L., Jacobson, E.L., and Jacobson, M.K. (2004b). Human poly(ADP-ribose) glycohydrolase is expressed in alternative splice variants yielding isoforms that localize to different cell compartments. Exp. Cell Res. *297*, 521–532.
Meyer-Ficca, M.L., Ihara, M., Bader, J.J., Leu, N.A., Beneke, S., and Meyer, R.G. (2015). Spermatid head elongation with normal nuclear shaping requires ADP-ribosyltransferase PARP11 (ARTD11) in mice. Biol. Reprod. *92*, 80.
Min, W., Bruhn, C., Grigaravicius, P., Zhou, Z.-W., Li, F., Krüger, A., Siddeek, B., Greulich, K.-O., Popp, O., Meisezahl, C., et al. (2013). Poly(ADP-ribose) binding to Chk1 at stalled replication forks is required for S-phase checkpoint activation. Nat Commun *4*, 2993.
Miura, K., Sakata, K., Someya, M., Matsumoto, Y., Matsumoto, H., Takahashi, A., and Hareyama, M. (2012). The combination of olaparib and camptothecin for effective radiosensitization. Radiat Oncol *7*, 62.
Mordes, D.A., and Cortez, D. (2008). Activation of ATR and related PIKKs. Cell Cycle *7*, 2809–2812.
Moss, J., Stanley, S.J., Nightingale, M.S., Murtagh, J.J., Monaco, L., Mishima, K., Chen, H.C., Williamson, K.C., and Tsai, S.C. (1992). Molecular and immunological characterization of ADP-ribosylarginine hydrolases. J. Biol. Chem. *267*, 10481–10488.
Moudry, P., Watanabe, K., Wolanin, K.M., Bartkova, J., Wassing, I.E., Watanabe, S., Strauss, R., Troelsgaard Pedersen, R., Oestergaard, V.H., Lisby, M., et al. (2016). TOPBP1 regulates RAD51 phosphorylation and chromatin loading and determines PARP inhibitor sensitivity. J. Cell Biol. *212*, 281–288.
Mourón, S., Rodriguez-Acebes, S., Martínez-Jiménez, M.I., García-Gómez, S., Chocrón, S., Blanco, L., and Méndez, J. (2013). Repriming of DNA synthesis at stalled replication forks by human PrimPol. Nat. Struct. Mol. Biol. *20*, 1383–1389.
Mueller-Dieckmann, C., Kernstock, S., Lisurek, M., von Kries, J.P., Haag, F., Weiss, M.S., and Koch-Nolte, F. (2006). The structure of human ADP-ribosylhydrolase 3 (ARH3) provides insights into the reversibility of protein ADP-ribosylation. Proc. Natl. Acad. Sci. U.S.A. *103*, 15026–15031.
Munnur, D., and Ahel, I. (2017). Reversible mono-ADP-ribosylation of DNA breaks. FEBS J.
Murai, J., Huang, S.N., Das, B.B., Renaud, A., Zhang, Y., Doroshow, J.H., Ji, J., Takeda, S., and Pommier, Y. (2012). Trapping of PARP1 and PARP2 by Clinical PARP Inhibitors. Cancer Res. *72*, 5588–5599.

Murai, J., Huang, S.-Y.N., Renaud, A., Zhang, Y., Ji, J., Takeda, S., Morris, J., Teicher, B., Doroshow, J.H., and Pommier, Y. (2014). Stereospecific PARP trapping by BMN 673 and comparison with olaparib and rucaparib. Mol. Cancer Ther. *13*, 433–443.
de Murcia, G., and Ménissier de Murcia, J. (1994). Poly(ADP-ribose) polymerase: a molecular nick-sensor. Trends Biochem. Sci. *19*, 172–176.
de Murcia, G., Huletsky, A., Lamarre, D., Gaudreau, A., Pouyet, J., Daune, M., and Poirier, G.G. (1986). Modulation of chromatin superstructure induced by poly(ADP-ribose) synthesis and degradation. J. Biol. Chem. *261*, 7011–7017.
Nagy, Z., Kalousi, A., Furst, A., Koch, M., Fischer, B., and Soutoglou, E. (2016a). Tankyrases Promote Homologous Recombination and Check Point Activation in Response to DSBs. PLoS Genet. *12*, e1005791.
Nagy, Z., Kalousi, A., Furst, A., Koch, M., Fischer, B., and Soutoglou, E. (2016b). Tankyrases Promote Homologous Recombination and Check Point Activation in Response to DSBs. PLoS Genet. *12*, e1005791.
Nakadate, Y., Kodera, Y., Kitamura, Y., Tachibana, T., Tamura, T., and Koizumi, F. (2013). Silencing of poly(ADP-ribose) glycohydrolase sensitizes lung cancer cells to radiation through the abrogation of DNA damage checkpoint. Biochem. Biophys. Res. Commun. *441*, 793–798.
Nam, E.A., and Cortez, D. (2011). ATR signalling: more than meeting at the fork. Biochem. J. *436*, 527–536.
Naus, P.J., Henson, R., Bleeker, G., Wehbe, H., Meng, F., and Patel, T. (2007). Tannic acid synergizes the cytotoxicity of chemotherapeutic drugs in human cholangiocarcinoma by modulating drug efflux pathways. J. Hepatol. *46*, 222–229.
Neal, J.A., Sugiman-Marangos, S., VanderVere-Carozza, P., Wagner, M., Turchi, J., Lees-Miller, S.P., Junop, M.S., and Meek, K. (2014). Unraveling the complexities of DNA-dependent protein kinase autophosphorylation. Mol. Cell. Biol. *34*, 2162–2175.
Neelsen, K.J., and Lopes, M. (2015). Replication fork reversal in eukaryotes: from dead end to dynamic response. Nat. Rev. Mol. Cell Biol. *16*, 207–220.
Nepal, M., Che, R., Ma, C., Zhang, J., and Fei, P. (2017). FANCD2 and DNA Damage. Int J Mol Sci *18*.
Neuvonen, M., and Ahola, T. (2009). Differential activities of cellular and viral macro domain proteins in binding of ADP-ribose metabolites. J. Mol. Biol. *385*, 212–225.
Nicolae, C.M., Aho, E.R., Vlahos, A.H.S., Choe, K.N., De, S., Karras, G.I., and Moldovan, G.-L. (2014). The ADP-ribosyltransferase PARP10/ARTD10 interacts with proliferating cell nuclear antigen (PCNA) and is required for DNA damage tolerance. J. Biol. Chem. *289*, 13627–13637.
Niere, M., Mashimo, M., Agledal, L., Dölle, C., Kasamatsu, A., Kato, J., Moss, J., and Ziegler, M. (2012). ADP-ribosylhydrolase 3 (ARH3), not poly(ADP-ribose) glycohydrolase (PARG) isoforms, is responsible for degradation of mitochondrial matrix-associated poly(ADP-ribose). J. Biol. Chem. *287*, 16088–16102.
Nikiforov, A., Kulikova, V., and Ziegler, M. (2015). The human NAD metabolome: Functions, metabolism and compartmentalization. Crit. Rev. Biochem. Mol. Biol. *50*, 284–297.
Noël, G., Giocanti, N., Fernet, M., Mégnin-Chanet, F., and Favaudon, V. (2003). Poly(ADP-ribose) polymerase (PARP-1) is not involved in DNA double-strand break recovery. BMC Cell Biol. *4*, 7.
Noll, A., Illuzzi, G., Amé, J.-C., Dantzer, F., and Schreiber, V. (2016). PARG deficiency is neither synthetic lethal with BRCA1 nor PTEN deficiency. Cancer Cell Int. *16*, 53.
Norquist, B., Wurz, K.A., Pennil, C.C., Garcia, R., Gross, J., Sakai, W., Karlan, B.Y., Taniguchi, T., and Swisher, E.M. (2011). Secondary somatic mutations restoring BRCA1/2 predict chemotherapy resistance in hereditary ovarian carcinomas. J. Clin. Oncol. *29*, 3008–3015.
Oberoi, J., Richards, M.W., Crumpler, S., Brown, N., Blagg, J., and Bayliss, R. (2010). Structural basis of poly(ADP-ribose) recognition by the multizinc binding domain of checkpoint with forkhead-associated and RING Domains (CHFR). J. Biol. Chem. *285*, 39348–39358.
Oei, S.L., and Ziegler, M. (2000). ATP for the DNA ligation step in base excision repair is generated from poly(ADP-ribose). J. Biol. Chem. *275*, 23234–23239.
Oestergaard, V.H., and Lisby, M. (2016). TopBP1 makes the final call for repair on the verge of cell division. Mol Cell Oncol *3*, e1093066.
Ohashi, S., Kanai, M., Hanai, S., Uchiumi, F., Maruta, H., Tanuma, S., and Miwa, M. (2003). Subcellular localization of poly(ADP-ribose) glycohydrolase in mammalian cells. Biochem. Biophys. Res. Commun. *307*, 915–921.
Ojha, N.K., and Lole, K.S. (2016). Hepatitis E virus ORF1 encoded macro domain protein interacts with light chain subunit of human ferritin and inhibits its secretion. Mol. Cell. Biochem. *417*, 75–85.
Okita, N., Ashizawa, D., Ohta, R., Abe, H., and Tanuma, S. (2010). Discovery of novel poly(ADP-ribose) glycohydrolase inhibitors by a quantitative assay system using dot-blot with anti-poly(ADP-ribose). Biochem. Biophys. Res. Commun. *392*, 485–489.

Oksenych, V., and Coin, F. (2010). The long unwinding road: XPB and XPD helicases in damaged DNA opening. Cell Cycle *9*, 90–96.
Olson, E., Nievera, C.J., Klimovich, V., Fanning, E., and Wu, X. (2006). RPA2 is a direct downstream target for ATR to regulate the S-phase checkpoint. J. Biol. Chem. *281*, 39517–39533.
O'Neil, N.J., van Pel, D.M., and Hieter, P. (2013). Synthetic lethality and cancer: cohesin and PARP at the replication fork. Trends Genet. *29*, 290–297.
Ono, T., Kasamatsu, A., Oka, S., and Moss, J. (2006). The 39-kDa poly(ADP-ribose) glycohydrolase ARH3 hydrolyzes O-acetyl-ADP-ribose, a product of the Sir2 family of acetyl-histone deacetylases. Proc. Natl. Acad. Sci. U.S.A. *103*, 16687–16691.
Orrenius, S., Nicotera, P., and Zhivotovsky, B. (2011). Cell death mechanisms and their implications in toxicology. Toxicol. Sci. *119*, 3–19.
Ozaki, Y., Matsui, H., Asou, H., Nagamachi, A., Aki, D., Honda, H., Yasunaga, S. 'ichiro, Takihara, Y., Yamamoto, T., Izumi, S., et al. (2012). Poly-ADP ribosylation of Miki by tankyrase-1 promotes centrosome maturation. Mol. Cell *47*, 694–706.
Pachkowski, B.F., Tano, K., Afonin, V., Elder, R.H., Takeda, S., Watanabe, M., Swenberg, J.A., and Nakamura, J. (2009). Cells deficient in PARP-1 show an accelerated accumulation of DNA single strand breaks, but not AP sites, over the PARP-1-proficient cells exposed to MMS. Mutat. Res. *671*, 93–99.
Paddock, M.N., Bauman, A.T., Higdon, R., Kolker, E., Takeda, S., and Scharenberg, A.M. (2011). Competition between PARP-1 and Ku70 control the decision between high-fidelity and mutagenic DNA repair. DNA Repair (Amst.) *10*, 338–343.
Palazzo, L., Daniels, C.M., Nettleship, J.E., Rahman, N., McPherson, R.L., Ong, S.-E., Kato, K., Nureki, O., Leung, A.K.L., and Ahel, I. (2016). ENPP1 processes protein ADP-ribosylation in vitro. FEBS J. *283*, 3371–3388.
Palle, K., and Vaziri, C. (2011). Rad18 E3 ubiquitin ligase activity mediates Fanconi anemia pathway activation and cell survival following DNA Topoisomerase 1 inhibition. Cell Cycle *10*, 1625–1638.
Panda, S., Poirier, G.G., and Kay, S.A. (2002). tej defines a role for poly(ADP-ribosyl)ation in establishing period length of the arabidopsis circadian oscillator. Dev. Cell *3*, 51–61.
Pankotai, T., Bonhomme, C., Chen, D., and Soutoglou, E. (2012). DNAPKcs-dependent arrest of RNA polymerase II transcription in the presence of DNA breaks. Nat. Struct. Mol. Biol. *19*, 276–282.
Pascal, J.M., and Ellenberger, T. (2015). The rise and fall of poly(ADP-ribose): An enzymatic perspective. DNA Repair (Amst.) *32*, 10–16.
Patel, A.G., Sarkaria, J.N., and Kaufmann, S.H. (2011). Nonhomologous end joining drives poly(ADP-ribose) polymerase (PARP) inhibitor lethality in homologous recombination-deficient cells. PNAS *108*, 3406–3411.
Patel, C.N., Koh, D.W., Jacobson, M.K., and Oliveira, M.A. (2005a). Identification of three critical acidic residues of poly(ADP-ribose) glycohydrolase involved in catalysis: determining the PARG catalytic domain. Biochem. J. *388*, 493–500.
Patel, N.S.A., Cortes, U., Di Poala, R., Mazzon, E., Mota-Filipe, H., Cuzzocrea, S., Wang, Z.-Q., and Thiemermann, C. (2005b). Mice lacking the 110-kD isoform of poly(ADP-ribose) glycohydrolase are protected against renal ischemia/reperfusion injury. J. Am. Soc. Nephrol. *16*, 712–719.
Patrick, S.M., Oakley, G.G., Dixon, K., and Turchi, J.J. (2005). DNA damage induced hyperphosphorylation of replication protein A. 2. Characterization of DNA binding activity, protein interactions, and activity in DNA replication and repair. Biochemistry *44*, 8438–8448.
Paudyal, S.C., and You, Z. (2016). Sharpening the ends for repair: mechanisms and regulation of DNA resection. Acta Biochim. Biophys. Sin. (Shanghai) *48*, 647–657.
Pellegrino, S., and Altmeyer, M. (2016). Interplay between Ubiquitin, SUMO, and Poly(ADP-Ribose) in the Cellular Response to Genotoxic Stress. Front Genet *7*, 63.
Perry, J., and Kleckner, N. (2003). The ATRs, ATMs, and TORs are giant HEAT repeat proteins. Cell *112*, 151–155.
Pettitt, S.J., Rehman, F.L., Bajrami, I., Brough, R., Wallberg, F., Kozarewa, I., Fenwick, K., Assiotis, I., Chen, L., Campbell, J., et al. (2013). A genetic screen using the PiggyBac transposon in haploid cells identifies Parp1 as a mediator of olaparib toxicity. PLoS ONE *8*, e61520.
Piao, L., Fujioka, K., Nakakido, M., and Hamamoto, R. (2018). Regulation of poly(ADP-Ribose) polymerase 1 functions by post-translational modifications. Front Biosci (Landmark Ed) *23*, 13–26.
Pines, A., Vrouwe, M.G., Marteijn, J.A., Typas, D., Luijsterburg, M.S., Cansoy, M., Hensbergen, P., Deelder, A., de Groot, A., Matsumoto, S., et al. (2012). PARP1 promotes nucleotide excision repair through DDB2 stabilization and recruitment of ALC1. J. Cell Biol. *199*, 235–249.
Pleschke, J.M., Kleczkowska, H.E., Strohm, M., and Althaus, F.R. (2000). Poly(ADP-ribose) Binds to Specific Domains in DNA Damage Checkpoint Proteins. J. Biol. Chem. *275*, 40974–40980.

Poirier, G.G., de Murcia, G., Jongstra-Bilen, J., Niedergang, C., and Mandel, P. (1982). Poly(ADP-ribosyl)ation of polynucleosomes causes relaxation of chromatin structure. Proc. Natl. Acad. Sci. U.S.A. *79*, 3423–3427.
Poli, J., Gasser, S.M., and Papamichos-Chronakis, M. (2017). The INO80 remodeller in transcription, replication and repair. Philos. Trans. R. Soc. Lond., B, Biol. Sci. *372*.
Polo, S.E., and Jackson, S.P. (2011). Dynamics of DNA damage response proteins at DNA breaks: a focus on protein modifications. Genes Dev. *25*, 409–433.
Polo, S.E., Kaidi, A., Baskcomb, L., Galanty, Y., and Jackson, S.P. (2010). Regulation of DNA-damage responses and cell-cycle progression by the chromatin remodelling factor CHD4. EMBO J. *29*, 3130–3139.
Pommier, Y., Leo, E., Zhang, H., and Marchand, C. (2010). DNA topoisomerases and their poisoning by anticancer and antibacterial drugs. Chem. Biol. *17*, 421–433.
Pommier, Y., Huang, S.N., Gao, R., Das, B.B., Murai, J., and Marchand, C. (2014). Tyrosyl-DNA-phosphodiesterases (TDP1 and TDP2). DNA Repair (Amst.) *19*, 114–129.
Pommier, Y., O'Connor, M.J., and de Bono, J. (2016). Laying a trap to kill cancer cells: PARP inhibitors and their mechanisms of action. Sci Transl Med *8*, 362ps17.
Poot, R.A., Bozhenok, L., van den Berg, D.L.C., Steffensen, S., Ferreira, F., Grimaldi, M., Gilbert, N., Ferreira, J., and Varga-Weisz, P.D. (2004). The Williams syndrome transcription factor interacts with PCNA to target chromatin remodelling by ISWI to replication foci. Nat. Cell Biol. *6*, 1236–1244.
Poot, R.A., Bozhenok, L., van den Berg, D.L.C., Hawkes, N., and Varga-Weisz, P.D. (2005). Chromatin remodeling by WSTF-ISWI at the replication site: opening a window of opportunity for epigenetic inheritance? Cell Cycle *4*, 543–546.
Popp, O., Veith, S., Fahrer, J., Bohr, V.A., Bürkle, A., and Mangerich, A. (2013). Site-specific noncovalent interaction of the biopolymer poly(ADP-ribose) with the Werner syndrome protein regulates protein functions. ACS Chem. Biol. *8*, 179–188.
Posavec Marjanović, M., Crawford, K., and Ahel, I. (2017). PARP, transcription and chromatin modeling. Semin. Cell Dev. Biol. *63*, 102–113.
Prabakaran, S., Lippens, G., Steen, H., and Gunawardena, J. (2012). Post-translational modification: nature's escape from genetic imprisonment and the basis for dynamic information encoding. Wiley Interdiscip Rev Syst Biol Med *4*, 565–583.
Prasad, R., Dyrkheeva, N., Williams, J., and Wilson, S.H. (2015). Mammalian Base Excision Repair: Functional Partnership between PARP-1 and APE1 in AP-Site Repair. PLoS ONE *10*, e0124269.
Qi, G., Kudo, Y., Tang, B., Liu, T., Jin, S., Liu, J., Zuo, X., Mi, S., Shao, W., Ma, X., et al. (2016). PARP6 acts as a tumor suppressor via downregulating Survivin expression in colorectal cancer. Oncotarget *7*, 18812–18824.
Quan, J., and Yusufzai, T. (2014). HARP preferentially co-purifies with RPA bound to DNA-PK and blocks RPA phosphorylation. Epigenetics *9*, 693–697.
Rack, J.G.M., Perina, D., and Ahel, I. (2016). Macrodomains: Structure, Function, Evolution, and Catalytic Activities. Annu. Rev. Biochem. *85*, 431–454.
Raghunandan, M., Chaudhury, I., Kelich, S.L., Hanenberg, H., and Sobeck, A. (2015). FANCD2, FANCJ and BRCA2 cooperate to promote replication fork recovery independently of the Fanconi Anemia core complex. Cell Cycle *14*, 342–353.
Raval-Fernandes, S., Kickhoefer, V.A., Kitchen, C., and Rome, L.H. (2005). Increased susceptibility of vault poly(ADP-ribose) polymerase-deficient mice to carcinogen-induced tumorigenesis. Cancer Res. *65*, 8846–8852.
Ray Chaudhuri, A., and Nussenzweig, A. (2017). The multifaceted roles of PARP1 in DNA repair and chromatin remodelling. Nat. Rev. Mol. Cell Biol. *18*, 610–621.
Ray Chaudhuri, A., Ahuja, A.K., Herrador, R., and Lopes, M. (2015). Poly(ADP-Ribosyl) Glycohydrolase Prevents the Accumulation of Unusual Replication Structures during Unperturbed S Phase. Mol Cell Biol *35*, 856–865.
Rector, J., Kapil, S., Treude, K.J., Kumm, P., Glanzer, J.G., Byrne, B.M., Liu, S., Smith, L.M., DiMaio, D.J., Giannini, P., et al. (2017). S4S8-RPA phosphorylation as an indicator of cancer progression in oral squamous cell carcinomas. Oncotarget *8*, 9243–9250.
Reinhardt, H.C., and Yaffe, M.B. (2013). Phospho-Ser/Thr-binding domains: navigating the cell cycle and DNA damage response. Nat. Rev. Mol. Cell Biol. *14*, 563–580.
Reynolds, P., Cooper, S., Lomax, M., and O'Neill, P. (2015). Disruption of PARP1 function inhibits base excision repair of a sub-set of DNA lesions. Nucleic Acids Res. *43*, 4028–4038.
Rippmann, J.F., Damm, K., and Schnapp, A. (2002). Functional characterization of the poly(ADP-ribose) polymerase activity of tankyrase 1, a potential regulator of telomere length. J. Mol. Biol. *323*, 217–224.
Rissel, D., Heym, P.P., Thor, K., Brandt, W., Wessjohann, L.A., and Peiter, E. (2017). No Silver Bullet - Canonical Poly(ADP-Ribose) Polymerases (PARPs) Are No Universal Factors of Abiotic and Biotic Stress Resistance of Arabidopsis thaliana. Front Plant Sci *8*, 59.

Rivera-Calzada, A., Spagnolo, L., Pearl, L.H., and Llorca, O. (2007). Structural model of full-length human Ku70-Ku80 heterodimer and its recognition of DNA and DNA-PKcs. EMBO Rep. *8*, 56–62.
Robert, I., Dantzer, F., and Reina-San-Martin, B. (2009). Parp1 facilitates alternative NHEJ, whereas Parp2 suppresses IgH/c-myc translocations during immunoglobulin class switch recombination. J. Exp. Med. *206*, 1047–1056.
Robert, I., Gaudot, L., Rogier, M., Heyer, V., Noll, A., Dantzer, F., and Reina-San-Martin, B. (2015). Parp3 negatively regulates immunoglobulin class switch recombination. PLoS Genet. *11*, e1005240.
Robert, I., Gaudot, L., Yélamos, J., Noll, A., Wong, H.-K., Dantzer, F., Schreiber, V., and Reina-San-Martin, B. (2017). Robust immunoglobulin class switch recombination and end joining in Parp9-deficient mice. Eur. J. Immunol. *47*, 665–676.
Robu, M., Shah, R.G., Purohit, N.K., Zhou, P., Naegeli, H., and Shah, G.M. (2017). Poly(ADP-ribose) polymerase 1 escorts XPC to UV-induced DNA lesions during nucleotide excision repair. Proc. Natl. Acad. Sci. U.S.A. *114*, E6847–E6856.
Rodríguez-Vargas, J.M., Ruiz-Magaña, M.J., Ruiz-Ruiz, C., Majuelos-Melguizo, J., Peralta-Leal, A., Rodríguez, M.I., Muñoz-Gámez, J.A., de Almodóvar, M.R., Siles, E., Rivas, A.L., et al. (2012). ROS-induced DNA damage and PARP-1 are required for optimal induction of starvation-induced autophagy. Cell Res. *22*, 1181–1198.
Rosenthal, F., Feijs, K.L.H., Frugier, E., Bonalli, M., Forst, A.H., Imhof, R., Winkler, H.C., Fischer, D., Caflisch, A., Hassa, P.O., et al. (2013). Macrodomain-containing proteins are new mono-ADP-ribosylhydrolases. Nat. Struct. Mol. Biol. *20*, 502–507.
Rosidi, B., Wang, M., Wu, W., Sharma, A., Wang, H., and Iliakis, G. (2008). Histone H1 functions as a stimulatory factor in backup pathways of NHEJ. Nucleic Acids Res. *36*, 1610–1623.
Rouillon, C., and White, M.F. (2011). The evolution and mechanisms of nucleotide excision repair proteins. Res. Microbiol. *162*, 19–26.
Rouleau, M., McDonald, D., Gagné, P., Ouellet, M.-E., Droit, A., Hunter, J.M., Dutertre, S., Prigent, C., Hendzel, M.J., and Poirier, G.G. (2007). PARP-3 associates with polycomb group bodies and with components of the DNA damage repair machinery. J. Cell. Biochem. *100*, 385–401.
Rouleau, M., Saxena, V., Rodrigue, A., Paquet, E.R., Gagnon, A., Hendzel, M.J., Masson, J.-Y., Ekker, M., and Poirier, G.G. (2011). A key role for poly(ADP-ribose) polymerase 3 in ectodermal specification and neural crest development. PLoS ONE *6*, e15834.
Ruscetti, T., Lehnert, B.E., Halbrook, J., Le Trong, H., Hoekstra, M.F., Chen, D.J., and Peterson, S.R. (1998). Stimulation of the DNA-dependent protein kinase by poly(ADP-ribose) polymerase. J. Biol. Chem. *273*, 14461–14467.
Saberi, A., Hochegger, H., Szuts, D., Lan, L., Yasui, A., Sale, J.E., Taniguchi, Y., Murakawa, Y., Zeng, W., Yokomori, K., et al. (2007). RAD18 and poly(ADP-ribose) polymerase independently suppress the access of nonhomologous end joining to double-strand breaks and facilitate homologous recombination-mediated repair. Mol. Cell. Biol. *27*, 2562–2571.
Sala, A., La Rocca, G., Burgio, G., Kotova, E., Di Gesù, D., Collesano, M., Ingrassia, A.M.R., Tulin, A.V., and Corona, D.F.V. (2008). The nucleosome-remodeling ATPase ISWI is regulated by poly-ADP-ribosylation. PLoS Biol. *6*, e252.
Sale, J.E. (2012). Competition, collaboration and coordination--determining how cells bypass DNA damage. J. Cell. Sci. *125*, 1633–1643.
Sale, J.E., Lehmann, A.R., and Woodgate, R. (2012). Y-family DNA polymerases and their role in tolerance of cellular DNA damage. Nat. Rev. Mol. Cell Biol. *13*, 141–152.
Satoh, M.S., and Lindahl, T. (1992). Role of poly(ADP-ribose) formation in DNA repair. Nature *356*, 356–358.
Savage, N. (2015). Proteomics: High-protein research. Nature *527*, S6-7.
Schlacher, K., Wu, H., and Jasin, M. (2012). A distinct replication fork protection pathway connects Fanconi anemia tumor suppressors to RAD51-BRCA1/2. Cancer Cell *22*, 106–116.
Schreiber, V., Amé, J.-C., Dollé, P., Schultz, I., Rinaldi, B., Fraulob, V., Ménissier-de Murcia, J., and de Murcia, G. (2002). Poly(ADP-ribose) polymerase-2 (PARP-2) is required for efficient base excision DNA repair in association with PARP-1 and XRCC1. J. Biol. Chem. *277*, 23028–23036.
Schreiber, V., Dantzer, F., Ame, J.-C., and de Murcia, G. (2006). Poly(ADP-ribose): novel functions for an old molecule. Nat. Rev. Mol. Cell Biol. *7*, 517–528.
Schuhwerk, H., Bruhn, C., Siniuk, K., Min, W., Erener, S., Grigaravicius, P., Krüger, A., Ferrari, E., Zubel, T., Lazaro, D., et al. (2017). Kinetics of poly(ADP-ribosyl)ation, but not PARP1 itself, determines the cell fate in response to DNA damage in vitro and in vivo. Nucleic Acids Res.
Schultz, N., Lopez, E., Saleh-Gohari, N., and Helleday, T. (2003). Poly(ADP-ribose) polymerase (PARP-1) has a controlling role in homologous recombination. Nucleic Acids Res. *31*, 4959–4964.

Serrano, M.A., Li, Z., Dangeti, M., Musich, P.R., Patrick, S., Roginskaya, M., Cartwright, B., and Zou, Y. (2013). DNA-PK, ATM and ATR collaboratively regulate p53-RPA interaction to facilitate homologous recombination DNA repair. Oncogene *32*, 2452–2462.
Shahrour, M.A., Nicolae, C.M., Edvardson, S., Ashhab, M., Galvan, A.M., Constantin, D., Abu-Libdeh, B., Moldovan, G.-L., and Elpeleg, O. (2016). PARP10 deficiency manifests by severe developmental delay and DNA repair defect. Neurogenetics *17*, 227–232.
Shall, S., and de Murcia, G. (2000). Poly(ADP-ribose) polymerase-1: what have we learned from the deficient mouse model? Mutat. Res. *460*, 1–15.
Shao, R.G., Cao, C.X., Zhang, H., Kohn, K.W., Wold, M.S., and Pommier, Y. (1999). Replication-mediated DNA damage by camptothecin induces phosphorylation of RPA by DNA-dependent protein kinase and dissociates RPA:DNA-PK complexes. EMBO J. *18*, 1397–1406.
Sharifi, R., Morra, R., Appel, C.D., Tallis, M., Chioza, B., Jankevicius, G., Simpson, M.A., Matic, I., Ozkan, E., Golia, B., et al. (2013). Deficiency of terminal ADP-ribose protein glycohydrolase TARG1/C6orf130 in neurodegenerative disease. EMBO J. *32*, 1225–1237.
Shen, X., Wang, W., Wang, L., Houde, C., Wu, W., Tudor, M., Thompson, J.R., Sisk, C.M., Hubbard, B., and Li, J. (2012). Identification of genes affecting apolipoprotein B secretion following siRNA-mediated gene knockdown in primary human hepatocytes. Atherosclerosis *222*, 154–157.
Shi, W., Feng, Z., Zhang, J., Gonzalez-Suarez, I., Vanderwaal, R.P., Wu, X., Powell, S.N., Roti, R., L, J., Gonzalo, S., et al. (2010). The role of RPA2 phosphorylation in homologous recombination in response to replication arrest. Carcinogenesis *31*, 994–1002.
Shibata, A. (2017). Regulation of repair pathway choice at two-ended DNA double-strand breaks. Mutat. Res. *803–805*, 51–55.
Shieh, W.M., Amé, J.C., Wilson, M.V., Wang, Z.Q., Koh, D.W., Jacobson, M.K., and Jacobson, E.L. (1998). Poly(ADP-ribose) polymerase null mouse cells synthesize ADP-ribose polymers. J. Biol. Chem. *273*, 30069–30072.
Shiloh, Y., and Ziv, Y. (2013). The ATM protein kinase: regulating the cellular response to genotoxic stress, and more. Nat. Rev. Mol. Cell Biol. *14*, 197–210.
Shimokawa, T., Masutani, M., Nagasawa, S., Nozaki, T., Ikota, N., Aoki, Y., Nakagama, H., and Sugimura, T. (1999). Isolation and cloning of rat poly(ADP-ribose) glycohydrolase: presence of a potential nuclear export signal conserved in mammalian orthologs. J. Biochem. *126*, 748–755.
Shimoyama, M., Ohota, M., Kakehi, K., and Ueda, I. (1970). Increase of NAD glycohydrolase activity and decrease of NAD concentration in rat liver during fasting. Biochim. Biophys. Acta *215*, 207–209.
Shiomi, N., Mori, M., Tsuji, H., Imai, T., Inoue, H., Tateishi, S., Yamaizumi, M., and Shiomi, T. (2007). Human RAD18 is involved in S phase-specific single-strand break repair without PCNA monoubiquitination. Nucleic Acids Res *35*, e9.
Sibanda, B.L., Chirgadze, D.Y., Ascher, D.B., and Blundell, T.L. (2017). DNA-PKcs structure suggests an allosteric mechanism modulating DNA double-strand break repair. Science *355*, 520–524.
Sims, J.L., Berger, S.J., and Berger, N.A. (1983). Poly(ADP-ribose) Polymerase inhibitors preserve nicotinamide adenine dinucleotide and adenosine 5'-triphosphate pools in DNA-damaged cells: mechanism of stimulation of unscheduled DNA synthesis. Biochemistry *22*, 5188–5194.
Slade, D., Dunstan, M.S., Barkauskaite, E., Weston, R., Lafite, P., Dixon, N., Ahel, M., Leys, D., and Ahel, I. (2011). The structure and catalytic mechanism of a poly(ADP-ribose) glycohydrolase. Nature *477*, 616–620.
Slama, J.T., Aboul-Ela, N., Goli, D.M., Cheesman, B.V., Simmons, A.M., and Jacobson, M.K. (1995). Specific inhibition of poly(ADP-ribose) glycohydrolase by adenosine diphosphate (hydroxymethyl)pyrrolidinediol. J. Med. Chem. *38*, 389–393.
Sokka, M., Parkkinen, S., Pospiech, H., and Syväoja, J.E. (2010). Function of TopBP1 in genome stability. Subcell. Biochem. *50*, 119–141.
Song, I.Y., Palle, K., Gurkar, A., Tateishi, S., Kupfer, G.M., and Vaziri, C. (2010). Rad18-mediated translesion synthesis of bulky DNA adducts is coupled to activation of the Fanconi anemia DNA repair pathway. J. Biol. Chem. *285*, 31525–31536.
Spagnolo, L., Barbeau, J., Curtin, N.J., Morris, E.P., and Pearl, L.H. (2012). Visualization of a DNA-PK/PARP1 complex. Nucleic Acids Res. *40*, 4168–4177.
Spivak, G. (2016). Transcription-coupled repair: an update. Arch. Toxicol. *90*, 2583–2594.
Stadler, J., and Richly, H. (2017). Regulation of DNA Repair Mechanisms: How the Chromatin Environment Regulates the DNA Damage Response. Int J Mol Sci *18*.
von Stechow, L., and Olsen, J.V. (2017). Proteomics insights into DNA damage response and translating this knowledge to clinical strategies. Proteomics *17*.

Steffen, J.D., Coyle, D.L., Damodaran, K., Beroza, P., and Jacobson, M.K. (2011). Discovery and structure-activity relationships of modified salicylanilides as cell permeable inhibitors of poly(ADP-ribose) glycohydrolase (PARG). J. Med. Chem. *54*, 5403–5413.
Steffen, J.D., Tholey, R.M., Langelier, M.-F., Planck, J.L., Schiewer, M.J., Lal, S., Bildzukewicz, N.A., Yeo, C.J., Knudsen, K.E., Brody, J.R., et al. (2014). Targeting PARP-1 allosteric regulation offers therapeutic potential against cancer. Cancer Res. *74*, 31–37.
Steiner, E., Holzmann, K., Elbling, L., Micksche, M., and Berger, W. (2006). Cellular functions of vaults and their involvement in multidrug resistance. Curr Drug Targets *7*, 923–934.
Stilmann, M., Hinz, M., Arslan, S.C., Zimmer, A., Schreiber, V., and Scheidereit, C. (2009). A nuclear poly(ADP-ribose)-dependent signalosome confers DNA damage-induced IkappaB kinase activation. Mol. Cell *36*, 365–378.
Strickfaden, H., McDonald, D., Kruhlak, M.J., Haince, J.-F., Th'ng, J.P.H., Rouleau, M., Ishibashi, T., Corry, G.N., Ausio, J., Underhill, D.A., et al. (2016). Poly(ADP-ribosyl)ation-dependent Transient Chromatin Decondensation and Histone Displacement following Laser Microirradiation. J. Biol. Chem. *291*, 1789–1802.
Sugimura, K., Takebayashi, S.-I., Taguchi, H., Takeda, S., and Okumura, K. (2008). PARP-1 ensures regulation of replication fork progression by homologous recombination on damaged DNA. J. Cell Biol. *183*, 1203–1212.
Sukhanova, M., Khodyreva, S., and Lavrik, O. (2010). Poly(ADP-ribose) polymerase 1 regulates activity of DNA polymerase beta in long patch base excision repair. Mutat. Res. *685*, 80–89.
Sun, Y., Zhang, T., Wang, B., Li, H., and Li, P. (2012). Tannic acid, an inhibitor of poly(ADP-ribose) glycohydrolase, sensitizes ovarian carcinoma cells to cisplatin. Anticancer Drugs *23*, 979–990.
Sy, S.M.H., Huen, M.S.Y., and Chen, J. (2009). PALB2 is an integral component of the BRCA complex required for homologous recombination repair. Proc. Natl. Acad. Sci. U.S.A. *106*, 7155–7160.
Symington, L.S. (2016). Mechanism and regulation of DNA end resection in eukaryotes. Crit. Rev. Biochem. Mol. Biol. *51*, 195–212.
Taglialatela, A., Alvarez, S., Leuzzi, G., Sannino, V., Ranjha, L., Huang, J.-W., Madubata, C., Anand, R., Levy, B., Rabadan, R., et al. (2017). Restoration of Replication Fork Stability in BRCA1- and BRCA2-Deficient Cells by Inactivation of SNF2-Family Fork Remodelers. Mol. Cell *68*, 414–430.e8.
Talens, F., Jalving, M., Gietema, J.A., and Van Vugt, M.A. (2017). Therapeutic targeting and patient selection for cancers with homologous recombination defects. Expert Opin Drug Discov *12*, 565–581.
Talhaoui, I., Lebedeva, N.A., Zarkovic, G., Saint-Pierre, C., Kutuzov, M.M., Sukhanova, M.V., Matkarimov, B.T., Gasparutto, D., Saparbaev, M.K., Lavrik, O.I., et al. (2016). Poly(ADP-ribose) polymerases covalently modify strand break termini in DNA fragments in vitro. Nucleic Acids Res. *44*, 9279–9295.
Tallis, M., Morra, R., Barkauskaite, E., and Ahel, I. (2014). Poly(ADP-ribosyl)ation in regulation of chromatin structure and the DNA damage response. Chromosoma *123*, 79–90.
Tanuma, S., Sakagami, H., and Endo, H. (1989). Inhibitory effect of tannin on poly(ADP-ribose) glycohydrolase from human placenta. Biochem. Int. *18*, 701–708.
Tavassoli, M., Tavassoli, M.H., and Shall, S. (1985). Effect of DNA intercalators on poly(ADP-ribose) glycohydrolase activity. Biochim. Biophys. Acta *827*, 228–234.
Teloni, F., and Altmeyer, M. (2016). Readers of poly(ADP-ribose): designed to be fit for purpose. Nucleic Acids Res. *44*, 993–1006.
Tentori, L., Leonetti, C., Scarsella, M., Muzi, A., Vergati, M., Forini, O., Lacal, P.M., Ruffini, F., Gold, B., Li, W., et al. (2005). Poly(ADP-ribose) glycohydrolase inhibitor as chemosensitiser of malignant melanoma for temozolomide. Eur. J. Cancer *41*, 2948–2957.
Teoh, S.T., and Lunt, S.Y. (2017). Metabolism in cancer metastasis: bioenergetics, biosynthesis, and beyond. Wiley Interdiscip Rev Syst Biol Med.
Tercero, J.A., and Diffley, J.F. (2001). Regulation of DNA replication fork progression through damaged DNA by the Mec1/Rad53 checkpoint. Nature *412*, 553–557.
Thompson, E.L., Yeo, J.E., Lee, E.-A., Kan, Y., Raghunandan, M., Wiek, C., Hanenberg, H., Schärer, O.D., Hendrickson, E.A., and Sobeck, A. (2017). FANCI and FANCD2 have common as well as independent functions during the cellular replication stress response. Nucleic Acids Res.
Thorslund, T., von Kobbe, C., Harrigan, J.A., Indig, F.E., Christiansen, M., Stevnsner, T., and Bohr, V.A. (2005). Cooperation of the Cockayne syndrome group B protein and poly(ADP-ribose) polymerase 1 in the response to oxidative stress. Mol. Cell. Biol. *25*, 7625–7636.
Thorvaldsen, T.E. (2017). Targeting Tankyrase to Fight WNT-dependent Tumours. Basic Clin. Pharmacol. Toxicol. *121*, 81–88.
Tikoo, K., Sane, M.S., and Gupta, C. (2011). Tannic acid ameliorates doxorubicin-induced cardiotoxicity and potentiates its anti-cancer activity: potential role of tannins in cancer chemotherapy. Toxicol. Appl. Pharmacol. *251*, 191–200.

Timinszky, G., Till, S., Hassa, P.O., Hothorn, M., Kustatscher, G., Nijmeijer, B., Colombelli, J., Altmeyer, M., Stelzer, E.H.K., Scheffzek, K., et al. (2009). A macrodomain-containing histone rearranges chromatin upon sensing PARP1 activation. Nat Struct Mol Biol *16*, 923–929.
Tischler, J., Lehner, B., and Fraser, A.G. (2008). Evolutionary plasticity of genetic interaction networks. Nat Genet *40*, 390–391.
Toledo, L.I., Altmeyer, M., Rask, M.-B., Lukas, C., Larsen, D.H., Povlsen, L.K., Bekker-Jensen, S., Mailand, N., Bartek, J., and Lukas, J. (2013). ATR prohibits replication catastrophe by preventing global exhaustion of RPA. Cell *155*, 1088–1103.
Tong, L., and Denu, J.M. (2010). Function and metabolism of sirtuin metabolite O-acetyl-ADP-ribose. Biochim. Biophys. Acta *1804*, 1617–1625.
Tripathi, K., Mani, C., Clark, D.W., and Palle, K. (2016). Rad18 is required for functional interactions between FANCD2, BRCA2, and Rad51 to repair DNA topoisomerase 1-poisons induced lesions and promote fork recovery. Oncotarget *7*, 12537–12553.
Tsai, Y.J., Abe, H., Maruta, H., Hatano, T., Nishina, H., Sakagami, H., Okuda, T., and Tanuma, S. (1991). Effects of chemically defined tannins on poly (ADP-ribose) glycohydrolase activity. Biochem. Int. *24*, 889–897.
Tsanov, N., Kermi, C., Coulombe, P., Van der Laan, S., Hodroj, D., and Maiorano, D. (2014). PIP degron proteins, substrates of CRL4Cdt2, and not PIP boxes, interfere with DNA polymerase η and κ focus formation on UV damage. Nucleic Acids Res. *42*, 3692–3706.
Tubbs, A., and Nussenzweig, A. (2017). Endogenous DNA Damage as a Source of Genomic Instability in Cancer. Cell *168*, 644–656.
Tucker, J.A., Bennett, N., Brassington, C., Durant, S.T., Hassall, G., Holdgate, G., McAlister, M., Nissink, J.W.M., Truman, C., and Watson, M. (2012). Structures of the human poly (ADP-ribose) glycohydrolase catalytic domain confirm catalytic mechanism and explain inhibition by ADP-HPD derivatives. PLoS ONE *7*, e50889.
Tuduri, S., Crabbé, L., Conti, C., Tourrière, H., Holtgreve-Grez, H., Jauch, A., Pantesco, V., De Vos, J., Thomas, A., Theillet, C., et al. (2009). Topoisomerase I suppresses genomic instability by preventing interference between replication and transcription. Nat. Cell Biol. *11*, 1315–1324.
Tulin, A., Naumova, N.M., Menon, A.K., and Spradling, A.C. (2006). Drosophila poly(ADP-ribose) glycohydrolase mediates chromatin structure and SIR2-dependent silencing. Genetics *172*, 363–371.
Tuncel, H., Tanaka, S., Oka, S., Nakai, S., Fukutomi, R., Okamoto, M., Ota, T., Kaneko, H., Tatsuka, M., and Shimamoto, F. (2012). PARP6, a mono(ADP-ribosyl) transferase and a negative regulator of cell proliferation, is involved in colorectal cancer development. Int. J. Oncol. *41*, 2079–2086.
Tuncer, S.K., Altinel, S., Toygar, M., Istanbulluoglu, H., Ates, K., Ogur, R., Altinel, O., Karslioglu, Y., Topal, T., Korkmaz, A., et al. (2016). Poly-ADP-ribose polymerase inhibition provides protection against lung injury in a rat paraquat toxicity model. Inflammopharmacology *24*, 155–161.
Tutt, A., Robson, M., Garber, J.E., Domchek, S.M., Audeh, M.W., Weitzel, J.N., Friedlander, M., Arun, B., Loman, N., Schmutzler, R.K., et al. (2010). Oral poly(ADP-ribose) polymerase inhibitor olaparib in patients with BRCA1 or BRCA2 mutations and advanced breast cancer: a proof-of-concept trial. Lancet *376*, 235–244.
Uchida, K., Uchida, M., Hanai, S., Ozawa, Y., Ami, Y., Kushida, S., and Miwa, M. (1993a). Isolation of the poly(ADP-ribose) polymerase-encoding cDNA from Xenopus laevis: phylogenetic conservation of the functional domains. Gene *137*, 293–297.
Uchida, K., Suzuki, H., Maruta, H., Abe, H., Aoki, K., Miwa, M., and Tanuma, S. (1993b). Preferential degradation of protein-bound (ADP-ribose)n by nuclear poly(ADP-ribose) glycohydrolase from human placenta. J. Biol. Chem. *268*, 3194–3200.
Vainonen, J.P., Shapiguzov, A., Vaattovaara, A., and Kangasjärvi, J. (2016). Plant PARPs, PARGs and PARP-like Proteins. Curr. Protein Pept. Sci. *17*, 713–723.
Vanderauwera, S., De Block, M., Van de Steene, N., van de Cotte, B., Metzlaff, M., and Van Breusegem, F. (2007). Silencing of poly(ADP-ribose) polymerase in plants alters abiotic stress signal transduction. Proc. Natl. Acad. Sci. U.S.A. *104*, 15150–15155.
Varnaitė, R., and MacNeill, S.A. (2016). Meet the neighbors: Mapping local protein interactomes by proximity-dependent labeling with BioID. Proteomics *16*, 2503–2518.
Vassin, V.M., Wold, M.S., and Borowiec, J.A. (2004). Replication protein A (RPA) phosphorylation prevents RPA association with replication centers. Mol. Cell. Biol. *24*, 1930–1943.
Vazquez, B.N., Thackray, J.K., and Serrano, L. (2017). Sirtuins and DNA damage repair: SIRT7 comes to play. Nucleus *8*, 107–115.
Veith, S., and Mangerich, A. (2015). RecQ helicases and PARP1 team up in maintaining genome integrity. Ageing Res. Rev. *23*, 12–28.

van de Ven, R.A.H., Santos, D., and Haigis, M.C. (2017). Mitochondrial Sirtuins and Molecular Mechanisms of Aging. Trends Mol Med *23*, 320–331.
Venkannagari, H., Fallarero, A., Feijs, K.L.H., Lüscher, B., and Lehtiö, L. (2013). Activity-based assay for human mono-ADP-ribosyltransferases ARTD7/PARP15 and ARTD10/PARP10 aimed at screening and profiling inhibitors. Eur J Pharm Sci *49*, 148–156.
Verdone, L., La Fortezza, M., Ciccarone, F., Caiafa, P., Zampieri, M., and Caserta, M. (2015). Poly(ADP-Ribosyl)ation Affects Histone Acetylation and Transcription. PLoS ONE *10*, e0144287.
Verheugd, P., Forst, A.H., Milke, L., Herzog, N., Feijs, K.L.H., Kremmer, E., Kleine, H., and Lüscher, B. (2013). Regulation of NF-κB signalling by the mono-ADP-ribosyltransferase ARTD10. Nat Commun *4*, 1683.
Verheugd, P., Bütepage, M., Eckei, L., and Lüscher, B. (2016). Players in ADP-ribosylation: Readers and Erasers. Curr. Protein Pept. Sci. *17*, 654–667.
Vermeulen, M., Mulder, K.W., Denissov, S., Pijnappel, W.W.M.P., van Schaik, F.M.A., Varier, R.A., Baltissen, M.P.A., Stunnenberg, H.G., Mann, M., and Timmers, H.T.M. (2007). Selective anchoring of TFIID to nucleosomes by trimethylation of histone H3 lysine 4. Cell *131*, 58–69.
Veuger, S.J., Curtin, N.J., Smith, G.C.M., and Durkacz, B.W. (2004). Effects of novel inhibitors of poly(ADP-ribose) polymerase-1 and the DNA-dependent protein kinase on enzyme activities and DNA repair. Oncogene *23*, 7322–7329.
Vida, A., Márton, J., Mikó, E., and Bai, P. (2017). Metabolic roles of poly(ADP-ribose) polymerases. Semin. Cell Dev. Biol. *63*, 135–143.
Villén, J., Beausoleil, S.A., Gerber, S.A., and Gygi, S.P. (2007). Large-scale phosphorylation analysis of mouse liver. Proc. Natl. Acad. Sci. U.S.A. *104*, 1488–1493.
Virág, L. (2013). 50Years of poly(ADP-ribosyl)ation. Molecular Aspects of Medicine *34*, 1043–1045.
Virág, L., Robaszkiewicz, A., Rodriguez-Vargas, J.M., and Oliver, F.J. (2013). Poly(ADP-ribose) signaling in cell death. Mol. Aspects Med. *34*, 1153–1167.
Vlastaridis, P., Kyriakidou, P., Chaliotis, A., Van de Peer, Y., Oliver, S.G., and Amoutzias, G.D. (2017). Estimating the total number of phosphoproteins and phosphorylation sites in eukaryotic proteomes. Gigascience *6*, 1–11.
Vodenicharov, M.D., Sallmann, F.R., Satoh, M.S., and Poirier, G.G. (2000). Base excision repair is efficient in cells lacking poly(ADP-ribose) polymerase 1. Nucleic Acids Res. *28*, 3887–3896.
Vyas, S., Chesarone-Cataldo, M., Todorova, T., Huang, Y.-H., and Chang, P. (2013). A systematic analysis of the PARP protein family identifies new functions critical for cell physiology. Nat Commun *4*, 2240.
Vyas, S., Matic, I., Uchima, L., Rood, J., Zaja, R., Hay, R.T., Ahel, I., and Chang, P. (2014). Family-wide analysis of poly(ADP-ribose) polymerase activity. Nat Commun *5*, 4426.
Wacker, D.A., Frizzell, K.M., Zhang, T., and Kraus, W.L. (2007). Regulation of chromatin structure and chromatin-dependent transcription by poly(ADP-ribose) polymerase-1: possible targets for drug-based therapies. Subcell. Biochem. *41*, 45–69.
Wang, H., Li, S., Luo, X., Song, Z., Long, X., and Zhu, X. (2017). Knockdown of PARP6 or survivin promotes cell apoptosis and inhibits cell invasion of colorectal adenocarcinoma cells. Oncol. Rep. *37*, 2245–2251.
Wang, M., Wu, W., Wu, W., Rosidi, B., Zhang, L., Wang, H., and Iliakis, G. (2006). PARP-1 and Ku compete for repair of DNA double strand breaks by distinct NHEJ pathways. Nucleic Acids Res. *34*, 6170–6182.
Wang, Y., Kim, N.S., Li, X., Greer, P.A., Koehler, R.C., Dawson, V.L., and Dawson, T.M. (2009a). Calpain activation is not required for AIF translocation in PARP-1-dependent cell death (parthanatos). J. Neurochem. *110*, 687–696.
Wang, Y., Dawson, V.L., and Dawson, T.M. (2009b). Poly(ADP-ribose) signals to mitochondrial AIF: a key event in parthanatos. Exp. Neurol. *218*, 193–202.
Wang, Y., Kim, N.S., Haince, J.-F., Kang, H.C., David, K.K., Andrabi, S.A., Poirier, G.G., Dawson, V.L., and Dawson, T.M. (2011a). Poly(ADP-ribose) (PAR) binding to apoptosis-inducing factor is critical for PAR polymerase-1-dependent cell death (parthanatos). Sci Signal *4*, ra20.
Wang, Y., Kim, N.S., Haince, J.-F., Kang, H.C., David, K.K., Andrabi, S.A., Poirier, G.G., Dawson, V.L., and Dawson, T.M. (2011b). Poly(ADP-ribose) (PAR) binding to apoptosis-inducing factor is critical for PAR polymerase-1-dependent cell death (parthanatos). Sci Signal *4*, ra20.
Wang, Z., Michaud, G.A., Cheng, Z., Zhang, Y., Hinds, T.R., Fan, E., Cong, F., and Xu, W. (2012). Recognition of the iso-ADP-ribose moiety in poly(ADP-ribose) by WWE domains suggests a general mechanism for poly(ADP-ribosyl)ation-dependent ubiquitination. Genes Dev. *26*, 235–240.
Wang, Z., Gagné, J.-P., Poirier, G.G., and Xu, W. (2014). Crystallographic and biochemical analysis of the mouse poly(ADP-ribose) glycohydrolase. PLoS ONE *9*, e86010.
Wang, Z.Q., Stingl, L., Morrison, C., Jantsch, M., Los, M., Schulze-Osthoff, K., and Wagner, E.F. (1997). PARP is important for genomic stability but dispensable in apoptosis. Genes Dev. *11*, 2347–2358.

Watanabe, F., Fukazawa, H., Masutani, M., Suzuki, H., Teraoka, H., Mizutani, S., and Uehara, Y. (2004). Poly(ADP-ribose) polymerase-1 inhibits ATM kinase activity in DNA damage response. Biochem. Biophys. Res. Commun. *319*, 596–602.
Weinfeld, M., Mani, R.S., Abdou, I., Aceytuno, R.D., and Glover, J.N.M. (2011). Tidying up loose ends: the role of polynucleotide kinase/phosphatase in DNA strand break repair. Trends Biochem. Sci. *36*, 262–271.
Weinstein, I.B. (2002). Cancer. Addiction to oncogenes--the Achilles heal of cancer. Science *297*, 63–64.
Welsby, I., Hutin, D., Gueydan, C., Kruys, V., Rongvaux, A., and Leo, O. (2014). PARP12, an interferon-stimulated gene involved in the control of protein translation and inflammation. J. Biol. Chem. *289*, 26642–26657.
Whatcott, C.J., Meyer-Ficca, M.L., Meyer, R.G., and Jacobson, M.K. (2009). A specific isoform of poly(ADP-ribose) glycohydrolase is targeted to the mitochondrial matrix by a N-terminal mitochondrial targeting sequence. Exp. Cell Res. *315*, 3477–3485.
Wojtowicz, K., Januchowski, R., Nowicki, M., and Zabel, M. (2017). vPARP Adjusts MVP Expression in Drug-resistant Cell Lines in Conjunction with MDR Proteins. Anticancer Res. *37*, 3015–3023.
Wollmann, Y., Schmidt, U., Wieland, G.D., Zipfel, P.F., Saluz, H.-P., and Hänel, F. (2007). The DNA topoisomerase IIbeta binding protein 1 (TopBP1) interacts with poly (ADP-ribose) polymerase (PARP-1). J. Cell. Biochem. *102*, 171–182.
Wright, R.H.G., Castellano, G., Bonet, J., Le Dily, F., Font-Mateu, J., Ballaré, C., Nacht, A.S., Soronellas, D., Oliva, B., and Beato, M. (2012). CDK2-dependent activation of PARP-1 is required for hormonal gene regulation in breast cancer cells. Genes Dev. *26*, 1972–1983.
Wu, B., Li, L., Huang, Y., Ma, J., and Min, J. (2017). Readers, writers and erasers of N(6)-methylated adenosine modification. Curr. Opin. Struct. Biol. *47*, 67–76.
Wu, X., Yang, Z., Liu, Y., and Zou, Y. (2005). Preferential localization of hyperphosphorylated replication protein A to double-strand break repair and checkpoint complexes upon DNA damage. Biochem. J. *391*, 473–480.
Xu, G., Chapman, J.R., Brandsma, I., Yuan, J., Mistrik, M., Bouwman, P., Bartkova, J., Gogola, E., Warmerdam, D., Barazas, M., et al. (2015). REV7 counteracts DNA double-strand break resection and affects PARP inhibition. Nature *521*, 541–544.
Yamada, T., Horimoto, H., Kameyama, T., Hayakawa, S., Yamato, H., Dazai, M., Takada, A., Kida, H., Bott, D., Zhou, A.C., et al. (2016). Constitutive aryl hydrocarbon receptor signaling constrains type I interferon-mediated antiviral innate defense. Nat. Immunol. *17*, 687–694.
Yan, Q., Dutt, S., Xu, R., Graves, K., Juszczynski, P., Manis, J.P., and Shipp, M.A. (2009). BBAP monoubiquitylates histone H4 at lysine 91 and selectively modulates the DNA damage response. Mol. Cell *36*, 110–120.
Yan, Q., Xu, R., Zhu, L., Cheng, X., Wang, Z., Manis, J., and Shipp, M.A. (2013). BAL1 and its partner E3 ligase, BBAP, link Poly(ADP-ribose) activation, ubiquitylation, and double-strand DNA repair independent of ATM, MDC1, and RNF8. Mol. Cell. Biol. *33*, 845–857.
Yang, X., and Qian, K. (2017). Protein O-GlcNAcylation: emerging mechanisms and functions. Nat. Rev. Mol. Cell Biol. *18*, 452–465.
Yang, C.-S., Jividen, K., Spencer, A., Dworak, N., Ni, L., Oostdyk, L.T., Chatterjee, M., Kuśmider, B., Reon, B., Parlak, M., et al. (2017a). Ubiquitin Modification by the E3 Ligase/ADP-Ribosyltransferase Dtx3L/Parp9. Molecular Cell *66*, 503–516.e5.
Yang, L., Ma, X., He, Y., Yuan, C., Chen, Q., Li, G., and Chen, X. (2017b). Sirtuin 5: a review of structure, known inhibitors and clues for developing new inhibitors. Sci China Life Sci *60*, 249–256.
Yang, Y., Liu, Z., Wang, F., Temviriyanukul, P., Ma, X., Tu, Y., Lv, L., Lin, Y.-F., Huang, M., Zhang, T., et al. (2015). FANCD2 and REV1 cooperate in the protection of nascent DNA strands in response to replication stress. Nucleic Acids Res. *43*, 8325–8339.
Yang, Y.-G., Cortes, U., Patnaik, S., Jasin, M., and Wang, Z.-Q. (2004). Ablation of PARP-1 does not interfere with the repair of DNA double-strand breaks, but compromises the reactivation of stalled replication forks. Oncogene *23*, 3872–3882.
Yata, K., Lloyd, J., Maslen, S., Bleuyard, J.-Y., Skehel, M., Smerdon, S.J., and Esashi, F. (2012). Plk1 and CK2 act in concert to regulate Rad51 during DNA double strand break repair. Mol. Cell *45*, 371–383.
Ying, S., Chen, Z., Medhurst, A.L., Neal, J.A., Bao, Z., Mortusewicz, O., McGouran, J., Song, X., Shen, H., Hamdy, F.C., et al. (2016). DNA-PKcs and PARP1 Bind to Unresected Stalled DNA Replication Forks Where They Recruit XRCC1 to Mediate Repair. Cancer Res. *76*, 1078–1088.
Yoshizaki, H., and Okuda, S. (2014). Elucidation of the evolutionary expansion of phosphorylation signaling networks using comparative phosphomotif analysis. BMC Genomics *15*, 546.
Yu, M., Schreek, S., Cerni, C., Schamberger, C., Lesniewicz, K., Poreba, E., Vervoorts, J., Walsemann, G., Grötzinger, J., Kremmer, E., et al. (2005). PARP-10, a novel Myc-interacting protein with poly(ADP-ribose) polymerase activity, inhibits transformation. Oncogene *24*, 1982–1993.

Yu, Y., Wang, W., Ding, Q., Ye, R., Chen, D., Merkle, D., Schriemer, D., Meek, K., and Lees-Miller, S.P. (2003). DNA-PK phosphorylation sites in XRCC4 are not required for survival after radiation or for V(D)J recombination. DNA Repair (Amst.) *2*, 1239–1252.
Yung, T.M.C., Sato, S., and Satoh, M.S. (2004). Poly(ADP-ribosyl)ation as a DNA damage-induced post-translational modification regulating poly(ADP-ribose) polymerase-1-topoisomerase I interaction. J. Biol. Chem. *279*, 39686–39696.
Zabka, T.S., Singh, J., Dhawan, P., Liederer, B.M., Oeh, J., Kauss, M.A., Xiao, Y., Zak, M., Lin, T., McCray, B., et al. (2015). Retinal toxicity, in vivo and in vitro, associated with inhibition of nicotinamide phosphoribosyltransferase. Toxicol. Sci. *144*, 163–172.
Zaja, R., Mikoč, A., Barkauskaite, E., and Ahel, I. (2012). Molecular Insights into Poly(ADP-ribose) Recognition and Processing. Biomolecules *3*, 1–17.
Zaniolo, K., Desnoyers, S., Leclerc, S., and Guérin, S.L. (2007). Regulation of poly(ADP-ribose) polymerase-1 (PARP-1) gene expression through the post-translational modification of Sp1: a nuclear target protein of PARP-1. BMC Mol. Biol. *8*, 96.
Zaremba, T., and Curtin, N.J. (2007). PARP inhibitor development for systemic cancer targeting. Anticancer Agents Med Chem *7*, 515–523.
Zellweger, R., Dalcher, D., Mutreja, K., Berti, M., Schmid, J.A., Herrador, R., Vindigni, A., and Lopes, M. (2015). Rad51-mediated replication fork reversal is a global response to genotoxic treatments in human cells. J Cell Biol *208*, 563–579.
Zeman, M.K., and Cimprich, K.A. (2014). Causes and consequences of replication stress. Nat. Cell Biol. *16*, 2–9.
Zhang, F., Chen, Y., Li, M., and Yu, X. (2014). The oligonucleotide/oligosaccharide-binding fold motif is a poly(ADP-ribose)-binding domain that mediates DNA damage response. Proc. Natl. Acad. Sci. U.S.A. *111*, 7278–7283.
Zhang, F., Shi, J., Bian, C., and Yu, X. (2015a). Poly(ADP-Ribose) Mediates the BRCA2-Dependent Early DNA Damage Response. Cell Rep *13*, 678–689.
Zhang, F., Shi, J., Chen, S.-H., Bian, C., and Yu, X. (2015b). The PIN domain of EXO1 recognizes poly(ADP-ribose) in DNA damage response. Nucleic Acids Res *43*, 10782–10794.
Zhang, Y., Liu, S., Mickanin, C., Feng, Y., Charlat, O., Michaud, G.A., Schirle, M., Shi, X., Hild, M., Bauer, A., et al. (2011). RNF146 is a poly(ADP-ribose)-directed E3 ligase that regulates axin degradation and Wnt signalling. Nat. Cell Biol. *13*, 623–629.
Zhang, Y., Mao, D., Roswit, W.T., Jin, X., Patel, A.C., Patel, D.A., Agapov, E., Wang, Z., Tidwell, R.M., Atkinson, J.J., et al. (2015c). PARP9-DTX3L ubiquitin ligase targets host histone H2BJ and viral 3C protease to enhance interferon signaling and control viral infection. Nat. Immunol. *16*, 1215–1227.
Zhou, H., Kawamura, K., Yanagihara, H., Kobayashi, J., and Zhang-Akiyama, Q.-M. (2017). NBS1 is regulated by two kind of mechanisms: ATM-dependent complex formation with MRE11 and RAD50, and cell cycle-dependent degradation of protein. J. Radiat. Res. *58*, 487–494.
Zhou, Z., Chan, C.H., Xiao, Z., and Tan, E. (2011). Ring finger protein 146/Iduna is a poly(ADP-ribose) polymer binding and PARsylation dependent E3 ubiquitin ligase. Cell Adh Migr *5*, 463–471.
Zhou, Z.-W., Liu, C., Li, T.-L., Bruhn, C., Krueger, A., Min, W., Wang, Z.-Q., and Carr, A.M. (2013). An essential function for the ATR-activation-domain (AAD) of TopBP1 in mouse development and cellular senescence. PLoS Genet. *9*, e1003702.
Zhu, Q., and Wani, A.A. (2017). Nucleotide Excision Repair: Finely Tuned Molecular Orchestra of Early Pre-incision Events. Photochem. Photobiol. *93*, 166–177.
Zhu, Y., and Gao, G. (2008). ZAP-mediated mRNA degradation. RNA Biol *5*, 65–67.
Zou, L., and Elledge, S.J. (2003). Sensing DNA damage through ATRIP recognition of RPA-ssDNA complexes. Science *300*, 1542–1548.
Zou, Y., Liu, Y., Wu, X., and Shell, S.M. (2006). Functions of human replication protein A (RPA): from DNA replication to DNA damage and stress responses. J. Cell. Physiol. *208*, 267–273.

APPENDIX

Appendix I:

Héberlé, E., Amé, J.-C., Illuzzi, G., Dantzer, F., and Schreiber, V. (2015). Discovery of the PARP Superfamily and Focus on the Lesser Exhibited But Not Lesser Talented Members. In PARP Inhibitors for Cancer Therapy, N.J. Curtin, and R.A. Sharma, eds. (Springer International Publishing), pp. 15–46.

Appendix II:

Schreiber, V., Illuzzi, G., Héberlé, E., and Dantzer, F. (2015). De la découverte du poly(ADP-ribose) aux inhibiteurs PARP en thérapie du cancer. Bulletin Du Cancer *102*, 863–873.

Appendix III:

Amé, J.-C., Héberlé, É., Camuzeaux, B., Dantzer, F., and Schreiber, V. (2017). Purification of Recombinant Human PARG and Activity Assays. Methods Mol. Biol. *1608*, 395–413.

Appendix IV:

French translation of the introductions and discussions of each project.

Chapter 2
Discovery of the PARP Superfamily and Focus on the Lesser Exhibited But Not Lesser Talented Members

Eléa Héberlé, Jean-Christophe Amé, Giuditta Illuzzi, Françoise Dantzer and Valérie Schreiber

Abstract Poly(ADP-ribosyl)ation is a post-translational modification of proteins in which ADP-ribose units are sequentially transferred from the substrate NAD^+ to acceptor proteins on glutamate, aspartate or lysine residues. The enzymes that catalyse this process are commonly called poly(ADP-ribose) polymerases or PARPs. In human, 17 proteins have been gathered in the PARP superfamily, based on their sequence homology with the catalytic domain of its founding member, PARP-1. In the first part of this chapter, we will recapitulate the history of the discovery of the PARP superfamily. Several excellent reviews have already presented biological processes involving PARP proteins, describing their involvement in DNA repair, transcription, post-transcriptional regulation, stress immunity and inflammation or cancer (Feijs KL, Verheugd P, Luscher B (2013) Expanding functions of intracellular resident mono- ADP-ribosylation in cell physiology. FEBS J 280(15):3519–3529; Kleine H, Luscher B (2009) Learning how to read ADP-ribosylation. Cell 139(1):17–19; Gibson BA, Kraus WL (2012) New insights into the molecular and cellular functions of poly(ADP-ribose) and PARPs. Nat Rev Mol Cell Biol 13(7):411–424; Welsby I, Hutin D, Leo O (2012) Complex roles of members of the ADP-ribosyl transferase super family in immune defences: looking beyond PARP1. Biochem Pharmacol 84(1):11–20; Chambon P, Weill JD, Mandel P (1963) Nicotinamide mononucleotide activation of new DNA-dependent polyadenylic acid synthesizing nuclear enzyme. Biochem Biophys Res Commun 11:39–43). During the past decades, researchers' attention has mainly focused on the DNA-damage dependent PARPs and on tankyrases. In the second part of this chapter, we have chosen to present an exhaustive and thorough description of each PARP family member that has not been widely portrayed so far. For this reason, we will not describe the DNA-damage dependent PARPs, PARP-1, -2 and -3, reviewed in two other chapters of this book (Chap. 3). We will also not detail the tankyrases TNKS1 and TNKS2, objects of a distinct chapter too (Chap. 4). We will

V. Schreiber (✉) · E. Héberlé · J.-C. Amé · G. Illuzzi · F. Dantzer
Biotechnology and Cell Signalling, UMR7242 CNRS, Université de Strasbourg, IREBS, Laboratory of Excellence Medalis, Equipe Labellisée Ligue contre le Cancer, ESBS, 300 Blvd Sébastien Brant, CS 10413, 67412 Illkirch, France
e-mail: valerie.schreiber@unistra.fr

© Springer International Publishing Switzerland 2015

N. J. Curtin, R. A. Sharma (eds.), *PARP Inhibitors for Cancer Therapy,*
Cancer Drug Discovery and Development 83, DOI 10.1007/978-3-319-14151-0_2

highlight the possible therapeutic avenues opened by the new biological roles that emerged for these highly promising PARP family members but still rather poorly characterized.

Keywords PARP family · MART · Macro domain · Zinc finger · Cancer · Immunity · Transcription · Antiviral activity · RNA metabolism · Stress response

2.1 Discovery of the PARP Superfamily (History, Characteristics, MART/PARPs, Nomenclature)

The activity of poly(ADP-ribosyl)ation (PARylation) responsible for the synthesis of poly(ADP-ribose) was first described by Chambon et al. [1] as a "new DNA-dependent polyadenylic acid synthesising nuclear enzyme" in rat liver nuclear extracts. This new compound was then identified as being poly(ADP-ribose) or PAR [2]. The first description of PARP was made by Sugimura et al. [3] and for almost 30 years, PARP was thought to be the only enzymatic activity responsible for that post-translational modification reaction, and has been studied initially mostly related to the DNA damage response. In response to DNA breaks, PARP uses NAD^+ to synthesise a linear or multibranched polymer of ADP-ribose onto various nuclear acceptor proteins or itself in an automodification reaction. The major benefit of this modification is that it facilitates DNA repair trough the opening of the chromatin structure, by modifying the histones and the recruitment of DNA repair proteins complexes to the DNA damaged sites. The importance of PARP in this process has been clearly demonstrated by the independent generation of PARP-deficient mouse models [4–6]. These animals or their derived cells showed hypersensitivity to DNA damage treatments (ionizing radiation, alkylating agents) [7]. However, the extensive analyses made with the embryonic fibroblasts derived from PARP-deficient mice unexpectedly showed that some PAR was still able to accumulate following treatment with the DNA alkylating agent MNNG as demonstrated by the Jacobson's lab in 1998 [8]. This result and other unpublished reports strongly suggested the existence of at least another enzymatic activity similar to that of PARP. In the plant *Arabidopsis thaliana* the first PARP-related polypeptide (APP) had a smaller molecular weight, 72 kDa, and displayed 60% similarity with the mammalian PARP [9]. Then a second gene was discovered with a molecular weight and a primary structure close to that of PARP and containing the classical Zn-fingers of the DNA binding site [10]. It became clear that PARP activity could exist as multiple forms but with representative sequence similarities at the level of the catalytic domain of the protein. A short time later, Tankyrase was identified and localized to human telomeres [11]. This protein of 142 kDa contains numerous ankyrin repeats with a C-terminal PARP catalytic domain capable to synthesise PAR independently from the presence of DNA. PARP-2 [12, 13] and PARP-3 were successively characterized, the first one responding to DNA damage in the nucleus, and the second, being localised to the centrosome [14]. The founding member of the PARP family was

therefore renamed PARP-1. Around the same time, vPARP (PARP-4) was identified in a two-hybrid screen as part of the vault particles, that are large ribonucleoprotein complexes [15].

Following 30 years of PARP-1 domination in the PARylation field, within 2 years four new members of the PARP family, with distinct primary structures, subcellular localizations and functions, were discovered by several research groups indicating that poly(ADP-ribosyl)ation is a more ubiquitous post-translational modification than first expected. Soon after, the fast accumulation of new sequences from human and mouse origins, provided by EST sequencing and human genome sequencing projects, has allowed to extensively search for new PARP related sequences. Finally a super family of 17 members has emerged [16]. These PARP domain-containing proteins are detailed in Table 2.1 and illustrated in Fig. 2.1.

An additional surprise was the variety of new domains associated with the PARP domain, suggesting their possible implication in many biological functions and likely in different subcellular locations (Table 2.1). Some domains or protein sequence motifs, like the WWE domain and the macro-domains are repeatedly found in a few of the PARPs. Another interesting aspect is that some similar functions, like the DNA binding function of the three DNA-dependent PARPs, are achieved with completely different protein domains, such as a combination of zinc fingers for PARP-1 and two very different N-terminal domains (in terms of primary sequence) for PARP-2 and PARP-3. Whereas the two tankyrases differ from each other only in their N-terminal HPS domain, absent in TNKS2, their functions seem to be very specific, as the knockdown of their expression revealed very different phenotypes with an essential regulatory function in mitotic segregation for TNKS1 [11, 17, 18] and a role in the basal metabolism for TNKS2 [19, 20].

The first structural studies have shown that the PARP catalytic domain binds NAD^+ via a unique protein fold similar to that of bacterial exotoxins (like diphtheria toxin) and different from the Rossmann fold of other NAD^+-binding enzymes (like the dehydrogenases) [21]. In addition, the coordination mode of NAD^+ within the catalytic site is conserved from the bacterial exotoxins to eukaryotic PARPs [22]. Some very important amino acid residues have been defined to be essential for the catalytic function, the catalytic glutamate (E988) being essential for the elongation activity of PARP-1 [23]. The alignment of the sequences of the catalytic domain of the 17 PARPs reveals major conservation blocks that defined the "PARP signature" corresponding to key secondary structures constituting the active site [16]. Notably, the catalytic residue E988 is not conserved in all the PARPs. Of note, PARP-10, lacking this residue achieves catalysis through a substrate-assisted mechanism [24]. Based on structural homology with the diphtheria toxin and sequence analysis of active ADP-ribosyl transferases, it has been concluded that three amino acids within the PARP signature were crucial for NAD^+ recognition and the elongating activity: a histidine (H862 in PARP-1), a tyrosine (Y896 in PARP-1) and a glutamate (E988 in PARP-1) forming a triad motif 'H-Y-E' (see Table 2.1) that appears in PARylating PARPs (PARP-1, PARP-2, PARP-3, PARP-4 and the tankyrases (PARP-5a and 5b) [24–26]. In the other PARPs the E is replaced by either an I, Y, T, V, L predicting a mono(ADP-ribosyl)ating activity of the enzyme

Table 2.1 The PARP family: *aa* amino acid; *ARTD* ADP-ribosyl transferase Diphtheria Toxin like; *BAL* B-aggressive lymphoma protein, *COAST6* collaborator of signal transducer and activator of transcription 6; *ND* not determined; *PARP* poly(ADP-ribose) polymerase; *vPARP* vault PARP; *ZAP1* zinc-finger antiviral protein 1; *ZC3HAV1* zinc-finger CCCH-type antiviral protein 1; *ZC3HDC1* zinc-finger CCCH domain-containing protein 1

PARP family member	Alternative name	Transferase name[a]	Subclass	Size[b] (aa)	Chromosome	Isoforms[c]	Uniprot Accession	Subcellular localization	Triad motif	Enzymatic activity[d]	Key functional motifs and domains
PARP1		ARTD1	DNA-dependent	1014	1q41-42	1	P09874	Nucleus	H-Y-E	P, B	WGR, zinc-fingers, BRCT
PARP2		ARTD2	DNA-dependent	583	14q11.2	2(1)	Q9UGN5	Nucleus	H-Y-E	P, B	DBD, WGR
PARP3		ARTD3	DNA-dependent	533	3p21.2	2(1)	Q9Y6F1	Nucleus, centrosomes	H-Y-E	P	WGR
PARP4	vPARP	ARTD4		1724	13q11	1	Q9UKK3	Cytoplasm, nucleus	H-Y-E	P(p)	BRCT
PARP5A	Tankyrase 1, TNKS1	ARTD5	Tankyrase	1327	8p23.1	2(1)	O95271	Nucleus, cytoplasm	H-Y-E	P, O	Ankyrin sequence repeats, SAM
PARP5B	Tankyrase2, TNKS2	ARTD6	Tankyrase	1166	10q23.3	1	Q9H2K2	Nucleus, cytoplasm	H-Y-E	P, O	Ankyrin sequence repeats, SAM
PARP6		ARTD17		630	15q22.3	3(1)	Q2NL67	ND	H-Y-Y	M(p)	
PARP7	TIPARP	ARTD14	CCCH PARP	657	3q25.31	1	Q7Z3E1	ND	H-Y-I	M	Zinc-fingers, WWE
PARP8		ARTD16		854	5q11.2	2(1)	Q8N3A8	ND	H-Y-I	M (p)	
PARP9	BAL1	ARTD9	macroPARP	854	3q21	3(1)	Q8IXQ6	Nucleus, cytoplasm	Q-Y-T	M (p)	Macro-domain
PARP10		ARTD10		1025	8q24.3	1	Q53GL7	Nuclear, cytoplasm	H-Y-I	M	

Table 2.1 (continued)

PARP family member	Alternative name	Transferase name[a]	Subclass	Size[b] (aa)	Chromosome	Isoforms[c]	Uniprot Accession	Subcellular localization	Triad motif	Enzymatic activity[d]	Key functional motifs and domains
PARP11		ARTD11		331	12p13.3	3(1)	Q9NR21	ND	H-Y-I	M (p)	WWE
PARP12	ZC3HDC1	ARTD12	CCCH PARP	701	7q34	1	Q9H0J9	Nucleus	H-Y-I	M (p)	Zinc-fingers, WWE
PARP13	ZC3HAV1, ZAP	ARTD13	CCCH PARP	902	7q34	5(1)	Q7Z2W4	Cytoplasm (nucleus)	H-Y-V	M (p)	Zinc-fingers, WWE
PARP14	BAL2, COAST6	ARTD8	macroPARP	1801	3q21.1	6(6)	Q460N5	Nucleus, cytoplasm	H-Y-L	M	Macro-domain, WWE
PARP15	BAL3	ARTD7	macroPARP	678	3q21.1	2(1)	Q460N3	Nucleus	H-Y-L	M (p)	Macro-domain
PARP16		ARTD15		322	15q22.2	3(1)	Q8N5Y8	Nucleus, RE membranes	H-Y-I	M (p)	

[a] Based on the revised nomenclature of Hottiger et al. [26]
[b] Size of the human protein in amino acids
[c] Isoforms result of alternative splicing, and the reference isoform sequence is noted in parenthesis
[d] Known or predicted enzymatic activity: mono- (M), oligo- (O) or poly(ADP-ribosyl)ation (P), or branching (B), predicted (p)

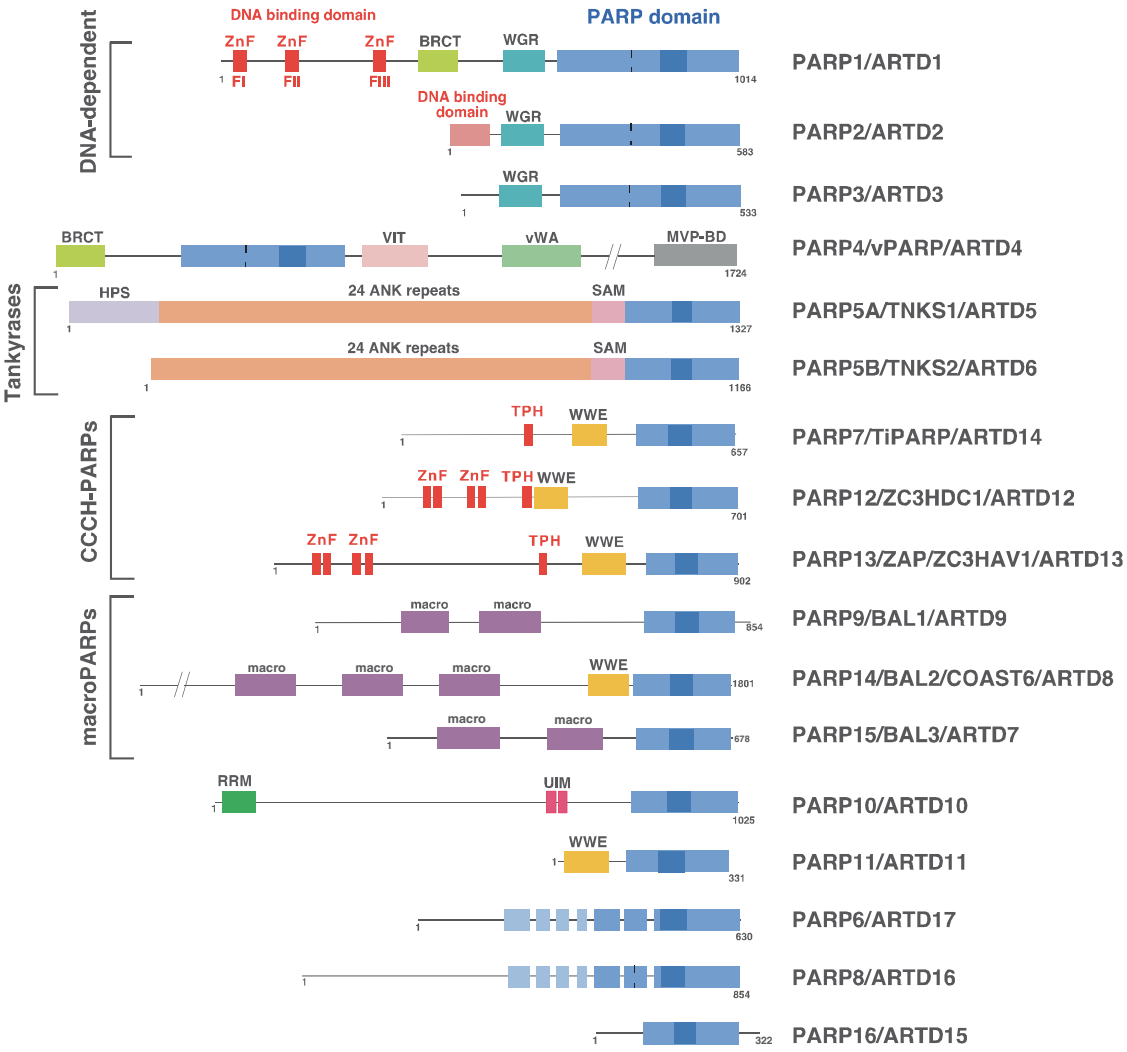

Fig. 2.1 Domain architecture of human poly(ADP-ribose) polymerase family members. Within each putative PARP domain, the region that is homologous to residues 859–908 of PARP-1—the PARP signature—is indicated by a *darker* colour. BRCT, SAM, UIM, MVP-BD, VWA and ANK are protein-interaction modules. *ANK* ankyrin; *BRCT* BRCA1-carboxy-terminus; *HPS* homopolymeric runs of His, Pro and Ser; macro, domain involved in ADP-ribose and poly(ADP-ribose) binding; *MVP-BD* MVP-binding; *PARP* poly(ADP-ribose) polymerase; *RRM* RNA-binding motif; *SAM* sterile α-motif; *TPH* TiPARP-homology; *UIM* ubiquitin-interacting motif; *VIT* vault inter-α-trypsin; *vWA* von Willebrand factor type A; *WGR* conserved W, G and R residues; *WWE* conserved W, W and E residues, domain involved in ADP-ribose and poly(ADP-ribose) binding; ZnF, DNA or RNA binding zinc fingers (except PARP-1 ZnFIII, which coordinates DNA-dependent enzyme activation)

and thus behaving like the mono-ADP-ribosyl transferases (mART). However it is still conceivable that these proteins could use alternative side chains in a slightly different geometry for catalysis. Indeed, PARP-14, -9, -10, -11, -13 and -7 display an aspartate at a position corresponding to the catalytic aspartate of a bacterial diphtheria toxin like ADP-ribosyl transferase, called rifampin ADP-ribosyltransferase (Arr). In this bacterial enzyme that shares three dimensional conformation similarities with PARP-1 NAD^+ -binding loop, the H and the Y of the triad were identified but not the conventional catalytic E residue. Instead this residue is replaced by

a D residue located in the neighbourhood within the substrate-binding loop and which fulfils the role of catalytic residue [26, 27]. To generalise and rationalise the nomenclature of the PARP family proteins, Hottiger et al. [26] have proposed to rename them with criteria based on the type of enzymatic reaction they catalyse, their structural features and on the rules for biochemical classifications, by removing the prefix "poly" and "mono" calling them 'ADP–Ribosyl Transferases Diphtheria Toxin like' or ARTDx, where x represents the specific number of the protein (see Table 2.1 for correspondence). The search of new members belonging to the PARP family, using the PARP signature domain of PARP-1, didn't pick any other ADP-ribosyl transferases (ART family) or NAD+ binding proteins (dehydrogenases), indicating that the PARP signature sequence is an extremely well defined and unique functional domain. Its conservation during evolution, with PARP-1 and tankyrases as key players (almost always found in any multicellular organisms), makes the function of this domain of vital importance. The evolution of the mammalian (and plant) genome complexity has required that the number of genes coding for PARP proteins be augmented to fulfil important new cellular functions. This evolution occurred alongside sequence modifications, with substitution of some key amino acid (E to Y, I, etc.) that modifies the extent of the PARP activity towards a mART activity, but the structural domain of these new PARPs remains overall similar. For simplicity in the following text, all the different names for each protein will be mentioned at the beginning of each chapter, then the original "PARP" nomenclature, used at the gene level, will be used throughout.

2.2 The macroPARPs: PARP-9, PARP-14, PARP-15

The macroPARP subfamily is composed of three members defined by the presence of 1–3 macro domains: PARP-9/ARTD9/BAL1 (B-aggressive lymphoma 1), PARP-14/ARTD8/BAL2/CoaSt6 (B-aggressive lymphoma 2, Collaborator of Stat6) and PARP-15/ARTD7/BAL3 (B-aggressive lymphoma 3). The three macroPARP genes and the gene encoding a binding partner of PARP-9, BBAP (B-lymphoma and BAL-associated protein) are localized within ~200 kbp in the 3q21 human chromosomal region, an area of known abnormalities in multiple haematological malignancies [28–30]. This region is syntenically conserved in mouse chromosome region 16B3, with the exception of the PARP-15 gene, absent in rodents and many other species [31]. This suggests that the macroPARP genes may be evolutionarily and/or functionally related or have coordinated expression.

PARP-9 and PARP-14 are predominantly expressed in normal mouse lymphoid tissues, but PARP-9 transcripts were also detected in developing and adult brain, intestine and colon [32]. Looking at PARP-15 expression in human cell lines database revealed that it is restricted to cells with haematological origin (http://www.broadinstitute.org/ccle/home). This preferential lymphoid pattern of expression suggests that macroPARPs function predominantly in the immune system. Whereas accumulating data support this hypothesis for PARP-9 and PARP-14, no functional data have been reported so far for PARP-15.

Each macroPARP gene encodes for two or more isoforms generated by alternative splicing. A major (short or S) and a minor (long or L) form were identified for PARP-9 [29] as well as two isoforms for PARP-15 and at least six are reported in the databases for PARP-14, with one even lacking the C-terminal PARP domain. The functional relevance of these putative isoforms remains an open question, but suggests that the complexity might be even higher than expected for the functional characterization of these proteins.

2.2.1 Structure/Domains of macroPARPs

PARP-14 and PARP-15, possessing a "HYL" triad motif, exhibit auto- and hetero-mART activity [24, 28, 33, 34] whereas PARP-9, with a "QYT" motif, is inactive [24]. The 3D structure of PARP-14 and PARP-15 PARP domains were solved, as apo-enzymes or bound to PARP inhibitors [35]. Subsequently a virtual screening identified small ligands of PARP-14 and PARP-15 catalytic sites [36]. An activity-based assay was also developed for PARP-15 and validated by screening a small inhibitor library of known ARTD inhibitors [34]. These are all first steps opening the way to further optimization for increased potency and selectivity of PARP-14 and PARP-15 inhibitors.

The macro domains of macroPARPs were first depicted as transcriptional repressor modules, at least for PARP-9 and PARP-15 [28]. Macro domains were initially described as ADP-ribose, or for some of them, O-acetyl-ADP-ribose, binding modules, able to either bind MARylated substrates or the last residue of PARylated substrates [37–42]. More recently, a hydrolysing activity towards MAR has been uncovered for several macro-domain containing proteins such as TARG1/C6orf130/OARD1, MacroD1/LRP16 and MacroD2/C20orf133, defining these domains as readers and erasers of MARylation [41, 43–45, 46]. In contrast to PARP-9 that can bind free PAR and PARylated PARP-1 via its macro domain 2 [37, 47], PARP-14 macro domains are not able to bind PARylated PARP-1 [42], despite being apparently recruited to laser-induced DNA damage sites [47]. However, PARP-14 macro domains 2 and 3, but not macro domain 1, can recognize MARylated substrates such as automodified PARP-10 or PARP-10 substrates [42] (see below). Of note, macro domain 1 of both PARP-9 and PARP-14 can neither bind PAR nor MAR [41, 42, 47]. However, up to now no hydrolysing activity has been reported for any of the macroPARP family members.

PARP-14 is the sole macroPARP possessing a WWE domain. WWE was characterized as a PAR binding module, recognizing the iso-ADP-ribose motif, with the WWE of RNF146/Iduna E3 ligase recognizing the distal ADP-ribose and ribose-ribose glycosidic bond [40, 48, 49]. PARP-14 WWE motifs is however unable to bind PAR. The solution structure of PARP-14 WWE domain by NMR revealed similarity with the WWE domains of RNF146 and PARP-11, displaying however structural differences, such as an additional ß-strand covering the hydrophobic pocket [49]. Together with the non-conservation of amino-acids playing a crucial role in the recognition of the adenine base of ADP-ribose, these specificities of PARP-14

WWE domain may explain the lack of binding to PAR and all ATP or ADP-ribose derivatives tested [48, 49]. The role of this non-functional WWE remains a mystery.

2.2.2 PARP-9

PARP-9 (experimentally identified as BAL1, B-aggressive lymphoma 1) was identified according to its differential expression in diffuse large B cell lymphomas (DLBCL), higher in some chemoresistant tumors with poor prognosis, particularly those associated with a brisk host inflammatory response [29, 30]. Overexpression of PARP-9 in a B-cell lymphoma cell line stimulates cell migration, suggesting a role for PARP-9 in the promotion of malignant B cell migration and dissemination in high risk DLBCL [29]. PARP-9 interacts with BBAP (B-lymphoma and BAL-associated protein), a ring finger E3 ligase of the DELTEX family, capable of heterodimerization with DELTEX members and self-ubiquitination [50]. DELTEX proteins participate in Notch signalling pathway that controls cell fate determination, notably in myogenesis, neurogenesis, lymphogenesis and intestinal homeostasis [51]. BBAP was proposed to regulate the subcellular localization of PARP-9, sequestering it within the cytoplasm [30]. PARP-9 was subsequently localized at the cell periphery where it colocalizes with actin filaments, but was also detected within the nucleus, at least in S-phase cells [52]. Of note, PARP-9 and BBAP genes are located head-to-head and partially overlapping, their mRNA are antisense through their respective 5′-extremities. The two genes are under the control of an IFNγ-responsive bidirectional promoter (see below) [30]. BBAP and PARP-9 are largely co-expressed in mouse during development and in adult animals [32]. However, some additional tissue-specific gene regulation may exist, with *PARP-9,* in contrast to *Bbap,* being expressed at higher levels in the developing gut than in brain, suggesting both common and independent tissue-specific regulations [32].

2.2.2.1 PARP-9, a Transcription Co-Factor in IFNγ Signalling, Promoting Tumour Development

PARP-9 and BBAP were highly expressed in primary host response (HR-)DLBCLs [30], tumours having increased expression of inflammatory mediators including interferon γ (IFNγ), mainly secreted by activated T lymphocytes and natural killer (NK) cells [53]. IFNγ regulates a variety of responses including antiviral state, inhibition of cellular proliferation, induction of apoptosis, activation of microbicidal effector functions and immunomodulation. The canonical Janus Kinase (JAK)/Signal Transducer and Activator of Transcription 1 (STAT1) pathway is the most common signalling route through which IFNγ potentiates its pleiotropic activity [54]. IFNγ modulates the host response to tumours in two opposite ways: at first, by preventing tumour development (immunosurveillance), but later by promoting the outgrowth of tumours with a reduced immunogenicity (immunoediting) [55].

Expression of PARP-9 and BBAP is induced by IFNγ in B-lymphoma cell lines, their bi-directional promoter containing functional STAT1 and IRF1 binding sites [30], thus defining PARP-9 and BBAP as IFN-stimulated genes (ISGs). PARP-9 itself acts as a transcriptional co-factor, its overexpression in a B-lymphoma cell lines modulating the expression of many type I and type II ISGs, or genes indirectly regulated by IFNγ [30]. Among these up-regulated genes were one of the masters regulators of type I and type II IFNγ response: IRF7 and STAT1 respectively, defining PARP-9 as an actor of the IFN signalling pathway. A recent study made a step forward in the elucidation of PARP-9's role in this process by examining the impact of the constitutive high expression of PARP-9 in HR-DLBCL cell lines [56]. Highly expressed PARP-9 is associated with intrinsic IFNγ signalling, with STAT1 being constitutively expressed and present in its activated phosphorylated form (STAT-Y701). PARP-9 stimulates the phosphorylation on Y701 of both STAT1 isoforms, the activating isoform STAT1α and the antagonistically acting and transcriptionally repressive isoform STAT1β, and interacted with both of them through its macrodomains in an ADP-ribosylation-dependent manner. PARP-9 promotes the nuclear accumulation of the repressive isoform STAT1β and together with STAT1β represses the expression of the tumour suppressor IRF1. Moreover, PARP-9 binds to the promoter of the STAT1-independent proto-oncogene BCL6 to enhance its expression. PARP-9 inhibition of the IRF1-mediated cell death and activation of the BCL6-mediated survival is associated with the increased expression of prosurvival factors PIM1, PIM2 and PARP-14 (see § 2.3), and decreased expression of the BCL6 antagonist BLIMP1 and of genes involved in cell cycle arrest or apoptosis such as p21, BAD, p53 and CASP3 [56]. Supporting these findings, PARP-9 knockdown strongly suppressed the proliferation of HR-DLBCL cell lines. Collectively, these results show that PARP-9 can promote proliferation, survival and chemoresistance in HR-DLBCL by suppressing the anti-proliferative and pro-apoptotic effects of IFNγ. The authors propose the appealing hypothesis that PARP-9 could induce a switch in STAT1 status, from tumour suppressor to oncogene in high-risk DLBCL. Therefore, in infiltrated DLBCL tumours, IFNγ production by dendritic cells could induce PARP-9 expression in tumour cells, leading to the up-regulation of genes involved in the inhibition of the anti-tumoural immune response, favouring tumour progression [56].

2.2.2.2 PARP-9 and the DNA Damage Response

The first indication that PARP-9 could be involved in the DNA damage response came with the discovery that its favourite partner BBAP was required for the efficient recruitment of the DNA damage response (DDR) factor 53BP1 to ionizing radiation (IR) or doxorubicin-induced DNA damages [57]. Histone H4 lysine 91 (H4K91) was identified as a substrate for BBAP E3 ligase activity, monoubiquitinated by BBAP in response to IR or doxorubicin, a prerequisite for histone H4K20 methylation. Since accumulation of the mediator protein 53BP1 at DSB depends on H4K20 methylation [58], this provides an explanation for the decreased 53BP1 recruitment to DNA damage sites in cells depleted in BBAP [57]. Next, the same

group studied the role of PARP-9 in the DSB repair [47]. Using laser microirradiation technology to locally introduce DNA damages, they revealed the fast but transient PARP-1 and PAR-dependent recruitment of PARP-9 to DNA breaks and demonstrated the critical role of the macro domain 2 in this process. Subsequently, PARP-9 recruits BBAP to the DNA damage sites. PARP-9-deficient cells showed increased sensitivity to doxorubicin and reduced repair of DNA breaks introduced by low-dose irradiation. The authors demonstrated that the PARP-1-BAL1-BBAP axis also favours the recruitment of BRCA1 and its binding partner RAP80, the ubiquitin-recognizing protein involved in DSB repair by homologous recombination [47]. In contrast, this axis is neither involved in the recruitment of ATM, MDC1 and RNF8 nor on H2AX phosphorylation at the damaged sites. The proposed model is that the PARP-1-BAL1-BBAP axis mediates ubiquitination of histone H4K91, increasing H4K20 methylation and thus favouring 53BP1 recruitment. Through its ubiquitin-interacting motifs (UIMs), RAP80 could also be recruited early to BBAP-mediated ubiquitinated targets, bringing BRCA1 with it. Next, the later accumulation or retention of RAP80/BRCA1 and 53BP1 at DNA breaks would rely on the RNF8/RNF168-mediated ubiquitination [59]. Moreover, BBAP can also ubiquitinate RAP80 on K43 and K48 for a yet unknown reason [47].

The mechanism proposed by Yan and colleagues [47] fits well with the current emerging view of a two-steps DSB repair process, in which initial recruitment of DDR factors occurs independently on H2AX phosphorylation, followed by sustained DDR factor retention or newly recruitment in a γH2AX-dependent manner [59, 60]. A growing body of studies reports the PARP-dependent initial recruitment of DSB repair factors and the PARP-independent retention at the DNA damage site, as described recently for BRCA1 (via its partner BARD1) or NBS1 [61, 62]. Regarding the PAR-dependent early recruitment of BRCA1, the relative contribution of the PAR-PARP-9-BBAP-ubiquitin-RAP80 axis with the PAR-BARD axis remains to be determined [47, 62].

2.2.3 PARP-14

2.2.3.1 PARP-14, a Transcription Co-Factor

PARP-14 was first described as a transcriptional regulator, through its functional interaction with the Signal Transducer and Activator of Transcription 6 (STAT6), and thus originally named COAST6 (*Co*ll*a*borator of *STAT6*) [63]. PARP-14 was shown to potentiate interleukin 4 (IL4) induced transcription of STAT6-dependent genes [63]. IL4 is a key cytokine that regulates lymphocytes differentiation, proliferation and survival in thymus and spleen. PARP-14 expression and subcellular localization are not modified by IL4 treatment at least in lymphoma cells [63], suggesting that IL4-dependent PARP-14 co-factor activity on STAT6 transcription is regulated at the protein level. PARP-14 activity is required for the IL4 dependent STAT6 transcription, since a catalytically inactive PARP-14 mutant is devoid of this stimulating activity [33]. STAT6 is not PARylated by PARP-14 whereas the

STAT6 cofactor p100 is [33]. PARP-14 was found associated with IL4- and STAT6-responsive promoters but not with STAT1- or STAT4-responsive promoters [64]. Further dissection of the underlying mechanism revealed that PARP-14 functions as a molecular switch, acting as a repressor to keep transcription off under non-stimulating conditions, by recruiting the histone deacetylases HDAC2 and HDAC3 to the promoters. Under IL4 stimulating conditions, PARP-14 turns to be activator, promoting the binding of STAT6, while PARylating itself and HDAC2/3, leading to their dissociation from each other and from the promoters [64]. ChIP analyses showed the association of PARP-14 with the STAT6-responsive promoters in absence of IL4, its dissociation upon IL4 treatment depending on PARP-14 activity [64]. But does PARP-14 directly bind DNA? Bioinformatics analyses of the promoter sequences of genes positively regulated by PARP-14 in TH2 cells, and identified by genome wide analyses, identified two putative PARP-14 DNA binding sites [65]. The interaction of PARP-14 with each motif was observed by *in vitro* DNA-pull down from cell extracts, but it remains to determine whether PARP-14 binds itself to these motifs, raising the question of the existence of a DNA-binding domain within PARP-14. Alternatively, PARP-14 could be tethered to these sites by a yet unknown transcriptional cofactor.

2.2.3.2 Roles of PARP-14 in Immune Response

Mice with a disrupted PARP-14 gene were generated, opening the way to physiological studies of PARP-14 function [66]. *PARP-14*$^{-/-}$ mice had normal numbers of B and T lymphocytes, but altered proportions of B-cell subsets in the spleen, with lesser marginal zone B cells and more follicular B cells. Consequently, the antigen-specific IgA response to immunization was decreased [66]. *PARP-14*$^{-/-}$ mice revealed a pro-survival role of PARP-14 in IL4-dependent protection of B cells from apoptosis induced by irradiation or growth factor withdrawal, requiring functional PARylation capacity [66]. PARP-14 regulated pro-survival genes, among them the serine/threonine kinase PIM1 and the antiapoptotic BCL2 family member protein MCL1. It is however unlikely that the PARP-14 pro-survival role completely relies on STAT6, since caspase-3 activation was higher in IL4 treated B cells from *PARP-14*$^{-/-}$ than from *Stat6*$^{-/-}$ mice. This suggests that PARP-14 might exert both STAT6 dependent and independent functions in response to IL4 [66]. A following study revealed that the PARP-14-dependent IL4 induced survival of B cells arises also from an enhancement of glycolysis and glucose oxidation [67] (see below).

PARP-14$^{-/-}$ mice showed protection from allergic airway disease (AAD). In this model of inflammation, PARP-14 supports the differentiation of T cells toward a T_H2 phenotype, by regulating the STAT6 dependent expression of the transcription factor Gata3 [68]. The PARP inhibitor PJ34 alleviates AAD, highlighting the potential therapeutic use of PARP inhibitors to treat asthma [68]. PJ34 is a general PARP inhibitor, but the fact that it did not decrease further the AAD phenotype of *PARP-14*$^{-/-}$ mice supports the interpretation that the protective effect of this PARP inhibitor can be inferred to PARP-14 inhibition. A genome wide analysis revealed that

PARP-14 enhances the expression of TH2 genes while repressing the expression of TH1-associated genes [65]. Not all the relevant target genes were affected by PJ34 inhibitor, indicating that some genes are regulated by PARP-14 independently on its activity. Consistent with the role of PARP-14 in STAT6 dependent transcription, several of the identified genes are regulated by the JAK-STAT pathway, positively or negatively [65].

Another research group reported that PARP-14 controls the class distribution, affinity repertoire, and recall capacity of antibody responses in diseases models of infection [69]. *PARP-14*$^{-/-}$ mice are impaired in the generation of IgE+B cells and in the amount of secreted IgE, due to defective B cell–intrinsic processes [69]. In contrast, the deficient antigen-specific IgA responses in *PARP-14*$^{-/-}$ mice result predominantly from B-cell extrinsic defects. The differentiation of naive CD4+T cells into Th17 cells, which promotes the IgA response [70], is less efficient in the absence of PARP-14 or if the PARP-14 MART activity is impaired. Upon T cell activation, PARP-14 enhances the expression of transcription factors involved in Th17 differentiation, such as RORa, Runx1, and Smad3 [69]. *PARP-14*$^{-/-}$ mice also showed reduced levels of CD103+dendritic cells in the gut, with a decreased expression of retinol aldehyde dehydrogenase and thus reduced levels of retinoic acid, also required for IgA production. Collectively, these results indicate that PARP-14 promotes the Th17 subset in an ADP-ribosylation–dependent manner [69]. In contrast to the study by Mehrotra et al. [68], Cho and collaborators did not observe an impact of PARP-14-deficiency on the pulmonary inflammation after the primary exposure to immune challenge, despite using the same model allergen ovalbumin, but upon recall challenge [69]. Beside probable differences in priming, these two studies however demonstrate that PARP-14 controls the allergic response, and support the idea that PARP-14 inhibitors could have therapeutic uses to treat allergy. PARP-14 expression was also shown to be higher in oesophageal biopsies of children suffering from eosinophilic esophagitis disease (EoE), whereas PARP-15 expression was reduced and PARP-9 did not change [71]. PARP-14, together with STAT6, regulates the production of the inflammatory chemokine CCL26. This study is the first illustrating a significant role of PARP-14 in the development of allergic inflammation in human.

2.2.3.3 PARP-14 and Cancer

Expression of PARP-14 is elevated in Myc-induced lymphoma samples compared with normal B cells [66]. In contrast, *PARP-14*$^{-/-}$ revealed delayed Eμ-Myc-induced lymphomagenesis [67]. PARP-14-deficiency impairs the sustained c-Myc driven effects such as increased cell size, persistent cell cycling and increased energy metabolism [67]. An increased expression of IL4 targets pro-survival genes is commonly observed in blood cancers. As mentioned above, PARP-14 stimulated the IL4-mediated expression of the pro-survival genes PIM1 and MCL1, known to contribute to the development of Eμ-Myc induced lymphomas [72, 73]. IL4 treatment also increased glucose uptake and mitochondrial activity in B cells, favouring cell

metabolism and proliferation. Interestingly, PARP-14 (and STAT6) were necessary for the glucose uptake into B cells in response to IL4, but not to lipopolysaccharide [67]. The PARP-14-dependent increase of glucose uptake leads to enhanced mitochondrial respiration. Therefore, by increasing the metabolic response, PARP-14 directly contributes to the pro-survival signalling of IL4. Of note, the first connexion between PARP-14 and glycolysis was established in an earlier study describing the interaction between PARP-14 and the phosphoglucose isomerase/autocrine motility factor (PGI/AMF), a cytosolic enzyme involved in glycolysis [74]. PARP-14 was shown to stabilize PGI/AMF, preventing its monoubiquitination and subsequent degradation by the endosome/lysosome pathway, thus favouring its accumulation and secretion. Targeting PARP-14 was therefore proposed as a therapeutic strategy to inhibit cancer cell migration and invasion during metastasis [74].

Expression of PARP-14 was also reported to correlate with disease progression and poor prognosis in multiple myeloma [75]. The pro-survival Jun N-terminal kinase 2 (JNK2) is constitutively activated in some multiple myeloma and suppresses the JNK1-mediated apoptosis. PARP-14 acts as a downstream effector of the JNK2-dependent pro-survival signal, by binding and inhibiting JNK1 pro-apoptotic function [75]. The PARP inhibitor PJ34 triggers JNK1 activation and increases apoptosis, enhancing the cytotoxicity of anti-myeloma agents like dexamethasone or bortezomib, opening the way to novel anti-myeloma therapeutic strategies [76].

Vyas and collaborators revealed the localization of PARP-14 to the ends of actin stress fibres in focal adhesions [52]. PARP-14 knockdown does not alter the focal adhesions assembly but their turnover, impairing the retraction of the highly elongated protrusions, thus increasing cell adherence to the substrate. It is tempting to speculate that the anticancer effects of PARP-14 inhibition would also partly result from an increased adhesiveness inhibiting metastasis.

Altogether, these studies suggest that PARP-14 could favour tumour promotion, by up-regulating pro-survival genes, by increasing cell metabolism through the elevation of glucose uptake and mitochondrial respiration, and by controlling cell adhesiveness. These findings open new avenues for anticancer strategies based on PARP-14 therapeutic targeting.

2.3 PARP-10

PARP-10/ARTD10 was the first enzymatically characterized MART, endowed with both automodification and heteromodification activity [24, 77]. Mechanistically, PARP-10 uses substrate-assisted catalysis to modify its substrate [24]. PARP-10 was initially identified as a binding partner of the proto-oncoprotein c-Myc, a key transcriptional regulator that controls cell proliferation [77]. PARP-10 is predominantly cytoplasmic but can shuttle between the cytoplasm and the nucleus, owing to the presence of a functional NES and of a non-conventional nuclear localization sequence [77, 78]. In both compartments, PARP-10 accumulates into dynamic bodies that contain poly-ubiquitin and are enriched in the autophagy adaptor protein,

poly-ubiquitin receptor p62/SQSTM1 [78]. PARP-10 can also accumulate within the nucleolus where it is phosphorylated in a CDK2-dependent manner during late-G1 to S phase [79]. *In vitro* studies revealed that the CDK2-cyclin E phosphorylation of PARP-10 increases its automodification activity [79].

The roles of PARP-10 appear to be multiple, in the regulation of cell proliferation, cell survival, transformation or viral infection. First, PARP-10 interacts with c-Myc and inhibits cell transformation induced by c-Myc/HA-Ras, but its catalytic activity is dispensable for this inhibitory effect [77]. In contrast, PARP-10 overexpression inhibits cell proliferation of primary and immortalized rodent fibroblasts and of human HeLa cells, promoting apoptosis dependent on PARP-10 activity [24, 77, 79, 80]. This observation could be regarded, in light of the recent discovery of PARP-10 overexpression inhibiting cellular translation [81]. In contrast, human HEK293 and U2OS cells were not sensitized by PARP-10 overexpression, suggesting that PARP-10 is not a general growth inhibitory protein [77]. Conversely, the depletion PARP-10 was also reported to affect cell proliferation and survival, with accumulation of PARP-10-deficient cells in the G1/S boundary and increased cell death [79]. Taken together, these studies suggest the need of tightly regulated PARP-10 levels for proper cell cycle progression and viability.

A further study reported that various DNA damaging agents induce PARP-10 cleavage by caspases during apoptosis [80]. A caspase cleavage site has been identified at position D406, preferentially recognized by Caspase 6 *in vitro*, and functional *in vivo*. Cleavage of PARP-10 inactivates its pro-apoptotic function that depends not only on its catalytic activity, but also on the N-terminal domain, containing an RRM RNA binding motif [80]. Accordingly, PARP-10 knockdown reduces UV- and doxorubicin-induced apoptosis, implicating PARP-10 in the cell response to DNA damages [80]. The fact that PARP-10 could be a novel DNA damage factor is further supported by the recent finding of PARP-10 being involved in the PCNA-mediated translesion DNA synthesis [82]. PARP-10 interacts with PCNA through a PCNA-interacting peptide (PIP)-box motif, and with mono-ubiquitinated PCNA through its ubiquitin-interacting motif (UIM). The interaction between PARP-10 and PCNA increases after UV-irradiation. PARP-10-deficient HeLa cells showed increased sensitivity to drugs affecting replication such as hydroxyurea, mitomycin C and UV, in contradiction with the observations made by Herzog et al. who used PARP-10-deprived U2OS cells [80], but no sensitivity to the DSB inducer bleomycin [82]. Recovery from S-phase specific damage is altered in the absence of PARP-10, with the accumulation of γH2AX foci likely reflecting the collapsing of stalled replication forks. PARP-10 increased the mutation frequency and favoured translesion synthesis by controlling the ubiquitylation status of PCNA, supporting a direct role of PARP-10 in the S-phase repair [82].

PARP-10 is also involved in the regulation of NF-kB signalling considering the study showing PARP-10 repressing the expression of NF-kB target genes in response to IL-1ß or TNFα [83]. This effect requires functional PARP-10 catalytic activity and intact UIM motifs. Mechanistically, the UIM motifs are able to recognize K63-poly-ubiquitin, a post-translational protein modification notably involved in NF-kB signalling and produced in response to IL-1ß or TNFα. PARP-10 binds

to and modifies the downstream target NEMO/IKKγ, preventing its K63 poly-ubiquitination and consequently inhibits NF-kB nuclear translocation into the nucleus, impairing the gene expression. This study highlights a role of PARP-10 in the inflammatory processes regulation, likely through a feedback mechanism aimed at terminating NF-kB signalling [83].

PARP-10 may also play an anti-viral activity. Its promoter contains an IFN-stimulated response element/virus response element (ISRE/VRE) that responds to IFNα and to infection by the Newcastle Disease Virus [84]. PARP-10 is a target of the non-structural protein NS1 of the H5N1 avian influenza virus during host infection [85]. NS1 interacts with PARP-10 and also down-regulates its expression, possibly by repressing the anti-proliferative and pro-apoptotic function of PARP-10. Finally, PARP-10 was shown to display inhibitory activity towards the replication of the Venezuelan equine encephalitis virus [86].

Another possible function of PARP-10 has been revealed, in lipid metabolism, since PARP-10 depletion reduces the secretion of apolipoprotein B in primary human hepatocytes, but the mechanism underlying this observation is not elucidated yet [87]. A broad screening approached based on protein microarray was also undertaken to search for PARP-10 substrates. Seventy-eight targets were identified, mainly kinases and signalling proteins [88]. Among them, the glycogen synthase kinase 3β (GSK3β) was found, a protein involved in many physiological processes. *In vitro*, MARylated GSK3β has a reduced kinase activity, compared to the non-modified protein, and *in vivo* the manipulation of PARP-10 levels impacts the GSK3ß activity. It remains however to determine in which cellular process PARP-10-dependent GSK3ß regulation is involved. Interestingly a concomitant protein microarray studies performed to identify PARP-14 substrates revealed that among the 142 candidates identified, 32 were also PARP-10 substrates [88]. Moreover, endogenous PARP-10 interacts with PARP-14 and both proteins colocalize into cytoplasmic foci that appear in cells treated with IFNα [42]. As mentioned above, PARP-14 macrodomains 2 and 3 were able to recognize auto-modified PARP-10, as well as the PARP-10 substrate Ran GTPase [42]. These findings highlight a functional crosstalk between the two MARTs PARP-10 and PARP-14.

2.4 The CCCH-PARPs: PARP-7, PARP-12, PARP-13

The CCCH PARP family contains 3 members (PARP-7/TiPARP/ARTD14, PARP-12/ARTD12 and PARP-13/ZC3HAV1/ZAP/ARTD13) sharing a similar domain organization, with C-X_7-C-X_5-C-X_3-H-type zinc fingers (CCCH), one or two WWE domains and a PARP domain (Table 2.1 and Fig. 2.1). PARP-12 and PARP-13 contain 4 CCCH-zinc fingers able to bind RNA [89, 90], and a fifth CCCH-zinc finger with unknown function but closely homolog to the one present in TiPARP, therefore named TPH (TiPARP homology) domain [91]. Whereas PARP-7 and PARP-12 are both endowed with MART activity, PARP-13 is one of the two inactive PARPs since it lacks residues crucial for catalytic activity [24, 92, 93]. PARP-12 and PARP-13

exist in (at least) 2 isoforms, a long (L) full length and a short one (S) that lacks the PARP domain.

2.4.1 PARP-7

PARP-7 was initially identified as a gene induced by 2,3,7,8-tetrachlorodibenzo-p-dioxin (TCDD) in hepatoma cells, and has been named TiPARP, for TCDD-inducible PARP [92]. TCDD is an environmental contaminant released by human activity, causing pleiotropic effects including deregulated lipid and glucose metabolism, skin disorders, carcinogenesis and dysfunction of the immune, reproductive and nervous systems [94]. The strong induction of TiPARP has led this gene to be considered as an efficient TCDD toxicity response marker [95–97].

TiPARP is an active enzyme, capable of automodification and heteromodification of histones, likely by MART activity considering the lack of the catalytic glutamate in the active site [92, 93]. TiPARP induction by TCDD depends on the dimerization of the aryl hydrocarbon receptor (ARH) with the aromatic hydrocarbon receptor nuclear translocator (ARNT) and their translocation to the nucleus where the complex activates transcription of responding genes. Inhibition of the proteasome 26S triggers TCDD-dependent super-induction of TiPARP expression, suggesting the existence of a labile factor that inhibits its transcription [98]. A xenobiotic response element (XRE), binding site for AHR/ARNT in regulatory regions of target genes, was identified in the first intron of TiPARP gene [99]. The mouse *Tiparp* gene overlaps head-to-head with a ncRNA (4931440P22Rik, also known as Tiparp-as1), of unknown function but also regulated by AHR [99].

Only recently studies regarding the protein function of TiPARP revealed that TiPARP is found in the cytoplasm, exhibiting punctate localization, but accumulates also into nuclear foci [52, 93]. RNAi depletion of TiPARP showed that TiPARP is a selective transcriptional repressor of AHR that can function simultaneously by impairing the transactivation of the receptor and by increasing its degradation by the proteasome. [93] AHR and TiPARP physically interact and colocalize, and the repression of AHR transactivation is dependent on the TiPARP zinc finger and catalytic domains. In agreement, *Tiparp*$^{-/-}$ mouse embryonic fibroblasts display increased TCDD-dependent AHR target transactivation and AHR protein levels [93]. Therefore, a regulatory feedback loop is established: the TCDD-induced and the AHR/ANRT-dependent induction of TiPARP lead to the repression of AHR transactivation activity.

TCDD induces a lethal wasting syndrome whose hallmark is the suppression of hepatic gluconeogenesis. TiPARP is directly involved in the process of TCDD toxicity effects, by inhibiting the transcription of phosphoenolpyruvate carboxykinase (PEPCK). This effect is mediated by NAD^+ level depletion and by decreasing sirtuin deacetylase-1 (SIRT1)-mediated activation of the peroxisome proliferator-activated receptor γ co-activator 1α (PGC1α), a PEPCK transcriptional activator [100]. The same team further showed that PEPCK is an ADP-ribosylation target of TiPARP [101]. Increased protein PARylation is detected upon TCDD treatment,

but this is unlikely due to the sole MART activity of TiPARP, since PAR is clearly produced and detected by anti-PAR antibodies [100, 101]. A TiPARP-dependent involvement of PARP-1 activity is a tempting hypothesis, owing to the fact that the observed phenotypes in the absence of TiPARP (suppression of the NAD^+ depletion, increase in SIRT1 activity on PGC1α) would also fit with a defective PARP-1 function [100, 102]. The TCDD-induced TiPARP-mediated suppression of gluconeogenesis seems independent of TiPARP ability to feedback and repress AHR transactivation [93]. However, AHR activation was clearly established in a model of non-alcoholic steatohepatitis: TiPARP expression, NAD^+ depletion, deactivation of the mitochondrial sirtuin deacetylase 3 (SIRT3) leading to increased SOD2 acetylation thereby decreasing its activity [103].

Besides its involvement in the AHR signaling, TiPARP might also be involved in other nuclear receptor signalling, such as the progesterone receptor (PR) and androgen receptor (AR). TiPARP expression is induced by progesterone analogue, in a PARP-1 and CDK2-dependent manner, in breast cancer cells [104] and its gene harbours a functional AR-binding site [105, 106]. Switching adherent hepatocytes to suspension cultures also up-regulates TiPARP expression [99]. TiPARP was also identified as a PDGF-target gene [107, 108]. The *Tiparp*$^{-/-}$ mice revealed no growth defects, but haemorrhages at late embryonic stages, kidney defects and abnormal skeletal morphology with craniofacial abnormalities, phenotypes that could at least partly be attributed to a defective PDGF signalling [108].

TiPARP knockdown has no impact on cell viability, but increases the length of pre-metaphase mitosis [52]. The human TiPARP gene maps at chromosome 3q25.31, a region defined as the Cyclin L (CCNL) amplicon, in which TiPARP is co-expressed with Cyclin L, linked with head and neck squamous cell carcinoma (HNSCC) [109]. Other association loci studies identified TiPARP as a susceptibility gene for ovarian cancer development [110] and oral squamous cell carcinoma [111]. But whether TiPARP, likely through its involvement in the AHR regulation, could constitute a target for anticancer strategies remains to be specifically addressed. Finally, a study revealed that TiPARP was induced by IFN and could inhibit the viral replication, possibly by acting on cellular translation, putting this CCH3-PARP into the subfamily of PARPs displaying antiviral activity (see below) [86].

2.4.2 PARP-13

PARP-13/ZAP/ZC3HAV1/ARTD13 comprises four conserved CCCH-type zinc fingers, a WWE domain, a NES and two NLS, allowing its dynamic relocalization in the cell between its main residence site, the cytoplasm and the nucleus where it can accumulate [112]. Within the cytoplasm, PARP-13 was further localized to RNA granules, stained both with markers of processing (P)-bodies and stress granules (SG) [113], see below). Human PARP-13 exists in two different forms resulting from alternative splicing. The long isoform, termed ZAP_L or PARP-13.1, contains the C-terminal PARP domain, whereas the shortest isoform, called ZAP, ZAP_S or PARP-13.2 lacks this domain [31, 91]. Nevertheless, all PARP-13 isoforms are in-

active because the PARP domain is either mutated (HEY to YYV) or absent [24, 114]. Both PARP-13 isoforms are expressed in a wide range of human tissues [91].

PARP-13 was initially identified in rat as a CCCH-type zinc finger polypeptide with antiviral activity, named ZAP for Zinc finger Antiviral Protein [115]. Of note, this polypeptide that did not contain the PARP domain selectively inhibited MMLV (Moloney Murine leukemia virus) infection by preventing the accumulation of viral mRNA in the cytoplasm [115]. It was shown later on, that the presence of the PARP-like domain in PARP-13.2/ZAP_L could enhance the antiviral effect compared to PARP-13.1/ZAP_S [91], but how this domain precisely contributes is not elucidated yet. Crystal structure of N-terminal conserved domain of rat ZAP revealed a tractor shape with the four CCCH zinc-finger motifs located at the bottom forming two RNA binding cavities [89]. ZAP binds RNA molecules as a dimer [89, 90]. The zinc-finger domain apparently recognizes a three dimensional folding predicted to form stem-loop structures rather than a consensus RNA sequence [116].

Antiviral activity was subsequently reported against a large collection of viruses (Sindbis virus, Semliki forest virus, Ross River virus, Venezuelan equine encephalitis virus, Ebola virus, Marburg virus…) but is not universal, since some viral strains were not affected by ZAP (vesicular stomatitis virus, poliovirus, yellow fever virus and herpes simplex virus type 1) [91, 117–120]). Contradictory results have been reported concerning putative antiviral activity on HIV [91, 119]. The generation of *PARP-13*$^{-/-}$ mice confirmed the antiviral activity of ZAP, since *PARP-13*$^{-/-}$ primary mouse fibroblasts displayed increase replication efficiency of murine leukemia virus (MLV) [113].

Several studies have contributed to elucidate mechanistically how ZAP blocks the replication after virus entry and uncoating, but before the amplification of newly synthesized genomic RNA [117–119, 121–127]. ZAP directly binds to viral RNA through its CCCH-type zinc fingers and recruits: (1) the cellular poly(A)-specific ribonuclease (PARN) to shorten the poly(A) tail of viral RNA; (2) the decapping components Dcp1a and Dcp2 and the p72 DEAD-box and DHX30 DEXH-box RNA helicases to help RNA unfolding and to initiate degradation from the 5′ end; (3) the RNA exosome, through binding to the exosome component hRrp46p, and degrading the RNA from the 3′ end.

ZAP also showed antiviral activity toward the DNA virus Murine Gamma Herpes Virus 68 (MHV-68), through the inhibition of the expression of the latency protein M2 [128]. In a subsequent study the same group showed that the ORF64 protein, essential for the lytic replication cycle, is also a target of ZAP regulation [129]. However, ZAP does not inhibit MHV-68 lytic replication, its activity is antagonized by the replication and trans-activator RTA viral protein, which is able to disrupt ZAP homodimerization and thus neutralize its antiviral activity. This mechanism could be conserved among other viruses and could explain how a virus escapes the ZAP-mediated immunity [129]. Replication of hepatitis B virus in hepatocytes is also inhibited by ZAP. In this case, both isoforms of ZAP exert antiviral effects, by acting on the viral pregenomic (pg)RNA itself [123].

ZAP expression was shown to increase in human hepatocytes treated with IFNα and in the liver of hepatitis B patients during immune active phase, confirming previous findings that ZAP is an IFN-stimulated gene (ISG) [123, 130]. The ZAP

promoter contains several distal interferon stimulated response elements (ISREs) and is a direct target and responder of IFR3, transcription factor in the antiviral response [125]. Moreover, ZAP synergizes with one or more other IFN-induced ISG to maximize the immunity response effect against virus [131, 132]. Expression of ZAP was indeed shown to correlate with the survival of chickens infected with recombinant highly pathogenic avian influenza viruses [133].

A recent study has discovered that ZAP_L, but not $ZAP_{S,}$ was S-farnesylated, a crucial modification for ZAP_L targeting to endolysosomes and to enhance its antiviral activity [134]. This study also pointed out different involvement of ZAP_S and ZAP_L in the antiviral activity, the former displaying higher blocking activity on viral translation, the latter acting on cellular membranes [134].

A further study described another mode of action of ZAP in the innate immunity response [135]. ZAP, mainly ZAP_S, favours the oligomerization and ATPase activity of RIG-1, a RNA helicase that subsequently activates the transcription factors IRF3 and NF-kB, thus efficiently inhibiting viral replication of Influenza A virus and Newcastle disease virus [136]. However, a study performed in primary mouse cells from *PARP-13*$^{-/-}$ mice did not confirm the involvement of ZAP in the RIG-1 dependent IFN response, suggesting that ZAP antiviral activity is exerted on an independent process [113].

Besides this extensive characterization of the antiviral function of PARP-13/ZAP, new physiological roles of PARP-13 have emerged, in the regulation of stress response and activity of microRNA (miRNA) in the cytoplasm [114]. PAR and several members of the PARP family (PARP-12, PARP-13.1/ZAP_L, PARP-13.2/ZAP_S, PARP-5a/TNKS1, PARP-14 and PARP-15) where detected in cytoplasmic RNA-enriched granules formed in response to stress, named the stress granules (SG), transiently formed organelles aimed to regulate stability and translation of mRNAs. Overexpression of these PARPs nucleated the formation of SG. PARP-13.2/ZAP_S isoform became highly PARylated upon stress suggesting trans-PARylation by another SG-PARP. PARP-5a/TNKS1, the only SG enzyme endowed with PARP activity is the most serious candidate, but could also be stimulated and/or regulated by PARP-12 [114, 137]. PAR is proposed to act as a scaffolding molecule to bridge mRNA and proteins into complexes but also to regulate protein functions within SG [114, 137]. After stress, several of the argonaute proteins, especially AGO2, that are involved in miRNA function, are ADP-ribosylated, correlating with relief of micro-RNA silencing. AGO2 modification was dependent on its mRNA binding capacity. PARP-13.1/ZAP_L and PARP-13.2/ZAP_S were the most efficient alleviators of microRNA silencing. A possible mechanism could be that the inactive PARP-13 isoforms nucleate the association of the catalytically active PARPs PARP-5a and/or PARP-12 to the mRNA/AGO2 complex to cooperatively promote AGO2 PARylation, its dissociation from mRNA, thus diminishing its silencing effect [114, 137].

In conclusion, PARP-13/ZAP is now considered as a broad range antiviral effector, acting both on the viral mRNAs and on the host proteins to stimulate the innate immunity defences. The challenge is now to rely on this knowledge to develop tools mimicking PARP-13/ZAP effect to fight against severe viral infections or dangerous viruses for which no treatment exists yet.

2.4.3 PARP-12

PARP-12/ARTD12 is far less described than its closest homolog PARP-13. Subcellular localization studies revealed co-localization with Golgi markers, whereas its overexpression disrupted Golgi structure and led to the accumulation of PARP-12 in stress granules [52, 81, 114]. Recent reports describe PARP-12 as an additional PARP member exhibiting antiviral activities [138]. First, PARP-12 was identified as an IFN-stimulated gene (ISG) overexpressed during clearance of the non-cytopathic alphavirus Venezuelan equine encephalitis virus [86]. The longest PARP-12 isoform, PARP-12_L but not the PARP-12_S shorter isoform lacking the PARP-domain, appeared to inhibit virus replication. PARP-12 has a broad antiviral effect, since it reduced viral replication of other classes of viruses with both negative- and positive-strand RNA genomes (vesicular stomatitis virus, encephalomyocarditis virus and Rift Valley fever virus) [86]. The same group further demonstrated that PARP-12_L negatively regulates cellular translation, activity requiring the functional PARP domain and resulting from direct binding of PARP-12_L to ribosomes and polysomes and complex formation with cellular RNAs [81]. This effect could explain the antiviral activity of PARP-12_L, but also its possible contribution to the cytotoxicity observed upon PARP-12 overexpression [52, 81].

In summary, several PARP family members turn out to be IFN-stimulated genes: PARP-7, PARP-12, PARP-13, PARP-10, PARP-9, PARP-14, PARP-15, with a clear antiviral activity demonstrated for some of them. Whether these proteins functionally and synergistically interact or play independent or redundant roles in the antiviral response remains a challenging question.

2.5 vPARP

PARP-4/ARTD4 is also known as vault-PARP (vPARP), as it has been originally described as a component of vault particles [15]. Vaults particles are the largest ribonucleoprotein particles ever described (12.9 MDa), playing roles in multidrug resistance, nucleo-cytoplasmic transport, formation of ribonucleoparticules, signal transduction pathways and immune response, although their precise functions are still not elucidated. Most of vPARP is associated with vaults particles, together with Major Vault Protein (MVP), telomerase-associated protein-1 (TEP1) and an untranslated small vault RNA. An interaction between vPARP and either TEP1 or MVP was reported [139, 140]. Cryoelectron microscopy and crystallography revealed the barrel-shaped structure of vaults [141–143]. Therefore, vPARP is mainly distributed in the cytoplasm, engaged in vaults but also present in cytoplasmic clusters named vPARP-rods, and can exchange between these two cytoplasmic structures [144]. In addition, there is also free non-vault vPARP localised inside the nucleus and at the mitotic spindle, suggesting a vault-independent role of vPARP [15].

vPARP is the only PARP family member whose PARP domain is not C-terminal but internal. It is active, able of PARylation as a single molecule as well as within the vault complex, modifying MVP and to a lesser extent itself [15]. PARP-4 also contains a BRCA1 C-terminal domain (BRCT), an inter-alpha-trypsin motif, a von Willebrand type A domain (vWA) [145] as well as a C-terminal interaction domain binding to MVP [139, 146]. A vault-free form of vPARP has been described in *Octopus vulgaris* brain, in which the sole PAR acceptor was actin, regulated by the ATP-dependent polymerization of the cytoskeleton protein, thus regulating a fundamental mechanism for synaptic plasticity [147].

The generation of *PARP-4*$^{-/-}$ mice revealed that vPARP is dispensable for normal development, telomerase function or telomere length maintenance and vault structure [140]. These mice however displayed increased carcinogen-induced tumours, by urethane in the lungs and by dimethylhydrazine in the colon [148]. In post-surgery ovarian cancer samples, vPARP protein levels, as well as the other vault proteins, are increased in the higher-grade tumours oppositely to the measured mRNA levels which were significantly decreased, suggesting a post-transcriptional regulation of vault component production [149]. Vaults have been associated with cellular processes involved in cancer development [150]. In addition, numerous studies have reported an expression of MVP correlated with the degree of malignancy in certain cancer types, suggesting a possible involvement of MVP and vaults in tumour development and/or progression [150]. But whereas vault levels may be a good predictor of drug resistance [151] it remains to determine if targeting vaults, and more particularly targeting vPARP, could be of interest for the fight against cancer.

2.6 PARP-16

PARP-16 is the only PARP displaying a putative C-terminal transmembrane domain. This domain addresses PARP-16 to the endoplasmic reticulum (ER) and the nuclear envelope [52, 152]. PARP-16 possesses auto-MART activity and crystal structure revealed the presence of a novel α-helical regulatory domain, distinct from the regulatory domain of PARP-1, that packs against its transferase domain [153].

In ER, PARP-16 is tail-anchored with its catalytic domain within the cytoplasm [152]. Karyopherin-β1 (KAPβ1), a component of the nuclear trafficking machinery, was identified by mass spectrometry as a substrate of PARP-16, but the function of this interaction is still unknown [152, 154]. PARP-16 was subsequently shown to regulate the unfolded protein response (UPR) through the activation of the functionally related ER stress sensors protein kinase RNA-like ER kinase (PERK) and inositol-requiring trans-membrane knase and endonuclease 1α (IRE1α) [155]. PARP-16 is activated during ER stress: it self-ADP-ribosylates before modifying PERK and IRE1α; these MARylations increase their kinase activity and the endonuclease activity of IRE1α, possibly due to the dissociation of the inhibitory protein BiP/GRP78 from PERK and IRE1α. The C-terminal luminal tail of PARP-16 is required for its function during ER stress, suggesting that it transduces stress sig-

nals from the ER to the cytoplasmic PARP catalytic domain [155]. In the absence of PARP-16, PERK and IRE1α cannot be activated upon UPR induction leading to cell death [155]. Knockdown of PARP-16 not only disrupts the organization of ER membrane, it also impacts the short-term viability, with accumulation of paired round cells, reminiscent of defective cytokinesis [52]. The link between PARP-16 role in UPR and cytokinesis is not established, but activation of the UPR is known to result in cytokinesis defects in *Saccharomyces cerevisiae* [52, 156]. Since cancer cells often exhibit increased protein folding capacities due to increased protein synthesis, PARP-16 could be an attractive target for therapeutic inhibition, as proposed by Vyas et al. [52].

2.7 PARP-6, PARP-8, PARP-11

PARP-8 has been localized to centrosomes throughout the cell cycle and to nuclear envelope where it colocalizes with Lamin A/C [52]. The defects in nuclear envelope structure and the strong impact on viability upon PARP-8 knockdown suggest that it is a critical nuclear envelope protein [52]. PARP-11 localizes to centrosomes only during mitosis to spindle poles [52]. The PARP-11 gene seems very weakly expressed [52]. The tridimensional structure of PARP-11 WWE domain has been solved, revealing its ability to recognize the terminal ADP-ribose, lacking the distal ribose in PAR, thus it could also recognize ADP-ribose, in contrast to the WWE domain of RNF146 which recognizes iso-ADP-ribose [49]. Concerning PARP-8 and PARP-11 functions, no studies have been reported until now.

Regarding PARP-6, a single study was published so far, revealing that it is a negative regulator of cell proliferation [157]. The growth suppression requires the catalytic domain, whereas the S-phase accumulation of PARP-6-overexpressing cells requires the N-terminal putative regulatory part of the protein. PARP-6 expression in colorectal cancer correlates with well-differentiated histology and good prognosis, defining PARP-6 as a possible tumour suppressor thanks to its role in the cell cycle control.

2.8 Conclusion: Targeting Novel PARP Family Members in Anticancer Strategies

Research over the last decades has provided ample evidence for the therapeutic opportunity of targeting the DNA-damage induced PAR metabolism in anticancer strategies, as exemplified in several following chapters of this book. So far, a considerable effort was and is still currently made on the generation and optimization of low molecular-weight inhibitors of PARP to increase their potency and selectivity. Efficient targeting of PARP-1 remains the major Grail, either to potentiate the cytotoxic effect of antitumor genotoxic drugs in chemo- or radiotherapy, or to selec-

tively kill repair-deficient tumours in a synthetic lethality approach. The emerging specific functions of some other members of the PARP family in genomic integrity, cell proliferation, cell division, inflammation and cell death make them potentially attractive alternative targets or possible markers for cancer therapy. Further work is needed to decipher the biological function and mode of action of each PARP family member. In addition, their biochemical and structural properties need to be clearly identified to open the way to the development of pharmacological inhibitors. Work is underway, full of promises.

References

1. Chambon P, Weill JD, Mandel P (1963) Nicotinamide mononucleotide activation of new DNA-dependent polyadenylic acid synthesizing nuclear enzyme. Biochem Biophys Res Commun 11:39–43
2. Chambon P, Weill JD, Doly J, Strosser MT, Mandel P (1966) On the formation of a novel adenylic compound by enzymatic extracts of liver nuclei. Biochem Biophys Res Commun 25(6):638–643
3. Yamada M, Miwa M, Sugimura T (1971) Studies on poly (adenosine diphosphate-ribose). X. Properties of a partially purified poly (adenosine diphosphate-ribose) polymerase. Arch Biochem Biophys 146(2):579–586
4. de Murcia JM, Niedergang C, Trucco C, Ricoul M, Dutrillaux B, Mark M, Oliver FJ, Masson M, Dierich A, LeMeur M, Walztinger C, Chambon P, de Murcia G (1997) Requirement of poly(ADP-ribose) polymerase in recovery from DNA damage in mice and in cells. Proc Natl Acad Sci U S A 94(14):7303–7307
5. Masutani M, Nozaki T, Nishiyama E, Shimokawa T, Tachi Y, Suzuki H, Nakagama H, Wakabayashi K, Sugimura M (1999) Function of poly(ADP-ribose) polymerase in response to DNA damage: gene-disruption study in mice. Mol Cell Biochem 193:149–152
6. Wang ZQ, Auer B, Stingl L, Berghammer H, Haidacher D, Schweiger M, Wagner EF (1995) Mice lacking ADPRT and poly(ADP-ribosyl)ation develop normally but are susceptible to skin disease. Genes Dev 9(5):509–520
7. Shall S, de Murcia G (2000) Poly(ADP-ribose) polymerase-1: what have we learned from the deficient mouse model? Mutat Res 460(1):1–15
8. Shieh WM, Ame JC, Wilson MV, Wang ZQ, Koh DW, Jacobson MK, Jacobson EL (1998) Poly(ADP-ribose) polymerase null mouse cells synthesize ADP-ribose polymers. J Biol Chem 273(46):30069–30072
9. Lepiniec L, Babiychuk E, Kushnir S, Van Montagu M, Inze D (1995) Characterization of an *Arabidopsis thaliana* cDNA homologue to animal poly(ADP-ribose) polymerase. FEBS Lett 364(2):103–108
10. Babiychuk E, Cottrill PB, Storozhenko S, Fuangthong M, Chen Y, O'Farrell MK, Van Montagu M, Inze D, Kushnir S (1998) Higher plants possess two structurally different poly(ADP-ribose) polymerases. Plant J 15(5):635–645
11. Smith S, Giriat I, Schmitt A, de Lange T (1998) Tankyrase, a poly(ADP-ribose) polymerase at human telomeres. Science 282(5393):1484–1487
12. Amé JC, Rolli V, Schreiber V, Niedergang C, Apiou F, Decker P, Muller S, Hoger T, Menissier-de Murcia J, de Murcia G (1999) PARP-2, A novel mammalian DNA damage-dependent poly(ADP-ribose) polymerase. J Biol Chem 274(25):17860–17868
13. Johansson M (1999) A human poly(ADP-ribose) polymerase gene family (ADPRTL): cDNA cloning of two novel poly(ADP-ribose) polymerase homologues. Genomics 57(3):442–445

14. Augustin A, Spenlehauer C, Dumond H, Menissier-De Murcia J, Piel M, Schmit AC, Apiou F, Vonesch JL, Kock M, Bornens M, De Murcia G (2003) PARP-3 localizes preferentially to the daughter centriole and interferes with the G1/S cell cycle progression. J Cell Sci 116(8):1551–1562
15. Kickhoefer VA, Siva AC, Kedersha NL, Inman EM, Ruland C, Streuli M, Rome LH (1999) The 193-kD vault protein, VPARP, is a novel poly(ADP-ribose) polymerase. J Cell Biol 146(5):917–928
16. Amé JC, Spenlehauer C, de Murcia G (2004) The PARP superfamily. Bioessays 26(8):882–893
17. Chang P, Coughlin M, Mitchison TJ (2005) Tankyrase-1 polymerization of poly(ADP-ribose) is required for spindle structure and function. Nat Cell Biol 7(11):1133–1139
18. Chang W, Dynek JN, Smith S (2005) NuMA is a major acceptor of poly(ADP-ribosyl)ation by tankyrase 1 in mitosis. Biochem J 391(2):177–184
19. Cook BD, Dynek JN, Chang W, Shostak G, Smith S (2002) Role for the related poly(ADP-Ribose) polymerases tankyrase 1 and 2 at human telomeres. Mol Cell Biol 22(1):332–342
20. Hsiao SJ, Poitras MF, Cook BD, Liu Y, Smith S (2006) Tankyrase 2 poly(ADP-ribose) polymerase domain-deleted mice exhibit growth defects but have normal telomere length and capping. Mol Cell Biol 26(6):2044–2054
21. Ruf A, Ménissier de Murcia J, de Murcia G, Schulz GE (1996) Structure of the catalytic fragment of poly(AD-ribose) polymerase from chicken. Proc Natl Acad Sci U S A 93(15):7481–7485
22. Ruf A, de Murcia G, Schulz GE (1998) Inhibitor and NAD+ binding to poly(ADP-ribose) polymerase as derived from crystal structures and homology modeling. Biochemistry 37(11):3893–3900
23. Marsischky GT, Wilson BA, Collier RJ (1995) Role of glutamic acid 988 of human poly-ADP-ribose polymerase in polymer formation. Evidence for active site similarities to the ADP-ribosylating toxins. J Biol Chem 270(7):3247–3254
24. Kleine H, Poreba E, Lesniewicz K, Hassa PO, Hottiger MO, Litchfield DW, Shilton BH, Luscher B (2008) Substrate-assisted catalysis by PARP10 limits its activity to mono-ADP-ribosylation. Mol Cell 32(1):57–69
25. Otto H, Reche PA, Bazan F, Dittmar K, Haag F, Koch-Nolte F (2005) In silico characterization of the family of PARP-like poly(ADP-ribosyl)transferases (pARTs). BMC Genomics 6:139
26. Hottiger MO, Hassa PO, Luscher B, Schuler H, Koch-Nolte F (2010) Toward a unified nomenclature for mammalian ADP-ribosyltransferases. Trends Biochem Sci 35(4):208–219
27. Baysarowich J, Koteva K, Hughes DW, Ejim L, Griffiths E, Zhang K, Junop M, Wright GD (2008) Rifamycin antibiotic resistance by ADP-ribosylation: structure and diversity of Arr. Proc Natl Acad Sci U S A 105(12):4886–4891
28. Aguiar RC, Takeyama K, He C, Kreinbrink K, Shipp M (2005) B-aggressive lymphoma (BAL) family proteins have unique domains that modulate transcription and exhibit Poly(ADP-ribose) polymerase activity. J Biol Chem 280(49):33756–33765
29. Aguiar RC, Yakushijin Y, Kharbanda S, Salgia R, Fletcher JA, Shipp MA (2000) BAL is a novel risk-related gene in diffuse large B-cell lymphomas that enhances cellular migration. Blood 96(13):4328–4334
30. Juszczynski P, Kutok JL, Li C, Mitra J, Aguiar RC, Shipp MA (2006) BAL1 and BBAP are regulated by a gamma interferon-responsive bidirectional promoter and are overexpressed in diffuse large B-cell lymphomas with a prominent inflammatory infiltrate. Mol Cell Biol 26(14):5348–5359
31. Schreiber V, Dantzer F, Ame JC, de Murcia G (2006) Poly(ADP-ribose): novel functions for an old molecule. Nat Rev Mol Cell Biol 7(7):517–528
32. Hakmé A, Huber A, Dollé P, Schreiber V (2008) The macroPARP genes PARP-9 and PARP-14 are developmentally and differentially regulated in mouse tissues. Dev Dyn 237(1):209–215
33. Goenka S, Cho SH, Boothby M (2007) Collaborator of Stat6 (CoaSt6)-associated Poly(ADP-ribose) polymerase activity modulates Stat6-dependent gene transcription. J Biol Chem 282(26):18732–18739

34. Venkannagari H, Fallarero A, Feijs KL, Luscher B, Lehtio L (2013) Activity-based assay for human mono-ADP-ribosyltransferases ARTD7/PARP15 and ARTD10/PARP10 aimed at screening and profiling inhibitors. Eur J Pharm Sci 49(2):148–156
35. Wahlberg E, Karlberg T, Kouznetsova E, Markova N, Macchiarulo A, Thorsell AG, Pol E, Frostell A, Ekblad T, Oncu D, Kull B, Robertson GM, Pellicciari R, Schuler H, Weigelt J (2012) Family-wide chemical profiling and structural analysis of PARP and tankyrase inhibitors. Nat Biotechnol 30(3):283–288
36. Andersson CD, Karlberg T, Ekblad T, Lindgren AEG, Thorsell A-G, Spjut S, Uciechowska U, Niemiec MS, Wittung-Stafshede P, Weigelt J, Elofsson M, Schüler H, Linusson A (2012) Discovery of ligands for ADP-ribosyltransferases via docking-based virtual screening. J Med Chem 55(17):7706–7718
37. Karras GI, Kustatscher G, Buhecha HR, Allen MD, Pugieux C, Sait F, Bycroft M, Ladurner AG (2005) The macro domain is an ADP-ribose binding module. Embo J 24(11):1911–1920
38. Ahel D, Horejsi Z, Wiechens N, Polo SE, Garcia-Wilson E, Ahel I, Flynn H, Skehel M, West SC, Jackson SP, Owen-Hughes T, Boulton SJ (2009) Poly(ADP-ribose)-dependent regulation of DNA repair by the chromatin remodeling enzyme ALC1. Science 325(5945):1240–1243
39. Gottschalk AJ, Timinszky G, Kong SE, Jin J, Cai Y, Swanson SK, Washburn MP, Florens L, Ladurner AG, Conaway JW, Conaway RC (2009) Poly(ADP-ribosyl)ation directs recruitment and activation of an ATP-dependent chromatin remodeler. Proc Natl Acad Sci U S A 106(33):13770–13774
40. Kalisch T, Ame JC, Dantzer F, Schreiber V (2012) New readers and interpretations of poly(ADP-ribosyl)ation. Trends Biochem Sci 37(9):381–390
41. Feijs KL, Forst AH, Verheugd P, Luscher B (2013) Macrodomain-containing proteins: regulating new intracellular functions of mono(ADP-ribosyl)ation. Nat Rev Mol Cell Biol 14(7):445–453
42. Forst AH, Karlberg T, Herzog N, Thorsell AG, Gross A, Feijs KL, Verheugd P, Kursula P, Nijmeijer B, Kremmer E, Kleine H, Ladurner AG, Schuler H, Luscher B (2013) Recognition of mono-ADP-ribosylated ARTD10 substrates by ARTD8 macrodomains. Structure 21(3):462–475
43. Sharifi R, Morra R, Appel CD, Tallis M, Chioza B, Jankevicius G, Simpson MA, Matic I, Ozkan E, Golia B, Schellenberg MJ, Weston R, Williams JG, Rossi MN, Galehdari H, Krahn J, Wan A, Trembath RC, Crosby AH, Ahel D, Hay R, Ladurner AG, Timinszky G, Williams RS, Ahel I (2013) Deficiency of terminal ADP-ribose protein glycohydrolase TARG1/C6orf130 in neurodegenerative disease. EMBO J 32(9):1225–1237
44. Rosenthal F, Feijs KL, Frugier E, Bonalli M, Forst AH, Imhof R, Winkler HC, Fischer D, Caflisch A, Hassa PO, Luscher B, Hottiger MO (2013) Macrodomain-containing proteins are new mono-ADP-ribosylhydrolases. Nat Struct Mol Biol 20(4):502–507
45. Jankevicius G, Hassler M, Golia B, Rybin V, Zacharias M, Timinszky G, Ladurner AG (2013) A family of macrodomain proteins reverses cellular mono-ADP-ribosylation. Nat Struct Mol Biol 20(4):508–514
46. Feijs KL, Verheugd P, Luscher B (2013) Expanding functions of intracellular resident mono-ADP-ribosylation in cell physiology. FEBS J 280(15):3519–3529
47. Yan Q, Xu R, Zhu L, Cheng X, Wang Z, Manis J, Shipp MA (2013) BAL1 and its partner E3 ligase, BBAP, link Poly(ADP-ribose) activation, ubiquitylation, and double-strand DNA repair independent of ATM, MDC1, and RNF8. Mol Cell Biol 33(4):845–857
48. Wang Z, Michaud GA, Cheng Z, Zhang Y, Hinds TR, Fan E, Cong F, Xu W (2012) Recognition of the iso-ADP-ribose moiety in poly(ADP-ribose) by WWE domains suggests a general mechanism for poly(ADP-ribosyl)ation-dependent ubiquitination. Genes Dev 26(3):235–240
49. He F, Tsuda K, Takahashi M, Kuwasako K, Terada T, Shirouzu M, Watanabe S, Kigawa T, Kobayashi N, Guntert P, Yokoyama S, Muto Y (2012) Structural insight into the interaction of ADP-ribose with the PARP WWE domains. FEBS Lett 586(21):3858–3864
50. Takeyama K, Aguiar RC, Gu L, He C, Freeman GJ, Kutok JL, Aster JC, Shipp MA (2003) The BAL-binding protein BBAP and related Deltex family members exhibit ubiquitin-protein isopeptide ligase activity. J Biol Chem 278(24):21930–21937

51. Artavanis-Tsakonas S, Rand MD, Lake RJ (1999) Notch signaling: cell fate control and signal integration in development. Science 284(5415):770–776
52. Vyas S, Chesarone-Cataldo M, Todorova T, Huang YH, Chang P (2013) A systematic analysis of the PARP protein family identifies new functions critical for cell physiology. Nat Commun 4:2240
53. Monti S, Savage KJ, Kutok JL, Feuerhake F, Kurtin P, Mihm M, Wu B, Pasqualucci L, Neuberg D, Aguiar RC, Dal Cin P, Ladd C, Pinkus GS, Salles G, Harris NL, Dalla-Favera R, Habermann TM, Aster JC, Golub TR, Shipp MA (2005) Molecular profiling of diffuse large B-cell lymphoma identifies robust subtypes including one characterized by host inflammatory response. Blood 105(5):1851–1861
54. Stark GR, Darnell JE Jr (2012) The JAK-STAT pathway at twenty. Immunity 36(4):503–514
55. Dunn GP, Old LJ, Schreiber RD (2004) The immunobiology of cancer immunosurveillance and immunoediting. Immunity 21(2):137–148
56. Camicia R, Bachmann SB, Winkler HC, Beer M, Tinguely M, Haralambieva E, Hassa PO (2013) BAL1/ARTD9 represses the anti-proliferative and pro-apoptotic IFNgamma-STAT1-IRF1-p53 axis in diffuse large B-cell lymphoma. J Cell Sci 126(9):1969–1980
57. Yan Q, Dutt S, Xu R, Graves K, Juszczynski P, Manis JP, Shipp MA (2009) BBAP monoubiquitylates histone H4 at lysine 91 and selectively modulates the DNA damage response. Mol Cell 36(1):110–120
58. Botuyan MV, Lee J, Ward IM, Kim JE, Thompson JR, Chen J, Mer G (2006) Structural basis for the methylation state-specific recognition of histone H4-K20 by 53BP1 and Crb2 in DNA repair. Cell 127(7):1361–1373
59. Lukas J, Lukas C, Bartek J (2011) More than just a focus: the chromatin response to DNA damage and its role in genome integrity maintenance. Nat Cell Biol 13(10):1161–1169
60. Polo SE, Jackson SP (2011) Dynamics of DNA damage response proteins at DNA breaks: a focus on protein modifications. Genes Dev 25(5):409–433
61. Li M, Lu LY, Yang CY, Wang S, Yu X (2013) The FHA and BRCT domains recognize ADP-ribosylation during DNA damage response. Genes Dev 27(16):1752–1768
62. Li M, Yu X (2013) Function of BRCA1 in the DNA damage response is mediated by ADP-ribosylation. Cancer Cell 23(5):693–704
63. Goenka S, Boothby M (2006) Selective potentiation of Stat-dependent gene expression by collaborator of Stat6 (CoaSt6), a transcriptional cofactor. Proc Natl Acad Sci U S A 103(11):4210–4215
64. Mehrotra P, Riley JP, Patel R, Li F, Voss L, Goenka S (2011) PARP-14 functions as a transcriptional switch for STAT6 dependent gene activation. J Biol Chem 286(3):1767–1776
65. Riley JP, Kulkarni A, Mehrotra P, Koh B, Perumal NB, Kaplan MH, Goenka S (2013) PARP-14 binds specific DNA sequences to promote Th2 cell gene expression. PLoS ONE 8(12):e83127
66. Cho SH, Goenka S, Henttinen T, Gudapati P, Reinikainen A, Eischen CM, Lahesmaa R, Boothby M (2009) PARP-14, a member of the B aggressive lymphoma family, transduces survival signals in primary B cells. Blood 113(11):2416–2425
67. Cho SH, Ahn AK, Bhargava P, Lee CH, Eischen CM, McGuinness O, Boothby M (2011) Glycolytic rate and lymphomagenesis depend on PARP14, an ADP ribosyltransferase of the B aggressive lymphoma (BAL) family. Proc Natl Acad Sci U S A 108(38):15972–15977
68. Mehrotra P, Hollenbeck A, Riley JP, Li F, Patel RJ, Akhtar N, Goenka S (2013) Poly (ADP-ribose) polymerase 14 and its enzyme activity regulates T(H)2 differentiation and allergic airway disease. J Allergy Clin Immunol 131(2):521–531 e521–512
69. Cho SH, Raybuck A, Wei M, Erickson J, Nam KT, Cox RG, Trochtenberg A, Thomas JW, Williams J, Boothby M (2013) B cell-intrinsic and -extrinsic regulation of antibody responses by PARP14, an intracellular (ADP-ribosyl)transferase. J Immunol 191(6):3169–3178
70. Hirota K, Turner JE, Villa M, Duarte JH, Demengeot J, Steinmetz OM, Stockinger B (2013) Plasticity of Th17 cells in Peyer's patches is responsible for the induction of T cell-dependent IgA responses. Nature Immunol 14(4):372–379

71. Krishnamurthy P, Sherrill JD, Parashette K, Goenka S, Rothenberg ME, Gupta S, Kaplan MH (2014) Correlation of increased PARP14 and CCL26 expression in biopsies from children with eosinophilic esophagitis. J Allergy Clin Immunol 133(2):577–580 e572
72. Allen JD, Berns A (1996) Complementation tagging of cooperating oncogenes in knockout mice. Semin Cancer Biol 7(5):299–306
73. Campbell KJ, Bath ML, Turner ML, Vandenberg CJ, Bouillet P, Metcalf D, Scott CL, Cory S (2010) Elevated Mcl-1 perturbs lymphopoiesis, promotes transformation of hematopoietic stem/progenitor cells, and enhances drug resistance. Blood 116(17):3197–3207
74. Yanagawa T, Funasaka T, Tsutsumi S, Hu H, Watanabe H, Raz A (2007) Regulation of phosphoglucose isomerase/autocrine motility factor activities by the poly(ADP-ribose) polymerase family-14. Cancer Res 67(18):8682–8689
75. Barbarulo A, Iansante V, Chaidos A, Naresh K, Rahemtulla A, Franzoso G, Karadimitris A, Haskard DO, Papa S, Bubici C (2013) Poly(ADP-ribose) polymerase family member 14 (PARP14) is a novel effector of the JNK2-dependent pro-survival signal in multiple myeloma. Oncogene 32(36):4231–4242
76. Bubici C, Papa S (2014) JNK signalling in cancer: in need of new, smarter therapeutic targets. Br J Pharmacol 171(1):24–37
77. Yu M, Schreek S, Cerni C, Schamberger C, Lesniewicz K, Poreba E, Vervoorts J, Walsemann G, Grotzinger J, Kremmer E, Mehraein Y, Mertsching J, Kraft R, Austen M, Luscher-Firzlaff J, Luscher B (2005) PARP-10, a novel Myc-interacting protein with poly(ADP-ribose) polymerase activity, inhibits transformation. Oncogene 24(12):1982–1993
78. Kleine H, Herrmann A, Lamark T, Forst AH, Verheugd P, Luscher-Firzlaff J, Lippok B, Feijs KL, Herzog N, Kremmer E, Johansen T, Muller-Newen G, Luscher B (2012) Dynamic subcellular localization of the mono-ADP-ribosyltransferase ARTD10 and interaction with the ubiquitin receptor p62. Cell Commun Signal 10(1):28
79. Chou HY, Chou HT, Lee SC (2006) Cdk-dependent activation of poly(ADP-ribose)polymerase member 10 (PARP10). J Biol Chem 281(22):15201–15207
80. Herzog N, Hartkamp JD, Verheugd P, Treude F, Forst AH, Feijs KL, Lippok BE, Kremmer E, Kleine H, Luscher B (2013) Caspase-dependent cleavage of the mono-ADP-ribosyltransferase ARTD10 interferes with its pro-apoptotic function. FEBS J 280(5):1330–1343
81. Atasheva S, Frolova EI, Frolov I (2014) Interferon-stimulated poly(ADP-Ribose) polymerases are potent inhibitors of cellular translation and virus replication. J Virol 88(4):2116–2130
82. Nicolae CM, Aho ER, Vlahos AH, Choe KN, De S, Karras GI, Moldovan GL (2014) The ADP-ribosyltransferase PARP10/ARTD10 interacts with Proliferating Cell Nuclear Antigen (PCNA) and is required for DNA damage tolerance. J Biol Chem 289(19):13627–13637
83. Verheugd P, Forst AH, Milke L, Herzog N, Feijs KL, Kremmer E, Kleine H, Luscher B (2013) Regulation of NF-kappaB signalling by the mono-ADP-ribosyltransferase ARTD10. Nat Commun 4:1683
84. Mahmoud L, Al-Saif M, Amer HM, Sheikh M, Almajhdi FN, Khabar KS (2011) Green fluorescent protein reporter system with transcriptional sequence heterogeneity for monitoring the interferon response. J Virol 85(18):9268–9275
85. Yu M, Zhang C, Yang Y, Yang Z, Zhao L, Xu L, Wang R, Zhou X, Huang P (2011) The interaction between the PARP10 protein and the NS1 protein of H5N1 AIV and its effect on virus replication. Virol J 8:546
86. Atasheva S, Akhrymuk M, Frolova EI, Frolov I (2012) New PARP gene with an anti-alphavirus function. J Virol 86(15):8147–8160
87. Shen X, Wang W, Wang L, Houde C, Wu W, Tudor M, Thompson JR, Sisk CM, Hubbard B, Li J (2012) Identification of genes affecting apolipoprotein B secretion following siRNA-mediated gene knockdown in primary human hepatocytes. Atherosclerosis 222(1):154–157
88. Feijs KL, Kleine H, Braczynski A, Forst AH, Herzog N, Verheugd P, Linzen U, Kremmer E, Luscher B (2013) ARTD10 substrate identification on protein microarrays: regulation of GSK3beta by mono-ADP-ribosylation. Cell Commun Signal 11(1):5

89. Chen S, Xu Y, Zhang K, Wang X, Sun J, Gao G, Liu Y (2012) Structure of N-terminal domain of ZAP indicates how a zinc-finger protein recognizes complex RNA. Nat Struct Mol Biol 19 (4):430–435
90. Law LMJ, Albin OR, Carroll J-WN, Jones CT, Rice CM, MacDonald MR (2010) Identification of a dominant negative inhibitor of human zinc finger antiviral protein reveals a functional endogenous pool and critical homotypic interactions. J Virol 84(9):4504–4512
91. Kerns JA, Emerman M, Malik HS (2008) Positive Selection and Increased Antiviral Activity Associated with the PARP-Containing Isoform of Human Zinc-Finger Antiviral Protein. PLoS Genet 4(1):e21
92. Ma Q, Baldwin KT, Renzelli AJ, McDaniel A, Dong L (2001) TCDD-inducible poly(ADP-ribose) polymerase: a novel response to 2,3,7,8-tetrachlorodibenzo-p-dioxin. Biochem Biophys Res Commun 289(2):499–506
93. MacPherson L, Tamblyn L, Rajendra S, Bralha F, McPherson JP, Matthews J (2013) 2,3,7,8-Tetrachlorodibenzo-p-dioxin poly(ADP-ribose) polymerase (TiPARP, ARTD14) is a mono-ADP-ribosyltransferase and repressor of aryl hydrocarbon receptor transactivation. Nucleic Acids Res 41(3):1604–1621
94. Matthews J (2013) Alternative negative feedback control in the Aryl hydrocarbon receptor signaling pathway. J Drug Metab Toxicol 4(e116)
95. de Waard PWJ, Peijnenburg AACM, Baykus H, Aarts JMMJG, Hoogenboom RLAP, van Schooten FJ, de Kok TMCM (2008) A human intervention study with foods containing natural Ah-receptor agonists does not significantly show AhR-mediated effects as measured in blood cells and urine. Chem Biol Interact 176(1):19–29
96. Boutros PC, Yao CQ, Watson JD, Wu AH, Moffat ID, Prokopec SD, Smith AB, Okey AB, Pohjanvirta R (2011) Hepatic transcriptomic responses to TCDD in dioxin-sensitive and dioxin-resistant rats during the onset of toxicity. Toxicol Appl Pharmacol 251(2):119–129
97. Ito T, Nagai H, Lin T-M, Peterson RE, Tohyama C, Kobayashi T, Nohara K (2006) Organic chemicals adsorbed onto diesel exhaust particles directly alter the differentiation of fetal thymocytes through arylhydrocarbon receptor but not oxidative stress responses. J Immunotoxicol 3(1):21–30
98. Ma Q (2002) Induction and superinduction of 2,3,7,8-tetrachlorodibenzo-rho-dioxin-inducible poly(ADP-ribose) polymerase: role of the aryl hydrocarbon receptor/aryl hydrocarbon receptor nuclear translocator transcription activation domains and a labile transcription repressor. Arch Biochem Biophys 404(2):309–316
99. Hao N, Lee KL, Furness SGB, Bosdotter C, Poellinger L, Whitelaw ML (2012) Xenobiotics and loss of cell adhesion drive distinct transcriptional outcomes by aryl hydrocarbon receptor signaling. Mol Pharmacol 82(6):1082–1093
100. Diani-Moore S, Ram P, Li X, Mondal P, Youn DY, Sauve AA, Rifkind AB (2010) Identification of the aryl hydrocarbon receptor target gene TiPARP as a mediator of suppression of hepatic gluconeogenesis by 2,3,7,8-tetrachlorodibenzo-p-dioxin and of nicotinamide as a corrective agent for this effect. J Biol Chem 285(50):38801–38810
101. Diani-Moore S, Zhang S, Ram P, Rifkind AB (2013) Aryl hydrocarbon receptor activation by dioxin targets phosphoenolpyruvate carboxykinase (PEPCK) for ADP-ribosylation via 2,3,7,8-tetrachlorodibenzo-p-dioxin (TCDD)-inducible poly(ADP-ribose) polymerase (TiPARP). J Biol Chem 288(30):21514–21525
102. Bai P, Canto C, Oudart H, Brunyanszki A, Cen Y, Thomas C, Yamamoto H, Huber A, Kiss B, Houtkooper RH, Schoonjans K, Schreiber V, Sauve AA, Menissier-de Murcia J, Auwerx J (2011) PARP-1 inhibition increases mitochondrial metabolism through SIRT1 activation. Cell Metab 13(4):461–468
103. He J, Hu B, Shi X, Weidert ER, Lu P, Xu M, Huang M, Kelley EE, Xie W (2013) Activation of the aryl hydrocarbon receptor sensitizes mice to nonalcoholic steatohepatitis by deactivating mitochondrial sirtuin deacetylase Sirt3. Mol Cell Biol 33(10):2047–2055
104. Wright RH, Castellano G, Bonet J, Le Dily F, Font-Mateu J, Ballare C, Nacht AS, Soronellas D, Oliva B, Beato M (2012) CDK2-dependent activation of PARP-1 is required for hormonal gene regulation in breast cancer cells. Genes Dev 26(17):1972–1983

105. Siddique HR, Mishra SK, Karnes RJ, Saleem M (2011) Lupeol, a novel androgen receptor inhibitor: implications in prostate cancer therapy. Clin Cancer Res 17(16):5379–5391
106. Bolton EC, So AY, Chaivorapol C, Haqq CM, Li H, Yamamoto KR (2007) Cell- and gene-specific regulation of primary target genes by the androgen receptor. Genes Dev 21(16):2005–2017
107. Chen WV, Delrow J, Corrin PD, Frazier JP, Soriano P (2004) Identification and validation of PDGF transcriptional targets by microarray-coupled gene-trap mutagenesis. Nat Genet 36(3):304–312
108. Schmahl J, Raymond CS, Soriano P (2007) PDGF signaling specificity is mediated through multiple immediate early genes. Nat Genet 39(1):52–60
109. Katoh M (2003) Identification and characterization of human TIPARP gene within the CCNL amplicon at human chromosome 3q25.31. Int J Oncol 23(2):541–547
110. Goode EL, Chenevix-Trench G, Song H, Ramus SJ, Notaridou M, Lawrenson K, Widschwendter M, Vierkant RA, Larson MC, Kjaer SK, Birrer MJ, Berchuck A, Schildkraut J, Tomlinson I, Kiemeney LA, Cook LS, Gronwald J, Garcia-Closas M, Gore ME, Campbell I, Whittemore AS, Sutphen R, Phelan C, Anton-Culver H, Pearce CL, Lambrechts D, Rossing MA, Chang-Claude J, Moysich KB, Goodman MT, Dork T, Nevanlinna H, Ness RB, Rafnar T, Hogdall C, Hogdall E, Fridley BL, Cunningham JM, Sieh W, McGuire V, Godwin AK, Cramer DW, Hernandez D, Levine D, Lu K, Iversen ES, Palmieri RT, Houlston R, van Altena AM, Aben KK, Massuger LF, Brooks-Wilson A, Kelemen LE, Le ND, Jakubowska A, Lubinski J, Medrek K, Stafford A, Easton DF, Tyrer J, Bolton KL, Harrington P, Eccles D, Chen A, Molina AN, Davila BN, Arango H, Tsai YY, Chen Z, Risch HA, McLaughlin J, Narod SA, Ziogas A, Brewster W, Gentry-Maharaj A, Menon U, Wu AH, Stram DO, Pike MC, Wellcome Trust Case-Control C, Beesley J, Webb PM, Australian Cancer S, Australian Ovarian Cancer Study G, Ovarian Cancer Association C, Chen X, Ekici AB, Thiel FC, Beckmann MW, Yang H, Wentzensen N, Lissowska J, Fasching PA, Despierre E, Amant F, Vergote I, Doherty J, Hein R, Wang-Gohrke S, Lurie G, Carney ME, Thompson PJ, Runnebaum I, Hillemanns P, Durst M, Antonenkova N, Bogdanova N, Leminen A, Butzow R, Heikkinen T, Stefansson K, Sulem P, Besenbacher S, Sellers TA, Gayther SA, Pharoah PD, Ovarian Cancer Association C (2010) A genome-wide association study identifies susceptibility loci for ovarian cancer at 2q31 and 8q24. Nat Genet 42(10):874–879
111. Cha JD, Kim HJ, Cha IH (2011) Genetic alterations in oral squamous cell carcinoma progression detected by combining array-based comparative genomic hybridization and multiplex ligation-dependent probe amplification. Oral Surg Oral Med Oral Pathol Oral Radiol Endod 111(5):594–607
112. Liu L, Chen G, Ji X, Gao G (2004) ZAP is a CRM1-dependent nucleocytoplasmic shuttling protein. Biochem Biophys Res Com 321(3):517–523
113. Lee H, Komano J, Saitoh Y, Yamaoka S, Kozaki T, Misawa T, Takahama M, Satoh T, Takeuchi O, Yamamoto N, Matsuura Y, Saitoh T, Akira S (2013) Zinc-finger antiviral protein mediates retinoic acid inducible gene I-like receptor-independent antiviral response to murine leukemia virus. Proc Natl Acad Sci U S A 110(30):12379–12384
114. Leung AKL, Vyas S, Rood JE, Bhutkar A, Sharp PA, Chang P (2011) Poly(ADP-Ribose) regulates stress responses and MicroRNA activity in the cytoplasm. Mol Cell 42(4):489–499
115. Gao G, Guo X, Goff SP (2002) Inhibition of retroviral RNA production by ZAP, a CCCH-type zinc finger protein. Science 297(5587):1703–1706
116. Huang Z, Wang X, Gao G (2010) Analyses of SELEX-derived ZAP-binding RNA aptamers suggest that the binding specificity is determined by both structure and sequence of the RNA. Protein Cell 1(8):752–759
117. Bick MJ, Carroll JWN, Gao G, Goff SP, Rice CM, MacDonald MR (2003) Expression of the zinc-finger antiviral protein inhibits alphavirus replication. J Virol 77(21):11555–11562
118. Müller S, Möller P, Bick MJ, Wurr S, Becker S, Günther S, Kümmerer BM (2007) Inhibition of filovirus replication by the zinc finger antiviral protein. J Virol 81(5):2391–2400

119. Zhu Y, Chen G, Lv F, Wang X, Ji X, Xu Y, Sun J, Wu L, Zheng Y-T, Gao G (2011) Zinc-finger antiviral protein inhibits HIV-1 infection by selectively targeting multiply spliced viral mRNAs for degradation. Proc Natl Acad Sci U S A 108(38):15834–15839
120. Zhu Y, Gao G (2008) ZAP-mediated mRNA degradation. RNA Biol 5(2):65–67
121. Guo X, Carroll J-WN, MacDonald MR, Goff SP, Gao G (2004) The zinc finger antiviral protein directly binds to specific viral mRNAs through the CCCH zinc finger motifs. J Virol 78(23):12781–12787
122. Jeong MS, Kim EJ, Jang SB (2010) Expression and RNA-binding of human zinc-finger antiviral protein. Biochem Biophys Res Commun 396(3):696–702
123. Mao R, Nie H, Cai D, Zhang J, Liu H, Yan R, Cuconati A, Block TM, Guo J-T, Guo H (2013) Inhibition of hepatitis B virus replication by the host zinc finger antiviral protein. PLoS Pathog 9(7):e1003494
124. Guo X, Ma J, Sun J, Gao G (2007) The zinc-finger antiviral protein recruits the RNA processing exosome to degrade the target mRNA. Proc Natl Acad Sci U S A 104(1):151–156
125. Wang X, Lv F, Gao G (2010) Mutagenesis analysis of the zinc-finger antiviral protein. Retrovirology 7:19
126. Chen G, Guo X, Lv F, Xu Y, Gao G (2008) p72 DEAD box RNA helicase is required for optimal function of the zinc-finger antiviral protein. Proc Natl Acad Sci U S A 105(11):4352–4357
127. Ye P, Liu S, Zhu Y, Chen G, Gao G (2010) DEXH-Box protein DHX30 is required for optimal function of the zinc-finger antiviral protein. Protein Cell 1(10):956–964
128. Xuan Y, Liu L, Shen S, Deng H, Gao G (2012) Zinc finger antiviral protein inhibits murine gammaherpesvirus 68 M2 expression and regulates viral latency in cultured cells. J Virol 86(22):12431–12434
129. Xuan Y, Gong D, Qi J, Han C, Deng H, Gao G (2013) ZAP inhibits murine gammaherpesvirus 68 ORF64 expression and is antagonized by RTA. J Virol 87(5):2735–2743
130. Zhang Y, Burke CW, Ryman KD, Klimstra WB (2007) Identification and characterization of interferon-induced proteins that inhibit alphavirus replication. J Virol 81(20):11246–11255
131. MacDonald MR, Machlin ES, Albin OR, Levy DE (2007) The zinc finger antiviral protein acts synergistically with an interferon-induced factor for maximal activity against alphaviruses. J Virol 81(24):13509–13518
132. Karki S, Li MM, Schoggins JW, Tian S, Rice CM, MacDonald MR (2012) Multiple interferon stimulated genes synergize with the zinc finger antiviral protein to mediate anti-alphavirus activity. PLoS ONE 7(5):e37398
133. Uchida Y, Watanabe C, Takemae N, Hayashi T, Oka T, Ito T, Saito T (2012) Identification of host genes linked with the survivability of chickens infected with recombinant viruses possessing H5N1 surface antigens from a highly pathogenic avian influenza virus. J Virol 86(5):2686–2695
134. Charron G, Li MMH, MacDonald MR, Hang HC (2013) Prenylome profiling reveals S-farnesylation is crucial for membrane targeting and antiviral activity of ZAP long-isoform. Proc Natl Acad Sci U S A 110(27):11085–11090
135. Hayakawa S, Shiratori S, Yamato H, Kameyama T, Kitatsuji C, Kashigi F, Goto S, Kameoka S, Fujikura D, Yamada T, Mizutani T, Kazumata M, Sato M, Tanaka J, Asaka M, Ohba Y, Miyazaki T, Imamura M, Takaoka A (2011) ZAPS is a potent stimulator of signaling mediated by the RNA helicase RIG-I during antiviral responses. Nat Immunol 12(1):37–44
136. Liu HM, Gale M (2011) ZAPS electrifies RIG-I signaling. Nat Immunol 12(1):11–12
137. Leung A, Todorova T, Ando Y, Chang P (2012) Poly(ADP-ribose) regulates post-transcriptional gene regulation in the cytoplasm. RNA Biol 9(5):542–548
138. Welsby I, Hutin D, Leo O (2012) Complex roles of members of the ADP-ribosyl transferase super family in immune defences: looking beyond PARP1. Biochem Pharmacol 84(1):11–20
139. van Zon A, Mossink MH, Schoester M, Scheffer GL, Scheper RJ, Sonneveld P, Wiemer EAC (2002) Structural domains of vault proteins: a role for the coiled coil domain in vault assembly. Biochem Biophys Res Com 291(3):535–541

140. Liu Y, Snow BE, Kickhoefer VA, Erdmann N, Zhou W, Wakeham A, Gomez M, Rome LH, Harrington L (2004) Vault poly(ADP-ribose) polymerase is associated with mammalian telomerase and is dispensable for telomerase function and vault structure in vivo. Mol Cell Biol 24(12):5314–5323
141. Kato K, Tanaka H, Sumizawa T, Yoshimura M, Yamashita E, Iwasaki K, Tsukihara T (2008) A vault ribonucleoprotein particle exhibiting 39-fold dihedral symmetry. Acta Crystallogr D Biol Crystallogr 64(5):525–531
142. Kong LB, Siva AC, Kickhoefer VA, Rome LH, Stewart PL (2000) RNA location and modeling of a WD40 repeat domain within the vault. Rna 6(6):890–900
143. Mikyas Y, Makabi M, Raval-Fernandes S, Harrington L, Kickhoefer VA, Rome LH, Stewart PL (2004) Cryoelectron microscopy imaging of recombinant and tissue derived vaults: localization of the MVP N termini and VPARP. J Mol Biol 344(1):91–105
144. van Zon A, Mossink MH, Schoester M, Houtsmuller AB, Scheffer GL, Scheper RJ, Sonneveld P, Wiemer EAC (2003) The formation of vault-tubes: a dynamic interaction between vaults and vault PARP. J Cell Sci 116 (Pt 21):4391–4400
145. Bateman A, Kickhoefer V (2003) The TROVE module: a common element in Telomerase, Ro and Vault ribonucleoproteins. BMC Bioinform 4:49
146. Zheng C-L, Sumizawa T, Che X-F, Tsuyama S, Furukawa T, Haraguchi M, Gao H, Gotanda T, Jueng H-C, Murata F, Akiyama S-I (2005) Characterization of MVP and VPARP assembly into vault ribonucleoprotein complexes. Biochem Biophys Res Com 326(1):100–107
147. De Maio A, Natale E, Rotondo S, Di Cosmo A, Faraone-Mennella MR (2013) Vault-poly-ADP-ribose polymerase in the Octopus vulgaris brain: a regulatory factor of actin polymerization dynamic. Comp Biochem Physiol B. Biochem Mol Biol 166(1):40–47
148. Raval-Fernandes S, Kickhoefer VA, Kitchen C, Rome LH (2005) Increased susceptibility of vault poly(ADP-ribose) polymerase-deficient mice to carcinogen-induced tumorigenesis. Cancer Res 65(19):8846–8852
149. Szaflarski W, Sujka-Kordowska P, Pula B, Jaszczyńska-Nowinka K, Andrzejewska M, Zawierucha P, Dziegiel P, Nowicki M, Ivanov P, Zabel M (2013) Expression profiles of vault components MVP, TEP1 and vPARP and their correlation to other multidrug resistance proteins in ovarian cancer. Int J Oncol 43(2):513–520
150. Steiner E, Holzmann K, Elbling L, Micksche M, Berger W (2006) Cellular functions of vaults and their involvement in multidrug resistance. Curr Drug Targets 7(8):923–934
151. Siva AC, Raval-Fernandes S, Stephen AG, LaFemina MJ, Scheper RJ, Kickhoefer VA, Rome LH (2001) Up-regulation of vaults may be necessary but not sufficient for multidrug resistance. Int J Cancer 92(2):195–202
152. Di Paola S, Micaroni M, Di Tullio G, Buccione R, Di Girolamo M (2012) PARP16/ARTD15 is a novel endoplasmic-reticulum-associated mono-ADP-ribosyltransferase that interacts with, and modifies karyopherin-ß1. PLoS ONE 7(6):e37352
153. Karlberg T, Thorsell A-G, Kallas Å, Schüler H (2012) Crystal structure of human ADP-ribose transferase ARTD15/PARP16 reveals a novel putative regulatory domain. J Biol Chem 287(29):24077–24081
154. Scarpa ES, Fabrizio G, Di Girolamo M (2013) A role of intracellular mono-ADP-ribosylation in cancer biology. FEBS J 280(15):3551–3562
155. Jwa M, Chang P (2012) PARP16 is a tail-anchored endoplasmic reticulum protein required for the PERK- and IRE1α-mediated unfolded protein response. Nat Cell Biol 14(11):1223–1230
156. Bicknell AA, Babour A, Federovitch CM, Niwa M (2007) A novel role in cytokinesis reveals a housekeeping function for the unfolded protein response. J Cell Biol 177(6):1017–1027
157. Tuncel H, Tanaka S, Oka S, Nakai S, Fukutomi R, Okamoto M, Ota T, Kaneko H, Tatsuka M, Shimamoto F (2012) PARP6, a mono(ADP-ribosyl) transferase and a negative regulator of cell proliferation, is involved in colorectal cancer development. Int J Oncol 41(6):2079–2086

Bull Cancer 2015; 102: 863–873

en ligne sur / *on line on*
www.em-consulte.com/revue/bulcan
www.sciencedirect.com

De la découverte du poly(ADP-ribose) aux inhibiteurs PARP en thérapie du cancer☆

Valérie Schreiber, Giuditta Illuzzi, Eléa Héberlé, Françoise Dantzer

Reçu le 14 juillet 2015
Reçu sous la forme révisée le 28 juillet 2015
Accepté le 28 juillet 2015
Disponible sur internet le : 15 septembre 2015

Université de Strasbourg, biotechnologie et signalisation cellulaire, UMR7242 CNRS, laboratoire d'excellence Medalis, équipe labellisée ligue 2011, ESBS, 300, boulevard Sébastien-Brant, CS 10413, 67412 Illkirch, France

Correspondance :
Valérie Schreiber, université de Strasbourg, biotechnologie et signalisation cellulaire, UMR7242 CNRS, laboratoire d'excellence Medalis, équipe labellisée ligue 2011, ESBS, 300, boulevard Sébastien-Brant, CS 10413, 67412 Illkirch, France.
valerie.schreiber@unistra.fr

Mots clés
Poly(ADP-ribose) polymérase
Inhibiteurs PARP
Réparation de l'ADN
Chimio- et radiothérapie
BRCA1/2
Létalité synthétique

Résumé

La poly(ADP-ribosyl)ation est une modification post-traductionnelle catalysée par les poly(ADP-ribose) polymérases. PARP-1 est un détecteur moléculaire des cassures dans l'ADN qui joue un rôle essentiel dans l'organisation spatiale et temporelle de leur réparation, contribuant ainsi au maintien de l'intégrité du génome et à la survie cellulaire. Son inhibition a été rapidement proposée comme une stratégie thérapeutique pour potentialiser l'action cytotoxique des radio- et chimiothérapies. De nombreux essais cliniques sont en cours, basés sur cette approche innovante. Les inhibiteurs PARP ont révélé une autre capacité remarquable, celle d'éliminer spécifiquement des cellules tumorales mutées pour BRCA1 ou BRCA2, altérées dans le mécanisme de réparation des cassures double brin par recombinaison homologue. Cette approche thérapeutique basée sur la létalité synthétique fait actuellement l'objet d'essais cliniques de phase III, et un inhibiteur PARP, l'olaparib, vient d'être approuvé pour le traitement de certains cancers de l'ovaire avancés mutés génétiquement pour BRCA1. Cette revue décrit la chronologie de la découverte de la poly(ADP-ribosyl)ation jusqu'aux applications thérapeutiques prometteuses de son inhibition dans des stratégies anticancéreuses innovantes. Les avantages et les espoirs de ces approches, mais aussi les obstacles rencontrés, sont discutés.

Keywords
Poly(ADP-ribose) polymerase
PARP inhibitors
DNA repair
Chemo- and radiotherapy
BRCA1/2
Synthetic lethality

Summary

From poly(ADP-ribose) discovery to PARP inhibitors in cancer therapy

Poly(ADP-ribosyl)ation is a post-translational modification catalyzed by poly(ADP-ribose) polymerases. PARP-1 is a molecular sensor of DNA breaks, playing a key role in the spatial and temporal organization of their repair, contributing to the maintenance of genome integrity and cell survival. The fact that PARP inhibition impairs efficacy of break repair has been exploited as anticancer strategies to potentiate the cytotoxicity of anticancer drugs and radiotherapy. Numerous clinical

☆ Cet article fait partie des communications sélectionnées pour le 2e Congrès de la SFC, juin 2015.

http://dx.doi.org/10.1016/j.bulcan.2015.07.012
© 2015 Société Française du Cancer. Publié par Elsevier Masson SAS. Tous droits réservés.

trials based on this innovative approach are in progress. PARP inhibition has also proved to be exquisitely efficient to kill tumour cells deficient in double strand break repair by homologous recombination, such as cells mutated for the breast cancer early onset genes BRCA1 or BRCA2, by synthetic lethality. Several phase III clinical trials are in progress for the treatment of breast and ovarian cancers with BRCA mutations and the PARP inhibitor olaparib has just been approved for advanced ovarian cancers with germline BRCA mutation. This review recapitulates the history from the discovery of poly(ADP-ribosyl)ation reaction to the promising therapeutic applications of its inhibition in innovating anticancer strategies. Benefits, hopes and obstacles are discussed.

Introduction

De la découverte du PAR à la famille PARP

Le poly(ADP-ribose), décrit pour la première fois en 1963, est une molécule complexe synthétisée par les poly(ADP-ribose) polymérases (PARP) [1,2] (*figures 1 et 2*). Dans cette réaction appelée poly(ADP-ribosyl)ation, ou PARylation, les PARP hydrolysent le NAD^+ et polymérisent des résidus d'ADP-ribose pour former un long polymère éventuellement branché, fortement chargé négativement, sur des protéines acceptrices (réaction d'hétéromodification), et sur elles-mêmes dans la réaction d'automodification (*figure 2*). Ce PAR peut être dégradé par les activités endo- et exo-hydrolases d'une autre enzyme, la poly(ADP-ribose) glycohydrolase (PARG). Pendant plus de 30 ans, PARP-1 et PARG ont été considérées comme les seules enzymes capables de respectivement synthétiser et dégrader le PAR. Cette modification post-traductionnelle si particulière a été alors largement étudiée pour son implication dans la réponse aux dommages à l'ADN, la surveillance et le maintien de l'intégrité du génome [1,2]. De nombreux travaux ont mis en évidence le rôle prépondérant du PAR dans l'organisation spatiale et temporelle de la réparation des cassures dans l'ADN, par l'ouverture locale de la chromatine par la poly(ADP-ribosyl)ation (PARylation) des histones, le recrutement de facteurs de réparation au site endommagé et le contrôle de la progression du cycle et de la survie cellulaire [1,2]. L'importance de PARP dans la réponse aux dommages a été clairement démontrée par la génération indépendante de modèles de souris $Parp^{-/-}$ déficientes en PARP, sensibles aux agents endommageant l'ADN.
La découverte inattendue d'une synthèse de PAR résiduelle dans les cellules $Parp^{-/-}$ traitées par un agent alkylant et l'identification simultanée par différents laboratoires de l'existence de nouvelles protéines possédant une activité de PARylation a totalement bouleversé le domaine. Ces PARP constituent une famille de 17 protéines [3], dont le membre fondateur, renommé PARP-1, reste non seulement le plus caractérisé à ce jour, mais aussi le plus actif. PARP-2 et PARP-3 sont à l'heure actuelle les seules nouvelles PARP à également être activées par l'ADN endommagé [4]. Toutefois, d'autres membres de la famille PARP

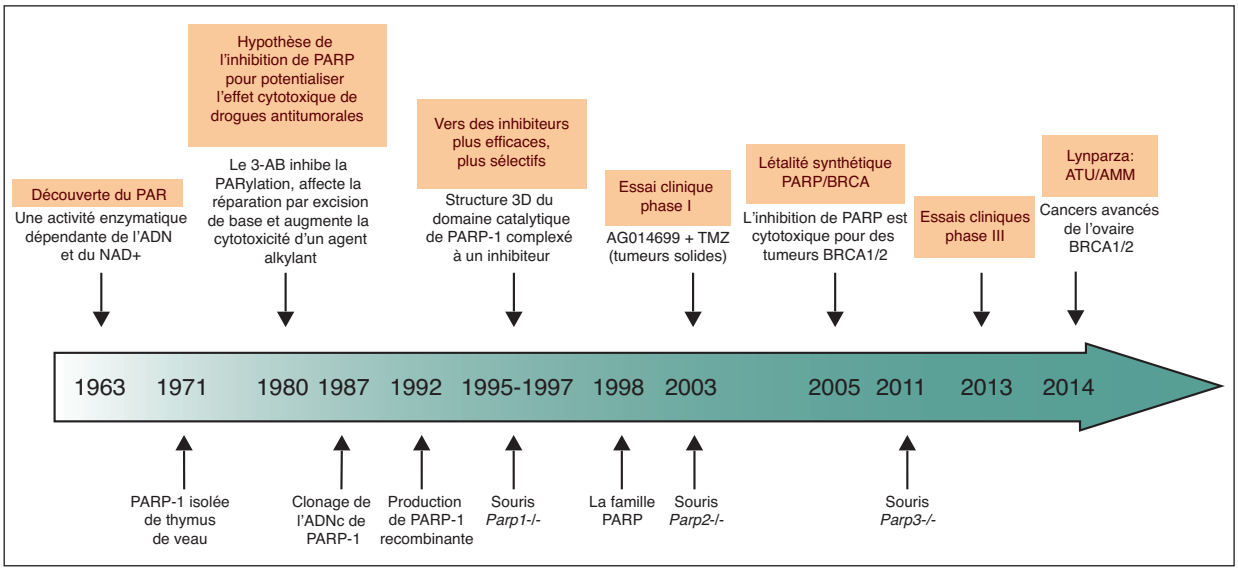

FIGURE 1

De la découverte du PAR aux essais cliniques, 50 ans d'efforts

Axe chronologique résumant les découvertes majeures dans le domaine de la PARylation.

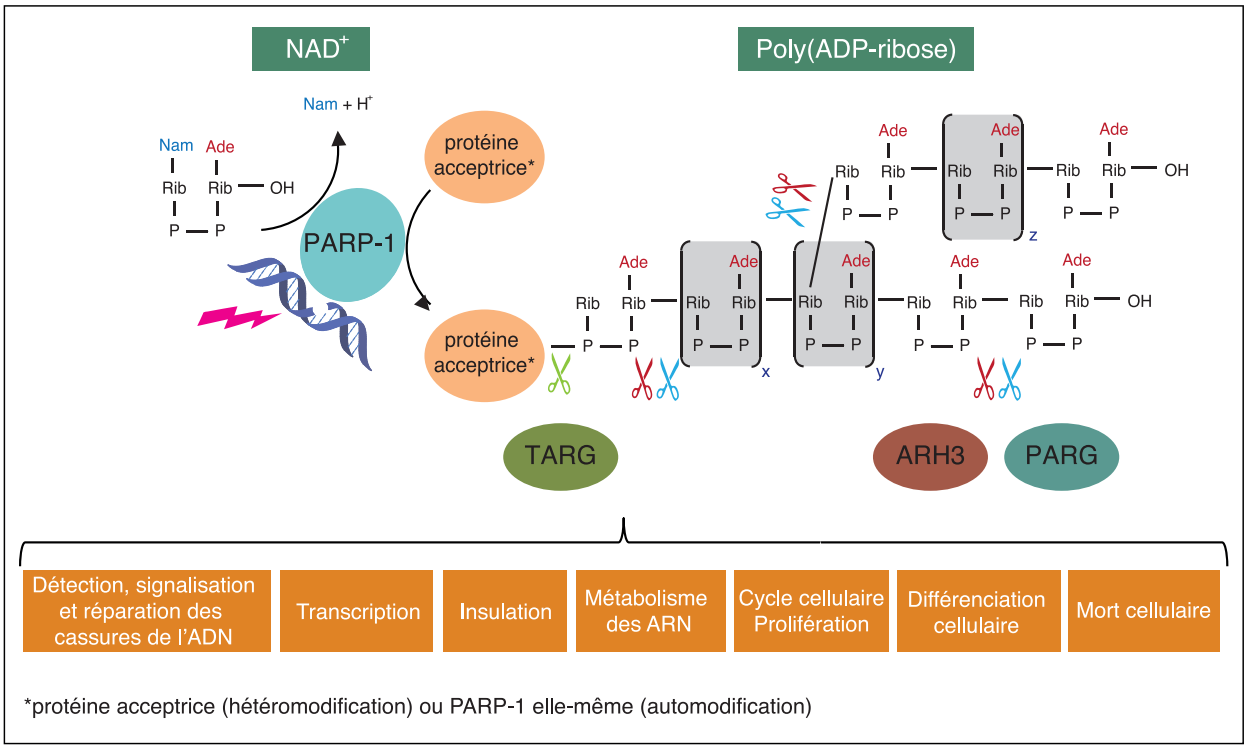

FIGURE 2

Synthèse et dégradation du PAR

PARP-1, activée par une cassure dans l'ADN, hydrolyse le NAD^+ et catalyse l'addition successive de résidus ADP-ribose sur elle-même (réaction d'automodification) ou sur des protéines acceptrices (réaction d'hétéromodification). Le PAR est hétérogène en taille et complexité, comme indiqué par les lettres x, y, z qui peuvent indiquer une valeur entre 0 et plus de 200. Les protéines PARG et ARH3 peuvent hydrolyser le PAR aux positions indiquées grâce à leurs activités endo- et exo-hydrolases. La protéine TARG hydrolyse la liaison entre le premier résidu ADP-ribose et la protéine. La PARylation est impliquée dans les divers processus cellulaires indiqués. Nam : nicotinamide ; Ade : adenine ; Rib : ribose.

ont été récemment impliqués dans la réponse aux dommages, les tankyrases TNK1 et TNK2, PARP-10, PARP-9 et PARP-14 [5–7]. Outre le fait que PARP-1 elle-même soit impliquée dans de nombreux processus cellulaires autres que la réponse aux dommages (transcription, signalisation, différenciation...), la diversité de fonction de ces nouvelles PARP a considérablement étendu le champ d'action de la PARylation.

Le PAR peut aussi interagir de façon non covalente avec des protéines possédant un domaine de liaison au PAR. Le premier motif peptidique de liaison au PAR (*PAR-binding module* [PBM]) a été décrit en 2000 et est retrouvé dans des facteurs de réparation de l'ADN, des facteurs de transcription, les histones ainsi que d'autres protéines de la chromatine. D'autres domaines de liaison au PAR ont été décrits depuis, tels que les doigts de zinc PBZ (*PAR-binding zinc finger*) et certains domaines macro, WWE, BRCT (*BRCA C-terminus*), FHA (*Forkhead associated*), RRM (*RNA recognition module*) et OB (*oligonucleotide/oligosaccharide-binding fold*) [8]. Une des fonctions principales de cette liaison non covalente au PAR est de permettre le recrutement et l'assemblage de complexes protéiques au site de synthèse du PAR.

PARylation et réponse cellulaire aux dommages à l'ADN

Comme mentionné ci-dessus, la fonction de PARP-1 la plus documentée à ce jour est la détection et la signalisation de cassures dans l'ADN pour initier la réponse cellulaire aux agressions génotoxiques (*figure 3*). PARP-1 s'active dès sa reconnaissance d'une interruption de l'ADN, s'autoPARyle et PARyle de nombreux accepteurs au voisinage de la lésion, en particulier les histones. Cette PARylation a de multiples conséquences, la première étant le remodelage de la chromatine au site endommagé. Ceci résulte à la fois de l'éviction des histones par le PAR, principalement l'histone H1, du recrutement grâce au PAR de facteurs de remodelage et de régulation de la structure de la chromatine, ainsi que des facteurs permettant d'instaurer localement un état transcriptionnel inactif, le temps que la lésion soit réparée. Parmi ces facteurs, on peut citer de façon non

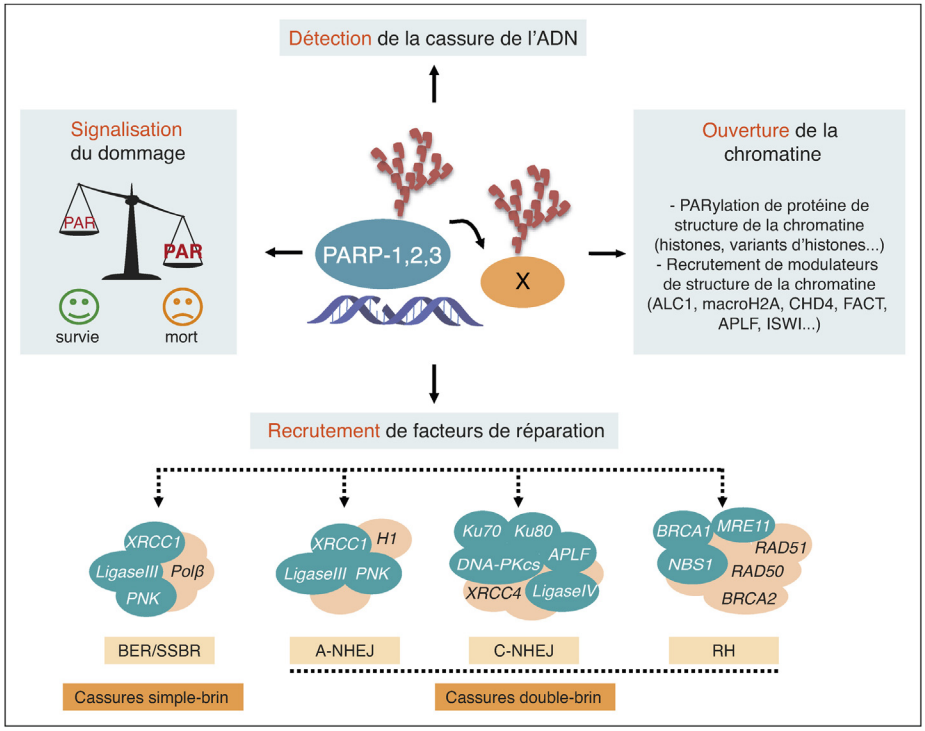

FIGURE 3

Fonctions du PAR dans la réponse aux dommages

Rôle de la PARylation dans la réponse aux dommages dans l'ADN. PARP-1 (et, dans certaines situations décrites dans le texte, PARP-2 et PARP-3) détecte les cassures dans l'ADN, signale leur présence en synthétisant localement sur elle-même et sur des protéines acceptrices (X) du PAR. La quantité de PAR produite, reflétant la sévérité du dommage, va permettre à la cellule d'adapter sa réponse en ouvrant des programmes de survie ou de mort cellulaire. Le PAR produit au site endommagé va permettre l'ouverture de la chromatine, par l'action combinée de l'éviction des histones par leur PARylation et le recrutement de facteurs de remodelage et de modification de la chromatine. Certains facteurs de réparation (indiqués en bleu) vont alors être recrutés par le PAR au site endommagé. Selon le type de lésion (cassure simple ou double brin), les facteurs présents dans la cellule, et la phase du cycle cellulaire, différentes machineries de réparation vont se charger de la restauration de l'intégrité de l'ADN (pour plus de détails, se reporter au texte).

exhaustive FACT, ALC1, macroH2A1.1, ISWI, SMARCA5, les protéines du complexe NuRD CHD4 et MTA1, l'histone chaperone APLF, les protéines polycomb EZH2, BMI1, CBX4 ou encore les déméthylases KDM5B, KDM4B et KDM4D [4,7]. Mais le PAR permet aussi le recrutement rapide au site endommagé de facteurs de réparation de l'ADN. Ainsi, XRCC1, la protéine centrale de la réparation des bases endommagées et des cassures simple brin (*base excision repair/single strand break repair* [BER/SSBR]) est recrutée en quelques secondes au site endommagé grâce au PAR synthétisé par PARP-1. La liste des facteurs de réparation dont le recrutement au site endommagé dépend du PAR, ou est accéléré par la présence de PAR, ne cesse de s'allonger, que ce soit pour réparer les cassures simple brin (XRCC1, DNA ligase III, PNK, APTX, TDP1, PCNA) ou double brin (ATM, BARD1, MRE11, NBS1, APLF) de l'ADN. Enfin, parmi les facteurs recrutés via le PAR au site endommagé, il faut encore citer la protéine RNF146/Iduna, une ubiquitine E3-ligase, qui poly-ubiquitinyle de façon PAR-dépendante certains facteurs de réparation pour les orienter vers une dégradation par le protéasome [9].

Les paragraphes ci-dessous ne font qu'apporter une description succincte du rôle de la PARylation dans les différentes voies de réparation des dommages à l'ADN. Pour plus de détails, se reporter aux diverses revues récentes et exhaustives sur le sujet [1,2,4,7,10].

Réparation des cassures simple brin et des bases endommagées (BER/SSBR)

C'est dans la voie de réparation par excision de base et des cassures simple brin (*base excision repair/single strand break repair* [BER/SSBR]) que l'implication de PARP-1 est la plus documentée. Celle-ci est étayée par la sensibilité des souris et cellules déficientes en PARP-1 à l'irradiation et aux agents alkylants et oxydants, ainsi que par le délai dans la réparation des cassures simple brin et des bases endommagées. PARP-1 est recrutée très rapidement, mais de façon transitoire, au site de

dommages introduits par micro-irradiation laser [11]. PARP-1 interagit physiquement et fonctionnellement avec de nombreux acteurs du BER/SSBR, à commencer par XRCC1, recruté par PARP-1 au site de dommage en quelques secondes. XRCC1 est le pivot du BER/SSBR, puisqu'il interagit fonctionnellement avec tous les acteurs de cette voie de réparation, pour stimuler leur(s) activité(s). PARP-1 interagit également avec bon nombre de ces acteurs et module pour certains leur activité par PARylation ou interaction non covalente avec le PAR, du moins in vitro. On peut citer notamment l'ADN glycosylase OGG1, l'ADN polymérase β, l'ADN ligase III, FEN1, APE1, PCNA et l'aprataxine [7]. PARP-1 peut se fixer sur des structures d'ADN mimant des intermédiaires de la réparation par BER/SSBR, comme les sites abasiques, les gaps et les structures dites en « flap », formées suite au déplacement par l'ADN polymérase β d'un ou de plusieurs nucléotides en aval de la lésion [7,12]. L'importance de PARP-1 dans le recrutement de facteurs du BER/SSBR est un fait établi, alors que son implication dans les étapes ultérieures reste controversée [13]. Si PARP-3 ne semble pas impliquée dans le BER/SSBR, PARP-2 l'est au contraire, comme l'atteste la sensibilité des souris et cellules à l'irradiation et aux agents alkylants, ainsi que le délai de réparation des cassures simple brin et des bases endommagées lorsque PARP-2 est absente [7,14]. PARP-2 n'est pas requise pour le recrutement de XRCC1. Étant recrutée plus tardivement que PARP-1 et interagissant avec des facteurs du BER/SSBR et des intermédiaires réactionnels de la réparation, elle pourrait intervenir dans des étapes ultérieures de la réparation [7].

Réparation des cassures double brin

Chez les mammifères, les cassures double brin, hautement toxiques et recombinogènes, sont majoritairement réparées tout au long du cycle cellulaire par religation d'extrémités non homologues (*non-homologous end-joining* [NHEJ]). Ce mécanisme, baptisé aujourd'hui C-NHEJ (NHEJ classique), met en jeu les protéines Ku70/Ku80, DNA-PK et le complexe de ligation ADN ligase IV/XRCC4/XLF [15]. En phases S et G2, les cassures peuvent être réparées par recombinaison homologue (RH), mécanisme impliquant notamment les protéines du complexe MRN (MRE11, NBS1, RAD50), RPA, BRCA1, BRCA2 et RAD51. Un mécanisme de réparation non homologue alternatif, ou A-NHEJ, a également été décrit, impliquant MRE11, l'histone H1 et les protéines du BER/SSBR XRCC1, DNA ligase III, et PARP-1 [15]. Ce mécanisme a été identifié dans des conditions où le C-NHEJ n'était pas ou plus fonctionnel. Le A-NHEJ (ou « backup » B-NHEJ) met en jeu une résection d'ADN au niveau de la cassure qui est plus importante que dans le C-NHEJ, afin de rechercher des micro-homologies de séquence, ce qui entraîne des micro-pertes de matériel génétique. Le A-NHEJ est donc encore moins fidèle que le C-NHEJ. Cette voie de réparation alternative permettrait toutefois d'assurer la diversification des anticorps lors de la commutation de classe par recombinaison, dans un contexte où la voie C-NHEJ est déficiente, au risque toutefois d'induire des anomalies chromosomiques et des translocations [15]. La façon dont, au niveau d'une cassure double brin, s'effectue le choix de la voie de réparation fait actuellement l'objet d'intenses recherches.

L'implication de PARP-1 dans la réparation des cassures double brin a été suggérée par sa capacité à se fixer sur et à être activée par ces extrémités, par la radiosensibilité des souris *Parp-1*$^{-/-}$ et surtout par les interactions physiques et fonctionnelles entre PARP-1 et certains acteurs du C-NHEJ, A-NHEJ ou de la RH. La relation entre PARP-1 et C-NHEJ est sans doute, à ce jour, la moins comprise. PARP-1 est décrite comme stimulant l'activité catalytique de DNA-PK, mais aussi comme un régulateur négatif du C-NHEJ, par compétition avec Ku70/Ku80 pour les cassures double brin. PARP-1 n'est toutefois pas un acteur essentiel du C-NHEJ, les souris Parp-1$^{-/-}$ ne présentant pas de défaut majeur de la recombinaison V(D)J lors de la maturation des lymphocytes B et T [4]. L'implication de PARP-1 dans le A-NHEJ est plus évidente, révélée, d'une part, par l'incapacité à réparer les cassures double brin dans des cellules déficientes en Ku, en absence de PARP-1 et, d'autre part, par la présence de PARP-1 dans le complexe multiprotéique du A-NHEJ. L'étude de la commutation de classe des immunoglobulines chez les souris *Parp-1*$^{-/-}$ révèle que PARP-1 favoriserait la réparation des régions de commutation par A-NHEJ [2]. PARP-1 pourrait ainsi contribuer au choix de la voie de réparation entre le C-NHEJ et le A-NHEJ. Enfin, le rôle de PARP-1 dans la RH est également sujet à débat. PARP-1 n'est apparemment pas requise pour le processus de recombinaison lui-même, comme l'atteste l'augmentation d'échanges de chromatides sœurs induits par des agents génotoxiques en absence de PARP-1. Là aussi, PARP-1 pourrait agir en amont, dans la régulation du choix de la voie de réparation, en facilitant le recrutement précoce de protéines impliquées dans le contrôle de la résection (MRE11, NBS1, BRCA1) [16]. Dans la réponse cellulaire au stress réplicatif, processus qui met en jeu la RH, PARP-1 a été décrite comme contrôlant le redémarrage des fourches de réplication bloquées et la prise en charge par la RH des fourches de réplication effondrées et converties en cassures double brin [17].

L'implication de PARP-2 dans la réparation des cassures double brin n'est pas évidente. Toutefois, PARP-2 aurait un rôle protecteur contre la recombinaison illégitime, puisque son invalidation chez la souris entraîne une persistance de cassures double brin non réparées lors de la recombinaison V(D)J, un défaut de réarrangement du récepteur des cellules T et une fréquence accrue de translocation entre le locus IgH et le proto-oncogène c-myc [2,4]. En revanche, plusieurs études désignent clairement PARP-3 comme agissant dans le C-NHEJ. PARP-3 favorise le recrutement de Ku70/80, une manière de limiter la résection de la cassure par MRE11, et recrute et interagit avec APLF pour accélérer l'étape de ligation catalysée par XRCC4/ligase IV [18]. De plus, PARP-3 participerait au choix de la voie de

réparation, en favorisant l'accès du facteur du C-NHEJ 53BP1, au détriment de la protéine de la RH, BRCA1 [18].

Ciblage de la PARylation dans des stratégies anticancéreuses

PARP-1 est donc un acteur clé dans l'organisation spatiale et temporelle de la réparation de l'ADN. Mais la synthèse de PAR, qui reflète la gravité du dommage, va aussi permettre à la cellule d'adapter sa réponse en conséquence et de l'orienter vers un processus de survie ou mort cellulaire (*figure 3*). En situation de stress génotoxique limité, induit par les sous-produits du métabolisme cellulaire ou par des agents exogènes, l'activation de PARP-1 va favoriser la réparation et la survie. En revanche, un stress génotoxique élevé va causer une sur-activation de PARP et entraîner un appauvrissement énergétique par diminution drastique du stock de NAD^+ disponible, fatal pour la cellule. Dans certaines situations ou types cellulaires, le PAR synthétisé peut même jouer un rôle actif dans la mort cellulaire, qui opère alors par un mécanisme particulier appelé parthanatose [19]. PARP-1 affiche donc une double facette : facteur de survie dans les cellules prolifératives, mais aussi acteur dans la mort cellulaire associée à l'inflammation. Une régulation fine et dynamique du taux de PAR produit est donc essentielle et s'opère à la fois au niveau de la synthèse du PAR par PARP-1, mais aussi par la dégradation du PAR par les endo/exo-glycohydrolases PARG et ARH3 [20]. Dans ces deux situations de stress génotoxique, limité ou élevé, l'inhibition de la synthèse de PAR est apparue comme une opportunité thérapeutique :

- en thérapie du cancer, pour potentialiser l'action cytotoxique d'agents génotoxiques anticancéreux en limitant la réparation des lésions ;
- dans les pathologies inflammatoires ou aiguës (maladies neurodégénératives, ischémie cardiaque ou cérébrale), pour limiter l'inflammation et la mort cellulaire induite par la synthèse de PAR [21].

La suite de cette revue se focalisera sur le ciblage de PARP dans des stratégies thérapeutiques anticancéreuses.

Inhibiteurs de PARP comme adjuvants en chimio- et radiothérapie du cancer

Dès la découverte en 1980 du rôle clé que semblait avoir la PARylation dans la réparation des cassures de l'ADN, une hypothèse a émergé, selon laquelle son inhibition pourrait avoir un intérêt thérapeutique pour potentialiser l'effet cytotoxique ou antiprolifératif de drogues anti-tumorales ciblant l'ADN, en empêchant la réparation des lésions générées par ces drogues [22] (*figures 1 et 3*). Cette hypothèse a été validée dans un grand nombre d'études, réalisées sur des cellules en culture ou des modèles de xénogreffes chez la souris et utilisant soit des inhibiteurs PARP, soit des cellules déficientes en PARP-1. Divers agents génotoxiques tels que les agents alkylants (témozolomide), les analogues du platine (cisplatine), les inhibiteurs de topoisomérase 1 (camptothécine) mais aussi les rayonnements ionisants (X, γ) se sont avérés être plus cytotoxiques en absence d'une PARP-1 fonctionnelle [23,24]. Les retombées prometteuses de cette potentialisation de la cytotoxicité des agents antitumoraux a rapidement stimulé les compagnies pharmaceutiques à développer de nouveaux inhibiteurs PARP plus efficaces, plus sélectifs. Le premier essai clinique a été initié en 2003, combinant le témozolomide avec l'inhibiteur PARP AG014699 (aussi appelé CO-338 ou rucaparib), pour traiter des tumeurs solides avancées (en particulier des mélanomes), révélant un bénéfice clinique prometteur et surtout, validant cette nouvelle stratégie thérapeutique [25]. Depuis, plusieurs dizaines d'essais cliniques de phase I et II ont été initiés, utilisant un inhibiteur PARP comme adjuvant en chimio- et radiothérapie pour traiter de nombreux types de cancers (http://clinicaltrials.gov) [24,26].

Inhibiteurs de PARP et létalité synthétique

En 2005, deux études publiées simultanément dans *Nature* ont révélé que les cellules mutées ou déficientes en BRCA1 ou BRCA2 (BRCA1/2) étaient extrêmement sensibles aux inhibiteurs PARP [27,28]. Ces deux gènes, fréquemment mutés dans des formes héréditaires de cancers du sein et de l'ovaire, codent pour des protéines impliquées dans la réparation des cassures double brin par RH. L'inhibition de PARP induit dans ces cellules une augmentation de l'instabilité chromosomique, un arrêt du cycle cellulaire et la mort par apoptose, appuyant la notion de létalité synthétique [29]. La létalité synthétique est une combinaison létale de deux effets qui, pris isolément, ne sont pas fatals. La létalité synthétique BRCA/PARP a été interprétée comme résultant de l'inefficacité de réparation des cassures simple brin spontanées dans les cellules traitées par un inhibiteur PARP, induisant la conversion de ces cassures simple brin en cassures double brin au cours de la réplication. Ces cassures double brin sont fatales dans les cellules mutées pour BRCA1/2, car elles ne peuvent être réparées, en raison de la non-fonctionnalité de la RH (*figure 4*). Les avantages de cette approche thérapeutique sont que :

- l'inhibiteur est administré seul, en monothérapie, limitant considérablement les effets secondaires possibles ;
- seules les cellules tumorales ayant les deux allèles BRCA1 ou BRCA2 mutés sont sensibles à l'inhibiteur PARP, les autres cellules du patient, ayant un allèle fonctionnel, étant toujours capables de réparer les cassures double brin générées.

La découverte remarquable de létalité synthétique entre PARP et BRCA1/2 a immédiatement eu un retentissement énorme et la littérature traitant de ce concept suit depuis une courbe exponentielle, ouvrant la voie aux essais cliniques pour le traitement de cancers mutés pour ces gènes. Mais, après un engouement des compagnies pharmaceutiques vis-à-vis de cette nouvelle approche thérapeutique, un coup d'arrêt a eu lieu en 2011/2012, suite aux résultats décevants du premier

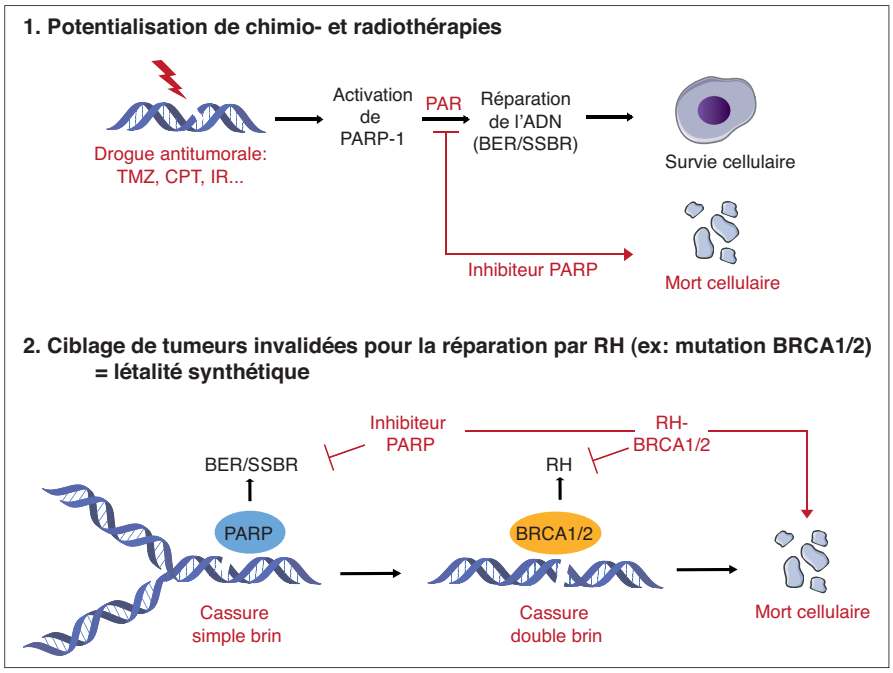

FIGURE 4

Principe du ciblage de la PARylation dans des stratégies anticancéreuses

1. Potentialisation de l'action cytotoxique des agents anti-tumoraux (témozolomide [TMZ], camptothécine [CPT]) et des radiations ionisantes (IR). En réponse aux cassures dans l'ADN, la synthèse de PAR par PARP-1 (et PARP-2) active le système de réparation par excision de bases et de cassures simple brin (BER/SSBR) pour assurer la survie cellulaire. Le traitement par un inhibiteur de PARP entraîne une persistance de cassures non réparées et la mort de la cellule tumorale. 2. Principe de l'inhibition de PARP-1 dans un protocole de létalité synthétique (cas des tumeurs mutées pour BRCA1 ou BRCA2). En présence d'un inhibiteur PARP, les cassures simple brin non réparées vont s'accumuler et être converties en cassures double brin au moment de la réplication. La réparation de ces cassures double brin va dépendre de la fonctionnalité du système de réparation par recombinaison homologue (RH). Les cellules tumorales portant une mutation BRCA1/2, incapables de réparer ces cassures double brin par RH, vont mourir.

essai clinique de phase III avec l'iniparib, mais aussi de plusieurs essais de phase II avec l'olaparib [30,31]. Lorsqu'il s'est avéré que l'iniparib était un inhibiteur médiocre de PARP, la course a été relancée, par AstraZeneca dans un premier temps, qui a repris le développement de l'olaparib. Les résultats obtenus en pré-clinique et clinique ont rapidement encouragé les compagnies pharmaceutiques à rouvrir leur programme « PARP ». Actuellement, plusieurs essais de phase III ciblés sur le traitement de cancers mutés génétiquement ou fonctionnellement pour BRCA1/2 sont en cours (http://clinicaltrials.gov). L'olaparib/lynparza a obtenu en août 2014 une autorisation temporaire d'utilisation (ATU) puis, 4 mois après, une autorisation de mise sur le marché (AMM) pour une utilisation en monothérapie pour le traitement d'entretien de patientes atteintes d'un cancer de haut grade de l'ovaire, des trompes de Fallope ou du péritoine, récidivant et sensible au platine, avec une mutation germinale et/ou somatique et qui présentent une réponse complète ou partielle à une chimiothérapie à base de platine. Il faut souligner que ce principe de létalité synthétique ne se limite pas aux gènes BRCA. De nombreux autres gènes ont été identifiés comme répondant au principe de létalité synthétique avec l'inhibition de PARP, parmi lesquels RAD51, ATRX, RPA1, NBN, ATR, ATM, CHEK1, CHEK2, PNKP, PALB2, CDK1, PTEN, FANCA, FANCM [29,32]. Leur point commun serait une diminution de l'efficacité de la RH, même si, pour certains d'entre eux, cet effet n'est pas clairement démontré, voire sujet à controverse. C'est notamment le cas de PTEN (*Phosphatase and TENsin homolog*), gène suppresseur de tumeur régulant la voie de signalisation PI3K/AKT, dont l'impact de la mutation sur la RH et sur la sensibilité aux inhibiteurs PARP a été remis en question [33]. Une étude récente vient même compliquer la donne, montrant qu'un défaut de PTEN ou BRCA1 altère bien la RH, alors qu'un défaut simultané de PTEN et BRCA1 restore une activité de RH et donc une résistance à l'inhibition de PARP [34]. Il reste donc de nombreuses pistes à explorer afin d'identifier quelles mutations génétiques et, surtout, quelles combinaisons de mutations peuvent bénéficier de cette stratégie thérapeutique d'inhibition de PARP.

Vers des inhibiteurs de PARP plus efficaces, plus spécifiques ?

Les inhibiteurs développés jusque-là et utilisés en essais cliniques sont essentiellement des dérivés du premier inhibiteur

PARP généré, le 3-aminobenzamide, peu efficace et surtout peu sélectif [22]. Ces inhibiteurs sont des analogues de la partie nicotinamide du NAD^+ et agissent comme des inhibiteurs compétitifs. C'est la résolution de la structure tridimensionnelle du domaine catalytique de PARP-1, en 1996, qui a permis d'améliorer la spécificité de ces inhibiteurs et d'augmenter leur l'efficacité de plus de 1000 fois pour atteindre des IC50 de l'ordre du nM [26,35]. Toutefois, bien que ces inhibiteurs de PARP aient été développés pour cibler PARP-1 en thérapie du cancer, la plupart d'entre eux s'avère inhiber un ou plusieurs autres membres de la famille PARP, au moins in vitro, mais à des doses généralement plus élevées [35,36]. Du fait de la forte similarité de structure entre les domaines catalytiques de PARP-1 et PARP-2, les inhibiteurs PARP sont rarement discriminants entre ces deux protéines et vont vraisemblablement inhiber ces deux PARP, voire même d'autres PARP, en particulier PARP-3, aux concentrations utilisées in vivo. De prime abord, il peut paraître avantageux d'inhiber simultanément PARP-1 et PARP-2, voire PARP-3, pour empêcher toute réparation des lésions d'ADN introduites par les agents anticancéreux et potentialiser d'autant plus leur action anti-tumorale. Le problème est que, plus on augmente le nombre de protéines ciblées, plus on augmente le risque d'apparition d'effets secondaires non souhaitables. La myélosuppression et l'anémie sont des effets secondaires fréquents de la combinaison inhibiteur PARP/agent de chimiothérapie. Ces effets pourraient être une conséquence de l'inhibition de PARP-2, les souris *Parp-2*$^{-/-}$ ayant révélé une sensibilité des cellules souches et progénitrices hématopoïétiques (cellules HSPC) aux faibles doses d'irradiation, entraînant une myélosuppression [37]. Ces souris s'avèrent également souffrir d'anémie chronique [38]. Aucun de ces phénotypes n'est observé chez les souris *Parp-1*$^{-/-}$. Ces résultats démontrent l'importance de connaître au mieux les fonctions biologiques de toutes les cibles d'un médicament et plaident pour le développement d'inhibiteurs spécifiques pour chaque PARP.

Une nouvelle piste explorée pour gagner en sélectivité est le développement d'inhibiteurs non compétitifs, mais allostériques. L'idée est de trouver des molécules capables d'interférer avec des interactions protéiques entre des domaines de PARP-1 nécessaires à son activation par les dommages à l'ADN. Effectivement, des mutants ponctuels de PARP-1, qui ne modifient pas sa capacité à se lier à l'ADN mais qui affectent l'activation catalytique par l'ADN, révèlent une capacité à sensibiliser les cellules à un agent anticancéreux dérivé du platine [39].

Une observation inattendue a été que les inhibiteurs de PARP en essais cliniques, bien que tous capables d'inhiber l'activité enzymatique de PARP-1 (et PARP-2) avec des IC50 de l'ordre du nM, s'avèrent avoir des capacités cytotoxiques très différentes. C'est le cas du talazoparib (BMN 673, BioMarin), niraparib (MK-4827, Tesaro), olaparib (AZD-2281, AstraZeneca), rucaparib (AG014699, Clovis) et véliparib (ABT-888, AbbVie). Le groupe de Pommier a trouvé l'explication dans la capacité variable qu'ont ces inhibiteurs à induire un « PARP trapping », c'est-à-dire le piégeage sur l'ADN de la PARP inhibée [40]. Les travaux de Satoh et Lindahl [41] avaient montré qu'une molécule de PARP-1 inactive reste fixée sur l'ADN endommagé du fait de l'absence d'automodification, ne pouvant être décrochée par répulsion électrostatique entre le PAR et l'ADN. L'idée que le piégeage de PARP puisse être responsable de l'effet cytotoxique des inhibiteurs PARP était déjà évoquée [13]. La nouveauté est que certains inhibiteurs induiraient un changement conformationnel allostérique de PARP-1 (et PARP-2), stabilisant son association avec l'ADN. PARP-1 inactivée obstrue physiquement la cassure, entraînant une perturbation massive de la réparation, mais aussi de la réplication et de la transcription [13,42]. Cette obstruction est critique pour la cytotoxicité, comme l'atteste le fait que les cellules dépourvues de PARP-1 (*Parp-1*$^{-/-}$ ou siPARP-1) sont beaucoup plus résistantes à l'olaparib ou au talazotarib que les cellules sauvages [43]. Le talazoparib a un effet cytotoxique 25 à 100 fois plus élevé que le rucaparib, l'olaparib et le niraparib et 1000 à 10 000 fois plus que le véliparib sur des cellules CAPAN-1 [40,42,44]. L'effet cytotoxique de ces inhibiteurs est directement corrélé à leur aptitude à stabiliser l'interaction PARP-1/ADN, aptitude qui découlerait de leur structure moléculaire et leur position dans le site actif de la protéine.

La question qui se pose maintenant est de savoir quel inhibiteur utiliser, pour quelle application thérapeutique ? Le piégeage de PARP-1 est-il systématiquement nécessaire pour atteindre l'effet toxique maximal ? La réponse à cette question semble être non, si on considère l'exemple de la combinaison entre l'inhibiteur PARP et la camptothécine (CPT), inhibiteur de la topoisomérase 1. Les cellules déficientes en PARP-1 ou traitées par un inhibiteur PARP sont effectivement hypersensibles aux inhibiteurs de topoisomérase 1 [45]. Les cellules de poulet DT40 dépourvues génétiquement de PARP-1 s'avèrent toutefois plus sensibles à la CPT que celles traitées par un inhibiteur PARP, que cet inhibiteur soit efficace en piégeage de PARP-1 (olaparib) ou non (véliparib) [46]. Cette potentialisation de la cytotoxicité de la CPT requiert donc uniquement l'inhibition de l'activité enzymatique de PARP-1. Ceci s'expliquerait par l'implication de la PARylation dans la prise en charge de la lésion formée par la topoisomérase 1, liée de façon covalente à l'ADN, lorsqu'elle est inhibée par la CPT [46,47]. C'est pourquoi l'effet synergique entre les inhibiteurs PARP et la CPT est observé même pour les inhibiteurs les moins piégeants comme le véliparib [46]. Dans cette stratégie thérapeutique, on pourrait donc privilégier les inhibiteurs non piégeants, qui, même si cela reste à démontrer, pourraient, de ce fait, être moins susceptibles d'entraîner des effets secondaires indésirables que des inhibiteurs piégeants. Considérons maintenant l'exemple de la combinaison entre l'inhibiteur PARP et le témozolomide (TMZ) dont l'effet synergique est largement documenté [21,42]. Cet agent alkylant génère des bases endommagées :

- des O^6-méthylguanines, létales sauf dans les tumeurs mutées pour la O^6-méthylguanine méthyltransférase (MGMT), résistantes au TMZ ;
- des N7-méthylguanines et N^3-méthyladenines, non létales, car réparées par BER/SSBR.

L'inhibition de PARP, en bloquant physiquement la réparation BER/SSBR, empêche leur réparation et les convertit en lésions létales. L'effet cytotoxique de l'inhibiteur est donc ici directement corrélé à sa capacité de piégeage de PARP-1 sur l'ADN et devrait donc être pris en compte dans les stratégies thérapeutiques basées sur cette approche [42,46].

Qu'en est-il des stratégies basées sur la létalité synthétique ? S'il a été longtemps admis que la létalité synthétique résultait de la conversion de cassures simple brin non réparées à cause de l'inhibition de PARP, en cassures double brin non réparables du fait de l'absence de BRCA1/2, plusieurs faits ne s'accordent pas avec ce schéma et le(s) mécanisme(s) conduisant à la mort cellulaire reste(nt) encore incompris. Ainsi, un simple défaut de réparation des cassures simple brin n'est pas suffisant pour expliquer l'effet cytotoxique de l'inhibiteur PARP, puisqu'une déplétion en XRCC1, qui abolit la voie du BER/SSBR, n'impacte pas la survie des cellules BRCA2 [48]. D'autre part, l'inhibition de PARP ne semble pas entraîner une augmentation spontanée des cassures simple brin [13]. Un autre modèle a été proposé, dans lequel l'inhibition de PARP-1 dans des cellules déficientes en RH serait à l'origine d'une dérégulation du NHEJ, favorisant l'instabilité génomique ainsi que des réarrangements chromosomiques qui conduiraient à la mort cellulaire [48]. L'invalidation du NHEJ diminue considérablement l'hypersensibilité des cellules déficientes en BRCA2 à l'inhibition de PARP [48]. Enfin, l'implication de PARP-1 et de BRCA1 dans le redémarrage des fourches de réplication bloquées pourrait également expliquer pourquoi le défaut simultané des deux protéines est létal [17]. Mais là encore, le piégeage de PARP-1 sur la lésion (cassure simple brin, fourche de réplication bloquée, voire effondrée, et générant une cassure double brin) pourrait être la clé du mécanisme. L'inhibition chimique de PARP s'avère plus cytotoxique pour des cellules déficientes en BRCA1/2 qu'une absence de PARP-1 [13,27,28,42]. Mais surtout, un inhibiteur PARP piégeant est plus toxique pour des cellules de poulet DT40 BRCA2$^{-/-}$ qu'un inhibiteur non piégeant [40]. Là encore, la capacité d'un inhibiteur à piéger PARP-1 sur l'ADN devrait être prise en compte dans les stratégies thérapeutiques ciblant les tumeurs déficientes en RH.

Problèmes de résistance

Un autre problème à ne pas occulter dans le développement clinique des inhibiteurs PARP, c'est l'apparition de résistance au traitement. De nombreuses études ont rapporté ce phénomène [29,49]. Dans le cas des tumeurs BRCA, l'apparition de mutations secondaires qui restaurent la fonction de BRCA1 ou BRCA2 ont été rapportées. Ces mutations peuvent toucher directement le gène BRCA1/2 et permettre de restaurer la fonction de la protéine dans la RH. Ces mutations peuvent aussi apparaître dans des gènes codant des facteurs du NHEJ, ce qui supprimerait l'instabilité génomique cytotoxique décrite ci-dessus [48]. De même, l'apparition de mutations affectant 53BP1, facteur qui régule avec BRCA1 la balance RH/NHEJ en favorisant le C-NHEJ, permettrait une restauration de la RH, qui fonctionnerait malgré l'absence de BRCA1 [50]. Une publication récente vient de démontrer qu'une mutation de la protéine REV7 conférerait également une résistance aux cellules BRCA1 traitées par un inhibiteur PARP [51]. Une des fonctions de REV7 est de limiter la résection et d'orienter la réparation vers le C-NHEJ. En son absence, la résection est stimulée, ce qui favorise la réparation par recherche d'homologies, le RH. À noter que si ce RH restauré est indépendant de BRCA1, il nécessite toujours un BRCA2 fonctionnel. Toutes ces situations favoriseraient l'échappement de la tumeur traitée par un inhibiteur PARP. Une autre situation décrite concerne l'augmentation de l'expression de la P-glycoprotéine (PgP), protéine de la pompe à efflux responsable de la résistance multidrogue, voire son activation [52]. Enfin, une perte de l'expression de PARP-1 peut également entraîner une perte de réponse à l'inhibiteur PARP, en particulier dans les stratégies anticancéreuses reposant sur l'effet piégeant de l'inhibiteur, comme la combinaison avec le TMZ mentionnée ci-dessus [46].

D'autres pistes à explorer ?

Les inhibiteurs PARP ont montré une cytotoxicité pour des cellules paraissant a priori non déficientes en BRCA ou en RH. C'est le cas des cellules de cancer du sein sporadique surexprimant HER2 (*human epidermal growth factor receptor 2*). L'inhibition de PARP pourrait altérer la fonction du facteur de transcription NF-κB, surexprimé dans ces cellules et connu pour être régulé par PARP-1 [53]. Après des résultats prometteurs montrant une sensibilité très élevée de cellules tumorales de sarcome d'Ewing portant une translocation EWSR-FL1, les résultats obtenus avec des xénogreffes chez la souris et, surtout, du premier essai clinique de phase II sont décevants [54]. Toutefois, l'espoir demeure avec une utilisation combinée d'inhibiteur PARP et de TMZ ou de radiothérapie [54]. Enfin, d'autres marqueurs prédictifs éventuels de sensibilité aux inhibiteurs PARP ont été identifiés (la kinase CDK12 dans les cancers de l'ovaire, la protéine de réparation par excision de nucléotides ERCC1 dans certains cancers du poumon), leur caractérisation est en cours [29].

Conclusion

Les inhibiteurs PARP sont donc porteurs d'un espoir qui ne cesse d'augmenter, que ce soit dans des stratégies de monothérapie ou de combinaison avec des agents chimio- ou radiothérapeutiques. Le défi à relever est de déterminer précisément quelles tumeurs bénéficieraient le mieux de ces stratégies. C'est pourquoi les recherches fondamentales, translationnelles et

cliniques doivent continuer à avancer de concert pour identifier de nouveaux marqueurs de prédiction d'une sensibilité aux inhibiteurs PARP. Une meilleure connaissance des fonctions biologiques, physiologiques mais aussi pathophysiologiques, des PARP ciblées par les inhibiteurs pharmacologiques, est indispensable pour anticiper les effets souhaités mais aussi indésirables de ces molécules à visée thérapeutique. D'autres membres de la famille PARP commencent à attirer l'attention, en révélant des propriétés qui les désigneraient à leur tour comme des cibles thérapeutiques prometteuses dans le traitement des cancers. C'est notamment le cas des tankyrases TNK1 et TNK2, impliquées dans la maintenance des télomères et la voie WNT, pour lesquelles des inhibiteurs spécifiques sont disponibles et testés pour leur action anti-tumorale dans le cancer du côlon [55,56]. L'inhibition ou invalidation de PARP-14, un régulateur de l'activité transcriptionnelle de Stat6, pourrait également contrarier la prolifération et la migration de cellules tumorales [57]. Le domaine de la PARylation est vaste, les opportunités de stratégies thérapeutiques nombreuses et prometteuses [58], les chercheurs et les compagnies pharmaceutiques n'ont donc pas dit leur dernier mot.

Remerciements : notre laboratoire est soutenu par le Centre national de la recherche scientifique, l'université de Strasbourg, la Ligue nationale contre le cancer (équipe labellisée), Électricité de France. Ce travail a été réalisé dans le cadre du LabEx ANR-10-LABX-0034_Medalis et a reçu à ce titre un soutien financier du ministère de la Recherche géré par l'Agence nationale de la recherche, programme d'investissement d'avenir. Nous nous excusons auprès de nos collègues dont nous n'avons pu citer les travaux, faute de place.

Déclaration d'intérêts : les auteurs déclarent ne pas avoir de conflits d'intérêts en relation avec cet article.

Références

[1] Luo X, Kraus WL. On PAR with PARP: cellular stress signaling through poly(ADP-ribose) and PARP-1. Genes Dev 2012;26:417–32.
[2] Robert I, Karicheva O, Reina-San-Martin B, Schreiber V, Dantzer F. Functional aspects of PARylation in induced and programmed DNA repair processes: preserving genome integrity and modulating physiological events. Mol Aspects Med 2013;34:1138–52.
[3] Amé JC, Spenlehauer C, de Murcia G. The PARP superfamily. Bioessays 2004;26:882–93.
[4] Beck C, Robert I, Reina-San-Martin B, Schreiber V, Dantzer F. Poly(ADP-ribose) polymerases in double-strand break repair: focus on PARP1, PARP2 and PARP3. Exp Cell Res 2014;329:18–25.
[5] Nicolae CM, Aho ER, Choe KN, Constantin D, Hu HJ, et al. A novel role for the mono-ADP-ribosyltransferase PARP14/ARTD8 in promoting homologous recombination and protecting against replication stress. Nucleic Acids Res 2015;43:3143–53.
[6] Yan Q, Xu R, Zhu L, Cheng X, Wang Z, et al. BAL1 and its partner E3 ligase, BBAP, link poly (ADP-ribose) activation, ubiquitylation, and double-strand DNA repair independent of ATM, MDC1, and RNF8. Mol Cell Biol 2013;33: 845–57.
[7] De Vos M, Schreiber V, Dantzer F. The diverse roles and clinical relevance of PARPs in DNA damage repair: current state of the art. Biochem Pharmacol 2012;84:137–46.
[8] Kalisch T, Ame JC, Dantzer F, Schreiber V. New readers and interpretations of poly(ADP-ribosyl)ation. Trends Biochem Sci 2012;37: 381–90.
[9] Kang HC, Lee YI, Shin JH, Andrabi SA, Chi Z, et al. Iduna is a poly(ADP-ribose) (PAR)-dependent E3 ubiquitin ligase that regulates DNA damage. Proc Natl Acad Sci U S A 2011;108:14103–08.
[10] Dantzer F, Noel G, Schreiber V. Inhibiteurs de PARP : des avancées significatives dans le traitement des cancers. Bull Cancer 2011;98: 277–90.
[11] Mortusewicz O, Ame JC, Schreiber V, Leonhardt H. Feedback-regulated poly(ADP-ribosyl)ation by PARP-1 is required for rapid response to DNA damage in living cells. Nucleic Acids Res 2007;35:7665–75.
[12] Khodyreva SN, Prasad R, Ilina ES, Sukhanova MV, Kutuzov MM, et al. Apurinic/apyrimidinic (AP) site recognition by the 5′-dRP/AP lyase in poly(ADP-ribose) polymerase-1 (PARP-1). Proc Natl Acad Sci U S A 2011;107:22090–95.
[13] Strom CE, Johansson F, Uhlen M, Szigyarto CA, Erixon K, et al. Poly(ADP-ribose) polymerase (PARP) is not involved in base excision repair but PARP inhibition traps a single-strand intermediate. Nucleic Acids Res 2011;39:3166–75.
[14] Boehler C, Gauthier LR, Mortusewicz O, Biard DS, Saliou JM, et al. Poly(ADP-ribose) polymerase 3 (PARP3), a newcomer in cellular response to DNA damage and mitotic progression. Proc Natl Acad Sci U S A 2011;108: 2783–8.
[15] Mladenov E, Iliakis G. Induction and repair of DNA double strand breaks: the increasing spectrum of non-homologous end joining pathways. Mutat Res 2011;711:61–72.
[16] Li M, Yu X. The role of poly(ADP-ribosyl) ation in DNA damage response and cancer chemotherapy. Oncogene 2015;34: 3349–56.
[17] Helleday T. The underlying mechanism for the PARP and BRCA synthetic lethality: clearing up the misunderstandings. Mol Oncol 2011;5:387–93.
[18] Beck C, Boehler C, Guirouilh Barbat J, Bonnet ME, Illuzzi G, et al. PARP3 affects the relative contribution of homologous recombination and nonhomologous end-joining pathways. Nucleic Acids Res 2014;42:5616–32.
[19] Fatokun AA, Dawson VL, Dawson TM. Parthanatos: mitochondrial-linked mechanisms and therapeutic opportunities. Br J Pharmacol 2014;171:2000–16.
[20] Mashimo M, Kato J, Moss J. ADP-ribosyl-acceptor hydrolase 3 regulates poly(ADP-ribose) degradation and cell death during oxidative stress. Proc Natl Acad Sci U S A 2013;110:18964–69.
[21] Curtin NJ, Szabo C. Therapeutic applications of PARP inhibitors: anticancer therapy and beyond. Mol Aspects Med 2013;34: 1217–56.
[22] Durkacz BW, Omidiji O, Gray DA, Shall S. (ADP-ribose)n participates in DNA excision repair. Nature 1980;283:593–6.
[23] Curtin NJ. DNA repair dysregulation from cancer driver to therapeutic target. Nat Rev 2012;12:801–17.
[24] Pernin V, Megnin-Chanet F, Pennaneach V, Fourquet A, Kirova Y, et al. Inhibiteurs de PARP et radiotherapie : rationnel et perspectives pour une utilisation en clinique. Cancer Radiother 2014;18:790–8.
[25] Plummer R, Jones C, Middleton M, Wilson R, Evans J, et al. Phase I study of the poly(ADP-ribose) polymerase inhibitor, AG014699, in combination with temozolomide in patients with advanced solid tumors. Clin Cancer Res 2008;14:7917–23.
[26] Curtin N. PARP inhibitors for anticancer therapy. Biochem Soc Trans 2014;42:82–8.

[27] Farmer H, McCabe N, Lord CJ, Tutt AN, Johnson DA, et al. Targeting the DNA repair defect in BRCA mutant cells as a therapeutic strategy. Nature 2005;434:917–21.

[28] Bryant HE, Schultz N, Thomas HD, Parker KM, Flower D, et al. Specific killing of BRCA2-deficient tumours with inhibitors of poly(ADP-ribose) polymerase. Nature 2005;434:913–7.

[29] Lord CJ, Tutt AN, Ashworth A. Synthetic lethality and cancer therapy: lessons learned from the development of PARP inhibitors. Annu Rev Med 2015;66:455–70.

[30] Kaye SB, Lubinski J, Matulonis U, Ang JE, Gourley C, et al. Phase II, open-label, randomized, multicenter study comparing the efficacy and safety of olaparib, a poly(ADP-ribose) polymerase inhibitor, and pegylated liposomal doxorubicin in patients with BRCA1 or BRCA2 mutations and recurrent ovarian cancer. J Clin Oncol 2012;30:372–9.

[31] Ledermann J, Harter P, Gourley C, Friedlander M, Vergote I, et al. Olaparib maintenance therapy in platinum-sensitive relapsed ovarian cancer. N Engl J Med 2012;366:1382–92.

[32] Turner NC, Lord CJ, Iorns E, Brough R, Swift S, et al. A synthetic lethal siRNA screen identifying genes mediating sensitivity to a PARP inhibitor. EMBO J 2008;27:1368–77.

[33] Fraser M, Zhao H, Luoto KR, Lundin C, Coackley C, et al. PTEN deletion in prostate cancer cells does not associate with loss of RAD51 function: implications for radiotherapy and chemotherapy. Clin Cancer Res 2012;18:1015–27.

[34] Peng G, Chun-Jen Lin C, Mo W, Dai H, Park YY, et al. Genome-wide transcriptome profiling of homologous recombination DNA repair. Nat Commun 2014;5:3361.

[35] Ekblad T, Camaioni E, Schuler H, Macchiarulo A. PARP inhibitors: polypharmacology versus selective inhibition. FEBS J 2013;280:3563–75.

[36] Wahlberg E, Karlberg T, Kouznetsova E, Markova N, Macchiarulo A, et al. Family-wide chemical profiling and structural analysis of PARP and tankyrase inhibitors. Nat Biotechnol 2012;30:283–8.

[37] Farres J, Martin-Caballero J, Martinez C, Lozano JJ, Llacuna L, et al. Parp-2 is required to maintain hematopoiesis following sublethal gamma-irradiation in mice. Blood 2013;122:44–54.

[38] Farres J, Llacuna L, Martin-Caballero J, Martinez C, Lozano JJ, et al. PARP-2 sustains erythropoiesis in mice by limiting replicative stress in erythroid progenitors. Cell Death Differ 2015;22:1144–57.

[39] Steffen JD, Tholey RM, Langelier MF, Planck JL, Schiewer MJ, et al. Targeting PARP-1 allosteric regulation offers therapeutic potential against cancer. Cancer Res 2014;74:31–7.

[40] Murai J, Huang SY, Das BB, Renaud A, Zhang Y, et al. Trapping of PARP1 and PARP2 by clinical PARP inhibitors. Cancer Res 2012;72:5588–99.

[41] Satoh MS, Lindahl T. Role of poly(ADP-ribose) formation in DNA repair. Nature 1992;356:356–8.

[42] Shen Y, Aoyagi-Scharber M, Wang B. Trapping PARP. J Pharmacol Exp Ther 2015;353:446–57.

[43] Pettitt SJ, Rehman FL, Bajrami I, Brough R, Wallberg F, et al. A genetic screen using the PiggyBac transposon in haploid cells identifies Parp1 as a mediator of olaparib toxicity. PLoS ONE 2013;8:e61520.

[44] Murai J, Huang SY, Renaud A, Zhang Y, Ji J, et al. Stereospecific PARP trapping by BMN 673 and comparison with olaparib and rucaparib. Mol Cancer Ther 2014;13:433–43.

[45] Bowman KJ, Newell DR, Calvert AH, Curtin NJ. Differential effects of the poly(ADP-ribose) polymerase (PARP) inhibitor NU1025 on topoisomerase I and II inhibitor cytotoxicity in L1210 cells in vitro. Br J Cancer 2001;84:106–12.

[46] Murai J, Zhang Y, Morris J, Ji J, Takeda S, et al. Rationale for poly(ADP-ribose) polymerase (PARP) inhibitors in combination therapy with camptothecins or temozolomide based on PARP trapping versus catalytic inhibition. J Pharmacol Exp Ther 2014;349:408–16.

[47] Das BB, Huang SY, Murai J, Rehman I, Ame JC, et al. PARP1-TDP1 coupling for the repair of topoisomerase I-induced DNA damage. Nucleic Acids Res 2014;42:4435–49.

[48] Patel AG, Sarkaria JN, Kaufmann SH. Non-homologous end joining drives poly(ADP-ribose) polymerase (PARP) inhibitor lethality in homologous recombination-deficient cells. Proc Natl Acad Sci U S A 2011;108:3406–11.

[49] Montoni A, Robu M, Pouliot E, Shah GM. Resistance to PARP-inhibitors in cancer therapy. Front Pharmacol 2013;4:18.

[50] Jaspers JE, Kersbergen A, Boon U, Sol W, van Deemter L, et al. Loss of 53BP1 causes PARP inhibitor resistance in Brca1-mutated mouse mammary tumors. Cancer Disc 2013;3:68–81.

[51] Xu G, Chapman JR, Brandsma I, Yuan J, Mistrik M, et al. REV7 counteracts DNA double-strand break resection and affects PARP inhibition. Nature 2015;521:541–4.

[52] Rottenberg S, Jaspers JE, Kersbergen A, van der Burg E, Nygren AO, et al. High sensitivity of BRCA1-deficient mammary tumors to the PARP inhibitor AZD2281 alone and in combination with platinum drugs. Proc Natl Acad Sci U S A 2008;105:17079–84.

[53] Nowsheen S, Cooper T, Bonner JA, LoBuglio AF, Yang ES. HER2 overexpression renders human breast cancers sensitive to PARP inhibition independently of any defect in homologous recombination DNA repair. Cancer Res 2012;72:4796–806.

[54] Vormoor B, Curtin NJ. Poly(ADP-ribose) polymerase inhibitors in Ewing sarcoma. Curr Opin Oncol 2014;26:428–33.

[55] Lau T, Chan E, Callow M, Waaler J, Boggs J, et al. A novel tankyrase small-molecule inhibitor suppresses APC mutation-driven colorectal tumor growth. Cancer Res 2013;73:3132–44.

[56] Riffell JL, Lord CJ, Ashworth A. Tankyrase-targeted therapeutics: expanding opportunities in the PARP family. Nat Rev Drug Discov 2012;11:923–36.

[57] Cho SH, Ahn AK, Bhargava P, Lee CH, Eischen CM, et al. Glycolytic rate and lymphomagenesis depend on PARP14, an ADP ribosyltransferase of the B aggressive lymphoma (BAL) family. Proc Natl Acad Sci U S A 2011;108:15972–77.

[58] Pujade-Lauraine É, Combe P. Olaparib dans les cancers de l'ovaire BRCA muté. Bull Cancer 2015;102(6 Suppl. 1):S82–4. http://dx.doi.org/10.1016/S0007-4551(15)31221-2.

Purification of Recombinant Human PARG and Activity Assays

Jean-Christophe Amé*, Éléa Héberlé, Barbara Camuzeaux, Françoise Dantzer, Valérie Schreiber

May 26, 2016

Groupe Poly(ADP-ribosyl)ation et Intégrité du Génome, UMR7242 du CNRS
École Supérieure de Biotechnologie de Strasbourg
Parc d'innovation, Boulevard Sébastien Brant
CS 10413
67412 ILLKIRCH CEDEX
France
tel.: +33 (0)3 68 85 47 05
Fax.: +33 (0)3 68 85 46 86

Contents

1 Introduction **3**

2 Materials **3**
2.1 Materials for Bacterial Growth and Protein Expression . . . 3
2.2 Materials for Purification of GST-hPARG . . . 4
2.3 Materials for PreScission Cleavage . . . 4
2.4 Materials for Large Scale PAR Synthesis . . . 4
2.5 Materials for SDS-PAGE . . . 5
2.6 Materials for Western Blot . . . 5
2.7 Detection of PARG activity in solution . . . 5
2.8 Materials for Electrophoresis on Sequencing Gel . . . 6
2.9 Materials for Detection of PARG Activity on Dot Blot . . . 6

3 Methods **7**
3.1 Purification Protocol Overview . . . 7
3.2 Bacterial Growth and Induction of Expression . . . 7
3.3 Cell Lysate Preparation . . . 8
3.4 Glutathione Sepharose 4B Affinity Chromatography . . . 9
3.5 PreScission Protease Cleavage . . . 9
3.6 Quality Control: SDS-PAGE . . . 10
3.7 Quality Control: Western Blot . . . 11
3.8 Detection of PARG Activity by Electrophoresis on Sequencing Gel . . . 11
3.8.1 Purification of Radioactive Poly(ADP-ribose) . . . 11
3.8.2 PARG Activity in Solution . . . 13
3.8.3 Electrophoresis on Sequencing Gel . . . 13
3.8.4 PARG Activity Dot Blot and Immuno-Detection of PAR . . . 15

4 Notes **16**

*Corresponding author, e-mail: jean-christophe.ame@unistra.fr

List of Figures

1 Schematic representation of the purification protocol of human PARG 7

2 **Details of the cloning region of hPARG expressing vector pGEX6P3-hPARGfl.** The N-terminal part of the GST is in green color and in a grey box. The preScission recognition site is in red and the cleavage position is depicted with the red arrow. The sequence of PARG is in bold and the purified protein is underlined. The PARG sequence was amplified by PCR using the forward and reverse oligonucleotides respectively: `5' gctcacagaattcaatgaatgcaggtccgggttgcg`, `5' ggtacccggggaattcttaggtaccggtacgttg`. The cloning sites are `EcoRI`. 8

3 **Purification of hPARG by affinity chromatography on Glutathione-Sepharose 4B.** *Left:* 10% SDS-PAGE of purification fractions. MW : molecular weight markers; 1, clear lysate (10 µl); 2, clear lysate after protamine sulfate precipitation (10 µl); 3, proteins bound to Glutathione-Sepharose beads after washing (10 µl); 4, free hPARG following overnight cleavage using 10 U of PreScission protease (10 U, 16 h et 4 °C) (20 µl/700 µl); 5, Proteins bound to the Glutathione-Sepharose beads after cleavage (20 µl). SDS-PAGE 10%, stained with Coomassie blue and scanned using the Li-COR Odyssey imaging system. *Right:* Detection of PARG by Western Blot. Same deposit as for SDS-PAGE but only 1/10-volume of previous deposit. After transfer, the nitrocellulose membrane was incubated overnight at 4 °C with a 1:10,000-dilution of anti-PARG monoclonal antibody (clone D8B10, Millipore) in PBS-0.05%-tween 5% fat-free dry milk. After three washes the membrane was incubated 2 h at room temperature with a 1:20,000-dilution of GAM-Alexa680-secondary antibody in PBS-0.05%-tween 5% fat-free dry milk. The membrane was scanned on a LI-COR Odyssey imaging system. 10

4 **Examples of PARG activity and detection by electrophoresis on 20% Acrylamide-7 M Urea sequencing gel.** Time course degradation of [^{32}P]-PAR by the human PARG purified from over-expressing *E. coli* BL21DE3. 2×10^5 cpm of purified [^{32}P]-PAR were incubated with 10 ng of purified human PARG. At each indicated time point, 10 µL of the reaction were taken and mixed with 10 µL of loading solution (95% formamide, 10 mM EDTA, 0.025% xylene cyanol, 0.025% bromophenol blue) to stop the reaction. 6 µL of each mixture was loaded and separated on a 0.35-mm sick 20% Acrylamide, 7 M Urea 40 cm high sequencing gel. The gel was exposed for 24 h on a phosphor screen. The phosphor screen was scanned on a Typhoon™ FLA 9500 Biomolecular Imager. 12

5 **Time-course evaluation of PARG activity using Dot Blot and detection of PAR with an anti-PAR antibody (10H).** Kinetic of digestion of un-labelled poly(ADP-ribose) by PARG. After the indicated time, 3 µL of the reaction containing 8 ng/µL of purified PAR was spotted onto the nitrocellulose membrane. *Top row:* reaction without PARG, *Bottom row:* reaction containing 0.48 ng/µL of purified human PARG. PAR was detected by immuno-detection using the 10H anti-PAR monoclonal antibody as primary antibody (1:1,000) and the Alexa680-conjugated goat anti-mouse secondary antibody (1:20,000). The signal was reveal by scanning the membrane using the LI-COR Odyssey imaging system. Dots were quantified using NIH ImageJ software and values were plotted using R statistical package (*Blue curve:* Variation of PAR intensity from reaction without PARG. Straight line showing the mean of PAR untreated values. *Red curve:* Variation of PAR intensity from reaction incubated with PARG.) 15

Abstract The purification of Poly(ADP-ribose) glycohydrolase (PARG) from over-expressing bacteria *Escherichia coli* is described here to a fast and reproducible one chromatographic step protocol. After cell lysis, GST-PARG-fusion proteins from the crude extract are affinity purified by a Glutathione 4B Sepharose chromatographic step. The PARG proteins are then freed from their GST-fusion by overnight enzymatic cleavage using the preScission protease. As described in the protocol, more than 500 µg of highly active human PARG can be obtained from 1.5 L of *E. coli* culture.

Key words: Poly(ADP-ribose) glycohydrolase, poly(ADP-ribose) metabolism, PARG purification

1 Introduction

Poly(ADP-ribosyl)ation is a post-translational modification of proteins mediated by poly(ADP-ribose) polymerases, or PARPs. It is present in higher eukaryotes and is involved in many physiological processes such as DNA repair, transcription, cell division and cell death. The widespread subcellular localisations of the 17 members of the PARP family underline the probable occurrence of this modification all over the cell (1, 2, 3, 4). Poly(ADP-ribose) is generated by polymerisation of ADP-ribose moieties from NAD^+ on acceptor proteins, either PARPs themselves, by automodification, or to heterologous substrates, by heteromodification. It regulates not only cell survival and cell-death programmes, but also an increasing number of other biological functions with which novel members of the PARP family have been associated. These functions include transcriptional regulation, telomere cohesion and mitotic spindle formation during cell division, intracellular trafficking and energy metabolism. At least three members of this family are activated in response to genotoxic stress: PARP-1, the founding member, PARP-2 and PARP-3. Many studies have shown that these proteins act in a complex response network that is driven by the cellular, molecular and chemical biology of poly(ADP-ribose) (PAR) thus these PARPs should be good targets for chemical therapeutics for several diseases (5, 6). Indeed, a number of PARP inhibitors are in advanced clinical development for BRCA-mutated breast cancer, and olaparib has recently been approved for BRCA-mutant advanced ovarian cancer.

Poly(ADP-ribosyl)ation is a transient modification of proteins, since poly(ADP-ribose) is efficiently and rapidly degraded by the endo- and exo-glycosidase activities of poly(ADP-ribose) glycohydrolase, (PARG). The unique PARG gene encodes a nuclear enzyme ($PARG^{111}$) as well as smaller isoforms showing cytoplasmic and mitochondrial localisations (7, 8). Many studies revealed the importance of PARP and PARG to control poly(ADP-ribose) levels regulating the balance between life-and-death in response to DNA injury (9, 10, 11), pointing that PARG could also be a good therapeutic target with the advantage that PARG inhibition, by limiting the recycling of ADP-ribose to NAD^+ provides an additional metabolic consequence that may affect cell survival (12). However, the currently available PARG inhibitors are questioned for their bioavailability or specificity, precluding from their evaluation in pre-clinical assays. Therefore, the design of PARG inhibitors requires that pure and high amount of this enzyme is easily available for enzymatic inhibition evaluation and co-crystallographic studies.

Here, we present a protocol specifically designed for the purification of the human full length PARG cloned in pGEX6P vectors in fusion with the GST tag and over-expressed in the bacterial system *Escherichia coli* BL21DE3. It results in a protein production of high purity suitable for studying the catalytic properties of the enzyme using biochemical or biophysical methods or for the induction of a specific immunogenic response for antibody production in the mouse or in the rabbit. We also present some tests to evaluate its activity in solution.

2 Materials

2.1 Materials for Bacterial Growth and Protein Expression

1. Sterile LB medium (10 g/L tryptone, 5 g/L Yeast Extract, 5 g/L NaCl, Sigma-Aldrich) (see Note 1).

2. 100 mg/mL Ampicillin (Sigma-Aldrich) stock solution in sterile water and stored in 1 mL aliquots at −20 °C.

3. Sterile 2-L flasks containing 500 mL of LB medium supplemented with the appropriate antibiotic (Ampicillin 100 µg/mL)

4. 1 M IPTG (Euromedex) stock solution prepared in sterile water and stored in 1 mL aliquots at −20 °C.

5. A Infors HT Minitron Incubator Shaker or equivalent for the culture during IPTG induction at 20 °C.

2.2 Materials for Purification of GST-hPARG

1. All the solutions are prepared using Milli-Q (18.2 MΩ.cm at 25 °C, 4 ppb TOC) water purified with a Millipore Advantage A10 water purification system connected to a source of reverse osmosis water.

2. Cell lysis buffer stock solution: prepare 250 mL of 25 mM Tris-HCl pH 8.0 buffer containing 50 mM glucose, 10 mM EDTA, 1 mM PMSF. Store it at 4 °C. Before use, prepare 20 mL aliquots containing two proteases inhibitor cocktail tablets .

3. Detergents: 100% Tween 20 (Sigma-Aldrich); 100% NP-40 (Sigma-Aldrich), 100% Triton® X100 (USB Corporation).

4. NaCl in powder and a 5 M stock solution (see Note 2).

5. Protamine sulfate 10 mg/mL in water (Sigma-Aldrich).

6. Proteases inhibitor cocktail tablets (CØmplete Mini, Roche Diagnostic Gmbh, Mannheim, Germany).

7. Glutathione Sepharose 4B from GE Healthcare.

8. Purification buffer: 50 mM Tris-HCl pH 8.0, 200 mM NaCl, 1 mM DTT, 0.1% Triton® X100.

2.3 Materials for PreScission Cleavage

1. PreScission protease (500 units, GE Healthcare).

2. PreScission cleavage buffer : 50 mM Tris-HCl pH 7.0, 150 mM NaCl, 1 mM EDTA, 1 mM DTT.

2.4 Materials for Large Scale PAR Synthesis

1. Siliconised 10 mL Sarstedt tubes: to prevent unspecific binding of the poly(ADP-ribose) to the plastic, the 10 mL Sarstedt screw cap tubes (round base) are siliconised by vortexing 1 mL of Sigmacote, (Sigma-Aldrich, St-Louis, MO, USA). Remove the solution and let it air-dry under the chemical hood (Sorbonne).

2. PARP activity buffer (10 ×): 500 mM Tris-HCl pH 8.0, 40 mM $MgCl_2$, 2 mM DTT, 500 µg/mL BSA, 20 µg/mL DNase I activated DNA, 4 mM NAD^+. This buffer can be kept in 200 µL aliquots for more than a year at −20 °C.

3. Radioactive NAD^+: [^{32}P]-NAD^+ (800 Ci/mmol, 5 µCi/µL, Perkin Elmer).

4. Purified PARP-1 (Enzo, Lausen, Switzerland).

5. 10 mg/mL solution of Proteinase K (Merk KGaA, Darmstadt, Germany), SDS 20%.

6. 0.2 M NaOH and 40 mM EDTA pH 8.0 solution. 0.2 M HCl solution.

7. Phenol/$CHCl_3$/isoamyl alcohol (25/24/1) mix (Roth GmbH, Karlsruhe, Germany).

8. 3 M potassium acetate pH 4.8 solution. 100% isopropyl alcohol (Fluka-Sigma-Aldrich, Germany).

9. TE buffer: 10 mM Tris-HCl pH 8.0, 1 mM EDTA pH 8.0.

2.5 Materials for SDS-PAGE

1. Separating buffer (4 ×): 1.5 M Tris-HCl, pH 8.8, 0.4% SDS. Store at 4 °C.
2. Stacking buffer (4 ×): 0.5 M Tris-HCl, pH 6.8, 0.4% SDS. Store at 4 °C.
3. Forty percent acrylamide/bis solution (37.5:1 with 2.6% C) (Bio-Rad) and N,N,N,N'-Tetramethylethylenediamine (TEMED, Euromedex) Store at 4 °C.
4. Ammonium persulfate (Sigma-Aldrich): prepare 10% solution in water and freeze in aliquots at −20°C.
5. Isopropanol.
6. Running buffer (5 ×): Tris-base 30 g/L, Glycine 144 g/L, SDS 5 g/L. The pH is not adjusted. Store at room temperature.
7. Prestained molecular weight markers (All blue Precision Plus Protein Prestained Standards, Bio-Rad).
8. Sample buffer: 50 mM Tris-HCl pH 6.8, Urea 6 M, SDS 3%, β-mercaptoethanol 6%. Add 3 mg of Bromophenol blue in 100 mL of sample buffer. Aliquot and store at −20 °C.
9. Coomassie blue staining solution: prepare 250 mL of 0.3% (w/v) Coomassie blue (Brilliant Blue G, Sigma-Aldrich) in 50% methanol, 10% acetic acid.
10. Coomassie blue destaining solution: Prepare 1 L of 50% methanol, 10% acetic acid in water.

2.6 Materials for Western Blot

1. Stock transfer buffer (10 ×): Tris base 30 g/L, glycine 144 g/L, SDS 10 g/L. The pH is not adjusted but should be 8.3. Store at room temperature.
2. Transfer buffer (1 ×): for a 1-L solution, mix in the following order 100 mL of 10 × stock transfer buffer, 700 mL of water, and 200 mL of 95% ethanol.
3. Nitrocellulose blotting membrane Amersham™ Protran™, 0.2 µm porosity (GE Healthcare), Whatman 3MM filter papers.
4. PBS buffer (10 ×): KH_2PO_4 10.6 mM, Na_2HPO_4, $2H_2O$ 30 mM, NaCl 1.54 M. Prepared with water and filtered 0.2 µm. Store at room temperature.
5. PBS-Tween buffer (1 ×): in a cylinder to make a 1-L solution, dilute 100 mL of 10 × PBS buffer, 500 µL of Tween-20, and complete with water.
6. Anti-PARG mouse monoclonal antibody (Millipore).
7. Horseradish peroxydase (HRP)-conjugated goat anti-rabbit secondary antibody (Sigma-Aldrich) or Alexa680-conjugated goat anti-rabbit secondary antibody (ThermoFisher Scientific).
8. Blocking buffer: 5% (w/v) nonfat dry milk in PBS.
9. Enhanced chemiluminescent reagents, ECL Plus Western Blotting Detection System, Amersham, GE Healthcare and BioMax MR film (Kodak, Rochester, NY) or Amersham Hyperfilm™ ECL (GE Healthcare) or a ImageQuant LAS 4000 imager (GE Healthcare) or an Odyssey® Imaging System (Li-Cor Biosciences).

2.7 Detection of PARG activity in solution

1. [^{32}P]-labelled-PAR (≃ 200,000 dpm, see § 3.8.1)
2. PARG activity buffer (10 ×): 500 mM Tris-HCl pH 8.0, 20 mM $MgCl_2$, 10 mM DTT, 1 M NaCl. The buffer is stored at −20 °C in small aliquots.
3. Purified recombinant human PARG.
4. Stop/Loading solution (95% formamide, 20 mM EDTA, 0.025% xylene cyanol, 0.025% bromophenol blue).

2.8 Materials for Electrophoresis on Sequencing Gel

1. Model S2 Sequencing Gel Electrophoresis Apparatus from Gibco BRL® or equivalent.
2. One pair of 33-cm wide glass plates (one short of 39 cm, one long of 42 cm).
3. Sigmacote, (Sigma-Aldrich, St-Louis, MO, USA).
4. One pair of 0.35-mm thick mylar side spacers.
5. A 0.35-mm thick mylar 32-square-toothed comb.
6. Binder Clips.
7. One pair of 122-cm DC power cords.
8. High voltage power supply (3,000 V/150 A).
9. 10 × TBE (890 mM Tris, 890 mM boric acid, 20 mM EDTA) electrophoresis buffer.
10. Urea.
11. Forty percent acrylamide/bis solution (38:2 with 3.3% C) (Bio-Rad) and N,N,N,N'-Tetramethylethylenediamine (TEMED, Euromedex) Store at 4 °C.
12. Ammonium persulfate (Sigma-Aldrich): prepare 10% solution in water and freeze in aliquots at −20 °C.
13. 250-mL Millipore Stericup® Millipore Express® Plus 0.22 µm PES.
14. Loading solution (95% formamide, 20 mM EDTA, 0.025% xylene cyanol, 0.025% bromophenol blue).
15. 35 × 3 cm band of Whatman 3MM filter paper.
16. Used autoradiographic Kodak acetate-film (minimum size 34 × 40 cm or an equivalent piece of rigid plastic that could accommodate the gel size after the electrophoresis).
17. Storage Phosphor ScreenImage and Typhoon™ FLA 9500 Biomolecular Imager (GE Healthcare).

2.9 Materials for Detection of PARG Activity on Dot Blot

1. Unlabelled purified poly(ADP-ribose) (200 ng/µL, determined by measuring the absorbance at 260 nm with a spectrophotometer and using the relationship A_{260}=1 ⇔ 40 µg/mL). Unlabelled PAR is obtained as in § 3.8.1, but the reaction is done without radioactive NAD^+ .
2. PARG activity buffer (10 ×): 500 mM Tris-HCl pH 8.0, 20 mM $MgCl_2$, 10 mM DTT, 1 M NaCl. The buffer is stored at −20 °C in small aliquots.
3. Purified recombinant human PARG.
4. Nitrocellulose membrane.
5. PBS-Tween buffer (1 ×): in a cylinder to make a 1-L solution, dilute 100 mL of 10 × PBS buffer, 500 µL of Tween-20, and complete with water.
6. Anti-poly(ADP-ribose) antibody polyclonal or monoclonal 10H (Trevigen).
7. Horseradish peroxydase (HRP)-conjugated goat anti-rabbit or anti-mouse secondary antibody (Sigma-Aldrich) or Alexa680-conjugated goat anti-rabbit or anti-mouse secondary antibody (ThermoFisher Scientific, Molecular Probes).
8. Blocking buffer: 5% (w/v) nonfat dry milk in PBS.
9. Enhanced chemiluminescent reagents, ECL Plus Western Blotting Detection System, Amersham, GE Healthcare and BioMax MR film (Kodak, Rochester, NY) or Amersham Hyperfilm™ ECL (GE Healthcare) or a ImageQuant LAS 4000 imager (GE Healthcare) or an Odyssey® Imaging System (Li-Cor Biosciences).

3 Methods

3.1 Purification Protocol Overview

A schematic representation of the purification protocol of human PARG is presented Fig. 1. It summarises the various steps needed to obtain a fairly pure and active human PARG from a *E. coli* culture over-expressing the protein.

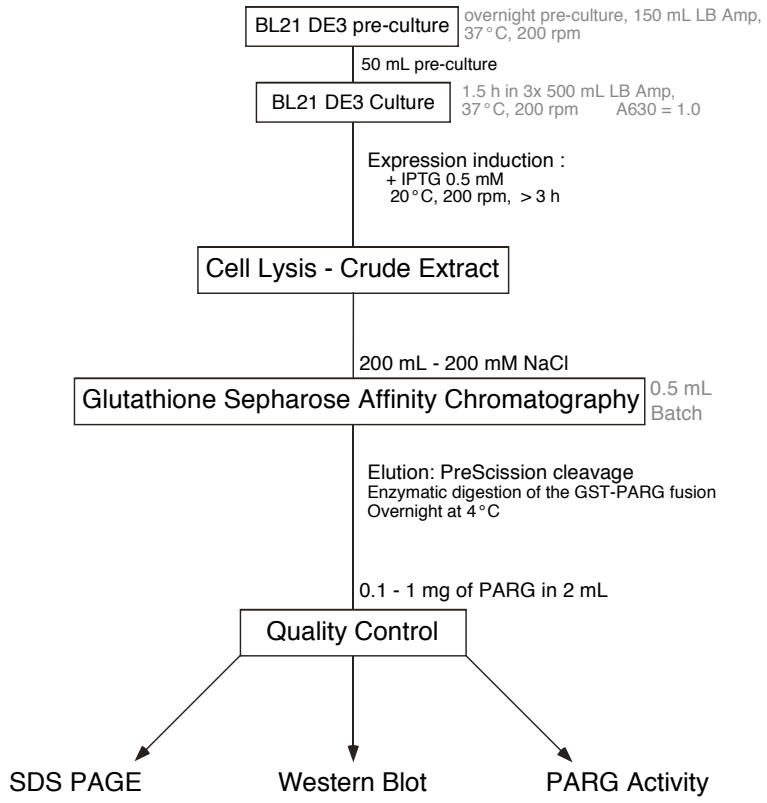

Fig. 1: Schematic representation of the purification protocol of human PARG

3.2 Bacterial Growth and Induction of Expression

The following protocol is suitable for the purification of the human recombinant PARG over-expressed in *Escherichia coli*. This system results in the expression of a GST-fusion protein facilitating it's purification by a single affinity chromatographic step using the Glutathione Sepharose 4B matrix. The fusion-protein bound to the purification matrix is then later cleaved by enzymatic cleavage with the preScission protease to elute the full length PARG from it's support. The expression of human PARG has been optimised by cloning into the expression plasmid pGEX6P3 a synthetic version of the human cDNA with codon usage adapted for expression in the bacteria *E. coli* (see Note 3).

1. The day before the culture a small pre-culture (3 mL) in LB containing the appropriate antibiotic (ampicillin at 100 µg/mL (LB-Amp)) is started with 30 µl from a stock of bacteria conserved at −80 °C previously transformed with the expressing plasmid (pGEX6P3 containing the cDNA of human PARG), shake at 37 °C.

2. After six hours, 100 µl of this culture is used to seed a 150 mL pre-culture (LB-Amp) in a 1-L flask, then shake at 200 rpm overnight at 37 °C.

3. The next day, three 2-L flasks containing 500 mL of LB-Amp are seeded with 50 mL of the overnight pre-culture each. The bacteria are grown for 2 h at 37 °C under agitation at 200 rpm.

4. The expression of the recombinant protein is induced by addition of 0.5 mM IPTG (275 µl of 1 M stock IPTG). The flasks are transferred to a Minitron shaker and cultivated for an additional 3 to 4 hours at 20 °C and 200 rpm agitation.

5. Following the expression of the protein, harvest the bacteria by centrifugation (9,000 × g, 15 min at room temperature) in 500-mL bottles (JA-10 Rotor, Avanti J25 centrifuge, Beckman).

6. Wash once with 80 mL of cold PBS 1 ×, transfer in two 50-mL Falcon tubes and harvest at 4 °C, 5,500 × g in a JA-12 rotor (Beckman). Discard the supernatant and dry freeze at −80 °C.

3.3 Cell Lysate Preparation

All the steps are performed at 4 °C ideally in the cold room or on ice.

1. The cells are quickly defrosted and resuspended by vortexing in 5 mL of cold cell lysis buffer (keep working in the same 50-mL Falcon tubes).

2. Moderately sonicate (40% power, 1.2-cm ⌀ probe) 3 × 20 sec in ice. Do not stop agitating during the sonication process to ensure a good lysis. The viscosity of the solution should disappear.

3. Add 0.2% of Triton® X100, 0.2% of NP40, 4 mL of 5 M NaCl.

4. Gently rotate the cell suspension for 20 min on a rotating wheel in the cold room.

5. Add 30 mL of ice-cold Tris-HCl 20 mM pH 7.5, rotate for an additional 20 min in the cold room.

6. Clear lysate from cellular debris by centrifugation at 22,300 × g for 60 min at 4 °C (rotor JA-12, Avanti J25, Beckman).

7. Add to the supernatant 1 mg/mL final of a 10 mg/mL protamine sulfate solution in water to precipitate the nucleic acids, invert the tubes several times and centrifuge at 22,300 × g for 60 min at 4 °C (rotor JA-12 Beckman).

8. Optional step : the crude protein solution can be clarified by filtration through a 0.22-µm vacuum filter (Steriflip®).

9. The protein solution is then diluted with Purification buffer to final volume of 50 mL (see Note 6) in a 50-mL Falcon tube.

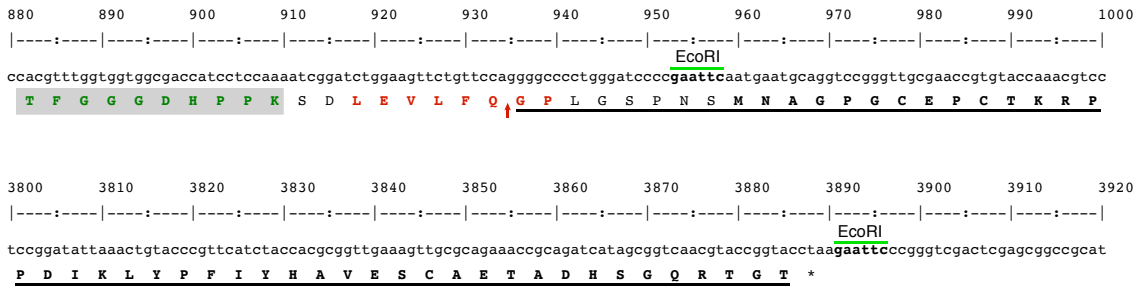

Fig. 2: **Details of the cloning region of hPARG expressing vector pGEX6P3-hPARGfl.** The N-terminal part of the GST is in green color and in a grey box. The preScission recognition site is in red and the cleavage position is depicted with the red arrow. The sequence of PARG is in bold and the purified protein is underlined. The PARG sequence was amplified by PCR using the forward and reverse oligonucleotides respectively: 5' gctcacagaattcaatgaatgcaggtccgggttgcg, 5' ggtacccggggaattcttaggtaccggtacgttg. The cloning sites are EcoRI.

3.4 Glutathione Sepharose 4B Affinity Chromatography

This chromatographic step performed in batch mode allows the rapid purification of the GST-PARG fusion protein in less than two hours. It ensures minimal protein contamination as extensive washing of the specific bound GST-PARG can be achieved using high salt concentration buffers thanks to the high affinity of GST for the Glutathione Sepharose matrix.

1. Wash three times in PBS 600 µL of 50% slurry of Glutathione Sepharose 4B beads in a 2-mL Eppendorf tube (see Note 4).
2. After the last wash, suspend the beads in 1 mL of Purification buffer and transfer into the tube containing the protein solution. Agitate softly by rotating on a wheel at 4 °C in a cold room for minimum 30 min.
3. Pellet the beads by centrifugation for 2 min at $500 \times g$ at 4 °C (rotor JA-12, Avanti J25, Beckman).
4. Carefully discard the supernatant, wash the hPARG-GST-Glutathione Sepharose 4B beads with 50 mL of Purification buffer. Repeat this washing step three times.
5. Transfer the beads in a 15-mL Falcon tube containing 12 mL of cold Purification buffer supplemented with NaCl to 1 M NaCl final. This step should eliminate any unspecific binding of protein.
6. Pellet the beads for 2 min at $500 \times g$ at 4 °C (Eppendorf centrifuge 5810R), carefully discard the supernatant. Suspend the beads in 14 mL of Purification buffer and pellet again the beads.
7. Transfer the beads in two 2.0-mL Eppendorf tubes, centrifuge for 1 min at $500 \times g$ at 4 °C (Eppendorf centrifuge 5415R), remove the supernatant.
8. Take off 5 µL of beads for further SDS-PAGE analysis of the bound proteins.
9. Tubes containing the hPARG-GST-Glutathione Sepharose 4B beads may be stored on ice or at 4 °C in the fridge for a few hours.

3.5 PreScission Protease Cleavage

PreScission Protease is a genetically engineered fusion protein consisting of human rhinovirus 3C protease and GST. This protease was specifically designed to facilitate removal of the protease by allowing simultaneous protease immobilisation and cleavage of GST fusion proteins produced from the pGEX-6P vectors. PreScission Protease specifically cleaves between the `Gln` and `Gly` residues of the recognition sequence of `LeuGluValLeuPheGln/GlyPro`.

1. Wash the beads twice with 1.5 mL of cold PreScission cleavage buffer.
2. Suspend the beads in 1.3 mL of cold PreScission cleavage buffer.
3. Add 10 units of PreScission protease to the beads, mix well by inverting several times the tubes. The cleavage reaction is then carried out at 4 °C by rotating the tubes on a wheel in the cold room overnight or for 10 to 12 h.
4. The GST-hPARG fusion cleavage should be complete after 10 to 12 h incubation. The supernatant should contain the free hPARG.
5. After centrifugation at $500 \times g$ at 4 °C for 2 min, collect as much of the supernatant as possible in a new 1.5 mL Eppendorf tube.
6. The beads are washed twice with 0.5 mL of cold PreScission buffer containing 0.2% Triton® X100 to recover most of the hPARG protein. The amount and the quality of the purified protein in each fraction is evaluated by SDS-PAGE, (see Fig. 3).
7. Add 10% glycerol final to the hPARG fractions. Aliquot and Store at −80 °C.

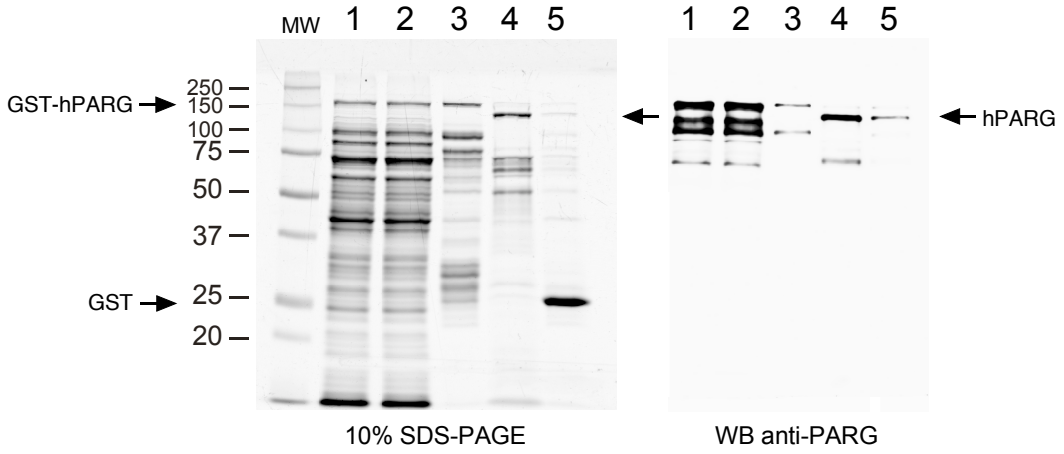

Fig. 3: **Purification of hPARG by affinity chromatography on Glutathione-Sepharose 4B.** *Left:* 10% SDS-PAGE of purification fractions. MW : molecular weight markers; 1, clear lysate (10 µl); 2, clear lysate after protamine sulfate precipitation (10 µl); 3, proteins bound to Glutathione-Sepharose beads after washing (10 µl); 4, free hPARG following overnight cleavage using 10 U of PreScission protease (10 U, 16 h et 4 °C) (20 µl/700 µl); 5, Proteins bound to the Glutathione-Sepharose beads after cleavage (20 µl). SDS-PAGE 10%, stained with Coomassie blue and scanned using the Li-COR Odyssey imaging system. *Right:* Detection of PARG by Western Blot. Same deposit as for SDS-PAGE but only 1/10-volume of previous deposit. After transfer, the nitrocellulose membrane was incubated overnight at 4 °C with a 1:10,000-dilution of anti-PARG monoclonal antibody (clone D8B10, Millipore) in PBS-0.05%-tween 5% fat-free dry milk. After three washes the membrane was incubated 2 h at room temperature with a 1:20,000-dilution of GAM-Alexa680-secondary antibody in PBS-0.05%-tween 5% fat-free dry milk. The membrane was scanned on a LI-COR Odyssey imaging system.

3.6 Quality Control: SDS-PAGE

1. The following instructions assume the use of a 11 by 10 cm gel system. They are easily adaptable to other formats. It is important that the glass plates are cleaned before use with a soft detergent (Teepol) and rinsed extensively with distilled water then 95% ethanol and air-dried.

2. Prepare a 1-mm thick, 10% gel by mixing 5 mL water with 2.5 mL of 4 × separating buffer, 2.5 mL acrylamide/*bis* solution, 68 µL ammonium persulfate solution, and 14 µL TEMED. Pour the gel, leaving space for a stacking gel, and carefully overlay with isopropanol. The gel should polymerise in about 10-15 min.

3. Pour off the isopropanol and rinse the top of the gel twice with distilled water.

4. Prepare the stacking gel by mixing 3.2 mL water with 1.25 mL of 4 × stacking buffer, 500 µL acrylamide/*bis* solution, 40 µL ammonium persulfate solution, and 8 µL TEMED. Pour the stack and insert the comb. The stacking gel should polymerise in about 10 min.

5. Prepare the running buffer by mixing 100 mL of the 10 × running buffer with 900 mL of water.

6. After polymerisation of the stacking gel, the comb is carefully removed and the wells are washed with 1 × running buffer using a 3-mL syringe fitted with a 22-gauge needle.

7. Add the running buffer to the lower chamber first, (avoid any bubbles which could be trapped between the glass plates on the bottom of the gel), then to the upper gel unit and load the 10 to 25 µL of each sample in a well. Include one well for pre-stained molecular weight markers.

8. Complete the assembly of gel unit and connect the power supply. The gel is run at 12 V/cm for 90 min at room temperature or until the dye front reaches the bottom of the gel.

9. Coomassie blue staining of the proteins separated by SDS-PAGE is performed by incubating the gel one hour in the Coomassie blue staining solution under shaking at room temperature. The proteins are revealed by destaining by washing the gel under shaking in the Coomassie

blue destaining solution. When this solution becomes blue, it must be replaced by a fresh one. This must be repeated until a gel with a clear background is obtained.

10. Rehydrate the gel in distilled water, change the water several times to remove the methanol/acetic acid solution.

3.7 Quality Control: Western Blot

1. The samples that have been separated by SDS-page are transferred to nitrocellulose membranes electrophoretically. Any transfer tank system can be used for this purpose. We use routinely a Mini Trans-Blot Electrophoretic Transfer Cell from Bio-Rad.

2. Prepare a tray of transfer buffer that is large enough to lay out a transfer cassette with its pieces of Scotch-brite® pads and with two sheets of Whatman® 3MM paper submerged on one side. Cut a sheet of the nitrocellulose just larger than the size of the gel (separating and stacking), wet and soak in the transfer buffer.

3. Disconnected the gel unit from the power supply and disassemble. Setup the sandwich from bottom to top: one side of the transfer cassette, a piece of Scotch-brite® pad, a sheet of Whatman® 3MM paper, the nitrocellulose membrane, the gel (ensuring that no bubbles are trapped between the membrane and the gel), a sheet of Whatman® 3MM paper, a piece of Scotch-brite® pad. The transfer cassette is then carefully closed.

4. Place the cassette into the transfer tank such as that the nitrocellulose membrane is between the gel and the anode (+). Fill up the tank with cold transfer buffer and add a magnetic stir bar. The electrophoretic transfer is performed in a cold chamber (4 °C) with the tank placed on top of a magnetic stirrer. Make sure that the magnetic stir bar rotates freely.

5. Put the lid on the tank and activate the power supply. The transfer is accomplished at 100 V (250 mA) for 1.5 h.

6. Once the transfer is completed, take out the cassette of the tank and carefully disassemble, with the top Scotch-brite® pad and sheets of 3MM paper removed. Do not forget to orientate the membrane. The gel can be discarded and the excess nitrocellulose cut off. The coloured molecular weight markers should be clearly visible on the membrane.

7. Incubate the nitrocellulose in 20 mL PBS-Tween for 5 min then in 20 mL blocking buffer for 20 min at room temperature on a rocking platform.

8. Discard the blocking buffer and replace by a minimum (10 mL) of blocking buffer containing an anti-PARG antibody (Millipore) at the working dilution (1:10,000). The incubation is performed at room temperature for 2 h or at 4 °C overnight on a rocking platform.

9. Remove the primary antibody. The dilution of antibody can be kept for further use and store at −20 °C. Wash the membrane three times for 10 min each with 20 mL PBS-Tween.

10. Discard the blocking buffer and replace with a minimum (10 mL) of PBS-Tween buffer containing a Goat anti-mouse Alexa Fluor 680 conjugate at the working dilution (1:20,000). The incubation is performed at room temperature for 60 min on a rocking platform.

11. Remove the secondary antibody solution. Wash the membrane three times each with 20 mL PBS-Tween at room temperature for 5 min and once with PBS for 5 min.

12. The membrane is scanned with the LI-COR Odyssey infrared imaging system. An example of the results produced is shown in Fig. 3.

3.8 Detection of PARG Activity by Electrophoresis on Sequencing Gel

3.8.1 Purification of Radioactive Poly(ADP-ribose)

The poly(ADP-ribose) synthesised as described below allows to obtain pure radioactive ([^{32}P] labelled) poly(ADP-ribose) (PAR) that can be separated by electrophoresis on sequencing gels and detected by autoradiography. It is also the substrate for PARG that can be used to evaluate its activity in various ways (see Note 5).

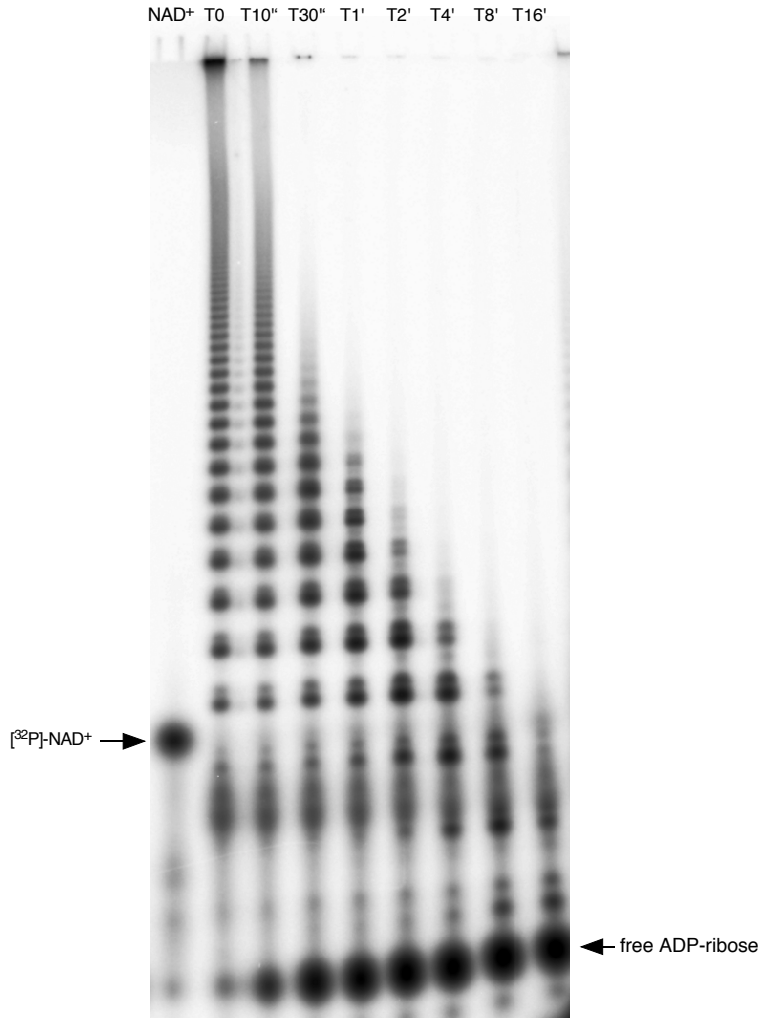

Fig. 4: **Examples of PARG activity and detection by electrophoresis on 20% Acrylamide-7 M Urea sequencing gel.** Time course degradation of [^{32}P]-PAR by the human PARG purified from over-expressing *E. coli* BL21DE3. 2×10^5 cpm of purified [^{32}P]-PAR were incubated with 10 ng of purified human PARG. At each indicated time point, 10 µL of the reaction were taken and mixed with 10 µL of loading solution (95% formamide, 10 mM EDTA, 0.025% xylene cyanol, 0.025% bromophenol blue) to stop the reaction. 6 µL of each mixture was loaded and separated on a 0.35-mm sick 20% Acrylamide, 7 M Urea 40 cm high sequencing gel. The gel was exposed for 24 h on a phosphor screen. The phosphor screen was scanned on a Typhoon™ FLA 9500 Biomolecular Imager.

1. The poly(ADP-ribosyl)ation reaction is performed in a siliconised 10-mL Sarstedt tubes that reduce unspecific binding of PAR to the plastic. For a 2-mL reaction add in the tube 1745 µL of water, 200 µL of 10 × PARP activity buffer, 5 µCi (1 µL) [^{32}P]-NAD$^+$ (800 Ci/mmol, 5 µCi/µL, Perkin Elmer), 10 µg PARP-1, gently vortex and incubate 1 h at 30 °C.

2. *DNase I digestion*: add to the reaction mix 4 µL of $CaCl_2$ 1 M and 4 µL of a 10 mg/mL solution of DNase I (Roche Diagnostics GmbH, Mannheim), mix and incubate 1 h at 37 °C.

3. *Proteinase K digestion* : add to the mix 935 µL of water, 15 µL of SDS 20% (0.1% final) and 50 µL of a 10 mg/mL solution of Proteinase K (Merck KGaA, Darmstadt, Germany). Mix and incubate 4 h or overnight at 37 °C.

4. Remove the amino acid residue covalently bound to the PAR by adding 2 mL of a 0.2 M NaOH and 40 mM EDTA pH 8.0 solution. Mix and incubate 1 h at 37 °C. Then, neutralise by adding 2 mL 0.2 M HCl.

5. *Phenol/$CHCl_3$ extraction*: the reaction mix is phenol/$CHCl_3$ extracted by adding 500 µL of Phenol/$CHCl_3$/isoamyl alcohol (25:24:1). Vortex and centrifuge at 3,000 × g. Carefully

transfer the upper phase to a new siliconised tube. Repeat the extraction until the organic/aqueous inter-phase is clean.

6. *PAR precipitation*: add to the aqueous phase 300 µL of 3 M potassium acetate pH 4.8 and 3.5 mL of isopropyl alcohol, mix and let the PAR precipitate 1 h at −20 °C. Centrifuge 30 min at 6,000 × g at 4 °C. The pellet is carefully washed twice with 3 mL of ice cold 80% ethanol. After centrifugation 30 min at 6,000 × g at 4 °C, air dry the pellet by leaving the tube open on the bench. The pellet is resuspended in TE buffer (≃ 20,000 dpm/µL).

3.8.2 PARG Activity in Solution

1. In a 1.5-mL Eppendorf, incubate the following reaction mixture at room temperature: 10 µL of 10× PARG activity buffer, 10 µL of [^{32}P]-labelled-PAR (≃ 200,000 dpm), an appropriate dilution of purified PARG (10 ng), water to 100 µL.

2. For a kinetic experiment, in a 1.5-mL tube prepare the reaction mixture but without PARG, then at various time-points (`T0, T10", T30", T1', T2', T4', T8', T16',` ...) after the addition of PARG, take off 10 µL of the mixture and stop the reaction in a new tube containing 10 µL of formamide Stop/Loading solution (see Note 7).

3.8.3 Electrophoresis on Sequencing Gel

Preparation of Glass Plates

1. Clean the glass plates thoroughly with a nonabrasive detergent and a plastic scouring pad. The cleaning solution should not leave a soap residue when rinsed thoroughly. Avoid scratching the surface of the glass plates.

2. Rinse the glass plates thoroughly with deionized water and wipe dry.

3. Treat the inside (acrylamide contact) surface of one or both glass plates (usually the short plate) with 2 mL of Sigmacote, wipe rapidly the entire surface with Kleenex tissue (see Note 8).

4. Before the assembly of plate, rinse the inside surfaces with ethanol and wipe them dry.

5. Assemble the glass plate the conventional manner : place the long glass plate inside-up on the bench, align the mylar side spacers at the sides such that you leave 1.5 to 2 cm free of spacer at the bottom of the plate (that will allow the insertion of the band of Whatman 3MM paper to seal the bottom of the plate assembly), and place the short glass plate inside-down on the side spacers. The spacers must be perfectly aligned with the glass plate edges.

6. Secure the assembly by clipping the plates with binder clips (5 or 6 on each sides).

7. Insert a band of Whatman 3MM filter paper at the bottom of the assembly, between the two plates. Make sure that the horizontal surface of the paper is perfectly in contact with the two side-spacers to avoid any leaks of acrylamide. Place binder clips at the bottom of the glass plate sandwich (see Note 9).

Pouring the Gel

1. Prepare 100 mL of 20% acrylamide-7 M Urea solution by mixing in a 250-mL beaker 42 g Urea, 10 mL TBE 10 × electrophoresis buffer and 50 mL acrylamide/bis-acrylamide 40% (38:2) stock solution (see Note 10).

2. Mix with a magnetic stirrer to complete dissolution, slightly heat the solution if necessary. Adjust the volume to 100 mL with water and vacuum filter using a 250-mL Millipore Stericup®. Keep the vacuum for a while to degas the solution as much as possible to reduce the possibility of bubbles formation during the polymerisation.

3. To pour the gel be ready with the following materials: a Pipetboy and a 35-mL or bigger disposable pipet, the ammonium persulfate 10% and TEMED solutions.

4. In the Stericup® add to the acrylamide solution, 600 µL ammonium persulfate 10% and 60 µL TEMED mix well by rotating the cup for a few seconds. Immediately, fill the pipet (using the Pipetboy) with the solution. Hold the assembled plate sandwich at a 45° angle on one bottom corner so that the gel solution flows evenly down along the lower side spacer. Maintain a constant, even flow to reduce the chance of forming bubbles in the solution.

5. As the gel sandwich fills, gradually lower the glass plates until they rest on the bottom edge, approximately at a 5° angle from the bench. The gel mold should be slightly overfilled to ensure complete polymerisation at the top (see Note 11).

6. Insert a well-forming comb into the top of the gel. Clip the top with Binder clips

7. Leave the glass plates in their near-horizontal position until the acrylamide has polymerised. The polymerisation should take a few minutes only.

8. The gel could be prepared the evening before the electrophoresis. If so, after polymerisation, pour some water on top of the comb to keep the gel wet, then cover the comb with Saran Wrap.

Pre-Electrophoresis

1. Remove the clips. Carefully slide the comb from between the plates.

2. Rinse the top of the gel with water to remove any un-polymerised acrylamide. Rinse the comb.

3. Place the gel sandwich in the sequencing apparatus with the short glass plate inward, so that the foam blocks on the side spacers form a seal with the gray silicone gasket. Rest the bottom edge of the sandwich on the ribbed gel support blocks in the lower buffer tray.

4. Secure the gel sandwich with the integral gel clamps along the sides of the sequencing apparatus.

5. Verify that the upper buffer chamber drain valve is closed, and fill the upper buffer chamber with approximately 450 mL of electrophoresis buffer (TBE 1 ×). Make sure no buffer is leaking from the upper buffer chamber. Fill the front chamber of the lower buffer tray with approximately 450 mL of electrophoresis buffer. The Whatman 3MM paper on the bottom of the gel will ensure good contact between the gel and the buffer and it should not be removed.

6. Close the upper and lower safety lids and connect the DC power cords to the sequencing apparatus and the DC power supply.

7. Before loading samples, pre-electrophorese the gel for 30 to 45 min. Set the output power to 80 W.

Electrophoresis

1. Prepare the samples in the formamide Stop/Loading solution by heating to a temperature of 90 °C to 100 °C for 3 to 5 min and then chilling on ice.

2. At the end of the pre-electrophoresis period, turn off the power supply and disconnect both DC power cords, first from the power supply and then from the sequencing apparatus, before opening the upper safety lid.

3. Immediately prior to loading the samples, rinse the wells of the gel with electrophoresis buffer. Use a syringe and a fine needle to wash away urea that has diffused into the wells.

4. Load samples (4 to 8 µL) onto the bottom of the wells with capillary comb.

5. After loading the samples, close the upper and lower safety lids and connect the DC power cords to the sequencing apparatus and the DC power supply. Set the output power to 70 W.

6. Monitor the progress of electrophoresis by following the migration of the bromophenol blue marker dye. Stop the electrophoresis when it reaches 1/3 from the bottom of the gel to ensure that no radioactive signal is lost.

7. Disassemble the gel sandwich by prying off the short (or siliconised) glass plate, working gently from a bottom corner with a thin spatula.

8. For autoradiography, transfer the gel to a solid backing, such as used film and cover it with Saran Wrap film. Because of the high acrylamide concentration (above 15%) the gel cannot be dried before exposure as it may crack during the procedure.

9. The gel may be exposed on a traditional [^{32}P]-type autoradiography film or on a Phosphor ScreenImage and revealed using a Typhoon™ FLA 9500 Biomolecular Imager (GE Healthcare). An example of such gel is shown Fig. 4.

3.8.4 PARG Activity Dot Blot and Immuno-Detection of PAR

1. In a 1.5-mL Eppendorf, incubate the following reaction mixture at room temperature: 5 µL of 10× PARG activity buffer, 400 ng of purified unlabelled-PAR, an appropriate dilution of purified PARG (24 ng), water to 50 µL.

2. For a kinetic experiment, in a 1.5-mL tube prepare the reaction mixture but without PARG, then at various time-points (`T0, T3', T6', T9', T12', T15', T18', T21',` ...) after the addition of PARG, take off 3 µL of the mixture and immediately deposit onto nitrocellulose to make regularly interspaced dots.

3. Dry the nitrocellulose, then crosslink 10 min under a 254 nm UV lamp at approximatively 100 millijoules/cm^2.

4. Incubate the membrane in 15 mL PBS-Tween buffer for 10 min at room temperature.

5. Incubate the membrane in 15 mL PBS-Tween buffer containing a 1:1,000 dilution of 10H monoclonal anti-PAR antibody for 60 min at room temperature.

6. Wash the membrane three times in 15 mL PBS-Tween buffer.

7. Incubate the membrane in 15 mL PBS-Tween buffer containing a 1:20,000 dilution of Alexa680-conjugated goat anti-mouse secondary antibody for 60 min at room temperature.

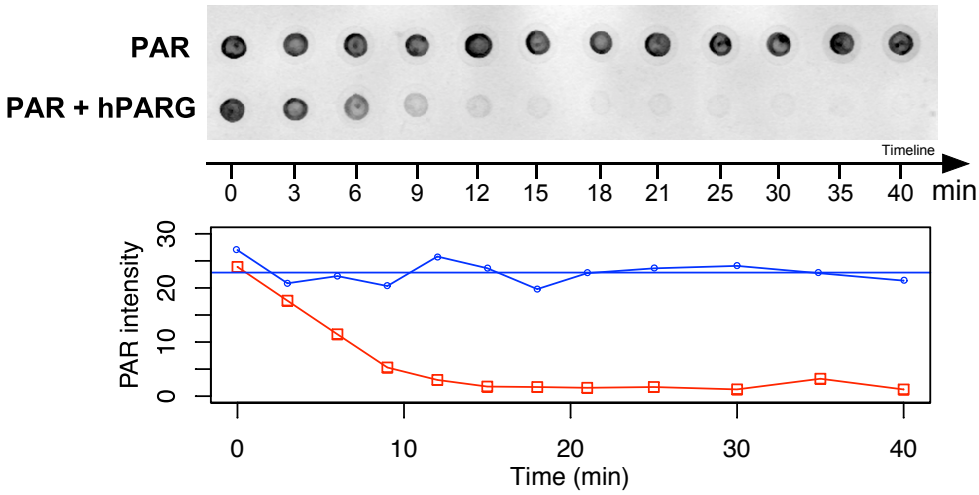

Fig. 5: **Time-course evaluation of PARG activity using Dot Blot and detection of PAR with an anti-PAR antibody (10H).** Kinetic of digestion of un-labelled poly(ADP-ribose) by PARG. After the indicated time, 3 µL of the reaction containing 8 ng/µL of purified PAR was spotted onto the nitrocellulose membrane. *Top row:* reaction without PARG, *Bottom row:* reaction containing 0.48 ng/µL of purified human PARG. PAR was detected by immuno-detection using the 10H anti-PAR monoclonal antibody as primary antibody (1:1,000) and the Alexa680-conjugated goat anti-mouse secondary antibody (1:20,000). The signal was reveal by scanning the membrane using the LI-COR Odyssey imaging system. Dots were quantified using NIH ImageJ software and values were plotted using R statistical package. *Blue curve:* Variation of PAR intensity from reaction without PARG. Straight line showing the mean of PAR untreated values. *Red curve:* Variation of PAR intensity from reaction incubated with PARG.

8. Wash the membrane three times in 15 mL PBS-Tween buffer.
9. Reveal the signal by scanning on a LI-COR Odyssey imaging system.
10. The signal can be quantified using the NIH ImageJ software.

4 Notes

1. Alternative culture media as 2 ×TY medium (16 g/L tryptone, 5 g/L Yeast Extract, 5 g/L NaCl) or Terrific Broth (11.8 g/L tryptone, 23.6 g/L Yeast Extract, 9.4 g/L K_2HPO_4, 2.2 g/L KH_2PO_4, 4 mL/L glycerol) could also be used instead of LB medium for higher cell density and higher protein expression. However it may result in protein of less solubility and less activity.
2. When available all the Sigma-Aldrich products provided in powder should be of the bioXtra quality. Lower quality grade (of TRIS and NaCl particularly) may interfere with protein stability and activity but also with the chromatographic results as the compound may absorb at 280 nm.
3. Sequence available upon request.
4. The volume of beads to take depends on the expression level of the protein. The indicated amount should be sufficient for most cases as the typical GST-protein binding capacity indicated by the manufacturer is up to 25 mg per mL of beads.
5. Radioactive materials must be handled with care for yourself and others. Only authorised persons should manipulate radioactivity accordingly to local laboratory regulations.
6. To avoid any protein degradation this protein solution should not be kept but should be promptly loaded onto the first chromatographic column to start the purification.
7. The tubes can be kept in the fridge for a few days if necessary.
8. This procedure must be done under a fume hood for protection against the highly volatile vapours.
9. This will help maintain uniform gel thickness while pouring the gel. It is important that the binder clips be placed over the side spacers only. Clamping unsupported glass will distort the thickness of the gel.
10. Acrylamide is a neurotoxic. It must be manipulated with care.
11. If a bubble forms while the gel is being poured, raise the glass plates into a vertical position, and either tip the gel solution away from the bubble or carefully tap the plate sandwich at the bubble to make it rise to the surface. Once all bubbles have been removed, return the glass plates to their previous position.

References

1. Kraus W. L (2015) PARPs and ADP-Ribosylation: 50 Years ... and Counting. Mol Cell 58:902–10.
2. Kraus W. L (2015) PARPs and ADP-Ribosylation Come Into Focus. Mol Cell 58:901.
3. Amé J.-C, Spenlehauer C, de Murcia G (2004) The PARP superfamily. Bioessays 26:882–893.
4. Schreiber V, Dantzer F, Ame J.-C, de Murcia G (2006) Poly(ADP-ribose): novel functions for an old molecule. Nat Rev Mol Cell Biol 7:517–528.
5. Gibson B. A, Kraus W. L (2012) New insights into the molecular and cellular functions of poly(ADP-ribose) and PARPs. Nat Rev Mol Cell Biol 13:411–24.
6. Gagné J.-P, Hendzel M. J, Droit A, Poirier G. G (2006) The expanding role of poly(ADP-ribose) metabolism: current challenges and new perspectives. Curr Opin Cell Biol 18:145–151.
7. Amé J. C, Jacobson E. L, Jacobson M. K (1999) Molecular heterogeneity and regulation of poly(ADP-ribose) glycohydrolase. Mol Cell Biochem 193:75–81.

8. Meyer-Ficca M. L, Meyer R. G, Coyle D. L, Jacobson E. L, Jacobson M. K (2004) Human poly(ADP-ribose) glycohydrolase is expressed in alternative splice variants yielding isoforms that localize to different cell compartments. Exp Cell Res 297:521–32.
9. Amé J.-C, Fouquerel E, Gauthier L. R, Biard D, Boussin F. D, Dantzer F, de Murcia G, Schreiber V (2009) Radiation-induced mitotic catastrophe in PARG-deficient cells. J Cell Sci 122:1990–2002.
10. Andrabi S. A, Kim N. S, Yu S.-W, Wang H, Koh D. W, Sasaki M, Klaus J. A, Otsuka T, Zhang Z, Koehler R. C, Hurn P. D, Poirier G. G, Dawson V. L, Dawson T. M (2006) Poly(ADP-ribose) (PAR) polymer is a death signal. Proc Natl Acad Sci U S A 103:18308–18313.
11. Feng X, Koh D. W (2013) Roles of poly(ADP-ribose) glycohydrolase in DNA damage and apoptosis.. International review of cell and molecular biology 304:227–281.
12. Stowell A, James D. I, Waddell I. D (2016) An HTS-compatible HTRF assay measuring the glycohydrolase activity of human PARG.. Analytical Biochemistry p. 10.1016/j.ab.2016.03.016.

Annex IV : French translation of selected sections

Objectifs de mon projet de recherche :

For the English version, see p.102.

Au fil des années, les nombreux rôles de la famille PARP (Poly (ADP-ribose) polymérase), et surtout des PARP ADN-dépendantes (PARP1, PARP2 et PARP3), ont été largement étudiés. Nous savons désormais que la PARylation joue un rôle important dans la réponse aux dommages de l'ADN, la réplication, la transcription, la biologie des télomères, le métabolisme de l'ARN, la régulation du cycle cellulaire, la différenciation et la mort cellulaire. Agissant comme un échafaudage moléculaire pour détecter, signaler et recruter des facteurs de réparation, le PAR est devenu une modification post-traductionnelle clé pour assurer le maintien de l'intégrité du génome. Mais, si la synthèse de polymère est effectivement un événement crucial pour la réparation des dommages à l'ADN et la survie cellulaire, sa dégradation est tout aussi importante. Les premières études concernant le rôle de PARG (Poly (ADP-ribose) glycohydrolase) dans la réparation de l'ADN proviennent de modèles animaux. PARG est codée par à un seul gène dans le génome humain, dont résultent cinq isoformes, de localisations subcellulaires différentes. De plus, la suppression simultanée de ces cinq isoformes est létale au stade embryonnaire chez la souris (Koh *et al.,* 2004). Pour ces deux raisons, il a été difficile d'évaluer avec précision la contribution de PARG dans la réparation de l'ADN. Depuis une dizaine d'années, les projets du laboratoire visent à élucider, au niveau moléculaire et cellulaire, le rôle et la régulation de PARG. Au cours de précédents travaux, le laboratoire a généré de nouveaux modèles de cellules HeLa déficientes en PARG, totalement viables, sur la base d'une stratégie d'inactivation par shRNA de toutes les isoformes. Ces lignées cellulaires présentaient une sensibilité accrue à l'irradiation, une réparation retardée des lésions simple et double brin de l'ADN et une augmentation de la mort cellulaire par catastrophe mitotique (Amé *et al.,* 2009). Le laboratoire a ensuite mis en évidence un lien fonctionnel entre PARG et le facteur de réparation /réplication PCNA, nécessaire pour la localisation efficace de l'isoforme PARG nucléaire (PARG^{111}) sur les sites endommagés par l'ADN et les foyers de réplication (Mortusewicz *et al.,* 2011). Cette étude a également montré que les deux isoformes cytoplasmiques de PARG (PARG102 et PARG99) pourraient être recrutés pour des dommages à l'ADN induits par micro-irradiation laser. L'identification d'une interaction entre PARG et PCNA a conduit à l'étude de la contribution de PARG dans le processus de réplication de l'ADN. Les résultats montrent que PARG est nécessaire pour assurer un contrôle étroit des niveaux de PAR produits lors d'un stress réplicatif prolongé, ce qui permet d'éviter un épuisement de la protéine RPA et l'accumulation de DSB (Illuzzi *et al.,* 2014).

Le but de mon projet était d'étudier le rôle, la régulation et le mécanisme d'action de la PARG humaine dans la réparation et la réplication de l'ADN, par la formation d'isoformes de localisations et de fonctions subcellulaires distinctes, ainsi que par des modifications post-traductionnelles.

Le premier objectif (**Objectif 1**) était de générer de nouveaux outils innovants permettant l'étude de la régulation PARG et la contribution précise de chaque isoforme à la réparation de l'ADN. J'ai généré une bibliothèque de lignées cellulaires stables U2OS, constitutivement invalidées pour toutes les isoformes de PARG endogènes et ré-exprimant une seule isoforme de PARG ou de l'une de ses versions mutées, de façon inductible. Quelques exemples d'applications possibles de ces constructions sont présentés.

Un autre objectif de mon projet (**Objectif 2**) était d'étudier si la PARG pouvait être régulée par des modifications post-traductionnelles. Ce projet a mené à la découverte d'un nouveau partenaire protéique, la protéine kinase DNA-PK, dépendante des dommages à l'ADN, capable de phosphoryler le PARG in vitro sur plusieurs sites, identifiés par spectrométrie de masse et par mutagenèse ciblée.

Dans la dernière partie de mon projet (**Objectif 3**), tirant parti de nos nouveaux modèles cellulaires et sachant que PARG et DNA-PK sont des partenaires protéiques, j'ai étudié le rôle de PARG dans la réponse cellulaire au stress réplicatif causé par un inhibiteur de la topoisomérase I, la camptothécine, qui est un médicament anticancéreux connu pour activer à la fois DNA-PK et la PARylation.

Les résultats obtenus pour chacun de ces objectifs sont présentés dans la section « Résultats » suivante.

Résultats

Objectif 1: Génération de nouveaux outils cellulaires pour l'étude de la contribution des isoformes de PARG dans la réparation de l'ADN

For the English version, see p.103.

Introduction

Afin de surmonter l'apparition de dommages de l'ADN, se produisant constamment dans le génome humain, les cellules doivent mobiliser des centaines de facteurs protéiques, en coordonnant étroitement leurs activités dans le temps et dans l'espace. La poly(ADP-ribosyl)ation, une modification post-traductionnelle catalysée principalement par la poly (ADP-ribose) polymérase 1 (PARP1), joue un rôle central dans la régulation de la réparation de l'ADN. Le catabolisme du PAR est principalement assuré par la poly (ADP-ribose) glycohydrolase (PARG), une protéine conservée chez les mammifères, les mouches, les vers et même les plantes (Amé *et al.,* 2000, Davidovic *et al.,* 2001). La protéine PARG est codée par un seul gène *parg*, qui fut cartographié très tôt sur le chromosome humain 10 (10q11.23, Amé *et al.,* 1999). Il partage un promoteur commun avec le gène *tim23* (Meyer *et al.,* 2003) et code cinq isoformes de tailles et de localisations subcellulaires différentes. Initialement, une longue isoforme nucléaire (110 kDa) et une courte isoforme cytoplasmique (65 kDa) ont été identifiées in vivo (Davidovic *et al.,* 2001). Il a ensuite été démontré qu'un épissage alternatif de l'ARNm du transcrit pouvait produire deux isoformes cytoplasmiques supplémentaires de 102 kDa (dépourvu d'exon 1) et de 99 kDa (dépourvu d'exon 1 et 2). Ces isoformes ont été décrites comme étant péri-nucléaires et présentes en grande quantité (Meyer-Ficca *et al.,* 2004). En fin de compte, deux formes mitochondriales (60 kDa et 55 kDa) ont été identifiées, qui pourraient également être produites par épissage

alternatif (Meyer *et al.,* 2007, Whatcott *et al.,* 2009). Ils ne présentent pas d'activité catalytique car l'ADP-ribosylhydrolase 3 (ARH3) a été décrite comme la principale enzyme dégradant le PAR dans la mitochondrie (Niere *et al.,* 2012). Les souris dont on a supprimé l'exon 4 du gène de PARG sont dépourvues de l'ensemble des isoformes, ce qui conduit à une mort précoce des embryons au jour 3,5 de leur développement. Les cellules souches trophoblastiques dérivées de ces embryons meurent par apoptose en raison d'une accumulation de PAR, et ne peuvent être maintenues en culture qu'après traitement avec un inhibiteur de PARP (Koh *et al.,* 2004). La déplétion des exons 2 et 3 du gène *parg* chez la souris conduit à des souris viables et fertiles, exprimant uniquement les isoformes courtes de PARG. Cependant, les cellules souches embryonnaires dérivées de ces souris sont plus sensibles à certains agents endommageant l'ADN et présentent des défauts de réparation de l'ADN (Cortes *et al.,* 2004, Gao *et al.,* 2007). La délétion de l'exon 1 du gène *parg* dans des cellules ES conduit à une sensibilité accrue aux agents endommageant l'ADN (Fujihara *et al.,* 2009). Les premiers modèles de cellules humaines disponibles utilisaient des stratégies de siRNA pour se débarrasser de toutes les isoformes de PARG et présentaient également une sensibilité accrue aux dommages à l'ADN (Blenn *et al.,* 2006, Fisher *et al.,* 2007). Notre laboratoire utilisait auparavant un modèle cellulaire HeLa, exprimant de manière stable un shRNA conduisant à une déplétion efficace de PARG (Amé *et al.,* 2009). Dans ces cellules, la surexpression des isoformes $PARG^{102}$ et $PARG^{99}$ marquées par la GFP a permis de démontrer qu'elles sont recrutées dans des foyers d'endommagement de l'ADN, induits par une micro-irradiation laser (Mortusewicz *et al.,* 2011). La capacité de translocation de ces isoformes cytoplasmiques vers le noyau a déjà été mentionnée dans une étude antérieure (Haince *et al.,* 2006). Malgré ces données, peu d'outils cellulaires pour déchiffrer la contribution précise de chaque isoforme à la réparation des dommages à l'ADN étaient disponibles. Dans l'article suivant, je propose de nouvelles lignées de cellules U2OS exprimant les ifosormes de PARG, ainsi que plusieurs exemples de leur utilisation dans le cadre de l'étude de la régulation des fonctions et de l'activité de PARG.

Discussion

For the English version, see p.128.

1. Choix de la lignée cellulaire

Notre laboratoire a précédemment décrit des lignées cellulaires HeLa déficientes en PARG, qui ont déjà été utilisées pour soulever plusieurs questions liées à la biologie de cette protéine (Amé *et al.,* 2009, Mortusewicz *et al.,* 2011, Illuzzi *et al.,* 2014). De plus, de nombreuses autres lignées cellulaires dépourvues de l'ensemble de isoformes de PARG, existent d'ores et déjà. Puisque nous voulions explorer le rôle des isoformes PARG dans la réparation de l'ADN, nous avons délibérément choisi de créer notre système d'induction stable dans la lignée U2OS (ATCC®HTB-96 ™). Les cellules U2OS (U-2 OS) sont des cellules adhérentes épithéliales humaines, dérivées de l' ostéosarcome d'une patiente caucasienne âgée de 15 ans. Elles sont facilement transfectables, largement utilisées pour des expériences de micro-irradiation laser et des études de réparation d'ADN en

général et semblent donc parfaitement correspondre à nos objectifs. Par ailleurs, nous avons constaté que, contrairement aux cellules U2OS, notre précédente lignée cellulaire HeLa dépourvue de PARG, présente une accumulation spontanée de γH2AX, même en l'absence de dommages. De plus, les cellules HeLa sont mutées pour p53, alors que les cellules U2OS sont p53 compétentes. Néanmoins, notre système à deux plasmides peut être utilisé de manière transitoire ou par le biais d'infections stables dans n'importe quelle lignée cellulaire. Dans l'étude, nous avons démontré que l'expression transitoire de nos plasmides dans les cellules Bosc ou les cellules Hela était suffisante pour induire l'expression de l'isoforme à la bonne taille et la localisation.

2. Efficacité de l'épuisement PARG

Dans notre nouveau modèle cellulaire, la déplétion de PARG avec le shRNA ciblant toutes les isoformes de PARG est non létale, et les cellules ne montrent aucune variation de croissance (données non présentées). Sur les transferts de Western, nous pouvons toujours voir que la déplétion PARG est efficace, soit après transfection transitoire ou après une infection stable avec le plasmide knockdown. Les cellules accumulent le PAR spontanément, et cette accumulation augmente après traitement au peroxide d'hydrogène (H202), induisant des dommages oxydatifs. Comme nous avons utilisé la même séquence de shRNA que dans les lignées cellulaires HeLa shPARG précédemment décrites dans Amé *et al.* 2009, nous pensons donc que l'épuisement PARG est efficace. Cependant, en examinant la cinétique d'accumulation de PAR après traitement au H202 et libération dans des lignées cellulaires flag-shPARG, soit par western blot, soit par immunofluorescence, nous avons observé que les niveaux de PAR diminuent avec le temps. Après 2h de recuperation après dommage, le polymère persiste, mais la quantité globale dans les cellules est réduite. Bien que d'autres enzymes dégradant le PAR puissent contribuer à la dégradation du PAR dans le noyau, comme ARH3 ou MacroD1 (Massimo *et al.,* 2013, Chen *et al.,* 2011; Fontana *et al.,* 2017), nous ne pouvons exclure une dépletion incomplète de la PARG dans notre modèle. Un moyen pratique d'éviter de telles questions aurait été de générer une lignée de cellules mutantes déficientes pour PARG avec le système CRISPR / Cas9. Au moment du démarrage du projet, CRISPR / Cas9 n'était pas encore totalement maîtrisé: la conception des ARN guides était compliquée par l'existence de pseudogènes de PARG dans le génome (JC-Amé, communication personnelle), beaucoup de d'arguments ont été reportés dans la littérature, et l'utilisation de mutants CRISPR impliquait la sélection d'une ou plusieurs populations clonales, situation que nous voulions éviter. Travailler avec une population cellulaire globale nous a semblé une meilleure solution, car il était alors possible de realiser des statistiques.

3. Niveaux d'expression des isoformes de PARG complétées

Nous devons signaler les difficultés majeures rencontrées lors de la génération de ces lignées cellulaires. Lors d'une transfection transitoire avec les vecteurs knockdown et de reconstitution, la transfection peut être hétérogène, et toutes les cellules n'expriment pas les isoformes aux mêmes niveaux, comme on le voit en immunofluorescence, ou par western blot. Le même problème se pose après une infection lentivirale, car nous

ne savons pas si les cellules ont intégré une ou plusieurs copies de chaque vecteur knockdown ou de reconstitution. Nous avons utilisé l'infection lentivirale plutôt que l'infection rétrovirale, car les lentivirus permettent l'infection simultanée des cellules en division et hors division, mais les deux systèmes permettent généralement l'intégration jusqu'à 10 sites dans le génome de l'hôte. De plus, nous ne maîtrisons pas les sites d'intégration de chaque construction, donc chaque cellule est susceptible d'afficher des niveaux d'expression très différents pour chaque vecteur intégré. Certaines cellules peuvent intégrer plusieurs copies du vecteur knockdown et quelques copies des vecteurs de reconstitution, générant une large gamme de motifs dans le profil d'expression. De plus, si les copies du vecteur de reconstitution sont intégrées dans des environnements de chromatine défavorables, avec une faible accessibilité pour la protéine rtTA lors de l'induction à la doxycycline, les cellules peuvent également présenter des niveaux d'expression hétérogènes. Pour surmonter ces problèmes, nous pourrions avoir des cellules rigoureusement sélectionnées pour un nombre de copies précis. Ceci pourrait impliquer la caractérisation des colonies cellulaires en effectuant des qPCR sur chaque population clonale (Charrier *et al.* 2010), mais ne nous informe pas plus sur le site d'intégration. De plus, travailler sur la population clonale est ce que nous voulions éviter. Alternativement, nous aurions pu concevoir nos vecteurs de clonage afin de sélectionner la population cellulaire pour ceux exprimant à la base la même quantité de protéine rtTA, et le même niveau de PARG reconstitué après induction à la doxycycline. A cette fin, nous aurions pu ajouter des marqueurs fluorescents aux isoformes rtTA et PARG, mais cela se fait toujours au détriment des canaux fluorescents disponibles pour les expériences. Néanmoins, bien que nos constructions fusionnées au tag flag ne soient pas prévues pour cet usage, des constructions PARG-GFP ont été générées afin d'étudier le motif d'interaction PIP2, et ont permis de trier les cellules pour former une population cellulaire plus homogène dans leur niveau de fluorescence. Pourtant, un autre problème subsistait concernant la maîtrise de l'induction à la doxycycline.

4. Fuite du système Tet

Notre stratégie de clonage dans le modèle cellulaire U2OS était basée sur l'expression sélective des isoformes de PARG lors de l'induction à la doxycycline. Cette stratégie est basée sur le système Tet-On classique, dérivé de la compréhension originale de l'opétron Tet bactérien sensible à la tétracycline, et est un outil largement utilisé en biologie, de la biologie moléculaire aux applications de thérapie génique (Das *et al.,* 2016). Le premier système Tet-On développé pour les cellules eucaryotes a été amélioré afin de réduire les niveaux de doxycycline nécessaires pour induire l'expression, et des promoteurs spéciaux appelés Tetracycline Responsive Elements (TRE) ont été conçus pour diminuer la liaison résiduelle de la protéine rtTA en absence de doxycycline (Gossen *et al.* 1995, Loew *et al.,* 2010). Bien que notre système vectoriel utilise l'un des promoteurs TRE de dernière génération, basé sur 7 répétitions de l'opérateur Tet, nos lignées cellulaires stables présentaient une fuite élevée, avec des isoformes s'exprimant même sans induction préalable par la doxycycline. Nous avons d'abord pensé que cela pouvait être dû à une contamination de notre milieu DMEM avec du sérum fœtal bovin contenant de la doxycycline résiduelle. Mais même en cultivant nos lignées cellulaires dans des milieux contenant du sérum sans doxycycline, cela n'a pas changé le schéma. Cette fuite observe en Western blot est probablement le résultat d'une sous-population de cellules dans laquelle le rapport entre la rtTA et le

promoteur TRE disponible est sous-optimal, pour les raisons discutées dans le paragraphe ci-dessus. Si tous les systèmes d'induction présentent des fuites basales, il est vrai que Tet-On a été décrit comme ayant les problèmes de fuite les plus élevés comparés aux modèles inductibles par les glucocorticoïdes ou inductibles par l'ecdysone (Meyer-Ficca *et al.,* 2004, b). Nous avons conservé le système Tet-On car nous voulions pouvoir moduler l'expression des gènes avec des concentrations croissantes de PARG dans nos expériences. De plus, les techniques quantitatives d'immunofluorescence que nous avons développé permettaient de considérer les cellules individuelles parmi la population globale, contournant ainsi les limites de notre modèle.

5. Niveaux de PARG endogènes VS PARG complémentés

Au départ, nous pensions que les niveaux de doxycycline permettraient un réglage très précis des niveaux d'isoformes de PARG dans nos modèles cellulaires. Encore une fois, nous avons été très déçus du comportement de nos lignées cellulaires, pour deux raisons : d'abord, parce que la fuite du système produisait déjà des taux de PARG reconstitués plus élevés que le niveau de PARG endogène dans certaines cellules ; puis parce que nous ne pouvions pas exprimer les isoformes à des niveaux similaires entre les lignées. Le protocole standard pour l'induction à la doxycycline est un traitement entre 24h-48h avec une concentration de 1µg/mL, produisant de très grandes quantités d'isoformes de PARG dans les cellules. Nous avons fait plusieurs tests afin d'ajuster la dose d'induction à la doxycycline, ainsi que le temps de traitement, pour réduire l'expression de PARG à un niveau proche des taux endogènes. Comme le montre la **figure 28**, il existe déjà une forte expression de $PARG^{102}$ et de $PARG^{99}$ même sans induction. $PARG^{111}$ et $PARG^{111cat}$ pourraient être induits à des niveaux raisonnables, après 4h d'induction à 1µg/mL ou après 16h d'induction à 1ng/mL.

Ceci est un problème, car le PARG a une activité très élevée, et même des quantités indétectables de la protéine endogène sont suffisantes pour dégrader efficacement le polymère dans les cellules. Dans notre test de dégradation PAR, nous avons obtenu des résultats similaires entre des cellules induites ou non induites (données non présentées). Afin de tenter de corréler les niveaux d'expression du marqueur flag et la dégradation PAR, l'analyse de cellules individuelles était probablement le seul moyen de réduire le biais intimement lié aux défauts du système. Cependant, lorsque nous avons essayé, nous n'avons pas pu observer de corrélation. Ceci suggère en effet que la dégradation PAR peut se produire, même en l'absence de signal flag détectable.

Toutefois, l'expression des versions non marquées des isoformes de PARG, indépendamment de leurs niveaux d'expression, nous a permis de confirmer que $PARG^{102}$ était l'isoforme la plus abondante dans les cellules U2OS. C'est également le cas des cellules Hela, des cellules HEK293T, des cellules BOSC et des cellules HCT116. Étant donné que $PARG^{102}$ peut contribuer à la dégradation nucléaire du PAR après les dommages, et qu'il se déplace vers le noyau (Mortusewicz *et al.,* 2011; Haince *et al.,* 2006), la production et la stabilisation du $PARG^{102}$ et la régulation de sa translocation nucléo-cytoplasmique pourraient être un moyen pour les cellules de réguler le niveau basique des dommages, tandis que la production de $PARG^{111}$ en très faibles quantités pourrait être utilisée pour traiter des dommages plus graves produisant des niveaux plus élevés de PAR. Alternativement, puisque $PARG^{111}$ est associé aux foyers de réplication, il pourrait avoir une fonction spécifique pendant la

réplication, en réponse au stress réplicatif. Parce que le PARG est une protéine de très faible abondance dans les cellules, l'étude de ces questions nécessiterait d'autres méthodes et stratégies et pourrait faire l'objet d'un autre projet de recherche en soi. Une stratégie de knock-in via CRIPSR-Cas9 serait probablement la méthode la plus intéressante pour introduire des rapporteurs fusionnés à la PARG humaine, afin d'affiner notre compréhension de la situation endogène.

6. PCNA contient-elle un PIP-degron?

Pour le projet PCNA (développé par G. Illuzzi), nous avons essayé de nous débarrasser des cellules «leaky» en sélectionnant une population GFP-négative par FACS avant l'induction à la doxycycline. Après 24 h d'induction avec 1 µg/mL de doxycycline, deux populations de «GFP élevée» et de «GFP faible» ont été sélectionnées pour leur capacité d'induction appropriée. A partir de ces cellules induites, il a fallu 72 heures pour que les niveaux de GFP diminuent après l'élimination de la doxycycline, suggérant que la protéine PARG[111] est hautement stable. Une telle stabilité complique l'étude fonctionnelle du motif PIP2. Nous avons supposé que le motif PIP2 pourrait agir comme un PIP-degron, un motif peptidique permettant l'interaction entre PCNA et l'adressage efficace des protéines interagissant avec le PCNA vers le protéasome pour médier leur dégradation, par le recrutement de l'U3 Ubiquitine Ligase CRL4 (Havens et Walter, 2009; Tsanov *et al.,* 2014). En effet, le motif PIP a montré une similitude avec d'autres PIP-degrons (p21, p12, hSet8 ...) sauf qu'il ne présente pas l'arginine basique ou le résidu lysine dans sa position +4. De plus, nous avons découvert une interaction entre PARG et les sous-unités Cullin4A et Cullin4B de l'enzyme CRL4 (données non présentées). Cependant, malgré de nombreux efforts, nous n'avons observé aucune dégradation significative, ni au cours de la progression en phase S, ni après traitement avec divers agents endommageant l'ADN (H202, MNNG, CPT), contrairement à la protéine p21-PIP-degron utilisée comme un contrôle (données non présentées). Seulement après un long traitement au HU, les niveaux de PARG semblaient diminuer, mais ceci était indépendant du motif PIP-degron, puisque sa mutation ne supprimait pas cette diminution. En ce qui concerne la difficulté d'établir une procédure expérimentale efficace pour étudier la dégradation de PARG en interaction avec PCNA, cette problématique reste ouverte.

Conclusion

Malgré toutes les limitations décrites ci-dessus, notre système de clonage et la bibliothèque de vecteurs et de lignées cellulaires générés ont permis de faire la lumière sur plusieurs aspects de la biologie de PARG. Aucun modèle n'est parfait, et nous devrions toujours garder à l'esprit les limites de chaque méthode utilisée dans la recherche. Cependant, nous avons réussi à générer une nouvelle boîte à outils moléculaire pour étudier de manière sélective la contribution des isoformes PARG dans la réparation de l'ADN. Bien que nous nous soyons limités au suivi de la dégradation PAR après les dommages oxydatifs, nous avons également pu quantifier les marqueurs de dommages à l'ADN comparativement, dans chaque lignée cellulaire et en réponse à d'autres types de dommages. Beaucoup d'autres applications restent possibles, et il sera souhaitable de les mener à

bien, car nous manquons encore de nombreux éléments pour comprendre pleinement les rôles de la protéine PARG dans les cellules humaines.

Objectif deux: Etude de la régulation du PARG par des modifications post-traductionnelles.

For the English version, see p. 135

Introduction

PARP1 et PARG sont deux enzymes portant des activités catalytiques opposées, effectuant respectivement la catalyse et de la dégradation du Poly (ADP-ribose), une modification post-traductionnelle (PTM) versatile, conservée à travers les organismes eucaryotes. Le Poly (ADP-ribose), en tant que molécule ayant des propriétés similaires aux acides nucléiques, agit comme un modulateur de l'activité des protéines et comme un échafaudage pour le recrutement de nombreux facteurs protéiques. Son rôle important dans la réparation, la transcription, la réplication, la mort cellulaire et le maintien de l'intégrité du génome doit être finement régulé dans le temps et l'espace (pour une revue, voir Martin-Hernandez *et al.,* 2016 ; Chaudhuri et Nussenzweig , 2017). Plus important encore, cette modification doit être dynamiquement induite ou supprimée, en réponse à toute forme de stress cellulaire. Il a été démontré que la cinétique de PARylation était cruciale pour déterminer le devenir des cellules après une lésion sur l'ADN, et que si de petites quantités transitoires de PAR sont bénéfiques, car elles activent la réparation de l'ADN, une accumulation prolongée de PAR est au contraire préjudiciable (Schuhwerk *et al.* 2017, Amé *et al.,* 2009, Illuzzi *et al.,* 2014). Cette régulation stricte de l'homéostasie du PAR est principalement réalisée par la régulation directe et dynamique des activités catalytiques de ses catalyseurs et dégradeurs, principalement PARP1 et PARG.

PARP1 a une structure modulaire, dont la modification par modification post-traductionnelle permet un réarrangement dynamique de ses différents domaines d'acides aminés (Gibson et Kraus, 2012). Parmi toutes les PTM, la phosphorylation est l'exemple le mieux décrit pour réguler PARP1. Par exemple, le ciblage de la sérine 372 et de la thréonine 373 par la kinase ERK1 / 2 réduit l'activité de PARP1 (Kauppinen *et al.,* 2006, Cohen-Armon *et al.,* 2007), tandis que la phosphorylation de la sérine 785 et de la sérine 786 par CDK2 est essentielle pour améliorer l'activité de PARP1 (Wright *et al.,* 2012). Plusieurs autres exemples ont été rapportés, de modifications permettant une régulation dynamique de PARP1 (revue dans Piao *et al.,* 2017). De nombreux autres sites ont été identifiés dans une analyse protéomique des sites de phosphorylation de PARP1, mais les rôles pour chacun d'entre eux ne sont pas encore caractérisés (Gagné *et al.,* 2008). Les preuves de la phosphorylation du PARG ont rarement été recueillies à partir de plusieurs expériences protéomiques générales (Beausoleil *et al.,* 2006, Villén *et al.,* 2007, Imami *et al.,* 2008), mais à ce jour, une seule étude portait sur la phosphorylation de PARG en elle même (Gagné *et al.,* 2008). Cette étude a montré que la phosphorylation de PARG était prédite principalement dans le domaine de régulation N-terminal présentant une structure dépliée (prédites en tant que NORS, un type de structure secondaire irrégulière, Liu et Rost, 2003) et révélait plusieurs sites de phosphorylation ciblés par la kinase CDKII. Dans ce projet, mon objectif était de trouver de nouvelles kinases capables de phosphoryler PARG, d'identifier des résidus phosphorylés et

d'étudier le rôle fonctionnel de la phosphorylation de PARG. Les résultats que j'ai obtenus sont affichés dans le brouillon de l'article de recherche suivant.

Discussion

For the English version, see p.157

1. Nouveaux partenaires protéiques pour PARG

Une première analyse de piégeage-GFP et de spectrométrie de masse dans des cellules HEK293T réalisées en laboratoire a permis de trouver des centaines de partenaires protéiques potentiels, parmi lesquels nous avons pu trouver des douzaines de kinases (J-C. Amé, communication personnelle). Parmi ceux-ci, nous avons retenu la protéine DNA-PK, parce que nous l'avons retrouvée de façon reproductible dans plusieurs expériences de spectrométrie de masse indépendantes. De plus, nous l'avons également identifié comme interagissant avec le fragment 1-87-GFP PARG, et DNA-PK avait déjà été signalée comme une protéine partenaire de PARP1. En effet, PARP1 se trouve dans un complexe DNA-PK et Ku (Spagnolo *et al.,* 2012), la phosphorylation de la DNA-PK peut réguler l'activité de PARP1 et inversement, la PARylation de DNA-PK par PARP1 peut réguler son activité (Ruscetti *et al.,* 1999). Nous avons remarqué que lorsque la DNA-PK était récupérée dans nos ensembles de données, les peptides Ku80 étaient moins abondants, et inversement (données non présentées). Cela pourrait suggérer que la PARG et la DNA-PK entrent en compétition pour la liaison de Ku80, de la même manière que le fait PARP1. Bien que notre étude se soit concentrée sur la DNA-PK, d'autres partenaires intéressants ont été identifiés dans nos ensembles de données.

Par exemple, PARG-GFP était associé à FAK1 (Focal adhesion kinase 1), une kinase qui active plusieurs voies de signalisation importantes comme la voie PI3K-AKT-mTOR dans laquelle la PARylation a un rôle à jouer (Philip *et al.,* 2017). Plk4 et Cdk1 ont également été récupérés, mais nous n'avons jamais détecté ces kinases par western blot après piégeage GFP de la construction 1-87-PARG marquée à la GFP. Un autre exemple intéressant est WSTF (BAZ1B), une protéine tyrosine kinase qui s'associe à PCNA (Poot *et al.,* 2004), et qui adresse le complexe de remodelage ISWI aux foyers de réplication, régulant le recrutement de la topoisomérase I (TOP1) aux fourches de réplication (Ribeyre *et al.,* 2016). Dans la littérature, on retrouve que la PARylation serait capable de réguler le complexe de remodelage nucléosomique ISWI, et on sait que PARP1 contribue fortement au remodelage de la chromatine (Sala *et al.,* 2008, Hinz et Czaja, 2015, Posavec Marjanovic *et al.,* 2017). De cette façon, PARG pourrait également être un acteur important dans ces processus.

Nous avons également co-purifié la protéine RUVBL1, une ATPase du complexe de remodelage INO80 qui a diverses fonctions dans le maintien de l'intégrité du génome (Poli *et al.,* 2017). RUVBL1 et RUVBL2 sont des régulateurs des PIKK kinases (parmi lesquels on trouve ATM, ATR et DNA-PK), et nos données préliminaires montrent que PARG et RUVBL1 co-immunoprécipitent, l'interaction augmentant après le traitement par H2O2 (voir **Figure 29**). Le signal RUVBL1 est détecté après co-purification avec la construction 1-87-GFP dans la lignée cellulaire HCT1116.

Collectivement, nos données confirment que PARG a de nombreux autres rôles et partenaires protéiques, mais peu de ces interactions sont caractérisées. L'analyse des ontologies géniques et les études antérieures lient la PARG avec des processus comme la biologie et le métabolisme de l'ARN, fonctions que nous avons également retrouvées dans nos ensembles de données (Gagné *et al.,* 2005, Gagné *et al.,* 2010).

2. Mesure d'interactions labiles et transitoires

Avec la DNA-PK comme nouveau partenaire putatif, nous avions l'intention de réaliser de nombreuses expériences de co-purification, en l'absence ou en présence de dommages à l'ADN. Lors de la purification de la DNA-PK endogène, nous n'avons jamais réussi à voir une co-précipitation de PARG endogène dans nos conditions. La PARG étant une protéine de très faible abondance, on peut imaginer que l'interaction putative reste inférieure au signal détectable en Western blot. Cependant, lors de la purification de PARG, il était possible de piéger DNA-PK. Cependant, les résultats étaient difficilement reproductibles, car il semble que DNA-PK soit une énorme protéine (469 kDa, Brewerton *et al.,* 2004). Des protéines énormes peuvent être déstabilisées à partir de complexes pendant l'IP, et transférer plus lentement pendant les opérations de transfert de Western. De plus, l'interaction des kinases avec leur substrat est très transitoire, ce qui complique encore la visualisation de l'interaction. Nous avons décidé de tirer parti de nos lignées de cellules PARG exprimant le marqueur (shPARG-flag et shPARG-111-flag, décrites dans l'Objectif 1), afin d'affiner notre compréhension de l'interaction entre PARG et DNA-PK directement dans les cellules, en utilisant la technique de « Proximity Ligation Assay » (PLA). Bien que cette méthode nécessite un certain calibrage avant de trouver le couple d'anticorps primaires le plus efficace à utiliser pour servir notre objectif, il s'agissait de la meilleure méthode pour observer et quantifier précisément l'interaction entre PARG et DNA-PK. Alternativement, nous aurions pu utiliser le BiFC, le FRET ou d'autres tests dépendant de la proximité des protéines entre elles (Lönn et Landergren, 2017). Pour avoir une compréhension complète de l'environnement protéique de PARG, nous aurions pu dériver notre modèle de cellule double plasmide afin de générer une fusion de PARG avec l'enzyme BirA, permettant le marquage biotine de toutes les protéines environnantes in vivo, pour les analyser par spectrométrie de masse. Cette méthode s'appelle BioID et a été fortement envisagée au cours de ce projet comme alternative au PLA (Varnaité et MacNeill, 2016). Dans les perspectives futures de ce projet, il sera primordial d'évaluer les variations de l'interaction entre PARG et DNA-PK en réponse à plusieurs types de stress cellulaires.

3. Identification des sites de phosphorylation: toujours un défi

Si l'identification et la validation des kinases partenaires était déjà une tâche difficile, l'identification des résidus subissant la phosphorylation était encore plus délicate. Dans cette étude, nous nous sommes concentrés sur les sites de phosphorylation de DNA-PK et dans le but d'identifier les résidus cibles, nous avons utilisé trois approches différentes. Le premier consiste à prédire tous les sites de phosphorylation sur PARG. Sur Phosphosite.org (voir **figure 30**), nous pouvons en effet voir que les événements de phosphorylation rapportés dans PARG sont concentrés dans la partie N-terminale, qui est une région acide (point isoélectrique,

pI = 6,0). La région entre les résidus 250 et 350 est encore plus acide, avec un pI de 3,94, alors que le domaine C-terminal catalytique est plus basique (pi = 8,63). Nos tests in vitro confirment que DNA-PK phosphoryle exclusivement la partie N-terminale de PARG.

Ces résultats sont confirmés par l'équipe de Gagné (Gagné *et al.,* 2008), dans un article dans lequel des prédictions similaires ont été trouvées avec d'autres algorithmes. Les phosphorylations trouvées dans cette étude sont résumées dans la figure ci-dessous (**Figure 31**).

Il est à noter que, parmi les kinases identifiées dans cet article et dans la littérature, un seul site est prédit comme étant une cible de DNA-PK avec l'algorithme de prédiction Phoscan kinase. Le même site peut évidemment être prédit comme une cible de la protéine kinase C (PKC) ou de la kinase CamK-II. Lorsque nous avons utilisé l'algorithme NetPhosK 1.0, nous n'avons pas obtenu les mêmes sites de phosphorylation. Des prédictions peuvent être faites sur la base de séquences peptidiques qui ont été identifiées dans des ensembles de données de spectrométrie de masse. La comparaison de telles séquences donne une idée de la similarité entre les sites cibles, et aide à générer ce qu'on appelle des «logos de séquence». Pour la DNA-PK, le logo de la séquence est montré ci-dessus (**figure 32**), et montre que la DNA-PK cible presque exclusivement les résidus sérine ou thréonine qui sont suivis par un résidu glutamine (Bennetzen *et al.,* 2010).

Trois de nos sérines correspondait à un contexte similaire à ce logo de séquence (S130, T143 et S335) mais nous ne pouvions pas exclure les autres, car nous connaissions plusieurs exemples de phosphorylation de DNA-PK survenant dans d'autres contextes de séquences, comme SL au lieu de SQ. Nous pouvons mentionner plusieurs exemples, notamment que DNA-PK phosphoryle la protéine Artemis in vitro, sur le résidu S503, dans un contexte ESLE (Soodarzi *et al.,* 2006). DNA-PK cible également la protéine SAF-A / hnRNP U sur le résidu S59 en réponse à une lésion de l'ADN dans un contexte GSLD, reliant ainsi la terminaison non homologue et le métabolisme de l'ARN (Britton *et al.,* 2009). Dans Ku80, le résidu S580 qui se place également dans un contexte SSLA est une cible pour la DNA-PK in vitro (Chan *et al.,* 1999), et la sérine S260 dans XRCC4, en contexte SSLD est également ciblée in vitro (Yu *et al.* 2003). Par conséquent, le choix des sites de phosphorylation ne doit pas reposer uniquement sur des prédictions, mais aussi sur des preuves directes en spectrométrie de masse. Les résidus S90, S95 ou S393 dans PARG n'étaient pas dans un contexte de séquence optimale mais ont néanmoins été identifiés dans nos expériences. Dans notre approche parallèle, consistant à disséquer la séquence N-terminale de la PARG en 7 fragments plus petits, nous avons détecté des signaux de phosphorylation faibles dans le Peptide 1, le Peptide 4 et le Peptide 5, où aucun site DNA-PK n'a été prédit, ni identifié en spectrométrie de masse. Nous n'avons pas pu détecter de signaux de phosphorylation forts dans le peptide 7, bien que la S392 ait été prédite. Dans le Peptide 2, nous n'avons pas pu déterminer si les sites S90 et S95 étaient de vrais sites de phosphorylation, car nous ne pouvions pas le tester in vitro après mutation, le peptide 2 étant très instable, pour des raisons inconnues, lorsque nous essayions de le purifier dans des bactéries.

Pour toutes ces raisons, le choix des mutations S130, S142 / T143 et S335 en résidus alanine était étayé pour des raisons théoriques et techniques, mais il s'agit tout de même d'un choix arbitraire. Ensuite, je dois mentionner que même si nous avons confirmé que les mutations simples S130A ou T143A diminuaient les niveaux de phosphorylation sur le peptide 3, la mutation simultanée de S130, S142 et T143 n'a pas diminué

davantage le signal en autoradiographie. Ceci suggère l'existence d'autres sites de phosphorylation de DNA-PK sur le peptide 3. En conséquence, si la mutation S335A diminue la phosphorylation du Peptide 6 in vitro, la mutation S333,334,335A n'a pas un impact plus fort. D'autres sites sont donc susceptibles d'exister, qui restent à identifier. Un alignement de séquence phylogénétique de la séquence PARG pourrait également nous aider à identifier des résidus conservés de sérine ou de thréonine qui pourraient correspondre à la spécificité de DNA-PK. La mutation de ces résidus dans la protéine tronquée N-ter et dans la PARG pleine longueur aiderait à confirmer les sites cibles de DNA-PK dans un contexte de séquence peptidique plus longue.

4. Impact fonctionnel de la phosphorylation de DNA-PK sur PARG

Bien que nous n'ayons pas identifié et confirmé tous les sites cibles de DNA-PK possibles in vitro, nous pouvons faire plusieurs hypothèses sur la façon dont ces modifications pourraient influencer l'activité de PARG. S130, qui a été prédit et confirmé dans notre test in vitro, mais n'a pas été retrouvé dans nos expériences de protéomiques, est localisé dans une séquence potentielle d'export nucléaire (NES) de PARG. Nous pourrions imaginer que la phosphorylation de ce cette séquence d'export pourrait réguler la localisation de PARG dans la cellule. En effet, notre laboratoire et d'autres avons montré que $PARG^{102}$ et $PARG^{99}$ étaient des isoformes cytoplasmiques, capables de se déplacer au noyau afin de dégrader le polymère nucléaire (Haince *et al.,* 2006, Mortusewicz *et al.,* 2011, Objectif 1). Alors que nous n'avons détecté aucun impact sur la localisation subcellulaire de $PARG^{111}$ lors de l'inhibition de DNA-PK (données non présentées), il serait intéressant d'étudier la localisation de $PARG^{102}$ et de $PARG^{99}$ dans les mêmes conditions.

Le site S335 que nous avons identifié se situe entre la S316 ciblée par CK-II dans les sites de clivage de la caspase3 de PARG (Gagné *et al.,* 2008) et un second NLS bipartite présumé, conservé dans plusieurs organismes (421-441, Amé *et al.,* 1999). Potentiellement, ceci pourrait également avoir un impact biologique.

Alternativement, la phosphorylation pourrait réguler l'activité de PARG ou la stabilité de la protéine. Bien que notre méthode de dot-blot ne nous ait pas permis de conclure (pour des raisons discutées dans l'article), nous pourrions comparer in vitro les activités de dégradation du PAR par des versions de PARG purifiée, ou même évaluer l'impact de la reconstitution de phosphomutant ou des versions phosphomimétiques de constructions PARG-flag ou PARG-GFP, en complétant nos lignées cellulaires U2OS déficientes en PARG, générées dans l'objectif 1. Étant donné que des modifications post-traductionnelles dans des domaines clés de PARG (ex: motif PIP) peuvent influencer son interaction avec d'autres partenaires protéiques tels que PCNA (Kaufmann *et al.,* 2017), il serait intéressant de surveiller des modifications dans l'interactome de ces mutants.

5. PARG et interaction fonctionnelle avec DNA-PK

Nos résultats montrent que dans des conditions basales, l'inhibition ou la déplétion de DNA-PK par siRNA dans des cellules déficientes en PARG n'affecte pas significativement la viabilité cellulaire dans un test de viabilité cellulaire par clonogénicité. La viabilité à court terme, après transfection avec un siDNA-PK, cependant, diminue légèrement par rapport à une transfection shCTRL. Les résultats préliminaires de la viabilité à court

terme et des essais clonogéniques effectués sur des cellules déficientes en DNA-PK M059J-Fus9, comparativement aux cellules Fus1, qui sont complémentées par une portion du chromosome 8 portant le gène DNA-PK (Hoppe *et al.,* 2000) suggèrent également que l'absence de DNA-PK sensibilise les cellules à la déplétion de siRNA de PARG (données non présentées). Dans nos mains cependant, le taux de croissance des cellules Fus9 était beaucoup plus faible que celui des cellules Fus1, compliquant le travail et nous empêchant d'avoir des résultats clairs et présentables. Puisque les protéines PARG et DNA-PK sont deux enzymes liées à la réparation de l'ADN, l'importance de cette interaction serait probablement mieux mise en évidence dans un contexte de dommages, comme le suggère l'augmentation des foyers d'interactions PLA après traitement à la néocarcinostatine (NCZ). D'autres données intéressantes disponibles en laboratoire suggèrent que le recrutement de PARG aux foyers de micro-irradiation laser induites est plus lent dans les cellules de souris 3T3 déficientes en DNA-PK, et que PARG reste plus longtemps aux les foyers de réparation. Bien que ces expériences doivent être confirmées, l'hypothèse selon laquelle la phosphorylation de la DNA-PK peut affecter la mobilité du PARG pourrait être une piste très intéressante pour de futures recherches.

6. DNA-PK et PARylation

Au fil des années, des preuves de plus en plus nombreuses montrent que PARP1 et DNA-PK sont fonctionnellement liées, même au-delà de leur interaction physique (Spagnolo *et al.,* 2012) et de leur capacité à catalyser mutuellement des modifications post-traductionnelles l'une sur l'autre (Ruscetti *et al.,* 1999). La DNA-PK est en effet un composant clé de la voie du NHEJ, en interaction avec les protéines KU70 / KU80. PARP1 a été identifiée dans un complexe avec KU ainsi qu'avec DNA-PK (Li *et al.,* 2004), et PARP régule la voie du NHEJ par une compétition avec KU au niveau des cassures double brin (Wang *et al.,* 2006). Dans le modèle décrit, la présence de Ku80 à des cassures double brin favorise le NHEJ classique, tandis que PARP1 favorise la voie NHEJ alternative (Audebert *et al.,* 2004, Hochegger *et al.,* 2006, Mansour *et al.*, 2013). Les liens étroits entre les composants des voies de la PARylation et du NHEJ ont même été décrits comme une voie alternative pour la médiation de la létalité synthétique de l'inhibiteur PARP dans les cellules déficientes pour la recombinaison homologue (Patel *et al.,* 2011) et inversement, la déficience en NHEJ dans les cellules cancéreuses de l'ovaire provoque leur résistance aux inhibiteurs de PARP (McCormick et *al.,* 2017). Il est à noter que l'utilisation combinée d'inhibiteurs de PARP et de DNA-PK sensibilise les cellules aux rayonnements ionisants et inhibe la réparation de l'ADN, émergeant ainsi comme une stratégie puissante pour cibler les tumeurs dans le contexte des radiothérapies (Veuger *et al., 2003,* Miura *et al.,* 2012, Arad *et al.,* 2014).
Par conséquent, un effet potentiel de la déplétion de PARG sur DNA-PK pourrait être médié par un effet indirect sur KU, ce qui est une hypothèse que nous n'avons pas exploré.

Conclusions

Dans cet article, nous avons fourni des preuves que les 87 premiers acides aminés du domaine N-terminal de PARG étaient suffisants pour interagir avec des kinases qui co-purifient, et notamment DNA-PK, qui est un

nouveau partenaire protéique pour PARG. Nous avons identifié trois résidus (S130, S142 / T143 et S335) qui sont ciblés par DNA-PK in-vitro. Bien que nous n'ayons pas élucidé l'impact fonctionnel de ces sites de phosphorylation, la modification de PARG sur ces positions pourrait s'avérer être un levier efficace pour la modulation rapide et réversible de sa localisation, de sa stabilité ou de l'activité catalytique de ses isoformes. Bien que PARP1 ait déjà été démontré comme un partenaire protéique de DNA-PK (*Spagnolo et al., 2012*), ce projet a démontré que PARG et DNA-PK interagissent également, et suggère que l'interaction augmente dans les conditions de dommages à l'ADN. Nous savons maintenant que DNA-PK est étroitement liée à la réparation des cassures double brin et au stress réplicatif (Ashley *et al.,* 2014, Ying *et al.*, 2016). Les anomalies du complexe DNA-PK déclenchent le syndrome SCID (Severe Combined Immunity Deficiency), car il est impliqué dans la recombinaison V (D) J. La protéine a des fonctions dans l'apparition du cancer, car elle protège les cellules de l'instabilité génomique (Grundy *et al.,* 2014, Goodwin et Knudsen, 2014). Puisqu'il s'agit maintenant d'une cible potentielle pour traiter les cancers, il est maintenant essentiel de comprendre ses interactions avec les voies de PARylation (Harnor *et al.,* 2017). Dans le chapitre suivant, nous étudions le lien entre la déficience en PARG et l'ADN-PK dans la réponse cellulaire à la camptothécine anticancéreuse (**Aim3**).

Objectif trois: Impact de la déficience en PARG sur la réponse cellulaire au DSB induit par la camptothécine

Introduction

For the English version, see p. 164

Dans la première partie de ce projet de thèse, j'ai généré de nouveaux outils pour l'étude de PARG (voir **objectif 1**). Parmi ces outils, des modèles cellulaires U2OS ont été établis, exprimant de manière stable un shRNA dirigé contre le domaine C-terminal de PARG, partagé par toutes ses isoformes. Ce shRNA avait déjà été utilisé avec succès pour générer une lignée de cellules HeLa dérives PARG (Amé *et al.* 2009). Notre modèle de cellules U2OS shPARG peut être complémenté par des versions d'isoformes de PARG fusionnées à la GFP ou marquée avec un tag flag. Ces modèles cellulaires nous ont permis d'étudier de nombreuses questions liées à la biologie PARG. En particulier, nous avons confirmé que DNA-PK était un nouveau partenaire protéique de PARG in vivo (voir **Aim2**). DNA-PK est une sérine / thréonine kinase de la famille PI3-K, qui joue un rôle central dans la réparation des cassures double brin (DSB), en coordination avec ATR et ATM, dans le maintien de l'intégrité génomique (pour une revue, voir Blackford et Jackson , 2017). Nous nous sommes intéressés à cette interaction, car plusieurs rapports indiquent que DNA-PK interagit avec PARP1 et que la PARylation pourrait stimuler son activité (Spagnolo *et al.,* 2012, Ruscetti *et al.*, 1998). Bien que l'activité kinase de DNA-PK soit principalement impliquée dans la voie non homologue, elle peut également réguler la recombinaison homologue et de nombreuses autres voies, du métabolisme à l'immunité, en passant par la recombinaison V (D) J (Kong *et al.* 2011). Les inhibiteurs de DNA-PK sont à présent des candidats sérieux pour le développement

de nouvelles thérapies contre le cancer (pour une revue, voir Harnor *et al.,* 2017). Fait important, DNA-PK est capable de cibler la sous-unité 32kDa du complexe RPA, RPA2, et de réaliser son hyperphosphorylation. La phosphorylation de la position S4/S8 est une étape importante dans la recombinaison homologue, et elle est également déclenchée par le stress réplicatif causé par le traitement au HU ou la CPT, ce qui conduit à la génération de DSB (Liaw *et al.* 2011, Ashley *et al.,* 2014). Notre laboratoire a déjà montré que le déficit en PARG entraîne une forte réduction de la phosphorylation de RPA2-S4S8 lors d'un traitement prolongé à l'HU, ce qui était attribuable à des niveaux élevés de PAR empêchant le chargement de RPA2 sur l'ADNsb au niveau de la chromatine (Illuzzi *et al.,* 2014). Pour toutes ces raisons, et tirant profit de notre nouveau modèle U2OS shPARG, nous avons décidé d'étudier le rôle de PARG dans la réponse cellulaire à l'agent anticancéreux qu'est la camptothécine (CPT). La CPT déclenche un stress réplicatif lorsque les fourches de réplication entrent en collision avec un complexe de clivage de Topoisomérase I bloquée sur l'ADN (*Pommier et al.,* 2010).
Afin de déchiffrer le rôle de PARG après traitement CPT, nous avons décidé d'étudier plusieurs marqueurs de stress et de réponse aux dommages (activation des checkpoints, dommages à l'ADN ...) juste après un traitement aigu et lors d'une libération cinétique après traitement au CPT (**Figure 33**). Les résultats obtenus sont présentés dans le troisième et dernier article de cette thèse.

Discussion et perspectives

For the English version, see p.200

1. Echapper au stress réplicatif : une tâche délicate.

Les résultats et les conséquences du stress de réplication sont des mécanismes complexes (Zeman et Cimprich, 2014), et compte tenu des données incomplètes que nous fournissons dans cet article, nous ne pouvons formuler que quelques hypothèses quant à ce qui pourrait arriver à chaque étape de la réponse à la CPT. La figure 34 schématise plusieurs voies pouvant être utilisées pour surmonter les lésions CPT. Dans cette discussion, je vais discuter certaines des hypothèses pour expliquer comment les cellules shPARG parviennent à échapper au stress réplicatif, même en absence de l'hyperphosphorylation de RPA. A chaque étape, je discturerai également la contribution potentielle de PARP1 et de DNA-PK.

A) Le traitement par CPT entraîne le piégeage de l'enzyme topoisomérase 1 (TOP1) dans un complexe de clivage (Top1-cc), bloquant son activité de coupure pour dégager la tension des torsions sur les brins d'ADN. Ceci conduit à la formation d'un brin d'ADN ouvert (Pommier *et al.* 2010). Cette situation initiale de blocage de la TOP1 peut avoir des résultats différents, qui dépendront de plusieurs facteurs.

B) Le moyen le plus rapide et le plus consensuel de réparer les lésions TOP1 est de les dégrader par une voie dépendante de l'ubiquitine, en adressant la protéine vers le protéasome (Desai *et al.* 1997). TOP1 et PARP1 interagissent et co-localisent dans les cellules et la PARylation de TOP1 influence sa distribution et son activité

dans le noyau (Das *et al.* 2016; Yung *et al.* 2004). En parallèle, l'augmentation de la PARylation après traitement à la CPT favorise également le recrutement du complexe TDP1 / XRCC1. Les cellules TDP1 knock-out sont très sensibles à la CPT, et une étude a démontré que TDP1 joue un rôle central dans la voie du NHEJ, au travers de la liaison du complexe XLF (Li *et al.* 2017). En effet, TDP1 lie PARP1 et peut exciser directement Top1-cc, générant une cassure simple brin qui peut être réparée par excision de base, en raison de la présence de XRCC1 (Das *et al.* 2014). De plus, TDP1 est capable de promouvoir l'assemblage du complexe des protéines du NHEJ. Il interagit avec Ku70 / Ku80, favorise la liaison à l'ADN du complexe XLF et stimule l'activité de DNA-PK (Heo *et al.* 2015). La phosphorylation par DNA-PK et ATM de la S81 de TDP1 est nécessaire pour médier l'association de XLF et nécessaire pour une activité de TDP1 optimale (Das *et al.,* 2009). Puisque DNA-PK phosphoryle également XRCC1 après irradiation, DNA-PK pourrait agir dans la voie du SSBR après une lésion induite par la CPT (Lévy *et al.,* 2006). En ce qui concerne le lien entre DNA-PK, PARP1 et la réparation de cassures simple brin, nous avons émis l'hypothèse que la carence en PARG pourrait conduire à une réparation altérée des dommages induits par la CPT, via la voie TDP1. Cependant, nous ne pouvions pas l'évaluer précisément en raison de considérations techniques, comme discuté dans l'article.
Cet aspect de la réponse au CPT fait défaut dans notre étude, car TDP1 répare principalement les complexes Top1-cc couplés à la transcription (Shiloh *et al.,* 2013). Ici, nous n'avons pas du tout considéré l'impact des lésions Top1-cc couplées à la transcription, même si une déficience en PARG est susceptible de déclencher des altérations du taux de transcription, et donc d'augmenter la quantité de dommages à l'ADN.

C) En cas de collision avec la fourche de réplication, un type important de lésion est généré: des DSB à extrémité unique (seDSB). Les cellules doivent éviter d'utiliser NHEJ pour réparer ce type de lésion, car il n'y a pas de brin complémentaire pour la réparation. Chanut *et al.* (2016) ont décrit un modèle dans lequel Ku80 et DNA-PK reconnaissent d'abord le DSB à extrémité unique, puis sont expulsés par les actions coordonnées du complexe MRN et de l'endonucléase CtIP qui vont provoquer la résection des brins permettant le chargement de Rad51 et la recombinaison homologue (RH) (Chanut *et al.,* 2016). Puisque PARP1 et PAR ont un rôle démontré dans la régulation de la résection, une déficience en PARG pourrait nuire à cette étape. En outre, les brins ayant subi une résection doivent être rapidement couverts par RPA2 afin de les protéger des nucléases, et la phosphorylation de RPA2 est un événement important pour la RH puisque l'hyperphosphorylation de RPA2 augmente son affinité avec Rad51 et favorise son remplacement (Wu *et al.,* 2005). Une version de RPA2 impossible à phosphoryler induite une réduction de la formation des foyers Rad51 et diminue la fréquence de la recombinaison homologue (Shi *et al.,* 2010), ce qui explique pourquoi l'hyperphosphorylation de RPA2 favorise la résistance à la CPT (Anantha *et al.,* 2007). Par conséquent, alors que le HR devrait être la voie principale pour surmonter les lésions TOP1 et permettre le chargement efficace de Rad51 dans nos cellules CTRL affichant un signal RPA2-P-S4S8, notre modèle shPARG semble être défectueux pour cette voie. Cependant, les résultats préliminaires de la formation de foyers Rad51 n'indiquent aucune réduction dans les cellules shPARG (données non présentées).

D) Alternativement au chargement classique de Rad51 et à un échange d'affinité avec la protéine RPA2 hyperphosphorylée, plusieurs mécanismes ont été proposés, pour permettre une charge efficace de Rad51.
L'E3-ubiquitine ligase Rad18 a des fonctions importantes pour la voie de synthèse translésionnelle (TLS), en régulant la monoubiquitination de PCNA, un événement qui favorise un changement de polymérase, en recrutant des polymérases spécialisées capables de contourner les lésions de l'ADN (Song *et al.* 2010). En soi, il a également été démontré que Rad18 se lie à Rad51 (Huang *et al.,* 2009).
En plus de son rôle direct sur Rad51, Rad18 régule la voie de l'anémie de Fanconi (Palle et Vaziri, 2011). Cette voie intervient principalement dans la réparation des cross-link entre brins, mobilisant des dizaines de protéines, parmi lesquelles un complexe de 8 protéines Fanconi Anemia, un complexe central ID2 composé des complexes FANCI et FANCD2, pouvant servir de plateforme de recrutement pour des effecteurs en aval comme XPF, BRCA2 ou Rad51 (pour une revue, voir Ceccaldi *et al.,* 2016). Au cours des dernières années, il y a de plus en plus de preuves du rôle de la voie FANC dans la stabilisation des fourches de réplication en arrêt, la promotion du redémarrage des fourches et l'inhibition des nouvelles origines de réplication (Schlaker *et al.* 2012, Raghunandan *et al.* 2015; Chaudury *et al.* 2013). En outre, chez la levure, la polymérase trans-lésionnelle REV1, en coopération avec FANCD2, est capable de stabiliser les filaments Rad51 (Yang *et al.,* 2015), et une autre étude chez l'homme a montré que FANCD2 est important pour le redémarrage de la fourche de réplication dépendant de Rad51 (Thompson *et al.* 2017). En l'absence de Rad18 ou de FANCD2, le nombre de foyers BRCA2 et Rad51 diminue après un traitement à la CPT (Tripathi *et al.,* 2016).
Dans les cellules DT40 de poulet, l'invalidation simultanée PARP1 et de Rad18 a un effet synergique et sensibilise les cellules au traitement CPT, suggérant qu'elles collaborent pour se remettre du traitement génotoxique (Saberi *et al.,* 2007). Rad18 est également impliqué dans le SSBR (Shiomi *et al.,* 2007), une voie dans laquelle PARP1 est centrale. En ce qui concerne le lien étroit entre PARG et PCNA, nous pouvons émettre l'hypothèse qu'en l'absence de PARG, Rad18 et / ou FANCD2 pourraient agir plus efficacement pour permettre un recrutement indépendant de Rad51 par RPA.

E) TOPBP1 (Topoisomerase IIB binding protein 1) est une protéine de structure, dotée de fonctions essentielles à la stabilité du génome (Sokka *et al.,* 2010). La littérature rapporte qu'elle améliore l'activité d'ATR en interagissant avec la protéine partenaire ATRIP (Kumagai *et al.,* 2006, Mordes *et al.,* 2008) et est impliqué dans la RH par son interaction avec la protéine NSB1 du complexe MRN (Morishima *et al.* 2007).
TOPBP1 interagit avec PARP1 (Wollmann *et al.,* 2007) et est un déterminant de la sensibilité aux inhibiteurs de PARP (Moudry *et al.,* 2016). Mécanistiquement, il a été montré que TOPBP1 se lie à et active la PLK1 pour phosphoryler Rad51 sur la position Ser14 (Moudry *et al.,* 2016), un pré-requis pour la phosphorylation de Rad51 par CK2 sur la position T13 et le chargement ultérieur de RAD51 sur la chromatine (Yata *et al.,* 2012). Ce chargement RAD51 promu par TOPBP1 est indépendant du complexe BRCA1 / PALB2 / BRCA2 (Sy *et al.,* 2009) nécessaire pour les étapes classiques de HR (Moudry *et al.,* 2016). L'absence de TOPBP1 a un impact sur le recrutement de RAD51, sans affecter la résection et le chargement de RPA (Moudry *et al.,* 2016). Fait intéressant, PLK1 est une kinase que nous avons trouvée associée à PARG dans nos ensembles de données de spectrométrie de masse (données non présentées), CK2 est une kinase qui phosphoryle PARG (Gagné *et al.,*

2008) et d'autres données préliminaires suggèrent que PARG et TOPBP1 interagissent physiquement et que cette interaction est réduite lors du traitement CPT (données non présentées). Au total, l'absence de PARG pourrait favoriser le chargement de Rad51 favorisé par TOPBP1, indépendamment de la phosphorylation de RPA2. Cette hypothèse est actuellement à l'étude.

F) Un autre dernier scénario de l'intoxication à la CPT est que les fourches peuvent s'inverser en des jonctions à quatre voies appelées «pied de poule». L'inversion de la fourche est fortement favorisée par PARP1, car elle inhibe le redémarrage de la fourche de replication dependant de l'hélicase RECQ1 (Berti *et al.,* 2013). Cette hypothèse, détaillée ci dessous, mérite également plus d'attention.

2. Inversion de la fourche de réplication en tant que réponse générale au stress réplicatif.

Des études distinctes et concordantes ont été publiées dans la littérature, qui ont conduit à considérer l'inversion de la fourche comme un mécanisme conservé au cours de l'évolution pour échapper au stress réplicatif (Ray Chaudhuri *et al.,* 2012), et qui peut survenir après différents types de traitement tout en reposant sur la présence de Rad51. Fait intéressant, bien que le CPT ne devrait pas déclencher de découplement à la fourche, Zellweger *et al.* 2015 a démontré que des doses légères de CPT pouvaient favoriser la formation d'ADNsb plus long aux jonctions d'inversion de la fourche. Ils montrent qu'un appauvrissement de Rad51 par expression d'un siRNA supprime le ralentissement de la fourche et l'inversion après le traitement CPT, et pourrait donc être un élément clé pour stabiliser les fourches inversées. La dernière étude utilisant des modèles déficients en PARG montre que sur les situations de base, en l'absence de traitement, la déplétion de PARG conduit à une augmentation du niveau spontané d'inversion de la fourche (Ray Chaudhuri *et al.,* 2015). C'est une observation importante, car elle pourrait être le mécanisme clé pour expliquer pleinement nos propres résultats. En effet, l'accumulation de l'inversion de la fourche dépend de l'activité de PARP1 et des niveaux de polymère (Berti *et al.,* 2013). Par conséquent, l'augmentation des évènements d'inversion spontanée de la fourche pourraient résulter de l'accumulation de PAR à dans nos cellules shPARG.
De plus, l'inversion de fourche aurait un rôle protecteur pour les fourches de réplication, agissant comme un «frein d'urgence» dans les cellules, afin de donner du temps aux mécanismes de réparation pour intervenir et ainsi surmonter le stress réplicatif et faciliter le redémarrage de la fourche (Higgins et al., 1976 ; Berti et Vindigni, 2013). Étant donné que 1) nos cellules U2OS sont plutôt protégées contre les traitements CPT; 2) comme discuté ci-dessus, l'absence de PARG pourrait favoriser un recrutment de Rad51, indépendant de RPA aux fourches, à travers la voie TOPBP1 ou FANCD2; 3) Rad51 est nécessaire pour l'inversion de la fourche (Zellweger *et al.,* 2015); Dans l'ensemble, nous pourrions décrire une situation où la déficience en PARG favorise la stabilisation dépendante de Rad51 des fourches inversées, pour surmonter le stress réplicatif induit par CPT, indépendamment de l'hyperphosphorylation de RPA.

3. Le redémarrage de la fourche comme voie de survie ?

Après l'inversion de la fourche, la fourche de réplication peut soit redémarrer en remodelant la structure de la jonction à quatre voies, soit altérer la réplication, générant ainsi des fossés simple brin post-réplicatifs (Heller *et al.,* 2006), qui doivent également être couverts par RPA et réparés ensuite par remplissage avec des polymérases trans-lésionnelles spécialisées, à travers la voie de synthèse translésionnelle (TLS) (Daigaku *et al.,* 2010). Chez l'homme, la protéine PrimPol peut reprendre la réplication après la fourche endommagée (Mouron *et al.,* 2013), et les polymérases translésionnelles (PolH, REV1, POLK, POLI, REV3L, REV7, POLN et POLQ, (pour une revue voir Sale *et al.,* 2012), peuvent réparer ces anomalies, puisque PARG et PCNA interagissent (Mortusewicz *et al.,* 2011; Kaufmann *et al.,* 2017) et que PCNA joue un rôle clé dans TLS (pour une revue, voir Kanao et Masutani, 2017), Nous pouvons suggérer que l'absence de PARG pourrait en quelque sorte favoriser la fonction TLS après traitement à la CPT. Les cellules HeLa déficientes en PARG présentent des patchs simple brins étendus après un traitement à la CPT nul ou très léger (Ray Chaudhuri *et al.,* 2015), ce qui pourrait s'expliquer par une plus forte proportion de redémarrage des fourches, directement liée à une plus grande proposition de ralentissement de fourches et d'évènements de réversion. Bien que nous n'ayons pas mesuré la vitesse à la fourche ni les lacunes d'ADN simple brin dans notre modèle de cellules U2OS, la déplétion de PARG a entraîné de tels phénotypes dans Ray Chaudhuri *et al.,* 2015.

Avec nos données actuelles et la compréhension actuelle de la question, je propose cette hypothèse pour expliquer pourquoi les cellules shPARG peuvent échapper au stress réplicatif en l'absence de phosphorylation de RPA (Figure 35). Alors que la lignée shCTRL présente une réponse médiée par HR normale après CPT, la lignée shPARG pourrait favoriser la stabilisation par Rad51 et PARP1 des événements d'inversion de la fourche, conduisant ainsi à un redémarrage de la fourche, sans besoin d'hyperphosphorylation de RPA. L'accumulation d'espaces ssDNA post-réplicatifs dans shPARG pourrait alors expliquer que la perte de RPA-S4S8 n'est pas couplée avec un recrutement altéré de RPA sur la chromatine.

4. L'absence de phosphorylation sur RPA-P-S4S8 résulte d'un effet direct sur RPA

Dans le modèle précédent, j'ai décrit comment les cellules shPARG pouvaient échapper au stress réplicatif sans avoir besoin de phosphorylation de RPA, mais cela n'explique pas entièrement les origines de cette diminution de phosphorylation.

Dans un travail antérieur, notre laboratoire avait démontré que l'activité PARG était nécessaire pour éviter l'accumulation délétère de PAR sur l'RPA, en cas de stress prolongé de réplication induit par l'HU (Illuzzi *et al.,* 2014). Le fait que le traitement à la CPT n'induise pas autant de synthèse de polymère que dans le traitement par HU s'oppose à l'hypothèse d'une suraccumulation de PAR sur RPA. Cependant, nous avons testé à la fois une immunoprécipitation de PAR, afin de révéler RPA et une immunoprécipitation de RPA pour révéler PAR, après traitement à la CPT. Dans les deux cas, nos données préliminaires n'ont pas révélé de RPA PARylée (données non présentées).

Dans un autre scénario, on peut imaginer la contribution d'une hélicase à ce mécanisme. Récemment, il a été montré que HARP / SMARCAL1, une hélicase dépendante de l'ATP, est capable de réenrouler la structure de l'ADN en se liant au RPA. Fait intéressant, HARP co-purifie avec RPA lié à DNA-PK et bloque la phosphorylation de RPA (Quan *et al.,* 2014). Il serait intéressant de voir si HARP est PARylé dans les cellules shPARG, et si cela pourrait favoriser la stabilisation d'une forme non phosphorylée de RPA.

Nous avons voulu suivre l'activité des kinases, mais l'impact de chacune d'entre elles sur la protéine RPA n'était pas clair dans la littérature, et la phosphorylation du RPA est sous le contrôle d'une régulation complexe, et dépend à la fois du type de dommage ADN et du cycle cellulaire (Maréchal et Zou, 2015). Certains des événements de phosphorylation doivent être "amorcés" par des cycline kinases. Une étude a montré que l'activité de Cdk5 favorisait l'activation du point de contrôle de la réplication par phosphorylation du RPA et était un déterminant de la sensibilité de l'inhibiteur de la PARP. Les cellules HeLa et U2OS déficientes en Cdk5 présentent une sensibilité plus élevée à l'irradiation en phase S. Cela est dû à un amorçage réduit des marques de phosphorylation Ser23, Ser29 et Ser33, qui entraîne des niveaux plus faibles de phosphorylation de RPA-S4S8 et est associé à une augmentation des dommages à l'ADN (Chiker *et al.,* 2015). Savoir si nos cellules shPARG peuvent présenter un défaut dans l'amorçage de l'hyperphosphorylation de RPA requiert une enquête plus approfondie.

Plusieurs études ont suggéré que la DNA-PK est la principale kinase impliquée dans l'hyperphosphorylation de RPA (Shao *et al.,* 1999), ciblant principalement S33 et T21 ou S4S8 (Ashley *et al.,* 2014). Dans notre étude, nous avons montré que ATM était la principale kinase responsable de la phosphorylation de RPA-S4S8 après CPT dans les cellules U2OS, mais son activité n'était pas altérée, comme révélé par l'activation efficace de Chk2. Nous ne pouvons pas exclure que l'activité ATM soit stimulée par des événements de réversion de fourche. L'activation d'ATR a été légèrement retardée, et comme un excès d'ADNss a été lié à l'activation de l'ATR (Zou et Elledge, 2003), on peut imaginer que dans les shPARG cela est dû à l'accumulation d'interstices d'ADN simple brin plutôt qu'à une résection. Cela donne du poids supplémentaire à l'hypothèse selon laquelle après le traitement à la CPT dans les shPARG, la signalisation ATM / ATR peut être couplée à l'accumulation de dommages à l'ADN (Ray Chaudhuri *et al.,* 2015). L'activité de DNA-PK a été évaluée uniquement par son autophosphorylation dans S2056. DNA-PK affiche plusieurs groupes de phosphorylation qui ont des impacts différents sur son activité dans la réparation de l'ADN. Par exemple, la phosphorylation de Ser2056 dans le groupe «PQR» est censée restreindre l'accès de DNA-PK aux extrémités de l'ADN, tandis que la phosphorylation de Thr2609 dans le cluster «ABCD» favorise l'accès aux extrémités de l'ADN et favorise la voie du NHEJ (Chan *et al.,* 2002). Par conséquent, le suivi de la phosphorylation de la Ser2056 uniquement, en tant que marqueur de l'activité DNA-PK est limitante. Nous avons pensé à tester la phosphorylation de p53 comme une meilleure preuve de l'activité de DNA-PK. Cependant, une étude a montré que la phosphorylation simultanée de p53 par ATR et ATM, et RPA par DNA-PK est nécessaire pour perturber l'interaction p53-RPA, leur permettant d'effectuer leur fonction dans la réparation de dommages à l'ADN, de sorte que même la phosphorylation p53 pourrait ne pas être un marqueur efficace pour conclure (Serrano *et al.,* 2013).

5. La technique IPond comme solution ?

Tout au long de cette étude, nous nous sommes concentrés sur le stress réplicatif déclenché lors de la collision de la fourche de réplication avec des complexes de clivage TOP1-cc, mais sans tenir compte du rôle de Top1 dans la prévention de la formation de structures en R-loop qui peuvent également altérer la transcription (Tuduri *et al.* 2009).

Les techniques de protéomique sur l'ADN en cours de synthèse sont une méthode efficace pour ébaucher le réseau complexe de protéines qui sont recrutées sur des fourches de réplication actives ou endommagées (Sirbu *et al.,* 2011 ; Drungralawa *et al.,* 2015). En 2016, l'équipe de Ribeyre et al. Ont montré que plusieurs facteurs protéiques sont recrutés dans la fourche de réplication, jouant un rôle à la fois sur les dommages et la réplication de l'ADN (ADN-PK, Ku80, Ligase 1, Ligase 3), la transcription et le traitement de l'ARN et la structure de la chromatine (SMARCA5, BAZ1B, NUMA1). Toutes ces fonctions sont étroitement liées à la Poly (ADP-ribosylation). Il est intéressant de noter que BAZ1B / WSTF est étroitement associé à PCNA (Poot *et al.* 2004, Poot *et al.* 2005), un partenaire démontré de PARG (Mortusewicz *et al.* 2011; Kauffmann *et al.* 2017). Des données préliminaires dans notre laboratoire ont également montré que la PARG pouvait directement co-immunoprécipiter avec WSTF (G. Illuzzi, communication personnelle). Parce que la déplétion de WSTF par siRNA entraîne une réduction de la phosphorylation de γH2AX, ainsi qu'une légère réduction de la phosphorylation de Chk1 et RPA2-S4S8, nous pourrions supposer que l'absence de PARG pourrait provoquer la diminution du recrutement de WSTF aux fourches de réplication.

Une autre étude intéressante utilisant la technique de l'IPOND a révélé la cinétique de plusieurs facteurs protéiques après le stress de réplication induit par l'HU (Drungralawa *et al.,* 2015). Cette étude montre que si les niveaux de PARP1 sont stables aux fourches de réplication, PARG est évincé de la fourche, tandis que H2A.1 et H2A.2, recrutés par le PAR (Khurana *et al.,* 2014) sont en augmentation, contribuant éventuellement à la création d'un environnement permissif de la chromatine permettant la réparation et le redémarrage de la fourche en arrêt. De manière générale, un prétraitement avec un inhibiteur de PARP avant l'exposition à la CPT a complètement rétabli le niveau de phosphorlation de RPA-S4S8 dans shPARG (données non présentées). Comme l'inhibition de la PARP sensibilise également les cellules au traitement CPT, cela prouve que l'accumulation du PAR au voisinage de la fourche de réplication est nécessaire pour un redémarrage correct de la fourche et qu'elle joue un rôle protecteur (Amé *et al.* 2009)

La meilleure méthode pour suivre ce qui se passe dans nos cellules shPARG serait d'utiliser la technique IPOND, couplée à la spectrométrie de masse, comme décrit dans Sirbu *et al.* 2011 et Drungralawa *et al.* 2015

Conclusion

Dans cette étude, nous avons utilisé une nouvelle lignée cellulaire U2OS déficient en PARG pour analyser la réponse à plusieurs agents endommageant l'ADN ou inducteurs de stress réplicatifs. Dans ces cellules shPARG, nous avons observé un défaut dramatique dans la phosphorylation de RPA-S4S8 qui n'était pas associé à une forte diminution des dommages à l'ADN, ou à une signalisation défectueuse des dommages. Ni le chargement

de RPA sur la chromatine, ni l'activité des kinases de la famille PI3-K associées à la phosphorylation de RPA2-S4S8 ou T21 n'a été altéré. Bien que nous ayons supposé que le défaut de phosphorylation de RPA reflète une résection altérée, couplée à un niveau diminué de recombinaison homologue aux fourches de réplication effondrées, nos résultats suggèrent que ces processus ne sont pas affectés de manière dramatique, et l'inhibition PARG ne diminue pas la viabilité cellulaire. Ceci suggère que les cellules déficientes en PARG utilisent des voies alternatives pour compenser ce défaut de RPA-S4S8. De façon plus globale, ces résultats aident à comprendre les mécanismes liant l'activité Top1 et la PARylation, deux caractéristiques fondamentales de l'intégrité génomique qui peuvent s'avérer être un ami ou un ennemi des cellules de mammifères (Kim et Jinks-Robertson, 2017).

Conclusion générale:

Durant ce projet de thèse, je me suis concentrée sur trois axes de recherche: le but initial de mon projet (**Objectif 1**) était de générer de nouveaux modèles cellulaires innovants permettant l'étude de la régulation PARG et la contribution précise de chaque isoforme à la réparation de l'ADN. En utilisant la technologie Golden Gate, j'ai généré plusieurs lignées cellulaires stables dans un contexte U2OS permettant le knockdown de toutes les isoformes de PARG endogènes et l'induction sélective de chacune des isoformes de PARG (**article de recherche n ° 1, non publié**). Le projet a également abouti à l'élaboration d'une nouvelle méthodologie à haut débit pour mesurer la dynamique de la dégradation des PAR dans les lignées cellulaires exprimant les isoformes. En utilisant ces outils, nous avons fourni de nouvelles preuves confirmant que $PARG^{102}$ est l'isoforme la plus abondante dans les cellules humaines, et qu'elle peut contribuer à la réparation de l'ADN.

Un autre objectif de mon projet (**Objectif 2**) était d'étudier si le PARG pouvait être régulé par des modifications post-traductionnelles. Ce projet a permis de découvrir un nouveau partenaire protéique, la DNA-PK, qui pourrait phosphoryler PARG in vitro sur plusieurs sites cibles identifiés, et dont l'interaction avec PARG augmente après lésion de l'ADN (**Article de recherche n ° 2, non publié**). Bien que la pertinence fonctionnelle des sites de phosphorylation nécessite une investigation supplémentaire, ce travail fournit une preuve supplémentaire que PARG, de même que PARP1, peut probablement être régulé par des kinases importantes jouant dans la réponse aux dommages de l'ADN.

Dans la dernière partie de mon projet, profitant de nos nouveaux modèles cellulaires et sachant que PARG et DNA-PK étaient des partenaires protéiques, j'ai eu l'intention d'étudier le rôle de PARG dans la réponse cellulaire à la camptothécine (**Objectif 3**). Ce projet était basé sur une investigation systématique de plusieurs marqueurs de réparation de l'ADN, lors d'une cinétique suite à un traitement aigu à la CPT, un médicament utilisé dans les thérapies anticancéreuses (**article de recherche n ° 3, non publié**). Nos résultats suggèrent que les cellules shPARG, bien qu'elles présentent un fort défaut de phosphorylation de RPA, sont capables d'utiliser des voies alternatives pour surmonter le stress réplicatif induit par la CPT.

Les résultats obtenus dans les différentes parties de ce manuscrit de thèse fournissent de nouvelles preuves que PARG, en tant que l'une des principales enzymes responsable de l'homéostasie du PAR, a une régulation complexe. La génération d'isoformes et les modifications post-traductionnelles sont susceptibles d'influencer

l'interaction entre PARG et d'autres facteurs protéiques impliqués dans le maintien de l'intégrité du génome. Au total, ce projet constitue une étape supplémentaire dans notre compréhension du rôle de la PARG en réponse aux dommages à l'ADN et au stress réplicatif. Cette connaissance sera précieuse pour l'élaboration de nouvelles stratégies pour le ciblage thérapeutique de lignées cellulaires cancéreuses déficientes dans le processus de réparation de l'ADN avec l'utilisation combinée d'agents génotoxiques et d'inhibiteurs de protéines.

Abstract:

Poly(ADP-ribosyl)ation is a post-translational modification of proteins involved in a wide number of biological processes including DNA repair. The function and mode of action of poly(ADP-ribose) (PAR) polymerase-1 (PARP1) activated in response to DNA damage is well established and PARP inhibitors have entered the clinics for the treatment of advanced breast and ovarian cancers. Far less is known about the function and regulation of the PAR degrading enzyme poly(ADP-ribose) glycohydrolase (PARG). Its study has been complicated by the existence of five low abundant isoforms, and the lack of functional tools to study them. Indeed, PARG is encoded as a single gene generating five different isoforms (the nuclear PARG^{111}, cytoplasmic PARG^{102}, PARG^{99} and PARG^{60} and mitochondrial PARG^{55}). In this thesis project, we describe new stable PARG deficient U2OS cell lines, allowing the inducible complementation with each of PARG isoforms in order to assess their contribution to nuclear PAR degradation induced by oxidative stress. In an attempt to identify functional partners and regulators of PARG, we performed mass spectrometry and identified the DNA-damage dependent kinase DNA-PK as a new partner of PARG, which is able to phosphorylate PARG on multiple target residues. We examined the functional interaction between PARG and DNA-PK using U2OS PARG deficient cell lines, in response to the anticancer drug camptothecin (CPT), a topoisomerase I inhibitor that triggers the activation of both PARP1 and DNA-PK. PARP inhibitors strengthen the cytotoxic effect of CPT, phenomenon which is now exploited in clinical trials. We show that in contrast to PARP inhibition, PARG deficiency does not impair cell survival after CPT treatment and only slightly reduces checkpoint activation and double strand-break formation. Intriguingly, PARG deficiency triggers a dramatic delay in RPA2-S4S8 phosphorylation, generally attributed to DNA-PK catalytic activity, suggesting that tolerance to CPT in the absence of PARG could rely on alternative mechanisms than the consensual homology-directed replication fork repair or restart, to escape replication stress.

Résumé :

La Poly(ADP-ribosyl)ation est une modification post-traductionnelle de protéines, impliquée dans un grand nombre de processus biologiques, dont la réparation de l'ADN. La fonction et le mode d'action de la Poly(ADP-ribose) (PAR) Polymérase 1 (PARP1), activée en réponse aux dommages de l'ADN sont bien compris et les inhibiteurs de PARP1 sont utilisés en clinique pour le traitement de cancers du sein et de l'ovaire avancés. En revanche, on en sait beaucoup moins sur la fonction et la régulation de l'enzyme de dégradation du PAR, la Poly(ADP-ribose) glycohydrolase (PARG). L'existence de cinq isoformes de faible abondance (la PARG^{111} nucléaire, les PARG^{102}, PARG^{99} et PARG^{60} cytoplasmiques et la PARG^{55} mitochondriale), ainsi que l'absence d'outils pour les étudier de manière comparative a longtemps compliqué l'analyse de PARG. Dans le contexte de ce projet de thèse, nous décrivons de nouvelles lignées U2OS stables, déficientes pour toutes les isoformes de PARG, permettant la complémentation inductible avec chacun des isoformes de PARG, dans le but d'évaluer leur contribution respective à la dégradation du PAR nucléaire induit par un stress oxydatif. Des expériences de spectrométrie de masse, réalisées dans le but de trouver de nouveaux partenaires fonctionnels et de nouveaux régulateurs de PARG nous ont permis d'identifier la protéine kinase dépendante des dommages de l'ADN (DNA-PK) comme un nouvel interactant, capable de phosphoryler PARG sur plusieurs acides aminés cibles. Nous avons exploré l'interaction fonctionnelle entre PARG et DNA-PK dans le contexte de la réponse cellulaire à la camptothécine (CPT), un agent anticancéreux inhibant la topoisomérase I et provoquant l'activation simultanée de PARP1 et DNA-PK. Les inhibiteurs de PARP renforcent l'effet cytotoxique de la CPT, un effet exploité dans le cadre d'essais cliniques. Nous montrons que, contrairement à l'inhibition de PARP, l'absence de PARG ne compromet pas la survie des cellules après traitement à la CPT et ne diminue que légèrement l'activation des points de contrôle et la formation de cassures double brin. En revanche, l'absence de PARG provoque une réduction drastique de la phosphorylation de RPA2-S4S8, généralement attribuée à l'activité catalytique de DNA-PK, suggérant que en absence de PARG, la tolérance à la CPT puisse dépendre de mécanismes alternatifs pour échapper au stress réplicatif, autres que la réparation ou le redémarrage des fourches par des voies consensuelles de recombinaison homologue.